

**INVESTIGATIONS OF THE BIOLOGICAL ROLES  
OF SUBSTITUTED CYCLOHEXADIENES**

A Dissertation

by

BENNIE JOHN BENCH

Submitted to the Office of Graduate Studies of  
Texas A&M University  
in partial fulfillment of the requirements for the degree of

DOCTOR OF PHILOSOPHY

December 2009

Major Subject: Chemistry

**INVESTIGATIONS OF THE BIOLOGICAL ROLES  
OF SUBSTITUTED CYCLOHEXADIENES**

A Dissertation

by

BENNIE JOHN BENCH

Submitted to the Office of Graduate Studies of  
Texas A&M University  
in partial fulfillment of the requirements for the degree of

DOCTOR OF PHILOSOPHY

Approved by:

Chair of Committee,  
Committee Members,

Head of Department,

Coran M. H. Watanabe  
Daniel A. Singleton  
Wenshe Liu  
Gary Kunkel  
David H. Russell

December 2009

Major Subject: Chemistry

## ABSTRACT

Investigations of the Biological Roles of Substituted Cyclohexadienes

(December 2009)

Bennie John Bench, B.S., Southeastern Oklahoma State University

Chair of Advisory Committee: Dr. Coran M. H. Watanabe

In recent years there have been two cycloterpenals, molecules consisting of a cyclohexadienal core, isolated from nature. Cyclocitral, the condensation product of citral, has been isolated from the North Sea bryozoans *Flustra foliacea*. In the human eyes, cycloretinal has been isolated and is a toxic by product of the vision cycle. This retinal dimer is believed to contribute to age related macular degeneration, the leading cause of blindness in the elderly. In 1992, it was discovered that if  $\beta$ -ionylideneacetaldehyde was incubated with beta-lactoglobulin ( $\beta$ -LG), the principal whey protein in dairy milk, that it would mediate the formation of cyclo- $\beta$ -ional. No follow up studies were performed on this protein mediated reaction or what biological activities these cycloterpenals may possess.

This dissertation investigates the biological roles of substituted cyclohexadienes including cycloterpenals and cyclohexadiene enaminonitriles. To mimic the protein mediated reaction, we developed a synthetic procedure to produce a wide array of cycloterpenal by utilizing L-proline. Over 100 cycloterpenals were synthesized and screened for their biological activities against an array of cell based screens. The phenotypic effects of these cycloterpenals were screened against a PC12

assay where dramatic effects were observed on neurite outgrowth. During the synthesis of starting materials for the production of our cycloterpenal library, it was discovered that if excess base was added to the Horner-Wadsworth-Emmons reaction between a methyl-ketone and diethyl-(cyanomethyl)-phosphonate, conversion of the  $\alpha$ - $\beta$ -unsaturated nitrile into an enamionitrile was observed. This new synthetic procedure was optimized to generate a library of enamionitriles as well as their quinazoline derivatives.

The work within also includes the investigation of the  $\beta$ -LG mediated reaction formation of cycloterpenals with natural and unnatural  $\beta$ -methyl aldehydes. We were able to demonstrate that  $\beta$ -LG could mediate the conversion of  $\alpha$ , $\beta$ -unsaturated aldehydes into their corresponding cycloterpenal. *In vitro* analysis was also performed with store bought milks and the  $\beta$ -LG present was able to mediate the formation of cyclocitral. An *in vivo* experiment was also performed by utilizing New Zealand White rabbits to demonstrate the formation of cycloretinal within the blood stream by feeding a source of  $\beta$ -LG with retinal.

Interestingly, in human blood,  $\beta$ -LG is present at concentrations of 0.7-1.2 g/dL. The protein has been identified within drusen pigments and lipofuscin granules that accumulate in the retina of macular degeneration patients. As humans do not produce beta-lactoglobulin, the source of this protein is from milk and milk products. With these experiments, we clearly demonstrate that under the appropriate conditions, cycloretinal can be produced with  $\beta$ -LG. We have clearly established a direct link between  $\beta$ -LG chemistry and age-related macular degeneration.



## **DEDICATION**

To:

My Family, Friends, the ones I've lost, and God

## ACKNOWLEDGMENTS

First off, I would like to thank my second family, the Watanabe group, for their support over the years. I have to thank those who have persevered with me over the years: Dr. Scott Angell, EunJin Kim, Jennifer Foulke-Abel, Dr. Vasudha Sharma, Dr. Chaomin Liu, and Hillary Agbo. Very special thanks to my good buddy, Dr. Gilbert Thom Kelly, whose encouragement, friendship, advice, and company (especially our “crazy hours”) has allowed me to get to where I am today. We went through everything in and out of the lab and survived. I also have to thank my friends outside the lab who have kept me sane over the years: Chris Hobbs, Victor Suarez and my bubba, Dr. Brandon Hudder.

I would like to thank my advisor, Dr. Coran M. H. Watanabe, for allowing me the freedom to do research in her group. I appreciate her for letting me explore my ideas and do the science that has enabled me to produce this dissertation and stop drinking chocolate milk.

I have to also thank all of those who have helped me along the way in collaborative efforts during my time at Texas A&M. I would like to recognize: Dr. Shane Tichy for his mass spectrometry expertise, Dr. Lisa Perez for her computational assistance and guidance, Dr. Vincent Gresham for his assistance during the rabbit study, and Dr. Bill Russell for going above and beyond during the study of beta-lactoglobulin.

For their service on my committee and helpful suggestions, I thank Dr. Dan Singleton, Dr. Weinshe Lui, and Dr. Gary Kunkel.

I would like to thank both sides of my family for all of their love and support throughout the years. If it were not for them, I would not be where I am at today. They have been a constant source of encouragement and have had my back during this entire endeavor. I would especially like to thank my Grandma Dot and Grandpa John for their constant love and support. Every day I would call grandma and give her the update and she would pass it along to the rest of the family. I have to give special thanks to my Aunts, Debbie and Denise and my Uncles, Brad and Frank for all of their support and shoulders to lean on in times of need. I cannot forget to thank them for the cookies and other goodies during my birthday. You can keep that up, I will not mind. I thank my lovely cousins Amber, Derek, Brooke, Terra, and Trevor. You are all my brothers and sisters and have supported me through all of the tough times. You have all grown up to be successful in each of your endeavors and I know that I have missed out on a lot over the past six years, but you know that I have always been cheering you on and given you my constant support. Now we just have to get Trevor through school. I also must thank their significant others as they have had to put up with me since coming into the family. So to Heather, Derek Ford, Caleb, and the newly enlisted Cody, I thank you for your support and the slaps on the back. To my Uncle Danny, you have always been the big brother I never had and I thank you for all of support over the years. I look forward to our future hunting and fishing trips together and catching up on lost time.

On the Bench side of things, I thank each and every one of you for your support and love. I have to give a special thanks to my Uncle Tot for his support throughout the years. I am ready to do some fishing that you owe me for getting

Jaime that scholarship. To Jaime, my little sissy, keep your head up and you can succeed. You have grown up to be a strong and successful woman. Keep it up. You do not know how proud I am of you. I have to thank my two cousins who I am in constant contact with. Mark, I am ready to hang out and go riding. I appreciate you having my back and being there through the tough times. We have both leaned on each other during our hard times. To Cory, I am glad that we have grown close and I look forward to all of our fun times to come. I appreciate all of your support and the laughs over the phone.

To my little baby cousins: Kaylee, Addison, Laynee, Hanna, and Lauren stay in school and study hard. You can achieve anything that you want out of life.

To my boys from Oklahoma, you guys are the best friends anyone could ask for. You all have been there for me during some tough times during my graduate career. I have to give shout outs to Daniel, Randy, Piggy, Rance, Casey, and my boy Bryan. We have been great friends for many years and I look forward to all of us growing old with each other and all the fishing and hunting to come. When I thank you guys, I have to thank your supporting casts of Crystal, Cris, and Karie for their support and chocolate delights. I have to give a special thanks to Del Holt for his support over the past couple of years and for being there for my mother. You have accepted me as one of your own and I greatly appreciate that. To Lara Butler, thank you for all of your love and support and putting up with me during some hard times.

Unfortunately during my tenure at A&M, I have lost some very special people in my life. Clint Williams, you were one of my best friends and a true American hero. You were a tragic loss to not only me but to the boys back home. I know we talked

about you coming to school here as soon as your time was done in the Army and I was looking forward to that time. I'll never forget the phone calls from overseas to see how school was going and how we would encourage each other to keep our heads up. Larry Bench, you were a constant source of encouragement and support. Our daily emails to each other were a highlight of my day. We all know that you were taken too soon. Dustin Bench, even though you have been gone for a few years, I always knew something was not right. I guess it was that brotherly instinct. I regret that we did not get to spend as much time together as we got into our later teens. The day I heard that they may have found your bones, I knew it was you my brother. I am glad we finally got to lay your bones to rest. It has been tough dealing with your losses, but I know that each of you have been with me as I think of you all each day and that has helped keep me driven. All of this work would not be possible if it was not for my parents, Bennie and Donna Bench. The support that I had from each of them was astounding. If I had one wish granted to me today, it would be that my father was here to see his son reach a major goal in his life that he helped encourage. I made him two promises right before he took his last breath and one has been fulfilled. To my mom, your constant love and support is what kept me strong throughout the years. Your hopes for my future have come true and I am very proud to be your son. I love you so much and thanks for everything. I am forever indebted to you.

I am proof that with a lot of hard work and persistence, any of your dreams can come true. Being a country boy from a small town in podunk Oklahoma, I have come a long ways. I will finally become "Dr. B.J. Bench" and I can say once again, Uncle Danny and Cousin Derek, "Who's the man now?"

## TABLE OF CONTENTS

	Page
ABSTRACT .....	iii
DEDICATION .....	v
ACKNOWLEDGMENTS .....	vi
TABLE OF CONTENTS .....	x
LIST OF FIGURES .....	xii
LIST OF SCHEMES .....	xvi
LIST OF TABLES .....	xviii
 CHAPTER	
I     INTRODUCTION .....	1
Introduction.....	1
Statement of Purpose .....	16
 II    INVESTIGATIONS OF THE BIOLOGICAL ROLES OF $\beta$ - LACTOGLOBULIN.....	 18
Introduction.....	18
Results and Discussion .....	21
Conclusion .....	52
Experimental.....	53
 III   SYNTHESIS AND BIOLOGICAL EVALUATION OF SELF- CONDENSATION CYCLOTERPENALS .....	 67
Introduction.....	67
Results and Discussion .....	71
Conclusion .....	91
Experimental.....	93

CHAPTER	Page
IV SYNTHESIS AND BIOLOGICAL EVALUATION OF HETERODIMERIC CYCLOTERPENALS.....	124
Introduction.....	124
Results and Discussion .....	126
Conclusion .....	157
Experimental.....	158
V SYNTHESIS OF CYCLOHEXADIENE ENAMINONITRILES AND QUINAZOLINES .....	214
Introduction.....	214
Results and Discussion .....	222
Conclusion .....	237
Experimental.....	237
VI CONCLUSION.....	255
REFERENCES .....	259
APPENDIX A .....	272
APPENDIX B .....	321
APPENDIX C .....	461
VITA.....	479

## LIST OF FIGURES

	Page
Figure 1. Graphical representation of drugs developed in the U.S. ....	1
Figure 2. Structures of carotenoids lycopene, vitamin E, and $\beta$ -carotene.....	6
Figure 3. Biologically relevant retinoids.....	6
Figure 4. Structures of cycloretinal, cyclocitral, and C-30 dimer. ....	8
Figure 5. Native BLG crystal structure. ....	12
Figure 6. The dimer interface viewed perpendicular to strand I. ....	12
Figure 7. Macular degeneration affects central vision. ....	13
Figure 8. Tunneling electron microscopy representation of drusen build-up. ....	14
Figure 9. Atomic force micrograph of RLF granules.....	15
Figure 10. Chemical structures of cyclo- $\beta$ -ional, cyclocitral, and cycloretinal. ....	21
Figure 11. $^1\text{H}$ -NMR of aldehyde region of cyclo- $\beta$ -ional formation. ....	22
Figure 12. Various concentrations of $\beta$ -LG observing cyclocitral production versus citral starting material. ....	23
Figure 13. Temperature optimization at room temperature (25°C) versus body temperature (37°C).....	24
Figure 14. pH effects on the self-condensation of BLG with citral. ....	26
Figure 15. pH profile color changes.....	27
Figure 16. BSA control spectra indicating no cyclocitral formation. ....	28
Figure 17. <i>E. coli</i> control indicating no metabolites in region of interest and after citral treatment. ....	29
Figure 18. Proposed routes to the synthesis of 1,2,4-trisubstituted cyclohexadienals. ....	33



	Page
Figure 19. Rate of formation for cyclocitral at various concentrations.....	36
Figure 20. $\beta$ -LG sequence with fragments containing active lysine residues.....	38
Figure 21. TK*IPAVFK fragmentation pattern. ....	39
Figure 22. IDALNENK*VLVLDTDYKK fragmentation pattern.....	40
Figure 23. Dimer bound IDALNENK**VLVLDTKYK fragmentation pattern. ....	40
Figure 24. Native $\beta$ -LG crystal structure depicting K77 and K91.....	41
Figure 25. $\beta$ -LG crystal structure depicting K77 and K91 with palmitate bound.....	42
Figure 26. $\beta$ -LG crystal structure depicting K77 and K91 with retinol bound. ....	42
Figure 27. Amino acid sequences for $\beta$ -LGs from various species with conserved K77 and K91 .....	44
Figure 28. Various milks incubated with citral for four days .....	45
Figure 29. $^1\text{H}$ -NMR of cyclocitral being produced from store bought milk after four days .....	46
Figure 30. $^1\text{H}$ -NMR overlay of rabbit feedings.....	50
Figure 31. SDS-PAGE gel of rabbit feedings. ....	51
Figure 32. $^1\text{H}$ -NMR overlay of blood experiment .....	52
Figure 33. Structures of relevant carotenoids.....	68
Figure 34. Biologically active retinoids .....	68
Figure 35. Structures of relevant homodimers .....	69
Figure 36. Chemical structures of the homodimer cycloterpenals-based compound library .....	71
Figure 37. Products formed by treatment of citral with NaH.....	72

	Page
Figure 38. CD spectra of menthylhydrazone derivatives. ....	75
Figure 39. Proposed routes to the synthesis of 1,2,4-trisubstituted cyclohexadienals. ....	78
Figure 40. Schematic diagram depicting Michael donor and acceptor interactions. ....	80
Figure 41. Time course analysis of retinal homodimerization by NMR. ....	81
Figure 42. Mass spectra of cycloretinal intermediates. ....	83
Figure 43. Citral mass spectra. ....	85
Figure 44. Numerical notation of citral homodimer 15. ....	86
Figure 45. Stimulation of neurite outgrowth. ....	89
Figure 46. Stimulation of neurite outgrowth by homodimer stereoisomers. ....	91
Figure 47. Structures of representative retinoid compounds. ....	125
Figure 48. Structures of cycloretinal, cyclocitral, and C-30 dimer. ....	125
Figure 49. Substituted heterodimeric cyclohexadienals generated by proline-mediated condensation of $\alpha,\beta$ -unsaturated aldehydes. ....	127
Figure 50. Chemical structures of heterodimers made with a single $\beta$ -methyl substituted aldehyde. ....	128
Figure 51. Cinnamaldehyde and 4-dimethylaminocinnamaldehyde Schiff base formation. ....	133
Figure 52. 4-nitrocinnamaldehyde Schiff base formation. ....	134
Figure 53. Time course analysis of proline-promoted formation of biphenyl-cinnamaldehyde heterodimers. ....	137
Figure 54. Products resulting from reaction of cinnamaldehyde with citral. ....	139

	Page
Figure 55. Chemical structures of heterodimers made with two $\beta$ -methyl substituted aldehydes.....	140
Figure 56. Chemical structures of heterodimers made with a $\beta$ -ethyl substituted aldehyde. ....	142
Figure 57. $^1\text{H}$ NMR spectra of the proton on C-6 of the products of the reaction between citral and cinnamaldehyde. ....	149
Figure 58. NMR predictions.....	150
Figure 59. Representative set of fluorescing aromatized heterodimers. ....	151
Figure 60. Representative structures of other aromatic compounds. ....	152
Figure 61. Stimulation of neurite outgrowth by cyclohexadienal heterodimers. ....	154
Figure 62. Stimulation of neurite outgrowth by heterodimer stereoisomers.....	156
Figure 63. General enaminonitrile scaffolds. ....	214
Figure 64. Enaminonitriles active against mice ScN2a cells. ....	216
Figure 65. Known cyclohexadiene enaminonitriles. ....	216
Figure 66. Quinazolines used as therapeutic agents.....	217
Figure 67. Structures of quinoxaline antibiotics. ....	219
Figure 68. $^1\text{H}$ -NMR depicting the mixture of $\alpha,\beta$ -unsaturated nitrile with self-dimerization product. ....	221
Figure 69. Enaminonitrile compounds synthesized. ....	226
Figure 70. Quinoxaline compounds synthesized.....	231

## LIST OF SCHEMES

	Page
Scheme 1. Building blocks of terpenoids.....	2
Scheme 2. Malvinate biosynthesis of isopentenyl pyrophosphate.....	3
Scheme 3. The deoxyxylulose phosphate pathway for IPP. ....	3
Scheme 4. Head-to-tail condensation of IPP and DMAPP to produce GPP.....	4
Scheme 5. Tail-to-tail condensation of geranylgeranyl pyrophosphate.....	5
Scheme 6. Nakanishi's proposed formation of all-trans-retinal C-40 dimer .....	8
Scheme 7. A2E and iso-A2E form highly reactive epoxides.....	15
Scheme 8. $\beta$ -LG mediated formation of cycloterpenals from $\beta$ -methyl aldehydes. ....	21
Scheme 9. $\beta$ -LG mediated reaction products between citral and cinnamaldehyde.....	34
Scheme 10. Synthetic route for retinal.....	48
Scheme 11. General reaction scheme for homodimer production. ....	71
Scheme 12. Reaction intermediates for the formation of cycloretinal.....	82
Scheme 13. Reaction intermediates for the formation of cyclocitral.....	84
Scheme 14. Synthesis of benzylidene aldehyde.....	85
Scheme 15. Isolation of stereoisomers.....	90
Scheme 16. Reaction scheme for biphenyl aldehyde and cinnamaldehyde.....	134
Scheme 17. Isolation of stereoisomers.....	155
Scheme 18. Horner Wadsworth Emmons reaction. ....	220
Scheme 19. Quinazolines derived from a cyclohexadiene enamionitrile scaffold. ....	222
Scheme 20. Proposed reaction mechanism of enamionitrile synthesis.....	225

	Page
Scheme 21. Synthesis of enaminonitriles using LDA.....	227
Scheme 22. Synthesis of quinazolines. ....	232

## LIST OF TABLES

	Page
Table 1. Selected ligand binding data for bovine $\beta$ -lactoglobulin. ....	11
Table 2. Yields at various pHs. ....	26
Table 3. Dimerization yields from one to four days.....	32
Table 4. Reaction yields for citral/cinnamaldehyde $\beta$ -LG reaction. ....	35
Table 5. K <sub>d</sub> measurement for substrates used for dimerization observations.....	37
Table 6. Effects of various substrates on proline promoted homodimerization.....	74
Table 7. Effect of proline derivatives on homodimerization.....	76
Table 8. Hydrogen/Deuterium integrations for cyclocitral. ....	87
Table 9. Hydrogen/Deuterium integrations for cyclocitral at proton 2.....	88
Table 10. Reactions involving a single $\beta$ -methyl substituted aldehyde. ....	129
Table 11. Reaction between two $\beta$ -methyl substituted aldehydes.....	141
Table 12. Reactions with $\beta$ -ethyl substituted donor aldehydes.....	143
Table 13. Cross-condensation reactions.....	145
Table 14. Percent conversions and quantum yields of fluorescent cyclohexadienals.....	152
Table 15. Percent yields using NaH. ....	224
Table 16. Substrate effects with excess NaH. ....	228
Table 17. Substrate effects with LDA.....	230
Table 18. Quinazoline product yields .....	234
Table 19. Cytotoxic activities against Jurkats.....	235
Table 20. Anti-microbial activities of library.....	236

## CHAPTER I

### INTRODUCTION

#### INTRODUCTION

Nature is a masterful synthetic chemist, producing compounds with diverse architecture and functionality. Natural resources have been used since antiquity for their pharmacological benefits. The sources of medicinal drugs range from terrestrial plants, marine organisms, and various microorganisms. To date, over 100,000 different molecules have been isolated and identified with many possessing biological activities.<sup>1</sup> These metabolites have significantly impacted the pharmaceutical market in the United States. Over the past 25 years, 47% of pharmaceuticals in the U.S. were comprised of natural products or their isolated derivatives. Furthermore, 73% of new drugs were synthetic derivatives or were built upon the basic molecular scaffold of natural products previously identified (Figure 1).<sup>2,3</sup>

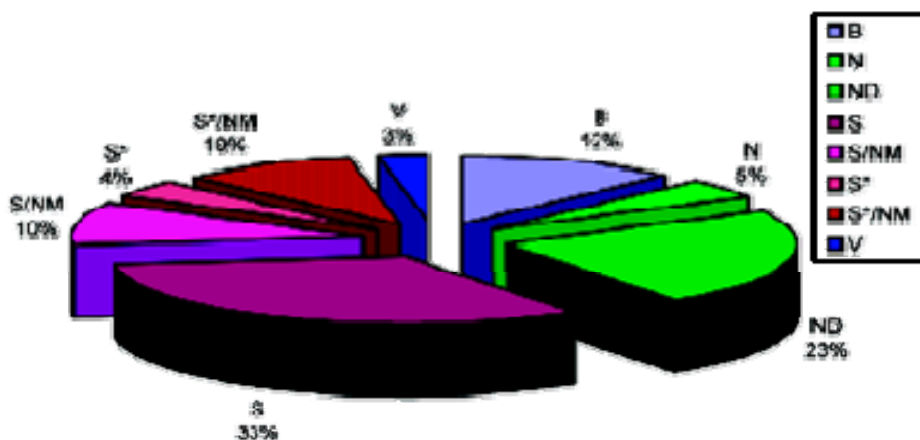
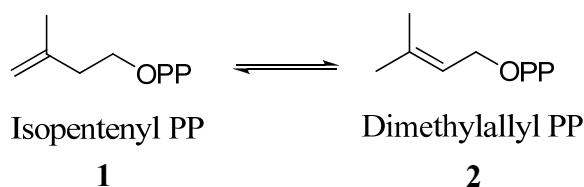


**Figure 1.** Graphical representation of drugs developed in the U.S.<sup>1</sup>

## Terpenoids

Among the classes of natural products, almost one-half of these molecules are isoprenoids, also referred to as terpenoids. The terpenoids are the oldest known biomolecules possessing many biological functions.<sup>4,5</sup> Examples of terpenoids in nature include the quinines in electron transport chains, components of membranes, plant defense, as hormones, and as photosynthetic pigments such as carotenoids and side chains of chlorophyll.<sup>6</sup> Terpenoids are synthesized in many species within the realms of eubacteria, archaebacteria, and eukaryotes via the condensation of isopentenyl pyrophosphate (IPP) **1** and its isomer dimethylallyl pyrophosphate (DMAPP) **2** (**Scheme 1**). These compounds are biosynthesized by two different routes. The pathway to IPP **1** in mammals and yeast begins with acetyl-CoA **3** with two other units being

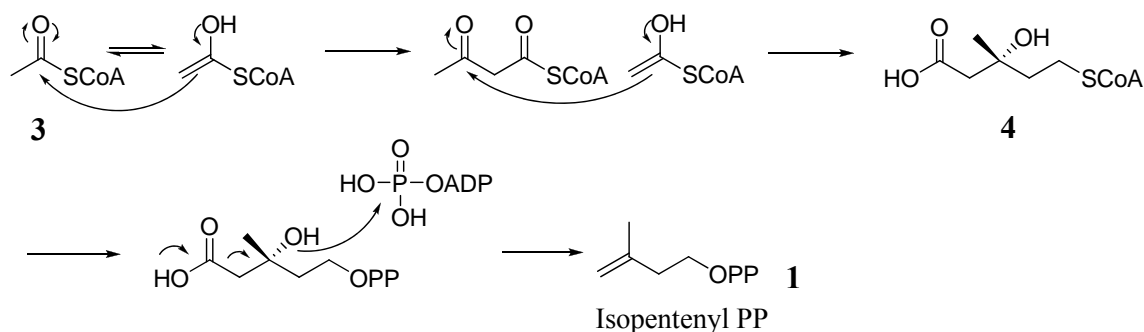
**Scheme 1.** Building blocks of terpenoids. After <sup>7</sup>



activated to the thioester and condensed in several steps to form hydroxymethylglutaryl-CoA (HMG-CoA) **4**. HMG-CoA **4** then undergoes dehydration, reduction, decarboxylation, and phosphorylation in multiple steps to produce IPP (**Scheme 2**).<sup>8,9</sup> The second pathway, termed the non-mevalonate pathway, was discovered in 1993 and many of the mechanistic details are still not well understood. It begins with the

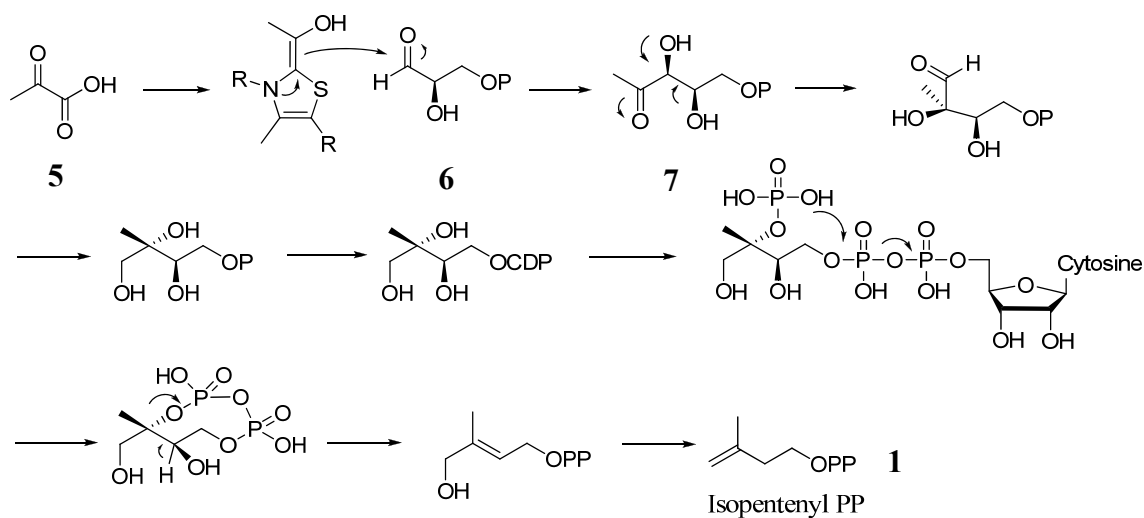


**Scheme 2.** Malvonnate biosynthesis of isopentenyl pyrophosphate. After <sup>7</sup>



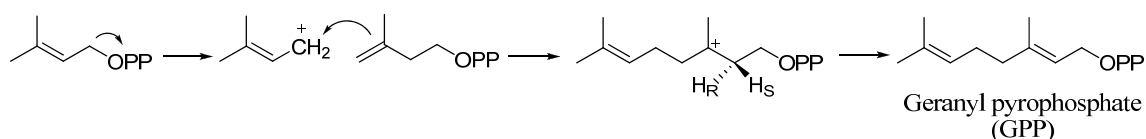
condensation of one unit of pyruvate **5** and one unit of glyceraldehydes-3-phosphate **6** to give 1-deoxy-D-xyulose-5-phosphate **7** (**Scheme 3**). **Scheme 3** demonstrates that 1-deoxy-D-xyulose-5-phosphate **7** undergoes several reductions and rearrangements to produce IPP **1**.<sup>10,11</sup>

**Scheme 3.** The deoxyxylulose phosphate pathway for IPP. After <sup>7</sup>



The production of terpenoids starts with the isomerization of IPP **1** to DMAPP **2** by IPP isomerase (**Scheme 1**).<sup>12,13</sup> The enzyme farnesyl diphosphate synthase catalyzes the coupling of the two substrates (IPP and DMAPP) giving geranyl diphosphate (GPP). This is performed in a head-to-tail fashion. First off, the reaction begins with a catalyzed ionization of the allyl pyrophosphate producing a carbocation intermediate. This carbon is attacked by the alkene of IPP to produce a tertiary carbocation. This intermediate is then deprotonated with the loss of the *pro-R* hydrogen (**Scheme 4**).<sup>13</sup> This enzyme can also add another C-5 unit to produce the sesquiterpene, farnesal (C<sub>15</sub>). This process can continue to give terpenes up to 25 carbons long. Triterpenes (C<sub>30</sub>) and tetraterpenes (C<sub>40</sub>) can also be generated by the coupling of C<sub>15</sub> and C<sub>20</sub> units.

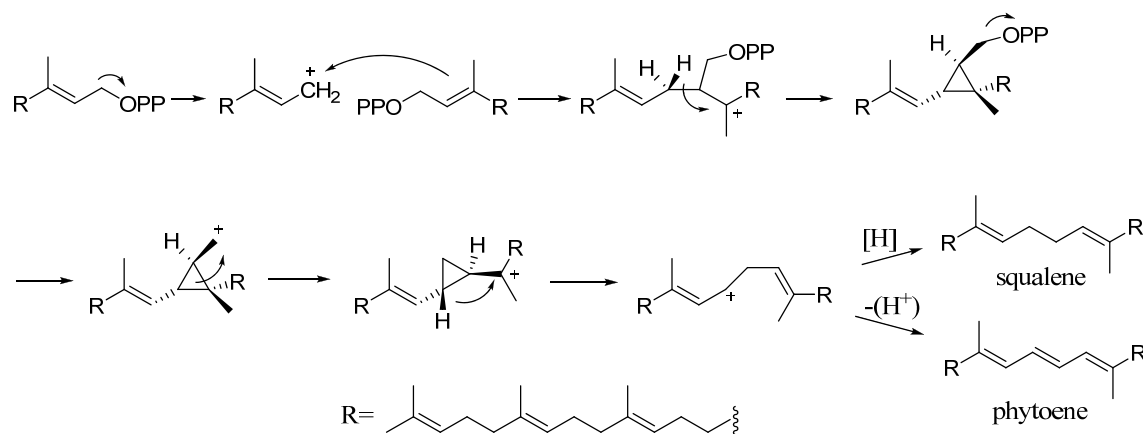
**Scheme 4.** Head-to-tail condensation of IPP and DMAPP to produce GPP. After<sup>7</sup>



IPP and DMAPP can also be condensed in a tail-to-tail fashion which leads to the terpenoids, squalene and phytoene.<sup>14-16</sup> There are two pathways in which these molecules are made. The first is a reductive pathway which results in two saturated methylene units at the connection point. This particular pathway leads to squalene which undergoes further metabolism to produce many compounds including steroids. The second pathway is a non-reductive pathway involving the formation of the triene

carotenoids, such as lycopene. This is due to the carbon-carbon bond forming from the two allylic alcohol positions.

**Scheme 5.** Tail-to-tail condensation of geranylgeranyl pyrophosphate. After <sup>7</sup>



## Carotenoids

The carotenoids form an important class of biologically active terpenoids and play a critical role in energy transfer processes such as photosynthesis or photoprotection. Carotenoids, such as lycopene **8** (**Figure 2**), act as a class of anti-oxidants which are responsible for the scavenging of free radicals within the human body.<sup>17</sup> For instance, **8** is 100 times more effective in singlet-oxygen quenching than vitamin E **9**.<sup>18</sup> Lycopene also acts as an important intermediate in the biosynthesis of  $\beta$ -carotene.  $\beta$ -carotene **10**, can be enzymatically cleaved by a  $\beta$ -carotene 15,15'-monooxygenase to form two retinals **11**.<sup>19-21</sup> Retinal **11** is important as it serves as the chromophore for the visual transduction cycle.<sup>22</sup> Retinal **11** can easily be oxidized to form retinol **12**, which is better known as vitamin A. Another key retinoid, retinoic acid **13**, can be made from retinal

via a retinal oxidase.<sup>23-26</sup> Retinol **12** and retinoic acid **13** (**Figure 3**) exhibit a variety of biological activities and are potent modulators of growth and differentiation.<sup>27-29</sup> Interestingly, **13** has been shown to differentiate embryonic stem cells into a neuron-like phenotype.<sup>30</sup> It has also been employed as a chemotherapeutic agent in the treatment of promyelocytic leukemia by causing terminal differentiation of the tumor cells.

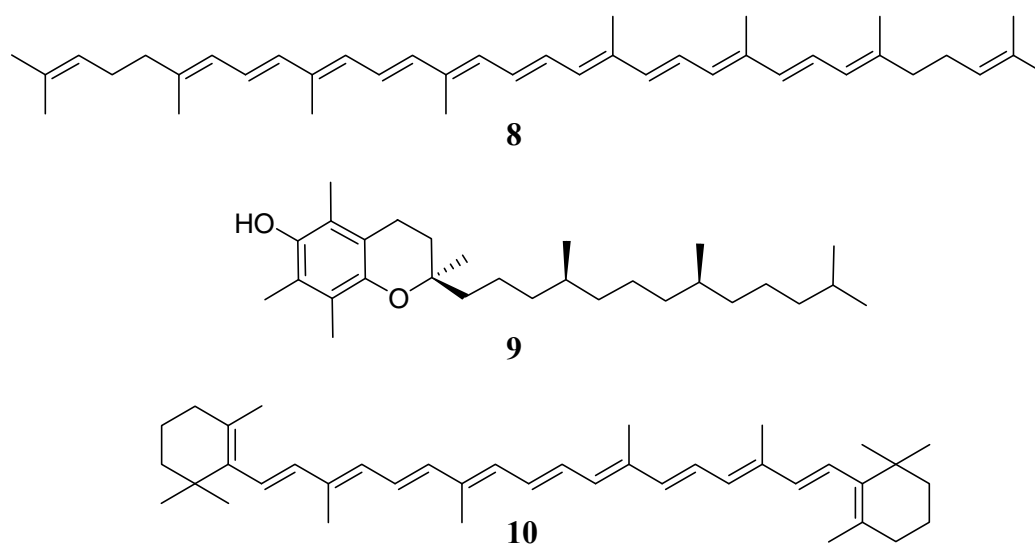


**Figure 2.** Structures of carotenoids lycopene, vitamin E, and  $\beta$ -carotene.

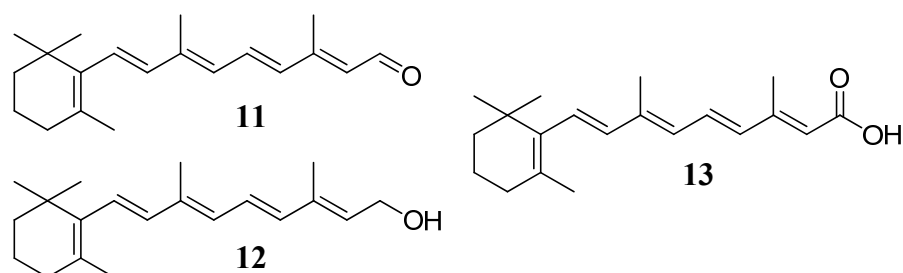


**Figure 3.** Biologically relevant retinoids.

### *Cycloterpenals in Nature*

An understudied subclass of the carotenoids is the cycloterpenals.<sup>31,32</sup> In nature, only two cycloterpenals (with a cyclohexadienal structural core) have been discovered. Interestingly, condensation of all-*trans*-retinal gives a C-40 ring-fused dimer **14** which is also known as cycloretinal (**Figure 4**). This molecule, along with other bisretinoids, is believed to act as a contributor of age-related macular degeneration, the leading cause of blindness in the elderly.<sup>33,34</sup> Since the isolation and identification of cycloretinal from the human eye in 2004, the formation of this metabolite has been under scrutiny.<sup>27</sup> In 2005, Nakanishi proposed that the C-40 dimer was formed with a protonated Schiff base conjugate with phosphatidylethanolamine (PE) (Scheme 6) supplied within retinal pigment epithelium (RPE) cells. The Schiff base then tautomerizes to react with free retinal via a Michael-type addition. After ring closure and elimination of the amino group of PE, the all-*trans* retinal dimer **14** is formed.<sup>28</sup>

The self-dimerization of citral has been suspected since the late 1890's.<sup>35,36</sup> The 1,2,4-trisubstituted structure **15** (**Figure 4**) was definitively ascribed in 1932.<sup>37</sup> Recently, citral dimer (cyclocitral) **15** was isolated from the North Sea bryozoan *Flustra foliacea*<sup>38,39</sup> and shown to exhibit antibacterial activity against *Roseobacter sp.* and *Sulfitobacter sp.* in an agar diffusion assay (100 µg resulted in a 0.5 and 1.0 cm zone of inhibition respectively). The formation of this metabolite in the bryozoans is unknown but it is speculated that a base catalyzed reaction is taking place as citral is also isolated from the bryozoans in substantial amounts.<sup>38,39</sup>

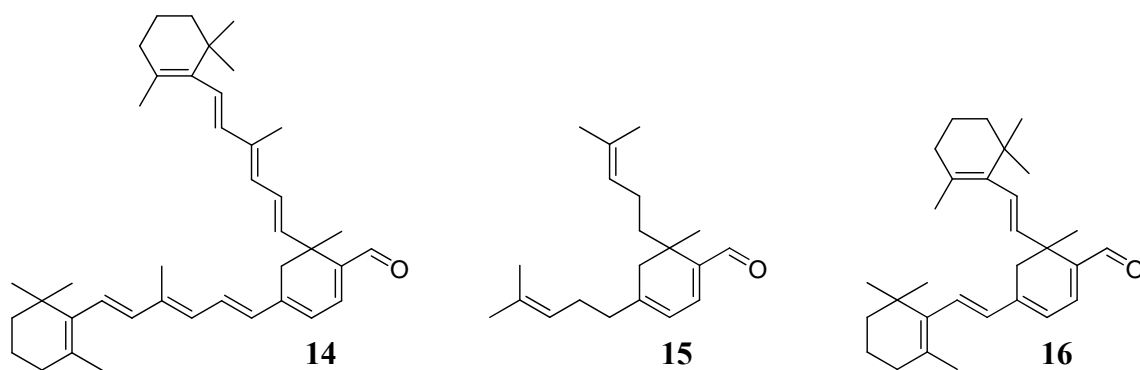
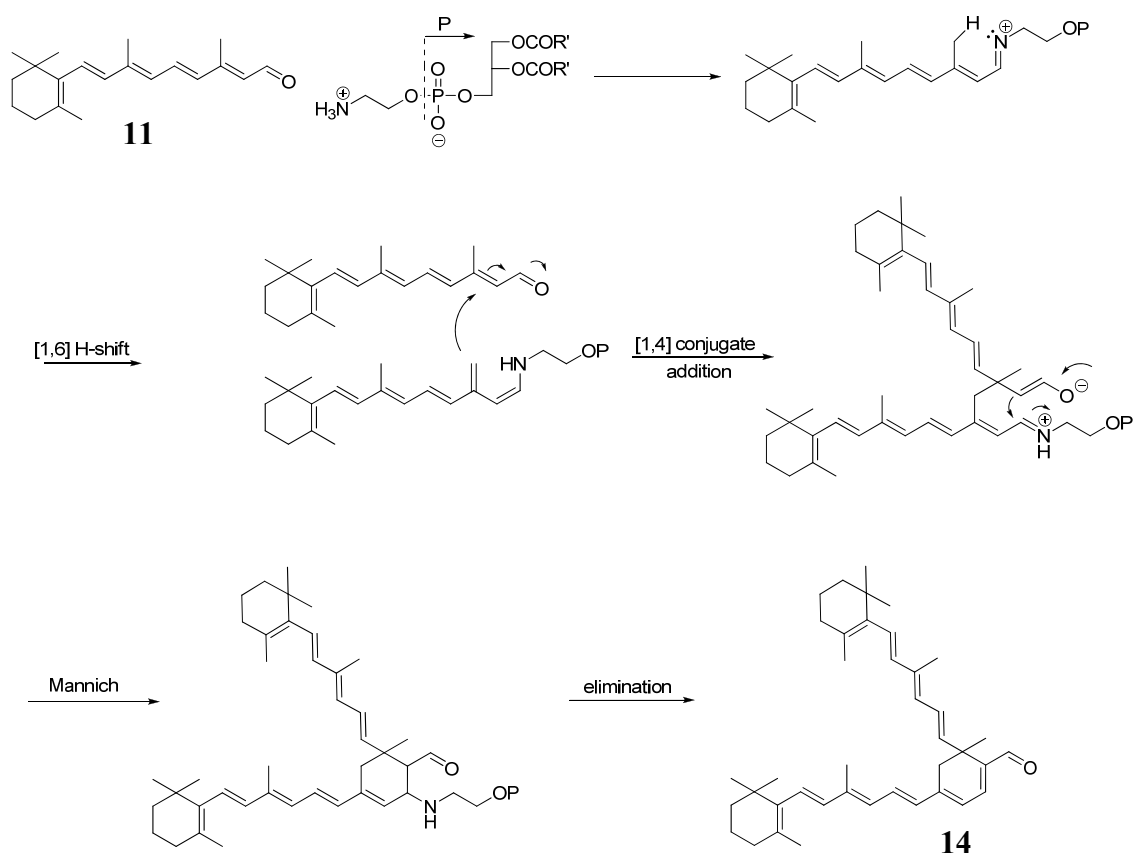


**Figure 4.** Structures of cycloretinal, cyclocitral, and C-30 dimer.

**Scheme 6.** Nakanishi's proposed formation of all-trans-retinal C-40 dimer.<sup>28</sup>



### *$\beta$ -LG Promotes Biosynthesis of Cycloterpenals*

Incubation of the principal milk protein  $\beta$ -lactoglobulin ( $\beta$ -LG) with  $\beta$ -ionylideneacetaldehyde has been shown to result in cyclohexadienal formation of its corresponding C-30 homodimer, cyclo- $\beta$ -ional **16 (Figure 4)**.<sup>40,41</sup> This protein mediated reaction was detected by UV-Vis and circular dichroism analyses with no further research being done to explore the phenomenon along with no follow up studies on the probable biological roles of these cycloterpenals. This is intriguing as  $\beta$ -LG is the principal whey protein in dairy milk. Protein analysis of blood samples reveal that levels of  $\beta$ -LG in the blood stream are on average between 0.7 to 1.2 g/dL. As humans do not possess a  $\beta$ -LG homolog, the source of this protein must be dietary. The lipocalin closest to  $\beta$ -LG in humans is glycodelin (also known as PP14 or pregnancy-associated endometrial glycoprotein). This protein is associated in the first trimester of pregnancy.<sup>42</sup> The exact function of glycodelin is also unknown.

### *Beta-Lactoglobulin*

Beta-lactoglobulin ( $\beta$ -LG) is the principal whey protein of ruminant species and is also present in many other species.<sup>43</sup> Based on its amino acid sequence and 3-dimensional structure, the protein is classified as a member of the lipocalin family. The lipocalin family is a large and diverse family of proteins with various functionalities ranging from insect camouflage to small hydrophobic molecule transport exemplified by the serum retinol-binding protein.<sup>44</sup>  $\beta$ -LG is the major whey protein in milk constituting 50-55% of the protein volume.<sup>43</sup> The protein has been studied extensively for its

physical and biochemical properties for over 70 years now because of its size, stability, and convenience (~3 g/liter of milk).<sup>43,45-47</sup>

To date, the biological function of  $\beta$ -LG is unknown. While  $\beta$ -LG may serve as a nutritional supplement,<sup>48</sup> the structural similarity to retinol-binding protein and fatty acid-binding protein suggests that it has a transport role for ligands such as retinoids and various fatty acids.<sup>44,49-52</sup> Binding studies have been performed with hydrophobic ligands examining a probable role in transport similar to that of other lipocalins with dissociation constants ranging from  $10^{-4}$  to  $10^{-9}$  M. Some examples can be seen for the binding of various fatty acids, retinoids, and steroids in **Table 1**.

$\beta$ -LG may also play a role in digestion of milk fats as ruminant  $\beta$ -LG has been isolated with fatty acids bound.<sup>54</sup> Not all  $\beta$ -LGs have the same properties. It has been shown that this is not the case for all  $\beta$ -LGs as mares and sows do not exhibit significant fatty acid binding. However,  $\beta$ -LG from all species bind retinol just as serum albumin and  $\alpha$ -lactalbumin, indicating that it is not highly specific.<sup>55</sup>

$\beta$ -LG is comprised of 162 amino acids with a molecular weight of ~18,400 Daltons.<sup>56</sup> The protein, with a predominant  $\beta$ -sheet configuration, contains nine anti-parallel  $\beta$ -strands (A-I) with one  $\alpha$ -helix. The calyx is comprised of two surfaces with  $\beta$ -strands A-D forming one side and strands E-H forming the other.  $\beta$ -strand I is located on the outer surface of the calyx (**Figure 5** and **Figure 6**).<sup>57-60</sup> The retinoid binding site for  $\beta$ -LG has been well established and lies inside the calyx of the protein.<sup>61</sup> Fatty acids and vitamin D have also been shown to bind directly to the calyx.<sup>60,62-64</sup> Recently, others have speculated upon the existence of other hydrophobic pockets within



**Table 1.** Selected ligand binding data for bovine  $\beta$ -lactoglobulin.

Ligand	$K_d$ (M)
Lauric	$7.0 \times 10^{-7}$
Palmitate	$1.0 \times 10^{-7}$
Retinoic Acid	$2.0 \times 10^{-7}$
Retinol	$2.0 \times 10^{-8}$
Vitamin D <sub>2</sub>	$4.91 \times 10^{-9}$
Stearate	$1.2 \times 10^{-7}$
Cholesterol	$3.49 \times 10^{-8}$

the protein. Biochemical binding assays performed with vitamin D showed uptake at a secondary binding site remote from the calyx.<sup>65-69</sup> In 2008, a crystal structure was obtained with vitamin D<sub>3</sub> binding within a secondary hydrophobic site of  $\beta$ -LG (residues 136-149),<sup>70</sup> while others have also speculated about other potential binding pockets within  $\beta$ -LG.<sup>71-73</sup>

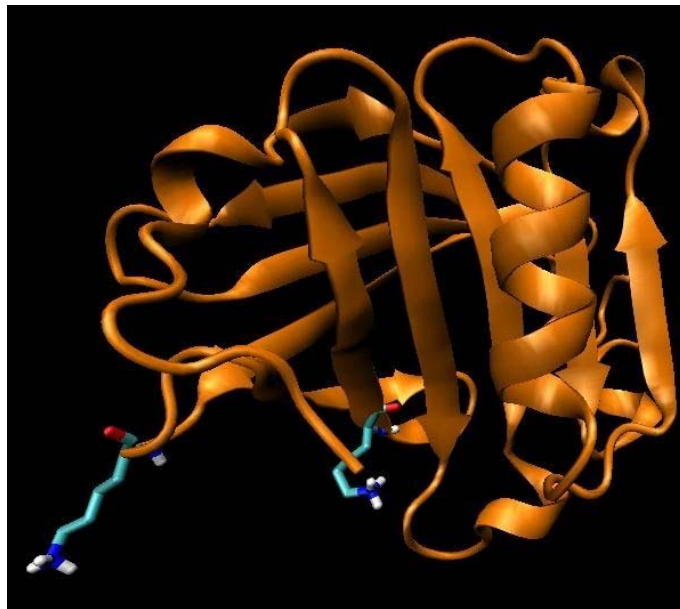


**Figure 5.** Native BLG crystal structure.<sup>49</sup>  
The diagram was prepared with VMB.

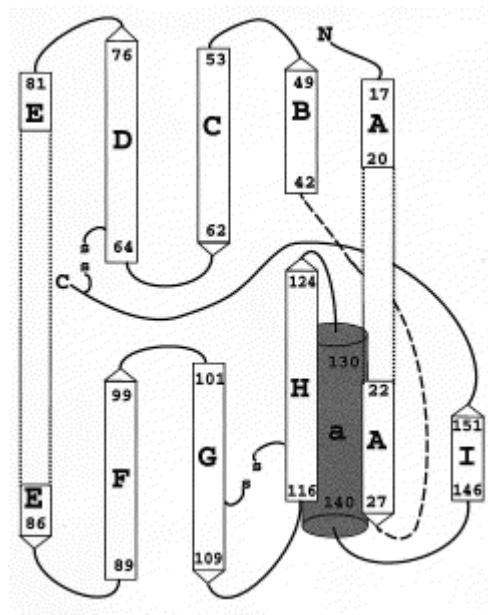


**Figure 6.** The dimer interface viewed perpendicular to strand I.<sup>57</sup>

### *Macular Degeneration and A2E*

Age-related macular degeneration affects 10-20% of people over the age of 65 in which the macula,<sup>74,75</sup> the inner lining of the eye, suffers thinning or atrophy. These events lead to the loss of central vision (**Figure 7**). AMD is defined as either “dry” or “wet”. Dry macular degeneration is the most common form of all AMD. A build-up



**Figure 7.** Macular degeneration affects central vision.<sup>74</sup>  
Photos courtesy of NIH National Eye Institute.

over time of drusen leads to small lesions within the central region of the macula. Drusen are tiny or white accumulations of extracellular material that build up in the Bruch's membrane of the eye (**Figure 8**).<sup>76,77</sup> Wet macular degeneration is less common accounting for 10% of all AMD cases. This form is characterized by choroidal neovascularization. This is the development of abnormal blood vessels under the retinal pigment epithelium (RPE) layer of the retina. This leads to intense scarring of the macula as these vessels continuously hemorrhage and bleed.<sup>78</sup> The overall progression of AMD is very slow. There are many influences on the disease ranging from genetic

benefactors to environmental risks including diet, cigarette smoking, and exposure to light.<sup>79</sup>

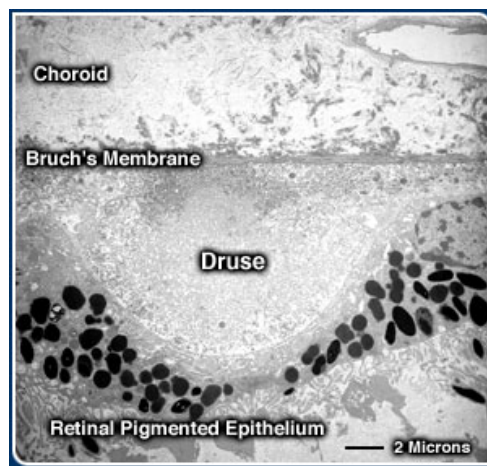


**Figure 8.** Tunneling electron microscopy representation of drusen build-up.<sup>77</sup>  
 Photo courtesy of The Center for the Study of Macular Degeneration Neuroscience Research Institute, University of California Santa Barbara.

AMD can also be associated with the build-up of retinal lipofuscin (RLF) granules (**Figure 9**). These granules begin to accumulate around the age of 20 and by the age of 80 they may constitute up to 20% of the cell volume.<sup>80</sup> These granules contain a mixture of proteins, lipids, and fluorescent bis-retinoid compounds. Proteomic studies were performed demonstrating that 41 different proteins including  $\beta$ -lactoglobulin were present within the granules.<sup>81</sup> Fluorescent compounds including cycloretinal and the bis-retinoid A2E **17** along with its isoform *iso*-A2E **18** (Scheme 7) have been isolated and characterized from RLF.<sup>81-83</sup> Evidence suggests that these toxic vision byproducts that accumulate in RLF contribute to the death of RPE eventually leading to the visual impairment of the individual through the oxidation of the

conjugated double bonds resulting in highly reactive epoxides **19** which lead to pathogenesis (**Scheme 7**).<sup>84-86</sup>

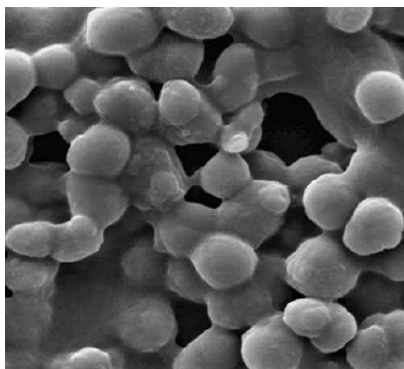
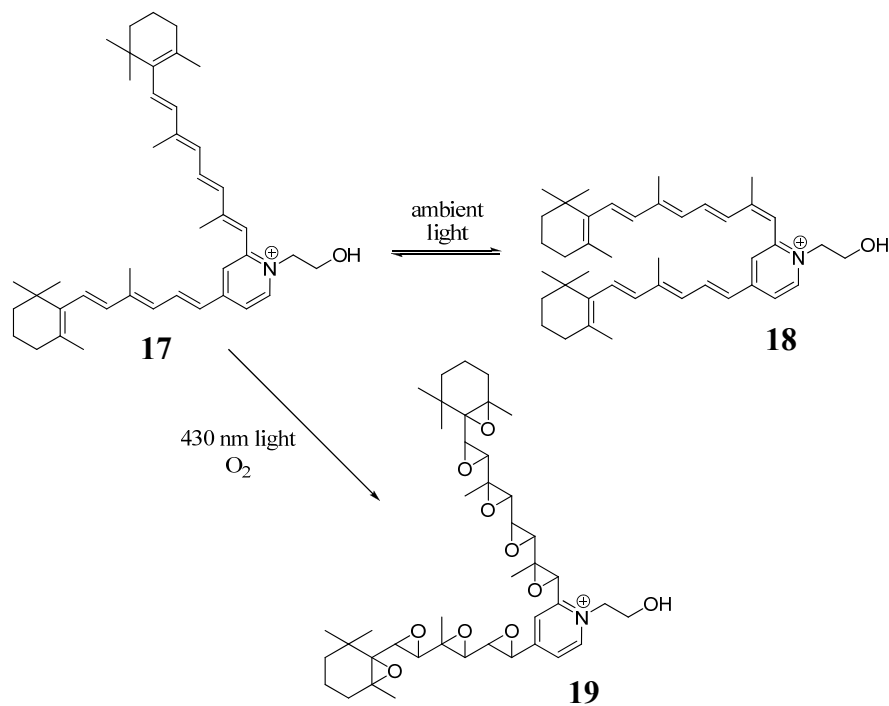


**Figure 9.** Atomic force micrograph of RLF granules.<sup>81</sup>

**Scheme 7.** A2E and iso-A2E form highly reactive epoxides.<sup>84-86</sup>



After 70 years of extensive research, the biological function of  $\beta$ -LG is still unknown. With experiments showing that it might be involved in the transport of essential metabolites, the possibility of other functions cannot be ruled out. The discovery of the  $\beta$ -LG mediated self-condensation of natural aldehydes in 1992 indicated that the protein might possess another biological role. With the generation of cycloterpenals from this reaction, it can be hypothesized that  $\beta$ -LG might play a role in developmental processes such as neuronal development or cellular differentiation. The isolation of cyclocitral and cycloretinal from nature provides evidence that this understudied class of cycloterpenals may play an essential role in nature as they may possess many biological attributes. In order to elucidate the functions of  $\beta$ -LG and cycloterpenals, a scheme must be designed to mimic the formation of cycloterpenals with  $\beta$ -LG to develop new compounds based on this cyclohexadienal motif. This is currently in development in Dr. Coran Watanabe's group to investigate the biological roles of cycloterpenals and thus elucidate another function of  $\beta$ -LG.

## **STATEMENT OF PURPOSE**

Natural products have become a staple in the everyday lives of humans. The carotenoids play an essential role in many biological functions and the recently discovered cycloterpenal class may possess unheard biological activities. The isolation of cycloretinal from the human eye in recent years has brought these cyclohexadiene core molecules to the attention of many scientists as this molecule along with other bis-retinoids from the human eye lead to the development of macular degeneration. With the ability of  $\beta$ -LG to condense natural  $\beta$ -methyl aldehydes such as retinal into

cycloretinal, one would have to believe that this protein mediated reaction can occur with other natural aldehydes that we consume on a daily bases, especially if one has a high intake of dairy products. Further analysis of this reaction could lead to the understanding of  $\beta$ -LGs biological roles as well as a better understanding as to the role the cycloterpenals play in nature.

## CHAPTER II

### INVESTIGATIONS OF THE BIOLOGICAL ROLES OF $\beta$ -LACTOGLOBULIN

#### INTRODUCTION

The lipocalin family is a large and diverse family of proteins with various functionalities ranging from insect camouflage to small hydrophobic molecule transport exemplified by the serum retinol-binding protein.<sup>44</sup> Bovine  $\beta$ -lactoglobulin ( $\beta$ -LG), a typical lipocalin, is a major whey protein in milk constituting 50-55% of the protein volume.<sup>43</sup>  $\beta$ -LG has been studied extensively for its physical and biochemical properties for over 70 years now because of its size, stability, and convenience ( $\sim 3$  g/liter of milk).<sup>43,45-47</sup> To date, the biological function of  $\beta$ -LG is unknown. While  $\beta$ -LG may serve as a nutritional supplement,<sup>48</sup> the structural similarity to retinol-binding protein and fatty acid-binding protein suggests that it has a transport role for ligands such as retinoids and various fatty acids.<sup>44,49-52</sup> Binding studies have been performed with ligands that are hydrophobic which in turn exemplifies a probable role in transport similar to that of other lipocalins with dissociation constants ranging from  $10^{-4}$  to  $10^{-9}$  M.<sup>53</sup>  $\beta$ -LG may also play a role in digestion of milk fats as ruminant  $\beta$ -LG has been isolated with fatty acids bound.<sup>54</sup> It has been shown this is not the case for all  $\beta$ -LGs as mares and sows do not exhibit significant fatty acid binding. However,  $\beta$ -LG from all species binds retinol just as serum albumin and  $\alpha$ -lactalbumin, indicating that it is not highly specific.<sup>55</sup>

$\beta$ -LG is comprised of 162 amino acids with a molecular weight of  $\sim 18,400$  Daltons.<sup>56</sup> The protein, with a predominant  $\beta$ -sheet configuration, contains nine anti-parallel  $\beta$ -strands (A-I) with one  $\alpha$ -helix. The protein is a dimeric structure comprised of



two surfaces with  $\beta$ -strands A-D forming one side of the calyx while strands E-H form the other.  $\beta$ -strand I is located on the outer surface of the calyx.<sup>57-60</sup> The retinoid binding site for  $\beta$ -LG has been well established and lies inside the calyx of the protein.<sup>61</sup> Fatty acids and vitamin D have also been shown to bind directly to the calyx.<sup>60,62-64</sup> Recently, there has been controversy towards the existence of other hydrophobic pockets within the protein. Biochemical binding assays performed with vitamin D showed uptake at a secondary binding site remote from the calyx.<sup>65-69</sup> In 2008, a crystal structure was obtained with vitamin D<sub>3</sub> binding within a secondary hydrophobic site of  $\beta$ -LG (residues 136-149).<sup>70</sup> Still, there are speculations of other potential binding pockets within  $\beta$ -LG.<sup>71-73</sup>

In the early 1990's, incubation of  $\beta$ -LG with  $\beta$ -ionylideneacetaldehyde resulted in cyclohexadienal formation of its corresponding C-30 homodimer, cyclo- $\beta$ -ional (**16**) (**Figure 10**).<sup>41,87</sup> This protein mediated reaction was detected by UV-Vis and circular dichroism analyses with no further studies performed to explain the phenomenon along with no follow up studies on the probable biological roles these cycloterpenals may possess. In our laboratory, we have developed synthetic strategies to make a vast library of molecules and investigated the probable biological roles of these cycloterpenals.<sup>31,32</sup> We broadly speculated that these molecules could be important in developmental processes such as neurite outgrowth. When our library was screened against PC12 cells, we observed the reduction of the cancerous proliferation as the cells began to differentiate into neurons.<sup>32</sup>

To date, there have only been two cycloterpenals discovered in nature. Cyclocitral (**15**), was recently isolated from the North Sea bryozoans *Flustra foliacea*

and shown to exhibit antibacterial activity.<sup>39,88,89</sup> Cycloretinal (**15**), condensation product of all-*trans*-retinal, has been isolated and characterized from the human eye (**Figure 10**).<sup>33,34</sup> Cycloretinal along with other bis-retinoids, A2E and its minor isomers, are believed to play a major role in death of retinal pigment epithelial (RPE) cells.<sup>90</sup> Accumulation of these toxic molecules occurs slowly over time in granules termed lipofuscin. These retinal lipofuscin (RLF) granules begin building up around the age of 20 and by 80 years constitutes up to 20% of the cell volume in RPE cells.<sup>80</sup> Evidence suggests that the toxic vision byproducts that accumulate in RLF contribute to the death of RPE eventually leading to the visual impairment of the individual.<sup>84-86</sup> How these toxic byproducts of the vision cycle are being formed is still a mystery. It has been shown that at high concentrations of all-*trans*-retinal, a fluorescent bis-retinoid adduct can form on lysine residues of rhodopsin in the rod outer segments.<sup>91</sup> This could be one possible way for these toxic molecules to form, but interestingly, the protein  $\beta$ -LG has been characterized within the human eye, particularly within the RLF granules that house these toxic molecules.<sup>81-83</sup> In this report, we demonstrate that  $\beta$ -LG mediates the formation of the toxic byproduct cycloretinal not only *in vitro* but also *in vivo* in a rabbit model where the metabolite was isolated in the blood. Other cycloterpenals can also be synthesized utilizing  $\beta$ -LG under optimal conditions.

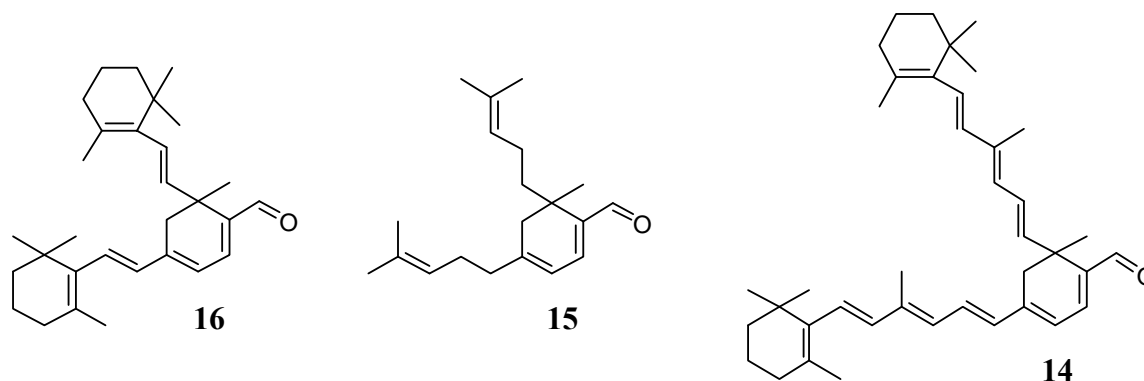


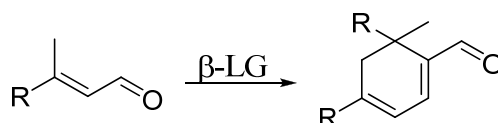
**Figure 10.** Chemical structures of cyclo- $\beta$ -ional, cyclocitral, and cycloretinal.

## RESULTS AND DISCUSSION

### *Optimization of $\beta$ -LG Mediated Synthesis of Cycloterpenals*

In 1990, it was reported that the incubation of  $\beta$ -LG with  $\beta$ -ionylideneacetaldehyde resulted in the formation of cyclo- $\beta$ -ional **16**.<sup>41,87</sup> This reaction was monitored with UV-Vis and circular dichroism spectroscopy with no further investigations to fully evaluate this protein mediated reaction, i.e. the scope of the reaction and mechanism of its formation (**Scheme 8**).

**Scheme 8.**  $\beta$ -LG mediated formation of cycloterpenals from  $\beta$ -methyl aldehydes.



To optimize the reaction, we followed the general conditions set forth by Li *et. al.* by utilizing a 0.2% solution of  $\beta$ -LG allowing the reaction to go overnight, incubating the protein solution at room temperature (with shaking) with  $\beta$ -ionylideneacetaldehyde

using a 1:2 protein to substrate molar ratio.<sup>41</sup> We scaled up the reaction in hopes of visualizing the homodimer by NMR and to our surprise after one day we saw trace amounts of **16** (**Figure 11**). The successful detection of the dimer product by NMR led us to further optimize the reaction by treating various

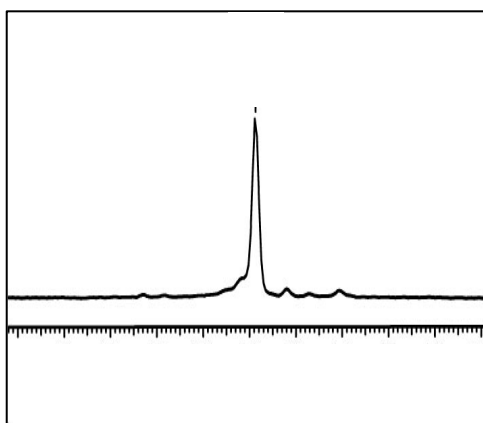


**Figure 11.** <sup>1</sup>H-NMR of aldehyde region for cyclo- $\beta$ -ional formation.

solutions of  $\beta$ -LG (0.2%-1.0%) with citral. These reactions were performed at room temperature over three days as seen in **Figure 12**. The production of cyclocitral increased with elevated concentrations with 1.0% giving the best production with an isolated yield of 29.1%. The yields for protein concentrations of 0.2%, 0.4%, 0.6%, and 0.8% were 8.2%, 13.4%, 17.9%, and 22.6%, respectively.

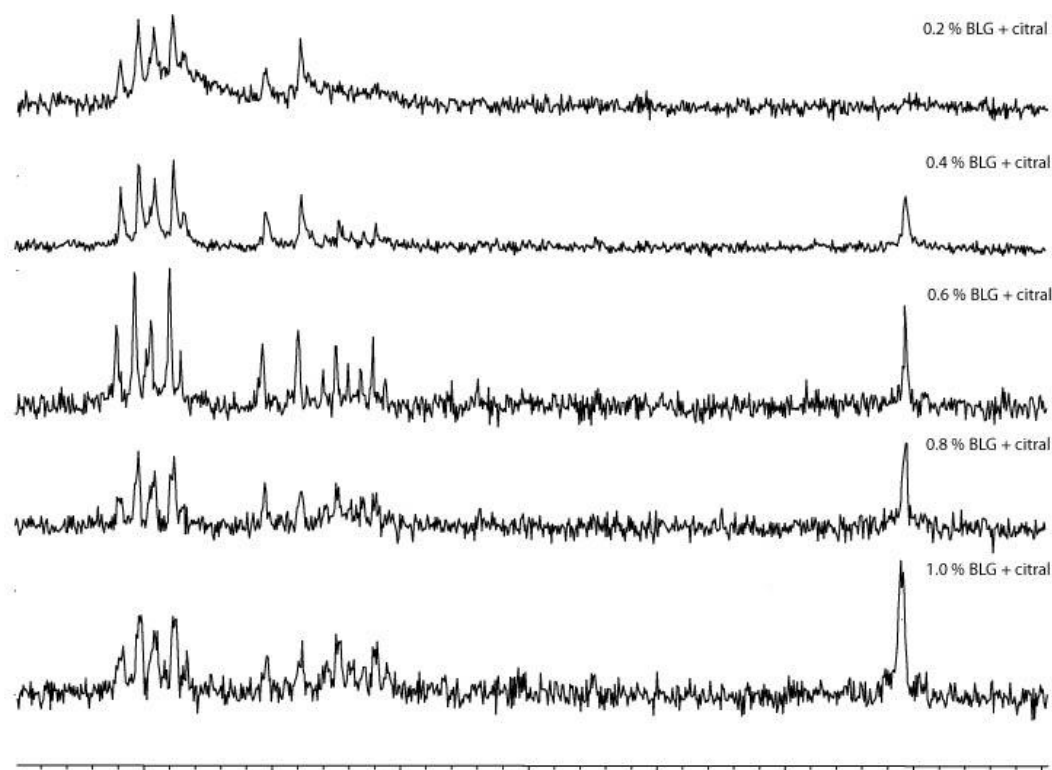


**Figure 12.** Various concentrations of  $\beta$ -LG observing cyclocitral production versus citral starting material.

Varying the protein to substrate ratio from 1:3 to 1:10 revealed that a protein to substrate concentration of 1:3 was optimal with an isolated yield of 58%. This is a dramatic improvement in yield as compared to product obtained with a 1:2 ratio, but when the ratio was increased to 1:4, the isolated yield was similar to that of 1:3. This was also the case for higher equivalents of substrate used. This is suggestive that the protein mediated reaction is a single turnover reaction resulting in dead protein after one reaction. Also, this indicates that there is another binding pocket available for the reaction to proceed. If the reaction was taking place within the central calyx, then only 2 equivalents would be necessary for production of the dimer. Worthy of note, the protein

remains yellow even after organic extraction which we believe to be the calyx bound substrate. Denaturation of the protein after reaction by boiling led to the recovery of the remainder of the starting material.

To further optimize this reaction, we looked at a comparison of the reaction carried out at room temperature (25°C) versus that of body temperature (37°C) since the protein is a component of the milk we drink. The production of cyclocitral was greater and faster at the higher temperature as shown in **Figure 13**. Evaluation of the reaction

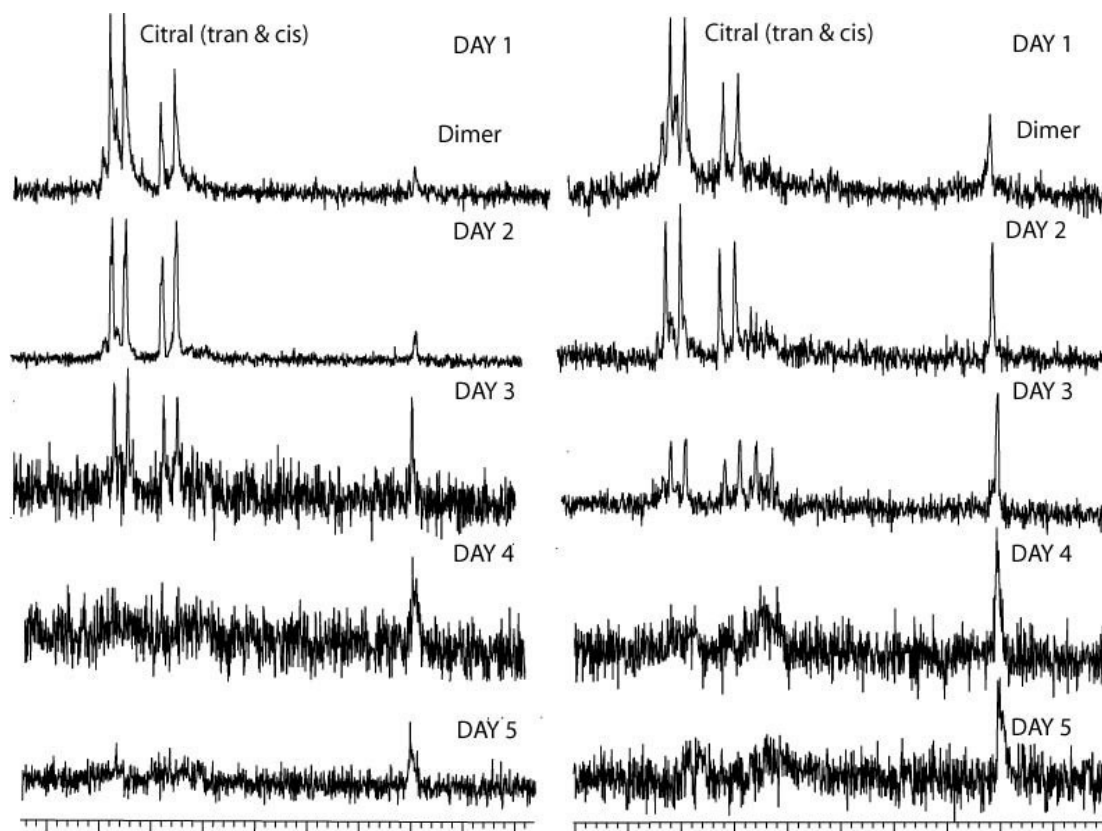


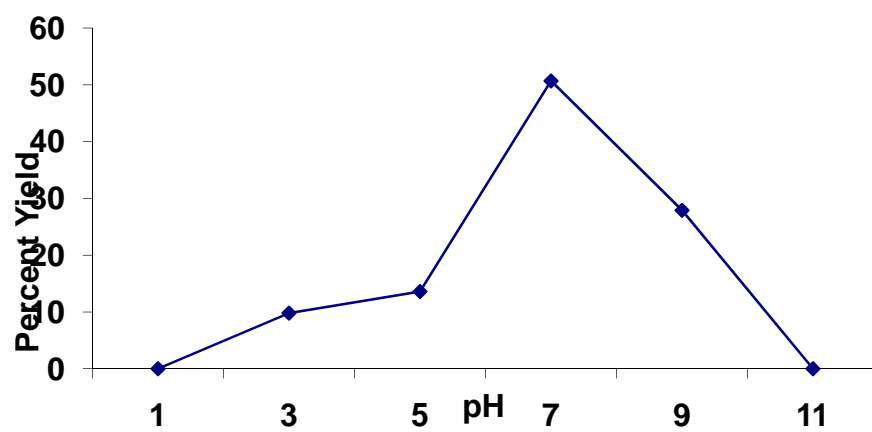
**Figure 13.** Temperature optimization at room temperature (25°C) (left) versus body temperature (37°C) (right).

progression revealed that the reaction was complete within a 4-day period, producing a 58% yield. The yields for days one thru three were 12.3%, 22.4%, and 36.2%, respectively. The reaction yield at five days was equivalent to that obtained at 4-days (58%).

Our next step in optimizing the reaction was to investigate the behavior of the reaction at various pHs. A pH profile (**Figure 14**) was carried out to observe the effects on the dimerization of citral. Yields diminished at pH values of 1.0 and 11.0 while pH 7.0 was found to be the optimal pH for the reaction. The equilibrium shifts at lower and higher pH values as the protonation state of the amine is affected. At pH 7.0, a yield of 58% was obtained while at pH values of 5.0 and 9.0 yields of 14% and 28% were isolated (**Table 2**). There was also a distinct color change at various pHs. At pH 7, the normal yellow color was observed with the uptake of citral. However, at acidic pHs, the color changes ranged from milky, pH 5, to clear as the pH was decreased. At basic conditions, and intense orange color was seen at pH 9, giving a slightly less intense color at pH 11 (**Figure 15**). The yield of cyclocitral was greater at pH 9 than that of pH 11 which would indicate a greater uptake at pH 9.

**Table 2.** Yields at various pHs.

pH	Percent Yield
1	0
3	9.8
5	13.6
7	50.7
9	27.9
11	0

**Figure 14.** pH effects on the self-condensation of BLG with citral.





**Figure 15.** pH profile color changes.

#### *Bovine Serum Albumin Control*

In order to determine specificity of the dimerization reaction to  $\beta$ -LG, we looked at one the most studied proteins in the world, bovine serum albumin (BSA). BSA contains 60 lysine residues. Various concentrations of BSA (0.2% to 1.0%) were treated with an excess amount of citral and cyclocitral formation followed. We allowed these reactions to go for four days before extraction. Interestingly in all cases, there was no dimerization observed as only unreacted citral was isolated.

#### *Microbial and RPE Controls*

Protein lysates from bacterias *E. coli*, *B. subtilis*, and yeast *S. cerevisiae* were screened for cyclocitral production, incubating each with excess citral. The lysates only yielded citral and no dimerization product was obtained. As control reactions, the lysates with no substrate present were extracted with ethyl acetate screened to ensure that no metabolites peaks would appear in the aldehyde region of interest (**Figure 17**). It should be noted that there are over 4000 proteins in each microbe's proteome.

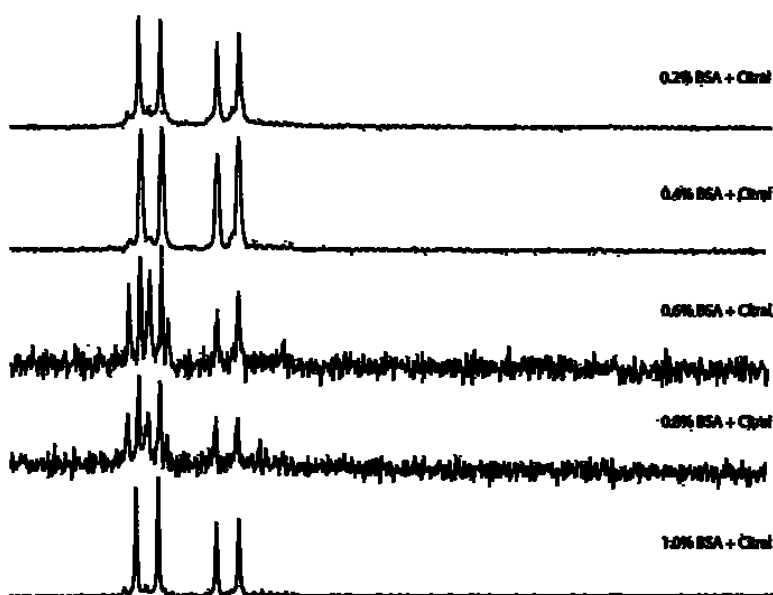


**Figure 16.** BSA control spectra indicating no cyclocitral formation.

Cycloretinal has been isolated from retinal pigment epithelial (RPE) cells in human eyes,<sup>33,34</sup> we examined whether the RPE cell protein lysate was capable of supporting dimer formation. We grew 10 plates of RPE cells to 95% confluency and used a dounce homogenizer to lyse the cells. A crude extract of the lysates indicated no presence of cycloretinal as well as A2E by  $^1\text{H}$ -NMR and mass spectrometry (MS).<sup>92</sup> After the RPE lysates were treated with citral for four days, there was no cyclocitral present via  $^1\text{H}$ -NMR and MS upon extraction. While this experiment shows that the lysates of RPE cells cannot perform the dimerization reaction, one might also speculate that rhodopsin may act as a player in cycloretinal formation as studies have shown that when retinal is at high concentrations, three lysine residues are modified with the addition of bis-retinoid adducts (A2-rhodopsin).<sup>91</sup> There is currently no evidence of cycloretinal adducts being attached to rhodopsin.

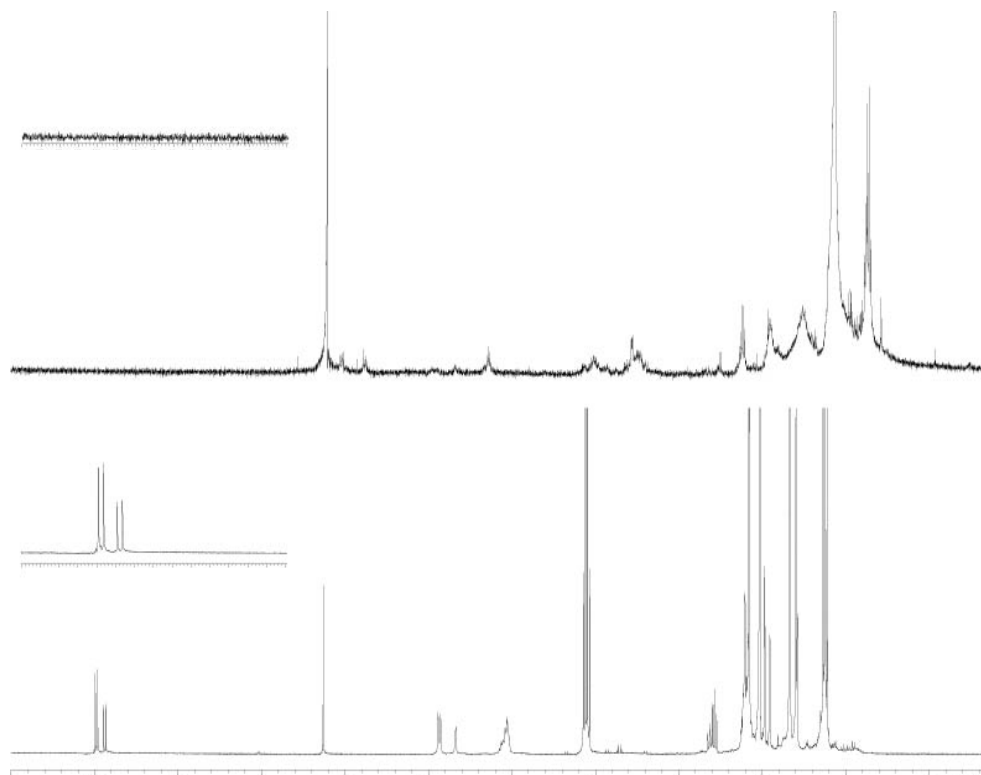


**Figure 17.** *E. coli* control indicating no metabolites in region of interest and after citral treatment.

### *Induced Protein Denaturation Experiments*

To inactivate  $\beta$ -LG, we utilized two different sources for the denaturation of our protein. The first experiment we performed was heat denaturation by taking 500 mL of a  $\beta$ -LG solution and boiling it for 10 minutes at 100 °C. Once the solution was cooled, the reaction was set up under optimal conditions with citral as substrate, and allowed to stir for four days at 37 °C. Upon extraction of the colorless solution, it was found that no cyclocitral was produced as only the starting material was isolated.

The other inactivation experiment that we performed was urea-induced denaturation. We treated  $\beta$ -LG with an excess amount of urea, to reduce the protein-protein and protein-water contacts,<sup>93</sup> over a two day period before we incubated the mixture with citral for an extra two days to observe cyclocitral formation. After two day post citral addition, extraction of the mixture yielded no cyclocitral.

#### *Production of Self-condensation Products with Various Aldehydes*

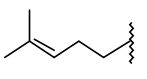
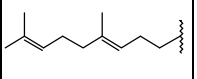
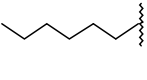
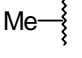
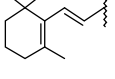
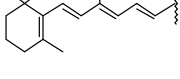
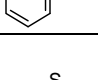
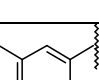
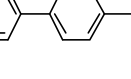

With our conditions optimized, we next looked at the effects of various substrates ranging from small aromatics, bulky aromatics, and long chain alkyl substrates over a four day period. We observed good conversion of the aldehyde to the dimer product. Percent conversion was monitored by <sup>1</sup>H-NMR after extraction where percent yield was determined by product isolation. With each of these reactions,  $\beta$ -LG would begin as a clear solution and darken overtime. For example, when  $\beta$ -LG is incubated with citral, the protein changes from clear to yellow and with retinal, the protein changes to a reddish-orange color. After extraction, boiling of the aqueous layer leads to isolation of the remaining substrate that remains bound to the protein following extraction. If 100% conversion is not achieved, it can be speculated that binding site interactions that facilitate the reaction are not optimal for that particular substrate. This was predominantly observed in the bulkier substrates and alkyl substrates. The reaction that gave the greatest yield (**Table 2**) after four days was the thiophene aldehyde with an isolated yield of 60.3%. The lowest isolated yield was the long alkyl chained farnesal at 23.4%. While the conversion of the naphthalene and biphenyl substrates after four days was fairly low, the overall yields (58.0% and 57.9% respectively) of the substrates

dimerized was significantly higher when compared to other substrates where their yields were actually lower. This can be seen when looking at the phenyl substrate as conversion was 77.0% with a meager isolated yield of 32.4% (**Table 3**).

#### *Proposed Reaction Mechanism*

The  $\beta$ -LG mediated reaction is thought to ensue by nucleophilic attack of the aldehyde with a terminal amine of lysine residues, resulting in the formation of a Schiff base **20** (**Figure 18**). Tautomerization, invoked by deprotonation of the  $\beta$ -methyl group of the imine, gives the  $\beta$ -methylenic lysine adduct **21** that can be visualized to dimerize with **20** following a Diels-Alder or Michael-like imine addition mechanism (pathway marked with green arrows). With the Michael-like imine addition, intermediate **22** is generated which then undergoes cyclization into reaction intermediate **23** (direct intermediate from Diels-Alder mechanism). From intermediate **23**, the lysine attached at C-4 of the cyclohexene ring readily dissociates leaving the cyclohexadiene intermediate **24**. Intermediate **24** then undergoes hydrolysis to give the 1,2,4-trisubstituted cyclohexadienal product **25**.

**Table 3.** Dimerization yields from one to four days.<sup>a</sup>Measured by <sup>1</sup>H-NMR. <sup>b</sup>Isolated yield.

	Day 1		Day 2		Day 3		Day 4	
	%	%	%	%	%	%	%	%
R group	conv. <sup>a</sup>	yield <sup>b</sup>	conv. <sup>a</sup>	yield <sup>b</sup>	conv. <sup>a</sup>	yield <sup>b</sup>	conv. <sup>a</sup>	yield <sup>b</sup>
	18.8	12.3	24.3	22.4	52.1	36.2	100.0	57.7
	24.6	11.1	47.3	11.5	51.0	16.3	100.0	23.6
	18.7	14.9	100.0	33.7	100.0	34.8	100.0	37.8
	2.4	15.6	30.1	30.5	100.0	54.9	100.0	55.3
	13.6	5.9	22.3	10.7	34.6	14.8	49.2	24.8
	19.5	23.6	17.5	31.9	19.7	43.1	20.0	44.2
	44.5	8.3	55.7	22.4	67.3	25.7	77.9	32.4
	10.8	7.1	58.8	27.3	100.0	51.8	100.0	60.3
	7.7	11.5	37.0	25.2	38.0	48.9	39.1	58.0
	34.9	8.4	45.1	27.5	44.1	38.9	52.5	57.9

### Heterodimer Formation Utilizing B-LG

Since  $\beta$ -LG has been proven to form cycloterpenals from  $\beta$ -methyl aldehydes, we also wanted to demonstrate that the protein could mediate the condensation reaction with a  $\beta$ -methyl substrate and an  $\alpha,\beta$ -unsaturated aldehyde. We decided to observe the dimerization between citral and cinnamaldehyde (**Scheme 9**) since previous studies have shown that this particular reaction will give not only products due to a proton abstraction from the  $\beta$ -methyl position (**26**) but also produce *cis* and *trans* diastereomers (**27** and **28** respectively) from the proton abstraction of the  $\gamma$ -methylene position, along with

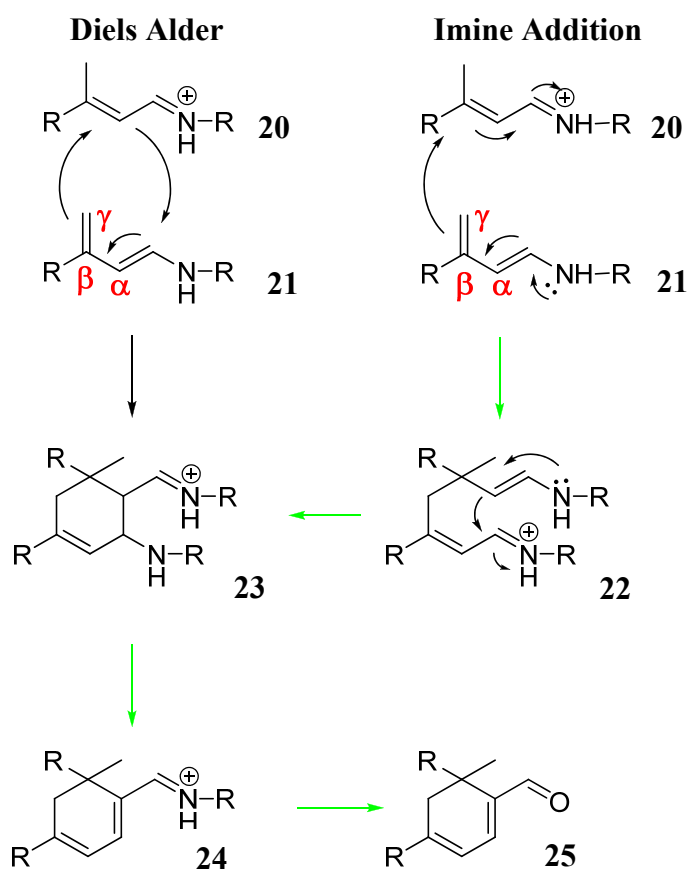
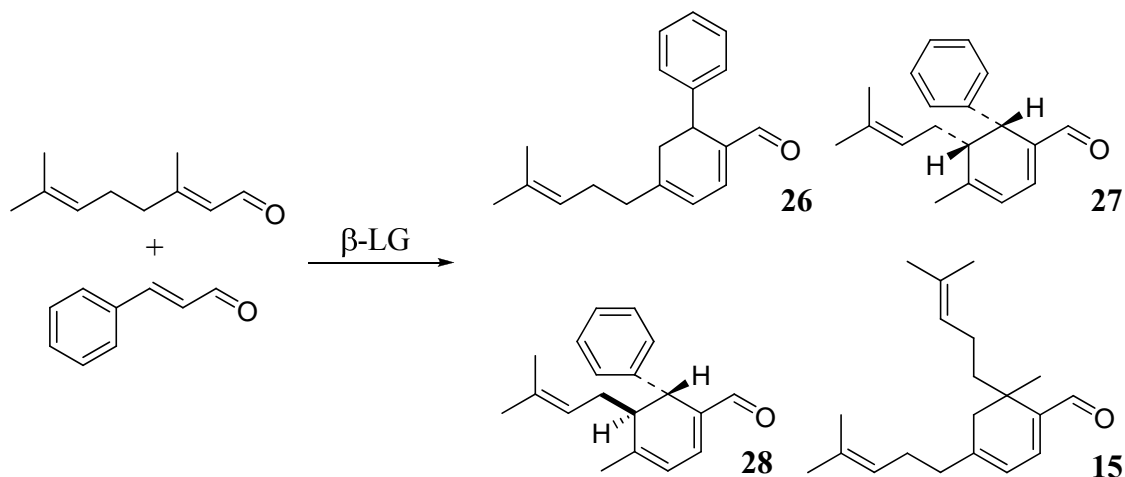


**Figure 18.** Proposed routes to the synthesis of 1,2,4-trisubstituted cyclohexadienals.

**Scheme 9.**  $\beta$ -LG mediated reaction products between citral and cinnamaldehyde.



cyclocitral **15** itself.<sup>32</sup> For the  $\beta$ -LG mediated reaction, we saw all four products produced.

For this particular reaction, we incubated  $\beta$ -LG with cinnamaldehyde and citral simultaneously. We were interested in observing the effects when the two substrates were at ratios of 1:1 or 1:2 to look at overall isolated yields of the various products shown in **Table 4**. Isolated yields varied in each case as there is a competition for the binding of the substrates to the active lysine residues. At both concentrations, the major product isolated was the *cis*-diastereomer **27** with yields after three days of 19% and yields of 22.2% and 28.3% for 1:1 and 1:2, respectively after four days. The other major product formed was cyclocitral with yields of 18% and 20% for 1:1 and slightly increasing to approximately 24% for time points at 1:2. In the formation of the *trans*-diastereomer from day three to four, we saw a slight increase in production at 1:1, but in for 1:2 the isolated yield was slightly diminished as the *cis* product had slightly increased.



**Table 4.** Reaction yields for citral/cinnamaldehyde  $\beta$ -LG reaction. Percent yields were determined by HPLC purification.

1:1	Day 3	Day 4	1:2	Day 3	Day 4
Compound	% yield	% yield	Compound	% yield	% yield
<b>26</b>	13.4	19.1	<b>26</b>	12.2	19.2
<b>27</b>	19.1	22.2	<b>27</b>	19.2	28.3
<b>28</b>	8.7	10.3	<b>28</b>	9.7	7.2
<b>15</b>	18.3	20.1	<b>15</b>	23.7	24.3

#### *Rate of $\beta$ -LG Mediated Reaction*

To determine the observed rate for the formation of cycloterpenals by  $\beta$ -LG, citral was used as a model substrate resulting in the formation of cyclocitral. The rate was determined by comparing integrated peak areas to a calibration curve to determine the amount of cyclocitral injected onto the column versus the resulting integrated peak area. Three different concentrations of citral were used to see if the increased amount of substrate had any effect on the rate of the formation of cyclocitral. In other words, was the protein mediated reaction catalytic or a single turnover event. Optimal substrate conditions were used (3x) as well as saturation conditions of 10X and 50X to that of the protein concentration. Interestingly, the results were similar for each concentration (**Figure 19**). This data corroborates well with previous experiments that indicated no increased yield when the protein was incubated with more than three equivalents of substrate. The rate of the reaction for cyclocitral formation is 0.034 M/min. To compare the rate of formation of cyclocitral to the other dimerization reactions, a comparison of the peak areas versus time was utilized. It was found that the reactions involving

thiophene, naphthalene, retinal, 3-methyl-2-butenal, and biphenyl were greater than citral. The other substrates were substantially less than that of the formation of cyclocitral.

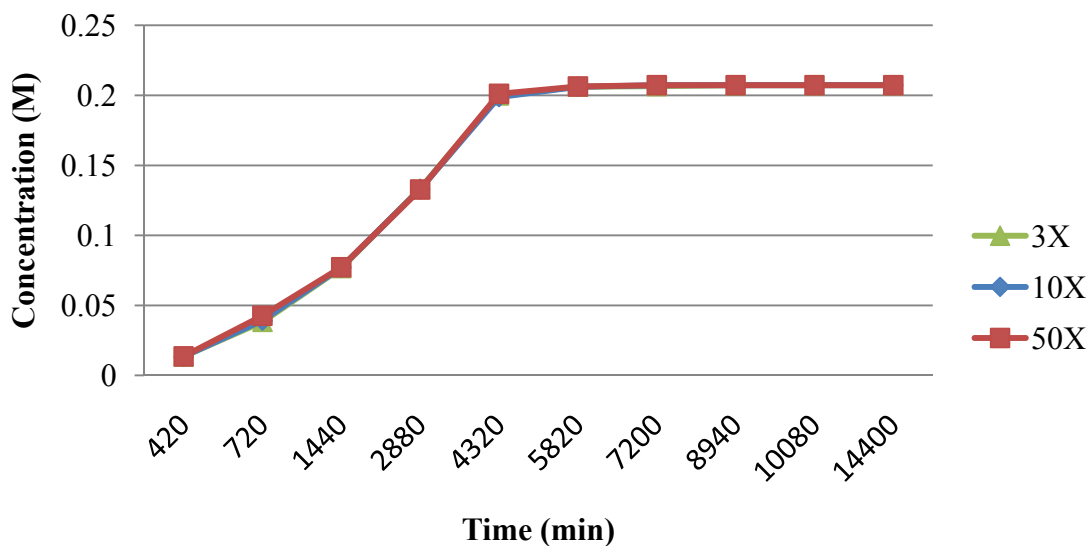


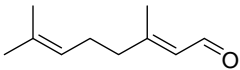
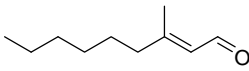
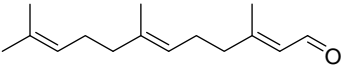
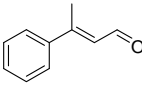
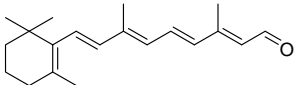
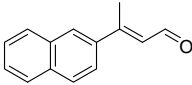
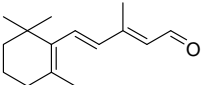
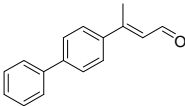
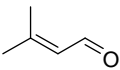
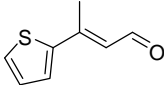
**Figure 19.** Rate of formation for cyclocitral at various concentrations.

#### *K<sub>D</sub> Measurements*

We measured the dissociation constants ( $K_d$ ) for each of the substrates mentioned above to determine how tightly the ligands bind to the main calyx of BLG. These measurements were performed using a fluorescent titration of each ligand at pH 7.0 in phosphate buffer saline (PBS). The  $K_d$  values (**Error! Not a valid bookmark self-reference.**) obtained were all in the micromolar range ( $10^{-6}$ ) with the exception of 3-methyl-2-butenal which displayed the highest affinity at  $9.83 \times 10^{-7}$  M. The values that we obtained for this series of  $\beta$ -methyl aldehydes is comparable to  $K_d$  values that have

been obtained for other molecules, ranging from  $10^{-4}$  to  $10^{-8}$  M by fluorescence microscopy.<sup>94</sup>

**Table 5.** K<sub>d</sub> measurement for substrates used for dimerization observations.

Substrate	K <sub>d</sub>	Substrate	K <sub>d</sub>
	$1.34 \times 10^{-6}$		$2.05 \times 10^{-6}$
	$2.88 \times 10^{-6}$		$1.15 \times 10^{-6}$
	$1.81 \times 10^{-6}$		$1.51 \times 10^{-6}$
	$1.35 \times 10^{-6}$		$1.63 \times 10^{-6}$
	$9.83 \times 10^{-7}$		$2.26 \times 10^{-6}$

### *Mass Spectrometric Evidence of Active Lysine Residues*

To gain an understanding of how  $\beta$ -LG is promoting this dimerization reaction, we decided perform a reductive amination with sodium cyano-borohydride ( $\text{NaCNBH}_3$ ) to crosslink citral to the protein. Two different treatments were performed. The first was to saturate the reaction with reductant and the second was to add the reductant after a small aliquot was taken from the reaction. Time points that were analyzed were at 6, 24, 48, 72, and 96 hours. Both mixtures were passed through a spin-column fitted with Sephadex resin to remove small molecules and borate salts. These samples were then

concentrated and digested with trypsin and subsequently analyzed by mass spectroscopy for residues containing a mass shift with citral or cyclocitral bound.

At the beginning of this investigation, we originally speculated that the reaction would take place in the central calyx of the protein (K60 and K69). Thus far, experimentation has led us to believe that other lysines within the protein may be performing the dimerization reaction. By our account, we found that 85% of the 15 lysine residues had citral reduced to them with one containing the dimerization product intermediate with MASCOT ion scores above 20. Lysines K8 and K142 were the only two not shown to display citral bound. The reduction of citral to multiple lysines was expected as previous studies have shown reductions of various substrates to as high as 95% of the 15 lysines.<sup>95-98</sup> As shown in **Figure 20**, the modified lysines that were consistently detected in each sample were from K77 and K91 (red) corresponding to the peptides TK\*IPAVFK (yellow) (MASCOT score of 40) and IDALNENK\*VLVLDTDYKK (blue) (MASCOT score of 101) (Please note that these modified residues were also found in peptides with slightly different sequences due to multiple missed tryptic cleavage sites). Modification of K77 was observed as fragment ions (M+citral) b3, b4, b5, b6, and b7 (**Figure 21**), while modification of K91 with citral gave mass ion fragments b8, b9, b10, b11, and b13 (**Figure 22**).

```

1 MIVTQTMKGLDIQKVAGTWYSLAMAASDISLLDAQSAPLRVYVEELKPTPE
52 GDLEILLQKWENGECQAQKKIIAEKTKIPAVFKIDALNENKVLVLDTDYKK
102 YLLFCMENSAEPEQSLACQCLVRTPEVDDEALEKFDKALKALPMHIRLSF
153 NPTQLEEQCHI

```

**Figure 20.**  $\beta$ -LG sequence with fragments containing active lysine residues.

We were also able to observe the dimer intermediate **24** bound to K91 within peptide fragment IDALNENK\*\*VLVLDTDYK (MASCOT score of 60). This result might suggest that upon a substrate molecule binding the calyx allowing K77 and K91 to get in close enough proximity that K77, which is on a flexible loop can interact with K91. To confirm this modification, mass fragment ions b8, b9, and b10 were observed (Figure 23).

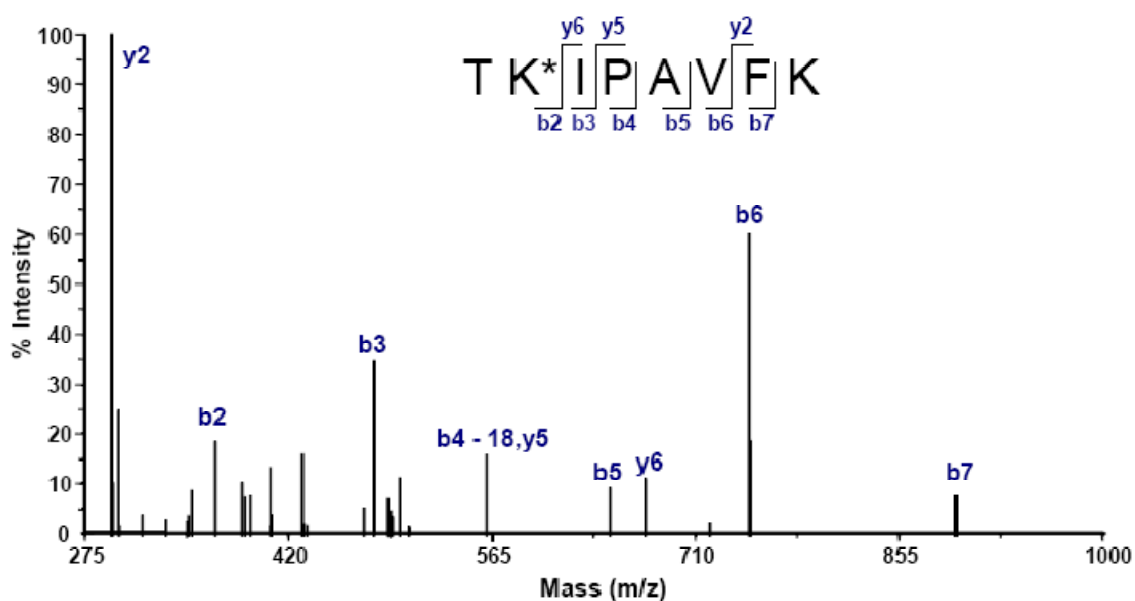


**Figure 21.** TK\*IPAVFK fragmentation pattern.

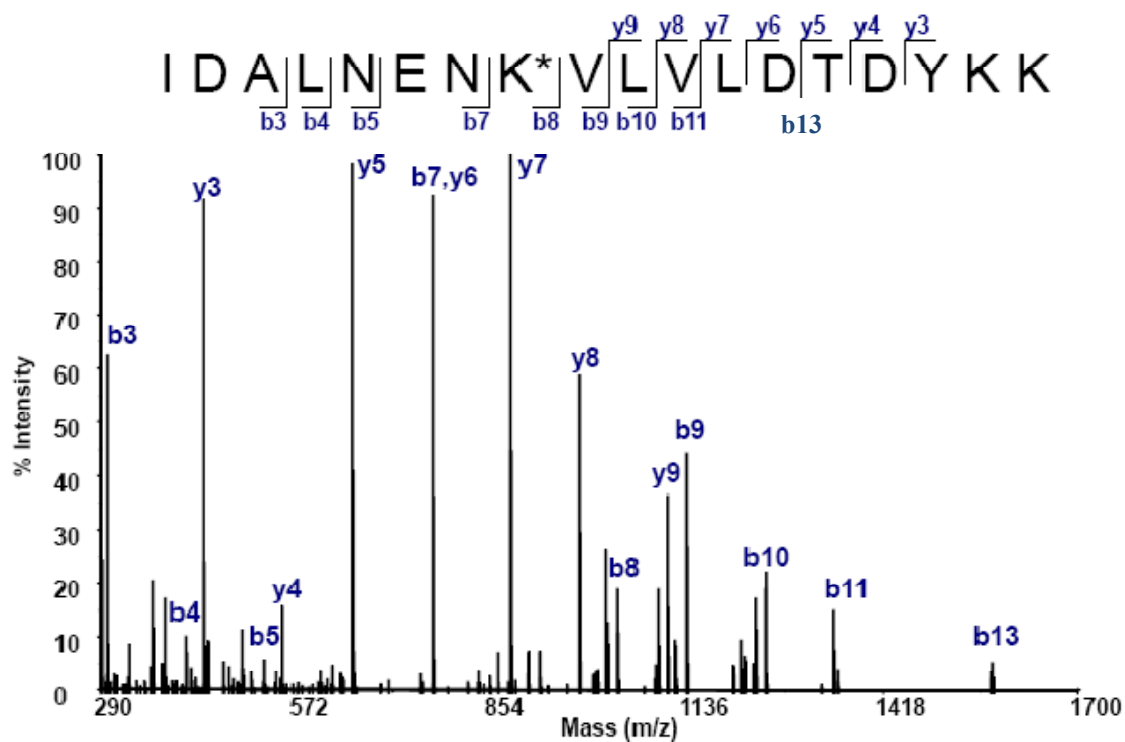


**Figure 22.** IDALNENK\*VLVLDTDYKK fragmentation pattern.

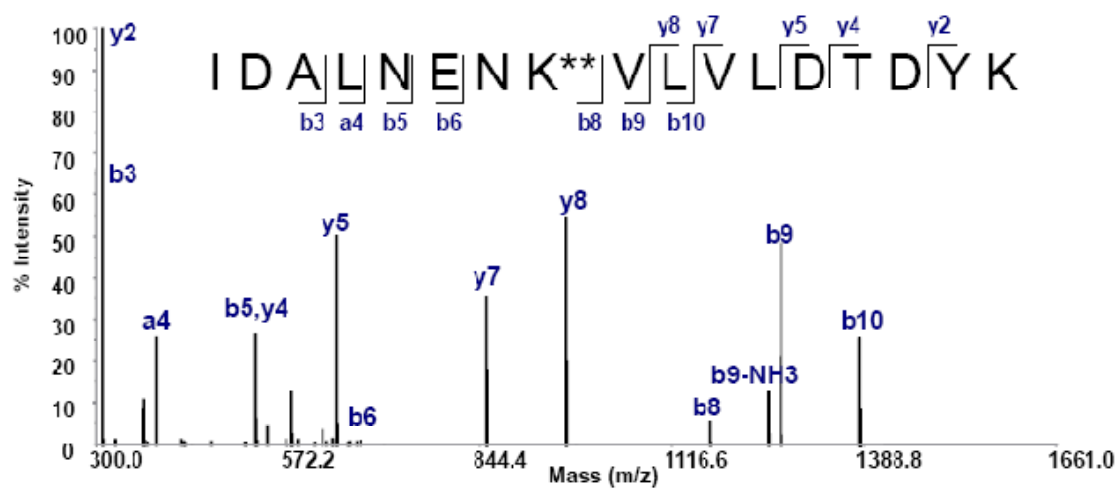


**Figure 23.** Dimer bound IDALNENK\*\*VLVLDTKYK fragmentation pattern.

With this information, we looked at the crystal structures of native  $\beta$ -LG, with palmitate bound, and retinol bound to look at the changes of the K77 and K91 residues upon binding of a substrate. In the native protein (**Figure 24**),<sup>49</sup> the terminal amines of the lysines are 16.09 Å apart. When a substrate is bound to the calyx, for instance palmitate,<sup>64</sup> the lysines move to 12.60 Å, which is a difference of 3.49 Å from the native protein (**Figure 25**). When you look at the structural change with the binding of retinol to the calyx,<sup>62</sup> the two lysine residues move within a distance of 12.10 Å of each other, a difference of 3.99 Å from the native protein (**Figure 26**).

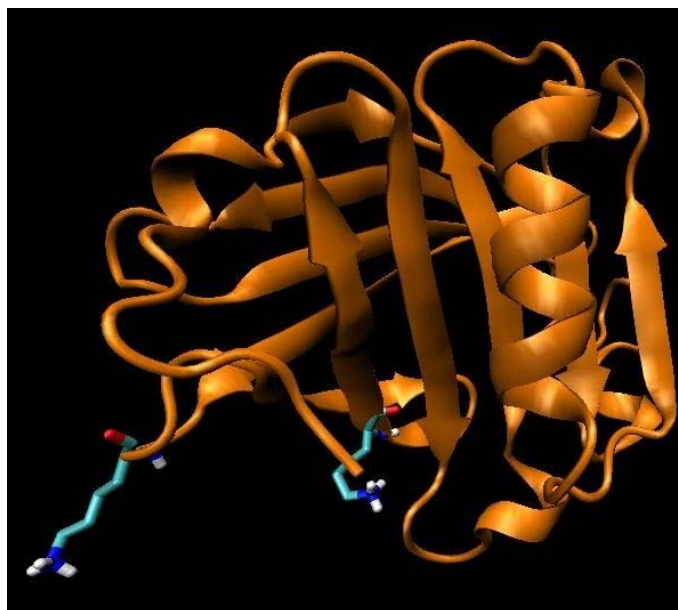


**Figure 24.** Native  $\beta$ -LG crystal structure depicting K77 and K91.<sup>49</sup>  
The diagram was prepared with VMB.

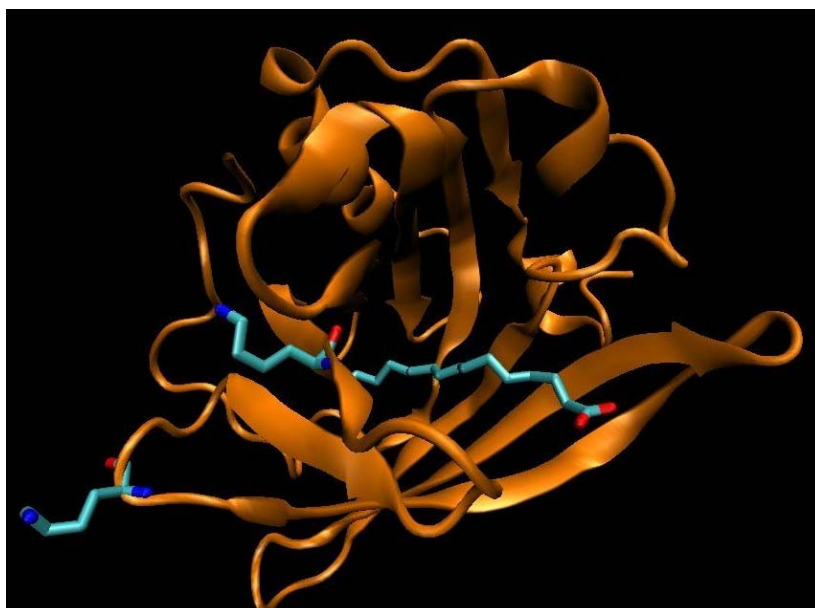


**Figure 25.**  $\beta$ -LG crystal structure depicting K77 and K91 with palmitate bound.<sup>64</sup>  
The diagram was prepared with VMB.



**Figure 26.**  $\beta$ -LG crystal structure depicting K77 and K91 with retinol bound.<sup>62</sup>  
The diagram was prepared with VMB.



### *Retinol/B-ionone Uptake Before Addition of Substrate*

So far, experimental evidence suggests that the dimerization reaction occurs in another location other than the primary active site of  $\beta$ -LG. To further probe this mechanism, incubation of the protein with substrates other than  $\beta$ -methyl aldehydes for two days was utilized. After the two day period, two equivalents of citral was added to see if the dimerization would still occur. In this series of experiments, we probed the calyx binding with the substrates retinol and  $\beta$ -ionone which have  $K_d$  values of  $1.5 \times 10^{-7}$  M and  $6.0 \times 10^{-7}$  M.<sup>94</sup> In order to ensure that the substrate was bound to the calyx,  $\beta$ -LG was incubated with 2 equivalents of substrate and was stirred at 37 °C for two days prior to the addition of citral. After two more days, the reaction mixture was extracted to find that the reaction had proceeded as normal. For retinol, the isolated yield of cyclocitral was 19.3% and with  $\beta$ -ionone the overall yield for the reaction was 17.1%. This data corroborates with that of the two day incubation with only citral and  $\beta$ -LG where the yield was 22%. As a control, a  $\beta$ -LG solution was stirred for two days at 37 °C with no substrate. After the two period, three equivalents of citral was added and the reaction was allowed to stir an additional two days. The reaction yield was 21.5%.

### *Sequence Comparison Amongst Similar B-LGs*

With the knowledge that K77 and K91 are likely responsible for the dimerization reaction, we looked at other  $\beta$ -LG sequences from other species to see if these two lysines were conserved. A comparison of the amino acid sequences of 20 various  $\beta$ -LGs was performed by Sawyer *et. al.*<sup>46</sup> in 2000 and based upon this only three other  $\beta$ -LGs had K77 and K91 conserved. These included buffalo, goat, and sheep (**Figure 27**).

While bovine lactoglobulin is the smallest of these proteins, the homology to the other three is varied by only two amino acids. The other proteins in the survey had amino acid substitutions at one of the sites or both amino acids modified. These included  $\beta$ -LGs from cat, dog, horse, donkey, dolphin, pig, baboon, wallaby, kangaroo, and possum.<sup>46</sup>

```

Buffalo MKCLLLALGLALACGAQAIVTQTMKGLDIQKVAGTWYSLAMAASDISLL
Cow B   -----MIVTQTMKGLDIQKVAGTWYSLAMAASDISLL
Goat    MKCLLLALGLALACGIQAIIVTQTMKGLDIQKVAGTWYSLAMAASDISLL
Sheep   MKCLLLALGLALACGVQAIIVTQTMKGLDIQKVAGTWYSLAMAASDISLL
          : ***** : *****

Buffalo DAQSAPLRVYVEELKPTPEGDLEILLQKWENGECQKKIIAEKTKIPAVF
Cow B   DAQSAPLRVYVEELKPTPEGDLEILLQKWENGECQKKIIAEKTKIPAVF
Goat    DAQSAPLRVYVEELKPTPEGNLEILLQKWENGECQKKIIAEKTKIPAVF
Sheep   DAQSAPLRVYVEELKPTPEGNLEILLQKWENGECQKKIIAEKTKIPAVF
          ***** : *****

Buffalo KIDALNENKVLVLDTDYKKYLLFCMENSAEPEQSLACQCLVRTPEVDDEA
Cow B   KIDALNENKVLVLDTDYKKYLLFCMENSAEPEQSLACQCLVRTPEVDDEA
Goat    KIDALNENKVLVLDTDYKKYLLFCMENSAEPEQSLACQCLVRTPEVDKEA
Sheep   KIDALNENKVLVLDTDYKKYLLFCMENSAEPEQSLACQCLVRTPEVDNEA
          ***** . **

```

**Figure 27.** Amino acid sequences for  $\beta$ -LGs from various species with conserved K77 and K91.

The SwissProt<sup>99</sup> databank entries are: buffalo, P02755; cow, P02754; goat, P02756; sheep, P02757.

### *Milk Promoted Biosynthesis of Cycloterpenals*

As previously mentioned,  $\beta$ -LG is able to survive the milk process even at elevated temperatures used during pasteurization (to kill bacteria). We have clearly demonstrated that  $\beta$ -LG undergoes the self dimerization of  $\beta$ -methyl aldehydes to cycloterpenals, so why would not the milk we drink also perform this dimerization reaction? In human blood,  $\beta$ -LG is present at concentrations of 0.7-1.2 g/dL. For this experiment, we took store bought milks such as whole (also chocolate), 2%, skim, half

& half, buttermilk, and fresh cow's milk and incubated it with excess citral for four days at 37 °C. These milks were then treated with excess citral as the exact concentration of  $\beta$ -LG present in each could not be determined. The color changes of the milks should be noted, especially in the case of skim milk, as it paralleled that seen with the  $\beta$ -LG solution (**Figure 28**). The color of the milk changed from a normal milk white color to

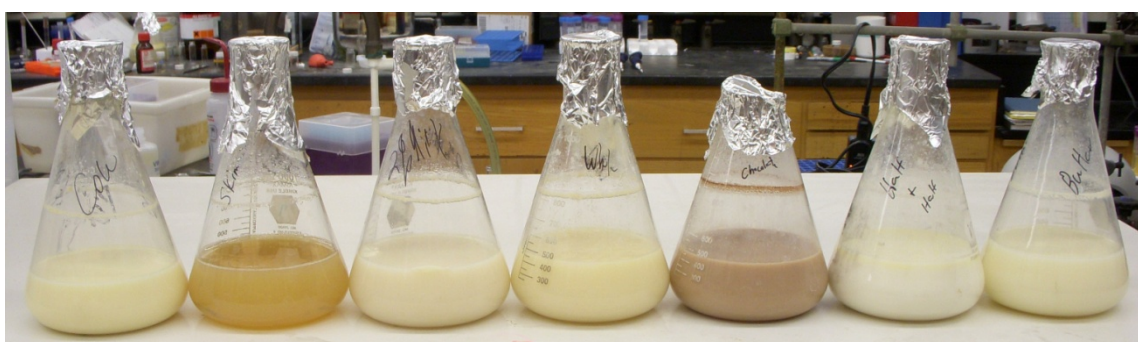
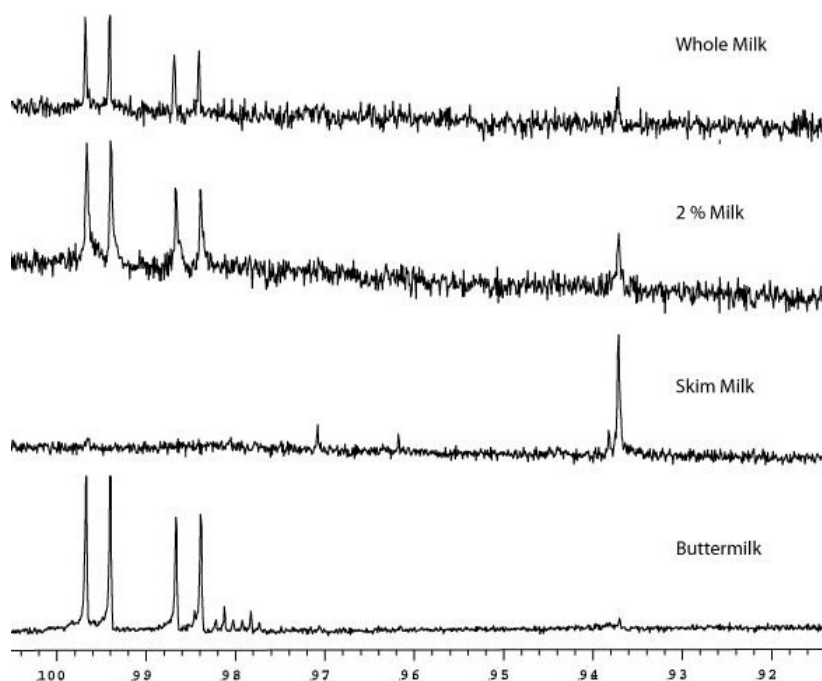


**Figure 28.** Various milks incubated with citral for four days.  
From left to right: Fresh cow's milk, skim, 2%, whole, chocolate, half & half, buttermilk.

that of a dark yellow, possibly reflecting Schiff base formation. The amount of fats, cholesterol, and sugars present in each milk sample could be affecting the amount of cyclocitral produced as the binding sites become occupied by small molecules. The uptake of citral by other proteins present in the milks could also have had an effect on overall yields. This is reflected in the isolated yields obtained for each of the milk reactions. As seen in **Figure 29**, the reaction product was observed with skim, and 2%, whole milk. Very little conversion was seen with buttermilk. The highest yielding was that of skim milk with a calculated yield (based on the amount of citral added) of 14.4%. The 2% milk exhibited a yield of 7.3% while whole and buttermilk gave a 4.8% and

1.2% yield, respectively. We were also able to detect cyclocitral in fresh cow's milk but only when adding a larger excess of citral to the milk. In the case of chocolate milk, the yield was comparable to that of whole milk with an isolated yield of 4.2%. For half & half, no dimerization product was detected.

In order to ensure that no small metabolites were responsible for the dimerization of citral to cyclocitral, 200 mL of skim, 2%, whole, and buttermilk was passed through a Sephadex G25 column. The flow through was then subjected to the exact same reaction conditions as used with the untreated milks. The yields for each reaction were unchanged indicating that only  $\beta$ -LG in the milks were responsible for the formation of the cyclocitral product.

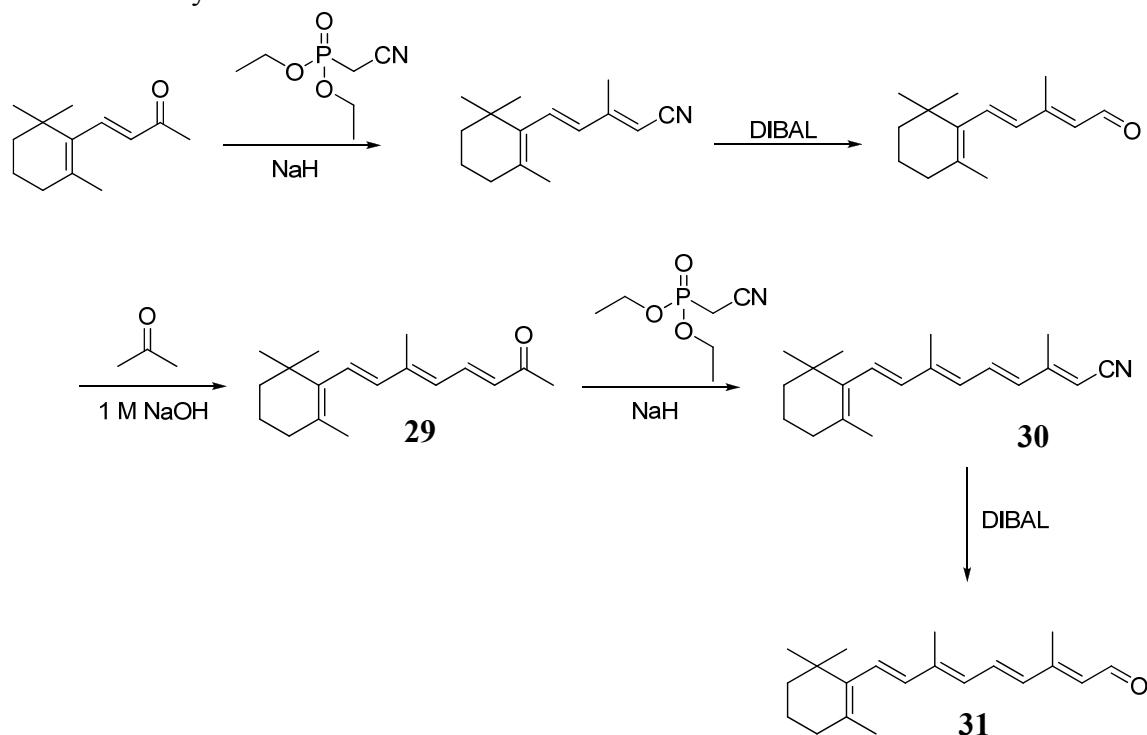


**Figure 29.**  $^1\text{H}$ -NMR of cyclocitral being produced from store bought milk after four days.

The two doublets at 9.85 and 9.95 correspond to citral and singlet at 9.38 is cyclocitral.

### *Synthesis of Retinal*

In order to perform our *in vivo* rabbit study, we needed to secure a source of retinal. We developed a synthetic scheme beginning with  $\beta$ -ionone with a five steps synthesis to generate all-*trans*-retinal (**Scheme 10**). The first step was to generate a stock pile of  $\beta$ -ionylideneacetaldehyde (C-15 aldehyde), which is synthesized in two steps from  $\beta$ -ionone. The C-15 aldehyde was then converted to all-*trans*-C-18 tetraene ketone **29** by utilizing an aldol condensation between acetone and  $\beta$ -ionylideneacetaldehyde in the presence of 1.0 M sodium hydroxide. This reaction gave us a yield of 92%.<sup>100</sup> A Horner-Wadsworth-Emmons reaction was then performed on the methyl-ketone by treating it with an ylide solution generated by treatment of diethyl-(cyanomethyl)-phosphonate with sodium hydride to give all-*trans*- C-20  $\beta$ -methyl nitrile **30** in an 88% yield.<sup>101,102</sup> This C-20 nitrile was then reduced with diisobutylaluminum hydride to give all-*trans*-retinal **31** in an 86% yield.<sup>101,103-105</sup>

**Scheme 10.** Synthetic route for retinal.

### *In Vivo Study Utilizing New Zealand White Rabbits*

We have demonstrated that cycloterpenal formation can occur with  $\beta$ -LG *in vitro* as demonstrated with isolated protein and the protein in various milks. As cycloretinal has been isolated from the human eye,<sup>33,34</sup> we set out to explore whether  $\beta$ -LG will form cycloretinal *in vivo* in a rabbit model. It has been shown that intact  $\beta$ -LG readily passes through the intestinal transepithelium cells in the rabbit's ileum. The absorption of intact  $\beta$ -LG into the blood stream is through intracellular transfer.<sup>106,107</sup> To do this, eight New Zealand White rabbits (2.5 kg) were randomly allocated to the control (basic diet) (n=1),  $\beta$ -LG/water control (n=1), skim milk control (n=1), retinal control (n=1),  $\beta$ -LG/water + retinal (n=2), and skim milk + retinal (n=2). Rabbits were fed twice daily for a period of one week their respective diets. All of the rabbits had free access to a

standard rabbit diet and water.  $\beta$ -LG/water was administered at 1.3 g/kg with the dosage of retinal being at 40 mg/kg for each feeding. After seven days, the rabbits were exsanguinated and the blood was removed for subsequent analyses. To probe for the formation of cycloretinal, the blood was extracted followed by characterization via  $^1\text{H}$ -NMR and MS. The control rabbit, with a normal diet, was used to ensure that no metabolites were in the aldehyde region of interest. The positive control rabbits yielded no cycloretinal. For the retinal feeding control, the substrate was absorbed into the blood stream with no cycloretinal present. As for the feedings involving either a  $\beta$ -LG solution or skim milk with retinal, the opposite was observed. We saw the *in vivo* formation of cycloretinal with each source. We were also able to see to absorption of retinal into the blood stream of the rabbits as each extract contained isomers of retinal **(Figure 30)**.

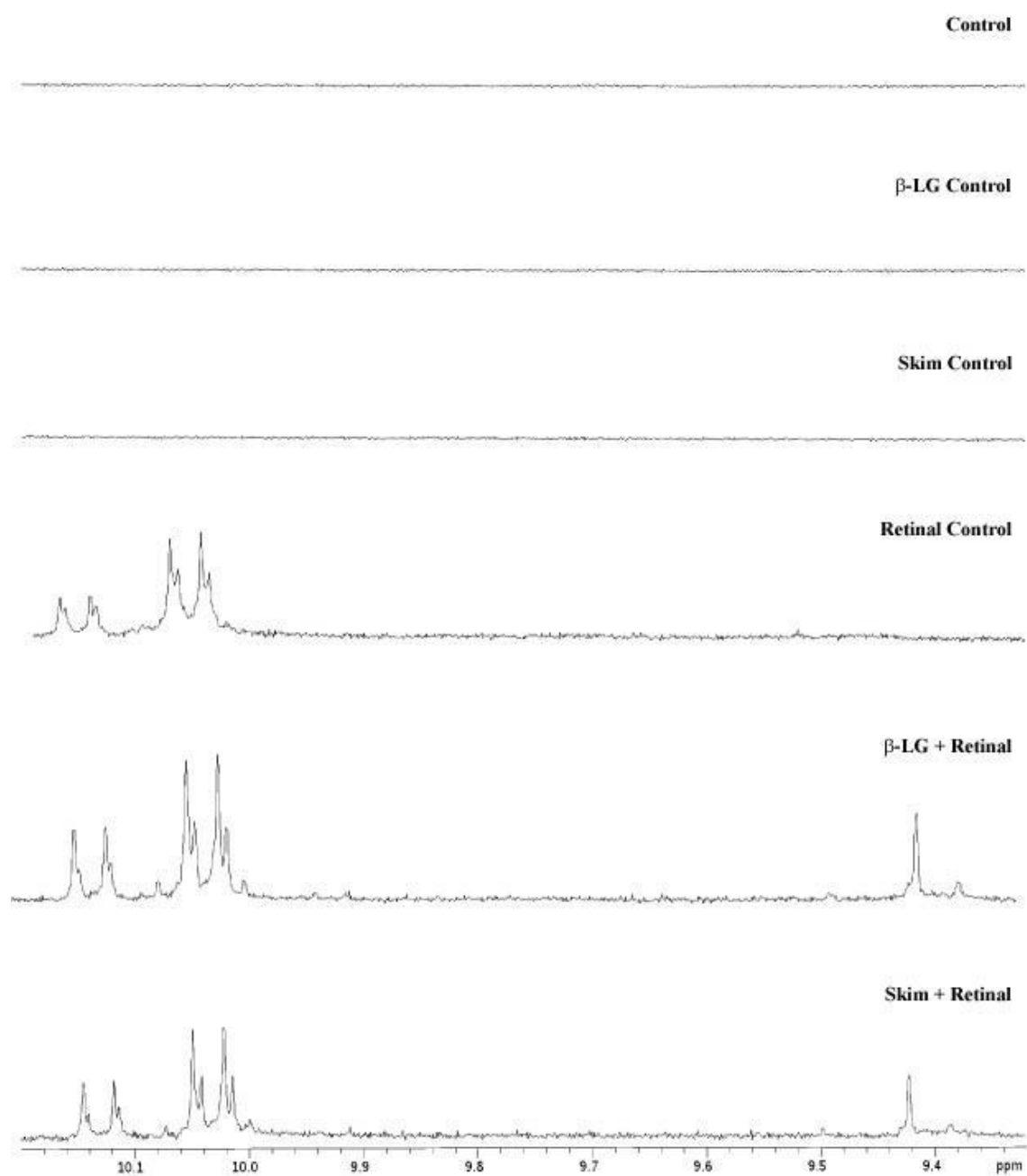


**Figure 30.**  $^1\text{H}$ -NMR overlay of rabbit feedings.



To assess  $\beta$ -LG uptake in the blood of rabbits, we looked at the serum of bloods from the  $\beta$ -LG/water and skim milk controls and feedings against the negative control (standard diet). A SDS-PAGE gel was ran with the serum (diluted 1:10) from each blood sample. The gel (**Figure 31**) showed that the  $\beta$ -LG was readily absorbed into the blood stream of the rabbits as each sample contained a band corresponding to the  $\beta$ -LG control at approximately 18 kD. However, the non-feeding control showed no traces of  $\beta$ -LG and looked like the other samples with the exception of the band at approximately 18 kD.

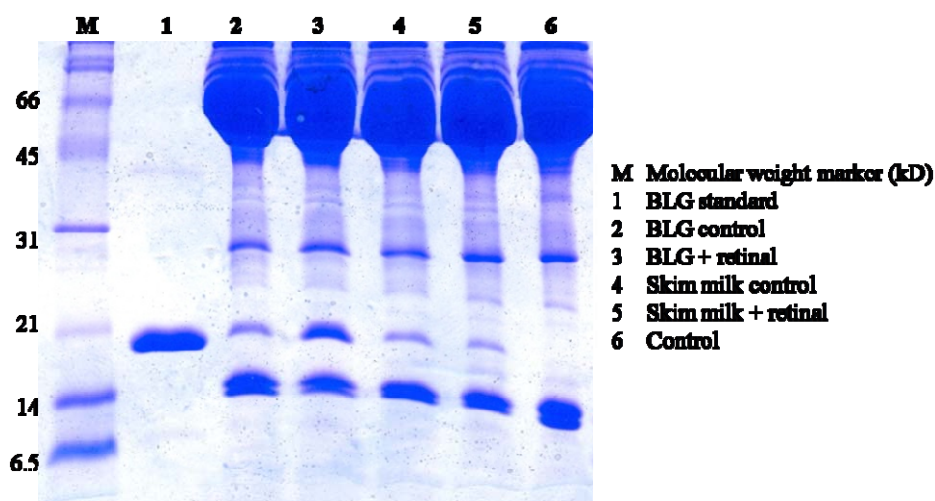


**Figure 31.** SDS-PAGE gel of rabbit feedings.

With SDS-PAGE gel confirmation of  $\beta$ -LG uptake, we next proceeded to demonstrate that the protein in the blood could perform the reaction *in vitro*. We took the  $\beta$ -LG/water control and the non-feeding control, 10 mL each, and incubated them with all-*trans*-retinal over a four day period at 37 °C. After four days, the mixture was

extracted and assayed for cycloretinal production. By  $^1\text{H}$ -NMR and MS, we observed  $\beta$ -LG (isolated from blood) could still perform the reaction. This experiment demonstrates the resiliency of  $\beta$ -LG. It clearly survives the acid environment of the stomach and makes it into the blood stream of rabbits. It leads one to speculate that it can survive in humans and make it way to eye where  $\beta$ -LG has been characterized in proteomic studies.

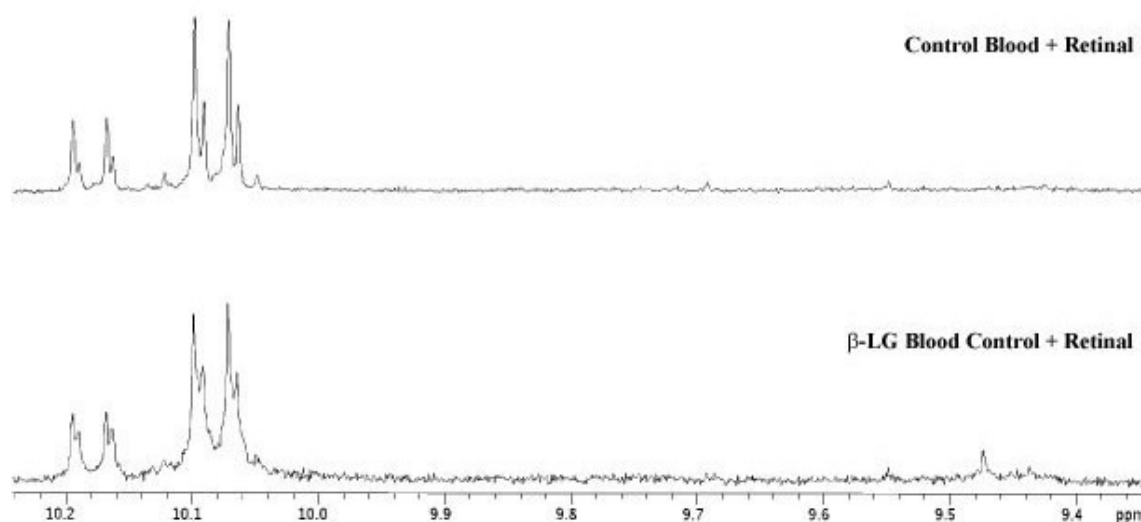


**Figure 32.**  $^1\text{H}$ -NMR overlay of blood experiment.

## CONCLUSION

The results in this chapter demonstrate that the major milk whey protein  $\beta$ -LG promotes the formation of cycloterpenals. We have shown that the reaction is amendable to various  $\beta$ -methyl substrates with moderate yields. The protein reaction was optimized and the mechanism of the reaction was probed with discovery of two lysines outside the central calyx of the protein being responsible for the dimerization. *In*

*vitro* experiments were also carried out on store bought milks where the dimerization of citral into cyclocitral was observed in skim, 2%, whole, and buttermilk. *In vivo* experiments were performed utilizing a rabbit model where the rabbits were fed sources of  $\beta$ -LG along with retinal which led to cycloretinal formation. In order to prove that  $\beta$ -LG can survive in the blood stream, the blood from the  $\beta$ -LG control rabbit was treated with retinal and cycloretinal was formed with the surviving protein. With this in mind,  $\beta$ -LG has been characterized in the human eye along with cycloretinal. The mechanism for this bis-retinoid formation has yet to be determined but it can be speculated that if  $\beta$ -LG is present under the right conditions, then the formation of cycloretinal is possible.

## EXPERIMENTAL

### *General*

Fresh THF was dried by passage through an MBRAUN solvent purification system and stored over molecular sieves. All other solvents and reagents were purchased and used without further purification unless noted.  $^1\text{H}$  (300 MHz) and  $^{13}\text{C}$  (75 MHz) spectra were recorded on a 300 MHz spectrometer. Chemical shifts for  $^1\text{H}$  and  $^{13}\text{C}$  NMR spectra are reported in ppm referenced to TMS (0 ppm) and coupling constants are reported in Hertz (Hz). MS spectra were recorded on an API QSTAR PULSAR (ES) apparatus. Chromatographic separations were achieved by flash silica chromatography (silica gel 60 mesh, EMD Biosciences). Fluorescence measurements were recorded on a PTI QuantaMaster series spectrofluorometer. HPLC separation were performed on a Varian ProStar system. Retinal **31**<sup>101,103,105</sup> and intermediates **29**<sup>100</sup> and **30**<sup>101</sup> have been previously synthesized and characterized. Initial experiments were

carried out using  $\beta$ -LG from Sigma (L3908, St. Louis, MO, 90%  $\beta$ -LG). The  $\beta$ -LG source that was used primarily for experimentation was obtained from Davisco Foods International, Inc. (JE-003-6-922, La Sueur, MN, 93.6%  $\beta$ -LG). All cycloterpenals have been fully characterized previously.<sup>31,32</sup>

### *Synthesis of A,B-Unsaturated Aldehydes*

$\alpha,\beta$ -unsaturated nitriles for the synthesis of the  $\alpha,\beta$ -unsaturated aldehydes used to produce the cyclohexadienals were synthesized following literature protocols<sup>102</sup> and purified by flash column chromatography (gradient of 2-10% ethyl acetate/hexanes).  $\alpha,\beta$ -Unsaturated aldehydes were prepared by reduction of their corresponding nitriles and purified by flash column chromatography (2%-10% ethyl acetate/hexanes).<sup>104</sup> Farnesal was synthesized from farnesol.<sup>108</sup> In each case, the *all-trans* isomer was utilized in the self-condensation reactions.

### *Organisms*

Retinal Pigment Epithelium (RPE) cells (CRL-2302) and *B. subtilis* strain 6633 were obtained from the American Type Culture Collection, Rockville, MD. The yeast *S. cerevisiae* wild-type strain [#404; BY4741; MATa his3 $\Delta$ 1 leu2 $\Delta$ 0 met15 $\Delta$ 0 ura3 $\Delta$ 0] was obtained from Dr. Michael Kladde at the Department of Biochemistry, Texas A&M University. The *E. coli* strain DH10B was obtained from Prof. Dennis Gross, Texas A&M University, Department of Plant Pathology.

### *Media Conditions*

- *LB* (Luria-Bertani) medium contained the following components per liter: Bacto-peptone, 10g; Yeast extract, 5g; Sodium chloride, 5g; and deionized water.
- *YPD* (Yeast Peptone Dextrose) medium contained the following components per liter: Yeast extract, 5g; Bacto-peptone, 5g; Glucose, 20 g; and deionized water.
- *NB* (Nutrient Broth) medium contained the following components per liter: Beef extract, 3g; Peptone, 5g; and deionized water.

Agar plates of the above media were prepared by adding 20 g/L bacto-agar. All media were autoclaved at 121 °C for 20 minutes.

### *RPE Cell Cultures*

A human adult RPE cell line (ARPE-19, ATCC) was maintained as stock cultures in BD Falcon (Catalog # 353003) 100 mm Cell Culture Dishes and was passaged weekly. The medium used for cell propagation was an ATCC-formulated Dulbecco's modified Eagles medium DMEM:F12 Medium (Catalog No. 30-2006) containing 10% fetal bovine serum (FBS, GIBCO, Catalog # 26140-079), propagated in a 5% carbon dioxide atmosphere at 37 °C.

### *General Procedure for B-LG Mediated Reactions*

In a 1000 mL Erlenmeyer flask, 500 mL of a 1%  $\beta$ -LG solution (PBS, pH 7.0) and three equivalents of substrate (0.5 M in absolute ethanol, 1.630 mL) were mixed together. This mixture was placed in a 37 °C shaker and stirred at 250 rpm for four days. The  $\beta$ -LG mixture was removed and 500 mL of ethyl acetate was added along

with a magnetic stir bar and the mixture stirred for 30 minutes at room temperature to extract the product. To avoid emulsions, the mixture was centrifuged at 9000 rpm at 4 °C for 30 minutes. The organic layer was collected, dried over anhydrous magnesium sulfate, and concentrated *in vacuo*.

#### *Heterodimer Formation Utilizing B-LG*

In a 1000 mL Erlenmeyer flask, 500 mL of a 1%  $\beta$ -LG solution (PBS, pH 7.0) and one equivalent of citral and cinnamaldehyde (0.5 M in absolute ethanol, 0.543 mL each) were mixed together. This mixture was placed in a 37 °C shaker and stirred at 250 rpm for three and four days, respectively. The  $\beta$ -LG mixture was removed and 500 mL of ethyl acetate was added along with a magnetic stir bar and the mixture stirred for 30 minutes at room temperature to extract the product. To avoid emulsions, the mixture was centrifuged at 9000 rpm at 4 °C for 30 minutes. The organic layer was collected, dried over anhydrous magnesium sulfate, and concentrated *in vacuo*. The crude material was subsequently purified via HPLC and products were characterized according to Bench *et al.*<sup>32</sup>

#### *pH Profile Experiment*

To determine the optimal pH for the protein reaction, we looked at a range of pHs which included 1.0, 3.0, 5.0, 7.0, 9.0 and 11.0. 500 mL of PBS, pH 7.0, was either buffered with 1.0 M HCl or 1.0 NaOH to obtain the desired pHs using a Seven Easy pH meter (Mettler-Toledo, Switzerland, Product # Z654280). Five grams of  $\beta$ -LG was then dissolved in each buffered PBS solution to give a 1% solution which was then treated

with three equivalents of citral (0.5 M in absolute ethanol, 1.630 mL). This mixture was placed in a 37 °C shaker and stirred at 250 rpm for four days. The  $\beta$ -LG mixture was removed, 500 mL of ethyl acetate was added along with a magnetic stir bar and the mixture was stirred for 30 minutes at room temperature to extract the product. To avoid emulsions, the mixture was centrifuged at 9000 rpm at 4 °C for 30 minutes. The organic layer was collected, dried over anhydrous magnesium sulfate, and concentrated *in vacuo*.

#### *Retinol/B-ionone Competition Experiment*

In a 1000 mL Erlenmeyer flask, 500 mL of a 1%  $\beta$ -LG solution (PBS, pH 7.0) and two equivalents of retinol or  $\beta$ -ionone (0.5 M in absolute ethanol, 1.086 mL) were mixed together. This mixture was placed in a 37 °C shaker and stirred at 250 rpm for 48 hours prior to the addition of two equivalents of citral (0.5 M in absolute ethanol, 1.086 mL). The reaction mixture was allowed to stir for the remaining two days. The  $\beta$ -LG mixture was removed and 500 mL of ethyl acetate was added along with a magnetic stir bar and the mixture stirred for 30 minutes at room temperature to extract the product. To avoid emulsions, the mixture was centrifuged at 9000 rpm at 4 °C for 30 minutes. The organic layer was collected, dried over anhydrous magnesium sulfate, and concentrated *in vacuo*.

#### *Rate Determination of B-LG*

To ten 250 mL Erlenmeyer flasks, 100 mL of 1%  $\beta$ -LG (PBS, pH 7.0) was mixed with three equivalents of citral (0.5 M in absolute ethanol, 0.326 mL). The solutions were placed in a 37 °C shaker at 250 rpm for 7, 12, 24, 48, 72, 97, 120, 149, 168, and

240 hours. When each mixture was removed, 125 mL of ethyl acetate was added along with a magnetic stir bar and the mixture stirred for 30 minutes at room temperature to extract the product. To avoid emulsions, the mixture was centrifuged at 9000 rpm at 4 °C for 30 minutes. The organic layer was collected, dried over anhydrous magnesium sulfate, and concentrated *in vacuo*. All HPLC procedures used a Varian ProStar 230 solvent delivery module. Elution was monitored at 240 nm with a Varian ProStar 330 Photodiode Array Detector. Integrals were determined by using Star Workstation for the ProStar 330 diode array detector. The stationary phase was a Phenomenex Luna 5 $\mu$  silica column (250 x 10 mm, part # 00G-4274-N0, Torrance, CA). The mobile phase was 100% dichloromethane at a flow rate of 3 mL/min. Under this condition, cyclocitral eluted at 5.55 minutes. The amount of cyclocitral was quantitated by comparing the integrated peak area to a calibration curve of the amount of pure cyclocitral injected onto the column versus the resulting integrated peak area. This same procedure was performed for the addition of ten equivalents (1.087 mL) and fifty equivalents (5.435 mL) of citral (0.5 M in absolute ethanol) to 100 mL of 1%  $\beta$ -LG.

#### *General Procedure for Heat Denaturation*

In a 1000 mL Erlenmeyer flask, 500 mL of a 1%  $\beta$ -LG solution (PBS, pH 7.0) was boiled for 10 minutes at 100 °C. Once the solution was cooled to the touch, three equivalents of citral (0.5 M in absolute ethanol, 1.630 mL) was added to the protein solution. This mixture was then placed in a 37 °C shaker and stirred at 250 rpm for four days. The  $\beta$ -LG mixture was removed and 500 mL of ethyl acetate was added along with a magnetic stir bar and the mixture stirred for 30 minutes at room temperature to



extract the product. To avoid emulsions, the mixture was centrifuged at 9000 rpm at 4 °C for 30 minutes. The organic layer was collected, dried over anhydrous magnesium sulfate, and concentrated *in vacuo*.

#### *General Procedure for Urea-Induced Denaturation*

In a 1000 mL Erlenmeyer flask, 500 mL of a 1%  $\beta$ -LG solution (PBS, pH 7.0) and ten equivalents of urea (0.5 M in absolute ethanol, 5.43 mL) were mixed together. This mixture was then placed in a 37 °C shaker and stirred at 250 rpm. After two days of incubation, three equivalents of citral (0.5 M in absolute ethanol, 1.630 mL) was added to the protein solution and stirred for an additional four days. The  $\beta$ -LG mixture was then removed and 500 mL of ethyl acetate was added along with a magnetic stir bar and the mixture stirred for 30 minutes at room temperature to extract the product. To avoid emulsions, the mixture was centrifuged at 9000 rpm at 4 °C for 30 minutes. The organic layer was collected, dried over anhydrous magnesium sulfate, and concentrated *in vacuo*.

#### *General Procedure for Microbial Protein Controls*

Microbes were grown on their respective plates under appropriate conditions. A single colony was picked and placed in a 3 mL culture and allowed to grow overnight before being transferred to a 500 mL culture. After 24 hours, the culture was centrifuged and the cell pellet flash frozen with liquid nitrogen before being stored at -80 °C. To lyse the cells, a Biospec Products Bead Beater (Biospec Products, Bartlesville, OK, Model 1107900) was utilized with 0.1 mm Glass Beads (Biospec Products, Bartlesville,

OK, Catalog # 11079101). To the frozen cell pellets, PBS (pH 7.0) was added and ten 30 second pulses with 1 minute intervals was performed to lyse the cells. Prior to performing dimerization screens, a metabolite control was generated where 40 mL of the protein extract was extracted with 200 mL of ethyl acetate, dried with anhydrous  $\text{MgSO}_4$ , and concentrated *in vacuo*. A  $^1\text{H}$ -NMR spectrum was produced to ensure that there were no metabolites in the aldehydic region of interest. Results were also confirmed by mass spectrometry. Protein concentration was measured by Bradford assay (Biorad, Hercules, CA, Catalog # 26140-079) and diluted to a 1% solution with PBS buffer. To establish whether crude protein extracts could support cycloterpenal formation, protein lysates were incubated with 0.5 M citral at 37 °C with shaking (250 rpm) for 4 days. As detailed previously, following incubation, the suspension was extracted with 300 mL of ethyl acetate, centrifuged, dried over anhydrous  $\text{MgSO}_4$ , and concentrated *in vacuo*.

#### *RPE Cell Screen for Dimerization*

RPE cells were subcultured until a total of 10 plates (95% cell coverage) were obtained. Cells were removed with 3 mL of a 0.05% (w/v) Trypsin- 0.53 mM EDTA solution (Gibco, Canada, Catalog # 25300-054) and placed in a 50 mL conical tube. Cells were pelleted for 20 minutes at 1000 rpm. To remove traces of medium, the cells were washed twice with DPBS, 1X without calcium and magnesium (Cellgro, Catalog # 21031187), and then resuspended in 10 mL of DPBS. The cell suspension was then lysed utilizing a 50 mL dounce homogenizer. Before a dimerization screen was performed, a metabolite control was performed where 5 mL of the protein lysate was

extracted with ethyl acetate (50 mL), dried with anhydrous  $\text{MgSO}_4$ , and concentrated *in vacuo*. A  $^1\text{H}$ -NMR was run to ensure that there were no metabolites in the aldehydic region of interest. Protein concentration was measured by Bradford assay (Biorad, Hercules, CA, Catalog # 26140-079) and diluted to a 1% solution with PBS buffer. To establish whether the crude protein extract could support cycloterpenal formation, protein lysates (10 mL) were incubated with 0.5 M citral at 37 °C with shaking (250 rpm) for 4 days. As detailed previously, following incubation, the suspension was extracted with 300 mL of ethyl acetate, centrifuged, dried over anhydrous  $\text{MgSO}_4$ , and concentrated *in vacuo*.

#### *Dimerization Utilizing Store Bought Milks*

To demonstrate the dimerization with processed milks, skim milk, 2% milk, whole milk, buttermilk, and half and half were purchased. We also looked at fresh cow's milk. The milks purchased contained approximately 8-9 grams of protein according to their labels. Initial experiments were performed with 200 mL of milk taken from the carton and diluted with 300 mL of PBS (pH 7.0) with 2.20 mL (3.80 mL for fresh cow's milk) of 0.5 M citral (in absolute ethanol) which was placed in a 37 °C shaker for 4 days being stirred at 250 rpm. After this time, the solutions were extracted with 300 mL of ethyl acetate and stirred with a magnetic stirrer for 30 minutes. The mixture was centrifuged for 30 minutes at 9000 rpm for 30 minutes at 4 °C. The organic layer was removed, dried with anhydrous  $\text{MgSO}_4$ , and concentrated *in vacuo*.

To ensure that there were no small metabolites responsible for the dimerization, each milk was passed through a Sephadex G25 (GE Healthcare, Uppsala, Sweden,

Product # 17-0033-01) column by measuring out 20 g of the powder and suspending it in 100 mL of PBS. This slurry was then poured into a 5.08 cm x 60 cm column with porosity disc sealed in. 200 mL of milk was passed through the column by the addition of PBS until a total volume of 500 mL was obtained. The filtered milk was retested using the same conditions as previously mentioned.

#### *In Vivo Study Utilizing New Zealand White Rabbits*

The following protocol (AUP#2008-70) was approved by the Texas A&M University Institutional Animal Care and Use Committee (IACUC). Eight adult New Zealand White rabbits (2.5 kg, Myrtle's Rabbitry, Thompsons Station, TN) were randomly allocated to the control (normal diet, n=1),  $\beta$ -LG/water control (n=1), skim milk control (n=1), retinal control (n=1),  $\beta$ -LG/water + retinal (n=2), and skim milk + retinal (n=2). All rabbits had free access to a standard rabbit diet and water. The rabbits were housed separately in standard cages in the LARR facility at Texas A&M University and maintained under standard conditions. Each day, the rabbits were provided the solutions by gavage twice daily for one week. Each solution was administered in 50 mL volumes with the exception of the retinal feeding in which a volume of 1 mL was fed. The  $\beta$ -LG/water solutions were supplied at 1.3 g/kg in 50 mL of water. The dosage of retinal used was 40 mg/kg dissolved in 150  $\mu$ L of absolute ethanol.

After seven days, the rabbits were anesthetized with a solution containing 10 mg/kg of ketamine with 3 mg/kg xylezine by intravenous injection allowing 5 minutes for the cocktail to take effect. Depth of anesthesia was monitored prior to blood removal by squeezing the foot of the subject. Cardiac blood was removed by opening the thorax

to visualize the heart before carrying out cardiac puncture, which also led to exsanguination of the rabbit. This process allowed us to obtain approximately 40-50 mL of blood from each subject. The blood (40 mL) was then processed by extraction with ethyl acetate (300 mL) assisted by stirring with a magnetic stirrer for one hour. This mixture was then centrifuged for 30 minutes at 9000 rpm for 30 minutes at 4 °C. The organic layer was removed, dried with anhydrous  $\text{MgSO}_4$ , and concentrated *in vacuo*.

To assess  $\beta$ -LG content in the samples, bloods from the control (normal diet),  $\beta$ -LG/water control,  $\beta$ -LG/water + retinal, skim milk control, and skim milk + retinal were centrifuged at 4000 rpm for 30 minutes at 4 °C to separate red blood cells from serum. After centrifugation, 1  $\mu\text{L}$  of serum was diluted with 9  $\mu\text{L}$  of PBS pH 8.0 and 10  $\mu\text{L}$  of 2x SDS-PAGE Treatment Buffer (125 mM Tris pH 6.8, 4% SDS, 20% glycerol, 0.2 mg/ml bromophenol blue, 0.2 mM DTT). Samples were heated to 90°C for 10 min and electrophoresed on a 15% SDS-PAGE gel at 200V for 35 min. Following electrophoresis, the gel was stained with Coomassie Blue to visualize protein bands.

To see if the  $\beta$ -LG absorbed within the blood could perform the dimerization of retinal to cycloretinal, 10 mL of blood from the  $\beta$ -LG/water control and 10 mL of blood from the control were incubated at 37 °C with 400 mg (dissolved in 1 mL of absolute ethanol) of retinal for 4 days. The blood was then processed by extraction with ethyl acetate (200 mL) where it was stirred with a magnetic stirrer for one hour. This mixture was then centrifuged for 30 minutes at 9000 rpm for 30 minutes at 4 °C. The organic layer was removed, dried with anhydrous  $\text{MgSO}_4$ , and concentrated *in vacuo*.

### *K<sub>D</sub> Measurements*

The  $K_d$  measurements were determined by utilizing the method set forth by Cho *et al.*<sup>61</sup> Fluorescence was measured on a PTI QuantaMaster series spectrofluorometer. Substrate, 2  $\mu$ L, (100  $\mu$ M in absolute ethanol) portion was added to 2 mL of  $\beta$ -LG (1.2  $\mu$ M subunit concentration) in PBS (pH 7.0) and mixed for 30 seconds. The tryptophan fluorescence was excited at 290 nm and was monitored at 334 nm at room temperature. The apparent dissociation constant,  $K_d'$  of a single binding site was calculated by the Cogan *et al.* method.<sup>109</sup> The following equation was utilized in the dissociation constants for our substrates.

$$P_o\alpha = (R_o/n)(\alpha/1-\alpha) - K_d'/n$$

where  $\alpha$  is the fraction of free binding sites,  $R_o$  is the total substrate concentration,  $P_o$  is the total protein concentration, and  $n$  is the apparent molar ratio of ligand to protein at saturation. The value of  $\alpha$  was calculated for every point on the titration curve using the following equation:

$$\alpha = (F - F_{\min})/(F_o - F_{\min})$$

where  $F = (I/I_o)$  represents the relative fluorescence intensity at a certain  $R_o$ ,  $F_{\min}$  represents the fluorescence intensity upon saturation of all the apoprotein molecules (with a 3-fold molar excess of ligand), and  $F_o$  is the initial fluorescence intensity. Addition of more than 1 mole of substrate/mole of  $\beta$ -LG caused no further reduction in the tryptophan fluorescence.

*Mass Spectroscopy for Reduction of Substrate to B-LG*

Five reactions consisting of 1%  $\beta$ -LG (1 mL) were incubated with 4X citral ( $5.0 \times 10^{-4}$  M, 4.35  $\mu$ L) and 10X NaCNBH<sub>3</sub> ( $5.0 \times 10^{-4}$  M, 10.9  $\mu$ L) and placed in a 37 °C shaker (250 rpm) to give time points of 6, 24, 48, 72, and 96 hours. At each time point, the mixture was removed and 2 x 75  $\mu$ L passed through a Bio Rad Micro Bio-Spin P-30 Tris chromatography column (Biorad, Hercules, CA, Catalog # 732-6233) to remove borate salts and excess substrate for a total volume of 150  $\mu$ L. Alternatively, another five reactions were setup but only incubated with 4X citral ( $5.0 \times 10^{-4}$  M, 4.35  $\mu$ L). At time points of 6, 24, 48, 72, and 96 hours, a 200  $\mu$ L aliquot was removed and treated with 10X NaCNBH<sub>3</sub> ( $5.0 \times 10^{-4}$  M, 10.9  $\mu$ L). This mixture was heated at 50 °C for 30 minutes prior to the removal of borate salts and excess substrate via a micro bio spin column.

$\beta$ -LG was diluted to a final concentration of 0.1 mg/mL in 50 mM Ammonium Bicarbonate buffer. This sample was reduced by adding dithiothreitol (DTT) to a final concentration of 5 mM followed by incubation at 60 °C for one hour. Alkylation was performed by adding iodoacetamide (20 mM final concentration) and the solution incubated at room temperature for ten minutes. Trypsin was added at an enzyme to protein ratio of 1:50 (w/w) and digestion was carried out at 37 °C overnight. A Hitachi High Technologies (Dallas, TX) NanoFrontier Liquid Chromatography Mass Spectrometer equipped with a nanoelectrospray ionization (nanoESI) source was used. 200 ng of the resulting digest was loaded and Liquid chromatography (LC) separation was achieved using Grace Vydac C18 column (150  $\times$  0.075 mm, 300 Å) (Deerfield, IL) at a flow rate of 200 nL min<sup>-1</sup>. Peptides were eluted using a gradient of (A): 98% water,

2% acetonitrile, 0.1% formic acid versus (B): 98% acetonitrile, 2% water, 0.1% formic acid. The gradient time table was as follows: 2% B for 5 min, 2-10% for 0.1 min, 10-40% for 29.9 min, 40-60% for 10 min, 60-98% for 5 min, held at 98% for 6 min, 98-2% for 1 min, held at 2% for 13 min, for a total run time of 70 min. The MS data was obtained on a linear quadrupole ion trap (LIT)-time-of-flight (TOF) mass spectrometer in positive ion mode (100-2000 Da) using a spray voltage of +2000 V and a micro channel plate (MCP) detector at +2100 V. Mascot ([www.matrixscience.com](http://www.matrixscience.com)) was used to analyze the data. Briefly, the raw data output was converted to a Mascot Generic File format and the data was searched against the Swiss Prot database with the following parameters.: 200 ppm peptide mass tolerance, +/- 0.5 Da fragment mass tolerance, 2 missed cleavages allowed for, variable modifications of Carbamidomethyl, Citral on Lysine (266.20 Da residue mass), and cyclocitral (400.32 Da residue mass). Tandem MS data was then interpreted manually using the NanoFrontier LD Data Processing program. Figures were created by deconvoluting the observed masses to the +1 charge state and labeling *b* and *y* fragment ions.



## CHAPTER III

### SYNTHESIS AND BIOLOGICAL EVALUATION OF SELF-CONDENSATION CYCLOTERPENALS \*

#### INTRODUCTION

Carotenoids form an important class of biologically active molecules and play a critical role in energy transfer processes such as photosynthesis or photoprotection. Carotenoids, such as lycopene **8** (**Figure 33**), act as a class of anti-oxidants which are responsible for the scavenging of free radicals within the human body.<sup>17</sup> For instance, **8** is 100 times more effective in singlet-oxygen quenching than vitamin E **9**.<sup>18</sup> Lycopene also acts as an important intermediate in the biosynthesis of  $\beta$ -carotene.  $\beta$ -carotene **10**, another important carotenoid, can be enzymatically cleaved by a  $\beta$ -carotene 15,15'-monooxygenase to form two retinals **11**.<sup>19-21</sup> Retinal **11** is important as it serves as the chromophore for the visual transduction cycle.<sup>22</sup> **11** can easily be oxidized to form retinol **12**, which is better known as vitamin A. The other important retinoid, retinoic acid **13**, can be made from retinal **11** via a retinal oxidase.<sup>23-26</sup> These retinoids (**Figure 34**) exhibit a variety of biological activities ranging from dermatological uses to cancer preventative agents, and are potent modulators of growth and differentiation.<sup>27-29</sup> Interestingly, **13** has been shown to differentiate embryonic stem cells into a neuron-like

---

\*Parts of this chapter are reprinted with permission from "Proline Promoted Synthesis of Ring-Fused Homodimers: Self-Condensation of  $\alpha,\beta$ -Unsaturated Aldehydes." Bench, B. J., Lui, C., Evett, C. R., Watanabe, C. M. H., 2006. *Journal of Organic Chemistry*, 71, 9458-9463, Copyright 2006 by American Chemical Society and from "Synthesis and Cellular Effects of Cycloterpenals: Cyclohexadienal-Based Activators of Neurite Outgrowth." Bench, B. J., Tichy, S. E., Perez, L. M., Benson, J., Watanabe, C. M. H., 2008. *Bioorganic & Medicinal Chemistry*, 16, 7573-7581, Copyright 2008 by Elsevier Ltd.

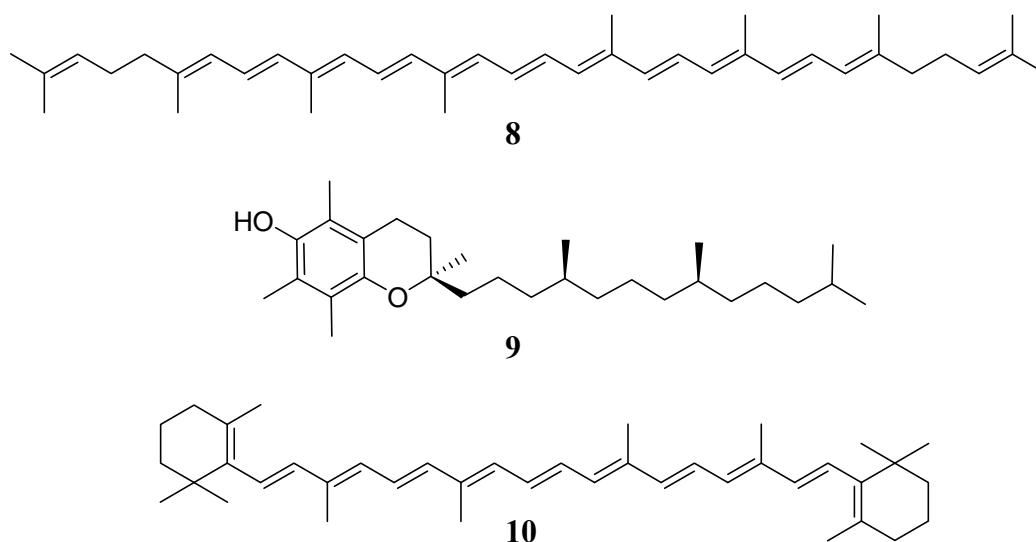


**Figure 33.** Structures of relevant carotenoids.

phenotype.<sup>30</sup> It has also been employed as a chemotherapeutic agent in the treatment of promyelocytic leukemia by causing terminal differentiation of the tumor cells.

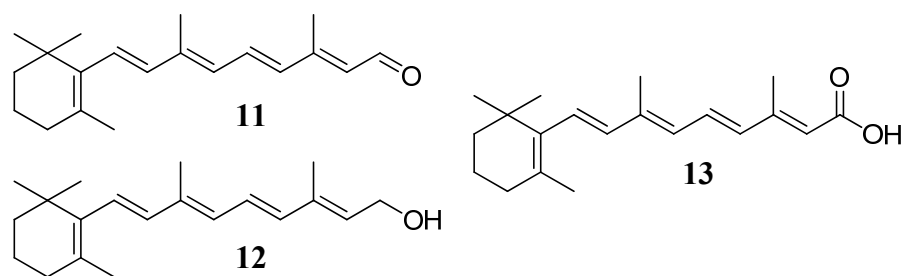


**Figure 34.** Biologically active retinoids.

Interestingly, condensation of all-*E*-retinal gives a C-40 ring-fused dimer **14** (with a cyclohexadienal structural core) which is also known as cycloretinal. This molecule, along with other bisretinoids, is believed to act as a contributor of age-related macular degeneration, the leading cause of blindness in the elderly.<sup>33,34</sup> The self-dimerization of citral has been suspected since the late 1890's.<sup>35,36</sup> The 1,2,4-

trisubstituted structure **15** was definitively ascribed in 1932.<sup>37</sup> Recently, citral dimer (cyclocitral) **15** was isolated from the North Sea bryozoans *Flustra foliacea*<sup>38,39</sup> and

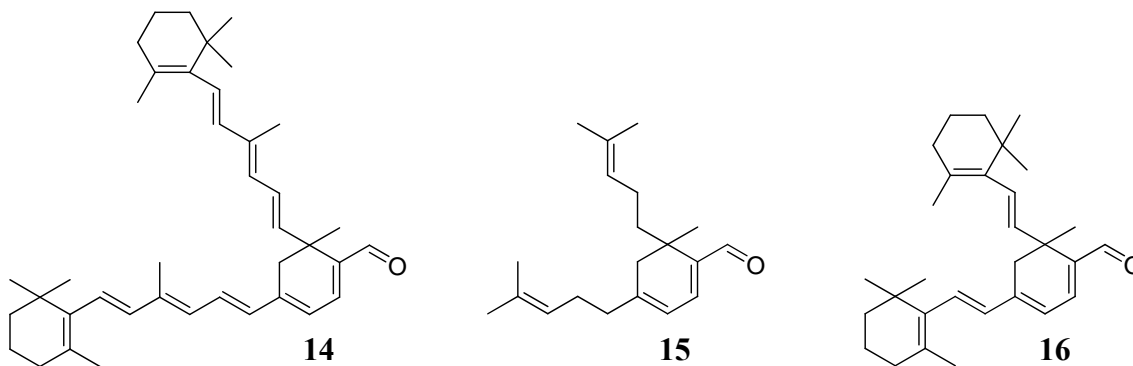


**Figure 35.** Structures of relevant homodimers.

shown to exhibit antibacterial activity against *Roseobacter sp.* And *Sulfitobacter sp.* in an agar diffusion assay (100  $\mu$ g resulted in a 0.5 and 1.0 cm zone of inhibition respectively). Furthermore, incubation of the principal milk protein  $\beta$ -lactoglobulin with  $\beta$ -ionylideneacetaldehyde has been shown to result in cyclohexadienal formation of its corresponding C-30 homodimer **16** (Figure 35).<sup>40</sup> While molecules with this structural scaffold are not unprecedented in nature, little is known regarding their biological function.

Over the past century, a variety of conditions have been used to develop facile synthetic routes to these self-condensation products. The general synthetic strategy has involved the use of strongly basic conditions such as lithium diisopropyl amide (LDA),<sup>110</sup> sodium hydride (NaH),<sup>111,112</sup> potassium hydride (KH),<sup>33,34,36,113</sup> potassium *tert*-

butoxide,<sup>113,114</sup> and others.<sup>115-117</sup> The problem with using these harsh basic conditions is that there is no degree of stereoselectivity.

Proline is a widely employed organocatalyst<sup>118,119</sup> as it is readily available and inexpensive.<sup>120,121</sup> It has been employed in a variety of asymmetric organic reactions including aldol,<sup>122-132</sup> Diels-Alder,<sup>133-138</sup> and Michael addition,<sup>126,139-144</sup> among many others.<sup>120,121</sup>

In this chapter, we fully investigate the use of L-proline as a chiral auxiliary to catalyze asymmetric self-condensation of a variety of  $\alpha,\beta$ -unsaturated aldehydes.<sup>87</sup> The scope of the reaction is investigated with 13  $\beta$ -methyl substituted substrates (and 1  $\beta$ -ethyl substituted substrate (**Figure 36**). Seven proline/proline-based catalysts and the reaction conditions were optimized. NMR and MS analyses as well as reactions with various proline derivatives also provide mechanistic insight into the reaction. In order to address the biological activity of this homodimer library, we tested it against PC12 cells where promising effects on neurite outgrowth were observed. We also screened the library for cytotoxic effects with an array of assays including Jurkats (human T-cell leukemia), yeast (*Saccharomyces cerevisiae*), and two bacterial strains (*Escherichia coli*, *Bacillus subtilis*).

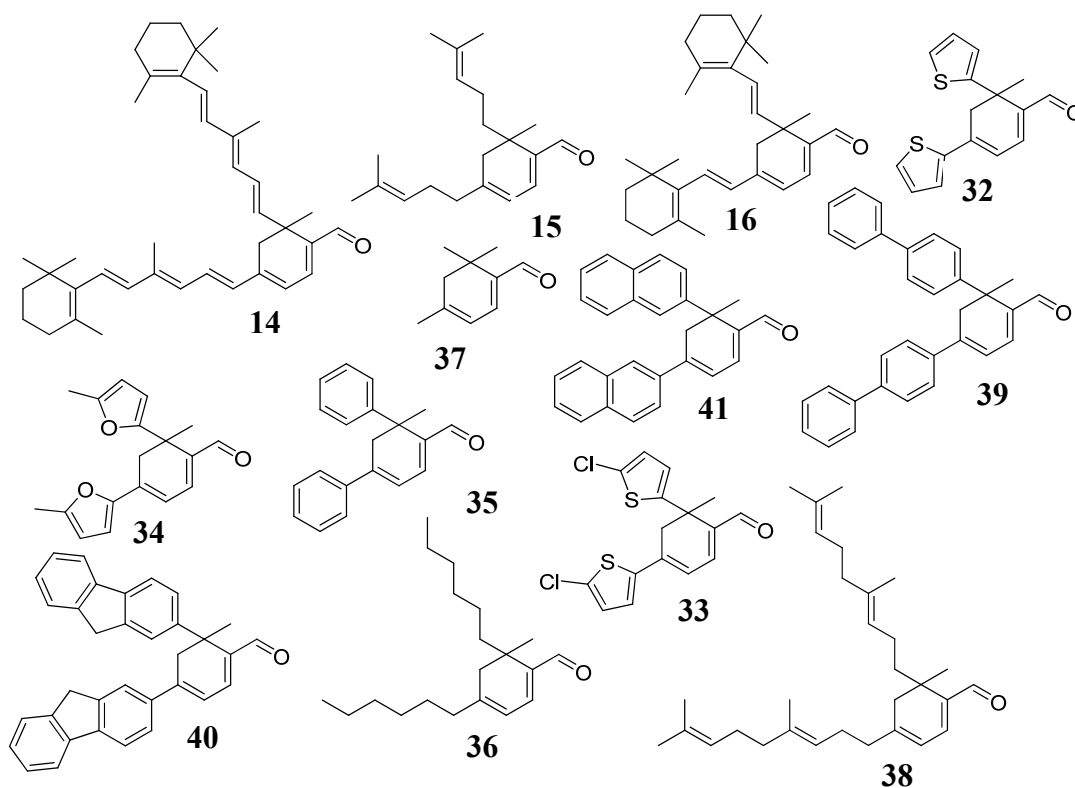


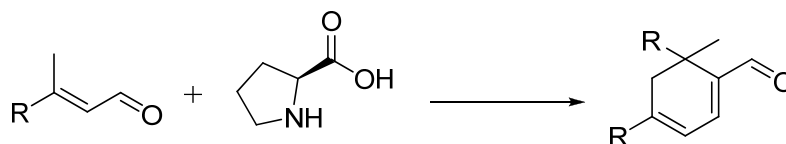
**Figure 36.** Chemical structures of the homodimer cycloterpenals-based compound library.

## RESULTS AND DISCUSSION

### *Optimization of Homodimer Synthesis*

Initially, we optimized conditions for these reaction (varying the temperature and substrate to catalyst ratios), utilizing citral **15** as a model substrate and L-proline to implement the reaction (**Scheme 11**). Reactions mediated with other amino acids (Trp,

**Scheme 11.** General reaction scheme for homodimer production.



His, Arg, Gly, and Ile) either fail or proceed to a lesser extent than proline.<sup>87</sup> Product yields were highest when the reactions were carried out at room temperature versus -20 to 0 °C or 50-100 °C. Cyclocitral (**15**) is typically isolated as the sole product in a 65% yield following 16-24 hours of incubation at room temperature using L-proline in ethanol (**Table 6**). This is in contrast to treatment of citral with NaH, which gives a mixture of the desired cyclocitral (**15**) along with a tetra-substituted cyclohexadienal (**15a**) in a 5:95 product ratio (**Figure 37**).<sup>111</sup> When the temperature is decreased (-20 to 0 °C), the reaction is sluggish and yields diminish to less than 5%. The majority of the starting

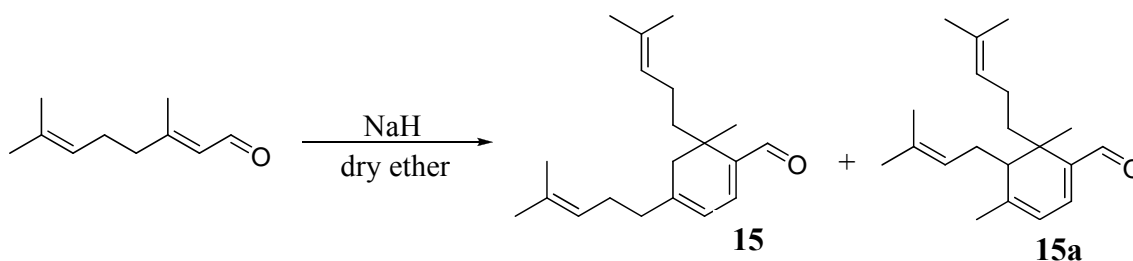


**Figure 37.** Products formed by treatment of citral with NaH.

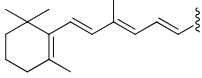
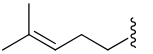
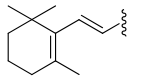
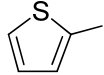
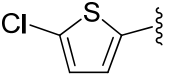
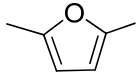
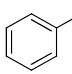
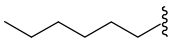
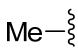
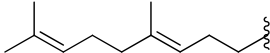
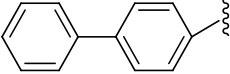
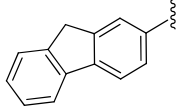
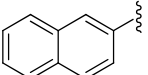
material remains as a Schiff base at 48 hours. On the contrary, when the temperature is increased, many unidentified byproducts begin to form within 1 hour and cyclocitral is obtained in less than 10% yield at 16 hours. Varying the substrate to auxiliary agent (L-proline) ratios also had a dramatic effect on reaction yields. We evaluated six different substrate-to-catalyst mol ratios: 1:0.5, 1:1, 1:1.25, 1:1.5, 1:1.75, and 1:2, respectively, whereby 1:1.5 molar concentrations exhibited the highest conversion rates (65%). At 1:0.5, 1:1, and 1:1.25 concentrations, the yields were <5%, 27%, and 42%, respectively.

Likewise, at higher proline concentrations, yields were diminished to 37% (1:1.75) and 35% (1:2).

### *Synthesis of Homodimers Utilizing L-proline*

Various substrates were tested utilizing these optimized conditions to investigate the generality of the reaction as illustrated in **Table 6**. Product yields ranged from 42% to 89% and ee values from 26% to 62%. Treatment of retinal (**14**) and  $\beta$ -ionylideneacetaldehyde (**16**) with ethanolic proline gave correspondingly higher yields than those originally reported, and yields are provided for the reaction with senecioaldehyde (**37**) and citral (**15**) that were not previously provided.<sup>87</sup> The new substrates examined included those of small aromatics such as thiophene (**32**), chlorothiophene (**33**), methyl-furan (**34**), and phenyl (**35**). We also looked at starting materials that contained aliphatic alkyl substituents (**36** and **38**), as well as bulky substituents such as biphenyl (**39**), fluorene (**40**), and naphthalene (**19**). Interestingly, the thiophene-substituted aldehyde (**33**) gave an unexpectedly lower yield than the methyl-furan-substituted (**34**) but gave a correspondingly higher ee. When the halogenated chlorothiophene (**33**) was tested, the yield was slightly higher than that of **32** with relatively equivalent ee values. The phenyl-substituted  $\alpha,\beta$ -unsaturated aldehyde (**35**) gave a moderate yield of 50% and an ee of 56%. Modest yields were obtained with the alkyl substituted 3-methyl-2-nonenal (**36**) and farnesal (**38**), presumably attributed to the flexibility of the groups versus the more rigid conjugated long chain substituents (**14** and **16**) where the highest yields were observed. We expected the biphenyl (**39**),

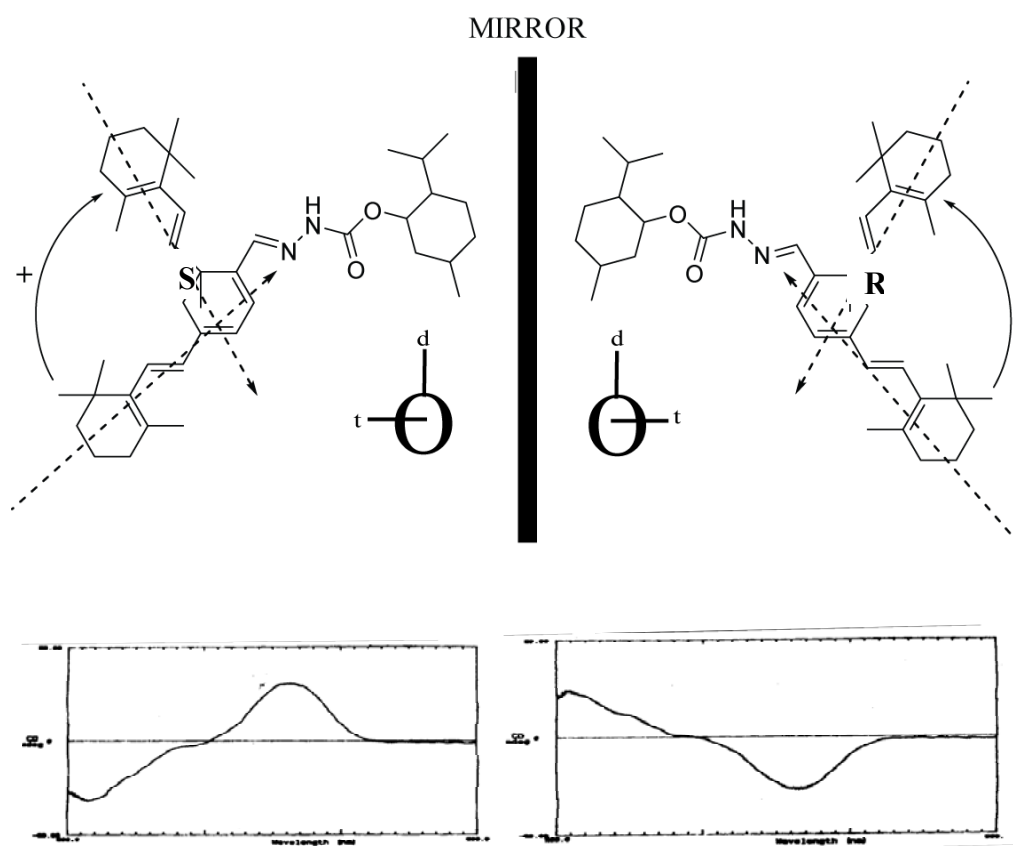
**Table 6.** Effects of various substrates on proline promoted homodimerization.

<b>R<sup>a</sup></b>	<b>Number</b>	<b>yield (%)<sup>b</sup></b>	<b>ee (%)<sup>c</sup></b>
	<b>14</b>	89	52
	<b>15</b>	65	50
	<b>16</b>	87	62
	<b>32</b>	47	40
	<b>33</b>	51	44
	<b>34</b>	60	26
	<b>35</b>	50	56
	<b>36</b>	73	54
	<b>37</b>	42	51
	<b>38</b>	52	46
	<b>39</b>	62	46
	<b>40</b>	57	42
	<b>41</b>	66	40

<sup>a</sup>Reaction conditions: 1 equiv of aldehyde and 1.5 equivs of L-proline dissolved in ethanol and stirred at room temperature for 16-24 hours. <sup>b</sup>Isolated yield. <sup>c</sup>Determined by Pr(hfc)<sub>3</sub> chiral shift reagent.



fluorene (**40**), and naphthalene (**41**) substituents to result in low transformation efficiencies due to steric hindrance which could be attributed to the bulkiness of the side chains. However, product yields were remarkably good when compared to others with yields of 52%, 62%, and 57% respectively. Circular dichroism (CD) analysis (**Figure 38**) of the menthylhydrazone derivatives of the C-30 dimer (formed through dimerization of **16**) suggests that the absolute configuration of the major isomer formed in these L-proline mediated reactions is the *S*-configuration as determined by the quadrant rule (chiral excitation theory).<sup>145</sup>

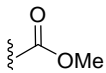
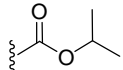
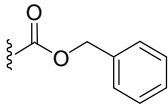
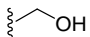
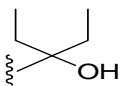
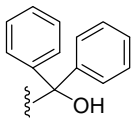


**Figure 38.** CD spectra of menthylhydrazone derivatives.

### Use of Proline Derivatives on Dimerization

Since the reaction appeared amenable to a variety of different substrates, we analyzed various proline derivatives to determine their effects on the enantioselectivity of the reaction. Previous work has shown that the reaction can be promoted by *trans*-4-hydroxy-L-proline, D-proline, and *cis*-4-hydroxy-D-proline.<sup>87</sup> Citral (**15**) was reacted with six different proline derivatives including L-proline methylester (**42**),<sup>146</sup> iso-propyl ester (**43**),<sup>146</sup> benzyl ester, (**44**),<sup>146</sup> prolinol (**45**),<sup>147</sup> diethyl prolinol (**46**),<sup>147</sup> and biphenyl

**Table 7.** Effect of proline derivatives on homodimerization.

R group <sup>a</sup>	catalyst	yield (%) <sup>b</sup>	time (h)	ee (%) <sup>c</sup>
	<b>42</b>	38	5	n/a
	<b>43</b>	43	34	n/a
	<b>44</b>	72	33	n/a
	<b>45</b>	78	23	13.4
	<b>46</b>	57	18	15.5
	<b>47</b>	49	30	14.8

<sup>a</sup>Reaction conditions: 1 equiv of aldehyde and 1.5 equivs of L-proline dissolved in ethanol and stirred at room temperature for 16-24 hours. <sup>b</sup>Isolated yield. <sup>c</sup>Determined by Pr(hfc)<sub>3</sub> chiral shift reagent.

prolinol (**47**) (**Table 7**). To our disappointment no stereoselectivity was observed, which was the case for the esters (**42-44**) that were synthesized. The highest selectivity was obtained with  $\alpha,\alpha$ -diethyl prolinol (**46**), which gave an enantiomeric excess of 15.5%. Reaction yields were moderate with the exceptions of the benzyl ester (**44**) and prolinol (**45**), which generated yields similar to that of L-proline. Solvent effects on citral dimerization were also examined with prolinol (**45**); THF, DMSO, DMF, and 2-propanol were each examined, but no improvement on enantiomeric selectivity was observed. As with the proline-assisted reaction, ethanol generated the highest yield of 78%.

#### *Reaction Mechanism for Homodimerization*

The proline promoted reaction is thought to commence by nucleophilic attack of the aldehyde with proline, resulting in the formation of a Schiff base **48** (**Figure 39**). Tautomerization, invoked by deprotonation of the  $\beta$ -methyl group, gives the  $\beta$ -methylenic proline adduct **49** that can be visualized to dimerize with **48** following a Diels-Alder or Michael-like imine addition mechanism (pathway marked with green arrows). During the Michael-like imine addition, intermediate **50** is generated and undergoes cyclization into reaction intermediate **51** (direct intermediate from Diels-Alder mechanism). From the di-proline intermediate **51**, the proline attached at C-4 of the cyclohexene ring readily dissociates leaving the cyclohexadiene intermediate **52**. Intermediate **52** then undergoes hydrolysis to give the 1,2,4-trisubstituted cyclohexadienal product **53**.

The need for 1.5 equivalents of chiral auxiliary (L-proline) in the reaction mixture is that it is necessary to convert all of the starting aldehyde to that of the Schiff base (accounting for 1 equivalent of L-proline), while the additional 0.5

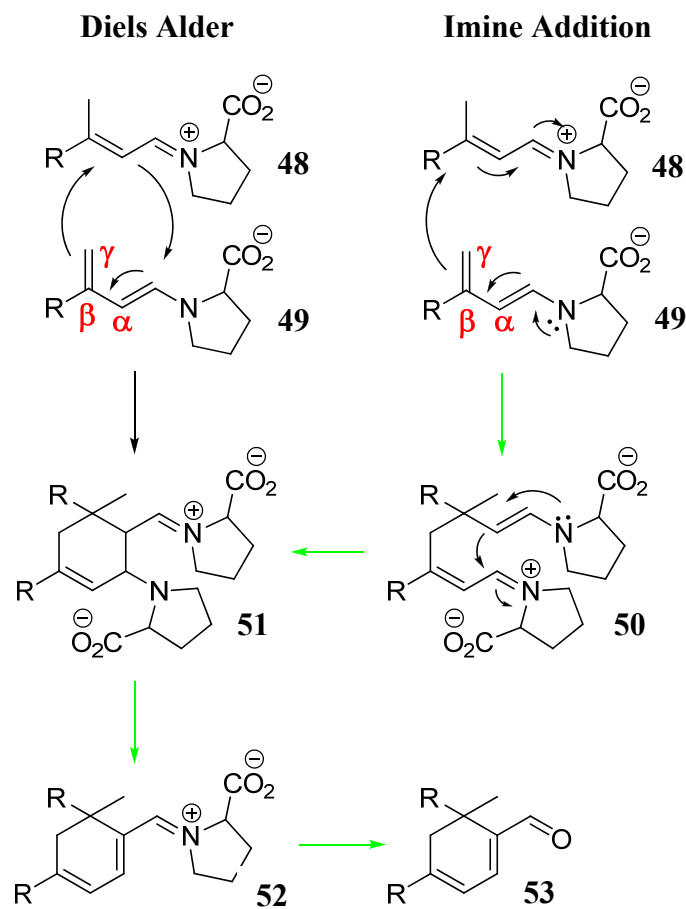


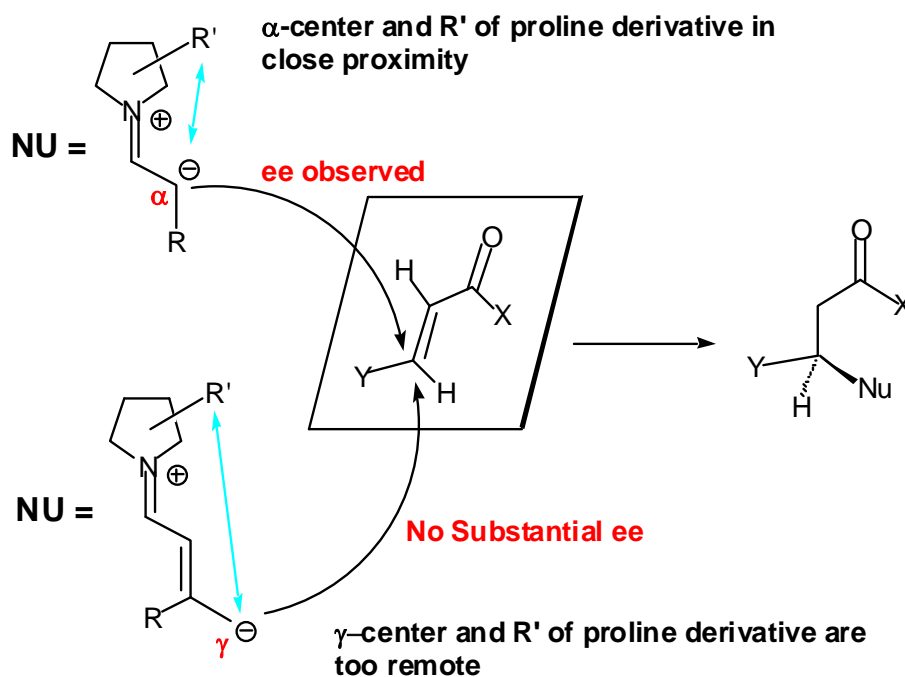
**Figure 39.** Proposed routes to the synthesis of 1,2,4-trisubstituted cyclohexadienals.

equivalents is needed to deprotonate the  $\beta$ -methyl group. In support of this mechanism, many of the proline derivatives listed in **Table 7** were capable of catalyzing the reaction in similar yields to that of L-proline. Therefore, proton abstraction is not an intramolecular process involving the proline carboxylate. Additionally, while proline

derivatives have been reported to give modest improvements in enantioselectivity over proline itself.<sup>120,121</sup> In our case no improvement was observed. Hence, the reactive center might be too remote for these derivatized proline chiral auxiliary agents to impart much of an impact. This in turn would suggest that the reaction likely proceeds through imine addition versus a Diels-Alder based mechanism.<sup>111,112,114-117</sup> The Diels-Alder approach involves the enamine and  $\gamma$ -positions of the diene in a more concerted type mechanism generating reaction intermediate 51 (Figure 39). On the contrary, the Michael-like imine addition involves only the  $\gamma$ -position, a remote carbon center of the cis-diene. The effect of the chiral auxiliary should be quite pronounced if the reaction followed a Diels-Alder reaction pathway. In further support of this notion, previous reports of proline-assisted Michael additions, where effects on ee values were observed, have involved addition by the  $\alpha$ -position of the donor molecule (Figure 40).<sup>126,139-144</sup> In our case, we are two carbon atoms removed (addition occurs with the  $\gamma$ -carbon of the donor molecule) and the chiral auxiliary is too far removed to elicit an effect.

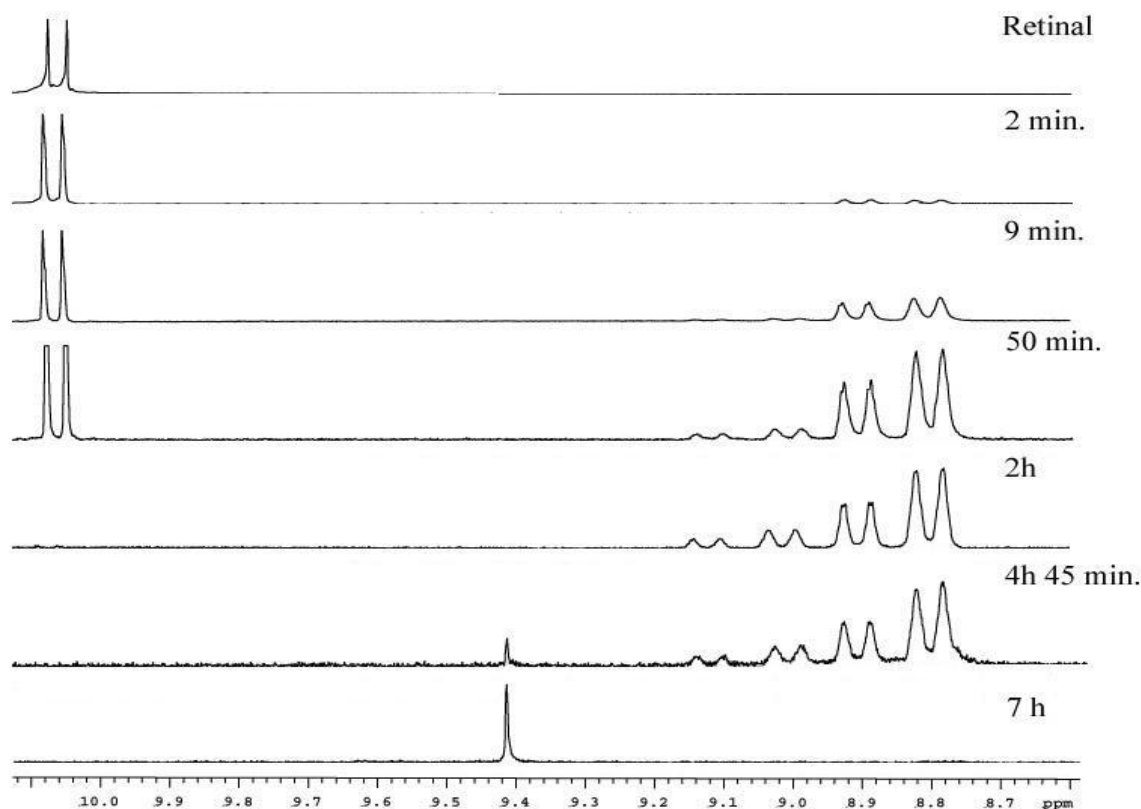
#### *Detection of Reaction Intermediates*

To provide additional experimental evidence for our proposed mechanism, we performed a time course analysis of this proline-assisted dimerization reaction by NMR and MS. The two experiments that were performed were with retinal for detection of reaction intermediates during the formation of **14** (requires addition of triethylamine) and citral to detect the formation of **15** (readily deprotonates with excess L-proline). The results for the dimerization of cycloretinal are provided here (**Figure 41**) while the



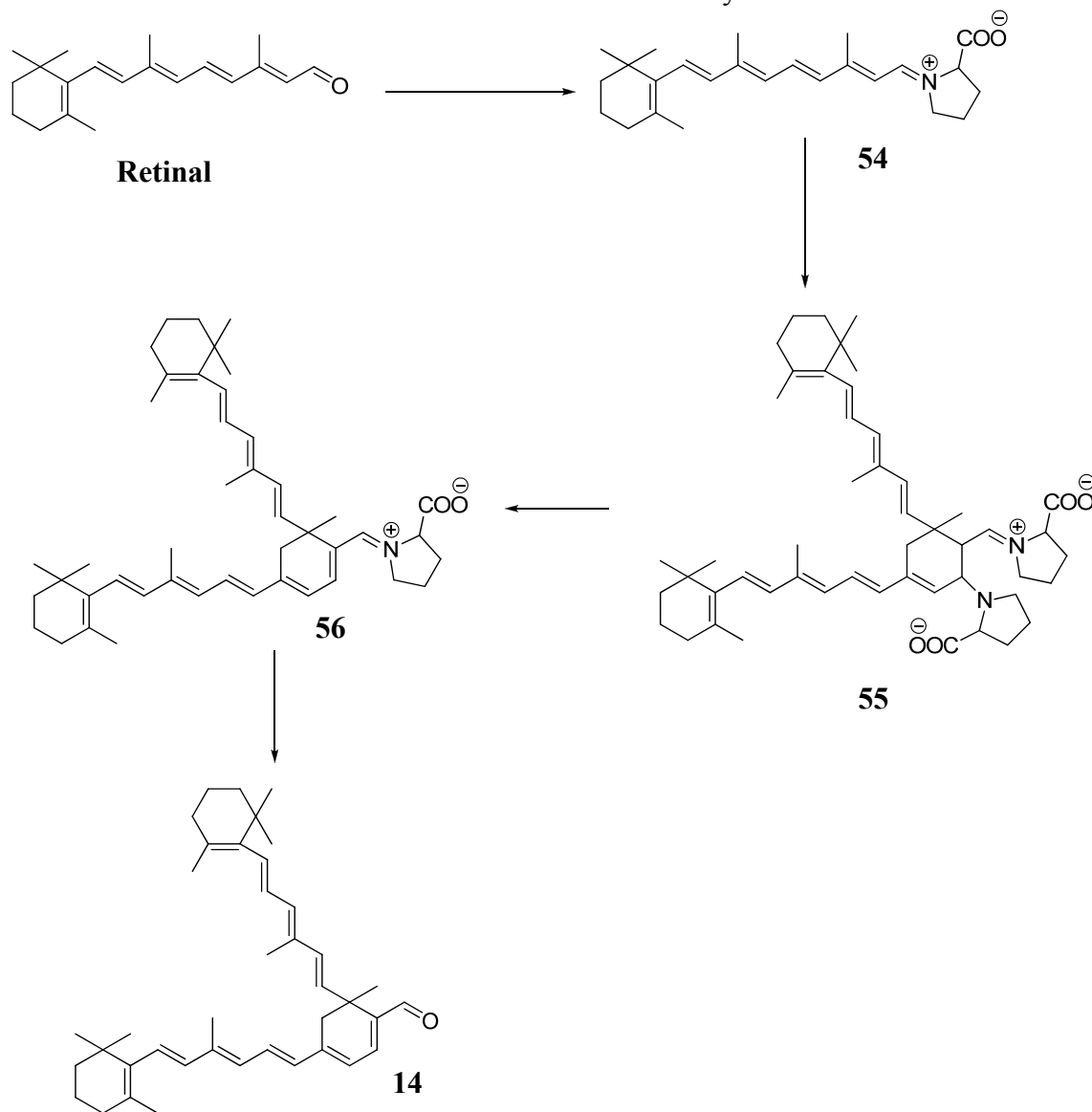
**Figure 40.** Schematic diagram depicting Michael donor and acceptor interactions.

results for citral can be found in the appendices for this chapter. After retinal and proline were mixed in a NMR tube, an immediate scan (2 minutes) revealed formation of the Schiff base (**54**), giving both cis and trans isomers ( $\alpha$ -carbon to the protonated imine) at 8.90 and 8.80 ppm, respectively.<sup>148</sup> After 9 minutes, two new pairs of peaks began to appear corresponding to cis/trans isomers at 9.01 and 9.11 ppm, respectively. We thought that it might correspond to the di-proline intermediate **55** but the C-6 proline readily dissociates to give intermediate **56**. Reaction intermediate corresponds to the new doublets being formed after 9 minutes. While full characterization of **56** could not be obtained due to convolution of the spectra, two additional pairs of doublets (7.25 and 7.57 ppm) were detected, corresponding to the coupled cyclohexadiene ring protons.



**Figure 41.** Time course analysis of retinal homodimerization by NMR.

Coupling of the protons was confirmed by H,H-COSY. Retinal was fully consumed by a time of 1 hour and 20 minutes postinduction with intermediates **54** and **56** remaining, providing evidence that the condensation reaction occurs between two proline adducts (**Figure 39**, condensation between **48** and **49**) as opposed to one proline adduct and one free floating aldehyde. After 3 hours, all of the retinal is consumed so triethylamine (1 equivalent) was added to facilitate dimer formation.<sup>87</sup> Traces of the cycloretinal product were apparent by 4 hours. Mass spectral analysis of the reaction was performed at four time points (30 minutes, 1 hour 30 minutes, 2 hours 30 minutes, and 4 hours and

**Scheme 12.** Reaction intermediates for the formation of cycloretinal.

30 minutes). The data points were consistent with the NMR results (**Figure 42**, reaction progression at 2 hours 30 minutes), showing detection of both the Schiff base **54** and intermediate **56** (**Scheme 13**). In the case for citral, similar results are observed with the exception of triethylamine needing to be added in order to facilitate the dimer formation. Formation of Schiff base **57** was observed just as in retinal while the bi-proline



intermediate **58** was not observed. Reaction intermediate **59** was characterized just as in the retinal reaction leading to formation of cyclocitral **14**. NMR and MS experiments paralleled those observed with retinal.

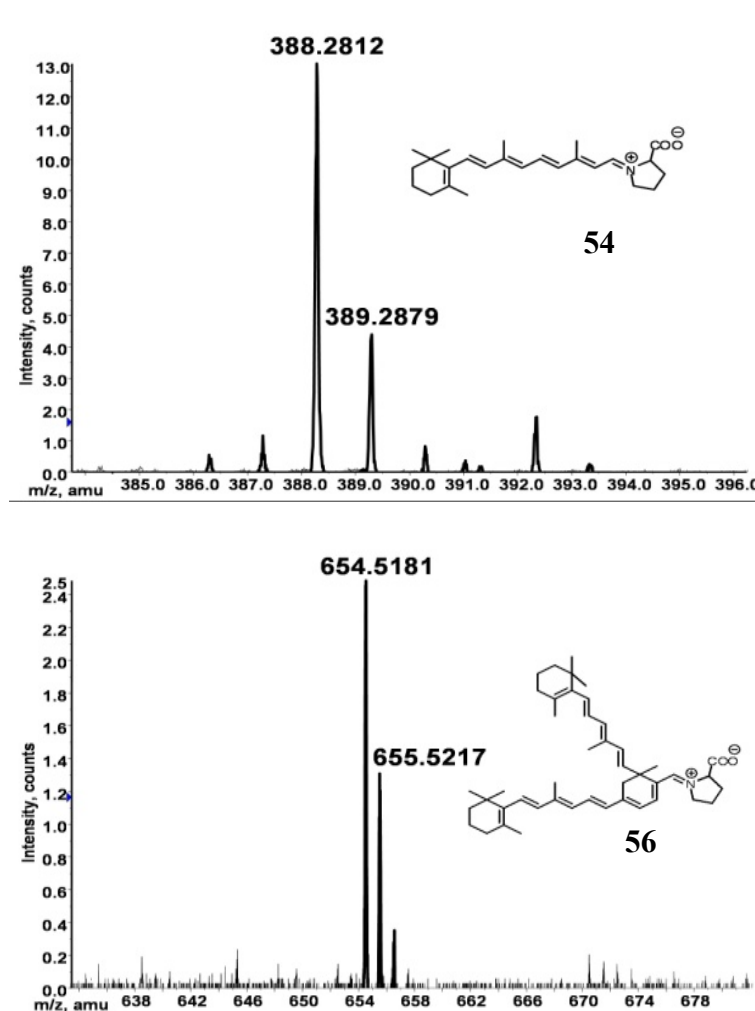
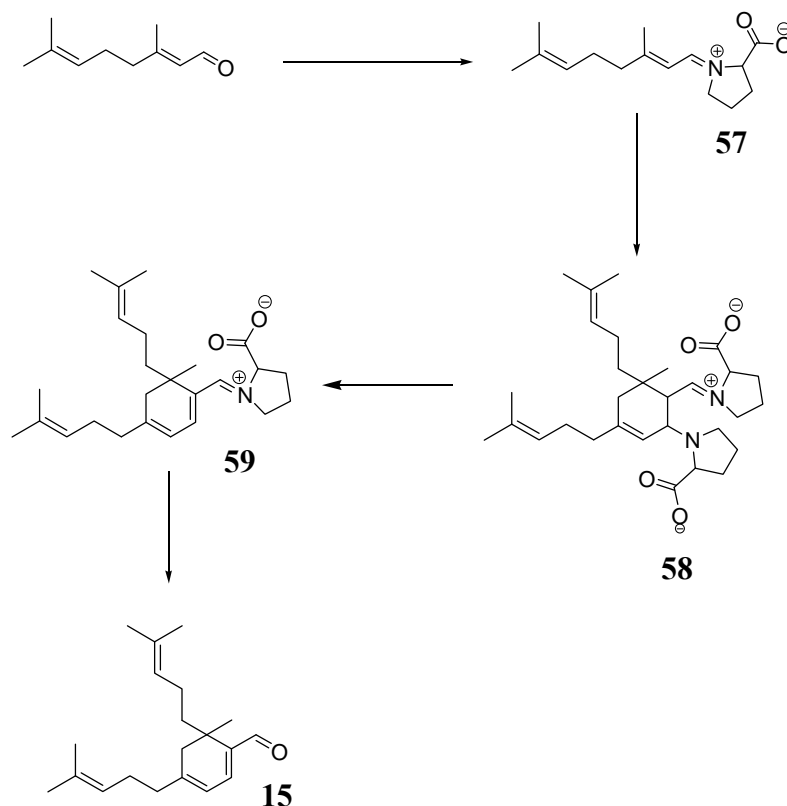


**Figure 42. Mass spectra of cycloretinal intermediates.**

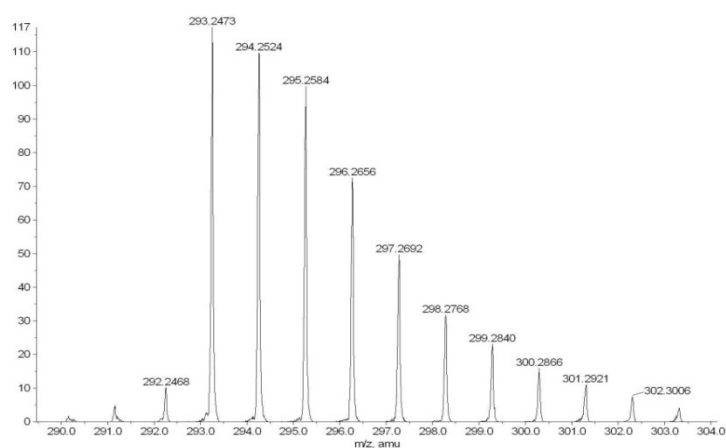
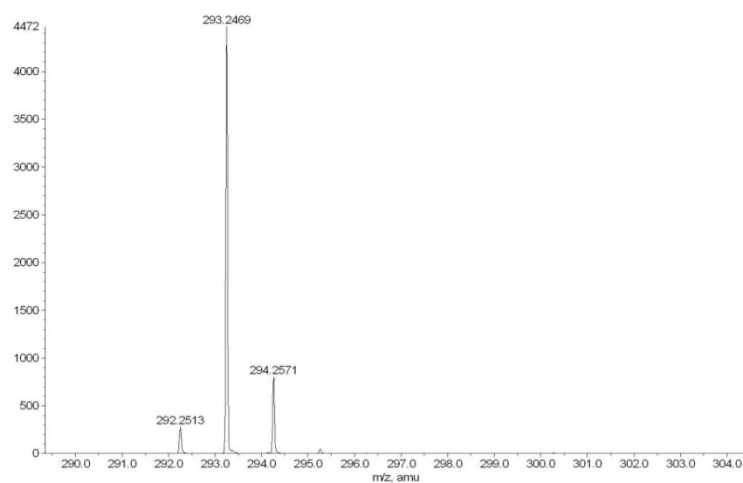
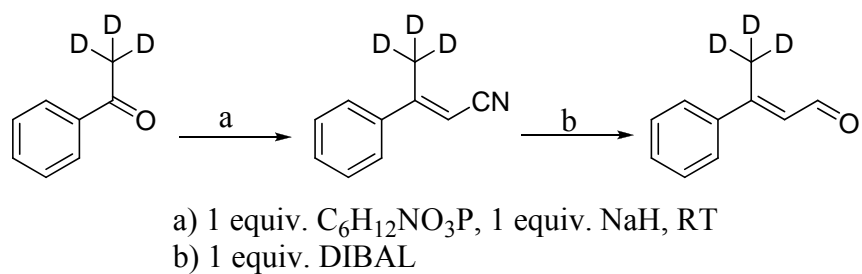
Mass spectral peaks ( $M + Li$ ) observed at 2h 30 min. post induction: (top) Schiff base **54** (388.2812 amu) and (bottom) intermediate **56** (654.5181 amu).

**Scheme 13.** Reaction intermediates for the formation of cyclocitral.



*Deuterium Exchange Experiments for Kinetic Isotope Effects*

Additionally, we synthesized a benzylidene nitrile **60** which we then reduced to a  $\beta$ -methyl substituted benzylidene aldehyde **61** in deuterated form with the intent of measuring a kinetic isotope effect for the homodimerization reaction (**Scheme 14**). However, a deuterium exchange experiment revealed significant solvent exchange by the reaction. Citral was reacted with L-proline in deuterated methanol and cyclocitral **15** was examined by both MS and NMR. MS analysis revealed the presence of cyclocitral **15** labeled with at least one and up to a possible 10 deuteriums atoms being exchanged (**Figure 43**).

**Scheme 14.** Synthesis of benzylidene aldehyde.**Figure 43.** Citral mass spectra.

Mass spectra (Top) of natural cyclocitral and (Bottom) of deuterated cyclocitral 15. Each m/z is (M+Li).

NMR analysis/integration of the peaks numbering scheme (**Figure 44**) confirmed the incorporation of deuterium at the aldehyde position as well as at C-3, C-3', C'3'', C-5, C-7, C-1'' (**Table 8** and **Table 9**). Two different sets of peaks were integrated with the percent deuterium incorporated values being relatively consistent. For example, at C-3, a value of 43.30% is observed with the hydrogen's on C-5', 6', 5'', and 6'' being integrated with an integral of 1200 being used. This value is used because we used an integral of 100 for each proton attached to the carbon (**Table 8**). When we used an integral of 100 for the hydrogen on C-2, a percent deuterium incorporated value of 43.06% was calculated (**Table 9**). The significant exchange observed during the course of this reaction hinders our ability to measure a kinetic isotope effect.

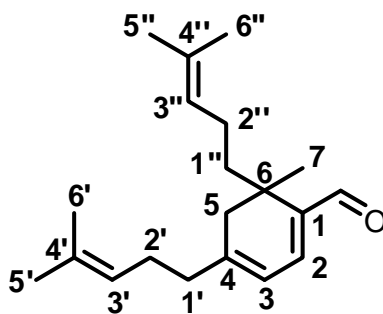


**Figure 44.** Numerical notation of citral homodimer 15.

**Table 8.** Hydrogen/Deuterium integrations for cyclocitral.  
Integrated at  $^1\text{H}$  5', 6', 5'', and 6'' (Integral=1200).

Carbon	$^1\text{H}$ (ppm)	Deuterated (D)	Natural (N)	% total hydrogen ((D/N)*100%)	% deuterium incorporated (100-%total hydrogen)
CHO	9.41		50.37	84.53	15.47
1		42.58			
2	6.67	41.12	41.29	99.59	0.41
3	5.92	31.99	56.42	56.70	43.30
4					
5a	2.36	66.22	105.17	62.96	37.04
5b	2.02	108.99	123.39	88.33	11.67
6					
7	1.19	138.97	177.44	78.32	21.68
1', 2'	2.18	263.62	267.32	98.62	1.38
3',3''	5.04-5.09	196.45	224.49	87.51	12.49
4'					
5', 6', 5'', 6''	1.51-1.72	1200.00	1200.00	100.00	0.00
1''a, 2''a, 2''b	1.74-1.94	228.27	286.27	79.74	20.26
1''b	1.31-1.41	234.41	538.43	43.54	56.46
4''					

#### *Effects on Neurite Outgrowth and General Cytotoxicity*

Given the demonstrated ability of retinoic acid and its analogs to modulate growth and cellular differentiation and the ability of a milk whey protein to generate cyclo- $\beta$ -ional, the cycloterpenal-based library of compounds was evaluated for their ability to stimulate neurite outgrowth in a PC12 assay. PC12 cells are a pluripotent cell line that was originally cloned in 1976 from a transplantable rat pheochromocytoma and exhibits the ability to differentiate into neurons. The PC12 assay is a widely

implemented method of identifying compounds that promote neurite outgrowth or survival.<sup>149</sup>

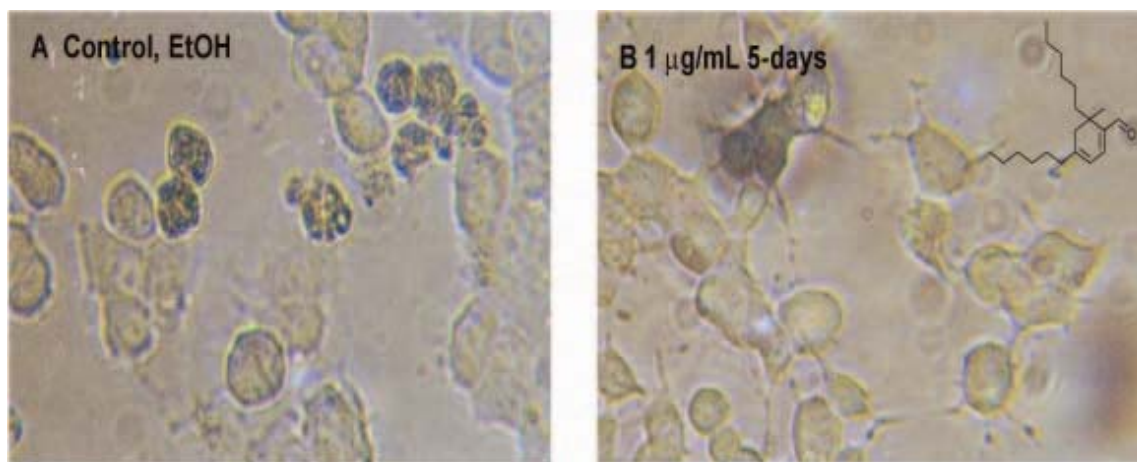
**Table 9.** Hydrogen/Deuterium integrations for cyclocitral at proton 2. Integrated at <sup>1</sup>H 2 (Integral=100).

Carbon	<sup>1</sup> H (ppm)	Deuterated (D)	Natural (N)	% total hydrogen ((D/N)*100%)	% deuterium incorporated (100-%total hydrogen)
CHO	9.41	103.57	121.99	84.90	15.10
1					
2	6.67	100	100.00	100.00	0.00
3	5.92	77.8	136.63	56.94	43.06
4					
5a	2.36	161.06	254.70	63.24	36.76
5b	2.02	265.07	298.85	88.70	11.30
6					
7	1.19	337.99	429.74	78.65	21.35
1', 2'	2.18	641.14	647.38	99.04	0.96
3',3"	5.04-5.09	477.79	543.68	87.88	12.12
4'					
5', 6', 5", 6"	1.51-1.72	2918.47	2926.21	99.74	0.26
1"a, 2"a, 2"b	1.74-1.94	555.16	693.29	80.08	19.92
1"b	1.31-1.41	570.1	1304.00	43.72	56.28
4"					

The PC12 cells were plated onto collagen Type IV plates at 10,000 cells /well, allowed to adhere for 24 hours, followed by the addition of compound at concentrations of 100, 10, and 1 µg/mL, respectively. The cells were monitored over a period of two weeks, where the most pronounced effects were observed at about one week of exposure. From our library of cyclohexadienals, one homodimer (**36**) was able to

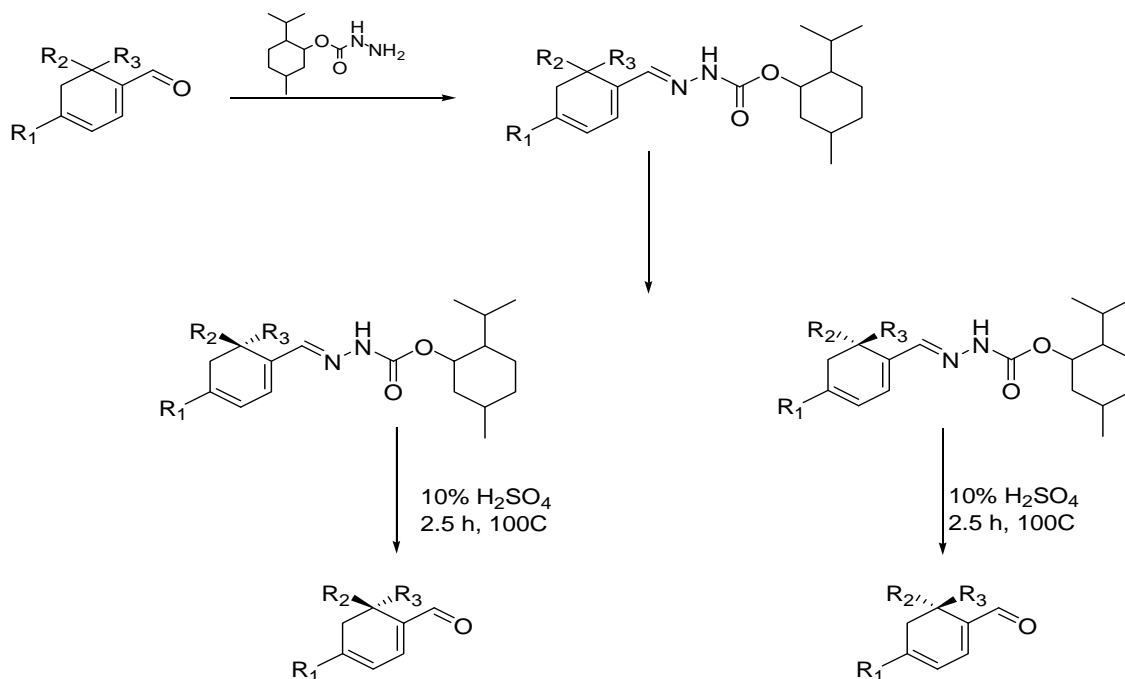
successfully stimulate neurite outgrowth (**Figure 45**). Therefore, neurite outgrowth activity appears to be associated with hydrocarbon chains.

To assess the degree to which stereochemistry dictates phenotype in the neurite outgrowth assay, the homodimer was derivatized into a menthylhydrazone derivative<sup>150</sup> to allow separation of the stereoisomers by HPLC (**Scheme 15**). Following HPLC purification, the compounds were each hydrolyzed giving each aldehyde in enantiomerically pure form. Upon reanalysis in the PC12 assay, the *R*-configuration was shown to be responsible for neurite outgrowth activity while the *S*-configuration exhibited no activity (**Figure 46**).



**Figure 45.** Stimulation of neurite outgrowth.

(A) Control, cells treated with absolute ethanol; (B) 3-Methyl-2-nonenal homodimer; 1 µg/mL at 5 days.

**Scheme 15.** Isolation of stereoisomers.

As cyclocitral **15** has been reported to possess antibiotic activity,<sup>39,88,151,152</sup> we also surveyed our cyclohexadienal library of compounds against bacterial strains (*Escherichia coli* and *Bacillus subtilis*) and yeast (*Saccharomyces cerevisiae*). All compounds were tested at three concentrations, 100, 10, and 1  $\mu\text{g/mL}$ . For the homodimer library, moderate to no inhibition was observed, where compounds exhibited MIC values  $>100$   $\mu\text{g/mL}$ . Against Jurkats, a human T-cell Leukemia cell line, the effects were again moderate for the compounds tested.



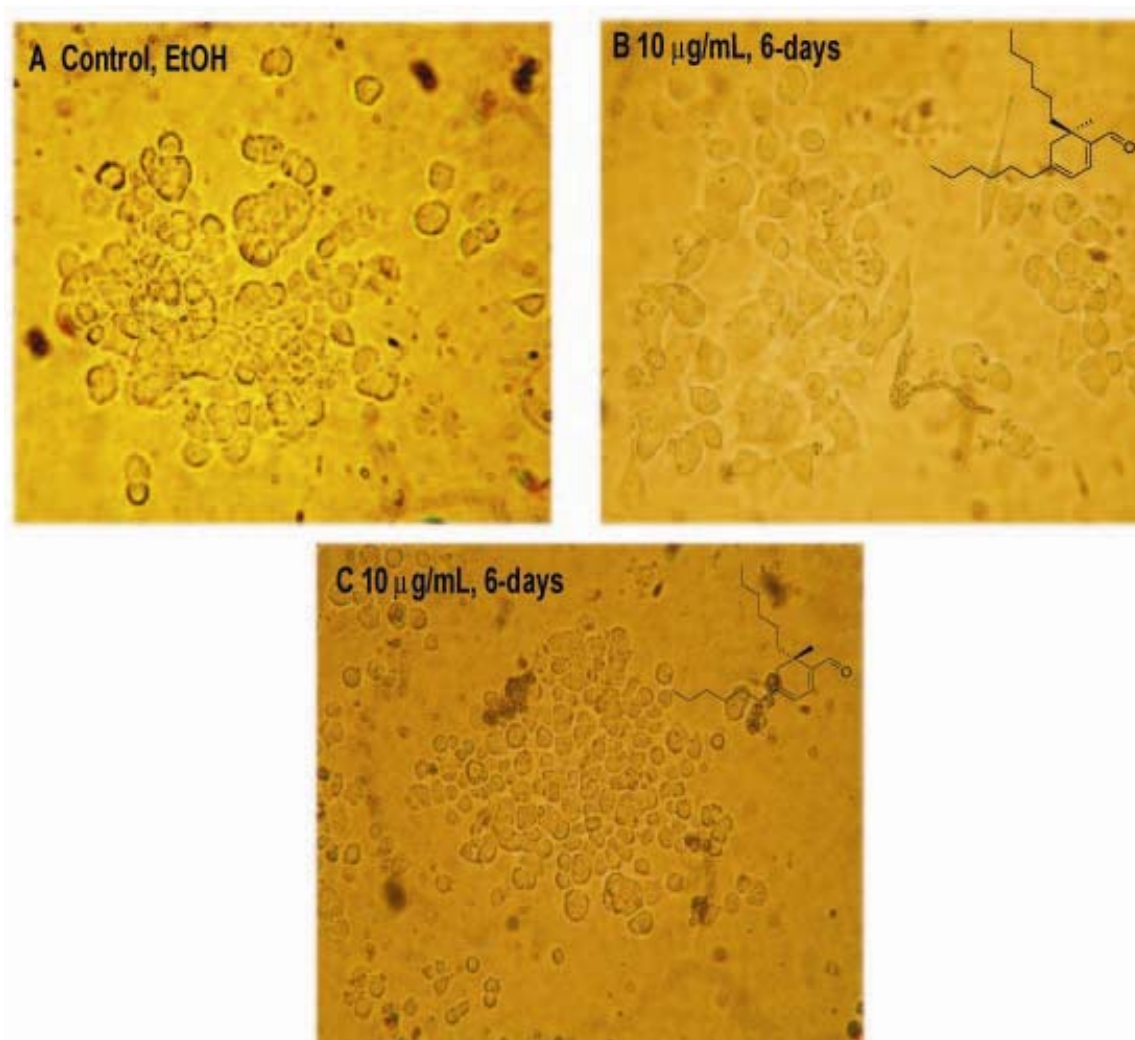


**Figure 46.** Stimulation of neurite outgrowth by homodimer stereoisomers. (A) Control, cells treated with absolute ethanol; (B) *R*-3-methyl-2-nonenal homodimer, 10 µg/mL at 6 days; (C) *S*-3-methyl-2-nonenal homodimer, 10 µg/mL at 6 days;

## CONCLUSION

The results in this chapter demonstrate the use of L-proline to promote asymmetric self-condensation of  $\alpha,\beta$ -unsaturated aldehydes to form trisubstituted cyclohexadiene products. Reaction conditions are mild and yet amendable to a variety of different substrates, yielding molecules with complex scaffolds from simple precursors.

Mechanistic hypotheses are presented involving condensation between two proline adducts through either a Diels-Alder or Michael-like imine addition. The progress of the reaction was monitored in time course analyses by NMR and MS, providing evidence for the intermediacy of Schiff base (**48**) and protonated imine (**52**). Moreover, these experiments revealed the complete loss of starting aldehyde during the reaction in support of a two proline adduct-based mechanism. Additionally, investigations with various proline derivatives gave similar yields to that of L-proline, suggesting that deprotonation and activation of the  $\beta$ -methyl group to give (**49**) is an intermolecular process and does not involve the proline carboxylate of the Schiff base (**48**). The moderate ee values exhibited by these proline chiral auxiliaries suggest that the reaction likely proceeds through imine addition versus a Diels-Alder based mechanism since a Diels-Alder would involve two reaction centers, the enamine and  $\gamma$ -positions of the diene (**Figure 39**), while imine addition would only involve the  $\gamma$ -position, a remote carbon center, of the *cis*-diene. The phenotypic effects of this library of homodimers were examined in a PC12 assay where dramatic effects were observed on neurite outgrowth. These results suggest that molecules with this cyclohexadienal motif might have applications in neurite regeneration, which plays a significant role in the treatment of neurodegenerative diseases or central nervous system injuries.

## EXPERIMENTAL

### *General*

Fresh THF was dried by passage through an MBRAUN solvent purification system and stored over molecular sieves. All other solvents and reagents were purchased and used without further purification.  $^1\text{H}$  (300 MHz) and  $^{13}\text{C}$  (75 MHz) spectra were recorded on a 300 MHz spectrometer. Chemical shifts for  $^1\text{H}$  and  $^{13}\text{C}$  NMR spectra are reported in ppm referenced to TMS (0 ppm) and coupling constants are reported in Hertz (Hz). MS spectra were recorded on an API QSTAR PULSAR (ES) apparatus. Infrared (IR) spectra were recorded with a FT-IR spectrometer. Chromatographic separations were achieved by flash silica chromatography (silica gel 60 mesh, EMD Biosciences). The nitrile, 3-phenyl-but-2-enenitrile, and aldehydes, 3-phenyl-but-2-enal and farnesal have been reported previously. *All-trans* retinal, citral, and senecioaldehyde used in preparation of dimers **14**, **15**, and **37** were each purchased from Aldrich.

### *Organisms*

PC12 neuronal cells (CRL 1721) and *B. subtilis* strain 6633 were obtained from the American Type Culture Collection, Rockville, MD. The yeast *S. cerevisiae* wild-type strain [#404; BY4741; MATa his3 $\Delta$ 1 leu2 $\Delta$ 0 met15 $\Delta$ 0 ura3 $\Delta$ 0] was obtained from Dr. Michael Kladde at the Department of Biochemistry, Texas A&M University. The *E. coli* strain DH10B was obtained from Prof. Dennis Gross, Texas A&M University, Department of Plant Pathology.

### *Media Conditions*

- *LB* (Luria-Bertani) medium contained the following components per liter: Bacto-peptone, 10g; Yeast extract, 5g; Sodium chloride, 5g; and deionized water.
- *YPD* (Yeast Peptone Dextrose) medium contained the following components per liter: Yeast extract, 5g; Bacto-peptone, 5g; Glucose, 20 g; and deionized water.
- *NB* (Nutrient Broth) medium contained the following components per liter: Beef extract, 3g; Peptone, 5g; and deionized water.

Agar plates of the above media were prepared by adding 20 g/L bacto-agar. All media were autoclaved at 121 °C for 20 minutes.

### *Neurite Outgrowth Assay*

PC12 cells were maintained in 100 mm Collagen Type IV dishes at 37 °C in a 5% CO<sub>2</sub>/air temperature. The cell culture medium consisted of RPMI 1640, with 10% heat-inactivated horse serum and 5% fetal bovine serum in a 10 mL volume. Cells were removed from the culture flasks by flushing with fresh culture medium. Cells were then transferred to a 15 mL falcon tube and centrifuged for 15 min. at 1000 rpm. The medium was removed and the cells were resuspended in fresh culture medium. The cells were counted with a hemocytometer and replated in a 96 well Collagen Type IV plate at 10,000 cells/well with enough fresh medium to bring the volume to 200 µL. The cells were allowed to adhere for 24 h prior to the addition of compound. Each cyclohexadienal compound was examined at three concentrations in duplicate, to give final concentrations of 100, 10 and 1 µg/mL respectively. Each well was visually

monitored over a period of 2 weeks for neurite outgrowth and intercellular connections. Only fresh medium was added when necessary. Photographs were taken with an Olympus SP-310 camera equipped with a modified lens piece that fits over the microscope eyepiece.

#### *Cytotoxicity Assay Against Jurkat Cell Line*

Jurkat cells were maintained in 75 cm<sup>2</sup> culture flasks at 37 °C under a 5% CO<sub>2</sub> atmosphere. The cell culture medium consisted of RPMI 1640 with 10% fetal bovine serum. Cells were harvested by centrifugation (20 min. at 1000 rpm), resuspended in fresh culture medium and counted on a hemocytometer. The cells (1 mL) were arrayed (200,000 cells/well) in 48 well plates to which compound was added to give final concentrations of 100, 10 and 1 µg/mL respectively. Cells were incubated for 24 h, transferred to 1.5 mL eppendorf tubes and centrifuged for 15 min. at 14,000 rpm. The medium was removed and the cell pellet resuspended in 1 mL of phosphate buffer saline (PBS) to wash the cells. The cells were again centrifuged for 15 min. at 14,000 rpm. The PBS was removed and the cell pellet resuspended in a lysis buffer (CyQuant Cell Proliferation Kit). The stock solution, 20X, should be diluted to a final concentration 1X with an 80 fold dilution of propidium iodide (Molecular Probes, P3566) in order to visualize 200,000 cells/well. The total volume prepared should be enough for entire assay. The lysed cells were then placed in a black 96 well plate and analyzed using a Bio-Tek fluorometer to measure relative fluorescence.

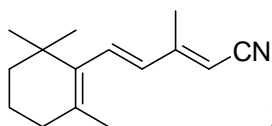
### *Anti-bacterial and Anti-fungal Assays*

Microbes (*Saccharomyces cerevisiae*, *Escherichia coli*, and *Bacillus subtilis* 6633) were cultured and maintained on agar plates (see supplemental material for media conditions). A single colony was used to inoculate 3 mL of culture medium and allowed to grow for 16 h. The cells (500  $\mu$ L) were diluted with 50 mL of fresh medium to an O.D. of 0.1 and aliquoted into a 96-well plate (100  $\mu$ L/well). The assays were set up in duplicate and the compounds tested to give final concentrations of 100, 10 and 1  $\mu$ g/mL. Plates were incubated (*E. coli* and *B. subtilis*, 37 °C; yeast, 30 °C) and shaken (250 rpm) for 16 h and cell density (O.D.) measured with a Bio-Tek microplate reader.

### *Synthesis of A,B-Unsaturated Nitriles*

Nitriles for the synthesis of the  $\alpha,\beta$ -unsaturated aldehydes used to produce the cyclohexadienals were synthesized following literature protocols<sup>102</sup> and purified by flash column chromatography (gradient of 2-10% ethyl acetate/hexanes).

### *Characterization of A,B-Unsaturated Nitriles*



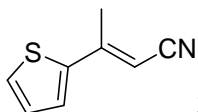
**3-Methyl-5-(2,6,6-trimethyl-cyclohex-1-enyl)-penta-2,4-dienitrile (62):**<sup>153</sup> Yield: 94%

$^1\text{H}$  NMR (300MHz,  $\text{CDCl}_3$ ,  $25^\circ\text{C}$ ),  $\delta$ : 6.54 (d, 1H,  $J = 16.2$  Hz), 6.11 (d, 1H  $J = 16.2$  Hz), 5.06 (s, 1H), 2.16 (d, 3H,  $J = 0.6$  Hz), 1.980-2.03 (m, 2H), 1.67 (d, 3H,  $J = 0.9$  Hz), 1.54-1.62 (m, 2H), 1.41-1.46 (m, 2H), 1.01 (s, 6H).

$^{13}\text{C}$  NMR (75 MHz,  $\text{CDCl}_3$ ,  $25^\circ\text{C}$ )  $\delta$ : 157.1 (C), 136.1 (C), 135.6 (CH), 132.9 (CH), 130.2 (C) 117.9 (C), 96.6 (CH), 39.6 ( $\text{CH}_2$ ), 34.3, (C), 33.3, ( $\text{CH}_2$ ), 29.0 (2 x  $\text{CH}_3$ ), 21.8 ( $\text{CH}_2$ ), 19.2 ( $\text{CH}_3$ ), 16.5 ( $\text{CH}_3$ )

IR (neat)  $\nu$  2925, 2855, 2210, 1738, 1614, 1585, 1455, 1375, 1365, 1217, 966  $\text{cm}^{-1}$

HRMS (ESI) for  $\text{C}_{15}\text{H}_{21}\text{NLi}$  ( $\text{M}+\text{Li}$ ) $^+$ : calcd 222.1834, found 222.1828.



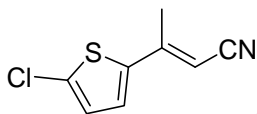
**3-Thiophen-2-yl-but-2-enenitrile (63):**<sup>154</sup> Yield: 83%

$^1\text{H}$  NMR (300MHz,  $\text{CDCl}_3$ ,  $25^\circ\text{C}$ ),  $\delta$ : 7.32 (dd, 1H,  $J = 1.2, 5.1$  Hz), 7.22 (dd,  $J = 1.2, 1\text{H}$  3.6 Hz), 7.00 (dd,  $J = 3.9, 1\text{H}, 5.1$  Hz), 5.5 (d, 1H,  $J = 1.2$ ), 2.34 (d, 3H,  $J = 1.2$  Hz).

$^{13}\text{C}$  NMR (75 MHz,  $\text{CDCl}_3$ ,  $25^\circ\text{C}$ )  $\delta$ : 152.27 (C), 142.03 (C), 128.83 (CH), 128.70 (CH), 128.12 (CH), 117.82 (C), 93.01 (CH), 20.13 ( $\text{CH}_3$ )

IR (neat)  $\nu$  3054, 2925, 2852, 2212, 1736, 1596, 1425, 1265, 705, 703  $\text{cm}^{-1}$

HRMS (ESI) for  $\text{C}_8\text{H}_7\text{NSLi}$  ( $\text{M}+\text{Li}$ ) $^+$ : calcd 156.0459, found 156.0479.



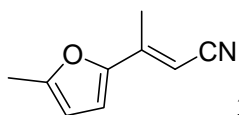
**3-(5-chlorothiophen-2-yl)-but-2-enenitrile (64):**

$^1\text{H}$  NMR (300 MHz,  $\text{CDCl}_3$ ,  $25^\circ\text{C}$ ),  $\delta$ -7.01, (d,  $J=3.9$  Hz, 1H), 6.81 (d,  $J=3.9$  Hz, 1H), 5.39 (q,  $J=0.9$  Hz, 1H), 2.31 (d,  $J=0.9$  Hz, 3H)

$^{13}\text{C}$  NMR (75 MHz,  $\text{CDCl}_3$ ,  $25^\circ\text{C}$ )  $\delta$ : 151.3 (C), 140.4 (C), 133.4 (C), 127.9 (CH), 127.7 (CH), 117.4 (C), 93.3 (CH), 19.5 ( $\text{CH}_3$ )

IR (neat)  $\nu$  3098, 3042, 2926, 2853, 2210, 1594, 1428, 1384, 989,  $786\text{ cm}^{-1}$

HRMS (ESI) for  $\text{C}_8\text{H}_6\text{CINSLi}$  ( $\text{M}+\text{Li}$ ) $^+$ : calcd 190.0070, found 190.0108.



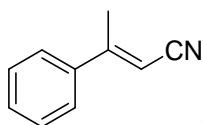
**3-(5-Methyl-furan-2-yl)-but-2-enenitrile (65):** Yield: 70%, yellow oil

$^1\text{H}$  NMR (300MHz,  $\text{CDCl}_3$ ,  $25^\circ\text{C}$ ),  $\delta$ : 6.48 (d, 1H,  $J = 3.3\text{ Hz}$ ), 6.04 (m, 1H), 5.54 (s, 1H), 2.26 (s, 3H), 2.17 (d, 3H,  $J = 0.9\text{ Hz}$ ),

$^{13}\text{C}$  NMR (75 MHz,  $\text{CDCl}_3$ ,  $25^\circ\text{C}$ )  $\delta$ : 155.8 (C), 150.8 (C), 146.1 (C), 118.3 (C), 114.2 (CH), 109.2 (CH), 89.8 (CH), 17.0 ( $\text{CH}_3$ ), 13.9 ( $\text{CH}_3$ )

IR (neat)  $\nu$  3009, 2925, 2855, 2210, 1730, 1640, 1610, 1578, 1513, 1263,  $703\text{ cm}^{-1}$

HRMS (ESI) for  $\text{C}_9\text{H}_9\text{NOLi}$  ( $\text{M}+\text{Li}$ ) $^+$ : calcd 154.0844, found 154.0844.



**(E)-3-phenyl-but-2-enenitrile (66):**<sup>155</sup>

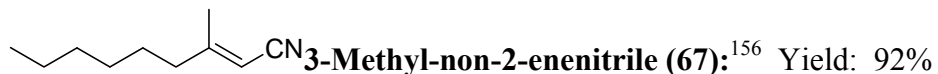
$^1\text{H}$  NMR (300MHz,  $\text{CDCl}_3$ ,  $25^\circ\text{C}$ ),  $\delta$ : 7.36-7.44 (m, 5H), 5.56 (q,  $J = 0.9, 2.1\text{ Hz}$ , 1H), 2.39 (d,  $J = 0.9\text{ Hz}$ , 3H)

$^{13}\text{C}$  NMR (75 MHz,  $\text{CDCl}_3$ ,  $25^\circ\text{C}$ )  $\delta$ : 159.8 (C), 138.3 (C), 130.6 (CH), 129.1 (2 x CH), 126.1 (2 x CH), 117.9 (C), 95.7 (CH), 20.3 ( $\text{CH}_3$ )

IR (neat)  $\nu$  3062, 2982, 2214, 1608, 1575, 1496, 1446, 1381, 1262, 1079, 1027, 921, 825, 754,  $690\text{ cm}^{-1}$



HRMS (ESI) for  $C_{10}H_9NLi$  ( $M+Li$ )<sup>+</sup>: calcd 150.0895, found 150.0884.

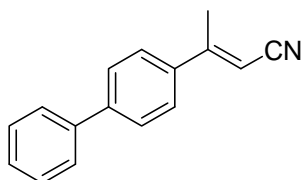


<sup>1</sup>H NMR (300MHz, CDCl<sub>3</sub>, 25°C),  $\delta$ : 5.05 (m, 1H), 2.12 (t, 2H,  $J=7.5$ ), 1.98 (d, 3H,  $J=0.9$ ), 1.28-1.50 (m, 11H)

<sup>13</sup>C NMR (75 MHz, CDCl<sub>3</sub>, 25°C)  $\delta$ : 165.4 (C), 117.1 (C), 94.9 (CH), 38.5 (CH<sub>2</sub>), 31.5 (CH<sub>2</sub>), 28.7 (CH<sub>2</sub>), 27.0 (CH<sub>2</sub>), 22.5 (CH<sub>2</sub>), 20.8 (CH<sub>3</sub>), 14.1 (CH<sub>3</sub>)

IR (neat)  $\nu$  3007, 2960, 2933, 2868, 2212, 1737, 1573, 1465, 738 cm<sup>-1</sup>

HRMS (ESI) for  $C_{10}H_{17}OLi$  ( $M+Li$ )<sup>+</sup>: calcd 158.1521, found 158.1520.



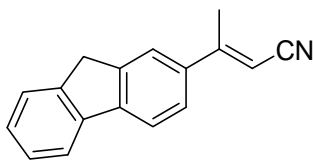
**3-Biphenyl-4-yl-but-2-enenitrile (68):**<sup>157</sup> Yield: 92%

<sup>1</sup>H NMR (300MHz, CDCl<sub>3</sub>, 25°C),  $\delta$ : 7.62-7.67 (m, 4H), 7.41-7.56 (m, 5H), 5.67 (d, 1H,  $J$  = 0.9 Hz), 2.50 (d, 3H,  $J=0.6$  Hz)

<sup>13</sup>C NMR (75 MHz, CDCl<sub>3</sub>, 25°C)  $\delta$ : 159.3 (C), 143.3 (C), 140.1 (C), 137.1 (C), 129.3 (2 x CH), 128.3 (CH), 127.7 (2 x CH), 127.3 (2 x CH), 126.64 (2 x CH), 118.04 (C), 95.48 (CH), 20.33 (CH<sub>3</sub>)

IR (neat)  $\nu$  3030, 2924, 2365, 2343, 2214, 2018, 1736, 1365, 1217, 811, 766, 690 cm<sup>-1</sup>

HRMS (ESI) for  $C_{16}H_{13}NLi$  ( $M+Li$ )<sup>+</sup>: calcd 226.1208, found 226.1210.



**3-(9H-Fluoren-2-yl)-but-2-enenitrile (69):** Yield: 94%, green

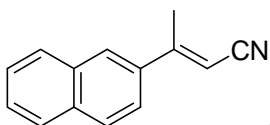
crystalline solid

$^1\text{H}$  NMR (300MHz,  $\text{CDCl}_3$ , 25°C),  $\delta$ : 7.34-7.82 (m, 7H), 5.67 (d, 1H,  $J = 1.2$  Hz), 3.90 (s, 2H), 2.52 (d,  $J = 1.2$  Hz, 3H)

$^{13}\text{C}$  NMR (75 MHz,  $\text{CDCl}_3$ , 25°C)  $\delta$ : 160.0 (C), 144.2 (C), 144.0 (C), 143.9 (C), 140.9 (C), 136.7 (C), 127.9 (CH), 127.3 (CH), 125.4 (CH), 125.1 (CH), 122.7 (CH), 120.7 (CH), 120.2 (CH), 118.2 (C), 94.9 (CH), 37.1 ( $\text{CH}_2$ ), 20.6 ( $\text{CH}_3$ )

IR (neat)  $\nu$  3057, 2922, 2853, 2210, 1736, 1598, 1457, 1440, 1263, 814, 735  $\text{cm}^{-1}$

HRMS (ESI) for  $\text{C}_{17}\text{H}_{13}\text{N}$  ( $\text{M}+\text{H}$ ) $^+$ : calcd 232.1126, found 232.1114.



**3-naphthalen-2-yl-but-2-enenitrile (70):**<sup>158</sup> Yield 82%, white solid

$^1\text{H}$  NMR (300MHz,  $\text{CDCl}_3$ , 25°C),  $\delta$ : 7.81-7.90 (m, 4H), 7.49-7.55 (m, 3H), 5.72 (q, 1H,  $J=0.9$  Hz), 2.5 (d, 3H,  $J=0.9$  Hz)

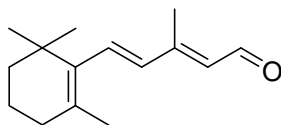
$^{13}\text{C}$  NMR (75 MHz,  $\text{CDCl}_3$ , 25°C)  $\delta$ : 159.4 (C), 135.3 (C), 134.2 (C), 133.2 (C), 129.0 (CH), 128.9 (CH), 127.9 (CH), 127.7 (CH), 127.2 (CH), 126.4 (CH), 123.0 (CH) 118.1 (C), 95.9 (CH), 20.3 ( $\text{CH}_3$ )

IR (neat)  $\nu$  3060, 2981, 2211, 1607, 1435, 1440, 1380, 1133, 809, 750  $\text{cm}^{-1}$

LRMS (ESI) for  $\text{C}_{14}\text{H}_{11}\text{N}$  ( $\text{M}+\text{H}$ ) $^+$ : calcd 194.1, found 194.0.

### Synthesis of *A,B*-Unsaturated Aldehydes

$\alpha,\beta$ -Unsaturated aldehydes were prepared by reduction of their corresponding nitriles and purified by flash column chromatography (2%-10% ethyl acetate/hexanes).<sup>104</sup> Farnesal was synthesized from farnesol.<sup>108</sup> In each case, the *all-trans* isomer was utilized in the self-condensation reactions.



**3-Methyl-5-(2,6,6-trimethyl-cyclohex-1-enyl)-penta-2,4-dienal**

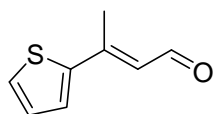
**(71):**<sup>153</sup> Yield: 97%

<sup>1</sup>H NMR (300MHz, CDCl<sub>3</sub>, 25°C),  $\delta$ : 10.09 (d, 1H,  $J$ = 8.1 Hz), 6.70 (d, 1H,  $J$ = 16.2 Hz), 6.17 (d, 1H,  $J$ =15.9 Hz), 5.89 (d, 1H,  $J$ =7.8 Hz), 2.27 (s, 3H), 2.00 (t, 2H,  $J$ =6.0 Hz), 1.68 (s, 3H), 1.52- 1.62 (m, 2H), 1.42-1.45 (m, 2H), 1.00 (s, 6H)

<sup>13</sup>C NMR (75 MHz, CDCl<sub>3</sub>, 25°C)  $\delta$ : 191.1 (CH), 157.2, (C), 136.1 (C), 135.6 (CH), 132.8 (CH), 132.5 (C), 130.2 (CH), 39.6 (CH<sub>2</sub>), 34.2 (C), 33.2 (CH<sub>2</sub>) 28.9 (2 x CH<sub>3</sub>), 21.7 (CH<sub>2</sub>), 19.1 (CH<sub>3</sub>), 16.5 (CH<sub>3</sub>)

IR (neat)  $\nu$  2930, 2865, 1738, 1665, 1606, 1448, 1376, 1364, 1216, 1206, 1116, 963, 764, 749, 732 cm<sup>-1</sup>

HRMS (ESI) for C<sub>15</sub>H<sub>22</sub>OLi (M+Li)<sup>+</sup>: calcd 225.1831, found 225.1835.



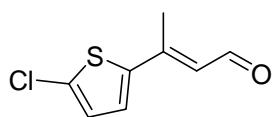
**3-Thiophen-2-yl-but-2-enal (72):**<sup>159</sup> Yield: 88%

<sup>1</sup>H NMR (300MHz, CDCl<sub>3</sub>, 25°C),  $\delta$ : 9.84 (d, 1H,  $J$ =7.5 Hz), 7.13-7.20 (m, 1H), 7.04 (dd, 1H,  $J$ =0.9, 3.9 Hz), 6.80-6.85 (m, 1H), 6.17 (dd, 1H,  $J$ =1.2, 7.8 Hz), 2.26 (d, 3H,  $J$ =1.2 Hz)

$^{13}\text{C}$  NMR (75 MHz,  $\text{CDCl}_3$ ,  $25^\circ\text{C}$ )  $\delta$ : 190.3 (CH), 149.7 (C), 144.5 (C), 129.1 (CH), 128.6 (CH), 128.2 (CH), 124.3 (CH), 15.9 ( $\text{CH}_3$ )

IR (neat)  $\nu$  3104, 3015, 2924, 2852, 2771, 2209, 1739, 1654, 1595, 1421, 1245, 1128, 745  $\text{cm}^{-1}$

HRMS (ESI) for  $\text{C}_8\text{H}_8\text{OSLi}$  ( $\text{M}+\text{Li}$ ) $^+$ : calcd 159.0456, found 159.0458.



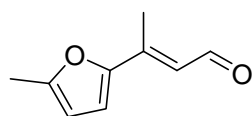
**(E)-3-(5-chlorothiophen-2-yl)but-2-enal (73):**

$^1\text{H}$  NMR (300MHz,  $\text{CDCl}_3$ ,  $25^\circ\text{C}$ ),  $\delta$ = 10.04 (d,  $J$ =7.8 Hz, 1H), 7.19, (d,  $J$ =3.9 Hz, 1H), 6.88 (dd,  $J$ =0.6, 3.9 Hz, 1H), 6.24 (dd,  $J$ =1.2, 7.8 Hz, 1H), 2.47 (d,  $J$ =1.2, 3H)

$^{13}\text{C}$  NMR (75 MHz,  $\text{CDCl}_3$ ,  $25^\circ\text{C}$ )  $\delta$ =190.6 (CH), 149.1 (C), 143.0 (C), 132.3 (C), 127.9 (CH), 127.8 (CH), 124.5 (CH), 15.6 ( $\text{CH}_3$ )

IR (neat)  $\nu$  3099, 2925, 2855, 1658, 1598, 1424, 1129, 1003, 909, 791, 730  $\text{cm}^{-1}$

HRMS (ESI) for  $\text{C}_8\text{H}_7\text{ClOSLi}$  ( $\text{M}+\text{Li}$ ) $^+$ : calcd 193.0066, found 193.0065.



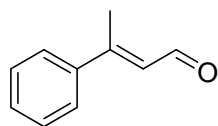
**3-(5-Methyl-furan-2-yl)-but-2-enal (74):**<sup>160</sup> Yield: 89%

$^1\text{H}$  NMR (300MHz,  $\text{CDCl}_3$ ,  $25^\circ\text{C}$ ),  $\delta$ : 10.04 (d, 1H,  $J$ =8.1 Hz), 6.68 (d, 1H,  $J$ =3.6 Hz), 6.43 (dd, 1H,  $J$ =0.9, 8.1 Hz), 6.08-6.10 (m, 1H), 2.35 (d, 3H,  $J$ =0.9), 2.31 (s, 3H)

$^{13}\text{C}$  NMR (75 MHz,  $\text{CDCl}_3$ ,  $25^\circ\text{C}$ )  $\delta$ =190.96 (CH), 156.29 (C), 152.09 (C), 144.34 (C), 121.33 (CH), 115.15 (CH), 109.40, (CH), 14.11 ( $\text{CH}_3$ ), 13.45 ( $\text{CH}_3$ )

IR (neat)  $\nu$  3010, 2924, 2853, 1649, 1608, 1578, 1513

HRMS (ESI) for  $C_9H_{10}O_2Li$  ( $M+Li$ )<sup>+</sup>: calcd 157.0841, found 157.0817.

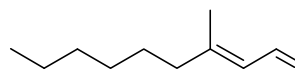


**(E)-3-phenyl-but-2-enal (75):**<sup>161</sup>

<sup>1</sup>H NMR (300MHz, CDCl<sub>3</sub>, 25°C), δ=10.12 (d, *J*=7.5 Hz, 1H), 7.48-7.52 (m, 5H), 6.33 (dq, *J*=1.35, 7.75 Hz, 1H), 2.48 (d, *J*=1.2 Hz, 3H)

<sup>13</sup>C NMR (75 MHz, CDCl<sub>3</sub>, 25°C) δ=191.4 (CH), 157.8 (C), 140.7 (C), 130.1 (CH), 128.8 (2 x CH), 127.3 (2 x CH), 126.5 (CH), 16.5 (CH<sub>3</sub>)

HRMS (ESI) for  $C_{10}H_{10}OLi$  ( $M+Li$ )<sup>+</sup>: calcd 153.0892, found 153.0882.



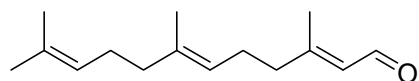
**3-Methyl-non-2-enal (76):**<sup>162,163</sup> Yield: 87%

<sup>1</sup>H NMR (300MHz, CDCl<sub>3</sub>, 25°C), δ: 9.97 (d, 1H, *J*=8.4 Hz), 5.88 (dd, 1H, *J*=0.3, 8.1 Hz), 2.57 (t, 2H, *J*=7.2 Hz), 1.98 (d, 3H, *J*=1.2 Hz), 1.50-1.6 (m, 8H), 0.87-0.92 (m, 3H)

<sup>13</sup>C NMR (75 MHz, CDCl<sub>3</sub>, 25°C) δ: 191.3 (CH), 164.5 (C), 127.3 (CH), 40.7 (CH<sub>2</sub>), 31.7 (CH<sub>2</sub>), 29.0 (CH<sub>2</sub>), 27.2 (CH<sub>2</sub>), 22.6 (CH<sub>2</sub>), 17.5 (CH<sub>3</sub>), 14.1 (CH<sub>3</sub>)

IR (neat) ν 3005, 2956, 2930, 2858, 1737, 1673, 1456, 1377, 1275, 1260, 1196, 764, 725 cm<sup>-1</sup>

HRMS (ESI) for  $C_{10}H_{18}OLi$  ( $M+Li$ )<sup>+</sup>: calcd 116.1518, found 161.1528.



**(2E,6E)-3,7,11-trimethyldodeca-2,6,10-trienal**

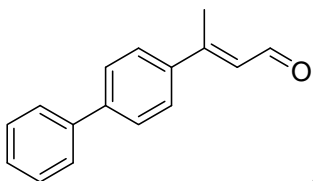
**(77):**<sup>108</sup> <sup>1</sup>H NMR (300MHz, CDCl<sub>3</sub>, 25°C), δ=9.85 (d, *J*=7.8 Hz, 1H), 5.74 (dd, *J*=1.4,

7.8 Hz, 1H), 4.97 (m, 2H), 2.10 (m, 4H), 2.05 (d,  $J=1.2$  Hz, 3H), 1.93 (m, 2H), 1.85 (m, 2H), 1.54 (s, 3H), 1.49 (s, 3H), 1.47 (s, 3H)

$^{13}\text{C}$  NMR (75 MHz,  $\text{CDCl}_3$ ,  $25^\circ\text{C}$ )  $\delta$ =191.1 (CH), 163.8 (C), 136.5 (C), 131.4 (C), 127.5 (CH), 124.3 (CH), 122.7 (CH), 40.7 ( $\text{CH}_2$ ), 39.8 ( $\text{CH}_2$ ), 26.7 ( $\text{CH}_2$ ), 26.6 ( $\text{CH}_3$ ), 25.8 ( $\text{CH}_2$ ), 17.7 ( $\text{CH}_3$ ), 17.6 ( $\text{CH}_3$ ), 16.1 ( $\text{CH}_3$ )

IR (neat)  $\nu$  2966, 2918, 1673, 1634, 1445, 1382, 1194, 1119  $\text{cm}^{-1}$

HRMS (ESI) for  $\text{C}_{15}\text{H}_{24}\text{OLi}$  ( $\text{M}+\text{Li}$ ) $^+$ : calcd 227.1987, found 227.1951.



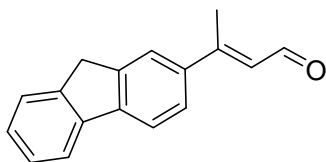
**3-Biphenyl-4-yl-but-2-enal (78):**<sup>164</sup> Yield: 90%

$^1\text{H}$  NMR (300MHz,  $\text{CDCl}_3$ ,  $25^\circ\text{C}$ ),  $\delta$ : 10.21 (d, 1H,  $J = 7.8$  Hz), 7.58-7.72 (m, 4H) 7.37-7.50 (m, 5H), 6.48 (dq, 1H,  $J = 1.2, 7.8$  HH), 2.60 (d, 3H,  $J = 1.2$  Hz)

$^{13}\text{C}$  NMR (75 MHz,  $\text{CDCl}_3$ ,  $25^\circ\text{C}$ )  $\delta$ =191.4 (CH), 157.2 (C), 143.2 (C), 140.2 (C), 139.4 (C), 129.2 (2 x CH), 128.2 (CH), 127.6 (2 x CH), 127.3 (2 x CH), 127.24 (CH), 127.0 (2 x CH), 16.5 ( $\text{CH}_3$ )

IR (neat)  $\nu$  3033, 2969, 2285, 1737, 1649, 1599, 1487, 1245, 1137, 831, 690  $\text{cm}^{-1}$

HRMS (ESI) for  $\text{C}_{16}\text{H}_{14}\text{OLi}$  ( $\text{M}+\text{Li}$ ) $^+$ : calcd 229.1205, found 229.0997.



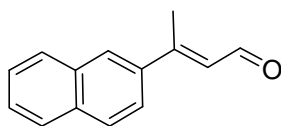
**3-(9H-Fluoren-2-yl)-but-2-enal (79):** Yield: 83%; yellow solid

$^1\text{H}$  NMR (300MHz,  $\text{CDCl}_3$ ,  $25^\circ\text{C}$ ),  $\delta$ : 10.20 (d, 1H,  $J = 7.8$  Hz), 7.73-7.82 (m, 3H), 7.55-7.60 (m, 2H), 7.32-7.43 (m, 2H), 6.49 (dq, 1H,  $J = 1.2, 8.1$  Hz), 3.92 (s, 2H), 2.62 (d, 3H,  $J = 1.2$  Hz)

$^{13}\text{C}$  NMR (75 MHz,  $\text{CDCl}_3$ ,  $25^\circ\text{C}$ )  $\delta$ =191.5 (CH), 158.1 (C), 144.1 (C), 144.0 (C), 143.9 (C), 141.0 (C), 139.0 (C), 127.8 (CH), 127.2 (CH), 127.0 (CH), 125.6 (CH), 125.4 (CH), 123.1 (CH), 120.6 (CH), 120.2 (CH), 37.2 ( $\text{CH}_2$ ), 16.7 ( $\text{CH}_3$ )

IR (neat)  $\nu$  3035, 2922, 2853, 2286, 2071, 1973, 1737, 1652, 1603, 1373, 1228, 828, 750  $\text{cm}^{-1}$

HRMS (ESI) for  $\text{C}_{17}\text{H}_{14}\text{OLi}$  ( $\text{M}+\text{Li}$ ) $^+$ : calcd 241.1205, found 241.1190.



**3-(naphthalen-2-yl)but-2-enal (80):**<sup>165</sup> Yield: 73% yield, yellow solid

$^1\text{H}$  NMR (300MHz,  $\text{CDCl}_3$ ,  $25^\circ\text{C}$ ),  $\delta$ : 10.24 (d,  $J=7.8$  Hz, 1H), 7.99 (d,  $J=1.5$  Hz, 1H), 7.81-7.88 (m, 3H), 7.61 (dd,  $J=1.8, 8.7$  Hz, 1H), 7.52-7.56 (m, 2H), 6.55 (d,  $J=1.2, 7.8$  Hz, 1H), 2.60 (d,  $J=1.2$  Hz, 3H)

$^{13}\text{C}$  NMR (75 MHz,  $\text{CDCl}_3$ ,  $25^\circ\text{C}$ ),  $\delta$ : 191.5 (CH), 157.4 (C), 137.8 (C), 134.3 (C), 133.3 (C), 129.1 (CH), 128.7 (CH), 127.9 (CH), 127.7 (CH), 127.6 (CH), 127.0 (CH), 126.6 (CH), 123.7 (CH), 16.5 ( $\text{CH}_3$ )

IR (neat)  $\nu$  3056, 2849, 2769, 1657, 1606, 1379, 1139, 851, 814, 747  $\text{cm}^{-1}$

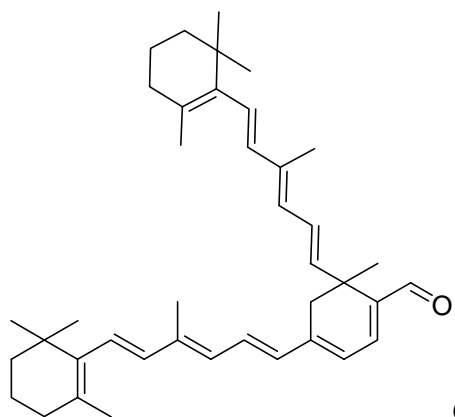
HRMS (ESI) for  $\text{C}_{14}\text{H}_{12}\text{OLi}$  ( $\text{M}+\text{Li}$ ) $^+$ : calcd 203.1048, found 203.1098.

### Synthesis of Self-Condensation Products

Ring-fused homodimers were generated by self-condensation of  $\alpha,\beta$ -unsaturated aldehydes, a modification of Asato *et al.*<sup>3</sup> The generalized approach is illustrated below for 6-Methyl-4,6-di-thiophen-2-yl-cyclohexa-1,3-dienecarbaldehyde (**32**).

To an oven-dried flask was added 3-Thiophen-2-yl-but-2-enal (**72**) (20 mg, 0.132 mmol) dissolved in 10 mL of 200 proof ethanol. To this solution, was added L-proline (23 mg, 0.200 mmol). The mixture was allowed to stir at RT for 24 h prior to quenching the reaction with D.I. H<sub>2</sub>O (30 mL) and extraction with hexanes (3 x 50 mL). The combined organics were washed with brine, dried over MgSO<sub>4</sub>, and concentrated *in vacuo*. Purification by flash chromatography (5% ethyl acetate/hexanes) afforded 17.7 mg of **32** as a red oil (47%).

### Characterization of Self-Condensation Products



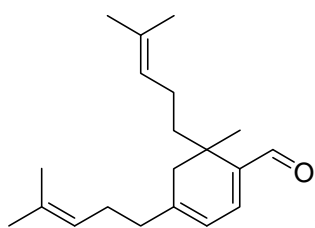
**6-Methyl-4,6-bis-[4-methyl-6-(2,6,6-trimethyl-cyclohex-1-enyl)-hexa-1,3,5-trienyl]-cyclohexa-1,3-dienecarbaldehyde (14):**<sup>112</sup>



$^1\text{H}$  NMR (300MHz,  $\text{CDCl}_3$ ,  $25^\circ\text{C}$ ),  $\delta=9.45$  (s, 1H), 6.97 (q,  $J=7.52$ , 13.98 Hz, 1H), 6.81 (d,  $J=6.10$  Hz, 1H), 6.42 (d,  $J=13.98$  Hz, 1H), 6.35 (q,  $J=10.40$ , 15.24 Hz, 1H), 6.30 (d,  $J=16.06$  Hz, 1H), 6.20 (d,  $J=7.52$  Hz, 1H), 6.16 (d,  $J=16.06$  Hz, 1H), 6.16 (d,  $J=6.10$  Hz, 1H), 6.08 (d,  $J=16.31$  Hz, 1H), 6.01 (d,  $J=16.31$  Hz, 1H), 6.00 (d,  $J=10.40$  Hz, 1H), 5.85 (d,  $J=15.24$  Hz, 1H), 2.69 (d,  $J=16.89$  Hz, 1H), 2.42 (d,  $J=16.89$  Hz, 1H), 2.02 (t,  $J=6.3$  Hz, 2H), 2.00 (s, 3H), 1.99 (t,  $J=6.3$  Hz, 2H), 1.85 (s, 3H), 1.73 (s, 3H), 1.66 (s, 3H), 1.60-1.64 (m, 4H), 1.48 (s, 3H), 1.45-1.47 (m, 4H), 1.04 (s, 6H), 0.98 (s, 6H)

$^{13}\text{C}$  NMR (75 MHz,  $\text{CDCl}_3$ ,  $25^\circ\text{C}$ )  $\delta=$  192.0 (CH), 144.1, 144.0, 141.4, 139.5, 138.2, 137.8, 137.8, 137.7, 137.3, 134.9, 132.6, 130.1, 130.1, 129.7, 129.3, 128.8, 128.6, 126.2, 123.7, 122.7, 39.5, 39.4, 38.5, 37.9, 34.2, 34.1, 33.1, 32.9, 28.9, 28.5, 24.3, 21.8, 21.6, 19.2, 12.9, 12.6

HRMS (ESI) for  $\text{C}_{40}\text{H}_{54}\text{OLi}$  ( $\text{M}+\text{Li}$ ) $^+$ : calcd 550.4175, found 550.4177.



**6-Methyl-4,6-bis-(4-methyl-pent-3-enyl)-cyclohexa-1,3-**

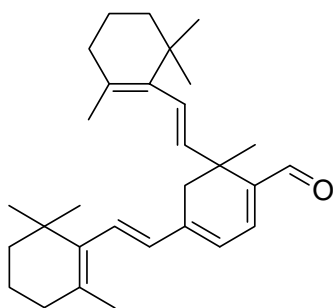
**dienecarbaldehyde (15):**<sup>113</sup>

$^1\text{H}$  NMR (300MHz,  $\text{CDCl}_3$ ,  $25^\circ\text{C}$ ),  $\delta=9.41$  (s, 1H), 6.67 (d,  $J=5.7$  Hz, 1H), 5.92 (d,  $J=6.0$  Hz, 1H), 5.04-5.09 (m, 2H), 2.36 (d,  $J=17.9$  Hz, 1H), 2.18 (d,  $J=3.0$  Hz, 4H), 2.02 (d,  $J=17.9$  Hz, 1H), 1.74-1.94 (m, 3H), 1.69 (s, 3H), 1.65 (s, 3H), 1.62 (s, 3H), 1.55 (s, 3H), 1.31-1.41 (m, 1H), 1.19 (s, 3H)

$^{13}\text{C}$  NMR (75 MHz,  $\text{CDCl}_3$ ,  $25^\circ\text{C}$ )  $\delta$ = 191.6 (CH), 151.1 (C), 146.2 (CH), 141.7 (C), 132.6 (C), 131.5 (C), 125.0 (CH), 123.5 (CH), 118.2 (CH), 42.1 ( $\text{CH}_2$ ), 38.6 ( $\text{CH}_2$ ), 38.0 ( $\text{CH}_2$ ), 36.5 (C), 25.9 ( $\text{CH}_3$ ), 25.8 ( $\text{CH}_3$ ), 25.4 ( $\text{CH}_2$ ), 24.1 ( $\text{CH}_2$ ), 19.5 ( $\text{CH}_3$ ), 18.0 ( $\text{CH}_3$ ), 17.8 ( $\text{CH}_3$ )

IR (neat)  $\nu$  2931, 2968, 1738, 1678, 1448, 1373, 1238, 1044  $\text{cm}^{-1}$

HRMS (ESI) for  $\text{C}_{20}\text{H}_{30}\text{OLi}$  ( $\text{M}+\text{Li}$ ) $^+$ : calcd 293.2457, found 293.2454.



**6-Methyl-4,6-bis-[2-(2,6,6-trimethyl-cyclohex-1-enyl)-**

**vinyl]-cyclohexa-1,3-dienecarbaldehyde (16):** <sup>87</sup>

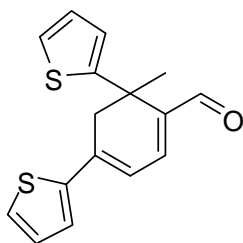
$^1\text{H}$  NMR (300MHz,  $\text{CDCl}_3$ ,  $25^\circ\text{C}$ ),  $\delta$ =9.48 (s, 1H), 6.83 (d,  $J$ =6.0 Hz, 1H), 6.52 (d,  $J$ =16.2 Hz, 1H), 6.20 (d,  $J$ =16.5 Hz, 1H), 6.09 (dd,  $J$ =1.8, 6.0 Hz, 1H), 5.63 (dd,  $J$ =1.2, 16.2 Hz, 1H), 5.33 (d,  $J$ =16.2 Hz, 1H), 2.66 (d,  $J$ = 16.8 Hz, 1H), 2.37 (dd,  $J$ =1.5, 17.1 Hz, 1H), 2.03 (t,  $J$ =6.0 Hz, 2H), 1.89 (t,  $J$ =5.4 Hz, 2H), 1.70 (s, 3H), 1.57-1.65 (m, 4H), 1.55 (s, 3H), 1.52 (s, 3H), 1.44-1.48 (m, 2H), 1.35-1.39 (m, 2H), 1.03 (s, 3H), 1.02 (s, 3H), 0.87 (s, 3H), 0.86 (s, 3H)

$^{13}\text{C}$  NMR (75 MHz,  $\text{CDCl}_3$ ,  $25^\circ\text{C}$ )  $\delta$ =192.6 (CH), 145.0 (CH), 144.6 (C), 141.8 (C), 137.7 (C), 137.5 (C), 137.5 (CH), 134.0 (CH), 131.9 (CH), 131.6 (C), 127.9 (C), 124.9 (CH), 121.9 (CH), 39.8 ( $\text{CH}_2$ ), 39.4 ( $\text{CH}_2$ ), 38.8 (C), 38.1 ( $\text{CH}_2$ ), 34.5 (C), 34.3 (C), 33.4

(CH<sub>2</sub>), 32.7 (CH<sub>2</sub>), 29.2 (2 x CH<sub>3</sub>), 28.8 (2 x CH<sub>3</sub>), 25.3 (CH<sub>3</sub>), 22.0 (CH<sub>3</sub>), 21.4 (CH<sub>3</sub>), 19.6 (CH<sub>2</sub>), 19.3 (CH<sub>2</sub>)

IR (neat)  $\nu$  2956, 2923, 2864, 1675, 1537, 1456, 1375, 1360, 1211, 1076, 967, 909, 733 cm<sup>-1</sup>

HRMS (ESI) for C<sub>30</sub>H<sub>42</sub>O (M+H)<sup>+</sup>: calcd 419.3314, found 419.3379.



**6-Methyl-4,6-di-thiophen-2-yl-cyclohexa-1,3-dienecarbaldehyde**

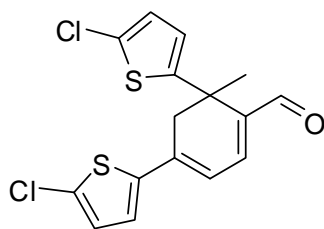
**(32):**

<sup>1</sup>H NMR (300MHz, CDCl<sub>3</sub>, 25°C),  $\delta$ : 9.49 (s, 1H), 7.35-7.40 (m, 1H) 7.28-7.30 (m, 2H), 7.05-7.14 (m, 3H), 6.93 (d, 1H,  $J$  = 6.0 Hz), 6.62 (dd, 1H,  $J$  = 0.9, 6.3 Hz), 3.21 (d, 1H,  $J$  = 17.4 Hz), 2.93 (dd, 1H,  $J$  = 1.5, 17.4 Hz), 1.84 (s, 3H)

<sup>13</sup>C NMR (75 MHz, CDCl<sub>3</sub>, 25°C)  $\delta$ : 192.0 (CH), 152.4 (C), 143.7 (CH), 143.6 (C), 142.2 (C), 141.5 (C), 138.8 (C), 128.6 (CH), 128.6 (CH), 127.9 (CH), 126.6 (CH), 126.2 (CH), 123.6 (CH), 45.2 (CH<sub>2</sub>), 29.9 (C), 27.2 (CH<sub>3</sub>)

IR (neat)  $\nu$  3006, 2928, 2855, 1738, 1455, 1365, 1217, 764 cm<sup>-1</sup>

HRMS (ESI) for C<sub>16</sub>H<sub>14</sub>OS<sub>2</sub>Li (M+Li)<sup>+</sup>: calcd 293.0646, found 293.0654.



**4,6-bis(5-chlorothiophen-2-yl)-6-methylcyclohexa-1,3-**

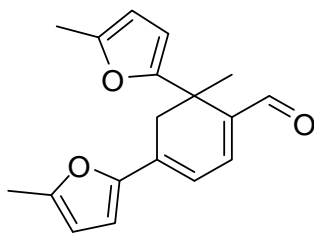
**dienecarbaldehyde (33):**

$^1\text{H}$  NMR (300MHz,  $\text{CDCl}_3$ ,  $25^\circ\text{C}$ ),  $\delta$ =9.52 (s, 1H), 7.08 (d,  $J$ =3.9 Hz, 1H), 6.91-6.98 (m, 2H), 6.64-6.70 (m, 2H), 6.52 (dd,  $J$ =1.8, 6.3 Hz, 1H), 3.06 (d,  $J$ =17.4 Hz, 1H), 2.86 (dd,  $J$ =2.1, 17.4 Hz, 1H), 1.82 (s, 3H)

$^{13}\text{C}$  NMR (75 MHz,  $\text{CDCl}_3$ ,  $25^\circ\text{C}$ )  $\delta$ =191.7 (CH), 149.2 (C), 143.8 (CH), 141.8 (C), 141.2 (C), 137.8 (C), 132.7 (C), 129.2 (C), 127.7 (CH), 125.8 (CH), 125.6 (CH), 123.0 (CH), 117.4 (CH), 44.0 ( $\text{CH}_2$ ), 39.2 (C), 26.8 ( $\text{CH}_3$ )

IR (neat)  $\nu$  2966, 2927, 2382, 2343, 1672, 1541, 1434, 792  $\text{cm}^{-1}$

LRMS (APCI) for  $\text{C}_{16}\text{H}_{12}\text{Cl}_2\text{OS}_2$  ( $\text{M}+\text{H}$ ) $^+$ : calcd 355.0, found 354.9.



**6-Methyl-4,6-bis-(5-methyl-furan-2-yl)-cyclohexa-1,3-**

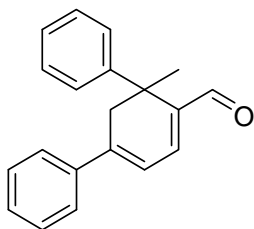
**dienecarbaldehyde (34):** Yield: 60%; red-yellow solid

$^1\text{H}$  NMR (300MHz,  $\text{CDCl}_3$ ,  $25^\circ\text{C}$ ),  $\delta$ : 9.47 (s, 1H), 7.00 (d, 1H,  $J$  = 6.0 Hz), 6.64 (d, 1H,  $J$  = 6.0 Hz), 6.50 (d, 1H,  $J$  = 3.0 Hz), 6.11 (dd, 1H,  $J$  = 0.9, 3.3 Hz), 6.00 (d, 1H,  $J$  = 3.3 Hz), 5.89 (m, 1H), 3.17 (d, 1H,  $J$ =1.8 Hz), 3.10 (d, 1H,  $J$ =1.8 Hz), 2.38 (s, 3H), 2.25 (s, 3H), 1.57 (s, 3H)

$^{13}\text{C}$  NMR (75 MHz,  $\text{CDCl}_3$ ,  $25^\circ\text{C}$ )  $\delta$ : 191.5 (CH), 157.1 (C), 155.1 (C), 151.9 (C), 151.0 (C), 143.5 (CH), 139.3 (C), 133.3 (C), 114.1 (CH), 112.3 (CH), 108.9 (CH), 106.1 (CH), 105.7 (CH), 38.9 ( $\text{CH}_2$ ), 37.1 (C), 22.6 ( $\text{CH}_3$ ), 14.2 ( $\text{CH}_3$ ), 13.8 ( $\text{CH}_3$ )

IR (neat)  $\nu$  3011, 2924, 2854, 1672, 1618, 1535, 1376, 1216, 1077, 1023,  $781\text{ cm}^{-1}$

HRMS (ESI) for  $\text{C}_{18}\text{H}_{18}\text{O}_3\text{Li}$  ( $\text{M}+\text{Li}$ ) $^+$ : calcd 289.1416, found 289.1418.



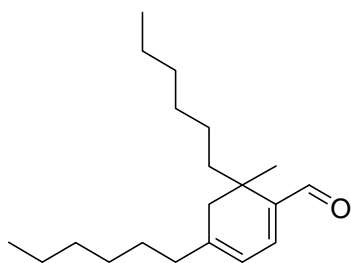
**6-methyl-4,6-diphenylcyclohexa-1,3-dienecarbaldehyde (35):**

NMR (300MHz,  $\text{CDCl}_3$ ,  $25^\circ\text{C}$ ),  $\delta$ =9.52 (s, 1H), 7.16-7.57 (m, 10H), 7.04 (d,  $J$ =6.0 Hz, 1H), 6.63 (dt,  $J$ =1.5, 6.0 Hz, 1H), 3.18 (dd,  $J$ = 1.5, 17.4 Hz, 1H), 2.85 (dd,  $J$ = 1.5, 17.4 Hz, 1H), 1.72 (s, 3H)

$^{13}\text{C}$  NMR (75 MHz,  $\text{CDCl}_3$ ,  $25^\circ\text{C}$ ),  $\delta$ =192.7 (CH), 147.4 (C), 145.0 (C), 144.3 (CH), 142.8 (C), 139.3 (C), 129.2 (CH), 129.1 (CH), 128.4 (2 x CH), 126.5 (CH), 126.3 (2 x CH), 126.1 (CH), 126.0 (2 x CH), 119.1 (CH), 44.9 ( $\text{CH}_2$ ), 41.0 (C), 20.4 ( $\text{CH}_3$ )

IR (neat)  $\nu$  3028, 2926, 2813, 2332, 1662, 1550, 1447, 1170, 757,  $696\text{ cm}^{-1}$

HRMS (ESI) for  $\text{C}_{20}\text{H}_{18}\text{Li}$  ( $\text{M}+\text{Li}$ ) $^+$ : calcd 281.1518, found 281.1528.



**4,6-Dihexyl-6-methyl-cyclohexa-1,3-dienecarbaldehyde (36):**

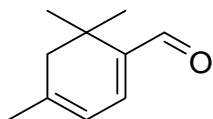
Yield: 50%; yellow oil

$^1\text{H}$  NMR (300MHz,  $\text{CDCl}_3$ ,  $25^\circ\text{C}$ ),  $\delta$ : 9.40 (s, 1H) 6.65 (d, 1H,  $J = 5.4$  Hz), 5.89-5.92 (m, 1H), 2.32 (d, 1H,  $J = 18$  Hz), 2.14 (t, 2H,  $J = 7.2$  Hz), 1.98 (d, 1H,  $J = 18.3$ ), 1.80-1.89 (m, 2H), 1.57 (s, 3H), 1.42-1.50 (m, 4H), 1.66-1.39 (m, 18H)

$^{13}\text{C}$  NMR (75 MHz,  $\text{CDCl}_3$ ,  $25^\circ\text{C}$ )  $\delta$ = 193.7 (CH), 148.9 (C), 146.2 (CH), 118.0 (CH), 42.0 ( $\text{CH}_2$ ), 38.6 ( $\text{CH}_2$ ), 38.0 ( $\text{CH}_2$ ), 34.9 ( $\text{CH}_2$ ), 31.8 (2 x  $\text{CH}_2$ ), 30.3 ( $\text{CH}_2$ ), 29.3 ( $\text{CH}_2$ ), 27.2 ( $\text{CH}_2$ ), 25.5 ( $\text{CH}_2$ ), 25.4 (C), 25.3 ( $\text{CH}_2$ ), 22.9 ( $\text{CH}_3$ ), 20.9 ( $\text{CH}_2$ ), 14.4 (2 x  $\text{CH}_3$ )

IR (neat)  $\nu$  3006, 2956, 2926, 1739, 1679, 1569,  $1366\text{ cm}^{-1}$

HRMS (ESI) for  $\text{C}_{20}\text{H}_{34}\text{O}$  ( $\text{M}+\text{H}$ ) $^+$ : calcd 291.2688, found 291.2669.



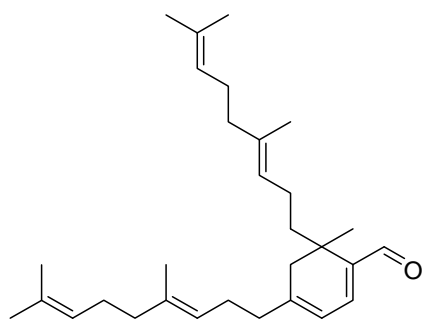
**4,6,6-trimethylcyclohexa-1,3-dienecarbaldehyde (37):** <sup>113</sup>

$^1\text{H}$  NMR (300MHz,  $\text{CDCl}_3$ ,  $25^\circ\text{C}$ ),  $\delta$ =9.39(s, 1H), 6.60 (d,  $J$ =5.4 Hz, 1H), 5.93-5.97 (m, 1H), 2.11 (d,  $J$ =0.9 Hz, 2H), 1.90 (d,  $J$ =0.9 Hz, 3H), 1.19 (s, 6H)

$^{13}\text{C}$  NMR (75 MHz,  $\text{CDCl}_3$ ,  $25^\circ\text{C}$ ),  $\delta$ =193.5 (CH), 147.4 (C), 145.3 (CH), 142.7 (C), 118.8 (CH), 46.8 ( $\text{CH}_2$ ), 33.0 (C), 26.3 (2 x  $\text{CH}_3$ ), 24.3 ( $\text{CH}_3$ )

IR (neat)  $\nu$  2925, 2852, 1675, 1542, 1513, 1457, 1378, 1261,  $810\text{ cm}^{-1}$

HRMS (ESI) for  $\text{C}_{10}\text{H}_{14}\text{OLi}$  ( $\text{M}+\text{Li}$ ) $^+$ : calcd 157.1205, found 157.1237.



**4,6-bis((E)-4,8-dimethylnona-3,7-dienyl)-6-**

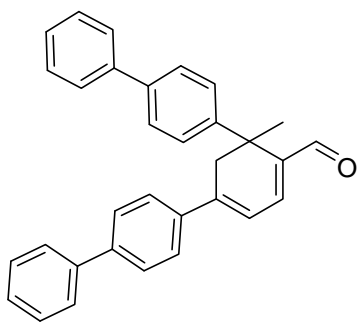
**methylcyclohexa-1,3-dienecarbaldehyde (38):**

$^1\text{H}$  NMR (300MHz,  $\text{CDCl}_3$ ,  $25^\circ\text{C}$ ),  $\delta$ =9.41 (s, 1H), 6.66 (d,  $J$ =5.7 Hz, 1H), 5.92 (d,  $J$ =5.4 Hz, 1H), 5.04-5.09 (m, 4H), 2.36 (d,  $J$ =18 Hz, 1H), 2.20 (s, 2H), 2.19 (s, 2H), 1.77-2.13 (m, 12 H), 1.66 (s, 6H), 1.61 (d,  $J$ =0.9 Hz, 3H), 1.59 (s, 6H), 1.54 (d,  $J$ =0.9 Hz, 3H), 1.31-1.41 (m, 1H), 1.19 (s, 3H)

$^{13}\text{C}$  NMR (75 MHz,  $\text{CDCl}_3$ ,  $25^\circ\text{C}$ ),  $\delta$ =193.6 (CH), 151.1 (C), 146.2 (CH), 141.7 (C), 136.2 (C), 135.1 (C), 131.6 (C), 131.5 (C), 124.8 (CH), 124.6 (CH), 124.4 (CH), 123.4 (CH), 118.2 (CH), 42.2 ( $\text{CH}_2$ ), 39.9 ( $\text{CH}_2$ ), 39.8 ( $\text{CH}_2$ ), 38.6 ( $\text{CH}_2$ ), 38.0 ( $\text{CH}_2$ ), 36.5 (C), 26.9 ( $\text{CH}_2$ ), 26.8 ( $\text{CH}_2$ ), 25.9 (2 x  $\text{CH}_3$ ), 25.7 ( $\text{CH}_2$ ), 25.5 ( $\text{CH}_3$ ), 24.0 ( $\text{CH}_2$ ), 17.9 ( $\text{CH}_3$ ), 17.9 ( $\text{CH}_3$ ), 16.3 ( $\text{CH}_3$ ), 16.2 ( $\text{CH}_3$ )

IR (neat)  $\nu$  2965, 2917, 2854, 2710, 1677, 1637, 1568, 1449, 1377, 1170, 831  $\text{cm}^{-1}$

HRMS (ESI) for  $\text{C}_{30}\text{H}_{46}\text{O}$  ( $\text{M}+\text{H}$ ) $^+$ : calcd 423.3627, found 423.3607.



**4,6-Bis-biphenyl-4-yl-6-methyl-cyclohexa-1,3-**

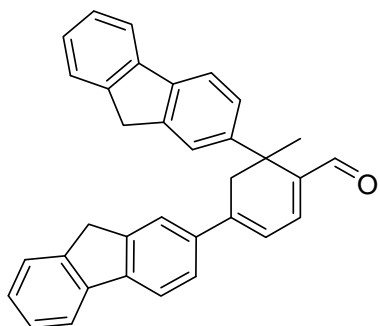
**dienecarbaldehyde (39):** Yield: 52%; yellow solid

$^1\text{H}$  NMR (300MHz,  $\text{CDCl}_3$ ,  $25^\circ\text{C}$ ),  $\delta$ : 9.60 (s, 1H), 7.30-7.74 (m, 16H), 7.12 (d, 1H,  $J$  = 6.0 Hz), 6.75 (d, 1H,  $J$  = 6.0 Hz), 3.25 (dd, 1H,  $J$  = 1.5, 17.7 Hz), 2.92 (dd, 1H,  $J$  = 1.2, 17.4 Hz), 1.56 (s, 3H)

$^{13}\text{C}$  NMR (75 MHz,  $\text{CDCl}_3$ ,  $25^\circ\text{C}$ )  $\delta$ : 192.7 (CH), 159.3 (C), 146.5 (C), 144.5 (C), 144.4 (CH), 142.8 (C), 142.1 (C), 140.4 (C), 139.3 (C), 138.0 (C), 129.1 (2 x CH), 128.9 (2 x CH), 128.0 (CH), 127.6 (2 x CH), 127.5 (CH), 127.3 (2 x CH), 127.2 (2 x CH), 127.1 (2 x CH), 126.8 (2 x CH), 126.4 (2 x CH), 119.1 (CH), 44.7 ( $\text{CH}_2$ ), 40.8 (C), 25.1 ( $\text{CH}_3$ )

IR (neat)  $\nu$  3006, 2970, 2922, 1739, 1678, 1365, 1276, 1261  $\text{cm}^{-1}$

HRMS (ESI) for  $\text{C}_{32}\text{H}_{26}\text{OLi}$  ( $\text{M}+\text{Li}$ ) $^+$ : calcd 433.2144, found 433.2151.



**4,6-Bis-(9H-fluoren-2-yl)-6-methyl-cyclohexa-1,3-**

**dienecarbaldehyde (40):** Yield: 62%; green crystalline solid

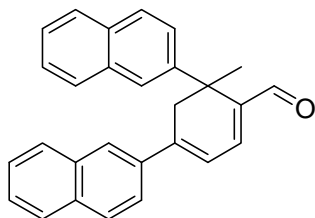


$^1\text{H}$  NMR (300MHz,  $\text{CDCl}_3$ ,  $25^\circ\text{C}$ ),  $\delta$ : 9.55 (s, 1H), 7.67-7.80 (m, 2H), 7.49-7.60 (m, 2H), 7.17-7.41 (m, 10H), 7.09 (d, 1H,  $J = 6.0$  Hz), 6.71-6.74 (m, 1Hz), 3.91 (s, 2H), 3.85 (s, 2H), 3.30 (d, 1H,  $J=18.6$  Hz), 2.95 (d, 1H,  $J = 18.0$  Hz), 1.56 (s, 3H)

$^{13}\text{C}$  NMR (75 MHz,  $\text{CDCl}_3$ ,  $25^\circ\text{C}$ )  $\delta=192.7$  (CH), 150.1 (C), 149.1 (C), 146.5 (2 x C), 145.0 (C), 144.3 (2 x C), 143.9 (2 x C), 143.6 (2 x C), 142.8 (C), 138.0 (CH), 127.5 (CH), 127.2 (CH), 126.8 (CH), 126.6 (CH), 125.4 (CH), 125.1 (CH), 125.0 (CH), 124.9 (CH), 123.1 (CH), 122.6 (CH), 120.4 (CH), 120.2 (CH), 120.0 (CH), 119.8 (CH), 118.7 (CH), 45.4 ( $\text{CH}_2$ ), 37.2 ( $\text{CH}_2$ ), 37.1 ( $\text{CH}_2$ ), 32.2 (C), 30.0 ( $\text{CH}_3$ )

IR (neat)  $\nu$  2955, 2922, 2853, 2126, 2016, 1976, 1739, 1457, 1375, 1366, 1229, 1217  $\text{cm}^{-1}$

HRMS (ESI) for  $\text{C}_{34}\text{H}_{26}\text{OLi}$  ( $\text{M}+\text{Li}$ ) $^+$ : calcd 457.2144, found 457.2136.



**6-methyl-4,6-di(naphthalen-2-yl)cyclohexa-1,3-**

**dienecarbaldehyde (41):**

$^1\text{H}$  NMR (300MHz,  $\text{CDCl}_3$ ,  $25^\circ\text{C}$ ),  $\delta=$  9.57 (s, 1H), 7.40-7.93 (m, 14H), 7.14,  $J=6.0$  Hz, 1H), 6.82 (d,  $J=6.0$  Hz, 1H), 3.40 (dd,  $J=1.5$ , 17.7 Hz, 1H), 3.02 (dd,  $J=1.5$ , 17.7 Hz, 1H), 1.85 (s, 3H)

$^{13}\text{C}$  NMR (75 MHz,  $\text{CDCl}_3$ ,  $25^\circ\text{C}$ ),  $\delta=192.6$  (CH), 144.8 (C), 144.3 (CH), 142.7 (C), 136.3 (C), 134.0 (C), 133.7 (C), 133.5 (C), 133.1 (C), 132.3 (C), 128.8 (CH), 128.7 (CH), 128.2 (CH), 127.9 (CH), 127.7 (CH), 127.4 (CH), 127.2 (CH), 127.1 (CH), 126.9

(CH), 126.2 (CH), 125.8 (CH), 125.5 (CH), 124.5 (CH), 123.5 (CH), 119.5 (CH), 44.7 (CH<sub>2</sub>), 41.3 (C), 24.9 (CH<sub>3</sub>)

IR (neat)  $\nu$  3056, 2925, 2852, 1675, 1542, 1513, 1457, 1378, 1261, 810 cm<sup>-1</sup>

HRMS (ESI) for C<sub>28</sub>H<sub>22</sub>O (M+Li)<sup>+</sup>: calcd 381.1831, found 381.1802.

#### *Determination of Absolute Configuration*

CD analysis of the menthylhydrazone derivatives of C-30 dimer suggests that the major isomer in these instances is in the *S*-configuration as determined by the quadrant rule (chiral excitation theory).<sup>145</sup>

#### *Preparation of Retinal Samples for NMR Analysis*

A 30 mg/mL solution of *all-trans* retinal, L-proline, and triethylamine was prepared by dissolving each in CD<sub>3</sub>OD. These were stored at -20°C until further use.

#### *NMR Analysis of Retinal Self-Condensation Reaction*

A 5 mm NMR tube was filled with 800  $\mu$ L of CD<sub>3</sub>OD and then placed in a 300 MHz NMR spectrometer. Once properly shimmed, another tube was filled with 500  $\mu$ L of *all-trans* retinal (30 mg/mL, 0.05278 mmol) and the instrument reshimmed. The reaction was started by ejecting the *all-trans* retinal and adding 304  $\mu$ L, 1.5 equivalents, of the L-proline solution (30 mg/mL, 0.07921 mmol), shaking the tube, reinserting the tube into the NMR, and immediately acquiring a spectrum that took a total time of 2

minutes. After the initial spectrum, the instrument was periodically reshimmed. After 3 hours 30 minutes, all of the *all-trans* retinal had been consumed and all that existed was Schiff base **54** and intermediate **56** at which time the NMR tube was removed and 180  $\mu\text{L}$  of triethylamine (30 mg/mL, 0.5340 mmol) was added followed by shaking and reinsertion of the tube. After a few minutes, formation of cycloretinal was present. After 2 hours 30 minutes, the reaction was complete. Spectra were acquired over an 8 hour period at various time points.

MS analysis of the reaction was taken at 30, 90, 150, and 270 minutes. Intermediates **54** ( $M + \text{Li} = 388.2812$  amu) and **56** ( $M + \text{Li} = 654.5181$  amu) were both observed.

#### *NMR Analysis of Citral Self-Condensation Reaction*

A 5 mm NMR tube was filled with 800  $\mu\text{L}$  of  $\text{CD}_3\text{OD}$  and was placed in a 300 MHz NMR for shimming purposes. Once properly shimmed, another tube was filled 400  $\mu\text{L}$  of citral (30 mg/mL, 0.07882 mmol) and the instrument was reshimmed. The reaction was started by ejecting the citral and adding 454  $\mu\text{L}$ , 1.5 eq., of the L-proline solution (30 mg/mL, 0.1183 mmol), shaking the tube, reinserting the tube into the NMR, and immediately acquiring a spectrum that took a total time of 2 minutes. After the initial spectrum and periodically throughout the experiment, the instrument was reshimmed. As with *all-trans* retinal, Schiff base formation initiates immediately just as observed with *all-trans* retinal and the reaction proceeds without the use of triethylamine. Spectra were acquired over an eight-hour period at various time points. However, during this time the

reaction did not come to a completion but the data can be paralleled to that of the all-trans retinal as intermediate **7** is also formed and can be seen via mass spectroscopy. Since citral is bought as a mixture of cis and trans isomers (see  $^1\text{H}$  NMR), the overall spectra of the reaction are complex just as that of the all-trans retinal limiting our ability to determine the structural characteristics of the various intermediates.

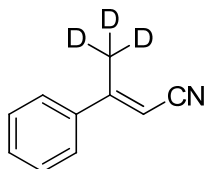
Mass spec also confirmed that seen by NMR analysis, where newly formed peaks belonged to that of intermediate **59** ( $M+H = 384.2803$  amu) and to the Schiff base **57** ( $M+H = 250.1620$  amu,  $M+Na = 272.1566$  amu).

#### *Hydrogen/Deuterium Exchange Experimental Procedure*

100.0 mg (0.6574 mmol) of citral was dissolved in  $\text{CD}_3\text{OD}$  followed by the addition of 115.5 mg (1.0032 mmol) of L-proline. This was stirred for 10 hours at room temperature and was quenched by dilution with hexanes. The mixture was washed with  $\text{D}_2\text{O}$  (3 x 15 mL), dried and evaporated. The crude mixture was purified via flash chromatography (10% ethyl acetate/hexanes) to yield cyclocitral. Samples were compared via mass spectroscopy (MS) and a NMR study was done to show incorporation which is correlated with MS. Each NMR integral was cut consistently and these were integrated against two separate regions,  $\text{CH}_3$  5', 6', 5'', 6'' (1.51-1.72 ppm) and as well as the CH at 2 (6.67 ppm) which is where exchange does not occur. Each integral was increased x100 to give extra decimal places.

### Synthesis of Deuterated Benzylidene Aldehyde

Synthesis of the corresponding benzylidene nitrile was synthesized following literature protocols and purified by flash column chromatography (10% ethyl acetate/hexanes).<sup>102</sup>



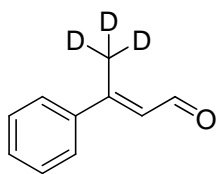
**3-phenylbut-2-enenitrile-β,β,β-d<sub>3</sub> (60):** 72% yield, colorless oil

<sup>1</sup>H NMR (300MHz, CDCl<sub>3</sub>, 25°C), δ=7.18-7.28 (m, 5H), 5.42 (s, 1H)

<sup>13</sup>C NMR (75 MHz, CDCl<sub>3</sub>, 25°C), δ=138.3 (C), 133.4 (C), 130.6 (CH), 129.1 (2 x CH), 126.1 (2 x CH), 117.9 (C), 95.8 (CH) 18.8-20.4 (sept, *J*= 19.55 Hz, CD<sub>3</sub>)

HRMS (ESI) for C<sub>10</sub>H<sub>6</sub>D<sub>3</sub>NLi (M+Li)<sup>+</sup>: calcd 153.1083, found 153.1049.

Deuterated benzylidene aldehyde **61** was synthesized by DIBAL reduction<sup>146</sup> of **60** followed by hydrolysis with a silica slurry containing 20% deuterium oxide (D<sub>2</sub>O) in ether.<sup>147</sup> The reaction was allowed to proceed to 75% completion (3 hours) prior to hydrolysis. After 30 minutes, the organics were filtered, dried over MgSO<sub>4</sub>, and evaporated. The crude material was subjected to flash chromatography with a gradient extending from 2-10% ethyl acetate/hexanes. Further purification was achieved by HPLC employing an isocratic gradient of 10% ethyl acetate/hexanes (the desired *all-trans* product, R<sub>t</sub> = 14.6 minutes; with the nitrile and *cis*-aldehyde at R<sub>f</sub> = 9.8 and R<sub>f</sub> = 12.3 minutes respectively).



**(E)-3-phenylbut-2-enal-  $\beta,\beta,\beta$ -d<sub>3</sub> (61):** 58% yield, colorless oil

<sup>1</sup>H NMR (300MHz, CDCl<sub>3</sub>, 25°C),  $\delta$ =10.19 (d,  $J$ =8.1 Hz, 1H), 7.53-7.58 (m, 2H), 7.41-7.45 (m, 3H), 6.41 (d,  $J$ =7.8 Hz, 1H)

<sup>13</sup>C NMR (75 MHz, CDCl<sub>3</sub>, 25°C),  $\delta$ =191.7 (CH), 158.1 (C), 142.3 (C), 130.4 (CH), 129.0 (2 x CH), 126.5 (2 x CH), 117.1 (CH), 15.1-16.5 (sept,  $J$ =19.4 Hz, CD<sub>3</sub>)

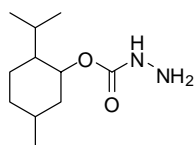
HRMS (ESI) for C<sub>10</sub>H<sub>7</sub>D<sub>3</sub>OLi (M+Li)<sup>+</sup>: calcd 156.1080, found 156.1076.

#### *Synthesis of 2-isopropyl-5-menthylcyclohexyl Hydrazinecarboxylate*

To synthesize 2-isopropyl-5-methylcyclohexyl hydrazinecarboxylate **81**,<sup>150</sup> ethyl 2-isopropyl-5-methylcyclohexyl carbonate was first prepared by reacting 25.0 g (1 equivalent) of L-menthol with 75 mL of ethyl chloroformate (7.3 equivalents) in the presence of pyridine (1 mL). The reaction was refluxed for 48 hours before the light brown product was poured over ice followed by dilution with 20 mL of water. The mixture was then extracted with ethyl ether (5 x 100 mL) with the organic layers combined, dried over MgSO<sub>4</sub>, and concentrated under vacuum. Assuming 100% conversion of the ethyl 2-isopropyl-5-methylcyclohexyl carbonate, 75 mL of 2-ethoxy ethanol was used to solubilize the starting material. Once completely dissolved, a two-fold excess of hydrazine monohydrate (20 mL) was added and the reaction mixture was poured over ice and extracted with ethyl ether (5 x 100 mL). The organic layers were combined, dried over MgSO<sub>4</sub>, and concentrated under vacuum. Once the ethyl ether was evaporated, 50 mL of hexanes was added and the solution was heated and left at -20°C

for 48 h in which white fluffy crystals were formed and were subsequently collected via vacuum filtration. The recrystallization was performed three more times yielding 12.7 g (51% yield).

*Characterization of 2-isopropyl-5-methylcyclohexyl Hydrazinecarboxylate*



**2-isopropyl-5-methylcyclohexyl hydrazinecarboxylate (81):**  $^1\text{H}$  NMR

(300 MHz,  $\text{CDCl}_3$ ,  $25^\circ\text{C}$ ),  $\delta$ =6.14 (s, 1H), 4.56 (dt,  $J$ =4.5, 21.9 Hz, 1H), 3.74 (s, 2H), 1.97-2.02 (m, 1H), 1.82-1.92 (m, 1H), 1.61-1.66 (m, 2H), 1.40-1.52 (m, 1H), 1.30 (t,  $J$ =10.8 Hz, 1H), 1.00-1.10 (m, 1H), 0.91-0.99 (m, 2H), 0.85-0.89 (m, 6H), 0.75 (d,  $J$ =6.9 Hz, 3H)

$^{13}\text{C}$  NMR (75 MHz,  $\text{CDCl}_3$ ,  $25^\circ\text{C}$ )  $\delta$ =159.0 (C), 75.7 (CH), 47.5 (CH), 41.6 ( $\text{CH}_2$ ), 34.4 ( $\text{CH}_2$ ), 31.6 (CH), 26.4 (CH), 23.7 ( $\text{CH}_2$ ), 22.2 ( $\text{CH}_3$ ), 21.0 ( $\text{CH}_3$ ), 16.6 ( $\text{CH}_3$ )

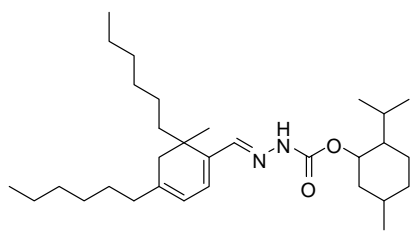
HRMS (ESI) for  $\text{C}_{11}\text{H}_{22}\text{N}_2\text{O}_2$  ( $\text{M}+\text{H}$ ) $^+$ : calcd 215.1760, found 215.1752.

*General Procedure for the Synthesis of the Menthylhydrazones*

Homodimer **36** (0.100 g, 1 equivalent) was dissolved in 200 proof ethanol (20 mL) with 1.5 equivalents of 2-isopropyl-5-methylcyclohexyl hydrazinecarboxylate **81** at room temperature. After 72 h, the reaction was extracted with 1:1 ethyl acetate/hexanes solution (2 x 100 mL), and was washed with brine. The organic layer was dried over magnesium sulfate ( $\text{MgSO}_4$ ) and concentrated under vacuum. The crude material was passed thru a silica plug with 10% ethyl acetate/hexanes as the mobile phase. The

mixture was then subjected to high pressure liquid chromatography (HPLC) with a mobile phase of 96% ethyl acetate/ 4% hexanes with a flow rate of 1.5 mL/minute. Two fractions were collected corresponding to the *R* and *S* stereoisomers respectively.

*Characterization of the Menthylhydrazones*



**2-isopropyl-5-methylcyclohexyl-2-((4,6-dihexyl-6-methylcyclohexa-1,3-dienyl)methylene)hydrazinecarboxylate (82):** HRMS (ESI) for  $\text{C}_{31}\text{H}_{54}\text{N}_2\text{O}_2$  ( $\text{M}+\text{H}$ )<sup>+</sup>: calcd 487.4264, found 487.4238.



*General Procedure for Conversion of Menthylhydrazones Back to Aldehyde*

Once the *R* and *S* stereoisomers were purified, each was dissolved in 20 mL of 1:1 water/ethanol with 5 mL of 10% sulfuric acid and boiled for 2.5 h in which a color change from clear to pink occurred within two hours. The reaction was removed from the heat source and allowed to cool when it was then extracted with ethyl ether (2 x 25 mL). The organic layer was then dried with  $\text{MgSO}_4$  and concentrated under vacuum. The crude mixture was then passed through a silica plug with a mobile phase of 10% ethyl acetate/hexanes.

## CHAPTER IV

### SYNTHESIS AND BIOLOGICAL EVALUATION OF HETERODIMERIC CYCLOTERPENALS\*

#### INTRODUCTION

The carotenoids are responsible for such processes as the inactivation of free radicals.<sup>17</sup> The retinoids, for example, the natural and synthetic derivatives of Vitamin A, serve as chromophores of the visual transduction system.<sup>166</sup> Retinoids also exhibit a variety of other biological activities. They are used extensively in dermatology for a variety of conditions, show activity as cancer preventative agents, and are potent modulators of growth and differentiation.<sup>27-29</sup> In this regard, *all-trans* retinoic acid **13** has been shown to differentiate embryonic stem cells into a neuron-like phenotype.<sup>30</sup> It has also been employed as a cancer chemotherapeutic in treatment of promyelocytic leukemia by causing terminal differentiation of the malignant cells.<sup>27</sup> Retinoic acid analogs TTNPB **83**, azulenic compounds **84** and **85** have been shown to possess biological activities as cancer chemopreventative agents (**Figure 47**).<sup>166</sup>

Interestingly, self-condensation of polyene aldehydes has been observed in nature resulting in terpenes with cyclodimeric structures. We defined these molecules as cycloterpenals as they are composed of a cyclohexadiene core formed by the condensation of two terpene aldehydes. Cyclocitral **15**, for example, was recently

---

\* Reprinted with permission from “Synthesis and Cellular Effects of Cycloterpenals: Cyclohexadienal-Based Activators of Neurite Outgrowth.” Bench, B. J., Tichy, S. E., Perez, L. M., Benson, J., Watanabe, C. M. H., 2008. *Bioorganic & Medicinal Chemistry*, 16, 7573-7581, Copyright 2008 by Elsevier Ltd.

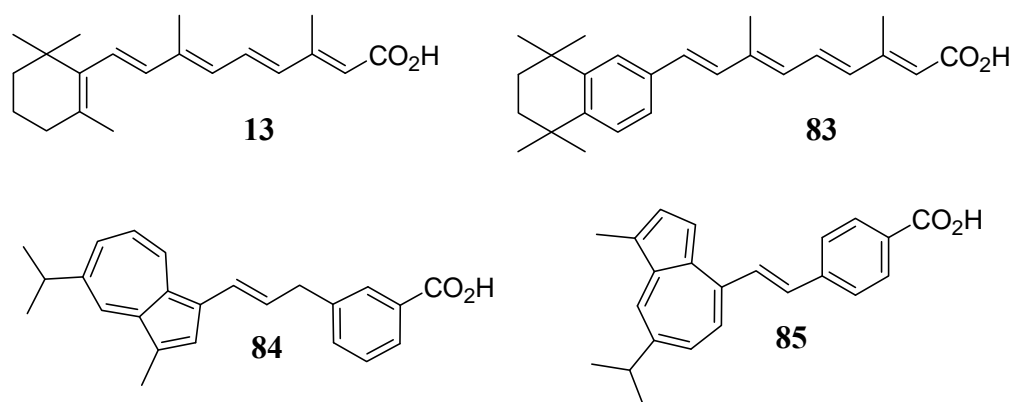


**Figure 47.** Structures of representative retinoid compounds.

isolated from the North Sea bryozoans *Flustra foliacea* and shown to exhibit antibiotic activity.<sup>39,88,89</sup> Cycloretinal **14** has been suggested as a contributor of age-related macular degeneration.<sup>33,34</sup> Furthermore, incubation of the milk whey protein  $\beta$ -lactoglobulin with  $\beta$ -ionylideneacetaldehyde has been shown to result in a C-30 ring-fused homodimer cyclo- $\beta$ -ional **16** (Figure 48).<sup>87</sup>

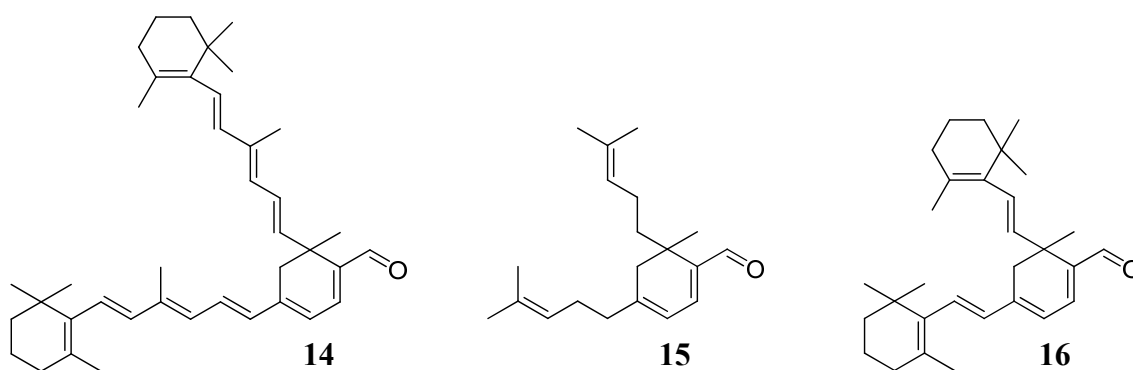


**Figure 48.** Structures of cycloretinal, cyclocitral, and C-30 dimer.

On these bases, we broadly speculate that some of these cycloterpenals or their structurally and functionally related analogs could be important in developmental processes such as neurite outgrowth. In this chapter, we designed a synthetic library of cyclohexadienals and tested the composite library (ring-fused heterodimers) against PC12 cells where promising effects were observed on neurite outgrowth. We also screened the library for cytotoxic effects with an array of assays including Jurkats (human T-cell leukemia), yeast (*Saccharomyces cerevisiae*), and two bacterial strains (*Escherichia coli*, *Bacillus subtilis*). In some instances, involving aromatic substitutions to the central ring, the cyclohexadiene ring system could be aromatized to give fluorescent molecules. In the future, some of these molecules or their respective derivatives might find use as fluorescent probes in protein target identification of a particular cyclohexadienal.

## RESULTS AND DISCUSSION

### *Synthesis of Asymmetric Cyclohexadienals*

The cycloterpenals-based compound library was generated by proline-promoted condensation of  $\alpha,\beta$ -unsaturated aldehydes giving mono-, di-, tri-, and tetra-substituted cyclohexadienals (**Figure 49**). The reaction involves condensation between a donor and acceptor aldehyde, where donor molecules require the presence of either a  $\beta$ -methyl or  $\beta$ -methylene group. Acceptor molecules exhibit a wider degree of flexibility, the single constraint owing to the presence of an  $\alpha,\beta$ -unsaturated aldehyde. The reaction proceeds by complete conversion of aldehyde to that of the Schiff base followed by a Diels-Alder or Michael-like imine addition.<sup>31</sup>

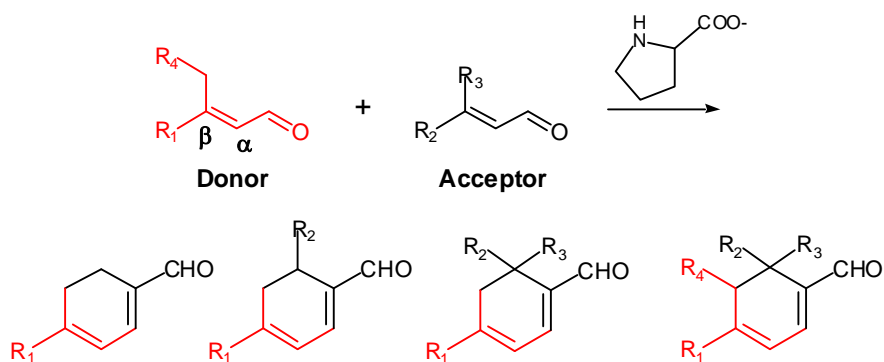


**Figure 49.** Substituted heterodimeric cyclohexadienals generated by proline-mediated condensation of  $\alpha,\beta$ -unsaturated aldehydes.

Here we detail optimal reaction conditions to favor heterodimer formation over competing homodimerization,<sup>31</sup> which is inherent to the reaction. Therefore, the reaction is not amendable to a one-pot synthetic strategy, unlike homodimerization, as minimal yields are obtained under such conditions. Moreover, we illustrate the scope of the reaction by invoking substrates that vary in function and architecture.

#### *Catalysis Involving a Single $\beta$ -methyl Substituted Substrate*

In order to synthesize this class of tri-substituted heterodimers (**Figure 50**), we first had to optimize the general reaction. Employing a one-pot strategy, reaction of 3-thiophen-2-yl-but-2-enal with 4-(dimethyl-amino)-cinnamaldehyde (in a 1:1 mol ratio) gave a 5% and 43% yield, respectively, of heterodimer **86** to the thiophene homodimer (**Table 10**). Likewise, skewing the ratio in favor of the acceptor aldehyde substrate over that of the  $\beta$ -methyl substituted aldehyde donor in a one-pot format gave poor yields of the heterodimer **86**. Therefore, we implemented this reaction as a model system and optimized its conditions in an effort to define a generalizable set of

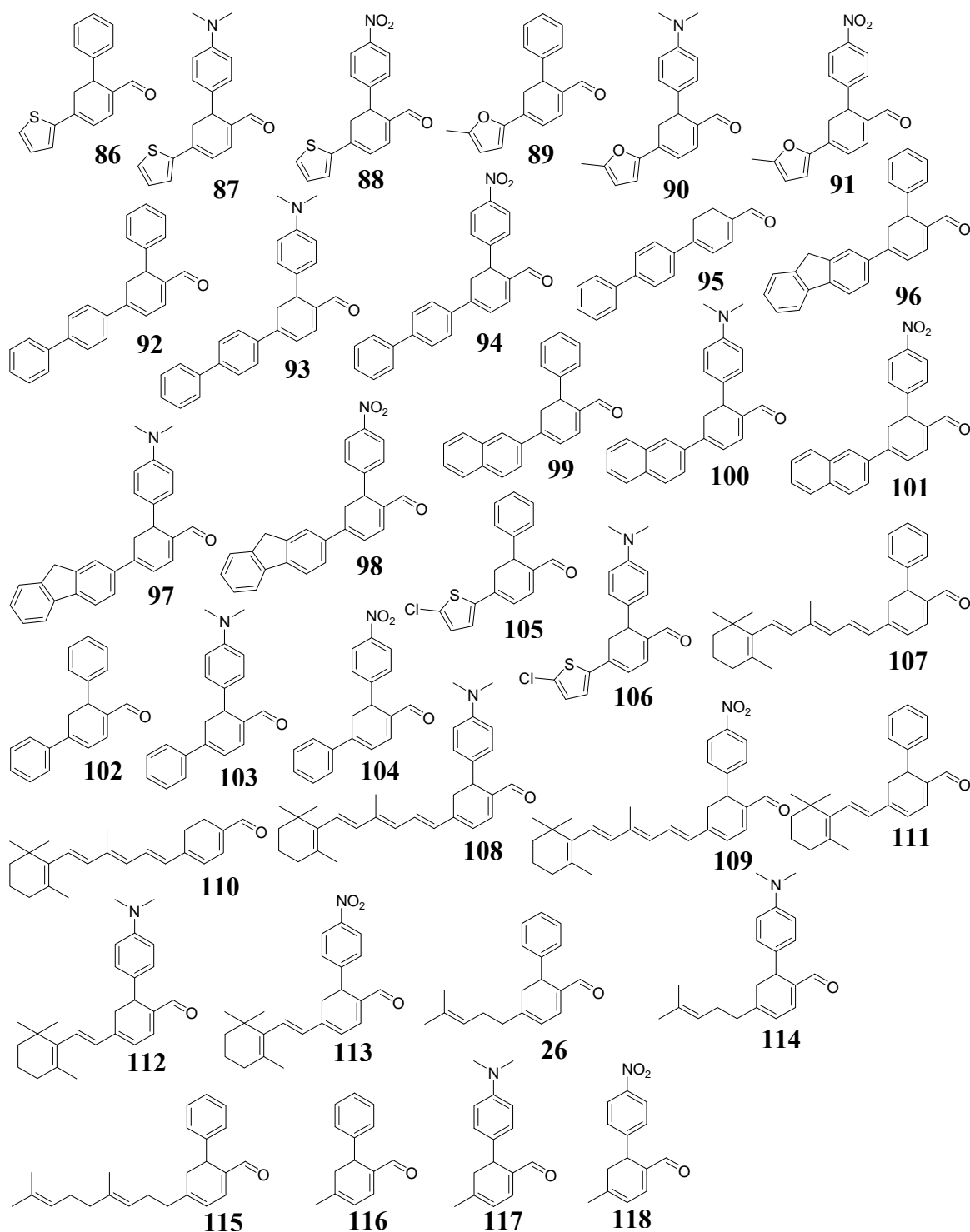
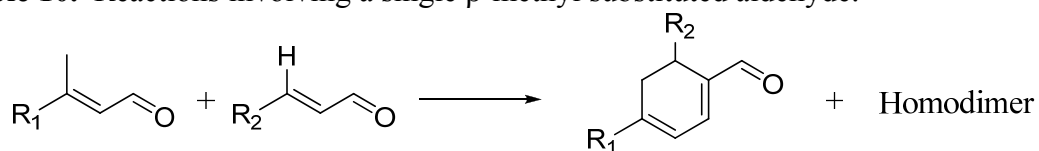


**Figure 50.** Chemical structures of heterodimers made with a single  $\beta$ -methyl substituted aldehyde.

reaction conditions to maximize heterodimer yields.

As  $\alpha,\beta$ -unsaturated aldehydes lacking a  $\beta$ -methyl group fail to self-dimerize (confirmed through ESI mass spectroscopy) and the reaction can be envisioned to proceed through formation of a Schiff base.<sup>31,87</sup> We examined the notion of pre-forming the proline Schiff base of the acceptor aldehyde (as monitored by TLC, the Schiff base appears at the base-line with concomitant loss of the starting aldehyde) prior to the addition of the donor aldehyde. Intuitively, this should minimize formation of the cyclic

**Table 10.** Reactions involving a single  $\beta$ -methyl substituted aldehyde.



<sup>a</sup> R1	<sup>a</sup> R2	Comp #	<sup>b</sup> Yield (%)	<sup>c</sup> ee (%)
thienyl	benzyl	<b>86</b>	48	56
thienyl	dimethylamino-benzyl	<b>87</b>	64	53
thienyl	nitrobenzyl	<b>88</b>	23	49
CH <sub>3</sub> furanyl	benzyl	<b>89</b>	48	63
CH <sub>3</sub> furanyl	dimethylamino-benzyl	<b>90</b>	62	72
CH <sub>3</sub> furanyl	nitrobenzyl	<b>91</b>	22	50
biphenyl	benzyl	<b>92</b>	45	52
biphenyl	dimethylamino-benzyl	<b>93</b>	75	62
biphenyl	nitrobenzyl	<b>94</b>	16	53
biphenyl	H-	<b>95</b>	57	—

**Table 10** continued.

fluorenyl	benzyl	<b>96</b>	47	43
fluorenyl	dimethylamino-benzyl	<b>97</b>	59	62
fluorenyl	nitrobenzyl	<b>98</b>	22	49
naphthyl	benzyl	<b>99</b>	50	57
naphthyl	dimethylamino-benzyl	<b>100</b>	58	54
naphthyl	nitrobenzyl	<b>101</b>	34	56
biphenyl	benzyl	<b>102</b>	53	64
biphenyl	dimethylamino-benzyl	<b>103</b>	64	54
biphenyl	nitrobenzyl	<b>104</b>	34	51
2-Cl thienyl	benzyl	<b>105</b>	42	36
2-Cl thienyl	dimethylamino-benzyl	<b>106</b>	56	41
retinyl	benzyl	<b>107</b>	55	56
retinyl	dimethylamino-benzyl	<b>108</b>	64	56
retinyl	nitrobenzyl	<b>109</b>	22	50
retinyl	H-	<b>110</b>	51	—
$\beta$ -ionyl	benzyl	<b>111</b>	47	56
$\beta$ -ionyl	dimethylamino-benzyl	<b>112</b>	57	59
$\beta$ -ionyl	nitrobenzyl	<b>113</b>	35	53
dimethylallyl	benzyl	<b>26</b>	12	52
dimethylallyl	dimethylamino-benzyl	<b>114</b>	5	40



**Table 10** continued.

farnesenyl	benzyl	<b>115</b>	15	62
methyl	benzyl	<b>116</b>	60	56
methyl	dimethylamino-benzyl	<b>117</b>	63	48
methyl	nitrobenzyl	<b>118</b>	47	54

<sup>a</sup>Reaction conditions: 1 (donor) : 1.5 (acceptor) : 3.4 (L-proline); the acceptor was dissolved in ethanol, reacted for 2 h to which donor was added and stirred at room temperature for 16-24 h.

<sup>b</sup>Isolated yield. <sup>c</sup>Determined by Pr(hfc)<sub>3</sub> chiral shift reagent.

homodimer, while maximizing heterodimer **87** yields. To our satisfaction, an overall enhancement in reaction yields (from 5% to 64%) was indeed obtained. Such a strategy greatly facilitates reaction yields. With this method, we were able to limit the formation of the homodimer product anywhere from 1% to 14% dependent upon the substrate.

To illustrate this strategy, we examined Schiff base formation of cinnamaldehyde and its derivatives by NMR to rationalize differences observed in reaction yields, *i.e.* while product yields for cinnamaldehyde and 4-dimethylamino-cinnamaldehyde were obtained in moderate yields. The yields for 4-nitro-cinnamaldehyde were considerably lower. Additionally, a difference in color change could also be visualized between that of cinnamaldehyde or dimethylamino-cinnamaldehyde and that of the nitro species. When the Schiff base is formed with cinnamaldehyde or the di-methylamino-substituted compound (in the presence of excess proline, 1:1.5 molar concentration), the reaction progresses from a clear solution to yellow and finally to red. The reaction is stirred for approximately 2 hours before the donor substrate is added (Schiff base formation monitored by TLC). However, when the reaction is performed with 4-

nitrocinnamaldehyde, the reaction goes from a yellowish hue to a light brown mixture with a slight precipitate forming within 20 minutes. In this case, the donor substrate is added and the reaction is stirred for 12-16 hours.

A time course analysis was performed by NMR to monitor conversion of the three cinnamaldehydes to their corresponding Schiff base products. Schiff base formation between proline and each aldehyde ensues immediately (as detected by NMR at 2 minutes). In **Figure 51**, cinnamaldehyde and 4-dimethylaminocinnamaldehyde Schiff base products are detected by the presence of two doublets, representing their *cis* and *trans* isomers ( $\alpha$ -carbon to the protonated imine), at 8.75 and 8.65 ppm and 8.34 and 8.29 ppm, respectively. By 2 h, all of the cinnamaldehyde substrate was converted to that of its Schiff base, while it took a total of 4 h for the 4-dimethylamino-cinnaladehyde reaction to come to completion. In contrast, in the case of 4-nitrocinnamaldehyde, unknown side reactions began to occur as the desired Schiff base formed (**Figure 52**). Schiff base formation began to form within 2 minutes as exhibited by the presence of the pair of *cis* and *trans* isomers at 8.85 and 8.74 ppm. However, at 13 minutes, a small singlet begins to appear at 9.74 ppm between the doublet of the 4-nitrocinnamaldehyde starting material. The intensity of the singlet continues to increase while the broad singlets at 8.85 and 8.74 ppm decrease over time. After 2 h and 45 minutes, this unknown product is entirely consumed leaving only an unknown product mixture.

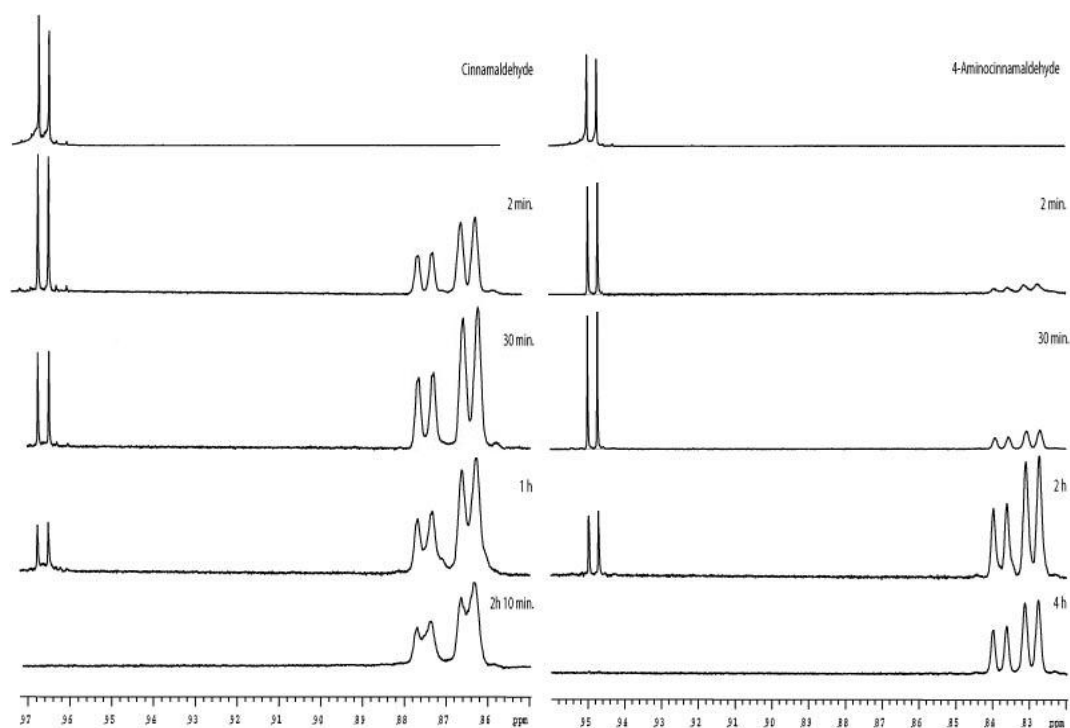


**Figure 51.** Cinnamaldehyde and 4-dimethylaminocinnamaldehyde Schiff base formation.

We also monitored the reaction by utilizing mass spectrometry to evaluate intermediate formation along with a time course as the reaction proceeds from Schiff base formation to the final product. The proline-promoted formation of 4-(biphenyl-4-yl)-6-phenylcyclohexa-1,3-dienecarbaldehyde involving cross-condensation between *trans*-cinnamaldehyde and (*E*)-3-(biphenyl-4-yl)but-2-enal was examined by LC/MS. The reaction is thought to proceed by complete conversion of the aldehyde group to that of their corresponding Schiff base (**Scheme 16**).

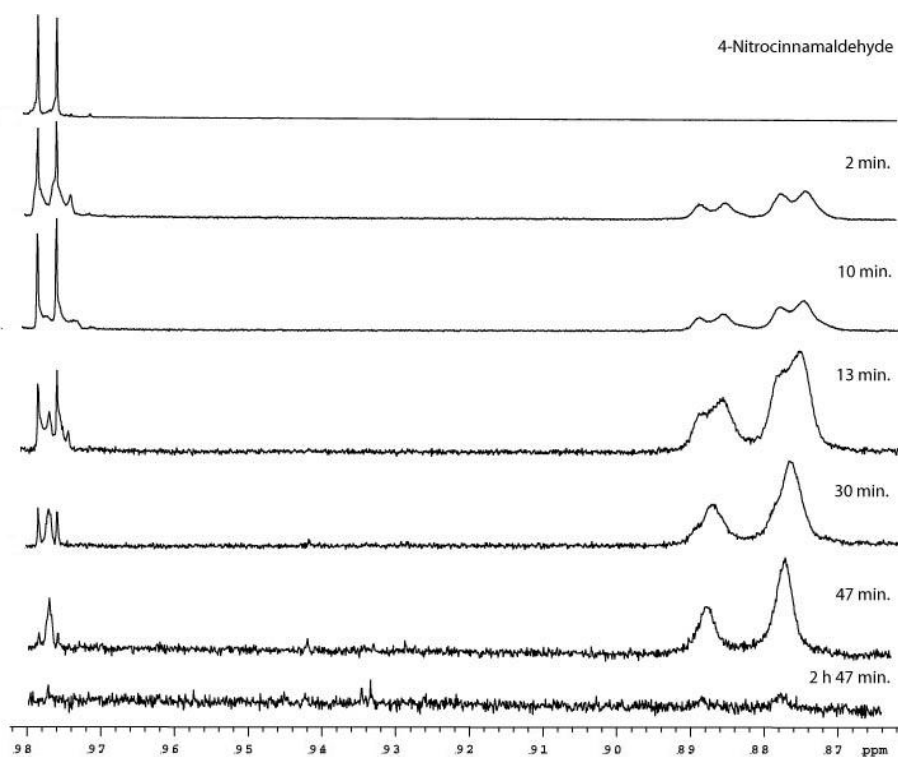
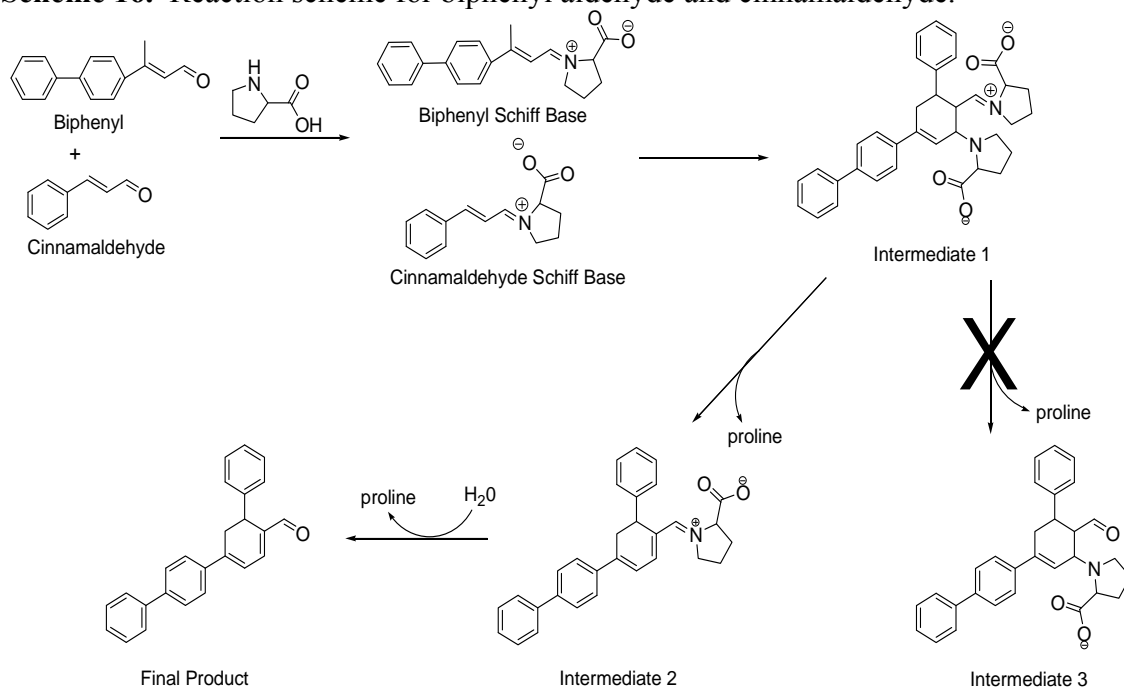


**Figure 52.** 4-nitrocinnamaldehyde Schiff base formation.

**Scheme 16.** Reaction scheme for biphenyl aldehyde and cinnamaldehyde.



Cross condensation occurs by deprotonation of the  $\beta$ -methyl group of the donor (biphenyl Schiff base), followed by addition to the  $\beta$ -position of the protonated imine of the acceptor (cinnamaldehyde Schiff Base), to give intermediate 1. The reaction can then proceed in one of two ways. Addition of water to the protonated imine would result in dissociation of proline and regeneration of the aldehyde group to give intermediate 3. Alternatively, dehydration might occur to give the cyclohexadiene ring system as a proline adduct (intermediate 2), where subsequent release of proline would yield the final product.

To evaluate this reaction, we first incubated cinnamaldehyde with an excess of L-proline overnight. (*E*)-3-(biphenyl-4-yl)but-2-enal was subsequently added and the progress of the reaction was monitored over time by LC/MS. Analysis revealed the formation of intermediate 2 but not of intermediate 3 based on their *m/z* ratios of Intermediate 2 and 3, 433.2 and 450.2 respectively. Unfortunately, we were unable to detect the formation of Intermediate 1 as the proline adduct undergoes rapid dissociation.

Time course analysis of the reaction over a 15 hour period allowed evaluation of reaction flux, the build-up and consumption of starting materials, and reaction intermediates (**Figure**). As cinnamaldehyde was already in its Schiff base form prior to the addition of the biphenyl acceptor aldehyde, as one would expect, biphenyl Schiff base formation steadily increases during the first 3 hours. Once formed, both cinnamaldehyde and biphenyl substrates (**Figure a and b**), Schiff bases decrease over time throughout the course of the reaction. As **Figure c** reveals, intermediate 2 increases during the first 9 hours of the reaction then decreases over time. Plotting intermediate 2

against the final reaction product (**Figure d**) reveals that as production of intermediate 2 rises, product formation also increases until intermediate 2 reaches its maximum at 9 hours.

Other factors found to influence the cross-condensation reaction included substrate (donor to acceptor) ratios and temperature effects. For instance, varying the ratio of donor to that of the acceptor (in a 1:1, 1:1.5, 1:2, and 1:3), at a set catalyst ratio (1:1.5 substrate to catalyst ratio, shown to be optimal from previous studies), gave surprisingly higher yields at 1:1 (21.4%) and 1:1.5 (64%) molar concentrations. At 1:2 and 1:3 molar concentrations, the overall heterodimer yields were 14.0% and 11.2%, respectively. Based upon these findings, we employed 1 (donor): 1.5 (acceptor): 3.8 (L-proline) molar concentration ratios to effect synthesis of the remainder of the heterodimers involving a single  $\beta$ -methylenic substrate.

Temperature effects on the reaction paralleled that observed with self-condensation reactions,<sup>31</sup> whereby product yields were highest at ambient temperature versus -20 to 0 °C or 50 to 100 °C. In all cases the concentration of catalyst, L-proline, in these reactions was held constant at 3.8 equivalents since these amounts were shown to give the greatest extents of conversion in homodimer reactions.<sup>31</sup> Use of L-proline (3.8 equivalents) maintains a substrate to catalyst ratio of 1:1.5, where substrate equals donor plus aldehyde.

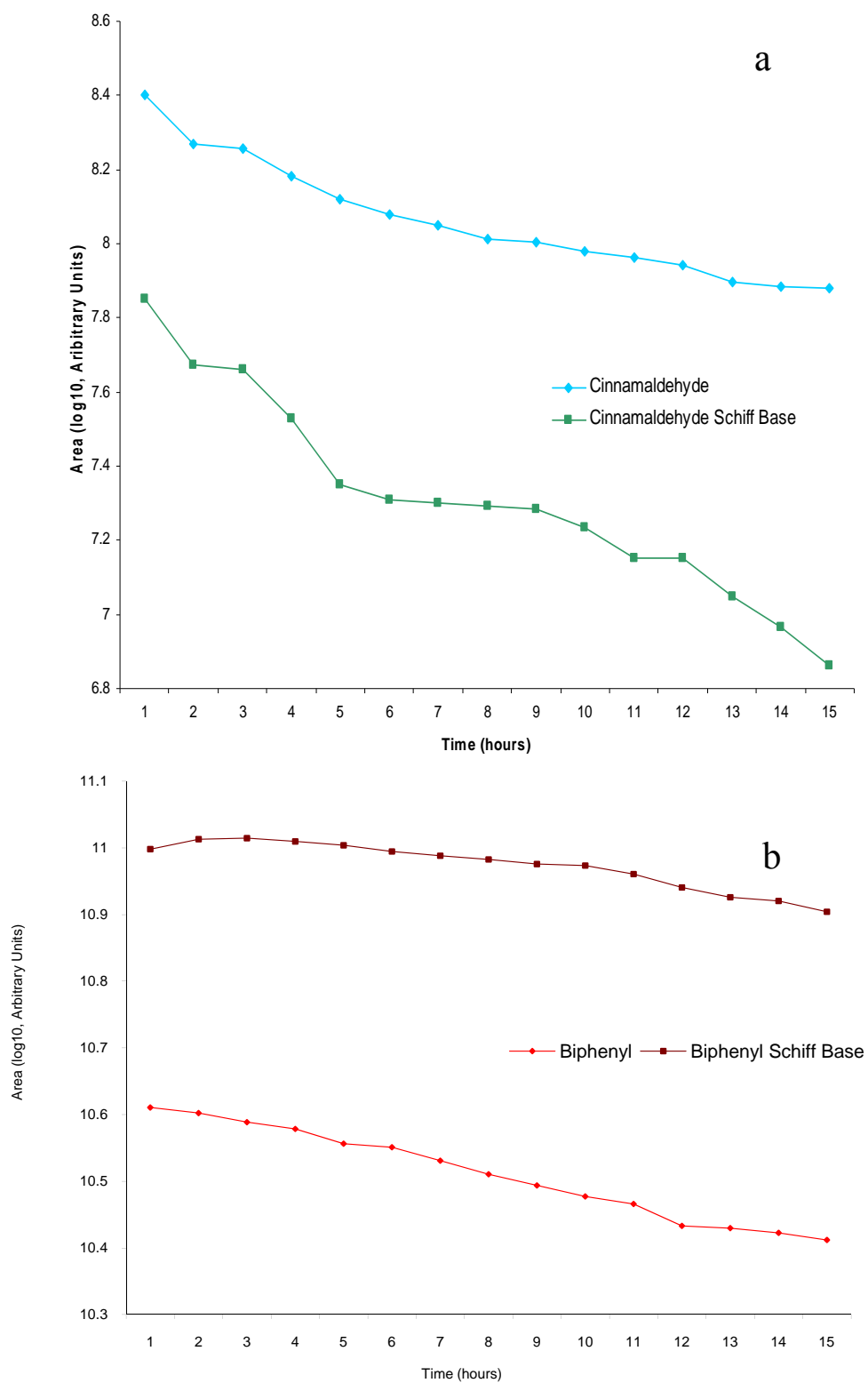


**Figure 53.** Time course analysis of proline-promoted formation of biphenyl-cinnamaldehyde heterodimers.

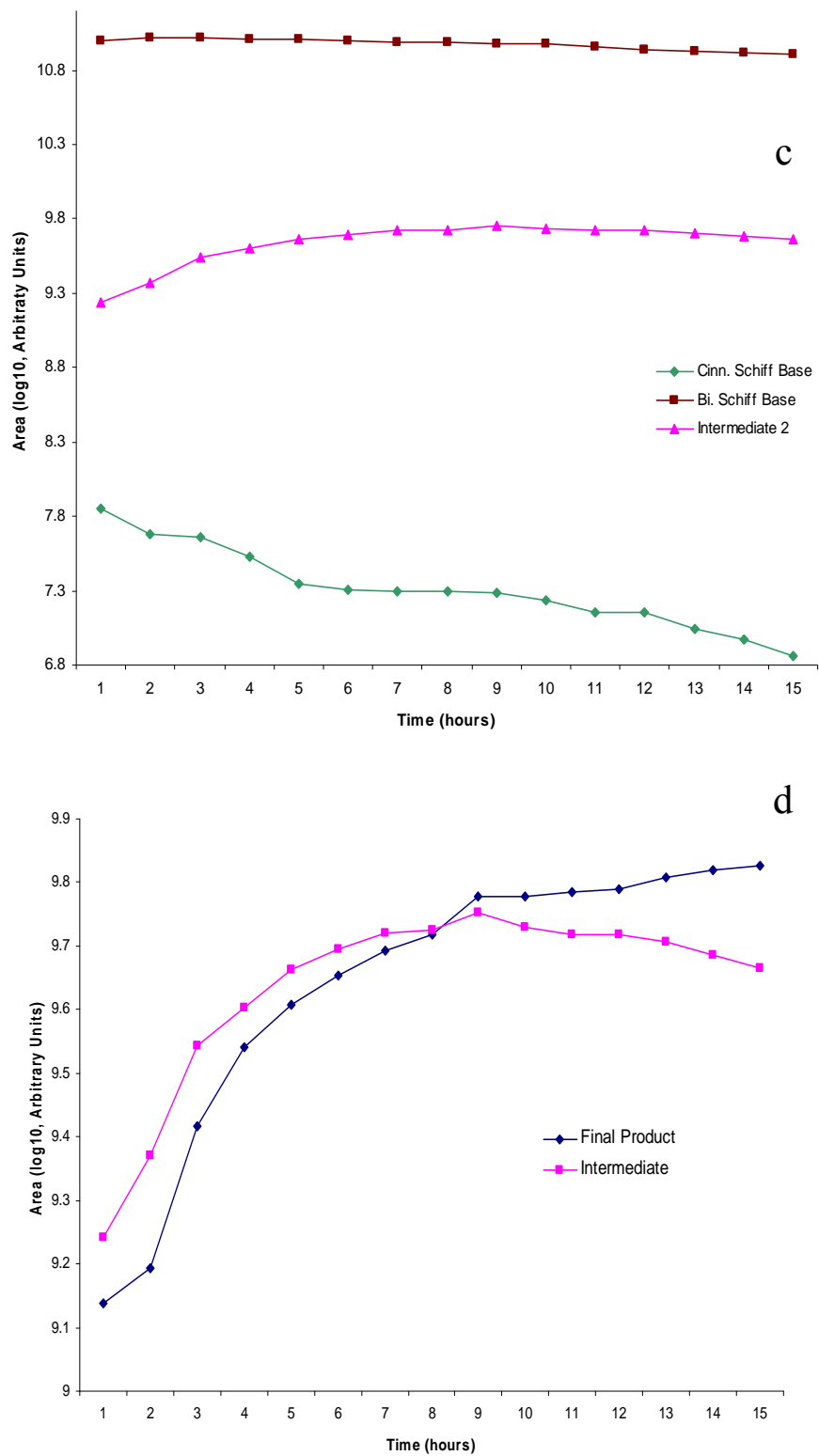
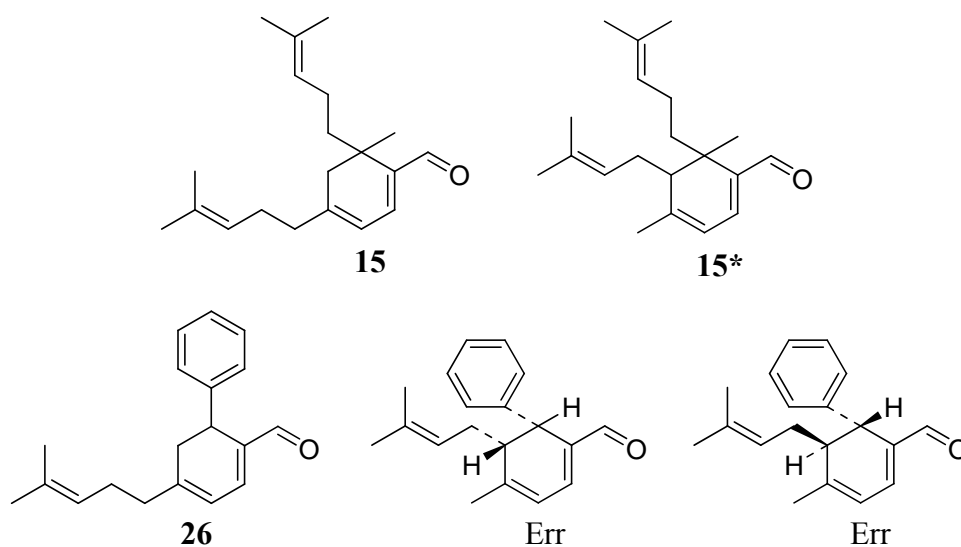


Figure 53 continued.



Utilizing these optimized conditions, we investigated the overall scope of the reaction as illustrated in **Table 10**. In most cases the heterodimers were generated in modest yields. The lowest yields were obtained with heterodimers bearing dimethylallyl-**26** and **114** or farnesenyl-**115** substituents giving reaction yields in the 5-15% range, which presumably is attributed to the flexibility of the side chains and competing reactions (**Figure 54**). Conversely, the highest yields were achieved with heterodimers bearing rigid substituents (aromatic or other conjugated systems). Such trends were also observed with homodimerization.<sup>31</sup> As expected, in almost all cases the cross-condensation reaction was favored by electron donating groups as opposed to electron withdrawing substituents. Homodimer yields ranged from 1% to 14% in each instance.



**Figure 54.** Products resulting from reaction of cinnamaldehyde with citral.

### *Catalysis Between Two $\beta$ -methyl Substituted Substrates*

Proline-promoted synthesis between two  $\beta$ -methylenic substrates would be expected to yield a mixture of substituted cyclohexadienals (**Figure 55**), corresponding to two homodimeric and two heterodimeric products (**Table 11**). To achieve these cross-condensation reactions, reaction conditions were modified slightly. A 1:1 ratio of each aldehyde substrate and 3 equivalents of L-proline were optimal. Skewing the ration (1:2) only enhanced homodimer formation of the more prevalent substrate.

Implementing these optimized conditions, we examined the generality of the reaction. Sterics appeared to govern these cross-condensations, as the only heterodimer product formed gave the bulkiest substituent at C-4 and the least hindered group at C-6

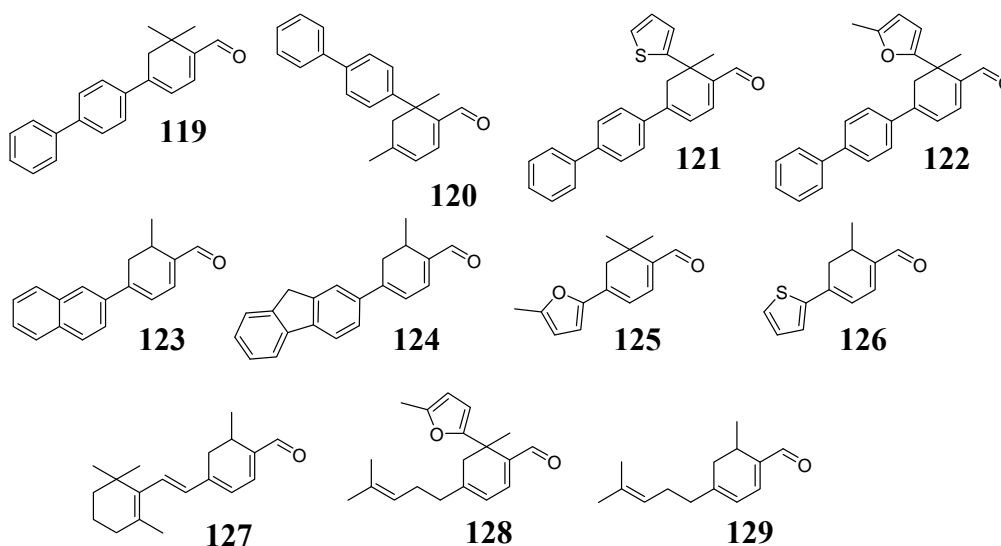
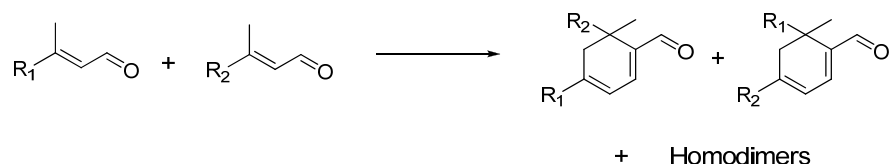


**Figure 55.** Chemical structures of heterodimers made with two  $\beta$ -methyl substituted aldehydes.

with the exception of **119** and **120**, in which both heterodimeric products were formed.

Likewise, reaction of citral and crotonaldehyde gave rise to tri-substituted

**Table 11.** Reaction between two  $\beta$ -methyl substituted aldehydes.



<sup>a</sup> R1	<sup>a</sup> R2	Comp #	<sup>b</sup> Yield (%)	<sup>c</sup> ee (%)
biphenyl	methyl	<b>119</b>	49	55
methyl	biphenyl	<b>120</b>	18	57
biphenyl	thienyl	<b>121</b>	14	54
biphenyl	CH <sub>3</sub> furanyl	<b>122</b>	29	50
naphthyl	H-	<b>123</b>	57	49
fluorenyl	H-	<b>124</b>	67	48
CH <sub>3</sub> furanyl	methyl	<b>125</b>	40	52
thienyl	H-	<b>126</b>	45	47
$\beta$ -ionyl	H-	<b>127</b>	39	44
dimethylallyl	CH <sub>3</sub> furanyl	<b>128</b>	23	46
dimethylallyl	H-	<b>129</b>	59	46

<sup>a</sup>Reaction conditions: 1 (donor) : 1 (acceptor) : 1.5 (L-proline) was dissolved in ethanol and stirred at room temperature for 16-24 h. <sup>b</sup>Isolated yield. <sup>c</sup>Determined by Pr(hfc)<sub>3</sub> chiral shift reagent.

cyclohexadienal **129**, with the dimethylallyl-linkage at C-4. Reaction yields ranged from

14% to as high as 67%, with the highest yields arising from condensation with an

acceptor aldehyde where  $R_2$  is H- or  $CH_3$ -. On the contrary, the lowest yields were obtained from reactions with an acceptor aldehyde where  $R_2$  is thienyl or methylfuranyl. While one might expect high level of homodimer to be formed with this one-pot strategy, the isolated yields ranged from 3% to 27% in each case.

*Catalysis Effected by the  $\beta$ -methylene Group of the Donor Aldehyde*

Interestingly, catalysis is not limited to reactions with  $\beta$ -methyl substituted aldehydes. A substitution at C-5 of the cyclohexadienal was readily observed as a result of deprotonation occurring from the  $\gamma$ -methylene position of the donor aldehyde (**Figure 56**). For instance, use of a  $\beta$ -ethyl substituted donor aldehyde gives methyl-substitution

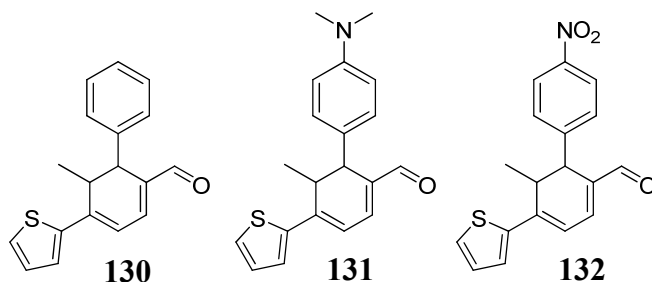
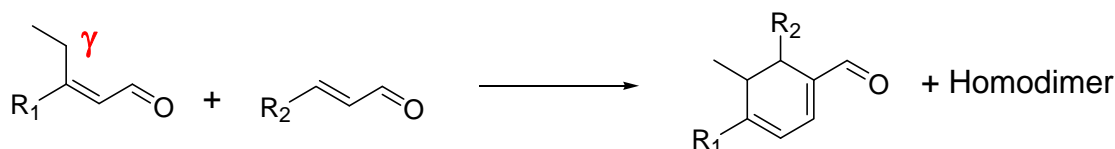


**Figure 56.** Chemical structures of heterodimers made with a  $\beta$ -ethyl substituted aldehyde.

at C-5 of the tri-substituted cyclohexadienal. In this regard, reaction of 3-thiophen-2-yl-pent-2-enal with three different  $\alpha,\beta$ -unsaturated aldehydes resulted in the formation of heterodimers shown in **Table 12** as the major product with yields ranging from 25% to 50% and approximately 10% homodimer in each instance. While it might be conceivable to generate the seven membered ring system by proton abstraction of the  $\delta$ -

methyl group, formation was not observed. Reaction conditions were the same as detailed previously and similar yields and ee values were observed.

**Table 12.** Reactions with  $\beta$ -ethyl substituted donor aldehydes.



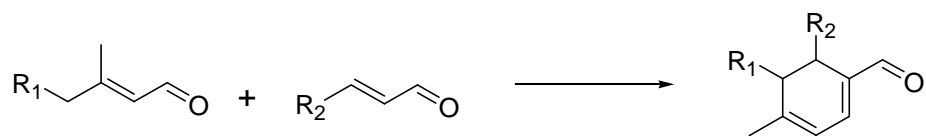
<sup>a</sup> R1	<sup>a</sup> R2	Comp #	<sup>b</sup> Yield (%)	<sup>c</sup> ee (%)
thienyl	benzyl	<b>130</b>	49	52
thienyl	dimethylamino benzyl	<b>131</b>	50	50
thienyl	nitrobenzyl	<b>132</b>	25	51

<sup>a</sup>Reaction conditions: 1 (donor) : 1.5 (acceptor) : 3.4 (L-proline); the acceptor was dissolved in ethanol, reacted for 2 h to which donor was added and stirred at room temperature for 16-24 h.

<sup>b</sup>Isolated yield. <sup>c</sup>Determined by Pr(hfc)<sub>3</sub> chiral shift reagent.

Likewise, reacting cinnamaldehyde with citral gave three heterodimer products (**Figure 54**), the expected di-substituted product **26** and two tri-substituted cyclohexadienals, *cis* and *trans* diastereomers (**27** and **28**), respectively. Previous work has actually shown that formation of homodimer **15** can be favored (95:5) in the presence of strong base, NaH resulting in a mixture of homodimers.<sup>111</sup> While we limited the formation of self-condensation products (**15** and **15\***) by allowing cinnamaldehyde to go to complete Schiff base formation prior to the addition of citral with homodimer **15** still observed in 9% yield. Heterodimers **26**, **27**, **28** were formed in 12%, 25%, and 4% yield respectively

(**Table 13**). As with previous systems, these reactions favored substituents with electron donating groups as opposed to those bearing electron with-drawing substituents. In this regard, reactions involving nitrobenzyl groups gave correspondingly lower yields than those involving benzyl or dimethylamino-benzyl substituents. These  $\beta$ -methylenic driven reactions were also demonstrated with farnsenal,  $\beta$ -methyl substituted nonenal in combination with acrolein, cinnamaldehyde, and its derivatives. In most instances only the *cis* product was formed; citral was purchased as a mixture of *cis* and *trans* isomers while all others were obtained as a single (*all-trans*) isomeric form. The compounds were assigned on the basis of computation analysis and NMR spectroscopy.

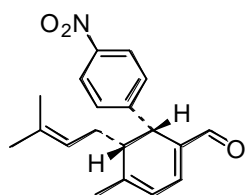
**Table 13.** Cross-condensation reactions.

<sup>a</sup> R1 & R2	Product	Comp #	<sup>b</sup> Yield (%)	<sup>c</sup> ee (%)
R1 dimethylallyl R2 benzyl		27	25	53
		28	4	62
R1 dimethylallyl R2 benzyl		133		33
		134	24	41

**Table 13** continued.

R1 dimethylallyl

R2 benzyl

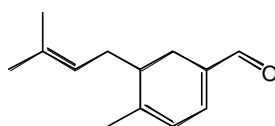
**135**

18

44

R1 dimethylallyl

R2 H-

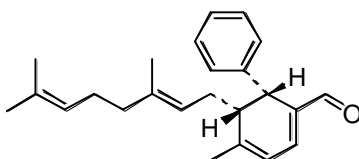
**136**

24

45

R1 farnesenyl

R2 benzyl

**137**

18

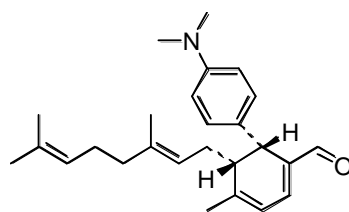
63

R1

farnesenyl

R2 dimethyl

aminobenzyl

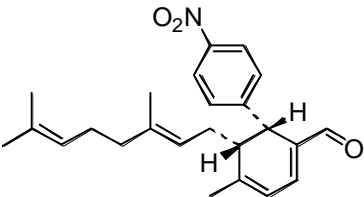
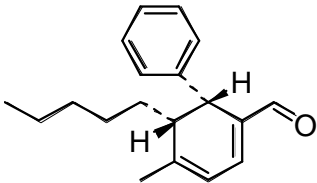
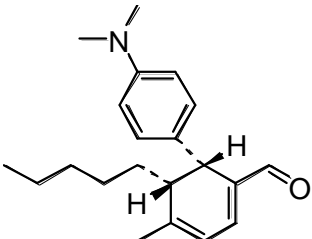
**138**

45

61



**Table 13** continued.

R1		<b>139</b>	23	55
farnesenyl				
R2 nitrobenzyl				
R1 pentyl				
R2 benzyl		<b>140</b>	29	57
R1 pentyl				
R2 dimethyl		<b>141</b>	31	55
aminobenzyl				

<sup>a</sup>Reaction conditions: 1 (donor) : 1.5 (acceptor) : 3.4 (L-proline) the acceptor was dissolved in ethanol, reacted for 2 h to which donor was added and stirred at room temperature for 16-24 h.

<sup>b</sup>Isolated yield. <sup>c</sup>Determined by Pr(hfc)<sub>3</sub> chiral shift reagent.

During the structural determination of the products from the citral/cinnamaldehyde reaction, we not only isolated the desired **26** compound but also two diastereomers, *cis* and *trans*, that occurred during the abstraction of a proton from the  $\gamma$ -methylene of citral. These two diastereomers gave interesting <sup>1</sup>H spectra as the proton on C-6 of the carbaldehyde ring (**Figure 57**). For the *trans* diastereomer **28**, a doublet ( $J=9.0$  Hz) was observed and a singlet for the *cis* diastereomer **27**. We decided

to investigate the relationship between these three products by performing B3LYP/6-31G(d') geometry optimizations by B3LYP/6-311++G(2d,p) for chemical shift and spin-spin coupling calculations for each product. These computational analyses can be used to confirm the structural assignment based on the NMR analyses.

For the  $\beta$ -methyl product **26**, we observed a chemical shift of 4.06 ppm giving rise to a doublet of doublets ( $J=1.5, 10.5$  Hz) experimentally. When NMR calculations are performed, we also see a chemical shift 4.06 ppm **Figure 58**. The bond lengths through space between the C-6 proton and the diastereomeric protons are 2.41 Å and 3.05 Å. For the *cis* and *trans* diastereomers, the comparison between experimental and calculation data gives us a difference of -0.47 and +0.34 ppm respectively. As previously mentioned, the *cis* diastereomer gives a singlet at 3.93 ppm while the *trans* diastereomer gives rise to a doublet 3.97 experimentally. The bond distance between the C-6 proton and the C-5 proton for the *cis* diastereomer is 3.05 Å. However, the bond length for the *trans* diastereomer is 2.38 Å.

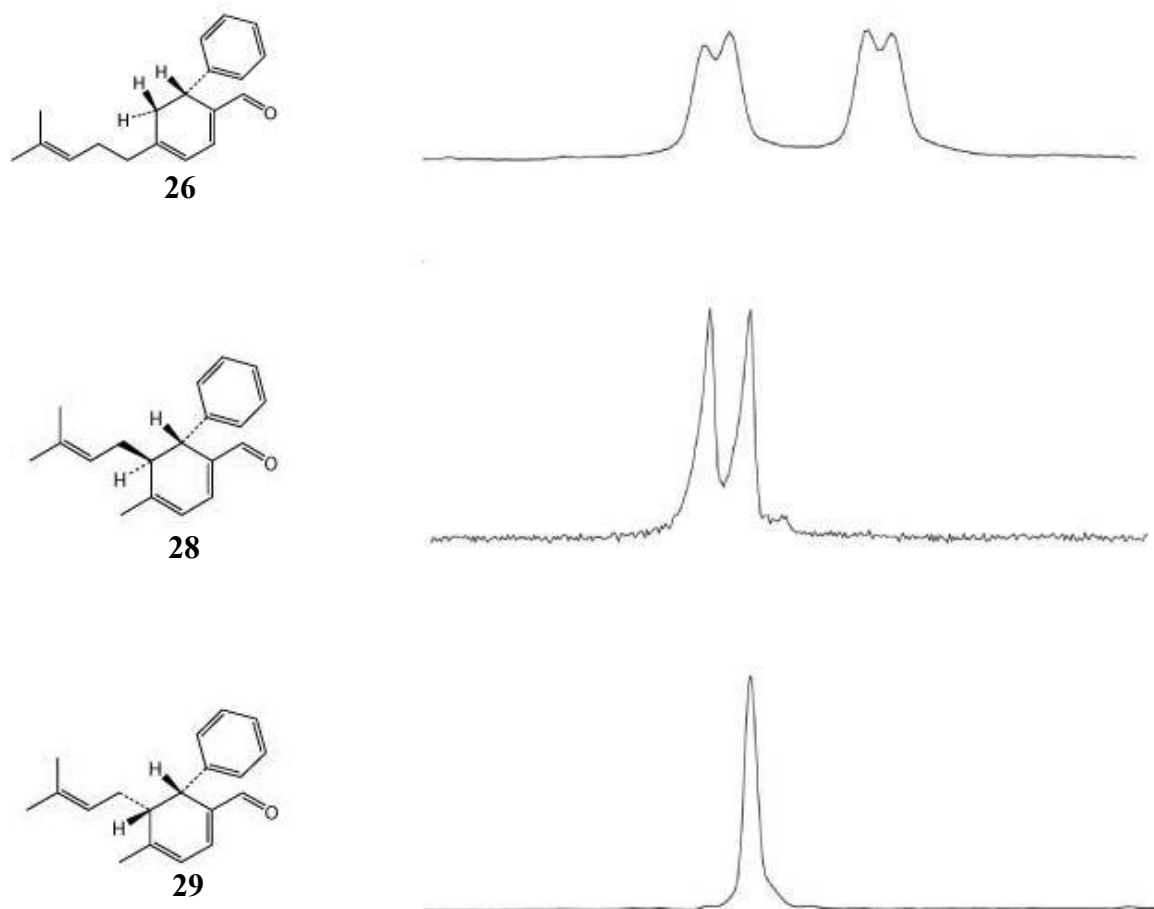


**Figure 57.**  $^1\text{H}$  NMR spectra of the proton on C-6 of the products of the reaction between citral and cinnamaldehyde.

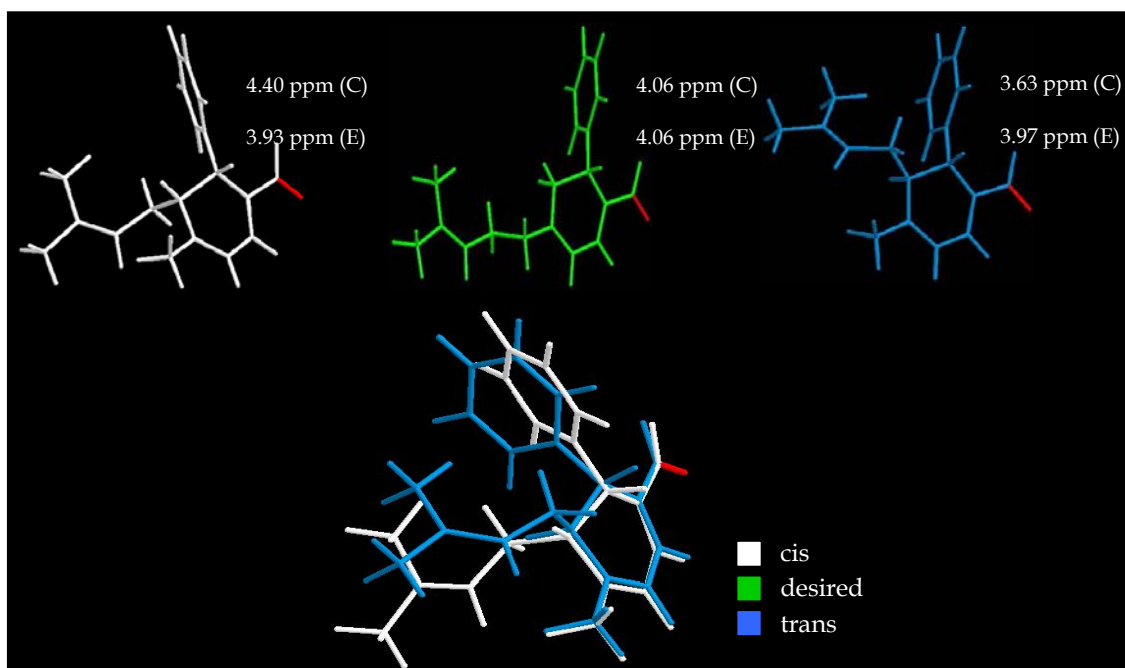
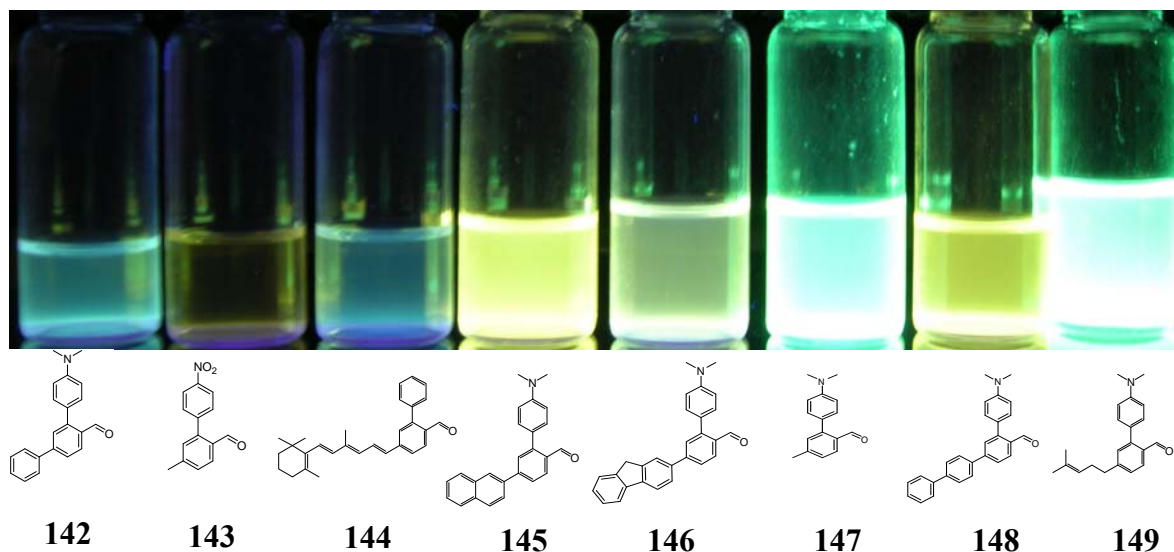


**Figure 58.** NMR predictions.

Citral with cinnamaldehyde products optimized conformations with an overlay of the cis and trans products. NMR predictions with computational (C) predictions with experimental (E) measurement of C-6 proton.

### *Aromatization and Fluorescence*

Interestingly, phenyl substituted cyclohexadienals, derived from cinnamaldehyde and its substituted analogs, were found to spontaneously aromatize (**Figure 59**) to give fluorescent molecules (over a period of one to several days) in about 5% to 15% conversion. Aromatization could also be invoked directly by reaction with potassium permanganate in quantitative yields.<sup>167</sup> With further experimentation, some of these molecules or their respective derivatives might therefore find use as fluorescent probes to identify the protein binding partner of a particular cyclohexadienal. Quantum yields<sup>168</sup>

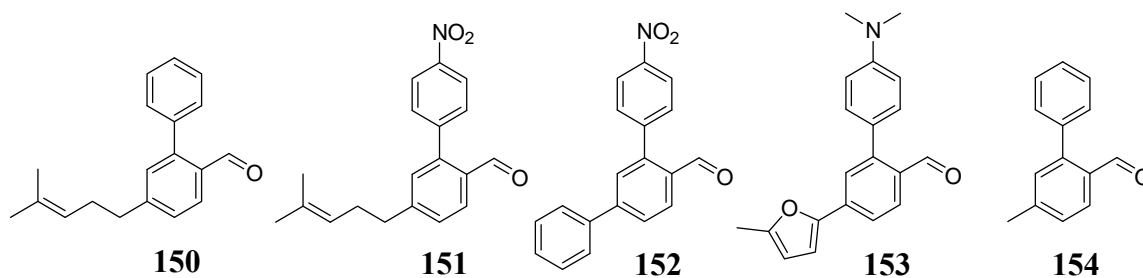


**Figure 59.** Representative set of fluorescing aromatized heterodimers.

were measured in dichloromethane and methanol (**Table 14**), for a subset of the molecules (**142-149**) including those that were most fluorescent as judged by exposure to UV light. Fluorescence measurements were not obtained for molecules **150-154** (**Figure 60**) as they demonstrated a small amount of fluorescence by UV light. In all cases, fluorescence of molecules was quenched in methanol. The highest quantum yields were obtained for compounds **147** and **149** (in dichloromethane), where the substituent at C-4 is not conjugated to the central aromatic ring. While nitro-substituted phenyl systems fluoresce mildly, the nitro-group was shown to significantly quench the quantum yield. Also, a crystal structure was obtained for compound **146** (See Appendix).

**Table 14.** Percent conversions and quantum yields of fluorescent cyclohexadienals.

Entry	% Conv.	<b>CH<sub>2</sub>Cl<sub>2</sub></b>			<b>MeOH</b>		
		$\lambda_{\text{abs}}$	$\lambda_{\text{em}}$	$\phi^a$	$\lambda_{\text{abs}}$	$\lambda_{\text{em}}$	$\phi^a$
<b>142</b>	10	368	490	0.025	360	503	0.008
<b>143</b>	14	368	559	0.016	368	413	0.002
<b>144</b>	7	368	474	0.042	374	598	0.056
<b>145</b>	13	374	520	0.112	384	434	0.005
<b>146</b>	14	368	526	0.046	368	497	0.044
<b>147</b>	11	363	502	0.699	354	396	0.002
<b>148</b>	15	368	519	0.088	368	515	0.005
<b>149</b>	8	368	501	0.312	368	522	0.010
<b>150</b>	7	--	--	--	--	--	--
<b>151</b>	5	--	--	--	--	--	--
<b>152</b>	14	--	--	--	--	--	--
<b>153</b>	11	--	--	--	--	--	--
<b>154</b>	6	--	--	--	--	--	--

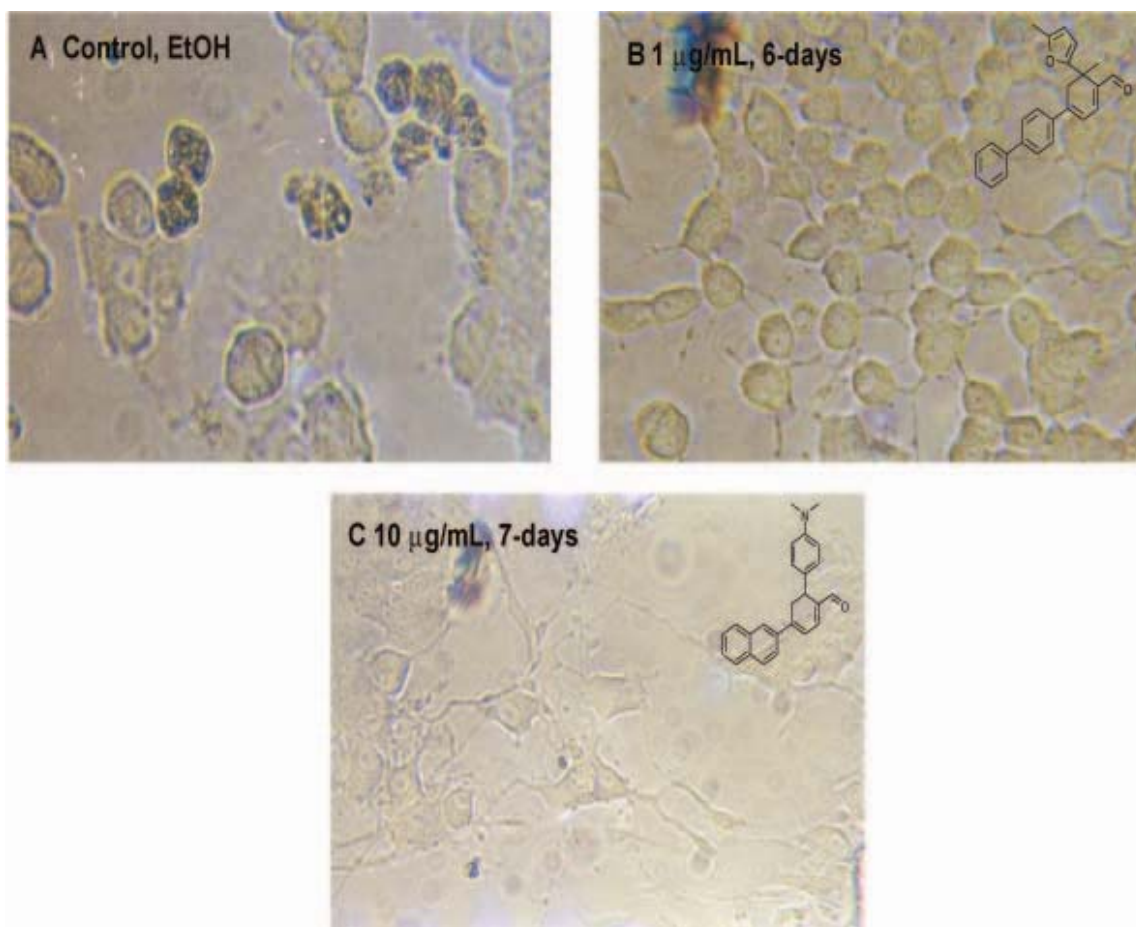
**Figure 60.** Representative structures of other aromatic compounds.*Effects on Neurite Outgrowth and General Cytotoxicity*

Given the demonstrated ability of retinoic acid and its analogs to modulate growth and cellular differentiation and the ability of a milk whey protein to generate cyclo- $\beta$ -ional, the cycloterpenal-based library of compounds was evaluated for their

ability to stimulate neurite outgrowth in a PC12 assay. PC12 cells are a pluripotent cell line that was originally cloned in 1976 from a transplantable rat pheochromocytoma and exhibits the ability to differentiate into neurons. The PC12 assay is a widely implemented method of identifying compounds that promote neurite outgrowth or survival.<sup>149</sup>

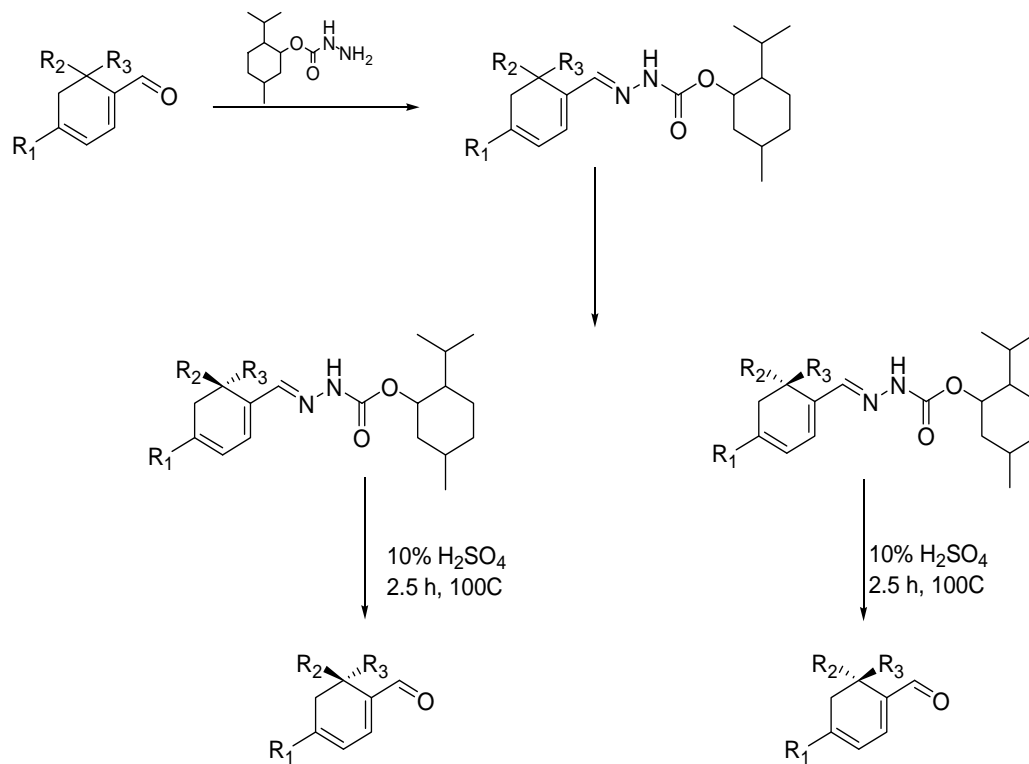
The PC12 cells were plated onto collagen Type IV plates at 10,000 cells /well, allowed to adhere for 24 hours, followed by the addition of compound at concentrations of 100, 10, and 1  $\mu\text{g/mL}$ , respectively. The cells were monitored over a period of two weeks, where the most pronounced effects were observed at about one week of exposure. From our library of cyclohexadienals, two heterodimers (**100** and **122**) were able to successfully stimulate neurite outgrowth (**Figure 61**). Therefore, neurite outgrowth activity appears to be associated with aromatic substituents. Intriguingly, biphenyl groups have been thought to serve as mimics of protein alpha helices.<sup>169</sup>

To assess the degree to which stereochemistry dictates phenotype in the neurite outgrowth assay, dimers **100** and **122** were derivatized into their corresponding menthylhydrazone derivatives<sup>150</sup> to allow separation of the stereoisomers by HPLC (**Scheme 17**). Following HPLC purification, the compounds were each hydrolyzed giving each aldehyde in enantiomerically pure form. Upon reanalysis in the PC12 assay, the *R*-configuration was shown to be responsible for neurite outgrowth activity while the *S*-configuration exhibited no activity (**Figure 46**). In the future, it will be interesting to establish whether the heterodimers that exhibit activity share the same target as the homodimers that possess neurite activity.



**Figure 61.** Stimulation of neurite outgrowth by cyclohexadienal heterodimers.  
(A) Control, cells treated with absolute ethanol; (B) methylfuran, biphenyl cyclohexadienals, 1 µg/mL at 6 days; (C) dimethylamino-phenyl, naphthyl-cyclohexadienal; 10 µg/mL at 7 days.



**Scheme 17.** Isolation of stereoisomers.

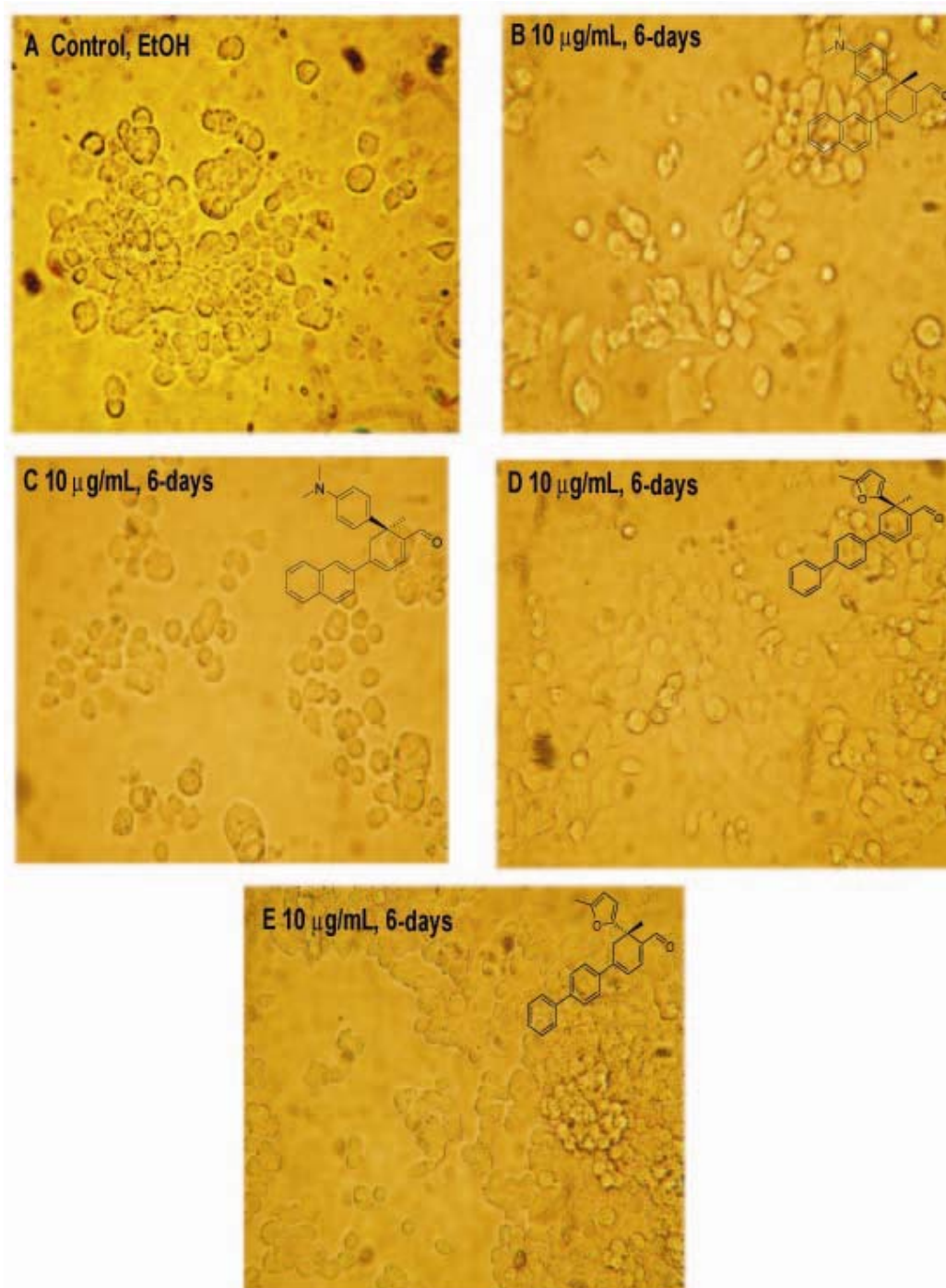


**Figure 62.** Stimulation of neurite outgrowth by heterodimer stereoisomers.

(A) Control, cells treated with absolute ethanol; (B) *R*-methylfuran, biphenyl cyclohexadienals, 10 µg/mL at 6 days; (C) *S*-methylfuran, biphenyl cyclohexadienals, 10 µg/mL at 6 days; (D) *R*-dimethylamino-phenyl, naphthyl-cyclohexadienal; 10 µg/mL at 6 days; (E) *S*-dimethylamino-phenyl, naphthyl-cyclohexadienal; 10 µg/mL at 6 days.

As cyclocitral **15** has been reported to possess antibiotic activity,<sup>39,88,151,152</sup> we also surveyed our cyclohexadienal library of compounds against bacterial strains (*Escherichia coli* and *Bacillus subtilis*) and yeast (*Saccharomyces cerevisiae*). All compounds were tested at three concentrations, 100, 10, and 1  $\mu\text{g/mL}$ . In most cases, moderate to no inhibition was observed, where compounds exhibited MIC values  $>100$   $\mu\text{g/mL}$ . Three compounds (**121**, **135**, and **147**) were reasonably active against *B. subtilis* with MIC values within the 10-25  $\mu\text{g/mL}$  range. Against Jurkats, a human T-cell Leukemia cell line, the effects were again moderate for the majority of compounds tested, a few (**94**, **98**, **106**, and **122**) demonstrated complete inhibition of growth at 1  $\mu\text{g/mL}$ .

## CONCLUSION

The retinoids have achieved prominence for their therapeutic benefits ranging from their ability to treat acne and skin blemishes to their ability to differentiate stem cells.<sup>17,27-30,166</sup> An unusual class of diterpenoid natural products, “cycloterpenals”, have been isolated from a variety of organisms including marine sponges and the human eye.<sup>33,34,39,88,89,151,152</sup> Moreover, incubation of the milk whey protein  $\beta$ -lactoglobulin with  $\beta$ -ionylideneacetaldehyde has been shown to give cycl- $\beta$ -ional.<sup>87</sup> As such, it is plausible that some of these cycloterpenals or their structurally and functionally related analogs could be important in developmental process such as neurite outgrowth.

In this chapter, we implemented a proline-promoted condensation reaction that enabled diversification of the cycloterpenals skeleton to give a library of molecules with varying degrees of substitution. Specific reaction conditions required to favor cross-

condensation as opposed to self-condensation were detailed. In the case of aromatic substituents, the cyclohexadiene ring system could be aromatized to give fluorescent molecules, which in the long term could lead to use of these molecules as probes in protein target identification of a particular cyclohexadienal.

The phenotypic effects of these cycloterpenals-based molecules were examined in a PC12 assay, where dramatic effects were observed on neurite outgrowth. These results suggest that molecules with this cyclohexadienal motif might have applications in neurite regeneration, which plays a significant role in the treatment of neurodegenerative diseases or central nervous system injuries.

## EXPERIMENTAL

### *General*

Fresh THF was dried by passage through an MBRAUN solvent purification system and stored over molecular sieves. All other solvents and reagents were purchased and used without further purification. Chemical shifts for  $^1\text{H}$  and  $^{13}\text{C}$  NMR spectra are reported in ppm referenced to TMS (0 ppm) and coupling constants are reported in Hertz (Hz). MS spectra were recorded on an API QSTAR PULSAR (ES) apparatus. IR spectra were recorded with a FT-IR spectrometer. Chromatographic separations were achieved by flash silica chromatography (silica gel 60 mesh, EMD Biosciences). The determination of ee's were done by  $\text{Pr}(\text{hfc})_3$  chiral shift reagent.  $\beta$ -methylenic aldehydes were synthesized by reduction of their corresponding nitriles,<sup>104</sup> which were derived from their respective methyl-ketone analogues.<sup>102</sup> In all cases, the

*all-trans* isomer was utilized except in the case of citral which was purchased as a mixture.

### *Organisms*

PC12 neuronal cells (CRL 1721) and *B. subtilis* strain 6633 were obtained from the American Type Culture Collection, Rockville, MD. The yeast *S. cerevisiae* wild-type strain [#404; BY4741; MATa his3 $\Delta$ 1 leu2 $\Delta$ 0 met15 $\Delta$ 0 ura3 $\Delta$ 0] was obtained from Dr. Michael Kladde at the Department of Biochemistry, Texas A&M University. The *E. coli* strain DH10B was obtained from Prof. Dennis Gross, Texas A&M University, Department of Plant Pathology.

### *Media Conditions*

- *LB* (Luria-Bertani) medium contained the following components per liter: Bacto-peptone, 10g; Yeast extract, 5g; Sodium chloride, 5g; and deionized water.
- *YPD* (Yeast Peptone Dextrose) medium contained the following components per liter: Yeast extract, 5g; Bacto-peptone, 5g; Glucose, 20 g; and deionized water.
- *NB* (Nutrient Broth) medium contained the following components per liter: Beef extract, 3g; Peptone, 5g; and deionized water.

Agar plates of the above media were prepared by adding 20 g/L bacto-agar. All media were autoclaved at 121 °C for 20 minutes.

### *Neurite Outgrowth Assay*

PC12 cells were maintained in 100 mm Collagen Type IV dishes at 37 °C in a 5% CO<sub>2</sub>/air temperature. The cell culture medium consisted of RPMI 1640, with 10%

heat-inactivated horse serum and 5% fetal bovine serum. Cells were removed from the culture flasks by flushing with fresh culture medium. Cells were then transferred to a 15 mL falcon tube and centrifuged for 15 min. at 1000 rpm. The medium was removed and the cells were resuspended in fresh culture medium. The cells were counted with a hemocytometer and replated in a 96 well Collagen Type IV plate at 10,000 cells/well with enough fresh medium to bring the volume to 200  $\mu$ L. The cells were allowed to adhere for 24 h prior to the addition of compound. Each cyclohexadienal compound was examined at three concentrations in duplicate, to give final concentrations of 100, 10 and 1  $\mu$ g/mL respectively. Each well was visually monitored over a period of 2 weeks for neurite outgrowth and intercellular connections. Fresh medium was added when necessary. Photographs were taken with an Olympus SP-310 camera equipped with a modified lens piece that fits over the microscope eyepiece.

#### *Cytotoxicity Assay Against Jurkat Cell Line*

Jurkat cells were maintained in 75 cm<sup>2</sup> culture flasks at 37 °C under a 5% CO<sub>2</sub> atmosphere. The cell culture medium consisted of RPMI 1640 with 10% fetal bovine serum. Cells were harvested by centrifugation (20 min. at 1000 rpm), resuspended in fresh culture medium and counted on a hemocytometer. The cells (1 mL) were arrayed (200,000 cells/well) in 48 well plates to which compound was added to give final concentrations of 100, 10 and 1  $\mu$ g/mL respectively. Cells were incubated for 24 h, transferred to 1.5 mL eppendorf tubes and centrifuged for 15 min. at 14,000 rpm. The medium was removed and the cell pellet resuspended in 1 mL of phosphate buffer saline (PBS) to wash the cells. The cells were again centrifuged for 15 min. at 14,000 rpm.

The PBS was removed and the cell pellet resuspended in a lysis buffer (CyQuant Cell Proliferation Kit). The stock solution, 20X, should be diluted to a final concentration 1X with an 80 fold dilution of propidium iodide in order to visualize 200,000 cells/well. The lysed cells were then placed in a black 96 well plate and analyzed using a Bio-Tek fluorometer to measure relative fluorescence.

#### *Anti-bacterial and Anti-fungal Assays*

Microbes (*Saccharomyces cerevisiae*, *Escherichia coli*, and *Bacillus subtilis* 6633) were cultured and maintained on agar plates (see supplemental material for media conditions). A single colony was used to inoculate 3 mL of culture medium and allowed to grow for 16 h. The cells (500  $\mu$ L) were diluted with 50 mL of fresh medium to an O.D. of 0.1 and aliquoted into a 96-well plate (100  $\mu$ L/well). The assays were set up in duplicate and the compounds tested to give final concentrations of 100, 10 and 1  $\mu$ g/mL. Plates were incubated (*E. coli* and *B. subtilis*, 37 °C; yeast, 30 °C) and shaken (250 rpm) for 16 h and cell density (O.D.) measured with a Bio-Tek microplate reader.

#### *NMR Analysis of Cinnamaldehyde Analogues-Schiff Base Reaction*

A 5 mm NMR tube was filled with 800  $\mu$ L of CD<sub>3</sub>OD and was placed in a 300 MHz NMR for shimming purposes. Once properly shimmed, another tube was filled 500  $\mu$ L of the various cinnamaldehyde derivatives (30 mg/mL) and the instrument was reshimmied. The reaction was started by ejecting the cinnamaldehyde and adding 1.5 eq. of the L-proline solution (30 mg/mL), shaking the tube, reinserting the tube into the NMR,

and immediately acquiring a spectrum that took a total time of 2 minutes. After the initial spectrum and periodically throughout the experiment, the instrument was reshimmed.

### *Theoretical Calculations*

The theoretical calculations were performed using the Gaussian 03 suite of programs.<sup>170</sup> All calculation were performed at the density functional theory (DFT)<sup>171</sup> level with the Becke three-parameter exchange functional (B3)<sup>172</sup> and the Lee-Yang-Parr correlation functional (LYP)<sup>173</sup> (B3LYP). Pople and co-workers' double- $\zeta$  quality basis set (BSI) with a polarization function on the heavy atoms (6-31G(d'))<sup>174-176</sup> was used for the geometry optimizations. All structures were fully optimized and frequency calculations were performed to guarantee that there were no imaginary modes. Pople's and co-workers' triple- $\zeta$  quality basis set with a diffuse function on heavy and light atoms, a double polarization functions on the heavy atoms and a polarization function on the light atoms (6-311++G(2d,p))<sup>176,177</sup> was employed for the NMR calculations. The d functions used spherical harmonic representations. The Gauge-Independent Atomic Orbital (GIAO) method<sup>178</sup> was used for the NMR calculations. Spin-spin coupling constants<sup>179</sup> were also calculated during the NMR calculations. Calculated proton chemical shifts were normalized again the average calculated proton chemical shifts for tetramethylsilane (TMS) ( $\delta = 31.77$  ppm).

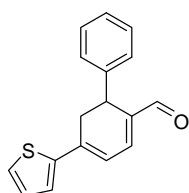
### *Synthesis of Cross-Condensation Productions*

The following is an example of the synthetic procedure for the synthesis of 4-(5-Methyl-furan-2-yl)-6-phenyl-cyclohexa-1,3-dienecarbaldehyde (**89**). The  $\alpha,\beta$ -



unsaturated compound cinnamaldehyde (33.0 mg, 1.5 equivalents) was dissolved in 200 proof ethanol (8 mL) with 3.4 equivalents (72.0 mg) of L-proline. After approximately 2 hours, at which point Schiff base formation is complete as monitored via thin layer chromatography (TLC), one equivalent of  $\beta$ -methylenic aldehyde 3-(5-methylfuran-2-yl)-but-2-enal (25 mg, 1 equivalent) was added to the reaction mixture and stirred at ambient temperatures for 18 hours. The reaction was monitored by TLC. Upon completion, the reaction was quenched by the addition of water (20 mL), extracted with a 1:1 ethyl acetate/hexanes solution (3 x 50 mL), and was washed with brine. The organic layer was dried over magnesium sulfate ( $\text{MgSO}_4$ ) and concentrated under vacuum. The crude product was purified by column chromatography (10% ethyl acetate/hexanes) to yield 12.7 mg of the final product (48% yield) as a red oil.

#### *Characterization of Cross Condensation Products*



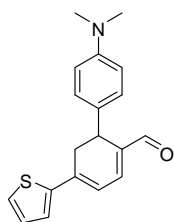
**6-phenyl-4-(thiophen-2-yl)cyclohexa-1,3-dienecarbaldehyde (86):**

$^1\text{H}$  NMR (300MHz,  $\text{CDCl}_3$ ,  $25^\circ\text{C}$ ),  $\delta$ =9.61 (s, 1H), 8.09-8.13 (m, 2H), 7.46 (d,  $J$ =9.0 Hz, 2H), 7.41 (d,  $J$ =5.1 Hz, 1H), 7.26-7.30 (m, 2H), 7.17 (d,  $J$ =6.0 Hz, 1H), 7.07-7.10 (m, 1H), 6.74 (dd,  $J$ =3.0, 6.0 Hz, 1H), 4.35 (dd,  $J$ =1.8, 9.6 Hz, 1H), 3.28 (qd,  $J$ =2.5, 9.6, 18.0 Hz, 1H), 3.12 (dd,  $J$ =1.9, 18.0 Hz, 1H)

$^{13}\text{C}$  NMR (75 MHz,  $\text{CDCl}_3$ ,  $25^\circ\text{C}$ )  $\delta$ =191.5 (CH), 150.2 (C), 144.1 (CH), 143.5 (C), 139.0 (C), 137.3 (C), 128.6 (2 x CH), 128.3 (2 x CH), 128.2 (CH), 126.5 (CH), 124.2 (2 x CH), 118.0 (CH), 34.6 ( $\text{CH}_2$ ), 33.9 (CH)

IR (neat)  $\nu$  3020, 2968, 2925, 2853, 2727, 1661, 1540, 1492, 1385, 1180, 844  $\text{cm}^{-1}$

HRMS (ESI) for  $\text{C}_{17}\text{H}_{14}\text{NOSLi}$  ( $\text{M}+\text{Li}$ ) $^+$ : calcd 273.0925, found 273.0833.



**6-(4-Dimethylamino-phenyl)-4-thiophen-2-yl-cyclohexa-1,3-**

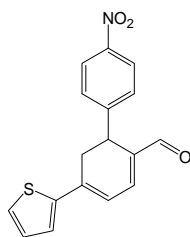
**dienecarbaldehyde (87):**

$^1\text{H}$  NMR (300MHz,  $\text{CDCl}_3$ ,  $25^\circ\text{C}$ ),  $\delta$ =9.55 (s, 1H), 7.33 (d,  $J$ =4.5 Hz, 1H), 7.24 (d,  $J$ =3.6 Hz, 1H), 7.17 (d,  $J$ =7.8 Hz, 2H), 7.02-7.05 (m, 1H), 6.99 (d,  $J$ =6.0 Hz, 1H), 6.58-6.70 (m, 3H), 6.14 (dd,  $J$ =3.9, 7.5 Hz, 1H), 3.12-3.15 (m, 2H), 2.88 (s, 6H)

$^{13}\text{C}$  NMR (75 MHz,  $\text{CDCl}_3$ ,  $25^\circ\text{C}$ )  $\delta$ =192.1 (CH), 145.8 (C), 142.9 (C), 142.0 (C), 139.2 (CH), 136.8 (C), 133.1 (C), 128.4 (2 x CH), 128.2 (CH), 128.0 (CH), 127.3 (CH), 126.1 (CH), 118.1 (2 x CH), 34.2 (2 x  $\text{CH}_3$ ) 33.6 ( $\text{CH}_2$ ), 29.9 (CH)

IR (neat)  $\nu$  2923, 2853, 1664, 1541, 1519, 1456, 1201, 1169, 969, 821, 701  $\text{cm}^{-1}$

HRMS (ESI) for  $\text{C}_{19}\text{H}_{19}\text{NOS}$  ( $\text{M}+\text{H}$ ) $^+$ : calcd 310.1266, found 310.1237.



**6-(4-Nitro-phenyl)-4-thiophen-2-yl-cyclohexa-1,3-dienecarbaldehyde**

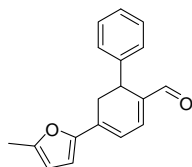
**(88):**

$^1\text{H}$  NMR (300MHz,  $\text{CDCl}_3$ ,  $25^\circ\text{C}$ ),  $\delta$ =9.57 (s, 1H), 8.07 (d,  $J$ =9.0 Hz, 2H), 7.43 (d,  $J$ =8.7 Hz, 2H), 7.37 (dd,  $J$ =0.9, 5.1 Hz, 1H), 7.24 (dd,  $J$ =1.2, 3.9 Hz, 1H), 7.14 (d,  $J$ =6.0 Hz, 1H), 7.03-7.06 (m, 1H), 6.70 (dd,  $J$ =2.4, 6.0 Hz, 1H), 4.31 (dd,  $J$ =2.1, 9.6 Hz, 1H), 3.24 (qd,  $J$ =2.7, 9.9, 17.7 Hz, 1H), 3.08 (dd,  $J$ =2.1, 18.0 Hz, 1H)

$^{13}\text{C}$  NMR (75 MHz,  $\text{CDCl}_3$ ,  $25^\circ\text{C}$ )  $\delta$ =191.5 (CH), 150.2 (C), 147.2 (C), 144.1 (CH), 143.4 (C), 139.0 (C), 137.2 (C), 128.6 (CH), 128.3 (2 x CH), 128.1 (CH), 126.5 (CH), 124.1 (2 x CH), 118.0 (CH), 34.5 (CH), 33.8 ( $\text{CH}_2$ )

IR (neat)  $\nu$  3108, 3075, 2924, 2817, 2717, 1738, 1659, 1539, 1512, 1341, 1168, 1027, 853, 826,  $698\text{ cm}^{-1}$

HRMS (ESI) for  $\text{C}_{17}\text{H}_{13}\text{NO}_3\text{S}$  ( $\text{M}+\text{Li}$ ) $^+$ : calcd 312.0694, found 312.0789.



**4-(5-Methyl-furan-2-yl)-6-phenyl-cyclohexa-1,3-dienecarbaldehyde**

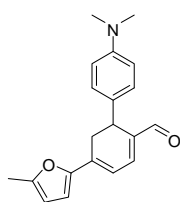
**(89):**

$^1\text{H}$  NMR (300MHz,  $\text{CDCl}_3$ ,  $25^\circ\text{C}$ ),  $\delta$ = 9.54 (s, 1H), 7.12-7.28 (m, 5H), 7.10 (d,  $J$ =6.3 Hz, 1H), 6.68 (dd,  $J$ = 2.6, 6.2 Hz, 1H), 6.45 (d,  $J$ =3.3 Hz, 1H), 6.05-6.06 (m, 1H), 4.19 (dd,  $J$ =1.8, 9.3 Hz, 1H), 2.87-3.09 (m, 2H), 2.34 (s, 3H)

$^{13}\text{C}$  NMR (75 MHz,  $\text{CDCl}_3$ ,  $25^\circ\text{C}$ )  $\delta$ =191.9 (CH), 155.2 (C), 151.9 (C), 144.1 (CH), 142.9 (C), 137.9 (C), 134.0 (C), 128.7 (2 x CH), 127.4 (2 x CH), 127.0 (CH), 115.1 (CH), 112.6 (CH), 108.9 (CH), 34.0 (CH), 31.5 ( $\text{CH}_2$ ), 14.2 ( $\text{CH}_3$ )

IR (neat)  $\nu$  3012, 2962, 2941, 2326, 1735, 1431, 1365, 1229, 1211, 1206, 913  $\text{cm}^{-1}$

HRMS (ESI) for  $\text{C}_{18}\text{H}_{16}\text{O}_2\text{Li}$  ( $\text{M}+\text{Li}$ ) $^+$ : calcd 271.1310, found 271.1365.



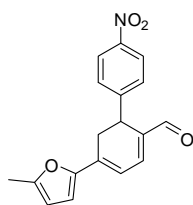
**6-(4-Dimethylamino-phenyl)-4-(5-methyl-furan-2-yl)-cyclohexa-1,3-**

**dienecarbaldehyde (90):**  $^1\text{H}$  NMR (300MHz,  $\text{CDCl}_3$ ,  $25^\circ\text{C}$ ),  $\delta$ =9.52 (s, 1H), 7.14 (d,  $J$ =8.7 Hz, 2H), 7.03 (d,  $J$ =6.0 Hz, 1H), 6.67 (dd,  $J$ =2.1, 6.0 Hz, 1H), 6.61 (d,  $J$ =8.7 Hz, 2H), 6.45 (d,  $J$ =3.3 Hz, 1H), 6.04-6.06 (m, 1H), 4.11 (dd,  $J$ =2.4, 9.3 Hz, 1H), 2.92-3.05 (m, 2H), 2.86 (s, 6H), 2.34 (s, 3H)

$^{13}\text{C}$  NMR (75 MHz,  $\text{CDCl}_3$ ,  $25^\circ\text{C}$ )  $\delta$ =192.2 (CH), 155.0 (C), 152.1 (C), 149.9 (C), 143.4 (CH), 138.5 (C), 134.1 (C), 131.2 (CH), 128.1 (2 x CH), 115.1 (2 x CH), 113.1 (CH), 112.4 (CH), 108.9 (CH), 41.0 (2 x  $\text{CH}_3$ ), 33.1 (CH), 31.5 ( $\text{CH}_2$ ), 14.2 ( $\text{CH}_3$ )

IR (neat)  $\nu$  3010, 2983, 2371, 1740, 1730, 1662, 1595, 1536, 1520, 1350, 1220  $\text{cm}^{-1}$

HRMS (ESI) for  $\text{C}_{20}\text{H}_{21}\text{NO}_2$  ( $\text{M}+\text{H}$ ) $^+$ : calcd 308.1651, found 308.1658.



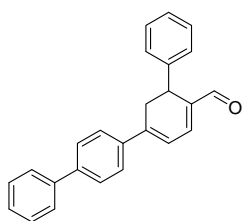
**4-(5-Methyl-furan-2-yl)-6-(4-nitro-phenyl)-cyclohexa-1,3-**

**dienecarbaldehyde (91):**  $^1\text{H}$  NMR (300MHz,  $\text{CDCl}_3$ ,  $25^\circ\text{C}$ ),  $\delta$ =9.56 (s, 1H), 8.09 (d,  $J$ =8.7 Hz, 2H), 7.44 (d,  $J$ =9.0 Hz, 2H), 7.20 (d,  $J$ =6.0, 1H), 6.73 (dd,  $J$ =2.6, 6.1 Hz, 1H), 6.50 (d,  $J$ =3.3 Hz, 1H), 6.08 (dd,  $J$ =0.6, 3.3 Hz, 1H), 4.25-4.30 (m, 1H), 3.08 (qd,  $J$ =2.7, 8.7 Hz, 1H), 2.87 (m, 1H), 2.35 (s, 3H)

$^{13}\text{C}$  NMR (75 MHz,  $\text{CDCl}_3$ ,  $25^\circ\text{C}$ )  $\delta$ =191.5 (CH), 155.8 (C), 151.4 (C), 150.3 (C), 144.7 (CH), 136.5 (C), 133.7 (C), 133.2 (C), 129.9 (CH), 128.3 (2 x CH), 124.0 (2 x CH), 115.0 (CH), 113.1 (CH), 34.1 ( $\text{CH}_2$ ), 31.2 (CH), 14.2 ( $\text{CH}_3$ )

IR (neat)  $\nu$  3006, 2990, 2925, 1720, 1662, 1538, 1521, 1345, 1276, 1261, 1173, 764, 750  $\text{cm}^{-1}$

HRMS (ESI) for  $\text{C}_{18}\text{H}_{15}\text{NO}_4\text{Li}$  ( $\text{M}+\text{Li}$ ) $^+$ : calcd 316.1161, found 316.1011.



**4-Biphenyl-4-yl-6-phenyl-cyclohexa-1,3-dienecarbaldehyde (92):**

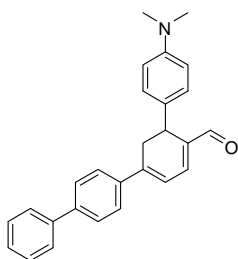
$^1\text{H}$  NMR (300MHz,  $\text{CDCl}_3$ ,  $25^\circ\text{C}$ ),  $\delta$ =9.63 (s, 1H), 7.56-7.66 (m, 5H), 7.29-7.53 (m, 6H), 7.16-7.25 (m, 3H), 7.14 (d,  $J$ =6.0 Hz, 1H), 7.75 (dd,  $J$ =2.4, 6.0 Hz, 1H), 4.27 (dd,  $J$ =2.7, 9.3 Hz, 1H), 3.14-3.32 (m, 2H)

$^{13}\text{C}$  NMR (75 MHz,  $\text{CDCl}_3$ ,  $25^\circ\text{C}$ )  $\delta$ =192.3 (CH), 145.2 (C), 143.7 (CH), 142.7 (C), 142.0 (C), 140.4 (C), 138.8 (C), 138.3 (C), 129.1 (2 x CH), 128.8 (2 x CH), 128.0 (CH),

127.6 (2 x CH), 127.4 (2 x CH), 127.2 (2 x CH), 127.1 (CH), 126.5 (2 x CH), 119.9 (CH), 34.6 (CH), 34.1 (CH<sub>2</sub>)

IR (neat)  $\nu$  3028, 2971, 2948, 2131, 1738, 1664, 1448, 1366, 1229, 1217, 1206, 896, 763, 696 cm<sup>-1</sup>

HRMS (ESI) for C<sub>25</sub>H<sub>20</sub>OLi (M+Li)<sup>+</sup>: calcd 343.1674, found 343.1673.



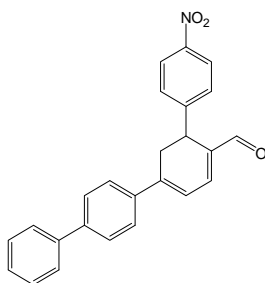
**4-(biphenyl-4-yl)-6-(4-(dimethylamino)phenyl)cyclohexa-1,3-**

**dienecarbaldehyde (93):** <sup>1</sup>H NMR (300MHz, CDCl<sub>3</sub>, 25°C),  $\delta$ =9.61 (s, 1H), 7.25-7.59 (m, 9H), 7.20-7.26 (m, 2H), 7.08 (d, J=5.7, 1H), 6.67-6.74 (m, 3H), 4.16-4.20 (m, 1H), 3.00-3.28 (m, 8H)

<sup>13</sup>C NMR (75 MHz, CDCl<sub>3</sub>, 25°C)  $\delta$ =192.6 (CH), 149.6 (C), 145.2 (C), 143.1 (CH), 141.9 (C), 140.5 (C), 139.4 (C), 138.5 (C), 131.4 (C), 129.1 (2 x CH), 128.1 (2 x CH), 127.5 (2 x CH), 127.2 (2 x CH), 126.5 (2 x CH), 122.0 (CH), 119.9 (CH), 113.3 (2 x CH), 41.1 (2 x CH<sub>3</sub>), 34.1 (CH<sub>2</sub>), 36.6 (CH)

IR (neat)  $\nu$  3008, 2971, 2382, 2354, 1739, 1670, 1366, 1275, 1217, 750 cm<sup>-1</sup>

HRMS (ESI) for C<sub>27</sub>H<sub>25</sub>NO (M+Li)<sup>+</sup>: calcd 386.2096, found 386.2049.



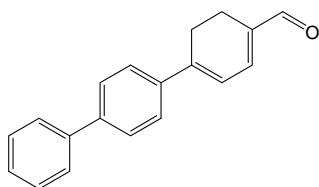
**4-Biphenyl-4-yl-6-(4-nitro-phenyl)-cyclohexa-1,3-**

**dienecarbaldehyde (94):**  $^1\text{H}$  NMR (300MHz,  $\text{CDCl}_3$ ,  $25^\circ\text{C}$ ),  $\delta$ =9.62 (s, 1H), 8.08 (d,  $J$ =8.7 Hz, 2H), 7.34-7.66 (m, 11H), 7.21 (d,  $J$ =6.0 Hz, 1H), 6.78 (dd,  $J$ =2.7, 6.0, 1H), 4.34 (dd,  $J$ =1.5, 9.9, 1H), 3.31 (qd,  $J$ =2.7, 9.9, 18.0, 1H), 3.13 (dd,  $J$ =1.8, 17.9, 1H)

$^{13}\text{C}$  NMR (75 MHz,  $\text{CDCl}_3$ ,  $25^\circ\text{C}$ )  $\delta$ =191.9 (CH), 150.2 (C), 147.2 (C), 145.1 (C), 144.3 (CH), 142.5 (C), 140.2 (C), 137.7 (C), 137.4 (C), 129.2 (2 x CH), 128.3 (2 x CH), 128.1 (CH), 127.7 (2 x CH), 127.2 (2 x CH), 126.5 (2 x CH), 124.1 (2 x CH), 119.9 (CH), 34.6 (CH), 33.7(CH<sub>2</sub>)

IR (neat)  $\nu$  3029, 2971, 2925, 1738, 1663, 1597, 1516, 1345, 1229, 1217, 1110, 832, 764, 697  $\text{cm}^{-1}$

HRMS (ESI) for  $\text{C}_{25}\text{H}_{19}\text{NO}_3\text{Li}$  ( $\text{M}+\text{Li}$ )<sup>+</sup>: calcd 388.1525, found 388.1575.



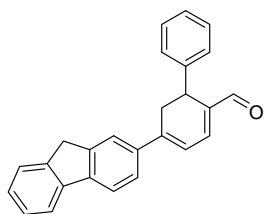
**4-Biphenyl-4-yl-cyclohexa-1,3-dienecarbaldehyde (95):**  $^1\text{H}$

NMR (300MHz,  $\text{CDCl}_3$ ,  $25^\circ\text{C}$ ),  $\delta$ =9.62 (s, 1H), 7.62-7.69 (m, 5H), 7.47-7.52 (m, 2H), 7.37-7.43 (m, 1H), 6.99 (d,  $J$ =5.7 Hz, 1H), 6.70 (d,  $J$ =5.7 Hz, 1H), 2.79-2.86 (m, 2H), 2.62-2.69 (m, 2H)

$^{13}\text{C}$  NMR (75 MHz,  $\text{CDCl}_3$ ,  $25^\circ\text{C}$ )  $\delta$ =192.7 (CH), 146.6 (C), 143.8 (CH), 141.8 (C), 140.5 (C), 138.5 (C), 136.7 (C), 129.2 (2 x CH), 127.9 (CH), 127.6 (2 x CH), 127.2 (2 x CH), 126.4 (2 x CH), 120.4 (CH), 25.9 ( $\text{CH}_2$ ), 19.1 ( $\text{CH}_2$ )

IR (neat)  $\nu$  3000, 2993, 2950, 1784, 1765, 1740, 1654, 1383, 1367, 1258, 1056,  $832\text{ cm}^{-1}$

HRMS (ESI) for  $\text{C}_{19}\text{H}_{16}\text{OLi}$  ( $\text{M}+\text{Li}$ ) $^+$ : calcd 267.1361, found 267.1423.



**4-(9H-fluoren-2-yl)-6-phenylcyclohexa-1,3-dienecarbaldehyde**

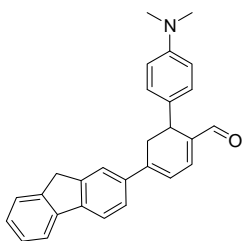
**(96):**  $^1\text{H}$  NMR (300MHz,  $\text{CDCl}_3$ ,  $25^\circ\text{C}$ ),  $\delta$ =9.62 (s, 1H), 7.74-7.80 (m, 2H), 7.67-7.68 (m, 1H), 7.52- 7.56 (m, 2H), 7.29-7.44 (m, 5H), 7.12-7.26 (m, 3H), 6.74 (dd,  $J$ =2.4, 6.0 Hz, 1H), 4.27 (dd,  $J$ =2.7, 9.0 Hz, 1H), 3.90 (s, 2H), 3.22-3.34 (m, 2H)

$^{13}\text{C}$  NMR (75 MHz,  $\text{CDCl}_3$ ,  $25^\circ\text{C}$ )  $\delta$ =192.3 (CH), 146.1 (C), 144.0 (C), 143.9 (CH), 143.0 (C), 142.9 (C), 141.2 (C), 138.6 (C), 138.5 (C), 138.0 (C), 128.8 (2 x CH), 127.5 (CH), 127.4 (2 x CH), 127.2 (CH), 127.1 (CH), 125.4 (CH), 125.1 (CH), 122.7 (CH), 120.4 (CH), 120.2 (CH), 119.6 (CH), 37.1 ( $\text{CH}_2$ ), 34.7 (CH), 34.4 ( $\text{CH}_2$ )

IR (neat)  $\nu$  3026, 2971, 2947, 2865, 1738, 1664, 1544, 1366, 1229, 1217, 1206, 1173,  $769\text{ cm}^{-1}$

HRMS (ESI) for  $\text{C}_{26}\text{H}_{20}\text{O}$  ( $\text{M}+\text{H}$ ) $^+$ : calcd 355.1674, found 355.1774.



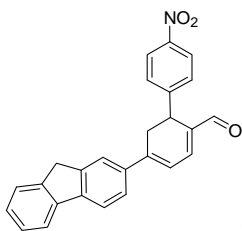


**6-(4-Dimethylamino-phenyl)-4-(9H-fluoren-2-yl)-cyclohexa-1,3-dienecarbaldehyde (97):**  $^1\text{H}$  NMR (300MHz,  $\text{CDCl}_3$ ,  $25^\circ\text{C}$ ),  $\delta=9.63$  (s, 1H), 7.73-7.83 (m, 3H), 7.59 (d,  $J=8.1$  Hz, 1H), 7.33-7.51 (m, 3H), 7.21 (d,  $J=8.4$  Hz, 2H), 7.10 (d,  $J=6.0$  Hz, 1H), 6.76 (dd,  $J=2.1, 6.0$  Hz, 1H), 6.72 (d,  $J=9.0$  Hz, 2H), 4.20 (dd,  $J=3.3, 8.1$  Hz, 1H), 3.93 (s, 2H), 3.26 (dd,  $J=2.1, 7.5$  Hz, 1H), 3.05-3.10 (m, 7H)

$^{13}\text{C}$  NMR (75 MHz,  $\text{CDCl}_3$ ,  $25^\circ\text{C}$ )  $\delta=192.6$  (CH), 154.3 (C), 152.7 (C), 146.2 (C), 144.0 (CH), 143.9 (C), 143.3 (C), 142.9 (C), 141.3 (C), 139.2 (C), 138.3 (C), 130.8 (2 x CH), 127.4 (CH), 127.2 (CH), 125.4 (CH), 125.1 (CH), 124.1 (CH), 122.7 (CH), 120.2 (CH), 119.6 (CH), 112.0 (2 x CH), 40.4 (2 x  $\text{CH}_3$ ), 37.2 ( $\text{CH}_2$ ), 34.4 ( $\text{CH}_2$ ), 33.7 (CH)

IR (neat)  $\nu$  3049, 2957, 2926, 2891, 2852, 1712, 1672, 1597, 1523, 1456, 1358, 1264, 1197, 1119, 823, 769, 735  $\text{cm}^{-1}$

HRMS (ESI) for  $\text{C}_{28}\text{H}_{25}\text{NO}$  ( $\text{M}+\text{H}$ ) $^+$ : calcd 392.2014, found 392.2039.



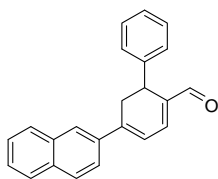
**4-(9H-Fluoren-2-yl)-6-(4-nitro-phenyl)-cyclohexa-1,3-dienecarbaldehyde (98):**  $^1\text{H}$  NMR (300MHz,  $\text{CDCl}_3$ ,  $25^\circ\text{C}$ ),  $\delta=9.66$  (s, 1H), 8.11 (d,  $J=8.7$  Hz, 2H), 7.79-7.89 (m, 2H), 7.53-7.73 (m, 2H), 7.49 (d,  $J=8.7$  Hz, 2H), 7.31-7.43

(m, 3H), 7.25 (d, J=6.3 Hz, 1H), 6.82 (dd, J=2.7, 5.7 Hz, 1H), 4.38 (dd, J=2.4, 10.2 Hz, 1H), 3.94 (s, 2H), 3.37 (qd, J=2.1, 10.2, 17.7 Hz, 1H), 3.20 (dd, J=2.1, 17.7 Hz, 1H)

$^{13}\text{C}$  NMR (75 MHz,  $\text{CDCl}_3$ , 25°C)  $\delta$ =191.9 (CH), 147.2 (C), 146.0 (C), 145.2 (C), 144.5 (C), 144.1 (CH), 143.9 (C), 143.5 (C), 141.1 (C), 137.4 (C), 137.2 (C), 128.4 (2 x CH), 127.7 (CH), 127.3 (CH), 125.4 (CH), 125.1 (CH), 124.1 (2 x CH), 123.9 (CH), 122.7 (CH), 120.6 (CH), 120.4 (CH), 37.2 ( $\text{CH}_2$ ), 34.7 ( $\text{CH}_2$ ), 34.1 (CH)

IR (neat)  $\nu$  3054, 3030, 2971, 2924, 2853, 1737, 1662, 1594, 1517, 1344, 1108, 854, 826, 733  $\text{cm}^{-1}$

HRMS (ESI) for  $\text{C}_{26}\text{H}_{19}\text{NO}_3$  ( $\text{M}+\text{H}$ ) $^+$ : calcd 394.1443, found 394.1412.



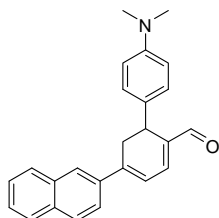
**4-(naphthalen-2-yl)-6-phenylcyclohexa-1,3-dienecarbaldehyde (99):**

$^1\text{H}$  NMR (300MHz,  $\text{CDCl}_3$ , 25°C),  $\delta$ =9.63 (s, 1H), 7.79-7.92 (m, 3H), 7.65 (dd, J=1.8, 8.7 Hz, 2H), 7.46-7.54 (m, 3H), 7.14-7.32 (m, 5H), 6.83 (dd, J=1.8, 6.0 Hz, 1H), 4.29 (dd, J=4.2, 12.0 Hz, 1H), 3.30 (m, 2H)

$^{13}\text{C}$  NMR (75 MHz,  $\text{CDCl}_3$ , 25°C),  $\delta$ =192.4 (CH), 145.4 (C), 143.6 (CH), 142.8 (C), 138.8 (C), 136.6 (C), 133.7 (C), 133.4 (C), 128.8 (2 x CH), 128.7 (CH), 128.6 (CH), 127.8 (CH), 127.4 (2 x CH), 127.1 (CH), 127.0 (CH), 126.8 (CH), 125.6 (CH), 123.6 (CH), 120.4 (CH), 34.6 (CH), 34.0 ( $\text{CH}_2$ )

IR (neat)  $\nu$  3055, 2924, 2810, 2717, 1666, 1547, 1395, 1374, 1169, 842, 814, 749, 699  $\text{cm}^{-1}$

HRMS (ESI) for C<sub>23</sub>H<sub>18</sub>O (M+Li)<sup>+</sup>: calcd 317.1518, found 317.1466.



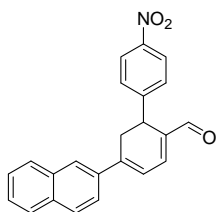
**6-(4-(dimethylamino)phenyl)-4-(naphthalen-2-yl)cyclohexa-1,3-**

**dienecarbaldehyde (100):** <sup>1</sup>H NMR (300MHz, CDCl<sub>3</sub>, 25°C), δ=9.61 (s, 1H), 7.94 (s, 1H), 7.82 (m, 3H), 7.67 (dd, J=1.8, 8.7 Hz, 1H), 7.47 (m, 2H), 7.18 (d, J=8.7 Hz, 2H), 7.07 (d, J=6.0, 1H), 6.81 (d, J=6.0 Hz, 1H), 6.58 (d, J=8.7 Hz, 2H), 4.19 (t, J=6.0 Hz, 1H), 3.28 (d, J=6.0 Hz, 2H), 2.84 (s, 6H)

<sup>13</sup>C NMR (75 MHz, CDCl<sub>3</sub>, 25°C), δ=192.6 (CH), 151.6 (C), 145.4 (C), 142.9 (CH), 140.9 (C), 137.8 (C), 135.7 (C), 134.1 (C), 133.5 (C), 128.7 (CH), 128.5 (CH), 128.1 (2 x CH), 127.8 (CH), 126.9 (CH), 126.8 (CH), 125.6 (CH), 123.7 (CH), 120.3 (CH), 112.9 (2 x CH), 40.8 (2 x CH<sub>3</sub>), 34.0 (CH<sub>2</sub>), 33.7 (CH)

IR (neat) ν 2932, 2850, 1668, 1547, 1521, 1169, 817 cm<sup>-1</sup>

HRMS (ESI) for C<sub>25</sub>H<sub>23</sub>NO (M+H)<sup>+</sup>: calcd 354.1858, found 354.1904.



**4-Naphthalen-2-yl-6-(4-nitro-phenyl)-cyclohexa-1,3-**

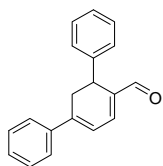
**dienecarbaldehyde (101):** <sup>1</sup>H NMR (300MHz, CDCl<sub>3</sub>, 25°C), δ=9.67 (s, 1H), 8.10 (d, J=9.0 Hz, 2H), 7.94 (s, 1H), 7.83-7.88 (m, 3H), 7.66 (dd, J=1.8, 8.7 Hz, 1H), 7.48-7.56

(m, 4H), 7.26 (d, J=6.0 Hz, 1H), 6.90 (dd, J=2.7, 6.0 Hz, 1H), 4.41 (dd, J=2.1, 9.6 Hz, 1H), 3.42 (qd, J=2.4, 9.6, 17.7 Hz, 1H), 3.28 (dd, J=2.1, 17.7 Hz, 1H)

$^{13}\text{C}$  NMR (75 MHz,  $\text{CDCl}_3$ , 25°C),  $\delta$ =192.0 (CH), 150.2 (C), 147.2 (C), 145.3 (C), 144.3 (CH), 137.5 (C), 136.0 (C), 133.9 (C), 133.4 (C), 128.9 (CH), 128.8 (CH), 128.4 (2 x CH), 127.9 (CH), 127.4 (CH), 127.1 (CH), 125.7 (CH), 124.1 (2 x CH), 123.4 (CH), 120.4 (CH), 37.7 ( $\text{CH}_2$ ), 33.8 (CH)

IR (neat)  $\nu$  3055, 2922, 2851, 1671, 1598, 1544, 1505, 1455, 1373, 1259, 1016, 857, 814, 788, 747  $\text{cm}^{-1}$

HRMS (ESI) for  $\text{C}_{235}\text{H}_{17}\text{NO}_3$  ( $\text{M}+\text{Li}$ ) $^+$ : calcd 362.1368, found 362.1384.



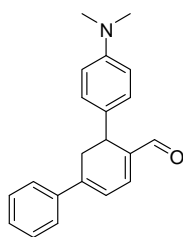
**4,6-diphenylcyclohexa-1,3-dienecarbaldehyde (102):**  $^1\text{H}$  NMR

(300MHz,  $\text{CDCl}_3$ , 25°C),  $\delta$ =9.61 (s, 1H), 7.45-7.50 (m, 2H), 7.32-7.41 (m, 3H), 7.28-7.30 (m, 1H), 7.20-7.24 (m, 2H), 7.17-7.19 (m, 2H), 7.12 (d, J=6.0 Hz, 1H), 6.67 (dd, J=2.7, 6.0 Hz, 1H), 4.24 (dd, J=2.1, 9.6 Hz, 1H), 3.08-3.29 (m, 2H)

$^{13}\text{C}$  NMR (75 MHz,  $\text{CDCl}_3$ , 25°C)  $\delta$ =191.2 (CH), 144.5 (C), 142.6 (CH), 141.4 (C), 138.3 (C), 137.5 (C), 128.0 (CH), 127.7 (2 x CH), 127.5 (2 x CH), 126.1 (2 x CH), 125.8 (CH), 124.8 (2 x CH), 118.8 (CH), 33.3 (CH), 33.0 ( $\text{CH}_2$ )

IR (neat)  $\nu$  3028, 2926, 2813, 2720, 2382, 2332, 2310, 1662, 1551, 1170, 757  $\text{cm}^{-1}$

HRMS (ESI) for  $\text{C}_{19}\text{H}_{16}\text{OLi}$  ( $\text{M}+\text{Li}$ ) $^+$ : calcd 267.1361, found 267.1368.



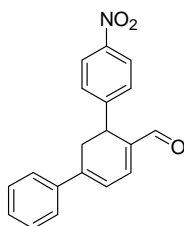
**6-(4-(dimethylamino)phenyl)-4-phenylcyclohexa-1,3-**

**dienecarbaldehyde (103):**  $^1\text{H}$  NMR (300MHz,  $\text{CDCl}_3$ ,  $25^\circ\text{C}$ ),  $\delta$ =9.60 (s, 1H), 7.44-7.50 (m, 2H), 7.32-7.41 (m, 5H), 7.18 (d,  $J$ =9.0 Hz, 2H), 7.13 (d,  $J$ =6.0 Hz, 1H), 6.67-6.70 (m, 1H), 4.22 (dd,  $J$ =1.5, 9.9 Hz, 1H), 3.19-3.30 (m, 1H), 3.08-3.10 (m, 1H), 3.04 (s, 6H)

$^{13}\text{C}$  NMR (75 MHz,  $\text{CDCl}_3$ ,  $25^\circ\text{C}$ )  $\delta$ =194.16 (CH), 152.6 (C), 145.8 (C), 143.2 (CH), 141.2 (C), 139.8 (C), 139.2 (C), 130.8 (2 x CH), 128.9 (CH), 128.2 (CH), 126.1 (CH), 124.0 (CH), 122.0 (CH), 120.0 (CH), 112.0 (2 x CH), 40.3 (2 x  $\text{CH}_3$ ), 34.2 ( $\text{CH}_2$ ), 33.7 (CH)

IR (neat)  $\nu$  2962, 2922, 2382, 2327, 2310, 1665, 1595, 1527, 1369, 1137, 809  $\text{cm}^{-1}$

LRMS (APCI) for  $\text{C}_{21}\text{H}_{21}\text{ON}$  ( $\text{M}+\text{H}$ ) $^+$ : calcd 304.2, found 304.3.



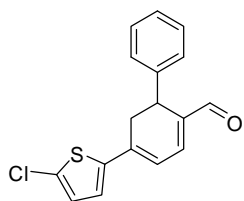
**6-(4-Nitro-phenyl)-4-phenyl-cyclohexa-1,3-dienecarbaldehyde (104):**

$^1\text{H}$  NMR (300MHz,  $\text{CDCl}_3$ ,  $25^\circ\text{C}$ ),  $\delta$ =9.62 (s, 1H), 8.07 (d,  $J$ =8.7 Hz, 2H), 7.34-7.48 (m, 7H), 7.20 (d,  $J$ =6.0 Hz, 1H), 6.71 (dd,  $J$ =2.7, 6.0 Hz, 1H), 4.32 (dd,  $J$ =1.8, 9.9 Hz, 1H), 3.29 (qd,  $J$ =2.7, 9.9, 17.7 Hz, 1H), 3.08 (dd,  $J$ =1.8, 17.7 Hz, 1H)

$^{13}\text{C}$  NMR (75 MHz,  $\text{CDCl}_3$ ,  $25^\circ\text{C}$ )  $\delta$ =191.9 (CH), 150.1 (C), 147.2 (C), 145.6 (C), 144.3 (CH), 139.0 (C), 137.5 (C), 129.7 (CH), 129.1 (2 x CH), 128.3 (2 x CH), 126.0 (2 x CH), 124.1 (2 x CH), 120.1 (CH), 34.6 (CH), 33.9 ( $\text{CH}_2$ )

IR (neat)  $\nu$  3057, 3029, 2971, 2925, 2854, 2825, 2719, 1739, 1662, 1596, 1551, 1514, 1343, 1171, 852, 766,  $696\text{ cm}^{-1}$

HRMS (ESI) for  $\text{C}_{19}\text{H}_{15}\text{O}_3\text{N}$  ( $\text{M}+\text{Li}^+$ ): calcd 312.1212, found 312.1198.



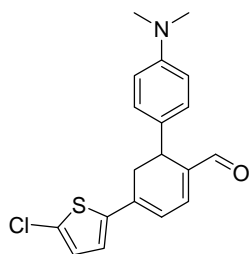
**4-(5-chlorothiophen-2-yl)-6-phenylcyclohexa-1,3-**

**dienecarbaldehyde (105):**  $^1\text{H}$  NMR (300MHz,  $\text{CDCl}_3$ ,  $25^\circ\text{C}$ ),  $\delta$ =9.56 (s, 1H), 7.46-7.50 (m, 1H), 7.14-7.24 (m, 4H), 7.03 (d,  $J$ =6.0 Hz, 1H), 6.98 (d,  $J$ =3.9 Hz, 1H), 6.84 (d,  $J$ =3.6 Hz, 1H), 6.53 (dd,  $J$ =2.7, 6.3 Hz, 1H), 4.22 (dd,  $J$ =2.7, 9.3 Hz, 1H), 2.98-3.16 (m, 2H)

$^{13}\text{C}$  NMR (75 MHz,  $\text{CDCl}_3$ ,  $25^\circ\text{C}$ )  $\delta$ =191.8 (CH), 142.9 (CH), 142.5 (C), 142.4 (C), 138.9 (C), 138.1 (C), 132.2 (C), 128.8 (2 x CH), 127.6 (CH), 127.3 (2 x CH), 127.2 (CH), 125.5 (CH), 118.2 (CH), 34.4 ( $\text{CH}_2$ ), 33.4 (CH)

IR (neat)  $\nu$  3095, 3028, 2928, 2868, 2715, 2383, 2343, 2310, 1664, 1542, 1434, 1421, 1168, 1003, 764,  $750\text{ cm}^{-1}$

LRMS (APCI) for  $\text{C}_{17}\text{H}_{13}\text{ClOS}$  ( $\text{M}+\text{H}^+$ ): calcd 301.0, found 301.3.



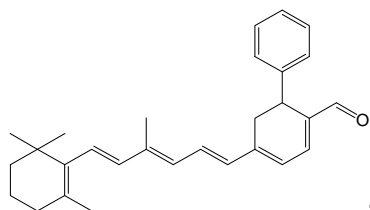
**4-(5-Chloro-thiophen-2-yl)-6-(4-dimethylamino-phenyl)-**

**cyclohexa-1,3-dienecarbaldehyde (106):**  $^1\text{H}$  NMR (300MHz,  $\text{CDCl}_3$ ,  $25^\circ\text{C}$ ),  $\delta$ =9.59 (s, 1H), 7.49-7.52 (m, 2H), 7.29-7.42 (m, 2H), 7.15 (d,  $J$ =8.7 Hz, 2H), 7.04 (d,  $J$ =6.0 Hz, 1H), 6.65 (dd,  $J$ =2.4, 6.0 Hz, 1H), 4.14 (dd,  $J$ =2.4, 9.0 Hz, 1H), 3.05-3.25 (m, 2H), 2.86 (s, 6H)

$^{13}\text{C}$  NMR (75 MHz,  $\text{CDCl}_3$ ,  $25^\circ\text{C}$ )  $\delta$ =192.6 (CH), 145.8 (C), 143.9 (C), 143.0 (CH), 142.8 (C), 139.8 (C), 139.4 (C), 138.2 (C), 129.1 (CH), 128.9 (2 x CH), 128.7 (CH), 128.0 (CH), 120.0 (CH), 113.1 (2 x CH), 41.0 (2 x  $\text{CH}_3$ ), 34.3 ( $\text{CH}_2$ ), 33.6 (CH)

IR (neat)  $\nu$  2981, 2890, 1674, 1473, 1463, 1382, 1275, 1261, 1151, 1073, 954,  $764\text{ cm}^{-1}$

LRMS (APCI) for  $\text{C}_{19}\text{H}_{18}\text{ClNOS}$  ( $\text{M}+\text{H}$ ) $^+$ : calcd 344.1, found 344.2.



**4-[4-Methyl-6-(2,6,6-trimethyl-cyclohex-1-enyl)-hexa-**

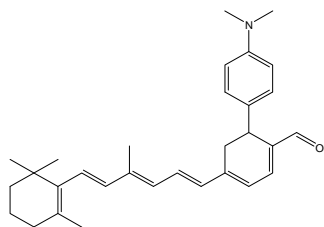
**1,3,5-trienyl]-6-phenyl-cyclohexa-1,3-dienecarbaldehyde (107):**  $^1\text{H}$  NMR (300MHz,  $\text{CDCl}_3$ ,  $25^\circ\text{C}$ ),  $\delta$ =9.51 (s, 1H), 7.13-7.27 (m, 5H), 6.99 (d,  $J$ =6.3 Hz, 1H), 6.89 (dd,  $J$ =11.7, 15.0 Hz, 1H), 6.41 (d,  $J$ =15.6 Hz, 1H), 6.24-6.32 (m, 2H), 6.10-6.18 (m, 2H), 4.19 (dd,  $J$ =2.1, 9.3 Hz, 1H), 3.01 (dd,  $J$ =2.4, 17.4 Hz, 1H), 2.84-2.94 (m, 1H), 2.02 (t,

$J=6.2$  Hz, 2H), 1.96 (s, 3H), 1.71 (s, 3H), 1.58-1.65 (m, 2H), 1.44-1.48 (m, 2H), 1.02 (s, 6H)

$^{13}\text{C}$  NMR (75 MHz,  $\text{CDCl}_3$ ,  $25^\circ\text{C}$ )  $\delta=191.8$  (CH), 144.9 (C), 143.8 (CH), 143.4 (C), 139.9 (C), 139.1 (C), 138.0 (C), 137.5 (CH), 133.0 (CH), 130.4 (C), 130.3 (CH), 129.7 (CH), 129.0 (CH), 128.7 (2 x CH), 127.4 (2 x CH), 127.0 (CH), 123.6 (CH), 39.8 ( $\text{CH}_2$ ), 34.5 (C), 34.4 (CH), 33.4 ( $\text{CH}_2$ ), 30.9 ( $\text{CH}_2$ ), 29.2 (2 x  $\text{CH}_3$ ), 22.0 ( $\text{CH}_3$ ), 19.4 ( $\text{CH}_2$ ), 13.2 ( $\text{CH}_3$ )

IR (neat)  $\nu$  3007, 2971, 1739, 1664, 1514, 1366, 1275, 1261, 1217, 765,  $750\text{ cm}^{-1}$

HRMS (ESI) for  $\text{C}_{29}\text{H}_{34}\text{O}$  ( $\text{M}+\text{Li}$ ) $^+$ : calcd 405.2770, found 405.2816.



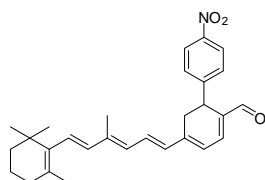
**6-(4-(dimethylamino)phenyl)-4-((1E,3E,5E)-4-methyl-6-(2,6,6-trimethylcyclohex-1-enyl)hexa-1,3,5-trienyl)cyclohexa-1,3-dienecarbaldehyde (108):**  $^1\text{H}$  NMR (300MHz,  $\text{CDCl}_3$ ,  $25^\circ\text{C}$ ),  $\delta=9.49$  (s, 1H), 7.15 (d,  $J=8.4$  Hz, 2H), 6.94 (d,  $J=6.0$  Hz, 1H), 6.85-6.89 (m, 1H), 6.59-6.66 (m, 2H), 6.41 (d,  $J=15.0$  Hz, 1H), 6.10-6.29 (m, 4H), 4.06-4.16 (m, 1H), 2.96-3.09 (m, 2H), 2.88 (s, 6H), 1.96-2.05 (m, 5H), 1.60 (m, 4H), 1.71 (s, 3H), 1.02 (s, 6H)

$^{13}\text{C}$  NMR (75 MHz,  $\text{CDCl}_3$ ,  $25^\circ\text{C}$ )  $\delta=192.1$  (CH), 145.0 (C), 143.3 (C), 139.9 (C), 138.0 (C), 137.6 (2 x CH), 136.8 (C), 133.3 (C), 133.2 (CH), 130.8 (C), 130.4 (2 x CH), 129.6 (CH), 128.9 (CH), 128.2 (CH), 123.6 (2 x CH), 39.8 (2 x  $\text{CH}_3$ ), 34.5 (CH), 33.5 ( $\text{CH}_2$ ), 33.4 ( $\text{CH}_2$ ), 30.8 ( $\text{CH}_2$ ), 29.9 (C), 29.2 (2 x  $\text{CH}_3$ ), 22.0 ( $\text{CH}_3$ ), 19.4 ( $\text{CH}_2$ ), 13.2 ( $\text{CH}_3$ )



IR (neat)  $\nu$  3010, 2958, 2888, 2820, 2383, 2326, 2300, 1661, 1596, 1527, 1371, 1135, 972, 812  $\text{cm}^{-1}$

HRMS (ESI) for  $\text{C}_{31}\text{H}_{39}\text{NO}$  ( $\text{M}+\text{H}$ ) $^{+}$ : calcd 442.3110, found 442.3122.



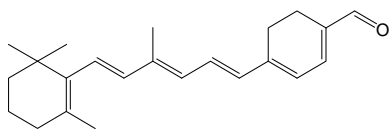
**4-((1E,3E,5E)-4-methyl-6-(2,6,6-trimethylcyclohex-1-enyl)hexa-**

**1,3,5-trienyl)-6-(4-nitrophenyl)cyclohexa-1,3-dienecarbaldehyde (109):**  $^1\text{H}$  NMR (300MHz,  $\text{CDCl}_3$ , 25°C),  $\delta$ =9.51 (s, 1H), 8.08 (d,  $J$ =9.0 Hz, 2H), 7.40 (d,  $J$ =8.4 Hz, 2H), 7.07 (d,  $J$ =6.3 Hz, 1H), 6.88 (dd,  $J$ =11.5, 15.0 Hz, 1H), 6.41 (d,  $J$ =15.3 Hz, 1H), 6.10-6.31 (m, 4H), 4.28 (t,  $J$ =5.7 Hz, 1H), 2.95 (d,  $J$ =5.7 Hz, 2H), 1.96 (s, 3H), 1.94 (t,  $J$ =6.9 Hz, 2H), 1.70 (s, 3H), 1.57-1.65 (m, 2H), 1.43-1.47 (m, 2H), 1.01 (s, 6H)

$^{13}\text{C}$  NMR (75 MHz,  $\text{CDCl}_3$ , 25°C)  $\delta$ =191.4 (CH), 150.7 (C), 144.7 (C), 144.5 (CH), 140.7 (C), 137.9 (C), 137.6 (C), 137.4 (CH), 135.0 (C), 132.5 (CH), 130.7 (C), 130.3 (CH), 130.1 (CH), 129.6 (CH), 128.3 (2 x CH), 124.1 (2 x CH), 123.3 (CH), 39.8 (CH<sub>2</sub>), 34.5 (C), 34.4 (CH), 33.4 (CH<sub>2</sub>), 30.6 (CH<sub>2</sub>), 29.2 (2 x CH<sub>3</sub>), 22.0 (CH<sub>3</sub>), 19.4 (CH<sub>2</sub>), 13.2 (CH<sub>3</sub>)

IR (neat)  $\nu$  3008, 2968, 1720, 1666, 1589, 1361, 978, 810  $\text{cm}^{-1}$

HRMS (ESI) for  $\text{C}_{29}\text{H}_{33}\text{NO}_3\text{Li}$  ( $\text{M}+\text{Li}$ ) $^{+}$ : calcd 450.2620, found 450.2625.



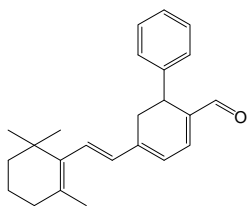
**4-[4-Methyl-6-(2,6,6-trimethyl-cyclohex-1-enyl)-hexa-**

**1,3,5-trienyl]-cyclohexa-1,3-dienecarbaldehyde (110):**  $^1\text{H}$  NMR (300MHz,  $\text{CDCl}_3$ ,  $25^\circ\text{C}$ ),  $\delta$ =9.50 (s, 1H), 6.86-6.95 (m, 2H), 6.39 (d,  $J$ =15.3 Hz, 1H), 6.28 (d,  $J$ =15.9 Hz, 1H), 6.12-6.19 (m, 3H), 2.55 (s, 4H), 2.00-2.04 (m, 5H), 1.72 (s, 3H), 1.58-1.66 (m, 2H), 1.41-1.49 (m, 2H), 1.03 (s, 6H)

$^{13}\text{C}$  NMR (75 MHz,  $\text{CDCl}_3$ ,  $25^\circ\text{C}$ )  $\delta$ =192.2 (CH), 146.3 (C), 144.1 (CH), 140.0 (2 x C), 138.0 (C), 137.5 (CH), 136.9 (C), 133.0 (CH), 130.3 (CH), 129.3 (CH), 128.8 (CH), 124.0 (CH), 39.4 ( $\text{CH}_2$ ), 34.5 (C), 33.4 ( $\text{CH}_2$ ), 29.2 (2 x  $\text{CH}_3$ ), 22.9 ( $\text{CH}_2$ ), 22.0 ( $\text{CH}_3$ ), 19.4 ( $\text{CH}_2$ ), 18.9 ( $\text{CH}_2$ ), 13.1 ( $\text{CH}_3$ )

IR (neat)  $\nu$  2954, 2926, 1717, 1664, 1514, 1400, 1221, 1082, 966, 866  $\text{cm}^{-1}$

HRMS (ESI) for  $\text{C}_{23}\text{H}_{30}\text{O}$  ( $\text{M}+\text{Li}$ ) $^+$ : calcd 329.24567, found 329.2466.



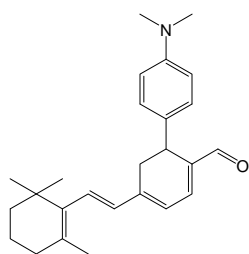
**6-Phenyl-4-[2-(2,6,6-trimethyl-cyclohex-1-enyl)-vinyl]-cyclohexa-**

**1,3-dienecarbaldehyde (111):**  $^1\text{H}$  NMR (300MHz,  $\text{CDCl}_3$ ,  $25^\circ\text{C}$ ),  $\delta$ =9.52 (s, 1H), 7.14-7.29 (m, 5H), 6.97 (d,  $J$ =5.7 Hz, 1H), 6.49 (d,  $J$ =16.2 Hz, 1H), 6.26 (d,  $J$ =16.2 Hz, 1H), 6.17 (dd,  $J$ =2.4, 6.0 Hz, 1H), 4.19 (dd,  $J$ =1.8, 9.6 Hz, 1H), 3.01 (dd,  $J$ =2.1, 17.7 Hz, 1H), 2.85 (qd,  $J$ =2.1, 9.6, 17.7 Hz, 1H), 2.03 (t,  $J$ =6.3 Hz, 2H), 1.72 (s, 3H), 1.56-1.65 (m, 2H), 1.43-1.48 (m, 2H), 1.02 (s, 3H), 1.01 (s, 3H)

$^{13}\text{C}$  NMR (75 MHz,  $\text{CDCl}_3$ ,  $25^\circ\text{C}$ )  $\delta$ =192.1 (CH), 145.2 (C), 144.1 (CH), 143.5 (C), 139.2 (C), 137.7 (C), 133.9 (CH), 132.5 (C), 128.7 (2 x CH), 127.4 (3 x CH), 126.9 (CH), 122.5 (CH), 39.9 ( $\text{CH}_2$ ), 34.5 ( $\text{CH}_2$ ), 34.3 (C), 33.6 (CH), 30.3 ( $\text{CH}_2$ ), 29.2 (2 x  $\text{CH}_3$ ), 22.1 ( $\text{CH}_3$ ), 19.3 ( $\text{CH}_2$ )

IR (neat)  $\nu$  2925, 2866, 1667, 1536, 1453, 1275, 1163, 1077, 751, 699  $\text{cm}^{-1}$

HRMS (ESI) for  $\text{C}_{24}\text{H}_{28}\text{O}$  ( $\text{M}+\text{Li}$ ) $^+$ : calcd 339.2300, found 339.2358.



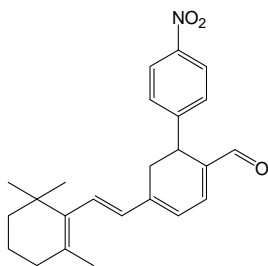
**6-(4-Dimethylamino-phenyl)-4-[2-(2,6,6-trimethyl-cyclohex-1-**

**enyl)-vinyl]-cyclohexa-1,3-dienecarbaldehyde (112):**  $^1\text{H}$  NMR (300MHz,  $\text{CDCl}_3$ ,  $25^\circ\text{C}$ ),  $\delta$ =9.50 (s, 1H), 7.14 (d,  $J$ =9.0 Hz, 2H), 6.90 (d,  $J$ =6.3 Hz, 1H), 6.61 (d,  $J$ =8.7 Hz, 2H), 6.52 (d,  $J$ =16.2 Hz, 1H), 6.26 (d,  $J$ =16.2 Hz, 1H), 6.15 (dd,  $J$ =2.4, 6.0 Hz, 1H), 4.09 (dd,  $J$ =1.5, 9.6 Hz, 1H), 3.00 (dd,  $J$ =1.8, 17.7 Hz, 1H), 2.89 (s, 6H), 2.74-2.86 (m, 1H), 2.04 (t,  $J$ =5.7 Hz, 2H), 1.73 (s, 3H), 1.57-1.65 (m, 2H), 1.43-1.48 (m, 2H), 1.03 (s, 6H)

$^{13}\text{C}$  NMR (75 MHz,  $\text{CDCl}_3$ ,  $25^\circ\text{C}$ )  $\delta$ =192.3 (CH), 149.9 (C), 145.3 (C), 143.3 (CH), 139.9 (C), 137.7 (C), 134.0 (CH), 132.1 (C), 132.1 (CH), 128.0 (2 x CH), 128.0 (C), 122.4 (CH), 113.0 (2 x CH), 41.0 (2 x  $\text{CH}_3$ ), 39.9 ( $\text{CH}_2$ ), 34.5 (C), 33.5 ( $\text{CH}_2$ ), 33.3 (CH), 30.3 ( $\text{CH}_2$ ), 29.2 (2 x  $\text{CH}_3$ ), 22.1 ( $\text{CH}_3$ ), 19.3 ( $\text{CH}_2$ )

IR (neat)  $\nu$  3005, 2926, 2863, 2806, 2713, 1738, 1663, 1613, 1519, 1444, 1356, 1275, 1200, 1160, 965, 819, 765, 750  $\text{cm}^{-1}$

HRMS (ESI) for  $\text{C}_{26}\text{H}_{33}\text{NO}$  ( $\text{M}+\text{Li}$ ) $^+$ : calcd 382.2722, found 382.2784.

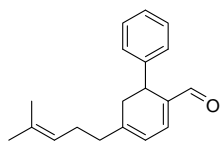


**6-(4-Nitro-phenyl)-4-[2-(2,6,6-trimethyl-cyclohex-1-enyl)-vinyl]-**

**cyclohexa-1,3-dienecarbaldehyde (113):**  $^1\text{H}$  NMR (300MHz,  $\text{CDCl}_3$ ,  $25^\circ\text{C}$ ),  $\delta$ =9.53 (s, 1H), 8.04-8.10 (m, 2H), 7.41 (d,  $J$ =9.3 Hz, 1H), 7.31 (d,  $J$ =8.7 Hz, 1H), 7.06 (d,  $J$ =5.7 Hz, 1H), 6.50 (d,  $J$ =16.5 Hz, 1H), 6.32 (dd,  $J$ =2.7, 6.0 Hz, 1H), 6.27 (d,  $J$ =16.2 Hz, 1H), 4.27 (dd,  $J$ =3.3, 8.1 Hz, 1H), 3.04 (d,  $J$ =17.1 Hz, 1H), 2.84-2.95 (m, 1H), 2.17-2.35 (m, 2H), 1.71 (s, 3H), 1.57-1.66 (m, 2H), 1.40-1.48 (m, 2H), 1.01 (s, 3H), 1.00 (s, 3H)

$^{13}\text{C}$  NMR (75 MHz,  $\text{CDCl}_3$ ,  $25^\circ\text{C}$ )  $\delta$ =191.5 (CH), 147.1 (C), 144.9 (C), 144.7 (CH), 137.8 (C), 137.5 (C), 133.4 (C), 133.1 (CH), 130.3 (C), 128.4 (CH), 128.3 (2 x CH), 124.0 (2 x CH), 122.3 (CH), 39.8 ( $\text{CH}_2$ ), 34.5 (C), 34.3 (CH), 33.6 (CH), 32.2 ( $\text{CH}_2$ ), 29.9 (2 x  $\text{CH}_3$ ), 22.1 ( $\text{CH}_3$ ), 19.2 ( $\text{CH}_2$ )

HRMS (ESI) for  $\text{C}_{24}\text{H}_{27}\text{NO}_3$  ( $\text{M}+\text{Li}^+$ ): calcd 384.2151, found 384.2158.



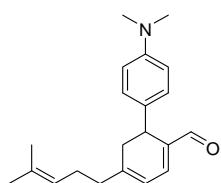
**4-(4-Methyl-pent-3-enyl)-6-phenyl-cyclohexa-1,3-**

**dienecarbaldehyde (26):**  $^1\text{H}$  NMR (300MHz,  $\text{CDCl}_3$ ,  $25^\circ\text{C}$ ),  $\delta$ = 9.52 (s, 1H), 7.10-7.24 (m, 5H), 6.96 (d,  $J$ =5.4 Hz, 1H), 6.03-6.07 (m, 1H), 4.94-5.00 (m, 1H), 4.06 (dd,  $J$ =1.5, 10.5 Hz, 1H), 2.79-2.89 (m, 1H), 2.48 (dd,  $J$ = 1.5, 18.0 Hz, 1H), 2.03-2.20 (m, 4H), 1.64 (s, 3H), 1.55 (s, 3H)

$^{13}\text{C}$  NMR (75 MHz,  $\text{CDCl}_3$ ,  $25^\circ\text{C}$ )  $\delta$ =192.4 (CH), 151.1 (C), 144.5 (CH), 143.0 (C), 132.7 (C), 128.6 (2 x CH), 127.3 (2 x CH), 126.9 (CH), 123.3 (CH), 119.1 (CH), 38.1 (CH<sub>2</sub>), 36.2 (CH<sub>2</sub>), 34.4 (CH<sub>2</sub>), 30.8 (C), 25.9 (CH<sub>3</sub>), 25.7 (CH<sub>2</sub>), 17.9 (CH<sub>3</sub>)

IR (neat)  $\nu$  3026, 2971, 2926, 2144, 1738, 1670, 1574, 1449, 1366, 1228, 1217, 1205, 698  $\text{cm}^{-1}$

HRMS (ESI) for  $\text{C}_{19}\text{H}_{22}\text{OLi}$  ( $\text{M}+\text{Li}$ )<sup>+</sup>: calcd 273.1831, found 273.1839 .



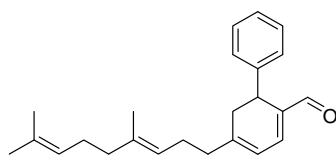
**6-(4-Dimethylamino-phenyl)-4-(4-methyl-pent-3-enyl)-cyclohexa-**

**1,3-dienecarbaldehyde (114):**  $^1\text{H}$  NMR (300MHz,  $\text{CDCl}_3$ ,  $25^\circ\text{C}$ ),  $\delta$ =9.43 (s, 1H), 7.13 (d,  $J$ =9.0 Hz, 2H), 6.77 (d,  $J$ =5.4 Hz, 1H), 6.60 (d,  $J$ =8.7 Hz, 2H), 6.07-6.12 (m, 1H), 5.12-5.20 (m, 1H), 3.89 (d,  $J$ =8.4 Hz, 1H), 2.88 (s, 6H), 2.24-2.37 (m, 2H), 1.99-2.20 (m, 4H), 1.89 (d,  $J$ =1.2 Hz, 3H), 1.71 (s, 3H)

$^{13}\text{C}$  NMR (75 MHz,  $\text{CDCl}_3$ ,  $25^\circ\text{C}$ )  $\delta$ =193.1 (CH), 151.8 (C), 142.7 (CH), 141.6 (C), 137.0 (C), 135.2 (C), 133.1 (C), 129.9 (2 x CH), 121.5 (CH), 119.1 (CH), 112.6 (2 x CH), 41.0 (2 x CH<sub>3</sub>), 38.2 (CH<sub>2</sub>), 37.6 (CH), 30.8 (CH<sub>2</sub>), 26.4 (CH<sub>2</sub>), 26.1 (CH<sub>3</sub>), 18.3 (CH<sub>3</sub>)

IR (neat)  $\nu$  2966, 2912, 2852, 2802, 2709, 2368, 1739, 1669, 1640, 1612, 1574, 1518, 1480, 1444, 1348, 1195, 1163, 947, 814  $\text{cm}^{-1}$

HRMS (ESI) for  $\text{C}_{21}\text{H}_{27}\text{NOLi}$  ( $\text{M}+\text{Li}$ )<sup>+</sup>: calcd 316.2253, found 316.2250.



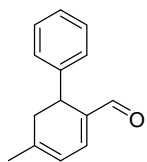
**4-(4,8-dimethylnona-3,7-dienyl)-6-phenylcyclohexa-1,3-**

**dienecarbaldehyde (115):**  $^1\text{H}$  NMR (300MHz,  $\text{CDCl}_3$ ,  $25^\circ\text{C}$ ),  $\delta$ =9.51 (s, 1H), 7.13-7.24 (m, 5H), 6.96 (d,  $J$ =5.4 Hz, 1H), 6.04-6.07 (m, 1H), 4.96-5.09 (m, 2H), 4.06 (dd,  $J$ =1.5, 10.5 Hz, 1H), 2.78-2.90 (m, 1H), 2.49 (dd,  $J$ =1.5, 17.7 Hz, 1H), 1.88-2.26 (m, 8H), 1.68 (s, 3H), 1.60 (s, 3H), 1.54 (s, 3H)

$^{13}\text{C}$  NMR (75 MHz,  $\text{CDCl}_3$ ,  $25^\circ\text{C}$ ),  $\delta$ =192.4 (CH), 151.1 (C), 144.5 (CH), 142.9 (C), 137.8 (C), 136.3 (C), 131.7 (C), 128.6 (2 x CH), 127.3 (2 x CH), 126.9 (CH), 124.4 (CH), 123.2 (CH), 119.1 (CH), 39.8 ( $\text{CH}_2$ ), 38.2 ( $\text{CH}_2$ ), 36.2 ( $\text{CH}_2$ ), 34.4 (CH), 26.8 ( $\text{CH}_2$ ), 26.0 ( $\text{CH}_2$ ), 25.5 ( $\text{CH}_3$ ), 17.9 ( $\text{CH}_3$ ), 16.2 ( $\text{CH}_3$ )

IR (neat)  $\nu$  2967, 2923, 2851, 2371, 2366, 2328, 1673, 1575, 1182  $\text{cm}^{-1}$

HRMS (ESI) for  $\text{C}_{24}\text{H}_{30}\text{O}$  ( $\text{M}+\text{H}$ ) $^+$ : calcd 341.2457, found 341.2485.



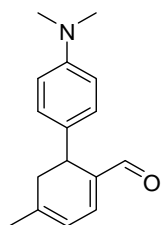
**4-methyl-6-phenylcyclohexa-1,3-dienecarbaldehyde (116):**  $^1\text{H}$  NMR

(300MHz,  $\text{CDCl}_3$ ,  $25^\circ\text{C}$ ),  $\delta$ =9.50 (s, 1H), 7.15-7.26 (m, 5H), 6.93 (d,  $J$ =5.4 Hz, 1H), 6.04-6.07 (m, 1H), 4.06 (d,  $J$ =10.5 Hz, 1H), 2.81-2.91 (dd,  $J$ =10.5, 18.3 Hz, 1H), 2.46 (d,  $J$ =18.3 Hz, 1H), 1.89 (s, 3H)

$^{13}\text{C}$  NMR (75 MHz,  $\text{CDCl}_3$ ,  $25^\circ\text{C}$ ),  $\delta$ =192.4 (CH), 147.6 (C), 144.5 (CH), 143.4 (C), 137.6 (C), 128.7 (2 x CH), 127.2 (2 x CH), 126.9 (CH), 119.7 (CH), 37.3 ( $\text{CH}_2$ ), 34.4 (CH), 24.4 ( $\text{CH}_3$ )

IR (neat)  $\nu$  3028, 2971, 2926, 2383, 2343, 2309, 1738, 1669, 1575, 1375, 1196, 756  $\text{cm}^{-1}$

HRMS (ESI) for  $\text{C}_{14}\text{H}_{14}\text{OLi}$  ( $\text{M}+\text{Li}$ ) $^{+}$ : calcd 205.1205, found 205.1236.



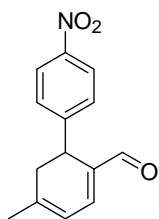
**6-(4-(dimethylamino)phenyl)-4-methylcyclohexa-1,3-dienecarbaldehyde**

**(117):**  $^1\text{H}$  NMR (300MHz,  $\text{CDCl}_3$ ,  $25^\circ\text{C}$ ),  $\delta$ =9.48 (s, 1H), 7.11 (d,  $J$ =9.0 Hz, 2H), 6.86 (d,  $J$ =5.7 Hz, 1H), 6.61-6.72 (m, 2H), 6.01- 6.04 (m, 1H), 3.97 (d,  $J$ =9.6 Hz, 1H), 3.07 (d,  $J$ =11.1 Hz, 1H), 2.89 (s, 6H), 2.44 (d,  $J$ =18.6 Hz, 1H), 1.89 (s, 3H)

$^{13}\text{C}$  NMR (75 MHz,  $\text{CDCl}_3$ ,  $25^\circ\text{C}$ ),  $\delta$ =192.7 (CH), 149.7 (C), 147.6 (C), 143.8 (CH), 138.2 (C), 131.8 (C), 127.9 (2 x CH), 119.6 (CH), 113. (2 x CH), 41.0 (2 x  $\text{CH}_3$ ), 37.3 ( $\text{CH}_2$ ), 33.5 (CH), 24.5 ( $\text{CH}_3$ )

IR (neat)  $\nu$  2923, 2851, 2382, 2342, 2327, 1670, 1612, 1596, 1577, 1520, 1253, 1165, 817, 736  $\text{cm}^{-1}$

HRMS (ESI) for  $\text{C}_{16}\text{H}_{19}\text{ONLi}$  ( $\text{M}+\text{Li}$ ) $^{+}$ : calcd 248.1627, found 248.1653.



**4-Methyl-6-(4-nitro-phenyl)-cyclohexa-1,3-dienecarbaldehyde (118):**  $^1\text{H}$

NMR (300MHz,  $\text{CDCl}_3$ ,  $25^\circ\text{C}$ ),  $\delta$ =9.53 (s, 1H), 8.11 (d  $J$ =8.7 Hz, 2H), 7.41 (d,  $J$ =8.4

Hz, 2H), 7.05 (d,  $J=5.7$  Hz, 1H), 6.12-6.15 (m, 1H), 4.17 (d,  $J=8.7$  Hz, 1H), 2.88-2.99 (m, 1H), 2.44 (dd,  $J=1.5, 18.3$  Hz, 1H), 1.93 (s, 3H)

$^{13}\text{C}$  NMR (75 MHz,  $\text{CDCl}_3$ ,  $25^\circ\text{C}$ ),  $\delta=192.0$  (CH), 150.9 (C), 147.5 (C), 147.1 (C), 145.0 (CH), 136.3 (C), 128.3 (2 x CH), 124.0 (2 x CH), 119.9 (CH), 36.9 (CH), 34.6 ( $\text{CH}_2$ ), 24.3 ( $\text{CH}_3$ )

IR (neat)  $\nu$  2971, 2925, 2819, 2717, 1738, 1666, 1575, 1514, 1342, 1195, 1155, 852, 827,  $697\text{ cm}^{-1}$

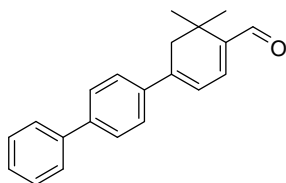
HRMS (ESI) for  $\text{C}_{14}\text{H}_{13}\text{O}_3\text{NLi}$  ( $\text{M}+\text{Li}$ ) $^+$ : calcd 250.1055, found 250.1017.

#### *Synthesis of Heterodimers Utilizing Two $\beta$ -methyl Substituted Substrates*

The following is an example of the synthetic procedure for the synthesis of 4-(9H-fluoren-2-yl)-6-methylcyclohexa-1,3-dienecarbaldehyde (**124**). In a dried 100 mL flask, 3-(9H-Fluoren-2-yl)-but-2-enal (100mg, 1 equivalent) and crotonaldehyde (30 mg, 1 equivalent) were dissolved in 15 mL of 200 proof ethanol. L-proline (300 mg, 3 equivalents) was added to facilitate the reaction. The reaction was stirred for 16 hours at room temperature before being quenched by the addition of 20 mL of water. The reaction mixture was extracted with a 1:1 ethyl acetate/hexanes solution (3 x 50 mL) and was washed with brine. The organic layer was dried over magnesium sulfate ( $\text{MgSO}_4$ ) and concentrated under vacuum. The crude product was purified by column chromatography (10% ethyl acetate/hexanes) to yield 57.6 mg of the final product (67% yield) as a green solid.



*Characterization of Heterodimers Utilizing Two  $\beta$ -methyl Substrates*



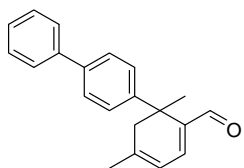
**4-(biphenyl-4-yl)-6,6-dimethylcyclohexa-1,3-**

**dienecarbaldehyde (119):**  $^1\text{H}$  NMR (300MHz,  $\text{CDCl}_3$ ,  $25^\circ\text{C}$ ),  $\delta=9.53$  (s, 1H), 7.60-7.63 (m, 5H), 7.43-7.49 (m, 2H), 7.34-7.40 (m, 2H), 6.83 (d,  $J=6.0$  Hz, 1H), 6.65 (dt,  $J=1.2$ , 6.0 Hz, 1H), 2.66 (d,  $J=1.2$  Hz, 2H), 1.31 (s, 6H)

$^{13}\text{C}$  NMR (75 MHz,  $\text{CDCl}_3$ ,  $25^\circ\text{C}$ )  $\delta=193.3$  (CH), 144.9 (C), 144.3 (CH), 144.1 (C), 141.8 (C), 140.5 (C), 138.6 (C), 129.1 (2 x CH), 127.9 (CH), 127.5 (2 x CH), 127.2 (2 x CH), 126.4 (2 x CH), 119.1 (CH), 43.5 ( $\text{CH}_2$ ), 33.4 (C), 26.1 (2 x  $\text{CH}_3$ )

IR (neat)  $\nu$  3030, 2924, 1678, 1596, 1487, 1262, 1184, 1135, 1006, 837, 765,  $697\text{ cm}^{-1}$

HRMS (ESI) for  $\text{C}_{21}\text{H}_{20}\text{OLi}$  ( $\text{M}+\text{Li}$ ) $^+$ : calcd 295.1674, found 295.1749.



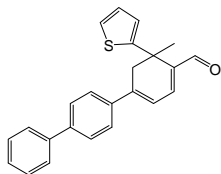
**6-(biphenyl-4-yl)-4,6-dimethylcyclohexa-1,3-dienecarbaldehyde**

**(120):**  $^1\text{H}$  NMR (300MHz,  $\text{CDCl}_3$ ,  $25^\circ\text{C}$ ),  $\delta=9.45$  (s, 1H), 7.54-7.58 (m, 2H), 7.48-7.51 (m, 2H), 7.30-7.43 (m, 5H), 6.87 (d,  $J=5.4$  Hz, 1H), 6.03 (dq,  $J=1.5$ , 5.4 Hz, 1H), 2.69 (d,  $J=18.0$  Hz, 1H), 2.40 (d,  $J=18.0$  Hz, 1H), 1.91 (d,  $J=1.2$  Hz, 3H), 1.67 (s, 3H)

$^{13}\text{C}$  NMR (75 MHz,  $\text{CDCl}_3$ ,  $25^\circ\text{C}$ )  $\delta=192.7$  (CH), 146.9 (C), 145.2 (CH), 141.5 (C), 141.1 (C), 140.0 (C), 139.1 (C), 128.9 (2 x CH), 127.2 (3 x CH), 127.1 (2 x CH), 126.6 (2 x CH), 119.0 (CH), 48.1 ( $\text{CH}_2$ ), 40.4 (C), 25.3 ( $\text{CH}_3$ ), 24.1 ( $\text{CH}_3$ )

IR (neat)  $\nu$  3051, 2923, 2854, 1655, 1602, 1455, 1422, 1253, 1163, 1142, 1124, 827, 769, 734  $\text{cm}^{-1}$

HRMS (ESI) for  $\text{C}_{21}\text{H}_{20}\text{OLi}$  ( $\text{M}+\text{Li}$ ) $^{+}$ : calcd 295.1674, found 295.1682.



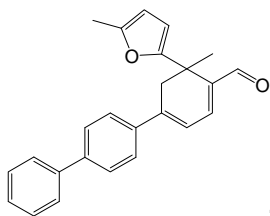
**4-Biphenyl-4-yl-6-methyl-6-thiophen-2-yl-cyclohexa-1,3-**

**dienecarbaldehyde (121):**  $^1\text{H}$  NMR (300MHz,  $\text{CDCl}_3$ ,  $25^\circ\text{C}$ ),  $\delta$ =9.56 (s, 1H), 7.28-7.63 (m, 10H), 7.09 (d,  $J$ =6.3 Hz, 1H), 7.00-7.06 (m, 2H), 6.72 (d,  $J$ =6.3 Hz, 1H), 3.20 (d,  $J$ =17.4 Hz, 1H), 2.92 (d,  $J$ =17.4 Hz, 1H), 1.77 (s, 3H)

$^{13}\text{C}$  NMR (75 MHz,  $\text{CDCl}_3$ ,  $25^\circ\text{C}$ )  $\delta$ =192.3 (CH), 153.9 (C), 144.5 (CH), 143.8 (C), 142.8 (C), 141.1 (C), 139.4 (C), 138.5 (C), 129.1 (2 x CH), 128.9 (2 x CH), 128.0 (CH), 127.6 (2 x CH), 127.2 (2 x CH), 126.8 (2 x CH), 126.4 (CH), 117.3 (CH), 44.7 ( $\text{CH}_2$ ), 40.8 (C), 25.1 ( $\text{CH}_3$ )

IR (neat)  $\nu$  3110, 2958, 2925, 2854, 1728, 1682, 1597, 1425, 1257, 1071, 701  $\text{cm}^{-1}$

HRMS (ESI) for  $\text{C}_{24}\text{H}_{20}\text{OSLi}$  ( $\text{M}+\text{Li}$ ) $^{+}$ : calcd 363.1395, found 363.1360.



**4-Biphenyl-4-yl-6-methyl-6-(5-methyl-furan-2-yl)-cyclohexa-1,3-**

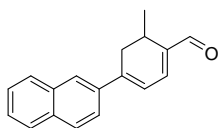
**dienecarbaldehyde (122):**  $^1\text{H}$  NMR (300MHz,  $\text{CDCl}_3$ ,  $25^\circ\text{C}$ ),  $\delta$ =9.49 (s, 1H), 7.30-7.71 (m, 9H), 6.97 (d,  $J$ =6.0 Hz, 1H), 6.60 (d,  $J$ =5.7 Hz, 1H), 6.07-6.08 (m, 1H), 5.85-5.87

(m, 1H), 2.60 (dd,  $J=1.35$ , 17.1 Hz, 1H), 2.48 (d,  $J=17.1$  Hz, 1H), 2.32 (s, 3H), 1.72 (s, 3H)

$^{13}\text{C}$  NMR (75 MHz,  $\text{CDCl}_3$ , 25°C)  $\delta=191.6$  (CH), 146.5 (C), 145.4 (C), 145.1 (C), 144.5 (CH), 143.6 (C), 143.1 (C), 142.1 (C), 139.3 (C), 131.2 (CH), 129.1 (2 x CH), 128.9 (CH), 127.6 (CH), 127.3 (2 x CH), 126.8 (CH), 126.4 (CH), 119.1 (CH), 108.9 (CH), 106.1 (CH), 44.7 ( $\text{CH}_2$ ), 31.8 (C), 22.6 ( $\text{CH}_3$ ), 14.4 ( $\text{CH}_3$ )

IR (neat)  $\nu$  2960, 2924, 2875, 2854, 1728, 1695, 1600, 1487, 1456, 1262, 1120, 766  $\text{cm}^{-1}$

HRMS (ESI) for  $\text{C}_{25}\text{H}_{22}\text{O}_2$  ( $\text{M}+\text{Li}$ ) $^{+}$ : calcd 361.1780, found 361.1745.



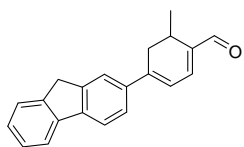
**6-methyl-4-(naphthalen-2-yl)cyclohexa-1,3-dienecarbaldehyde**

**(123):**  $^1\text{H}$  NMR (300MHz,  $\text{CDCl}_3$ , 25°C),  $\delta=9.58$  (s, 1H), 8.01-8.05 (m, 2H), 7.96-7.99 (m, 1H), 7.63-7.71 (m, 4H), 6.92 (d,  $J=6.0$  Hz, 1H), 6.75 (dd,  $J=2.7$ , 6.0 Hz, 1H), 3.73-3.77 (m, 1H), 2.95-3.18 (m, 2H), 1.05 (d,  $J=6.9$  Hz, 3H)

$^{13}\text{C}$  NMR (75 MHz,  $\text{CDCl}_3$ , 25°C),  $\delta=192.7$  (CH), 145.0 (C), 142.5 (CH), 141.9 (C), 137.3 (C), 133.6 (C), 133.4 (C), 128.5 (CH), 128.0 (CH), 127.4 (2 x CH), 126.8 (CH), 125.4 (CH), 123.7 (CH), 119.9 (CH), 33.6 ( $\text{CH}_2$ ), 24.4 (CH), 18.1 ( $\text{CH}_3$ )

IR (neat)  $\nu$  3053, 2926, 1665, 1548, 1177, 818, 749  $\text{cm}^{-1}$

HRMS (ESI) for  $\text{C}_{18}\text{H}_{16}\text{O}$  ( $\text{M}+\text{Li}$ ) $^{+}$ : calcd 255.1361, found 255.1411.



**4-(9H-fluoren-2-yl)-6-methylcyclohexa-1,3-dienecarbaldehyde**

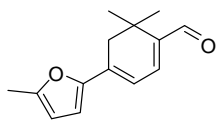
**(124):**  $^1\text{H}$  NMR (300MHz,  $\text{CDCl}_3$ , 25°C),  $\delta=9.56$  (s, 1H), 7.77-7.90 (m, 2H), 7.55-7.59

(m, 2H), 7.25-7.44 (m, 3H), 6.90 (d,  $J=6.0$  Hz, 1H), 6.65 (dd,  $J=2.7, 6.0$  Hz, 1H), 3.93 (s, 2H), 3.05-3.15 (m, 1H), 2.95 (dq,  $J=2.7, 8.4$  Hz, 1H), 2.76-2.78 (m, 1H), 1.04 (d,  $J=7.2$  Hz, 3H)

$^{13}\text{C}$  NMR (75 MHz,  $\text{CDCl}_3$ ,  $25^\circ\text{C}$ )  $\delta=192.6$  (CH), 145.7 (C), 143.9 (C), 143.8 (C), 142.8 (C), 142.7 (CH), 141.6 (C), 141.3 (C), 138.7 (C), 127.4 (CH), 127.2 (CH), 125.4 (CH), 125.0 (CH), 122.6 (CH), 120.4 (CH), 120.2 (CH), 119.1 (CH), 37.2 ( $\text{CH}_2$ ), 33.9 ( $\text{CH}_2$ ), 24.4 (CH), 18.1 ( $\text{CH}_3$ )

IR (neat)  $\nu$  3053, 2962, 2925, 2868, 1733, 1663, 1546, 1423, 1265, 1183, 1046, 825, 733, 703  $\text{cm}^{-1}$

HRMS (ESI) for  $\text{C}_{21}\text{H}_{18}\text{O}$  ( $\text{M}+\text{H}$ ) $^+$ : calcd 287.1436, found 287.1436.



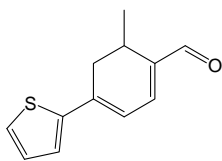
**6,6-dimethyl-4-(5-methylfuran-2-yl)cyclohexa-1,3-**

**dienecarbaldehyde (125):**  $^1\text{H}$  NMR (300MHz,  $\text{CDCl}_3$ ,  $25^\circ\text{C}$ ),  $\delta=9.44$  (s, 1H), 6.81 (d,  $J=6.0$  Hz, 1H), 6.58 (d,  $J=6.0$  Hz, 1H), 6.48 (d,  $J=3.6$  Hz, 1H), 6.07-6.10 (m, 1H), 2.41 (d,  $J=1.2$ , 2H), 2.36 (s, 3H), 1.26 (s, 6H)

$^{13}\text{C}$  NMR (75 MHz,  $\text{CDCl}_3$ ,  $25^\circ\text{C}$ )  $\delta=193.0$  (CH), 150.1 (C), 144.9 (C), 141.2 (C), 137.7 (CH), 136.4 (C), 126.6 (CH), 114.7 (CH), 109.1 (CH), 41.0 ( $\text{CH}_2$ ), 26.1 (2 x  $\text{CH}_3$ ), 23.0 (C), 14.2 ( $\text{CH}_3$ )

IR (neat)  $\nu$  3012, 2983, 1730, 1665, 1585, 1540, 1334, 1213  $\text{cm}^{-1}$

HRMS (ESI) for  $\text{C}_{14}\text{H}_{16}\text{O}_2$  ( $\text{M}+\text{Li}$ ) $^+$ : calcd 223.1310, found 223.1319.



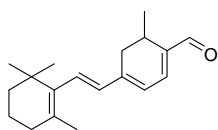
**6-Methyl-4-thiophen-2-yl-cyclohexa-1,3-dienecarbaldehyde (126):**

$^1\text{H}$  NMR (300MHz,  $\text{CDCl}_3$ ,  $25^\circ\text{C}$ ),  $\delta$ =9.52 (s, 1H), 7.35 (d,  $J$ =5.1 Hz, 1H), 7.28 (d,  $J$ =5.4 Hz, 1H), 7.07-7.09 (m, 1H), 6.85 (d,  $J$ =6.0 Hz, 1H), 6.60 (dd,  $J$ =2.4, 5.7 Hz, 1H), 3.02-3.12 (m, 1H), 2.81-2.91 (m, 1H), 2.65-2.72 (m 1H), 1.01 (d,  $J$ =7.2 Hz, 3H)

$^{13}\text{C}$  NMR (75 MHz,  $\text{CDCl}_3$ ,  $25^\circ\text{C}$ )  $\delta$ =192.2 (CH), 144.8 (C), 142.3 (C), 141.7 (C), 138.8 (C), 128.4 (CH), 127.2 (CH), 125.8 (CH), 117.6 (CH), 33.9 ( $\text{CH}_2$ ), 24.4 (CH), 18.3 ( $\text{CH}_3$ )

IR (neat)  $\nu$  3083, 3048, 3022, 2979, 2961, 1765, 1732, 1222, 1210, 764  $\text{cm}^{-1}$

HRMS (ESI) for  $\text{C}_{12}\text{H}_{12}\text{OS}$  ( $\text{M}+\text{H}$ ) $^+$ : calcd 211.0769, found 211.0732.



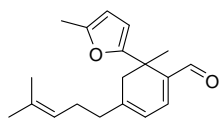
**6-Methyl-4-[2-(2,6,6-trimethyl-cyclohex-1-enyl)-vinyl]-cyclohexa-**

**1,3-dienecarbaldehyde (127):**  $^1\text{H}$  NMR (300MHz,  $\text{CDCl}_3$ ,  $25^\circ\text{C}$ ),  $\delta$ =9.47 (s, 1H), 6.79 (d,  $J$ =5.7 Hz, 1H), 6.50 (d,  $J$ =16.2 Hz, 1H), 6.26 (d,  $J$ =16.2 Hz, 1H), 6.09 (d,  $J$ =6.0 Hz, 1H), 2.96-3.07 (m, 1H), 2.52 (d,  $J$ =4.8 Hz, 2H), 1.74 (s, 3H), 1.60-1.66 (m, 2H), 1.45-1.50 (m, 4H), 1.05 (s, 6H), 0.96 (d,  $J$ =6.9 Hz, 3H)

$^{13}\text{C}$  NMR (75 MHz,  $\text{CDCl}_3$ ,  $25^\circ\text{C}$ )  $\delta$ =192.3 (CH), 144.6 (C), 143.1 (CH), 137.7 (C), 134.6 (CH), 131.9 (C), 131.7 (CH), 129.2 (C), 121.9 (CH), 39.9 ( $\text{CH}_2$ ), 34.5 ( $\text{CH}_2$ ), 33.5 ( $\text{CH}_2$ ), 30.4 (CH), 30.0 (C), 29.2 (2 x  $\text{CH}_3$ ), 24.1 ( $\text{CH}_3$ ), 19.3 ( $\text{CH}_3$ ), 18.4 ( $\text{CH}_2$ )

IR (neat)  $\nu$  3006, 2970, 2957, 2925, 2864, 1738, 1664, 1536, 1375, 1365, 1275, 1261, 1062, 764  $\text{cm}^{-1}$

HRMS (ESI) for  $\text{C}_{19}\text{H}_{26}\text{OLi}$  ( $\text{M}+\text{Li}$ ) $^{+}$ : calcd 277.2144, found 277.2134.



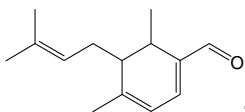
**6-methyl-6-(5-methylfuran-2-yl)-4-(4-methylpent-3-enyl)cyclohexa-**

**1,3-dienecarbaldehyde (128):**  $^1\text{H}$  NMR (300MHz,  $\text{CDCl}_3$ ,  $25^\circ\text{C}$ ),  $\delta$ =9.45 (s, 1H), 6.85 (d,  $J$ =6.0 Hz, 1H), 6.56 (d,  $J$ =6.0 Hz, 1H), 6.48 (d,  $J$ =3.3 Hz, 1H), 6.07-6.09 (m, 1H), 5.01-5.08 (m, 1H), 2.64 (dd,  $J$ =1.2, 17.1 Hz, 1H), 2.35 (s, 3H), 2.30 (dd,  $J$ =1.4, 17.3 Hz, 1H), 1.81-1.98 (m, 4H), 1.63 (s, 3H), 1.58 (s, 3H), 1.53 (s, 3H)

$^{13}\text{C}$  NMR (75 MHz,  $\text{CDCl}_3$ ,  $25^\circ\text{C}$ )  $\delta$ =193.1 (CH), 155.2 (C), 152.0 (C), 151.0 (C), 145.9 (CH), 141.9 (C), 132.4 (C), 124.9 (CH), 114.5 (CH), 112.0 (CH), 108.8 (CH), 43.7 (CH<sub>2</sub>), 38.4 (CH<sub>2</sub>), 37.7 (CH<sub>2</sub>), 32.2 (C), 24.0 (CH<sub>3</sub>), 23.0 (CH<sub>3</sub>), 21.3 (CH<sub>3</sub>), 14.4 (CH<sub>3</sub>)

IR (neat)  $\nu$  2920, 2851, 2171, 1737, 1541, 1454, 1375, 1265, 1049, 707, 703  $\text{cm}^{-1}$

HRMS (ESI) for  $\text{C}_{19}\text{H}_{24}\text{O}_2\text{Li}$  ( $\text{M}+\text{Li}$ ) $^{+}$ : calcd 291.1936, found 291.1957.



**4,6-Dimethyl-5-(3-methyl-but-2-enyl)-cyclohexa-1,3-**

**dienecarbaldehyde (129):**  $^1\text{H}$  NMR (300MHz,  $\text{CDCl}_3$ ,  $25^\circ\text{C}$ ),  $\delta$ =9.47 (s, 1 H), 6.66 (d,  $J$ =5.4 Hz, 1H), 5.93 (dq,  $J$ =1.5, 5.4 Hz, 1H), 5.02-5.09 (m, 1H), 2.78 (q,  $J$ =6.9 Hz, 1H), 1.83-1.96 (m, 6H), 1.69 (s, 3H), 1.48 (s, 3H), 0.97 (d,  $J$ =6.6 Hz, 3H)

$^{13}\text{C}$  NMR (75 MHz,  $\text{CDCl}_3$ ,  $25^\circ\text{C}$ ),  $\delta$ =192.9 (CH), 151.5 (C), 142.1 (CH), 139.3 (C), 134.3 (C), 121.5 (CH), 118.0 (CH), 47.1 (CH), 31.9 ( $\text{CH}_2$ ), 27.5 (CH), 25.8 ( $\text{CH}_3$ ), 23.6 ( $\text{CH}_3$ ), 22.7 ( $\text{CH}_3$ ), 17.8 ( $\text{CH}_3$ )

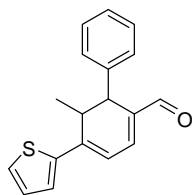
IR (neat)  $\nu$  2981, 2970, 1754, 1672, 1458, 1363, 1228, 1045  $\text{cm}^{-1}$

HRMS (ESI) for  $\text{C}_{14}\text{H}_{20}\text{O}$  ( $\text{M}+\text{Li}^+$ ): calcd 211.1674, found 211.1680.

### *Synthesis of Heterodimers with $\beta$ -ethyl Substituted Substrates*

The same synthetic procedure was utilized in the production of the tri-substituted cyclohexadienals that was used for the synthesis of the cross condensation products.

### *Characterization of Heterodimers Derived From $\beta$ -ethyl Substrates*



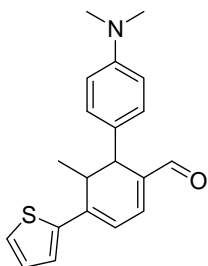
**5-methyl-6-phenyl-4-(thiophen-2-yl)cyclohexa-1,3-dienecarbaldehyde**

**(130):**  $^1\text{H}$  NMR (300MHz,  $\text{CDCl}_3$ ,  $25^\circ\text{C}$ ),  $\delta$ =9.62 (s, 1H), 7.11-7.28 (m, 6H), 7.02-7.16 (m, 2H), 6.62 (d,  $J$ =6.0 Hz, 1H), 3.94 (s, 1H), 3.19 (q,  $J$ =7.2 Hz, 1H), 1.22 (d,  $J$ =7.2 Hz, 3H)

$^{13}\text{C}$  NMR (75 MHz,  $\text{CDCl}_3$ ,  $25^\circ\text{C}$ ),  $\delta$ =192.6 (CH), 145.4 (C), 143.6 (C), 142.3 (CH), 142.2 (C), 137.2 (C), 128.8 (2 x  $\text{CH}_2$ ), 128.5 (CH), 127.5 (CH), 127.3 (2 x CH), 127.1 (CH), 126.0 (CH), 116.7 (CH), 42.3 (CH), 40.0 (CH), 20.7 ( $\text{CH}_3$ )

IR (neat)  $\nu$  3028, 2963, 2925, 2852, 2717, 1663, 1540, 1492, 1395, 1170, 845, 698  $\text{cm}^{-1}$

HRMS (ESI) for  $\text{C}_{18}\text{H}_{16}\text{OS}$  ( $\text{M}+\text{Li}^+$ ): calcd 287.1082, found 287.1063.



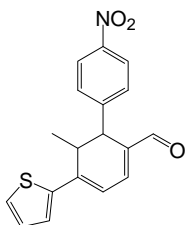
**6-(4-Dimethylamino-phenyl)-5-methyl-4-thiophen-2-yl-cyclohexa-**

**1,3-dienecarbaldehyde (131):**  $^1\text{H}$  NMR (300MHz,  $\text{CDCl}_3$ ,  $25^\circ\text{C}$ ),  $\delta$ =9.60 (s, 1H), 7.76 (d,  $J$ =5.4 Hz, 1H), 7.32 (dd,  $J$ =0.6, 5.1 Hz, 1H), 7.23 (dd,  $J$ =0.9, 3.9 Hz, 1H), 7.03 (d,  $J$ =9.0 Hz, 2H), 7.00 (d,  $J$ =6.0 Hz, 1H), 6.70 (d,  $J$ =9.0 Hz, 2H), 6.61 (d,  $J$ =6.0 Hz, 1H), 3.86 (s, 1H), 3.16 (q,  $J$ =7.5 Hz, 1H), 3.09 (s, 6H), 1.23 (d,  $J$ =7.5 Hz, 3H)

$^{13}\text{C}$  NMR (75 MHz,  $\text{CDCl}_3$ ,  $25^\circ\text{C}$ ),  $\delta$ =192.7 (CH), 149.5 (C), 149.2 (C), 147.3 (C), 145.4 (CH), 141.9 (C), 136.9 (C), 132.2 (CH), 128.5 (2 x CH), 127.5 (CH), 126.0 (CH), 166.6 (CH), 111.2 (2 x CH), 41.5 (CH), 40.3 (2 x  $\text{CH}_3$ ), 39.6 (CH), 20.6 ( $\text{CH}_3$ )

IR (neat)  $\nu$  3004, 2970, 2924, 2805, 2736, 1738, 1663, 1597, 1540, 1372, 1167, 765, 750  $\text{cm}^{-1}$

HRMS (ESI) for  $\text{C}_{20}\text{H}_{21}\text{ONS}$  ( $\text{M}+\text{H}$ ) $^+$ : calcd 324.1422, found 324.1452.



**5-Methyl-6-(4-nitro-phenyl)-4-thiophen-2-yl-cyclohexa-1,3-**

**dienecarbaldehyde (132):**  $^1\text{H}$  NMR (300MHz,  $\text{CDCl}_3$ ,  $25^\circ\text{C}$ ),  $\delta$ =9.66 (s, 1H), 8.07 (m, 2H), 7.55-7.60 (m, 1H), 7.39-7.46 (m, 2H), 7.26 (d,  $J$ =3.6 Hz, 1H), 7.18 (d,  $J$ =6.3 Hz,



1H), 7.04-7.10 (m, 1H), 6.69 (d, J=6.0 Hz, 1H), 4.06 (s, 1H), 3.18 (q, J=7.2 Hz, 1H), 1.22 (d, J=7.2 Hz, 3H)

<sup>13</sup>C NMR (75 MHz, CDCl<sub>3</sub>, 25°C), δ=192.2 (CH), 149.7 (C), 147.2 (C), 145.3 (C), 143.0 (CH), 143.0 (C), 135.8 (C), 133.3 (CH), 129.9 (2 x CH), 128.7 (CH), 128.2 (CH), 124.1 (2 x CH), 116.6 (CH), 42.2 (CH), 39.6 (CH), 20.7 (CH<sub>3</sub>)

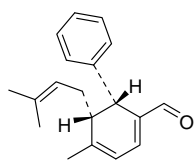
IR (neat) ν 3074, 2963, 2927, 2855, 1717, 1663, 1602, 1539, 1517, 1345, 1273, 1171, 852, 712 cm<sup>-1</sup>

HRMS (ESI) for C<sub>18</sub>H<sub>15</sub>O<sub>3</sub>NS (M+H)<sup>+</sup>: calcd 326.0851, found 326.0887.

#### *Synthesis of Heterodimers Effected by β-methylene Group*

The same synthetic procedure was utilized in the production of the tri-substituted cyclohexadienals that was used for the synthesis of the cross condensation products.

#### *Characterization of Heterodimers Effected by β-methylene Group*



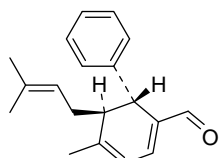
**(5R,6R)-4-methyl-5-(3-methylbut-2-enyl)-6-phenylcyclohexa-1,3-**

**dienecarbaldehyde (27):** <sup>1</sup>H NMR (300MHz, CDCl<sub>3</sub>, 25°C), δ=9.54 (s, 1H), 7.11-7.24 (m, 5H), 6.94 (d, J=5.7 Hz, 1H), 6.02-6.05 (m, 1H), 5.15-5.21 (m, 1H), 3.93 (s, 1H), 2.25 (dd, J=4.5, 12.6 Hz, 1H), 1.98-2.16 (m, 2H), 1.88 (s, 3H), 1.77 (s, 3H), 1.55 (s, 3H)

<sup>13</sup>C NMR (75 MHz, CDCl<sub>3</sub>, 25°C) δ= 192.9 (CH), 152.0 (C), 143.6 (CH), 142.7 (C), 136.4 (C), 135.6 (C), 128.7 (2 x CH), 127.3 (2 x CH), 126.8 (CH), 121.3 (CH), 119.2 (CH), 48.4 (CH), 38.2 (CH), 30.8 (CH<sub>2</sub>), 26.2 (CH<sub>3</sub>), 23.6 (CH<sub>3</sub>), 17.9 (CH<sub>3</sub>)

IR (neat)  $\nu$  3029, 2969, 2916, 2850, 2806, 2715, 2160, 1670, 1641, 1575, 1442, 1201, 1182  $\text{cm}^{-1}$

HRMS (ESI) for  $\text{C}_{19}\text{H}_{22}\text{OLi}$  ( $\text{M}+\text{Li}$ ) $^{+}$ : calcd 273.1831, found 273.1832.



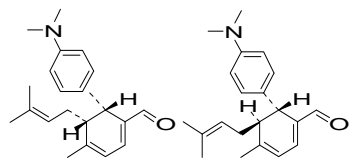
**(5S,6R)-4-methyl-5-(3-methylbut-2-enyl)-6-phenylcyclohexa-1,3-**

**dienecarbaldehyde (28):**  $^1\text{H}$  NMR (300MHz,  $\text{CDCl}_3$ ,  $25^\circ\text{C}$ ),  $\delta$ = 9.43 (s, 1H), 7.13-7.29 (m, 5H). 6.81 (d,  $J$ =5.7 Hz, 1H), 6.10-6.14 (m, 1H), 5.10-5.15 (m, 1H), 3.97 (d,  $J$ =9.0 Hz, 1H), 2.87-2.95 (m, 1H), 2.25-2.35 (m, 1H), 2.09-2.16 (m, 1H), 1.96 (s, 3H), 1.70 (s, 3H), 1.29 (s, 3H)

$^{13}\text{C}$  NMR (75 MHz,  $\text{CDCl}_3$ ,  $25^\circ\text{C}$ )  $\delta$ =192.3 (CH), 151.9 (C), 143.2 (CH), 141.1 (C), 138.9 (C), 133.4 (C), 129.2 (2 x CH), 128.2 (2 x CH), 127.0 (CH), 123.0 (CH), 121.6 (CH), 43.7 (CH), 38.5 (CH), 26.5 ( $\text{CH}_2$ ), 26.1 ( $\text{CH}_3$ ), 22.4 ( $\text{CH}_3$ ), 18.1 ( $\text{CH}_3$ )

IR (neat)  $\nu$  3029, 2917, 2852, 2713, 2165, 1670, 1571, 1452, 1169, 698  $\text{cm}^{-1}$

HRMS (ESI) for  $\text{C}_{19}\text{H}_{22}\text{OLi}$  ( $\text{M}+\text{Li}$ ) $^{+}$ : calcd 273.1831, found 273.1832.



**6-(4-Dimethylamino-phenyl)-4-methyl-5-(3-methyl-but-2-**

**enyl)-cyclohexa-1,3-dienecarbaldehyde(133 & 134):**  $^1\text{H}$  NMR (300MHz,  $\text{CDCl}_3$ ,  $25^\circ\text{C}$ ), trans product  $\delta$ =9.53 (s, 1H), 7.04 (d,  $J$ =8.7 Hz, 2H), 6.87 (d,  $J$ =5.7 Hz, 1H), 6.61

(d,  $J=8.7$  Hz, 2H), 6.00-6.06 (m, 1H), 5.15-5.21 (m, 1H), 3.85 (s, 1H), 2.88 (s, 6H), 2.27 (dd,  $J=4.5, 9.9$  Hz, 1H), 1.96-2.22 (m, 2H), 1.90 (s, 3H), 1.76 (s, 3H), 1.67 (s, 3H)

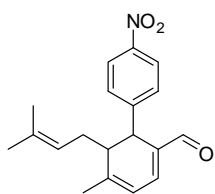
cis product  $\delta=9.50$  (s, 1H), 7.10 (d,  $J=9.0$  Hz, 2H), 6.87 (d,  $J=5.7$  Hz, 1H), 6.61 (d,  $J=8.7$  Hz, 2H), 6.00-6.06 (m, 1H), 5.15-5.21 (m, 1H), 4.99-5.04 (m, 1H), 3.98 (d,  $J=9.3$  Hz, 1H), 2.88 (s, 6H), 2.47 (dd,  $J=1.2, 18$ Hz, 1H), 1.96-2.22 (m, 2H), 1.90 (s, 3H), 1.76 (s, 3H), 1.67 (s, 3H)

$^{13}\text{C}$  NMR (75 MHz,  $\text{CDCl}_3$ ,  $25^\circ\text{C}$ ) trans product  $\delta=193.1$  (CH), 152.0 (C), 149.7 (C), 143.0 (CH), 137.1 (C), 135.2 (C), 131.1 (C), 128.0 (2 x CH), 121.6 (CH), 119.1 (CH), 113.0 (2 x CH), 48.4 (CH), 41.0 (2 x  $\text{CH}_3$ ), 37.4 (CH), 30.8 ( $\text{CH}_2$ ), 26.2 ( $\text{CH}_3$ ), 23.6 ( $\text{CH}_3$ ), 18.0 ( $\text{CH}_3$ )

cis product  $\delta=192.6$  (CH), 151.1 (C), 149.6 (C), 143.8 (CH), 138.4 (C), 132.6 (C), 131.4 (C), 127.9 (2 x CH), 123.5 (CH), 119.0 (CH), 113.0 (2 x CH), 48.4 (CH), 41.0 (2 x  $\text{CH}_3$ ), 33.5 (CH), 30.8 ( $\text{CH}_2$ ), 26.0 ( $\text{CH}_3$ ), 23.6 ( $\text{CH}_3$ ), 18.0 ( $\text{CH}_3$ )

IR (neat)  $\nu$  2966, 2909, 2805, 2715, 1672, 1641, 1614, 1576, 1519, 1444, 1349, 1196, 1162,  $815\text{ cm}^{-1}$

HRMS (ESI) for  $\text{C}_{21}\text{H}_{27}\text{NOLi}$  ( $\text{M}+\text{Li}$ ) $^+$ : calcd 316.2253, found 316.2273.



**4-methyl-5-(3-methylbut-2-enyl)-6-(4-nitrophenyl)cyclohexa-1,3-**

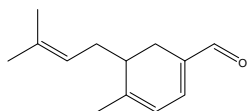
**dienecarbaldehyde (135):**  $^1\text{H}$  NMR (300MHz,  $\text{CDCl}_3$ ,  $25^\circ\text{C}$ ),  $\delta=9.55$  (s, 1H), 8.07 (d,  $J=8.7$  Hz, 2H), 7.27 (d,  $J=8.7$  Hz, 2H), 7.03 (d,  $J=5.4$  Hz, 1H), 6.08 (dd,  $J=1.5, 5.7$  Hz,

1H), 5.17-5.20 (m, 1H), 4.02 (s, 1H), 2.12-2.22 (m, 3H), 1.88 (s, 3H), 1.79 (s, 3H), 1.54 (s, 3H)

$^{13}\text{C}$  NMR (75 MHz,  $\text{CDCl}_3$ ,  $25^\circ\text{C}$ ),  $\delta$ =192.4 (CH), 151.8 (C), 150.3 (C), 145.8 (C), 144.1 (CH), 136.4 (C), 135.1 (C), 128.3 (2 x CH), 124.0 (2 x CH), 120.1 (CH), 119.3 (CH), 48.4 (CH), 38.1 (CH), 30.7 ( $\text{CH}_2$ ), 26.2 ( $\text{CH}_3$ ), 23.5 ( $\text{CH}_3$ ), 17.9 ( $\text{CH}_3$ )

IR (neat)  $\nu$  2967, 2928, 2382, 2327, 2335, 1673, 1576, 1520, 1346, 1110, 837  $\text{cm}^{-1}$

HRMS (ESI) for  $\text{C}_{19}\text{H}_{21}\text{NO}_3$  ( $\text{M}+\text{H}$ ) $^+$ : calcd 318.1681, found 318.1741.



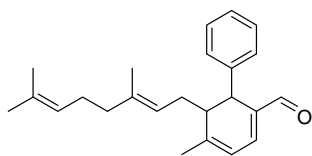
**4-Methyl-5-(3-methyl-but-2-enyl)-cyclohexa-1,3-**

**dienecarbaldehyde (136):**  $^1\text{H}$  NMR (300MHz,  $\text{CDCl}_3$ ,  $25^\circ\text{C}$ ),  $\delta$ =9.49 (s, 1H), 6.72 (dd,  $J$ =2.1, 5.4 Hz, 1H), 5.95 (dd,  $J$ =1.2, 5.4 Hz, 1H), 5.02-5.08 (m, 1H), 2.62 (dd,  $J$ =3.3, 17.1 Hz, 1H), 2.11-2.37 (m, 4H), 1.95 (s, 3H), 1.70 (s, 3H), 1.51 (s, 3H)

$^{13}\text{C}$  NMR (75 MHz,  $\text{CDCl}_3$ ,  $25^\circ\text{C}$ ),  $\delta$ =193.2 (CH), 153.2 (C), 132.7 (CH), 134.5 (C), 134.3 (C), 121.7 (CH), 119.7 (CH), 38.9 (CH), 29.9 ( $\text{CH}_2$ ), 29.3 ( $\text{CH}_2$ ), 26.1 ( $\text{CH}_3$ ) 23.0 ( $\text{CH}_3$ ), 17.8 ( $\text{CH}_3$ )

IR (neat)  $\nu$  2926, 2855, 1686, 1670, 1575, 1442, 1266, 735  $\text{cm}^{-1}$

HRMS (ESI) for  $\text{C}_{13}\text{H}_{18}\text{O}$  ( $\text{M}+\text{H}$ ) $^+$ : calcd 191.1436, found 191.1447.



**5-(3,7-dimethylocta-2,6-dienyl)-4-methyl-6-phenylcyclohexa-**

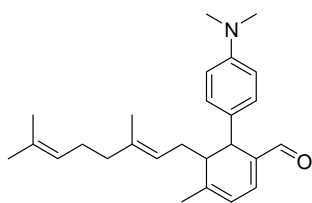
**1,3-dienecarbaldehyde (137):**  $^1\text{H}$  NMR (300MHz,  $\text{CDCl}_3$ ,  $25^\circ\text{C}$ ),  $\delta$ =9.54 (s, 1H), 7.12-

7.24 (m, 5H), 6.94 (d,  $J=5.7$ , 1H), 6.04 (dq,  $J=1.5$ , 5.7 Hz, 1H), 5.04-5.23 (m, 2H), 3.93 (s, 1H), 2.46 (t,  $J=6.9$  Hz, 1H), 2.23-2.30 (m, 1H), 1.95-2.17 (m, 5H), 1.88 (d,  $J=1.2$  Hz, 3H), 1.70 (d,  $J=1.2$  Hz, 3H), 1.63 (s, 3H), 1.58 (s, 3H)

$^{13}\text{C}$  NMR (75 MHz,  $\text{CDCl}_3$ , 25°C),  $\delta=192.8$  (CH), 151.9 (C), 143.6 (CH), 142.8 (C), 139.2 (C), 136.4 (C), 131.8 (C), 128.7 (2 x CH), 127.3 (2 x CH), 126.8 (CH), 124.4 (CH), 121.1 (CH), 119.2 (CH), 48.5 (CH), 40.2 ( $\text{CH}_2$ ), 38.3 (CH), 30.8 ( $\text{CH}_2$ ), 26.9 ( $\text{CH}_2$ ), 26.0 ( $\text{CH}_3$ ), 23.6 ( $\text{CH}_3$ ), 18.0 ( $\text{CH}_3$ ), 16.3 ( $\text{CH}_3$ )

IR (neat)  $\nu$  2972, 2924, 2851, 2370, 2328, 2318, 1702, 1674, 1578, 1261, 1077, 764, 699  $\text{cm}^{-1}$

HRMS (ESI) for  $\text{C}_{24}\text{H}_{30}\text{O}$  ( $\text{M}+\text{H}$ ) $^+$ : calcd 341.2457, found 341.2456.



**6-(4-Dimethylamino-phenyl)-5-(3,7-dimethyl-octa-2,6-**

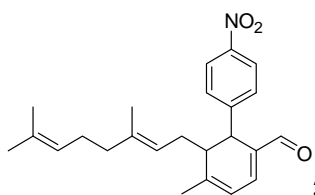
**dienyl)-4-methyl-cyclohexa-1,3-dienecarbaldehyde (138):**  $^1\text{H}$  NMR (300MHz,  $\text{CDCl}_3$ , 25°C),  $\delta=9.52$  (s, 1H), 7.03 (d,  $J=9.0$  Hz, 2H), 6.87 (d,  $J=5.4$  Hz, 1H), 6.60 (d,  $J=8.7$  Hz, 2H), 6.01 (dd,  $J=1.5$ , 5.7 Hz, 1H), 5.12-5.22 (m, 2H), 3.84 (s, 1H), 2.88 (s, 6H), 2.85 (dd,  $J=4.5$ , 9.1 Hz, 1H), 1.95-2.18 (m, 6H), 1.90 (s, 3H), 1.71 (s, 3H), 1.63 (s, 3H), 1.55 (s, 3H)

$^{13}\text{C}$  NMR (75 MHz,  $\text{CDCl}_3$ , 25°C),  $\delta=191.7$  (CH), 150.6 (C), 148.4 (C), 141.6 (CH), 137.6 (C), 135.8 (C), 130.5 (C), 129.8 (C), 126.7 (2 x CH), 123.2 (CH), 120.3 (CH),

117.8 (CH), 111.7 (2 x CH), 47.2 (CH), 39.7 (2 x CH<sub>3</sub>), 38.9 (CH<sub>2</sub>), 36.2 (CH), 29.6 (CH<sub>2</sub>), 25.7 (CH<sub>2</sub>), 24.7 (CH<sub>3</sub>), 22.4 (CH<sub>3</sub>), 16.7 (CH<sub>3</sub>), 15.0 (CH<sub>3</sub>)

IR (neat)  $\nu$  2926, 2865, 2823, 2720, 1735, 1664, 1613, 1519, 1357, 1200, 1160, 966, 820  $\text{cm}^{-1}$

HRMS (ESI) for C<sub>26</sub>H<sub>35</sub>NO (M+H)<sup>+</sup>: calcd 378.2797, found 378.2626.

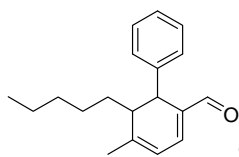


**5-(3,7-Dimethyl-octa-2,6-dienyl)-4-methyl-6-(4-nitro-phenyl)-cyclohexa-1,3-dienecarbaldehyde (139):** <sup>1</sup>H NMR (300MHz, CDCl<sub>3</sub>, 25°C),  $\delta$ =9.55 (s, 1H), 8.07 (d, J=8.7 Hz, 2H), 7.26 (d, J=8.7 Hz, 2H), 7.03 (d, J=5.4 Hz, 1H), 6.08 (d, J=5.4 Hz, 1H), 5.11-5.20 (m, 2H), 4.02 (s, 1H), 2.05-2.27 (m, 7H), 1.88 (s, 3H), 1.70 (s, 3H), 1.63 (s, 3H), 1.54 (s, 3H)

<sup>13</sup>C NMR (75 MHz, CDCl<sub>3</sub>, 25°C),  $\delta$ =192.3 (CH), 151.7 (C), 150.4 (C), 147.0 (C), 144.0 (CH), 140.1 (C), 135.2 (C), 132.0 (C), 128.3 (2 x CH), 124.2 (CH), 124.0 (2 x CH), 120.6 (CH), 119.3 (CH), 48.5 (CH), 40.1 (CH<sub>2</sub>), 38.2 (CH), 30.7 (CH<sub>2</sub>), 26.9 (CH<sub>2</sub>), 26.0 (CH<sub>3</sub>), 23.5 (CH<sub>3</sub>), 18.0 (CH<sub>3</sub>), 16.3 (CH<sub>3</sub>)

IR (neat)  $\nu$  2968, 2914, 2853, 2716, 1670, 1576, 1517, 1440, 1344, 1183, 837  $\text{cm}^{-1}$

HRMS (ESI) for C<sub>24</sub>H<sub>29</sub>NO<sub>3</sub> (M+Li)<sup>+</sup>: calcd 386.2307, found 386.2387.



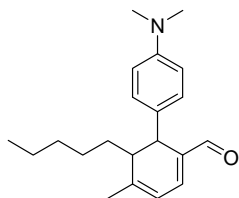
**4-Methyl-5-pentyl-6-phenyl-cyclohexa-1,3-dienecarbaldehyde**

**(140):**  $^1\text{H}$  NMR (300MHz,  $\text{CDCl}_3$ ,  $25^\circ\text{C}$ ),  $\delta=9.55$  (s, 1H), 7.06-7.27 (m, 5H), 6.96 (d,  $J=5.7$  Hz, 1H), 5.98-6.03 (m, 1H), 3.86 (s, 1H), 2.14 (t,  $J=7.2$  Hz, 1H), 1.90 (s, 3H), 1.20-1.42 (m, 8H), 0.84-0.90 (m, 3H)

$^{13}\text{C}$  NMR (75 MHz,  $\text{CDCl}_3$ ,  $25^\circ\text{C}$ ),  $\delta=192.4$  (CH), 152.3 (C), 143.6 (C), 143.8 (CH), 142.9 (C), 128.6 (2 x CH), 127.3 (2 x CH), 126.9 (CH), 119.0 (CH), 38.9 ( $\text{CH}_2$ ), 38.0 (CH), 32.2 (CH), 31.9 ( $\text{CH}_2$ ), 26.9 ( $\text{CH}_2$ ), 23.6 ( $\text{CH}_3$ ), 22.8 ( $\text{CH}_2$ ), 14.3 ( $\text{CH}_3$ )

IR (neat)  $\nu$  2955, 2926, 2856, 1725, 1674, 1577, 1453, 1378, 1274, 1181, 1031, 763, 698  $\text{cm}^{-1}$

HRMS (ESI) for  $\text{C}_{19}\text{H}_{24}\text{O}$  ( $\text{M}+\text{Li}$ ) $^+$ : calcd 275.1987, found 275.2025.



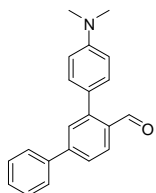
**6-(4-Dimethylamino-phenyl)-4-methyl-5-pentyl-cyclohexa-1,3-**

**dienecarbaldehyde (141):**  $^1\text{H}$  NMR (300MHz,  $\text{CDCl}_3$ ,  $25^\circ\text{C}$ ),  $\delta=9.51$  (s, 1H), 7.05-7.10 (m, 2H), 6.84 (d,  $J=5.4$  Hz, 1H), 6.61 (d,  $J=8.7$  Hz, 2H), 5.98-6.03 (m, 1H), 3.86 (s, 1H), 2.88 (s, 6H), 2.14 (t,  $J=7.2$  Hz, 1H), 1.88 (s, 3H), 1.19-1.42 (m, 8H), 0.84-0.91 (m, 3H)

$^{13}\text{C}$  NMR (75 MHz,  $\text{CDCl}_3$ ,  $25^\circ\text{C}$ ),  $\delta=193.1$  (CH), 152.3 (C), 143.9 (C), 143.1 (CH), 137.2 (C), 131.2 (C), 127.9 (2 x CH), 118.9 (CH), 113.0 (2 x CH), 40.9 (2 x  $\text{CH}_3$ ), 38.2 ( $\text{CH}_2$ ), 37.9 (CH), 33.5 (CH), 32.1 ( $\text{CH}_2$ ), 26.6 ( $\text{CH}_2$ ), 23.6 ( $\text{CH}_3$ ), 22.8 ( $\text{CH}_2$ ), 14.3 ( $\text{CH}_3$ )

HRMS (ESI) for  $C_{21}H_{29}NO$  ( $M+H$ )<sup>+</sup>: calcd 312.2327, found 312.2356.

*Characterization of Aromatic Heterodimers*



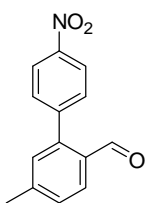
**4''-Dimethylamino-[1,1';3',1'']terphenyl-4'-carbaldehyde (142):**  $^1H$

NMR (300MHz,  $CDCl_3$ , 25°C),  $\delta$ =10.06 (1H), 8.07 (d,  $J$ =8.4 Hz, 1H), 7.65-7.69 (m, 2H), 7.30-7.52 (m, 7H), 6.83 (d,  $J$ =8.7 Hz, 2H), 3.04 (6H)

$^{13}C$  NMR (75 MHz,  $CDCl_3$ , 25°C)  $\delta$ =193.1 (CH), 150.6 (C), 147.5 (C), 144.5 (C), 142.4 (C), 140.2 (C), 134.7 (C), 132.7 (CH), 131.4 (2 x CH), 129.6 (CH), 129.2 (2 x CH), 128.5 (CH), 127.6 (2 x CH), 125.7 (CH), 112.3 (2 x CH), 40.7 (2 x  $CH_3$ )

IR (neat)  $\nu$  3063, 2957, 2919, 2850, 2382, 2366, 2330, 2326, 2310, 1682, 1600, 1396, 1263, 840  $cm^{-1}$

LRMS (APCI) for  $C_{21}H_{19}NO$  ( $M+H$ )<sup>+</sup>: calcd 302.2, found 302.2.



**5-Methyl-4'-nitro-biphenyl-2-carbaldehyde (143):**  $^1H$  NMR (300MHz,

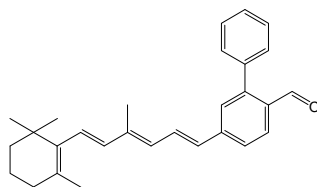
$CDCl_3$ , 25°C),  $\delta$ =10.38 (s, 1H), 8.37 (d,  $J$ =9.0 Hz, 2H), 7.97 (d,  $J$ =8.1 Hz, 1H), 7.81 (d,  $J$ =9.0 Hz, 2H), 7.65 (d,  $J$ =8.1 Hz, 1H), 7.56 (s, 1H), 2.81 (s, 3H)

$^{13}C$  NMR (75 MHz,  $CDCl_3$ , 25°C),  $\delta$ =192.4 (CH), 148.0 (C), 146.4 (C), 143.8 (C), 141.7 (C), 134.3 (C), 133.0 (CH), 131.1 (CH), 128.4 (2 x CH), 125.6 (CH), 124.5 (2 x CH), 20.0 ( $CH_3$ )



IR (neat)  $\nu$  3082, 2971, 2925, 2852, 2744, 1738, 1694, 1596, 1563, 1509, 1342, 1218, 1203, 1108, 851, 823, 753  $\text{cm}^{-1}$

HRMS (ESI) for  $\text{C}_{14}\text{H}_{11}\text{O}_3\text{NLi}$  ( $\text{M}+\text{Li}$ ) $^{+}$ : calcd 248.0899, found 248.0993.



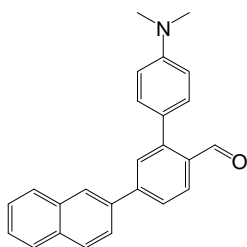
**5-[4-Methyl-6-(2,6,6-trimethyl-cyclohex-1-enyl)-hexa-1,3,5-**

**trienyl]-biphenyl-2-carbaldehyde (144):**  $^1\text{H}$  NMR (300MHz,  $\text{CDCl}_3$ ,  $25^\circ\text{C}$ ),  $\delta$ =9.91 (s, 1H), 7.99 (d,  $J$ =8.4 Hz, 1H), 7.39-7.55 (m, 7H), 7.35 (d,  $J$ =3.6 Hz, 1H), 6.60 (d,  $J$ =15.3 Hz, 1H), 6.14-6.32 (m, 3H), 2.05 (s, 3H), 2.03 (t,  $J$ =6.9 Hz, 2H), 1.73 (s, 3H), 1.58-1.66 (m, 2H), 1.46-1.49 (m, 2H), 1.04 (s, 6H)

$^{13}\text{C}$  NMR (75 MHz,  $\text{CDCl}_3$ ,  $25^\circ\text{C}$ ),  $\delta$ =191.9 (CH), 146.8 (C), 143.4 (C), 139.4 (C), 138.2 (C), 138.0 (C), 137.5 (CH), 137.4 (C), 132.4 (C), 130.5 (CH), 130.2 (2 x CH), 129.8 (CH), 129.3 (CH), 128.8 (CH), 128.4 (2 x CH), 128.6 (CH), 128.4 (CH), 128.3 (CH), 125.6 (CH), 39.8 ( $\text{CH}_2$ ), 34.5 (C), 33.3 ( $\text{CH}_2$ ), 29.2 (2 x  $\text{CH}_3$ ), 22.0 ( $\text{CH}_3$ ), 19.5 ( $\text{CH}_2$ ), 13.2 ( $\text{CH}_3$ )

IR (neat)  $\nu$  3028, 2958, 2925, 2859, 1738, 1683, 1583, 1445, 1361, 1258, 1208, 1118, 967, 806, 767, 702  $\text{cm}^{-1}$

HRMS (ESI) for  $\text{C}_{29}\text{H}_{32}\text{O}$  ( $\text{M}+\text{H}$ ) $^{+}$ : calcd 403.2613, found 403.2653.



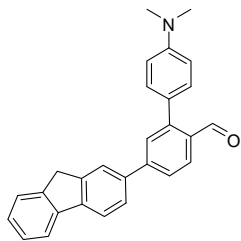
**4'-Dimethylamino-5-naphthalen-2-yl-biphenyl-2-carbaldehyde**

**(145):**  $^1\text{H}$  NMR (300MHz,  $\text{CDCl}_3$ ,  $25^\circ\text{C}$ ),  $\delta$ =10.08 (s, 1H), 8.10-8.14 (m, 2H), 7.86-7.96 (m, 3H), 7.75-7.82 (m, 3H), 7.49-7.58 (m, 2H), 7.35 (d,  $J$ =9.0 Hz, 2H), 8.84 (d,  $J$ =9.0 Hz, 2H), 3.04 (s, 6H)

$^{13}\text{C}$  NMR (75 MHz,  $\text{CDCl}_3$ ,  $25^\circ\text{C}$ ),  $\delta$ =192.0 (CH), 149.5 (C), 146.1 (C), 145.1 (C), 136.3 (C), 132.7 (C), 132.2 (C), 131.5 (C), 130.3 (C), 130.2 (2 x CH), 128.7 (CH), 127.8 (CH), 127.5 (2 x CH), 127.4 (CH), 126.8 (CH), 125.7 (2 x CH), 124.8 (CH), 124.3 (CH), 111.2 (2 x CH), 39.5 (2 x  $\text{CH}_3$ )

IR (neat)  $\nu$  2919, 2850, 1683, 1598, 1525, 1360, 1196, 816, 749  $\text{cm}^{-1}$

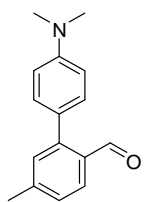
HRMS (ESI) for  $\text{C}_{25}\text{H}_{21}\text{NO}$  ( $\text{M}+\text{H}$ ) $^+$ : calcd 352.1701, found 352.1747.



**4'-Dimethylamino-5-(9H-fluoren-2-yl)-biphenyl-2-carbaldehyde**

**(146):**  $^1\text{H}$  NMR (300MHz,  $\text{CDCl}_3$ ,  $25^\circ\text{C}$ ),  $\delta$ =10.01 (s, 1H), 8.10 (d,  $J$ =7.8 Hz, 1H), 7.77-7.89 (m, 4H), 7.68-7.70 (m, 2H), 7.57 (d,  $J$ =7.2 Hz, 1H), 7.50 (d,  $J$ =7.8 Hz, 2H), 7.32-7.43 (m, 4H), 3.98 (s, 2H), 3.16 (s, 6H);  $^{13}\text{C}$  NMR (75 MHz,  $\text{CDCl}_3$ ,  $25^\circ\text{C}$ )  $\delta$ =193.1 (CH), 153.0 (C), 149.1 (C), 148.5 (C), 145.7 (C), 144.3 (C), 143.8 (C), 141.2 (C), 134.9 (C), 132.5 (C), 131.4 (2 x CH), 129.5 (CH), 128.4 (CH), 127.3 (2 x CH), 127.2 (CH),

126.5 (CH), 125.7 (CH), 125.4 (CH), 124.3 (CH), 120.5 (CH), 120.4 (CH), 112.5 (2 x CH), 40.8 (2 x CH<sub>3</sub>), 34.5 (CH<sub>2</sub>); IR (neat)  $\nu$  3046, 2985, 2954, 1677, 1589, 1458, 1265, 1119, 825, 771 cm<sup>-1</sup> HRMS (ESI) for C<sub>28</sub>H<sub>23</sub>NO (M+H)<sup>+</sup>: calcd 390.1858, found 390.1853.



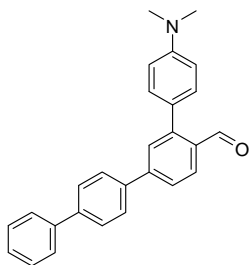
**4'-(dimethylamino)-5-methylbiphenyl-2-carbaldehyde (147):** <sup>1</sup>H NMR

(300MHz, CDCl<sub>3</sub>, 25°C),  $\delta$ =9.98 (s, 1H), 7.90 (d, J=7.8 Hz, 1H), 7.57 (d, J=9.0 Hz, 1H), 7.24-7.28 (m, 3H), 6.80 (d, J=8.7 Hz, 2H), 3.02 (s, 6H), 2.44 (s, 3H)

<sup>13</sup>C NMR (75 MHz, CDCl<sub>3</sub>, 25°C),  $\delta$ =193.1 (CH), 155.1 (C), 150.5 (C), 146.7 (C), 144.6 (CH), 141.3 (C), 133.1 (C), 131.5 (CH), 131.3 (2 x CH), 127.9 (CH), 112.3 (2 x CH), 40.7 (2 x CH<sub>3</sub>), 22.1 (CH<sub>3</sub>)

IR (neat)  $\nu$  2925, 2853, 2383, 2327, 2310, 1678, 1602, 1524, 1357, 1198, 817 cm<sup>-1</sup>

HRMS (ESI) for C<sub>16</sub>H<sub>17</sub>ONLi (M+Li)<sup>+</sup>: calcd 246.1470, found 246.1485.



**4'''-Dimethylamino-[1,1';4',1'';3'',1''']quaterphenyl-4''-**

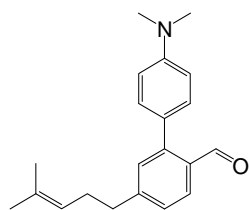
**carbaldehyde (148):** <sup>1</sup>H NMR (300MHz, CDCl<sub>3</sub>, 25°C),  $\delta$ =10.10 (s, 1H), 8.12 (d, J=8.4

Hz, 1H), 7.68-7.81 (m, 8H), 7.48-7.53 (m, 2H), 7.41-7.44 (m, 1H), 7.38 (d, J=9.0 Hz 2H), 6.87 (d, J=8.7 Hz, 2H), 3.08 (s, 6H)

$^{13}\text{C}$  NMR (75 MHz,  $\text{CDCl}_3$ ,  $25^\circ\text{C}$ )  $\delta$ = 193.0 (CH), 150.7 (C), 147.2 (C), 145.8 (C), 141.5 (C), 140.7 (C), 139.0 (C), 132.7 (C), 131.4 (2 x CH), 129.4 (CH), 129.1 (2 x CH), 128.6 (CH), 128.0 (2 x CH), 127.9 (2 x CH), 127.8 (CH), 127.3 (2 x CH), 125.6 (CH), 125.5 (C), 112.4 (2 x CH), 20.7 (2 x  $\text{CH}_3$ )

IR (neat)  $\nu$  3039, 2924, 2342, 2213, 1685, 1601, 1487, 1446, 1264, 1003, 817, 740, 734,  $692\text{ cm}^{-1}$

HRMS (ESI) for  $\text{C}_{27}\text{H}_{23}\text{NO}$  ( $\text{M}+\text{H}$ ) $^+$ : calcd 378.1858, found 378.1868.



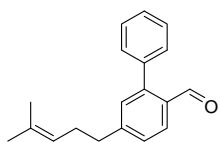
**4'-Dimethylamino-5-(4-methyl-pent-3-enyl)-biphenyl-2-**

**carbaldehyde (149):**  $^1\text{H}$  NMR (300MHz,  $\text{CDCl}_3$ ,  $25^\circ\text{C}$ ),  $\delta$ =10.24 (s, 1H), 7.85 (d, J=8.1 Hz, 1H), 7.53-7.60 (m, 3H), 7.45 (s, 1H), 6.81 (d, J=9.0 Hz, 2 H), 5.19-5.25 (m, 1H), 3.09 (t, J=7.2 Hz, 2H), 3.03 (s, 6H), 2.29-2.39 (m, 2H), 1.68 (s, 3H), 1.49 (s, 3H)

$^{13}\text{C}$  NMR (75 MHz,  $\text{CDCl}_3$ ,  $25^\circ\text{C}$ ),  $\delta$ =191.8 (CH), 145.7 (C), 133.4 (C), 133.3 (C), 132.2 (CH), 131.7 (C), 129.9 (C), 128.6 (CH), 128.2 (2 x CH), 127.4 (C), 124.1 (CH), 123.3 (CH), 112.7 (2 x CH), 40.6 (2 x  $\text{CH}_3$ ), 33.0 ( $\text{CH}_2$ ), 30.8 ( $\text{CH}_2$ ), 25.9 ( $\text{CH}_3$ ), 17.8 ( $\text{CH}_3$ )

IR (neat)  $\nu$  2968, 2918, 2850, 2350, 1736, 1667, 1594, 1515, 1457,  $1345\text{ cm}^{-1}$

HRMS (ESI) for  $\text{C}_{21}\text{H}_{25}\text{NO}$  ( $\text{M}+\text{Li}$ ) $^+$ : calcd 314.2096, found 314.2093.



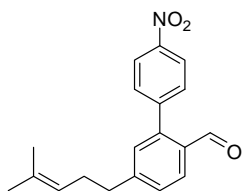
**5-(4-methylpent-3-enyl)biphenyl-2-carbaldehyde (150):**  $^1\text{H}$  NMR

(300MHz,  $\text{CDCl}_3$ ,  $25^\circ\text{C}$ ),  $\delta=9.94$  (s, 1H), 7.96 (d,  $J=8.1$  Hz, 1H), 7.20-7.50 (m, 7H), 5.13-5.19 (m, 1H), 2.74 (t,  $J=7.7$  Hz, 2H), 2.31-2.41 (m, 2H), 1.69 (s, 3H), 1.55 (d,  $J=1.8$  Hz, 3H)

$^{13}\text{C}$  NMR (75 MHz,  $\text{CDCl}_3$ ,  $25^\circ\text{C}$ )  $\delta=192.5$  (CH), 149.1 (C), 146.3 (C), 138.3 (C), 133.1 (C), 131.9 (C), 131.1 (CH), 130.3 (2 x CH), 128.6 (2 x CH), 128.3 (CH), 128.2 (CH), 127.9 (CH), 123.2 (CH), 36.5 ( $\text{CH}_2$ ), 29.8 ( $\text{CH}_2$ ), 25.9 ( $\text{CH}_3$ ), 17.9 ( $\text{CH}_3$ )

IR (neat)  $\nu$  2966, 2923, 2856, 2371, 2343, 2318, 1687, 1602, 1445, 1258, 1075, 831, 797, 768, 702  $\text{cm}^{-1}$

HRMS (ESI) for  $\text{C}_{19}\text{H}_{20}\text{O}$  ( $\text{M}+\text{H}$ ) $^+$ : calcd 265.1592, found 265.0790.



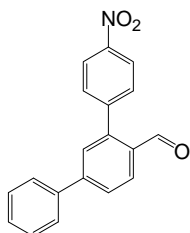
**5-(4-Methyl-pent-3-enyl)-4'-nitro-biphenyl-2-carbaldehyde (151):**

$^1\text{H}$  NMR (300MHz,  $\text{CDCl}_3$ ,  $25^\circ\text{C}$ ),  $\delta=9.71$  (s, 1H), 8.33 (d,  $J=9.0$  Hz, 1H), 8.17 (d,  $J=8.7$  Hz, 1H), 7.57 (d,  $J=9.0$  Hz, 1H), 7.53 (s, 1H), 7.42 (d,  $J=9.0$  Hz, 1H), 6.95 (d,  $J=16.8$  Hz, 1H), 6.81 (d,  $J=16.5$  Hz, 1H), 4.37 (t,  $J=7.6$  Hz, 1H), 3.28 (t,  $J=7.7$  Hz, 2H), 2.69-2.79 (m, 2H), 1.71 (s, 3H), 1.58 (s, 3H)

$^{13}\text{C}$  NMR (75 MHz,  $\text{CDCl}_3$ ,  $25^\circ\text{C}$ ),  $\delta=185.2$  (CH), 149.2 (C), 146.9 (C), 143.7 (C), 140.5 (C), 139.1 (C), 134.0 (C), 131.6 (CH), 126.5 (2 x CH), 124.5 (2 x CH), 124.0 (2 x CH), 120.9 (CH), 30.0 ( $\text{CH}_2$ ), 26.9 ( $\text{CH}_2$ ), 25.3 ( $\text{CH}_3$ ), 18.03 ( $\text{CH}_3$ )

IR (neat)  $\nu$  2928, 2850, 2324, 2218, 2027, 1995, 1734, 1667, 1592, 1515, 1458, 1343, 1109, 859  $\text{cm}^{-1}$

HRMS (ESI) for  $\text{C}_{19}\text{H}_{19}\text{NO}_3$  ( $\text{M}+\text{H}$ ) $^{+}$ : calcd 310.1443, found 310.1437.



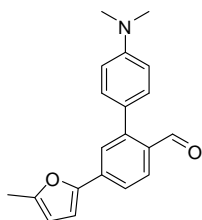
**4''-Nitro-[1,1';3',1'']terphenyl-4'-carbaldehyde (152):**  $^1\text{H}$  NMR

(300MHz,  $\text{CDCl}_3$ , 25°C),  $\delta$ =9.71 (s, 1H), 8.33 (d,  $J$ =8.7 Hz, 2H), 8.17 (d,  $J$ =9.0 Hz, 2H), 8.02-8.08 (m, 1H), 7.57 (d,  $J$ =8.7 Hz, 2H), 7.48-7.55 (m, 1H), 7.43 (d,  $J$ =9.0 Hz, 2H), 6.78-6.98 (m, 2H)

$^{13}\text{C}$  NMR (75 MHz,  $\text{CDCl}_3$ , 25°C)  $\delta$ =185.3 (CH), 149.2 (C), 143.7 (C), 140.5 (C), 131.7 (3 x CH), 131.2 (C), 129.9 (C), 126.5 (3 x CH), 124.5 (3 x CH), 124.0 (3 x CH), 120.9 (CH)

IR (neat)  $\nu$  2924, 2856, 1718, 1654, 1626, 1587, 1514, 1343, 1272, 1107, 941, 861  $\text{cm}^{-1}$

HRMS (ESI) for  $\text{C}_{19}\text{H}_{13}\text{NO}_3$  ( $\text{M}+\text{H}$ ) $^{+}$ : calcd 304.0974, found 304.1138.



**4'-(dimethylamino)-5-(5-methylfuran-2-yl)biphenyl-2-carbaldehyde**

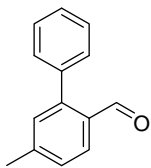
**(153):**  $^1\text{H}$  NMR (300MHz,  $\text{CDCl}_3$ , 25°C),  $\delta$ =9.78 (s, 1H), 7.99 (d,  $J$ =8.4 Hz, 1H), 7.63-

7.67 (m, 2H), 7.32 (d,  $J=8.4$  Hz, 2H), 6.79-6.87 (m, 2H), 6.73 (d,  $J=3.3$  Hz, 1H), 6.11-6.13 (m, 1H), 3.04 (s, 6H), 2.39 (s, 3H)

$^{13}\text{C}$  NMR (75 MHz,  $\text{CDCl}_3$ ,  $25^\circ\text{C}$ )  $\delta=192.6$  (CH), 153.9 (C), 151.5 (C), 150.7 (C), 145.8 (C), 140.4 (C), 135.6 (C), 131.3 (2 x CH), 129.0 (C), 128.5 (CH), 125.1 (CH), 121.6 (CH), 112.3 (2 x CH), 109.3 (CH), 108.6 (CH), 29.9 ( $\text{CH}_3$ ), 14.1 ( $\text{CH}_3$ )

IR (neat)  $\nu$  3063, 3013, 2979, 2371, 2362, 2318, 1739, 1436, 1365, 1266, 1216, 1201, 860  $\text{cm}^{-1}$

HRMS (ESI) for  $\text{C}_{20}\text{H}_{19}\text{NO}_2$  ( $\text{M}+\text{H}$ ) $^+$ : calcd 306.1416, found 306.1431.



**5-methylbiphenyl-2-carbaldehyde (154):**  $^1\text{H}$  NMR (300MHz,  $\text{CDCl}_3$ ,

$25^\circ\text{C}$ ),  $\delta=10.3$  (s, 1H), 7.88 (d,  $J=8.1$  Hz, 1H), 7.57-7.65 (m, 2H), 7.36-7.51 (m, 5H), 2.17 (s, 3H)

$^{13}\text{C}$  NMR (75 MHz,  $\text{CDCl}_3$ ,  $25^\circ\text{C}$ ),  $\delta=192.6$  (CH), 153.7 (C), 146.5 (C), 141.3 (C), 140.0 (C), 132.9 (CH), 130.7 (CH), 129.2 (2 x CH), 128.6 (CH), 127.6 (2 x CH), 125.3 (CH), 20.1 ( $\text{CH}_3$ )

IR (neat)  $\nu$  3027, 2963, 2384, 2363, 2324, 1698, 1605, 1448, 1261, 1093, 1053 800  $\text{cm}^{-1}$

HRMS (ESI) for  $\text{C}_{14}\text{H}_{12}\text{OLi}$  ( $\text{M}+\text{Li}$ ) $^+$ : calcd 203.1048, found 203.1058.

### *Determination of Quantum Yields*

Relative quantum yields<sup>168</sup> were obtained with a photon counting spectrofluorometer equipped with a photomultiplier tube, which is sensitive up to 850-

900 nm. The slit width was 0.5 nm for both excitation and emission sources. The quantum yield was calculated with the following equation:

$$\phi_x = \phi_{st}(I_x/I_{st})(A_{st}/A_x)(\eta_x^2/\eta_{st}^2)$$

where the x subscript denotes unknown, st denotes standard,  $\phi_{st}$  is the reported quantum yield of the standard,  $I$  is the integrated emission spectra,  $A$  is the absorbance at the excitation wavelength and  $\eta$  is the refractive index of the solvent used. Quinine sulfate ( $\phi = 0.55$  in 0.1 M H<sub>2</sub>SO<sub>4</sub>) was used as the standard.

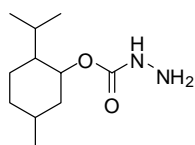
#### *Synthesis of 2-isopropyl-5-menthylcyclohexyl Hydrazinecarboxylate*

To synthesize 2-isopropyl-5-methylcyclohexyl hydrazinecarboxylate **81**,<sup>150</sup> ethyl 2-isopropyl-5-methylcyclohexyl carbonate was first prepared by reacting 25.0 g (1 equivalent) of L-menthol with 75 mL of ethyl chloroformate (7.3 equivalents) in the presence of pyridine (1 mL). The reaction was refluxed for 48 hours before the light brown product was poured over ice followed by dilution with 20 mL of water. The mixture was then extracted with ethyl ether (5 x 100 mL) with the organic layers combined, dried over MgSO<sub>4</sub>, and concentrated under vacuum. Assuming 100% conversion of the ethyl 2-isopropyl-5-methylcyclohexyl carbonate, 75 mL of 2-ethoxy ethanol was used to solubilize the starting material. Once completely dissolved, a two-fold excess of hydrazine monohydrate (20 mL) being added and then the reaction mixture was poured over ice and extracted with ethyl ether (5 x 100 mL) with the organic layers combined, dried over MgSO<sub>4</sub>, and concentrated under vacuum. Once the ethyl ether was evaporated, 50 mL of hexanes was added and the solution was heated



and left at -20°C for 48 h in which white fluffy crystals were formed and were subsequently collected via vacuum filtration. The recrystallization was performed three more times yielding 12.7 g (51% yield).

*Characterization of 2-isopropyl-5-methylcyclohexyl Hydrazinecarboxylate*



**2-isopropyl-5-methylcyclohexyl hydrazinecarboxylate (81):**  $^1\text{H}$  NMR

(300 MHz,  $\text{CDCl}_3$ , 25°C),  $\delta$ =6.14 (s, 1H), 4.56 (dt,  $J$ =4.5, 21.9 Hz, 1H), 3.74 (s, 2H), 1.97-2.02 (m, 1H), 1.82-1.92 (m, 1H), 1.61-1.66 (m, 2H), 1.40-1.52 (m, 1H), 1.30 (t,  $J$ =10.8 Hz, 1H), 1.00-1.10 (m, 1H), 0.91-0.99 (m, 2H), 0.85-0.89 (m, 6H), 0.75 (d,  $J$ =6.9 Hz, 3H)

$^{13}\text{C}$  NMR (75 MHz,  $\text{CDCl}_3$ , 25°C)  $\delta$ =159.0 (C), 75.7 (CH), 47.5 (CH), 41.6 ( $\text{CH}_2$ ), 34.4 ( $\text{CH}_2$ ), 31.6 (CH), 26.4 (CH), 23.7 ( $\text{CH}_2$ ), 22.2 ( $\text{CH}_3$ ), 21.0 ( $\text{CH}_3$ ), 16.6 ( $\text{CH}_3$ )

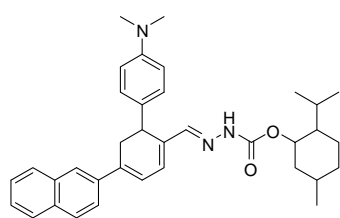
HRMS (ESI) for  $\text{C}_{11}\text{H}_{22}\text{N}_2\text{O}_2$  ( $\text{M}+\text{H}$ ) $^+$ : calcd 215.1760, found 215.1752.

*General Procedure for the Synthesis of the Menthylhydrazones*

Heterodimer 4-Biphenyl-4-yl-6-methyl-6-(5-methyl-furan-2-yl)-cyclohexa-1,3-dienecarbaldehyde **122** (0.100 g, 1 equivalent) was dissolved in 200 proof ethanol (20 mL) with 1.5 equivalents of 2-isopropyl-5-methylcyclohexyl hydrazinecarboxylate **81** at room temperature. After 72 h, the reaction was extracted with 1:1 ethyl acetate/hexanes solution (2 x 100 mL), and was washed with brine. The organic layer was dried over magnesium sulfate ( $\text{MgSO}_4$ ) and concentrated under vacuum. The crude material was

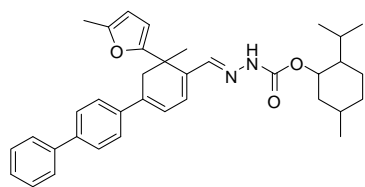
passed thru a silica plug with 10% ethyl acetate/hexanes as the mobile phase. The mixture was then subjected to high pressure liquid chromatography (HPLC) with a mobile phase of 96% ethyl acetate/ 4% hexanes with a flow rate of 1.5 mL/minute. Two fractions were collected corresponding to the R and S stereoisomers respectively.

*Characterization of the Menthylhydrazones*



**2-isopropyl-5-methylcyclohexyl-2-((6-(4-(dimethylamino)phenyl)-4-(naphthalen-2-yl)cyclohexa-1,3-**

**dienyl)methylene)hydrazinecarboxylate (155):** HRMS (ESI) for  $C_{36}H_{43}N_3O_2$  ( $M+H$ )<sup>+</sup>: calcd 550.3434, found 550.3424.



**2-isopropyl-5-methylcyclohexyl 2-((4-(biphenyl-4-yl)-6-methyl-6-(5-methylfuran-2-yl)cyclohexa-1,3-**

**dienyl)methylene)hydrazinecarboxylate (156):** HRMS (ESI) for  $C_{36}H_{42}N_2O_3$  ( $M+H$ )<sup>+</sup>: calcd 551.3274, found 551.3269.

*General Procedure for Conversion of Menthylhydrazones Back to Aldehyde*

Once the R and S stereoisomers were purified, each was dissolved in 20 mL of 1:1 water/ethanol with 5 mL of 10% sulfuric acid and boiled for 2.5 h in which a color change from clear to pink occurred within two hours. The reaction was removed from the heat source and allowed to cool when it was then extracted with ethyl ether (2 x 25 mL). The organic layer was then dried with  $\text{MgSO}_4$  and concentrated under vacuum. The crude mixture was then passed through a silica plug with a mobile phase of 10% ethyl acetate/hexanes.

## CHAPTER V

### SYNTHESIS OF CYCLOHEXADIENE ENAMINONITRILES AND QUINAZOLINES\*

#### INTRODUCTION

##### *Enaminonitriles*

Enaminonitriles (**Figure 63**) are useful scaffolds in the synthesis of a wide variety of heterocyclic systems with purposes ranging from pharmaceuticals, fungicides, and to solvatochromatic dyes, which are dyes that change in position and sometimes intensity of an electronic absorption or emission band, accompanying a change in the polarity of the medium.<sup>180-184</sup>

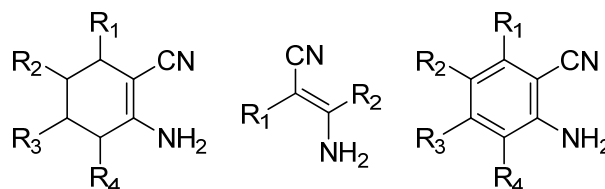


**Figure 63.** General enaminonitrile scaffolds.

An example of the pharmaceutical potential of this class of compounds comes from the recent advances toward an effective therapy for transmissible spongiform encephalopathies (TSEs) or prions diseases. These neurodegenerative diseases can be

---

\*Reprinted with permission from “An Efficient One-Pot Synthesis of Tethered Cyclohexadiene Enaminonitriles from Methyl-Ketones: An Effective Route to Quinazolines.” Bench, B.J., Suarez, V. H. Watanabe, C. M. H., 2008. *Bioorganic & Medicinal Chemistry Letters*, 18, 3126-3130, Copyright 2008 by Elsevier Ltd.

characterized by spongiform changes within the large vacuoles in the cortex, cerebellum, astrocytosis, neuronal death, and deposits of the pathological protein PrP<sup>Sc</sup> (the “scrapie form” of PrP). While this is mainly seen within the brain, it can also occur in other organs and tissues. In this category of diseases, one finds scrapie in sheep and goats, bovine spongiform encephalopathy (Mad Cow) in cattle, chronic wasting disease in deer, and Creutzfeldt-Jacob disease in humans,<sup>185</sup> which is attributed to the consumption of contaminated beef products.<sup>186-188</sup> To date though, there are currently no effective treatments for the prevention of infection or even disease progression.<sup>189</sup> However, enaminonitriles based on a pyridine dicarbonitrile scaffold (**Figure 64**) have been shown to bind to cell-surface glycosylphosphatidylinositol anchored protein PrP<sup>C</sup> which inhibits the posttranslation conversion of the anchor protein into its protease-resistant isoform PrP<sup>Sc</sup>.<sup>190</sup> This abnormal protein folding is quite rapid and leads to rapid progression of the disease.<sup>189</sup> Enaminonitriles, such as **157** and its analogs **158-160** (**Figure 64**) have shown biological activity (**157**, 18  $\mu$ M; **158**, 35  $\mu$ M; **159**, 19  $\mu$ M; **160**, 16  $\mu$ M) against scrapie-infected mouse neuroblastoma cells (ScN2a) inhibiting PrP<sup>Sc</sup>.<sup>190</sup>

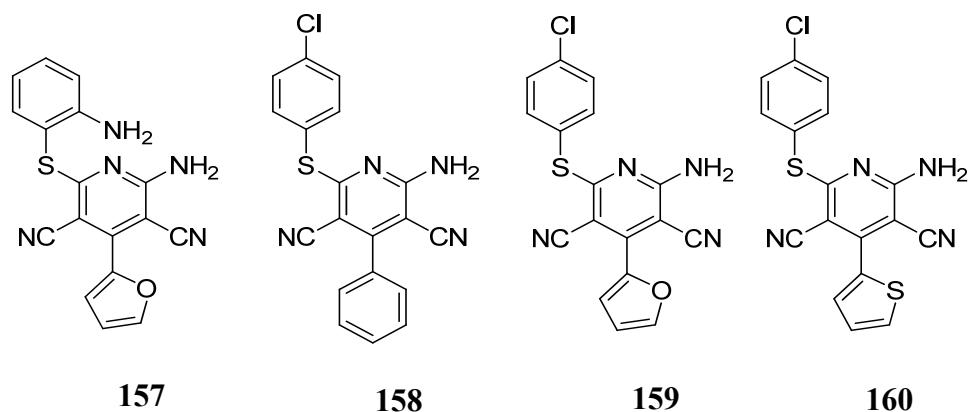


**Figure 64.** Enaminonitriles active against mice ScN2a cells.<sup>190</sup>

The self-dimerization of  $\alpha,\beta$ -unsaturated nitriles to cyclic enaminonitriles (**Figure 65**) has been previously performed utilizing lithium diisopropylamide (LDA)<sup>191</sup> as well as other strong bases (ethanolic KOH or piperidine) with moderate yields.<sup>192,193</sup> To date, only a small number of substituted cyclohexadiene enaminonitriles have been synthesized with no report on their biological activities.<sup>191,194</sup>

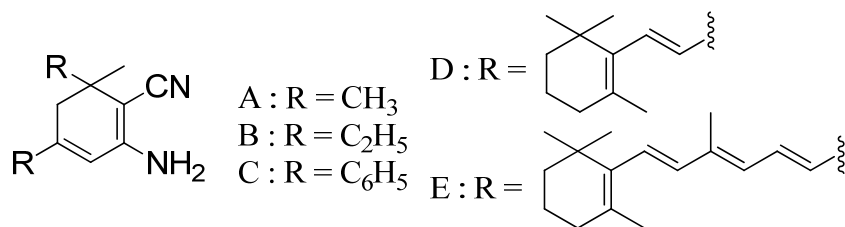


**Figure 65.** Known cyclohexadiene enaminonitriles.

### Quinazolines

In addition to inducing many biological effects, enaminonitriles are also important intermediaries in the synthesis of quinazolines. Quinazolines are used as dyes, antibiotics, and pharmaceuticals with many possessing biological activities.<sup>195-197</sup> The quinazolines (**Figure 66**), for example, have been employed in the treatments of hypertension and hyperplasia. Doxazosin **161**, known as Cardura<sup>®</sup>, is an alpha blocker used to treat high blood pressure by inhibiting the binding of norepinephrine to alpha receptors in the autonomic nervous system leading to the relaxation of the smooth vascular muscles.<sup>198</sup> Prazosin **162**, trade names Minipress<sup>®</sup> and Hypovase<sup>®</sup>, acts as an

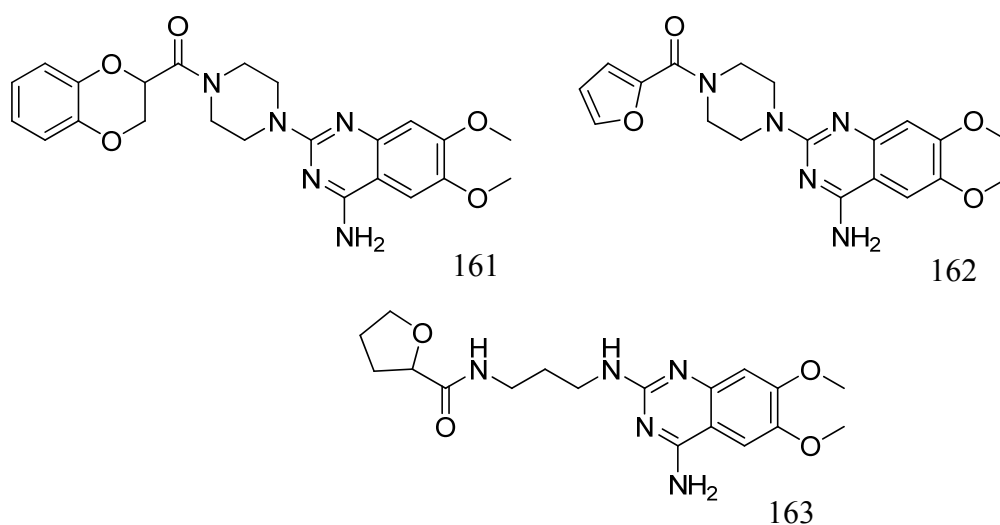
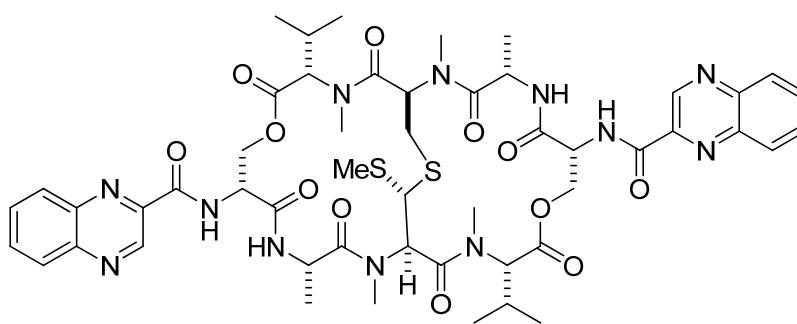


**Figure 66.** Quinazolines used as therapeutic agents.

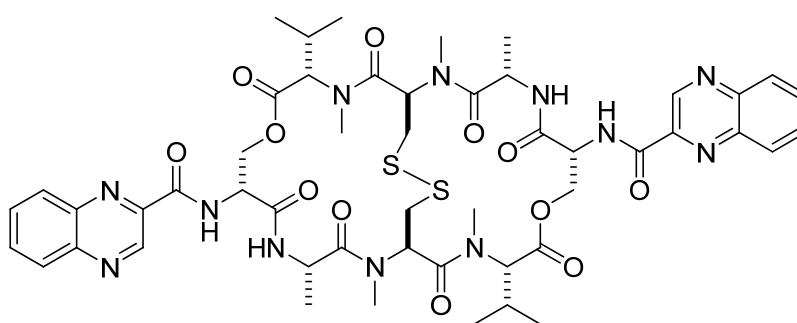
adrenergic alpha-1 antagonist used in the treatment of heart failure hypertension, pheochromocytoma (tumor of the adrenal gland), prostatic hypertrophy, and urinary retention.<sup>199</sup> Alfuzosin **163**, known as Uroxatral<sup>®</sup>, is used in the treatment of benign prostatic hyperplasia by relaxing the muscles in the prostate and the bladder neck making it easier to urinate. It employs the same mechanism just as **161** and **162** by blocking norepinephrine binding to alpha receptors.<sup>200</sup>

Naturally occurring quinoxaline antibiotics are produced by various species of streptomycetes and are distributed throughout nature.<sup>201,202</sup> Echinomycin **164** and triostin A **165** are two examples of the family of molecules that exhibit potent antibacterial, anticancer, and antiviral activities.<sup>203</sup> This class of antibiotics contains two quinoxaline-2-carboxyl moieties that are linked to a cross-bridge cyclic octapeptide dilactone core (**Figure 67**).<sup>204</sup> Echinomycin **164** is reported to be a strong inhibitor of DNA transcription<sup>205</sup> and synthesis.<sup>206</sup> **164** binds to double stranded DNA sandwiching two base pairs within its U-shaped conformation.<sup>207-210</sup>





Echinomycin: 164



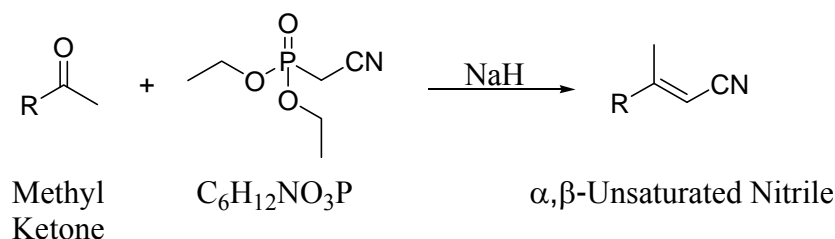
Triostin A: 165

**Figure 67.** Structures of quinoxoline antibiotics.*Discovery of New Self-Condensation Reaction*

In previous studies, we successfully synthesized a library of functionalized cyclohexadienals that have shown biological activities ranging from antimicrobial to neurite outgrowth activities against PC12 cells.<sup>211,212</sup> To construct our library of substituted cyclohexadienals, we utilized  $\beta$ -methylenic aldehyde starting materials, which were formed via the reduction of their corresponding  $\alpha,\beta$ -unsaturated nitriles. To synthesize these nitrile intermediates, we performed a Horner-Wadsworth Emmons

reaction by treating methyl-ketone substrates with a ylide solution generated by treatment with diethyl (cyanomethyl)-phosphonate ( $\text{C}_6\text{H}_{12}\text{NO}_3\text{P}$ ) and sodium hydride ( $\text{NaH}$ ) (Scheme 18) consisting of one equivalent of each of the three components.<sup>102</sup>

**Scheme 18.** Horner Wadsworth Emmons reaction.



However, when this reaction was treated with excess  $\text{NaH}$ , we discovered that the nitrile itself underwent a self-dimerization resulting in complex enamionitriles. This was first discovered during the production of 3-(thiophen-2-yl)but-2-enenitrile (**72**) from the treatment of 4-acetyl-biphenyl with  $\text{C}_6\text{H}_{12}\text{NO}_3\text{P}$ . During the setup of this reaction, excess  $\text{NaH}$  was added and upon review of the crude  $^1\text{H}$ -NMR, new peaks were observed within the spectrum. What was noticeable was the fact that there were peaks similar to that of the cyclohexadienals<sup>32,211</sup> that were mentioned in previous chapters. As you can see in the example spectrum (**Figure 68**) of 3-(biphenyl-4-yl)but-2-enenitrile (**78**), the peaks that first caught our attention were that of the diastereomer protons of the cyclohexadiene ring (2.9 and 3.3 ppm). This led us to believe that this might be a self-dimerization product due to the deprotonation of methyl group of the  $\alpha,\beta$ -unsaturated nitrile causing a self-dimerization with that of another  $\alpha,\beta$ -unsaturated nitrile. From

these results, we began to investigate this new reaction and developed a one-pot synthetic strategy towards the development of these new self-dimerization products.

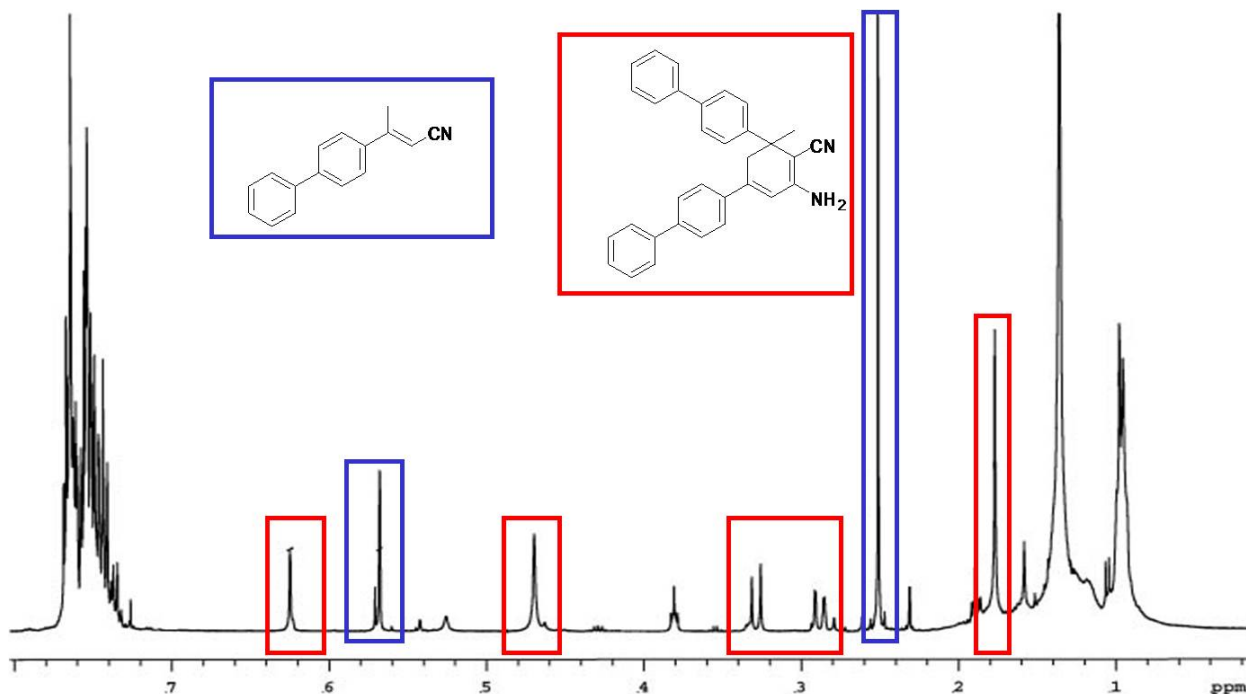
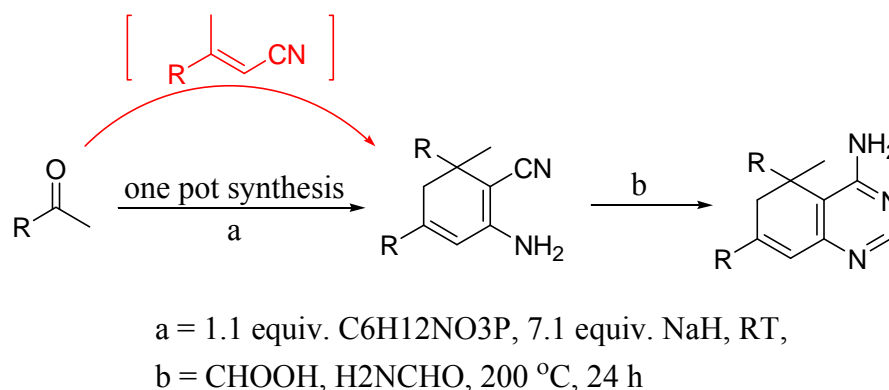


**Figure 68.** <sup>1</sup>H-NMR depicting the mixture of  $\alpha,\beta$ -unsaturated nitrile with self-dimerization product. The  $\alpha,\beta$ -unsaturated nitrile peaks are shown in blue while the self-dimerization product peaks are shown in red.

In this chapter, we describe a new one-pot strategy for the synthesis of tethered cyclohexadiene enaminonitriles via the reduction of the intermediate nitrile with excess NaH. We compare this synthetic methodology with that reported previously, where self-dimerization of the  $\alpha,\beta$ -unsaturated nitriles ensues upon LDA<sup>191</sup> treatment or other strong bases.<sup>192,193</sup> Additionally, we synthesized the quinazoline<sup>191</sup> derivatives (**Scheme**

19) of each enaminonitriles by heating the enaminonitrile with formic acid and formamide only to discover that the synthetic procedure described within the literature did not work as described. Here we provide new reaction conditions that produce the compounds in moderate yields. We additionally report on the biological activities of this library of compounds including their cytotoxic effects against bacteria (*E. coli* and *B. subtilis* 6633), yeast, and human T-cell leukemia (Jurkat).

**Scheme 19.** Quinazolines derived from a cyclohexadiene enaminonitrile scaffold.



## RESULTS AND DISCUSSION

### *Enaminonitrile Reaction Optimazation*

As previously mentioned, enaminonitriles can be generated in a one-pot format by implementation of a Horner-Wadsworth Emmons reaction where the methyl-ketone is treated with a ylide solution produced by the treatment of diethyl (cyanomethyl)-phosphonate with excess NaH.<sup>102</sup> To optimize the synthesis of our library of enaminonitriles, we employed a thiophene substrate as a model for the production of **166**, where we discovered that an excess of six equivalents of NaH were required to

facilitate the deprotonation of the nitriles (**Scheme 19**). This thiophene substrate was used because we first discovered the conversion of nitriles into enaminonitriles while synthesizing our library of cyclohexadienals<sup>212</sup> and it was high yielding. It was found that after four days a yield of 89% was obtained for **166**. Four days was required to reach 100 percent conversion of the  $\alpha,\beta$ -unsaturated nitrile into the corresponding enaminonitrile product. An analysis of the conversion of nitrile to enaminonitrile by <sup>1</sup>H-NMR, after one day a conversion of 74.5% was observed while 81.5% and 91.5% of the nitrile was converted after two and three days respectively. When fewer equivalents of NaH were used to facilitate the reaction, yields were drastically diminished (**Table 15**). When 0.5, 1.0, 1.25 and 2.0 equivalents were used to perform the reaction, no yield was observed as there was only total conversion of the methyl-ketone into the thiophene nitrile product intermediate. However, we began to see a small conversion of the nitrile into the product at 3.0 equivalents, but with a meager yield of 7%. An increase in yield began to occur at 4.0 equivalents giving an isolated yield of 43%. When we increased the amount of NaH over 7.0 equivalents, i.e. 8.0 and 10.0 equivalents, yields began to dramatically decrease to 41% and 10% respectively in comparison to the 89% yield observed with the optimum 7.0 equivalents.

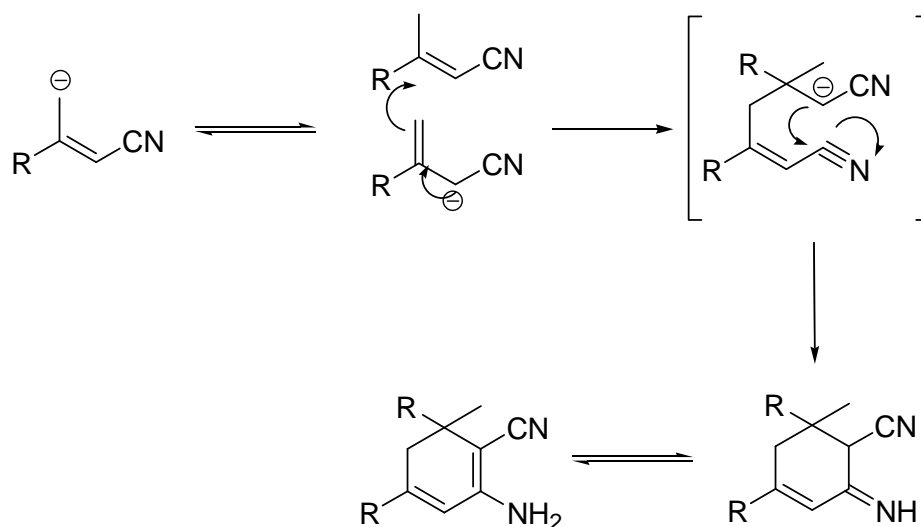
**Table 15.** Percent yields using NaH.

This table represents the overall yields based on the equivalents of NaH used to facilitate the reaction.

Equivalent	Percent Yield
0.5	0
1.0	0
1.25	0
2.0	0
3.0	7
4.0	43
7.0	89
8.0	41
10.0	10

#### *Enaminonitrile Reaction Mechanism*

To form enaminonitriles, deprotonation of the nitriles  $\beta$ -methyl has to occur leading to the formation of an allylic anion which can tautomerize making it capable of attacking another  $\beta$ -methyl nitrile in a Michael type reaction (**Scheme 20**). This would lead to an intermediate which undergoes a Thorpe-Ziegler cyclization forming an imine which then tautomerizes to give the final enaminonitrile product.

**Scheme 20.** Proposed reaction mechanism of enaminonitrile synthesis.

#### *Synthesis of Enaminonitriles Utilizing NaH*

With these optimized conditions in hand, various substrates (**Figure 69**) were analyzed to investigate the scope of the reaction as shown in **Table 16**. We were able to obtain moderate yields ranging from the lowest, 79%, and the highest, 96%. The substrates that were employed for this study ranged from small and large bulky aromatics to aliphatic alkyl containing substrates. However, the trend for this NaH mediated reaction indicated that the small and large aromatic substrates were capable of undergoing deprotonation forming the enaminonitrile product while the aliphatic alkyl chain substrates gave no yield. We first looked at the previously mentioned thiophene **166** and a bromo-substituted thiophene **167** which gave high yields of 89 % and 96 % respectively. The next set of compounds we evaluated was the unsubstituted phenyl, fluoro, and bromo substituted substrates. The un-substituted phenyl **168** and the 4-fluoro phenyl **169** substrates both gave yields of 88 % while the 4-bromo phenyl **170** starting

material gave a lower yield in comparison of 79%. With these results, we were skeptical of the bulkier biphenyl **171** and naphthalene **172** substrate's yields as we would expect diminished yields. However, they produced higher yields in comparison to the other small aromatic thiophene and phenyl substituted compounds other than the bromothiophene **167** substrate with yields of 93% and 90% respectively.

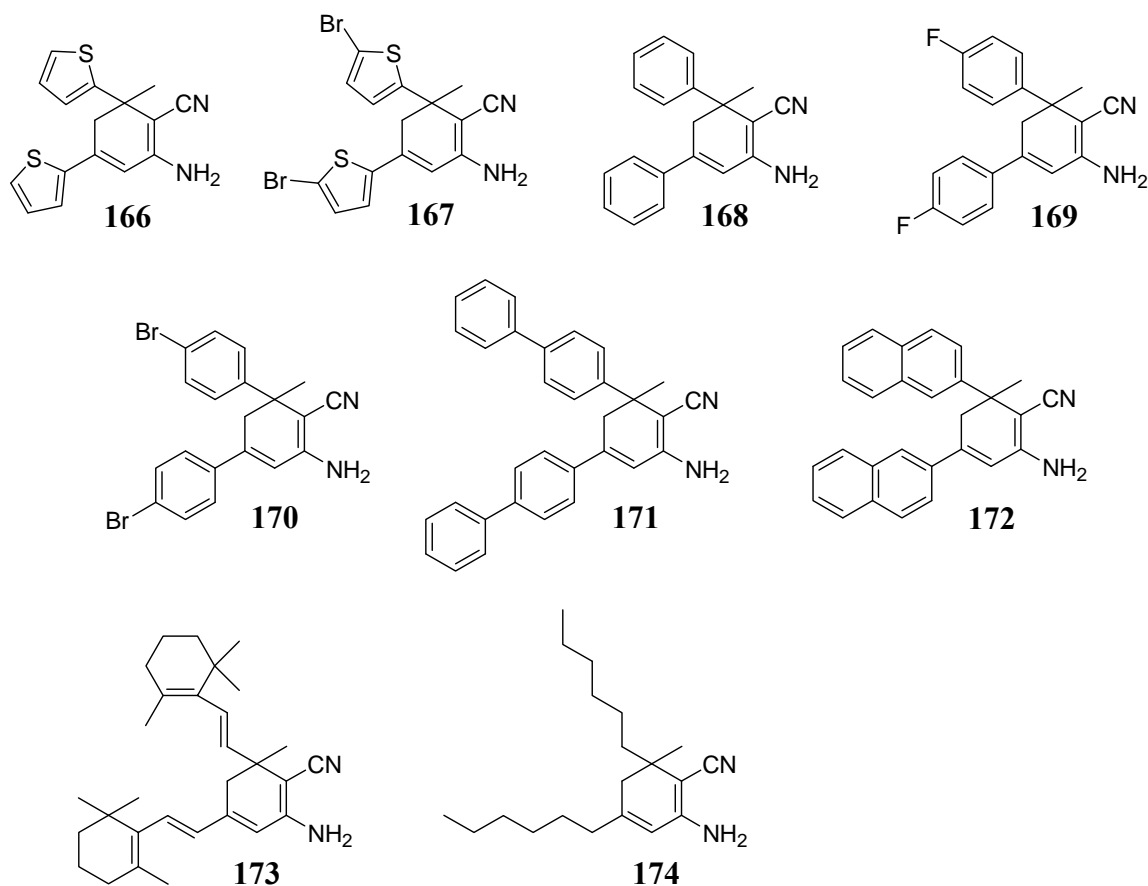


**Figure 69.** Enaminonitrile compounds synthesized.



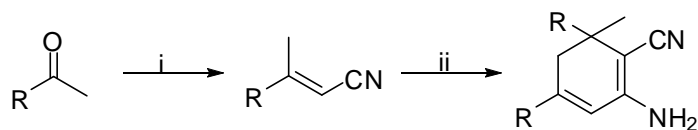
A limitation of this one-pot strategy is that it does not facilitate the dimerization of aliphatic alkyl substrates (**Table 16**). When we tested the  $\beta$ -ionone **173** and 2-octanone **174** substrates, we found that no enaminonitrile product was formed in the crude  $^1\text{H}$ -NMR. The only compound present in the spectrum was the nitrile intermediate itself. To evaluate if this was simply an equivalency issue, we employed higher NaH equivalents of 8.0, 10.0, and 12.0 but the result was still the same as on nitrile intermediate was present.. This could be attributed to the reduced stabilization of the resulting  $\beta$ -methyl anion after deprotonation requiring a much stronger base for the reaction to proceed to form the enaminonitrile product.

#### *Synthesis of Substituted Enaminonitriles Using LDA*

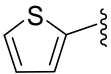
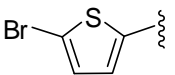
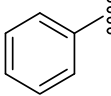
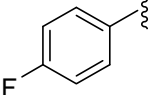
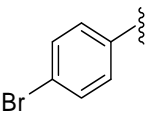
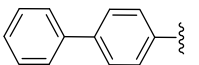
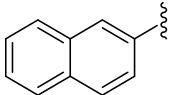
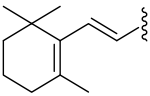
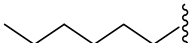
We compared our new NaH catalyzed reaction to the LDA reaction that was reported by Tucker in 1981. Tucker's work focused on treating small aliphatic nitriles with LDA in tetrahydrofuran (THF) resulting in the self-dimerization enaminonitriles.<sup>191</sup> For this set of experiments, we generated the corresponding nitriles from their methyl-ketones, purified them by flash chromatography, and subsequently reacted them with LDA in THF, thus producing their enaminonitrile product in two steps (**Scheme 21**).

#### **Scheme 21.** Synthesis of enaminonitriles using LDA.

Reagents and conditions: (i) 1.1 equivs.  $\text{C}_6\text{H}_{12}\text{NO}_3\text{P}$ , 1.1 equiv NaH; (ii) LDA.



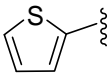
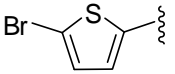
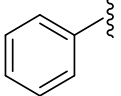
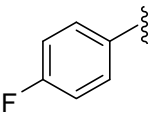
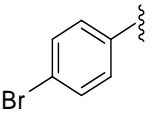
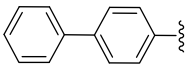
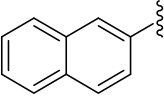
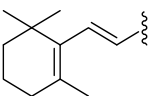
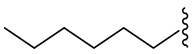
**Table 16.** Substrate effects with excess NaH.

R Group	Compound	Yield (%)
	<b>166</b>	89
	<b>167</b>	96
	<b>168</b>	88
	<b>169</b>	88
	<b>170</b>	79
	<b>171</b>	93
	<b>172</b>	90
	<b>173</b>	---
	<b>174</b>	---

Surprisingly we observed an inverse correlation with LDA compared to the trend with the NaH catalyzed reaction (**Table 17**). The NaH reaction readily self-dimerizes small and large aromatics in high yields, while LDA gives minimal yields. These results could be attributed to steric effects with LDA resulting in the lack of full dissociation of the catalyst prior to self-condensation. Conversely, reactions catalyzed with LDA seemed to favor long chain alkyl substrates while NaH failed to convert them into their enamionitrile products. Previous reports by Tucker demonstrated the LDA method with alkylidene malononitriles with included 3-methyl-2-butenenitrile and 3-methyl-2-pentenitrile which gave high to moderate yields of 90 % and 60 %, respectively.<sup>191</sup>

As mentioned, we observed lower yields with LDA (**Table 17**) in comparison to that of the NaH catalyzed reactions. For the small and large aromatics, we observed yields ranging from 12 % to 28 % for the LDA catalyzed reactions while the NaH catalyzed reactions gave us yields ranging from 79 % to 96 %. However, while we observed no conversion of the aliphatic nitriles with NaH, we did see a yield of 36 % for the C-15 nitrile **173** and 31 % for the 3-methyl-non-2-enenitrile **174** substrate. For thiophene **166**, we saw a yield of 28 % while the bromo-substituted thiophene **167** gave an overall yield of 24 % in comparison to 89 % and 96 % respectively using NaH in a one-pot fashion. The phenyl-substrates yields were even lower than the thiophene substrates as **168** gave a yield of 18% while the fluoro **169** and bromo **170** substituted phenyls demonstrated yields of 20% each. For the bulkier biphenyl **171** and naphthalene **172** substrates, the yields were diminished additionally with isolated yields of 12% and 13% respectively.

**Table 17.** Substrate effects with LDA.

<b>R Group</b>	<b>Compound</b>	<b>Yield (%)</b>
	<b>166</b>	28
	<b>167</b>	24
	<b>168</b>	18
	<b>169</b>	20
	<b>170</b>	20
	<b>171</b>	12
	<b>172</b>	13
	<b>173</b>	36
	<b>174</b>	31

### Synthesis of Quinazolines

The interesting aspect of the enamionitriles is the 1,2-relationship of the amino and nitrile groups. This can be exploited in the synthesis of the class of compounds known as quinazolines (**Figure 70**). From literature, these compounds can be synthesized via the heating in the presence of formic acid and formamide at 200°C (**Scheme 22**). While it was previously reported by Tucker that the reaction took one hour to go to completion, we were unable to isolate any quinazoline product under these conditions.<sup>191</sup>

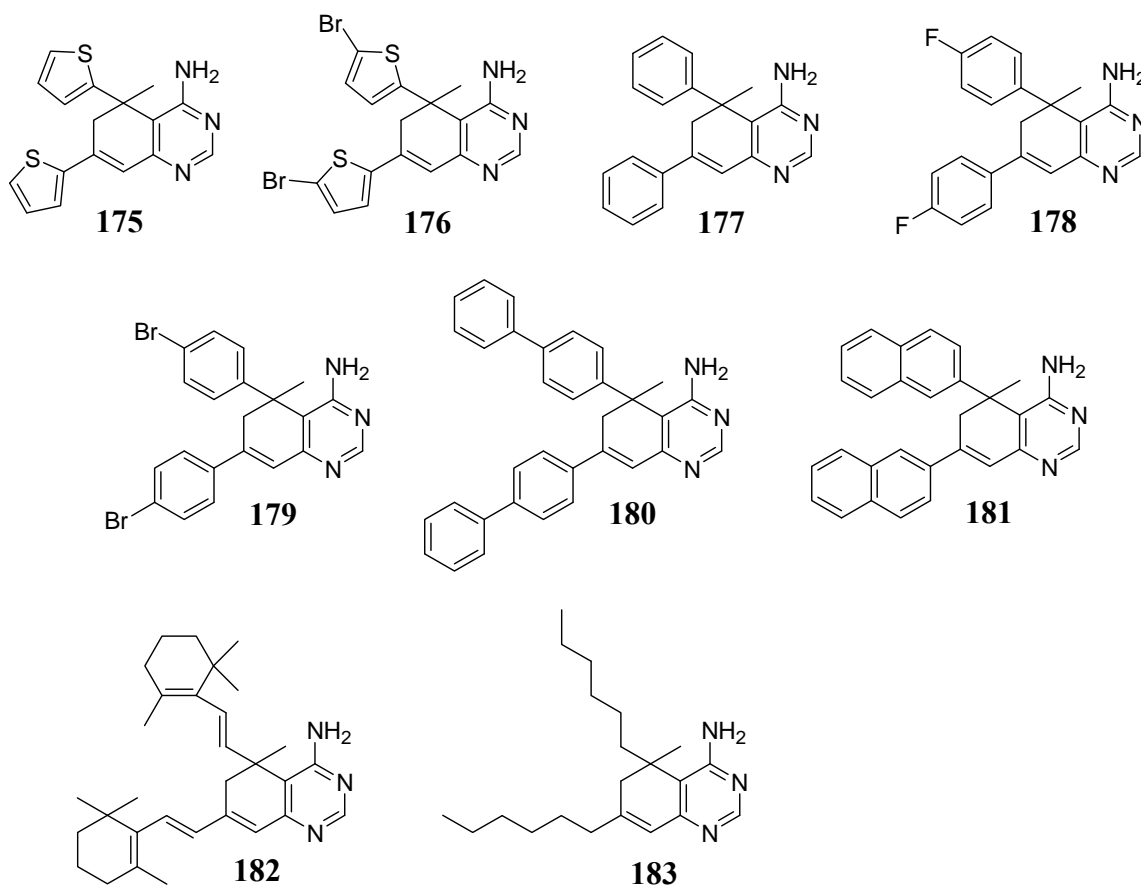
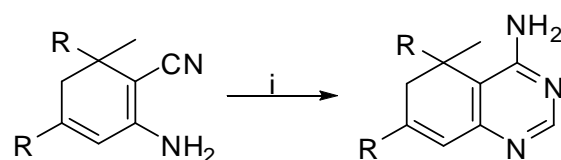


**Figure 70.** Quinazoline compounds synthesized.

We decided to optimize this reaction as the reported conditions offered little or no product formation based on crude  $^1\text{H-NMR}$ 's on the various substrates we examined. With formic acid having a low boiling point, we implemented a reflux set-up which was not used in Tucker's work. This may explain why we were seeing little product formation as the formic acid evaporates upon heating. By using the thiophene enaminonitrile **166** as a model substrate, we still observed a small trace of product formation after one hour according to the crude  $^1\text{H-NMR}$ . At 12 hours, approximately half of the starting material was converted into quinazoline and upon isolation and purification, a 37% yield was obtained. According to the crude  $^1\text{H-NMR}$ , the complete conversion of the enaminonitrile to the quinazoline was observed after 24 hours while affording a 73% isolated yield.

**Scheme 22.** Synthesis of quinazolines.

Reagents and conditions: (i)  $\text{CHOOH}$ ,  $\text{H}_2\text{NCHO}$ ,  $200^\circ\text{C}$ , 24 h.



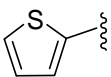
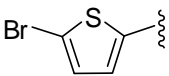
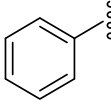
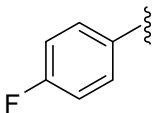
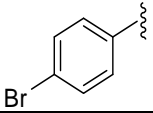
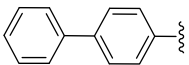
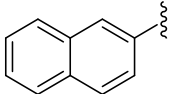
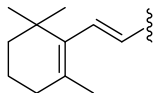
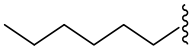
With conditions optimized, we synthesized our small library of quinazolines (**Table 18**) from our enaminonitriles utilizing our one-pot synthetic strategy with the exception of the aliphatic substrates **173** and **174** in which employed LDA to produce their enaminonitrile products. Overall yields for the quinazoline synthesis were moderate with a range from 54% to 78%. The alkyl aliphatics gave the lowest yields while the unsubstituted aromatic possessed a higher isolated yield when compared to the

fluoro or bromo-substituted substrates. For the thiophene **175**, a yield of 73% was observed while its bromo **176** analogue was at 60%. As for the phenyl substrates, the unsubstituted **177** substrate offered a yield of 74% while the fluoro **178** and bromo **179** substrates yields were 67% and 70% respectively. For this reaction, the bulkier substrates offered the highest yields in which the isolated yields for the biphenyl **180** and naphthalene **181** quinazolines were 78% and 74% respectively. As mentioned, the lowest yields for our scope were the aliphatic substrates and the isolated yields for **182** and **183** were 54% and 57% respectively.

#### *Biological Evaluation of Compounds*

The biological activities of the synthesized enamionitriles (**166-174**) and their quinazoline (**175-183**) derivatives were screened against an array of assays. We looked at their ability to inhibit the growth of Jurkats (a leukemic T-cell line) as well as bacterial strains (*E. coli* and *B. subtilis*) and yeast (*S. cerevisiae*). The most pronounced effects that we observed were against the Jurkats cell line, where in all cases the quinazolines were more active than their corresponding enamionitriles. The most effective compounds which exhibited  $IC_{50}$  values in the low micromolar range were quinazolines **178** (3.24  $\mu$ M), **181** (9.37  $\mu$ M), and **176** (9.51  $\mu$ M) were heterocyclic and in many instances, halogenated (**Table 19**). With the anti-microbial assays, we did not see much of an effect as all of the compounds displayed moderate activities. Minimal inhibition concentration (MIC) values were  $\geq 163$   $\mu$ M in *B. subtilis*,  $\geq 189$   $\mu$ M in *E. coli*, and  $\geq 197$   $\mu$ M against *S. cerevisiae* which can be seen in **Table 20**.

**Table 18.** Quinazoline product yields.

<b>R Group</b>	<b>Compound</b>	<b>Yield (%)</b>
	<b>175</b>	73
	<b>176</b>	60
	<b>177</b>	74
	<b>178</b>	67
	<b>179</b>	70
	<b>180</b>	78
	<b>181</b>	74
	<b>182</b>	54
	<b>183</b>	57



**Table 19.** Cytotoxic activities against Jurkats.

<b>Compound</b>	<b>IC50 (<math>\mu\text{g/ml}</math>)</b>	<b><math>\mu\text{M}</math></b>
<b>166</b>	51.485	172.15
<b>167</b>	6.424	13.93
<b>168</b>	4.342	15.13
<b>169</b>	6.257	19.37
<b>170</b>	9.213	20.52
<b>171</b>	8.478	19.31
<b>172</b>	7.35	18.99
<b>173</b>	5.452	12.65
<b>174</b>	14.166	46.75
<b>175</b>	5.008	15.36
<b>176</b>	4.586	9.51
<b>177</b>	5.522	17.59
<b>178</b>	1.133	3.24
<b>179</b>	5.962	12.69
<b>180</b>	4.848	10.4
<b>181</b>	3.881	9.37
<b>182</b>	5.849	12.8
<b>183</b>	4.148	12.61

**Table 20.** Anti-microbial activities of library.

<i>B. Subtilis 6633</i>			<i>E. coli</i>		Yeast	
Compound	IC50 (µg/ml)	µM	IC50 (µg/ml)	µM	IC50 (µg/ml)	µM
<b>166</b>	62.33	208.4	57.37	191.8	64.24	214.8
<b>167</b>	75.02	162.8	89.33	193.8	91.24	198
<b>168</b>	56.32	196.1	58.39	203.3	58.37	203.3
<b>169</b>	65.23	201.9	69.36	214.6	68.59	212.3
<b>170</b>	76.33	170	87.39	194.6	90.24	201
<b>171</b>	78.25	178.2	85.64	195	87.75	199.8
<b>172</b>	80.23	207.2	79.64	205.7	78.26	202.1
<b>173</b>	82.37	191	81.57	189.1	85.27	197.7
<b>174</b>	74.56	245.9	70.37	232	68.26	225.1
<b>175</b>	74.66	229	71.24	218.5	69.26	212.4
<b>176</b>	80.24	166.5	92.37	191.7	95.26	197.7
<b>177</b>	75.64	240.8	60.37	192.1	66.53	211.8
<b>178</b>	80.23	229.1	70.24	200.6	71.29	203.6
<b>179</b>	79.64	169.4	90.24	192	95.26	202.7
<b>180</b>	80.26	172.1	91.26	195.7	94.7	203.1
<b>181</b>	79.64	192.3	78.69	190	81.57	196.9
<b>182</b>	77.99	170.1	87.37	190.6	90.98	198.5
<b>183</b>	78.65	238.1	70.79	214.3	74.57	225.8

## CONCLUSION

These findings represent a new one-pot synthetic strategy in the preparation of cyclohexadiene enamionitriles. The reaction is high yielding with small aromatics and other bulky substrates thus complementing that of previously reported syntheses using LDA. The only instance to where the one-pot synthetic strategy cannot be implemented is with alkyl substrates. The cyclohexadiene enamionitrile were additionally implemented as precursors in the synthesis of quinazolines, a scaffold with demonstrated therapeutic activities. In this regard, we optimized reaction conditions reported in the literature which generated each quinazoline in moderate yields.

In cell-based assays, the quinazolines gave the most promising effects where  $IC_{50}$  values in the low micromolar range were measured against a human leukemic cell-line. The identification of the cellular targets of these lead compounds might direct the synthesis of functionally and structurally related analogs with more potent biological activities.

## EXPERIMENTAL

### *General*

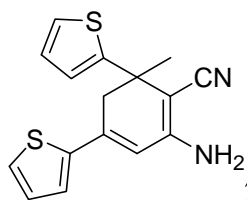
Fresh THF was dried by passage through an MBRAUN solvent purification system and stored over molecular sieves. All other solvents and reagents were purchased and used without further purification.  $^1H$  (300 MHz) and  $^{13}C$  (75 MHz) spectra were recorded on a 300 MHz spectrometer. Chemical shifts for  $^1H$  and  $^{13}C$  NMR spectra are reported in ppm referenced to TMS (0 ppm) and coupling constants are reported in Hertz (Hz). MS spectra were recorded on an API QSTAR PULSAR (ES) apparatus. Infrared (IR)

spectra were recorded with a FT-IR spectrometer. Chromatographic separations were achieved by flash silica chromatography (silica gel 60 mesh, EMD Biosciences).

#### *General Procedure for NaH Catalyzed Formation of Enaminonitriles*

To an oven dried flask, 7.1 equivalents of NaH was added and immediately flushed with pure nitrogen gas. Enough THF was added to dissolve the NaH and this solution was allowed to stir for five min. before 1.1 equivalents of diethyl (cyanomethyl)-phosphonate was added to create the ylide solution. After approximately ten minutes, 1 equivalent of methyl-ketone substrate was added and this reaction mixture was allowed to stir at room temperature for 4 days. After 4 days, the reaction mixture was quenched by the addition of water and extracted with ethyl ether and washed with ammonium sulfate, water, and brine before being dried over magnesium sulfate and evaporated under vacuum. The crude product was subsequently purified via flash chromatography with 100% dichloromethane.

#### *Characterization of Enaminonitriles*



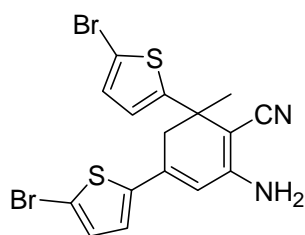
**2-Amino-6-methyl-4,6-di(thiophen-2-yl)cyclohexa-1,3-**

**dienecarbonitrile (166):**  $^1\text{H}$  NMR (300MHz,  $\text{CDCl}_3$ ,  $25^\circ\text{C}$ ),  $\delta$ =7.33 (d,  $J$ =3.0 Hz, 1H), 7.22 (d,  $J$ =3.9 Hz, 1H), 7.10-7.12 (m, 1H), 7.03-7.06 (m, 1H), 6.86-6.92 (m, 2H), 6.19 (d,  $J$ =2.1 Hz, 1H), 4.51 (s, 2H), 3.18 (d,  $J$ =16.8 Hz, 1H), 2.86 (dd,  $J$ =2.1, 16.8 Hz, 1H), 1.74 (s, 3H)

$^{13}\text{C}$  NMR (75 MHz,  $\text{CDCl}_3$ ,  $25^\circ\text{C}$ )  $\delta$ =152.6 (C), 142.9 (C), 142.7 (C), 138.8 (C), 128.4 (CH), 127.3 (CH), 126.8 (CH), 126.2 (CH), 123.8 (CH), 123.5 (CH), 120.0 (C), 115.3 (CH), 81.4 (C), 43.5 ( $\text{CH}_2$ ), 38.1 (C), 30.3 ( $\text{CH}_3$ )

IR (neat)  $\nu$  3466, 3352, 3234, 3100, 2968, 2925, 2863, 2169, 1635, 1552, 1407, 853, 827, 701  $\text{cm}^{-1}$

HRMS (ESI) for  $\text{C}_{16}\text{H}_{14}\text{N}_2\text{S}_2$  ( $\text{M}+\text{H}$ ) $^+$ : calcd 299.0677, found 299.0662.



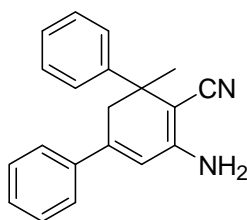
**2-Amino-4,6-bis(5-bromothiophen-2-yl)-6-methylcyclohexa-**

**1,3-dienecarbonitrile (167):**  $^1\text{H}$  NMR (300MHz,  $\text{CDCl}_3$ ,  $25^\circ\text{C}$ ),  $\delta$ =6.98 (d,  $J$ =3.9 Hz, 1H), 6.92 (d,  $J$ =3.9 Hz, 1H), 6.79 (d,  $J$ =3.6 Hz, 1H), 6.62 (d,  $J$ =3.9 Hz, 1H), 6.10 (d,  $J$ =2.1 Hz, 1H), 4.69 (s, 2H), 2.96 (d,  $J$ =16.8 Hz, 1H), 2.75 (dd,  $J$ =2.4, 16.8 Hz, 1H), 1.68 (s, 3H)

$^{13}\text{C}$  NMR (75 MHz,  $\text{CDCl}_3$ ,  $25^\circ\text{C}$ )  $\delta$ =153.9 (C), 152.9 (C), 144.0 (C), 137.7 (C), 131.4 (CH), 129.7 (CH), 126.6 (CH), 123.9 (CH), 119.7 (C), 115.7 (CH), 114.9 (C), 110.1 (C), 80.1 (C), 42.6 ( $\text{CH}_2$ ), 38.4 (C), 30.0 ( $\text{CH}_3$ )

IR (neat)  $\nu$  3466, 3348, 3236, 3095, 2968, 2931, 2866, 2169, 1635, 1552, 1435, 1408, 1216, 966, 792  $\text{cm}^{-1}$

HRMS (ESI) for  $\text{C}_{16}\text{H}_{12}\text{N}_2\text{Br}_2\text{S}_2$  ( $\text{M}+\text{Li}$ ) $^+$ : calcd 460.8969, found 460.8918.



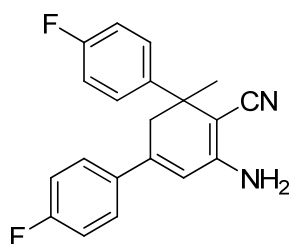
**2-Amino-6-methyl-4,6-diphenylcyclohexa-1,3-dienecarbonitrile**

(**168**):  $^1\text{H}$  NMR (300MHz,  $\text{CDCl}_3$ ,  $25^\circ\text{C}$ ),  $\delta=7.25\text{--}7.41$  (m, 9H), 7.15–7.21 (m, 1H), 6.13 (d,  $J=2.1$  Hz, 1H), 4.61 (s, 2H), 3.18 (d,  $J=16.8$  Hz, 1H), 2.82 (dd,  $J=2.1$ , 16.8 Hz, 1H), 1.67 (s, 3H)

$^{13}\text{C}$  NMR (75 MHz,  $\text{CDCl}_3$ ,  $25^\circ\text{C}$ )  $\delta=153.3$  (C), 147.1 (C), 145.7 (C), 139.1 (C), 129.2 (CH), 129.0 (2 x CH), 128.5 (2 x CH), 126.7 (CH), 126.2 (2 x CH), 125.9 (2 x CH), 121.9 (C), 118.0 (CH), 80.5 (C), 42.3 ( $\text{CH}_2$ ), 39.4 (C), 29.1 ( $\text{CH}_3$ )

IR (neat)  $\nu$  3477, 3355, 3036, 2961, 2165, 1637, 1556, 1496, 1401, 1265, 871, 763, 699  $\text{cm}^{-1}$

HRMS (ESI) for  $\text{C}_{20}\text{H}_{18}\text{N}_2$  ( $\text{M}+\text{H}^+$ ): calcd 287.1548, found 287.1574.



**2-Amino-4,6-bis(4-fluorophenyl)-6-methylcyclohexa-1,3-**

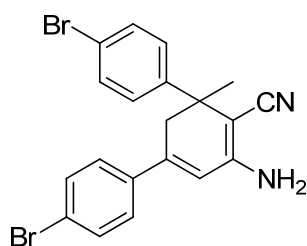
**dienecarbonitrile (169)**:  $^1\text{H}$  NMR (300MHz,  $\text{CDCl}_3$ ,  $25^\circ\text{C}$ ),  $\delta=7.30\text{--}7.38$  (m, 4H), 6.92–7.09 (m, 4H), 6.09 (d,  $J=2.4$  Hz, 1H), 4.63 (s, 2H), 3.07 (d,  $J=16.8$  Hz, 1H), 2.80 (dd,  $J=2.1$ , 16.8 Hz, 1H), 1.65 (s, 3H)

$^{13}\text{C}$  NMR (75 MHz,  $\text{CDCl}_3$ ,  $25^\circ\text{C}$ )  $\delta=165.0$  (C), 163.3 (C), 161.7 (C), 153.2 (C), 144.6 (C), 129.4 (d,  $J=8.0$  Hz, C), 127.8 (CH), 127.8 (CH), 127.7 (CH), 127.7 (CH), 120.6 (C),

117.7 (CH), 116.2 (CH), 115.9 (CH), 115.4 (CH), 115.1 (CH), 80.2 (C), 42.7 (CH<sub>2</sub>), 39.1 (C), 29.1 (CH<sub>3</sub>)

IR (neat)  $\nu$  3455, 3347, 3232, 3017, 2971, 2948, 2170, 1738, 1641, 1556, 1506, 1366, 1229, 1217, 1160, 908, 828, 729 cm<sup>-1</sup>

HRMS (ESI) for C<sub>20</sub>H<sub>16</sub>N<sub>2</sub>F<sub>2</sub> (M+H)<sup>+</sup>: calcd 323.1360, found 323.1370.



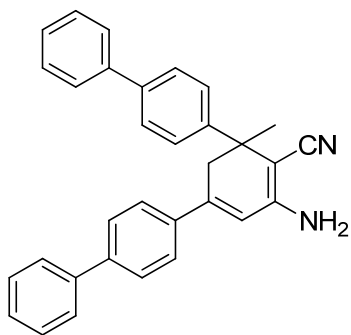
**2-Amino-4,6-bis(4-bromophenyl)-6-methylcyclohexa-1,3-**

**dienecarbonitrile (170):** <sup>1</sup>H NMR (300MHz, CDCl<sub>3</sub>, 25°C),  $\delta$ =7.21-7.48 (m, 8H), 6.15 (s, 1H), 4.71 (s, 2H), 3.04 (d,  $J$ =16.8 Hz, 1H), 2.79 (d,  $J$ =16.8 Hz, 1H), 1.63 (s, 3H)

<sup>13</sup>C NMR (75 MHz, CDCl<sub>3</sub>, 25°C)  $\delta$ =153.3 (C), 146.0 (C), 144.4 (C), 137.7 (C), 132.2 (2 x CH), 131.6 (2 x CH), 128.0 (2 x CH), 127.4 (2 x CH), 123.5 (C), 120.8 (C), 120.6 (C), 118.4 (CH), 79.9 (C), 42.1 (CH<sub>2</sub>), 39.3 (C), 29.0 (CH<sub>3</sub>)

IR (neat)  $\nu$  3468, 3346, 3234, 2965, 2929, 2870, 2173, 1642, 1557, 1488, 1393, 1078, 1007, 817 cm<sup>-1</sup>

HRMS (ESI) for C<sub>20</sub>H<sub>16</sub>N<sub>2</sub>Br<sub>2</sub> (M+Li)<sup>+</sup>: calcd 448.9840, found 448.9805.



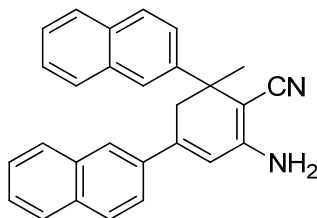
**2-Amino-4,6-di(biphenyl-4-yl)-6-methylcyclohexa-1,3-**

**dienecarbonitrile (171):**  $^1\text{H}$  NMR (300MHz,  $\text{CDCl}_3$ ,  $25^\circ\text{C}$ ),  $\delta$ =7.31-7.70 (m, 18 H), 6.22 (d,  $J$ =1.8 Hz, 1H), 4.64 (s, 2H), 3.27 (d,  $J$ =16.8 Hz, 1H), 2.88 (dd,  $J$ =1.8, 16.8 Hz, 1H), 1.75 (s, 3H)

$^{13}\text{C}$  NMR (75 MHz,  $\text{CDCl}_3$ ,  $25^\circ\text{C}$ )  $\delta$ =153.3 (C), 146.3 (C), 145.1 (C), 142.0 (C), 140.9 (C), 140.4 (C), 139.5 (C), 137.8 (C), 129.2 (2 x CH), 129.0 (2 x CH), 128.0 (CH), 127.6 (2 x CH), 127.5 (2 x CH), 127.3 (5 x CH), 126.7 (2 x CH), 126.4 (2 x CH), 121.0 (C), 117.8 (CH), 80.6 (C), 42.1 ( $\text{CH}_2$ ), 39.6 (C), 29.2 ( $\text{CH}_3$ )

IR (neat)  $\nu$  3462, 3347, 3057, 3028, 2965, 2928, 2872, 2170, 1638, 1551, 1486, 1396, 1274, 1006, 832, 763, 730, 696  $\text{cm}^{-1}$

HRMS (ESI) for  $\text{C}_{32}\text{H}_{26}\text{N}_2$  ( $\text{M}+\text{H}$ ) $^+$ : calcd 439.2174, found 439.2163.



**2-Amino-6-methyl-4,6-di-naphthalen-2-yl-cyclohexa-1,3-**

**dienecarbonitrile (172):**  $^1\text{H}$  NMR (300MHz,  $\text{CDCl}_3$ ,  $25^\circ\text{C}$ ),  $\delta$ =7.88 (d,  $J$ =1.2 Hz, 1H), 7.71-7.85 (m, 7H), 7.65 (dd,  $J$ =1.8, 8.4 Hz, 1H), 7.54 (d,  $J$ =2.1 Hz, 1H), 7.47-7.52 (m,

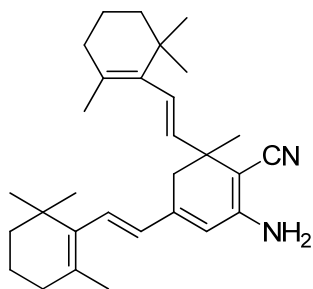


2H), 7.39-7.44 (m, 2H), 6.27 (d,  $J=1.8$  Hz, 1H), 3.46 (d,  $J=17.4$  Hz, 1H), 3.01 (dd,  $J=2.1, 16.8$  Hz, 1H), 1.81 (s, 3H)

$^{13}\text{C}$  NMR (75 MHz,  $\text{CDCl}_3$ ,  $25^\circ\text{C}$ )  $\delta=153.0$  (C), 145.6 (C), 144.3 (C), 136.2 (C), 133.7 (C), 133.5 (C), 133.4 (C), 132.4 (C), 128.7 (CH), 126.6 (CH), 128.4 (CH), 128.3 (CH), 127.9 (CH), 127.6 (CH), 127.0 (CH), 126.9 (CH), 126.2 (CH), 125.9 (CH), 125.4 (CH), 125.0 (CH), 124.5 (CH), 123.4 (CH), 120.5 (C), 118.2 (CH), 81.3 (C), 42.1 ( $\text{CH}_2$ ), 39.7 (C), 29.0 ( $\text{CH}_3$ )

IR (neat)  $\nu$  3472, 3346, 3229, 3054, 2963, 2168, 1638, 1554, 1505, 1404, 1275, 850, 815, 746  $\text{cm}^{-1}$

HRMS (ESI) for  $\text{C}_{28}\text{H}_{22}\text{N}_2$  ( $\text{M}+\text{H}^+$ ): calcd 387.1861, found 387.1830.



**2-Amino-6-methyl-4,6-bis-2-(2,6,6-trimethylcyclohex-1-**

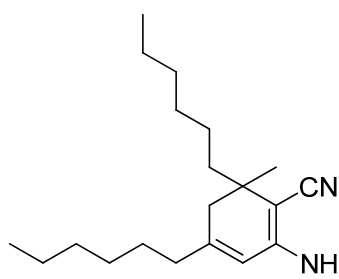
**enyl)vinyl)cyclohexa-1,3-dienecarbonitrile (173)**<sup>213</sup>:  $^1\text{H}$  NMR (300MHz,  $\text{CDCl}_3$ ,  $25^\circ\text{C}$ ),  $\delta=6.43$  (d,  $J=16.2$  Hz, 1H), 6.10 (d,  $J=16.2$  Hz, 1H), 5.75 (dd,  $J=1.2, 16.2$  Hz, 1H), 5.70 (s, 1H), 5.20 (d,  $J=15.9$  Hz, 1H), 4.33 (s, 2H), 2.59 (d,  $J=16.5$  Hz, 1H), 2.29 (dd,  $J=1.8, 16.5$  Hz, 1H), 1.89-2.03 (m, 4H), 1.67 (s, 3H), 1.52-1.62 (m, 9H), 1.40-1.47 (m, 2H), 1.39 (s, 3H), 1.00 (s, 3H), 0.99 (s, 3H), 0.91 (s, 3H), 0.90 (s, 3H)

$^{13}\text{C}$  NMR (75 MHz,  $\text{CDCl}_3$ ,  $25^\circ\text{C}$ )  $\delta=153.0$  (C), 144.0 (C), 138.6 (CH), 137.6 (C), 137.5 (C), 133.5 (CH), 131.8 (CH), 131.2 (C), 127.9 (C), 125.2 (CH), 120.4 (C), 119.1 (CH),

79.9 (C), 39.7 (CH<sub>2</sub>), 39.4 (CH<sub>2</sub>), 37.3 (C), 36.8 (CH<sub>2</sub>), 34.4 (C), 34.2 (C), 33.3 (CH<sub>2</sub>), 32.7 (CH<sub>2</sub>), 29.1 (CH<sub>3</sub>), 29.1 (CH<sub>3</sub>), 28.9 (2 x CH<sub>3</sub>), 28.3 (CH<sub>3</sub>), 21.9 (CH<sub>3</sub>), 21.5 (CH<sub>3</sub>), 19.5 (CH<sub>2</sub>), 19.3 (CH<sub>2</sub>)

IR (neat)  $\nu$  3474, 3359, 3233, 2958, 2926, 2865, 2171, 1738, 1636, 1553, 1456, 1361, 1217, 969 cm<sup>-1</sup>

HRMS (ESI) for C<sub>30</sub>H<sub>42</sub>N<sub>2</sub> (M+H)<sup>+</sup>: calcd 431.3426, found 431.3394.



**2-Amino-4,6-dihexyl-6-methylcyclohexa-1,3-**

**dienecarbonitrile (174):** <sup>1</sup>H NMR (300MHz, CDCl<sub>3</sub>, 25°C),  $\delta$ =5.52 (s, 1H), 4.25 (s, 2H), 2.06-2.16 (m, 3H), 1.96 (d,  $J$ =17.1 Hz, 1H), 1.20-1.42 (m, 18H), 1.09 (s, 3H), 0.83-0.87 (m, 6H)

<sup>13</sup>C NMR (75 MHz, CDCl<sub>3</sub>, 25°C)  $\delta$ =152.4 (C), 150.4 (C), 120.9 (C), 116.2 (CH), 79.4 (C), 41.0 (CH<sub>2</sub>), 40.5 (CH<sub>2</sub>), 37.8 (CH<sub>2</sub>), 34.4 (C), 32.1 (CH<sub>2</sub>), 31.9 (CH<sub>2</sub>), 30.2 (CH<sub>2</sub>), 29.2 (CH<sub>2</sub>), 27.0 (CH<sub>3</sub>), 26.8 (CH<sub>2</sub>), 24.7 (CH<sub>2</sub>), 22.9 (CH<sub>2</sub>), 22.8 (CH<sub>2</sub>), 14.3 (CH<sub>3</sub>), 14.3 (CH<sub>3</sub>)

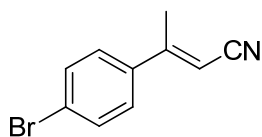
IR (neat)  $\nu$  3470, 3360, 3234, 2956, 2927, 2857, 2169, 1658, 1568, 1457, 1417, 1378, 911, 733 cm<sup>-1</sup>

HRMS (ESI) for C<sub>20</sub>H<sub>34</sub>N<sub>2</sub> (M+H)<sup>+</sup>: calcd 303.2800, found 303.2803.

*Synthesis of A,B-Unsaturated Nitriles*<sup>102</sup>

Nitriles **62-70** for LDA reactions were prepared following literature protocols and purified by flash column chromatography (gradient of 2-10% ethyl acetate/hexanes). Starting material **62-70** are found in Chapter III while **184** was synthesized for compounds of this chapter.

*Characterization of A,B-Unsaturated Nitriles*



**3-(5-bromothiophen-2-yl)but-2-enenitrile (184):** <sup>1</sup>H NMR

(300MHz, CDCl<sub>3</sub>, 25°C), δ=6.98 (d, *J*=3.3 Hz, 2H), 5.43 (q, *J*=0.9 Hz, 1H), 2.34 (d, *J*=0.9 Hz, 3H)

<sup>13</sup>C NMR (75 MHz, CDCl<sub>3</sub>, 25°C) δ=151.2 (C), 143.3 (C), 131.6 (CH), 128.4 (CH), 117.4 (C), 116.2 (C), 93.6 (CH), 19.67 (CH<sub>3</sub>)

IR (neat) ν 3095, 3050, 2995, 2925, 2852, 2210, 1660, 1593, 1411, 1269, 969, 790 cm<sup>-1</sup>

HRMS (ESI) for C<sub>8</sub>H<sub>6</sub>NBrS (M+H)<sup>+</sup>: calcd 227.9483, found 227.9463.

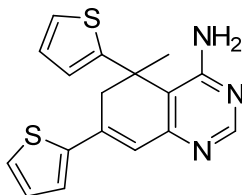
*General Procedure for LDA Self-Dimerizations*<sup>191</sup>

A solution of  $\alpha,\beta$ -unsaturated nitrile in THF was added to a stirred solution of lithium diisopropylamide (2.0 M) in THF that was cooled to -20°C. The reaction mixture was warmed to room temperature and stirred until the starting material was consumed (monitored via thin layered chromatography). The reaction was then quenched by the addition of water. The mixture was extracted with ethyl ether. The organic layer was washed with ammonium sulfate, water, and brine before being dried over magnesium sulfate and evaporated under vacuum. The crude product was purified via flash chromatography with 100% dichloromethane.

*General Procedure for Quinazolines*<sup>191</sup>

Enaminonitrile was dried over vacuum and dissolved with 2.0 equivalents of formic acid and 2.0 equivalents of formamide. This mixture was refluxed for 24 h at 200°C. Upon completion, the reaction mixture was brought back to room temperature and extracted with 100 mL (2 x 50 mL) of ethyl ether. The combined ether layers were washed with water and a concentrated brine solution before being dried over magnesium sulfate and concentrated *in vacuo*. The crude product was purified via flash chromatography with a gradient of 100% dichloromethane to 90% dichloromethane/10% methanol.

*Characterization of Quinazolines*



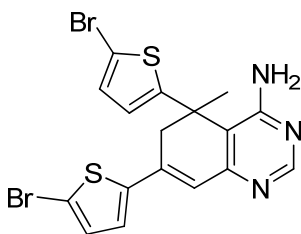
**5-Methyl-5,7-di(thiophen-2-yl)-5,6-dihydroquinazolin-4-amine**

(**175**):  $^1\text{H}$  NMR (300MHz,  $\text{CDCl}_3$ ,  $25^\circ\text{C}$ ),  $\delta$ =8.39 (s, 1H), 7.34-7.37 (m, 2H), 7.24 (dd,  $J$ =1.2, 3.6 Hz, 1H), 7.15 (dd,  $J$ =0.9, 3.6 Hz, 1H), 7.02-7.06 (m, 2H), 6.92 (d,  $J$ =2.4 Hz, 1H), 4.86 (s, 2H), 3.30 (dd,  $J$ =2.4, 16.8 Hz, 1H), 2.91 (d,  $J$ =16.8 Hz, 1H), 1.70 (s, 3H)

$^{13}\text{C}$  NMR (75 MHz,  $\text{CDCl}_3$ ,  $25^\circ\text{C}$ )  $\delta$ =165.7 (C), 160.0 (C), 153.2 (CH), 151.4 (C), 142.4 (C), 140.1 (C), 128.6 (CH), 128.6 (CH), 127.5 (CH), 126.9 (CH), 126.8 (CH), 125.5 (CH), 124.7 (C), 117.3 (CH), 46.5 ( $\text{CH}_2$ ), 39.4 (C), 22.3 ( $\text{CH}_3$ )

IR (neat)  $\nu$  3469, 3342, 3183, 3106, 3073, 3037, 2923, 2886, 1688, 1613, 1556, 1448, 1420, 1183, 1047, 852,  $700\text{ cm}^{-1}$

HRMS (ESI) for  $\text{C}_{17}\text{H}_{15}\text{N}_3\text{S}_2$  ( $\text{M}+\text{H}^+$ ): calcd 326.0786, found 326.0707.



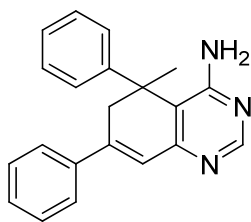
**5,7-Bis(5-bromothiophen-2-yl)-5-methyl-5,6-**

**dihydroquinazolin-4-amine (176)**:  $^1\text{H}$  NMR (300MHz,  $\text{CDCl}_3$ ,  $25^\circ\text{C}$ ),  $\delta$ =8.43 (s, 1H), 6.91-7.04 (m, 5H), 4.82 (s, 2H), 3.22 (dd,  $J$ =1.5, 17.1 Hz, 1H), 2.91 (d,  $J$ =17.1 Hz, 1H), 1.79 (s, 3H)

$^{13}\text{C}$  NMR (75 MHz,  $\text{CDCl}_3$ ,  $25^\circ\text{C}$ )  $\delta$ =159.9 (C), 157.4 (CH), 154.9 (C), 143.2 (C), 136.8 (C), 135.8 (C), 129.8 (CH), 128.2 (CH), 127.3 (CH), 125.3 (CH), 121.9 (2 x C), 121.5 (CH), 112.9 (C), 45.9 ( $\text{CH}_2$ ), 40.7 (C), 22.2 ( $\text{CH}_3$ )

IR (neat)  $\nu$  3469, 3388, 3294, 3159, 2967, 2927, 2854, 1618, 1554, 1421, 1049, 961, 797, 730, 703  $\text{cm}^{-1}$

HRMS (ESI) for  $\text{C}_{17}\text{H}_{13}\text{Br}_2\text{N}_3\text{S}_2$  ( $\text{M}+\text{H}$ ) $^+$ : calcd 481.8996, found 481.8980.



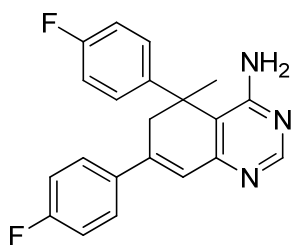
**5-Methyl-5,7-diphenyl-5,6-dihydroquinazolin-4-amine (177):**  $^1\text{H}$

NMR (300MHz,  $\text{CDCl}_3$ ,  $25^\circ\text{C}$ ),  $\delta$ =8.20 (s, 1H), 7.30-7.72 (m, 10H), 6.84 (s, 1H), 4.60 (s, 2H), 3.22 (dd,  $J$ =1.5, 17.7 Hz, 1H), 2.95 (dd,  $J$ =1.2, 17.7 Hz, 1H), 1.90 (s, 3H)

$^{13}\text{C}$  NMR (75 MHz,  $\text{CDCl}_3$ ,  $25^\circ\text{C}$ )  $\delta$ =158.0 (C), 153.0 (C), 150.6 (CH), 146.9 (C), 145.8 (C), 139.1 (C), 129.2 (CH), 129.0 (2 x CH), 128.5 (2 x CH), 126.7 (CH), 126.1 (2 x CH), 125.9 (2 x CH), 121.0 (C), 117.8 (CH), 42.3 ( $\text{CH}_2$ ), 39.4 (C), 29.1 ( $\text{CH}_3$ )

IR (neat)  $\nu$  3469, 3352, 3233, 3083, 3059, 3033, 2966, 2924, 1654, 1588, 1487, 1417, 1006, 832, 764, 697  $\text{cm}^{-1}$

HRMS (ESI) for  $\text{C}_{21}\text{H}_{19}\text{N}_3$  ( $\text{M}+\text{H}$ ) $^+$ : calcd 314.1657, found 314.1613.



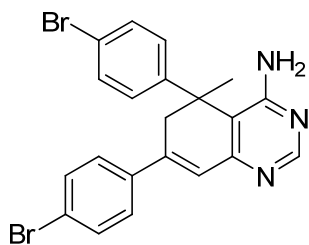
**5,7-Bis(4-fluorophenyl)-5-methyl-5,6-dihydroquinazolin-4-**

**amine (178):**  $^1\text{H}$  NMR (300MHz,  $\text{CDCl}_3$ ,  $25^\circ\text{C}$ ),  $\delta$ =8.18 (s, 1H), 7.28-7.51 (m, 3H), 6.88-7.19 (m, 7H), 6.70 (s, 1H), 5.80 (s, 2H), 3.07 (dd,  $J$ =1.5, 17.4 Hz, 1H), 2.85 (d,  $J$ =17.4 Hz, 1H), 1.83 (s, 3H)

$^{13}\text{C}$  NMR (75 MHz,  $\text{CDCl}_3$ ,  $25^\circ\text{C}$ )  $\delta$ = 165.1 (C), 163.1 (C), 159.2 (C), 157.9 (C), 147.6 (CH), 146.7 (C), 144.1 (C), 134.9 (C), 127.8 (CH), 127.7 (CH), 127.5 (CH), 127.4 (CH), 123.7 (C), 122.6 (CH), 116.1 (CH), 115.8 (CH), 115.3 (CH), 115.0 (CH), 44.8 ( $\text{CH}_2$ ), 40.9 (C), 25.1 ( $\text{CH}_3$ )

IR (neat)  $\nu$  3465, 3389, 3320, 3171, 3055, 2928, 2967, 1652, 1585, 1508, 1421, 1229, 1161, 1013, 828, 734  $\text{cm}^{-1}$

HRMS (ESI) for  $\text{C}_{21}\text{H}_{17}\text{F}_2\text{N}_2$  ( $\text{M}+\text{H}$ ) $^+$ : calcd 350.1469, found 350.1488.



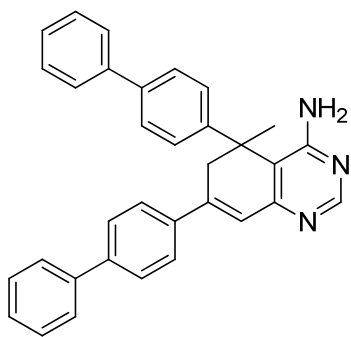
**5,7-Bis(4-bromophenyl)-5-methyl-5,6-dihydroquinazolin-4-**

**amine (179):**  $^1\text{H}$  NMR (300MHz,  $\text{CDCl}_3$ ,  $25^\circ\text{C}$ ),  $\delta$ =8.42 (s, 1H), 7.45-7.52 (m, 2H), 7.32-7.40 (m, 4H), 7.17-7.25 (m, 2H), 6.75 (s, 1H), 4.50 (s, 2H), 3.06 (dd,  $J$ =1.5, 17.7 Hz, 1H), 2.83 (dd,  $J$ =1.5, 17.7 Hz, 1H), 1.80 (s, 3H)

$^{13}\text{C}$  NMR (75 MHz,  $\text{CDCl}_3$ ,  $25^\circ\text{C}$ )  $\delta$ =162.1 (C), 157.8 (C), 147.6 (CH), 147.2 (C), 143.9 (C), 137.6 (C), 132.2 (2 x CH), 131.5 (2 x CH), 127.8 (2 x CH), 127.4 (2 x CH), 123.7 (C), 123.6 (C), 123.1 (CH), 120.3 (C), 44.3 ( $\text{CH}_2$ ), 41.1 (C), 24.6 ( $\text{CH}_3$ )

IR (neat)  $\nu$  3469, 3387, 3294, 3158, 3104, 2927, 2854, 1618, 1554, 1439, 1421, 1049, 961, 797,  $730\text{ cm}^{-1}$

HRMS (ESI) for  $\text{C}_{21}\text{H}_{17}\text{N}_3\text{Br}_2$  ( $\text{M}+\text{H}$ ) $^+$ : calcd 469.9867, found 469.9860.



**5,7-Di(biphenyl-4-yl)-5-methyl-5,6-dihydroquinazolin-4-**

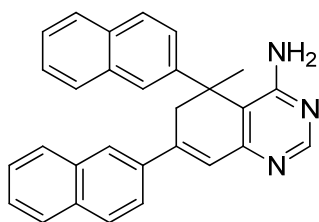
**amine (180):**  $^1\text{H}$  NMR (300MHz,  $\text{CDCl}_3$ ,  $25^\circ\text{C}$ ),  $\delta$ =8.40 (s, 1H), 7.51-7.70 (m, 8H), 7.29-7.49 (m, 10H), 7.15 (d,  $J$ =2.4 Hz, 1H), 4.76 (s, 2H), 3.31 (dd,  $J$ =2.4, 17.1 Hz, 1H), 2.92 (d,  $J$ =17.1 Hz, 1H), 1.71 (s, 3H)

$^{13}\text{C}$  NMR (75 MHz,  $\text{CDCl}_3$ ,  $25^\circ\text{C}$ )  $\delta$ =160.0 (C), 157.6 (C), 157.0 (2 x C), 153.1 (CH), 143.4 (2 x C), 140.6 (C), 137.0 (2 x C), 129.2 (CH), 129.1 (CH), 128.2 (2 x CH), 127.9 (CH), 127.6 (CH), 127.4 (CH), 127.3 (3 x CH), 127.2 (5 x CH), 126.3 (CH), 125.5 (CH), 125.0 (CH), 124.5 (C), 121.4 (CH), 46.7 ( $\text{CH}_2$ ), 40.3 (C), 22.6 ( $\text{CH}_3$ )

IR (neat)  $\nu$  3462, 3380, 3298, 3031, 2958, 2925, 2856, 1600, 1556, 1487, 1264, 832,  $765, 697\text{ cm}^{-1}$

HRMS (ESI) for  $\text{C}_{33}\text{H}_{27}\text{N}_3$  ( $\text{M}+\text{H}$ ) $^+$ : calcd 466.2283, found 466.2229.





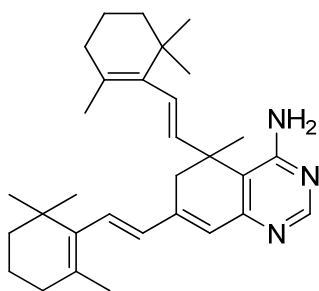
**5-Methyl-5,7-di(naphthalen-2-yl)-5,6-dihydroquinazolin-4-**

**amine (181):**  $^1\text{H}$  NMR (300MHz,  $\text{CDCl}_3$ ,  $25^\circ\text{C}$ ),  $\delta$ =8.48 (s, 1H), 8.05 (s, 1H), 7.76-7.93 (m, 8H), 7.67 (dd,  $J$ =1.8, 8.4 Hz, 1H), 7.54-7.62 (m, 2H), 7.40-7.53 (m, 4H), 7.11 (d,  $J$ =2.7 Hz, 1H), 4.39 (s, 2H), 3.47 (dd,  $J$ =2.7, 17.1 Hz, 1H), 2.97 (d,  $J$ =17.1 Hz, 1H), 1.85 (s, 3H)

$^{13}\text{C}$  NMR (75 MHz,  $\text{CDCl}_3$ ,  $25^\circ\text{C}$ )  $\delta$ =160.0 (C), 158.5 (C), 157.2 (C), 145.1 (CH), 142.9 (C), 136.2 (C), 133.7 (C), 133.6 (C), 133.4 (C), 132.7 (C), 129.7 (CH), 128.6 (3 x CH), 128.3 (CH), 128.0 (CH), 127.9 (CH), 127.1 (CH), 126.9 (CH), 126.9 (CH), 126.8 (CH), 126.1 (CH), 125.2 (CH), 124.4 (CH), 123.8 (C), 123.6 (CH), 45.5 ( $\text{CH}_2$ ), 42.5 (C), 21.1 ( $\text{CH}_3$ )

IR (neat)  $\nu$  3471, 3387, 3308, 3177, 3054, 2961, 2927, 2854, 1671, 1598, 1557, 1449, 1376, 1274, 1046, 854, 817, 747  $\text{cm}^{-1}$

HRMS (ESI) for  $\text{C}_{29}\text{H}_{23}\text{N}_3$  ( $\text{M}+\text{H}$ ) $^+$ : calcd 414.1970, found 414.1938.



**5-methyl-5,7-bis((E)-2-(2,6,6-trimethylcyclohex-1-**

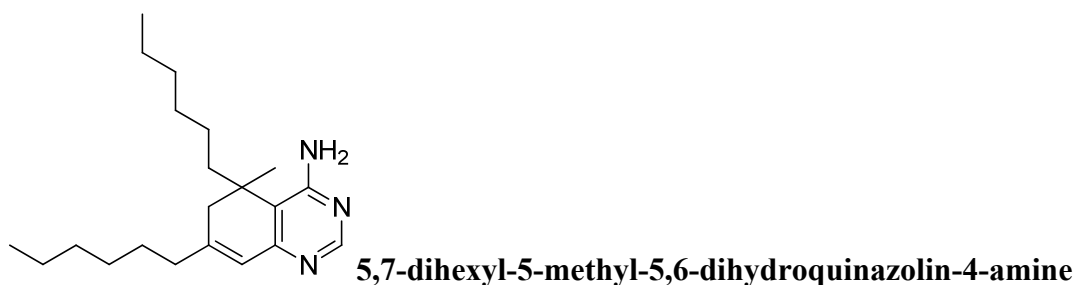
**enyl)vinyl)-5,6-dihydro-quinazolin-4-amine (182):**  $^1\text{H}$  NMR (300MHz,  $\text{CDCl}_3$ ,

25°C),  $\delta$ =8.20, (s, 1H), 6.75 (d,  $J$ =16.2 Hz, 1H), 6.60 (s, 1H), 6.35 (d,  $J$ =16.2 Hz, 1H), 6.00 (dd,  $J$ =1.2, 16.2 Hz, 1H), 5.30 (d,  $J$ =15.9 Hz, 1H), 4.40 (s, 2H), 2.58 (d,  $J$ =16.5 Hz, 1H), 2.18-2.20 (m, 1H), 1.88-2.03 (m, 4H), 1.67 (s, 3H), 1.52-1.62 (m, 9H), 1.40-1.47 (m, 2H), 1.39 (s, 3H), 1.00 (s, 3H), 0.99 (s, 3H), 0.91 (s, 3H), 0.90 (s, 3H)

$^{13}\text{C}$  NMR (75 MHz,  $\text{CDCl}_3$ , 25°C)  $\delta$ =161.8 (C), 159.8 (C), 151.8 (CH), 146.2 (C), 139.4 (CH), 138.4 (C), 138.3 (C), 134.3 (CH), 132.6 (CH), 132.0 (C), 128.7 (C), 126.0 (CH), 119.4 (C), 118.5 (CH), 40.4 ( $\text{CH}_2$ ), 40.1 ( $\text{CH}_2$ ), 37.9 (C), 37.5 ( $\text{CH}_2$ ), 35.1 (C), 34.9 (C), 34.0 ( $\text{CH}_2$ ), 33.4 ( $\text{CH}_2$ ), 29.8 ( $\text{CH}_3$ ), 29.6 ( $\text{CH}_3$ ), 29.6 (2 x  $\text{CH}_3$ ), 30.0 ( $\text{CH}_3$ ), 22.0 ( $\text{CH}_3$ ), 21.5 ( $\text{CH}_3$ ), 20.2 ( $\text{CH}_2$ ), 20.0 ( $\text{CH}_2$ )

IR (neat)  $\nu$  3472, 3360, 3243, 2958, 2928, 2866, 1704, 1636, 1555, 1345, 1217, 707  $\text{cm}^{-1}$

HRMS (ESI) for  $\text{C}_{31}\text{H}_{43}\text{N}_3$  ( $\text{M}+\text{H}$ ) $^+$ : calcd 458.3535, found 458.3543.



(**183**):  $^1\text{H}$  NMR (300MHz,  $\text{CDCl}_3$ , 25°C),  $\delta$ =8.2 (s, 1H), 6.08 (s, 1H), 5.18 (s, 2H), 1.96-2.27 (m, 4H), 1.49-1.54 (m, 2H), 1.16-1.42 (m, 19H), 0.88-1.02 (m, 6H)

$^{13}\text{C}$  NMR (75 MHz,  $\text{CDCl}_3$ , 25°C)  $\delta$ =162.9 (C), 158.2 (C), 151.7 (CH), 146.7 (C), 122.9 (CH), 121.6 (C), 41.5 ( $\text{CH}_2$ ), 40.3 ( $\text{CH}_2$ ), 38.5 ( $\text{CH}_2$ ), 37.7 ( $\text{CH}_2$ ), 31.1 ( $\text{CH}_2$ ), 31.9 ( $\text{CH}_2$ ), 30.4 ( $\text{CH}_2$ ), 29.3 ( $\text{CH}_2$ ), 27.0 ( $\text{CH}_3$ ), 25.9 ( $\text{CH}_2$ ), 25.4 ( $\text{CH}_2$ ), 23.2 ( $\text{CH}_2$ ), 22.9 ( $\text{CH}_2$ ), 14.3 (2 x  $\text{CH}_3$ )

IR (neat)  $\nu$  3470, 3360, 3234, 2956, 2927, 2857, 1655, 1578, 1457, 1378, 911  $\text{cm}^{-1}$

HRMS (ESI) for  $\text{C}_{21}\text{H}_{35}\text{N}_3$  ( $\text{M}+\text{H}$ )<sup>+</sup>: calcd 330.2909, found 330.2920.

### *Organisms and Cell Lines*

Jurkats (TIB-152) and *B. subtilis* strain 6633 were obtained from the American Type Culture Collection, Rockville, MD. The yeast *S. cerevisiae* wild-type strain [#404; BY4741; MATa his3 $\Delta$ 1 leu2 $\Delta$ 0 met15 $\Delta$ 0 ura3 $\Delta$ 0] was obtained from Dr. Michael Kladde at the Department of Biochemistry, Texas A&M University. The *E. coli* strain DH10B was obtained from Prof. Dennis Gross, Texas A&M University, Department of Plant Pathology.

### *Cytotoxicity Assay Against the Human T-cell Leukemia, Jurkat Cell Line*

Jurkat cells were maintained in 75  $\text{cm}^2$  culture flasks at 37 °C under a 5%  $\text{CO}_2$  atmosphere. The cell culture medium consisted of RPMI 1640 with 10% fetal bovine serum. Cells were harvested by centrifugation (20 min. at 1000 rpm), resuspended in fresh culture medium and counted on a hemocytometer. The cells (1 mL) were arrayed (200,000 cells/well) in 48 well plates to which compound was added to give final concentrations of 100, 10 and 1  $\mu\text{g}/\text{mL}$  respectively. Cells were incubated for 24 h, transferred to 1.5 mL eppendorf tubes and centrifuged for 15 min. at 14,000 rpm. The medium was removed and the cell pellet resuspended in 1 mL of phosphate buffer saline (PBS) to wash the cells. The cells were again centrifuged for 15 min. at 14,000 rpm. The PBS was removed and the cell pellet resuspended in a lysis buffer. The lysed cells

were placed in a black 96 well plate and analyzed using a Bio-Tek fluorometer to measure relative fluorescence.

#### *Anti-bacterial and Anti-fungal Assays*

Microbes (*Saccharomyces cerevisiae*, *Escherichia coli*, and *Bacillus subtilis* 6633) were cultured and maintained on agar plates (see supplemental material for media conditions). A single colony was used to inoculate 3 mL of culture medium and allowed to grow for 16 h. The cells (500  $\mu$ L) were diluted with 50 mL of fresh medium to an O.D. of 0.1 and aliquoted into a 96-well plate (100  $\mu$ L/well). The assays were set up in duplicate and the compounds tested to give final concentrations of 100, 10 and 1  $\mu$ g/mL. Plates were incubated (*E. coli* and *B. subtilis*, 37 °C; yeast, 30 °C) and shaken (250 rpm) for 16 h and cell density (O.D.) measured with a Bio-Tek microplate reader.

## CHAPTER VI

### CONCLUSION

In recent years, the advancements in the field of natural products have grown tremendously. The discovery of new drugs occurs on a daily basis with many of these possessing biological activities. Along with new drug discovery comes the discovery of new and unique molecular scaffolds. An example of this is the understudied class of compounds known as the cycloterpenals. The cycloterpenals possess a cyclohexadienal structural core and two have been isolated in nature thus far. The formation of cyclocitral has been suspected since the late 1890's and it was not until 1932 that the cyclohexadienal structure was ascribed.<sup>35,36</sup> Cyclocitral was recently isolated from the North Sea bryozoans *Flustra foliacea* and exhibited antibacterial activity against two bacterial strains.<sup>38,39</sup> Interestingly, cycloretinal was isolated from the human eye. This product is formed from the dimerization of the vision chromophore all-*trans*-retinal. This molecule, along with other bisretinoids that have been characterized in the eye, is believed to act as a contributor of age-related macular degeneration, the leading cause of blindness in the elderly.<sup>33,34</sup>

In the early 1990's, the formation of cyclo- $\beta$ -ional from  $\beta$ -ionylideneacetaldehyde was observed when the substrate was incubated with the milk protein  $\beta$ -lactoglobulin ( $\beta$ -LG).  $\beta$ -LG is the major whey protein in dairy milk constituting 50-55% of the protein volume.<sup>43</sup> The only function ascribed to  $\beta$ -LG after 70 years of extensive research is that it is involved as a carrier of essential nutrients such as fatty acids, retinoids, and steroids. Humans do not possess a homolog to  $\beta$ -LG so the only source of the protein in the human body is through the consumption of dairy

products. However, humans have a receptor in the small intestines where  $\beta$ -LG is absorbed into the blood stream. This protein is quite robust as it is able to survive the milk pasteurization process and the highly acidic environment within the stomach. Protein analysis of blood samples reveal that levels of  $\beta$ -LG in the blood stream are on average between 0.7 to 1.2 g/dL. In our investigations, we have revealed that  $\beta$ -LG can mediated the dimerization of natural and unnatural  $\beta$ -methyl aldehydes. Since  $\beta$ -LG is the principal whey protein in dairy milk, we set out to demonstrate that the protein in store bought milks could perform the reaction *in vitro*. To our amazement, the milk that we drink daily was able to facilitate the reaction of converting citral to cyclocitral. To demonstrate that the protein can mediate this reaction *in vivo*, we fed eight rabbits skim milk along with a  $\beta$ -LG solution. We fed the rabbits retinal along with these solutions only to discover that indeed cycloretinal was formed within the blood streams of the rabbits. These *in vivo* results help demonstrate how the slow accumulation of cycloretinal in the human eyes may be occurring as recent proteomic studies of various regions of the eyes has shown that  $\beta$ -LG is present.<sup>81</sup>

The reasons why  $\beta$ -methyl aldehydes can be dimerized by  $\beta$ -LG is not fully understood. Do these cycloterpenals possess other functionalities within the body? We hypothesized that since  $\beta$ -LG is the major whey protein in milk that these molecules may be involved in developmental processes such as cellular differentiation or neuronal development. The cycloterpenals are an understudied class of molecules so we set out to build a library of these molecules based on the cyclohexadienal scaffold. We incorporated various substituents in hopes of getting a glimpse into harnessing the power of these molecules. To do this, we developed a synthetic strategy that mimicked the

protein mediated reaction carried out by  $\beta$ -LG. By using L-proline, we were able to successfully synthesize over 100 cycloterpenals and screen for their biological activities. We established cell-based assays where we screened for antifungal/antimicrobial activities as well as a PC12 assay to screen for neurite outgrowth. Dramatic effects were observed with the PC12 assay where three molecules from our library stimulated neurite outgrowth and cell survival. The molecules possessing this activity contained aromatic substituents and long aliphatic chains. Biphenyl groups have been thought to serve as mimics of protein alpha helices while long aliphatic chains are capable of inserting into lipid bilayers.<sup>169</sup> In the case of the aromatic substituted cycloterpenals, the cyclohexadiene ring system could be aromatized to give fluorescent molecules. In the long term, these molecules could lead to protein target identification for a certain cycloterpenal.

During the synthesis of our  $\beta$ -methyl starting materials, we noticed the formation of a side product due to increased concentration of sodium hydride (NaH) that was utilized in a Horner-Wadsworth-Emmons reaction in the preparation of  $\alpha,\beta$ -unsaturated-nitriles. A characteristic of this side product was that it possessed diastereomeric protons similar to that of our cyclohexadienals. We isolated and characterized this side product to discover that the  $\beta$ -methyl-nitrile had self-condensated into a cyclohexadiene enamionitrile. Optimization of this reaction was pursued as this new synthetic strategy utilizing excess NaH gave yields from 80-96% in comparison to previous literature protocols which used lithium diisopropylamide (LDA). The yields for the LDA reactions were a meager 12-36% dependent upon substrate. These new cyclohexadiene enamionitriles were taken on step further to produce substituted quinazolines. This

class of molecules are important as antibacterial agents. We screened this library of 18 compounds against our cell-based screens where we saw  $CC_{50}$  values in the low micromolar range. The identification of the cellular targets of these compounds might direct the synthesis of functionally and structurally related analogues with more potent biological activities.

With our studies of substituted cyclohexadienes, we have established a direct link between  $\beta$ -LG and age-related macular degeneration. These findings could aid in the development of new therapeutics for the treatment of age-related macular degeneration. We have also discovered that the class of molecules known as cycloterpenals have therapeutic potential as they can be further developed in the treatment of neurodegenerative diseases or central nervous system injuries. This is only the tip of the iceberg as only two cycloterpenals have been isolated in nature with the growing possibility of others in the near future. These molecules may serve a purpose that we are uncertain at the present as the principal whey protein in dairy milk may play a larger role in living systems as it mediates the dimerization of natural aldehydes.



## REFERENCES

- (1) Rouhi, M. *Chemical & Engineering News* **Oct. 13 2003**, 77-91.
- (2) Newman, D. J.; Cragg, G. M. *Curr. Drug Targ.* **2006**, 7, 279-304.
- (3) Newman, D. J.; Cragg, G. M. *J. Nat. Prod.* **2007**, 70, 461-477.
- (4) Brocks, J. J.; Logan, G. A.; Buick, R.; Summons, R. E. *Science* **1999**, 285, 1033-1036.
- (5) Summons, R. E.; Janhnke, L. L.; Hope, J. M.; Logan, G. A. *Nature* **1999**, 400, 554-557.
- (6) Spurgeon, S. L.; Porter, J. W. In *Biosynthesis of Isoprenoid Compounds*; Vol. 1, Porter, J. W., Spurgeon, S. L., Eds.; Wiley: New York, 1981; p 1-46.
- (7) Dewick, P. M. *Medicinal Natural Products: A Biosynthetic Approach*; 2nd ed.; Wiley: Chichester, West Sussex, England, 2001.
- (8) Bochar, D. A.; Friesen, J. A.; Stauffacher, C. V.; Rodwell, V. W. *Biosynthesis of Mevalonic Acid from Acetyl CoA*; Vol. 2, Elsevier Science: Oxford, UK, 1999.
- (9) Davis, E. M.; Croteau, R. *Top. Curr. Chem.* **2000**, 209, 53-95.
- (10) Eisenreich, W.; Schwarz, M.; Cartayrade, A.; Arigoni, D.; Zenk, M. H.; Bacher, A. *Chem. Biol.* **1998**, 5, R221-R233.
- (11) Rohmer, M. In *Comprehensive Natural Product Chemistry*; Vol. 2, Elsevier Science: Oxford, UK, 1999; p 45-68.
- (12) Durbecq, V.; Sainz, G.; Oudjama, Y.; Clantin, B.; Bompard-Gilles, C.; Tricot, C.; Caillet, J.; Stalon, V.; Droogmans, L.; Villeret, V. *EMBO J.* **2001**, 20, 1530-1537.
- (13) Leyes, A. E.; Baker, J. A.; Poulter, C. D. *Org. Lett.* **1999**, 1, 1071-1073.
- (14) Dogbo, O.; Laferriere, A.; D' Harlingue, A.; Camara, B. *Proc. Natl. Acad. Sci. U. S. A.* **1988**, 85, 7054-7058.
- (15) Gu, P.; Ishii, Y.; Spencer, T. A.; Shechter, I. *J. Biol. Chem.* **1998**, 273, 12515-12525.
- (16) Radisky, E. S.; Poulter, C. D. *Biochemistry* **2000**, 39, 1748-1760.

- (17) Krinsky, N. I. *Pure Appl. Chem.* **1994**, *66*, 1003-1010.
- (18) Di Mascio, P.; Kaiser, S.; Sies, H. *Arch. Biochem. Biophys.* **1989**, *274*, 532-538.
- (19) Goodman, D. S.; Huang, H. S.; Kanai, M.; Shiratori, T. *J. Biol. Chem.* **1967**, *242*, 3543-3554.
- (20) Goodman, D. S.; Huang, H. S.; Kanai, M.; Shiratori, T. *J. Biol. Chem.* **1966**, *241*, 1929-1932.
- (21) Leuenberger, M. G.; Engeloch-Jarret, C.; Woggon, W. D. *Angew. Chem.* **2001**, *40*, 2614-2616.
- (22) Wald, G. *Nature* **1968**, *219*, 800-807.
- (23) Dockham, P. A.; Lee, M.-O.; Sladek, N. E. *Pharmacol.* **1992**, *43*, 2453-2469.
- (24) Lee, M.-O.; Manthey, C. L.; Sladek, N. E. *Pharmacol.* **1991**, *42*, 1279-1285.
- (25) Posch, K. C.; Burns, R. D.; Napoli, J. L. *J. Biol. Chem.* **1992**, *267*, 19676-19682.
- (26) Zhao, D.; McCaffery, P.; Ivins, K. J.; Neve, R. L.; Hogan, P.; Chin, W. W.; Drager, U. C. *Eur. J. Biochem.* **1996**, *240*, 15-22.
- (27) Bertram, J. S.; Kolonel, L. N.; Meyskens, F. L., Jr. *Cancer Res.* **1987**, *47*, 3012-3031.
- (28) Ganguly, J. *Biochemistry of Vitamin A*; Spriger : Boca Raton, FL 1989.
- (29) Huang, M.-E.; Ye, Y.-C.; Chen, S.-R.; Chai, J.-R.; Lu, J.-X.; Zhao, L.; Gu, L.-J.; Wang, Z.-Y. *Blood* **1988**, *72*, 567-572.
- (30) Jones-Villeneuve, E.; McBurney, M.; Rogers, K.; Kalnins, V. *J. Cell Biol.* **1982**, *94*, 253-262.
- (31) Bench, B. J.; Liu, C.; Evett, C. R.; Watanabe, C. M. H. *The Journal of Organic Chemistry* **2006**, *71*, 9458-9463.
- (32) Bench, B. J.; Tichy, S. E.; Perez, L. M.; Benson, J.; Watanabe, C. M. H. *Bioorg. Med. Chem.* **2008**, *16*, 7573-7581.
- (33) Fishkin, N.; Pescitelli, G.; Sparrow, J. R.; Nakanishi, K.; Berova, N. *Chirality* **2004**, *16*, 637-641.

- (34) Fishkin, N. E.; Sparrow, J. R.; Allikmets, R.; Nakanishi, K. *Proc. Natl. Acad. Sci. U S A* **2005**, *102*, 7091-7096.
- (35) Labbe, H. *Bull. Soc. Chim. Fr.* **1899**, *21*, 407.
- (36) Tiemann, F. *Berichte der deutschen chemischen Gesellschaft* **1898**, *31*, 3278-3296.
- (37) Fischer, F. G.; Löwenberg, K. *Justus Liebig's Annalen der Chemie* **1932**, *494*, 263-284.
- (38) Holst, P. B.; Anthoni, U.; Christophersen, C.; Nielsen, P. H.; Bock, K. *Acta Chem. Scand.* **1994**, *48*, 765-768.
- (39) Peters, L.; Wright, A. D.; Kehraus, S.; Gundisch, D.; Tilotta, M. C.; Konig, G. M. *Planta Med.* **2004**, *70*, 883-886.
- (40) Li, X.-y.; Asato, A. E.; Liu, R. S. H. *Tetrahedron Lett.* **1990**, *31*, 4841-4844.
- (41) Ariyaratne, K. A. N. S.; Brown, R.; Dasgupta, A.; de Jonge, J.; Jameson, G. B.; Loo, T. S.; Weinberg, C.; Norris, G. E. *Int.l Dairy J.*, **2002**, *12*, 311-318.
- (42) Garde, J.; Bell, S. C.; Eperon, I. C. *Proc. Natl. Acad. Sci. U. S. A.* **1991**, *88*, 2456-2460.
- (43) Hambling, S. G.; MacAlpine, A. S.; Sawyer, L. In *Advanced Dairy Chemistry II*; Fox, P. F., Ed.; Elsevier: Amsterdam, 1992, p 141-190.
- (44) Flower, D. R. *Biochem. J.* **1996**, *318*, 1-14.
- (45) Lyster, R. L. J. *J. Dairy Res.* **1972**, *39*, 279-318.
- (46) Sawyer, L.; Kontopidis, G. *Biochem. et Biophys. Acta* **2000**, *1482*, 136-148.
- (47) Tilley, J. M. A. *Dairy Sci. Abstr.* **1960**, *22*, 111-125.
- (48) Jost, R.; Maire, J. C.; Maynard, F.; Secretin, F. *Int. J. Food Sci. Technol.* **1999**, *34*, 533-542.
- (49) Brownlow, S.; Morais Cabral, J. H.; Cooper, R.; Flower, D. R.; Yewdall, S. J.; Polikarpov, I.; North, A. C. T.; Sawyer, L. *Structure* **1997**, *5*, 481-495.
- (50) Newcomer, M. E.; Jones, T. A.; Aqvist, J.; Sundelin, J.; Eriksson, U.; Rask, L.; Peterson, P. A. *EMBO J.* **1984**, *3*, 1451-1454.
- (51) Perez, M. D.; Calvo, M. J. *Dairy Sci.* **1995**, *78*, 978-988.

- (52) Rocha, T. L.; Brownlow, S.; Saddler, K. N.; Fothergill-Gilmore, L. A.; Sawyer, L. *J. Dairy Res.* **1996**, *63*, 575-584.
- (53) Papiz, M. Z.; Sawyer, L.; Eliopoulos, E. E.; North, A. C. T.; Findlay, J. B. C.; Sivaprasadarao, R.; Jones, T. A.; Newcomer, M. E.; Kraulis, P. J. *Nature* **1986**, *324*, 383-385.
- (54) Perez, M. D.; Sanchez, L.; Aranda, P.; Ena, J. M.; Oria, R.; Calvo, M. *Biochem. et. Biophys. Acta* **1991**, *1123*, 151-155.
- (55) Puyol, P.; Perez, M. D.; Ena, J. M.; Calvo, M. *Agric. Biol. Chem.* **1991**, *55*, 2515-2520.
- (56) Pervaiz, S.; Brew, K. *Science* **1985**, *228*, 335-337.
- (57) Kuwata, K.; Hoshino, M.; Forge, V.; Era, S.; Batt, C. A.; Goto, Y. *Protein Sci.* **1999**, *8*, 2541-2545.
- (58) Qin, B. Y.; Bewley, M. C.; Creamer, L. K.; Baker, E. N.; Jameson, G. B. *Protein Sci.* **1999**, *8*, 75-83.
- (59) Qin, B. Y.; Bewley, M. C.; Creamer, L. K.; Baker, H. M.; Baker, E. N.; Jameson, G. B. *Biochemistry* **1998**, *37*, 14014-14023.
- (60) Uhrinova, S.; Smith, M. H.; Jameson, G. B.; Uhrin, D.; Sawyer, L.; Barlow, P. N. *Biochemistry* **2000**, *39*, 3565-3574.
- (61) Cho, Y.; Batt, C.; Sawyer, L. *J. Biol. Chem.* **1994**, *269*, 11102-11107.
- (62) Kontopidis, G.; Holt, C.; Sawyer, L. *J. Mol. Biol.* **2002**, *318*, 1043-1055.
- (63) Qin, B. Y.; Creamer, L. K.; Baker, E. N.; Jameson, G. B. *FEBS Lett.* **1998**, *438*, 272-278.
- (64) Wu, S.-Y.; Perez, M. D.; Puyol, P.; Sawyer, L. *J. Biol. Chem.* **1999**, *274*, 170-174.
- (65) Muresan, S.; van der Bent, A.; de Wolf, F. A. *J. Agric. Food Chem.* **2001**, *49*, 2609-2618.
- (66) Wang, Q.; Allen, J. C.; Swaisgood, H. E. *J. Dairy Sci.* **1997**, *80*, 1054-1059.
- (67) Wang, Q.; Allen, J. C.; Swaisgood, H. E. *J. Dairy Sci.* **1997**, *80*, 1047-1053.

- (68) Wang, Q.; Allen, J. C.; Swaisgood, H. E. *J. Dairy Sci.* **1998**, *81*, 76-81.
- (69) Wang, Q.; Allen, J. C.; Swaisgood, H. E. *J. Dairy Sci.* **1999**, *82*, 257-264.
- (70) Yang, M.-C.; Guan, H.-H.; Liu, M.-Y.; Lin, Y.-H.; Yang, J.-M.; Chen, W.-L.; Chen, C.-J.; Simon J. T. Mao *Proteins: Structure, Function, and Bioinformatics* **2008**, *71*, 1197-1210.
- (71) Kontopidis, G.; Holt, C.; Sawyer, L. *J. Dairy Sci.* **2004**, *87*, 785-796.
- (72) Narayan, M.; Berliner, L. J. *Biochemistry* **1997**, *36*, 1906-1911.
- (73) Narayan, M.; Berliner, L. J. *Protein Science* **1998**, *7*, 150-157.
- (74) Ferris, F. L.; Fine, S. L.; Hyman, L. *Arch. Ophthalmol* **1984**, *102*, 1640-1642.
- (75) Klein, R.; Klein, B. E.; Linton, K. L. *Ophthalmology* **1992**, *99*, 933-943.
- (76) Eldred, G. E. *Gerontology* **1995**, *41*, 15-28.
- (77) Ishibashi, T.; Patterson, R.; Ohnishi, Y.; Inomata, H.; Ryan, S. J. *Am. J. Ophthalmol* **1986**, *101*, 342-353.
- (78) Abdelsalam, A.; Del Priore, L.; Zarbin, M. A. *Surv. Ophthalmol.* **1999**, *44*, 1-28.
- (79) Evans, J. R. *Prog. Retinal Eye. Res.* **2001**, *20*, 227-253.
- (80) Feeney-Burns, L.; Hilderbrand, E. S.; Eldridge, S. *Invest. Ophthalmol. Vis. Sci.* **1984**, *1984*, 195-200.
- (81) Warburton, S.; Southwick, K.; Hardman, R. M.; Secrest, A. M.; Grow, R. K.; Xin, H.; Woolley, A. T.; Burton, G. F.; Thulin, C. D. *Mol. Vis.* **2005**, *11*, 1122-1134.
- (82) Crabb, J. W.; Miyagi, M.; Gu, X.; Shadrach, K.; West, K. A.; Sakaguchi, H.; Kamei, M.; Hasan, A.; Yan, L.; Rayborn, M. E.; Salomon, R. G.; Hollyfield, J. G. *Proc. Natl. Acad. Sci. U. S. A.* **2002**, *99*, 14682-14687.
- (83) Ng, K.-P.; Gugi, B.; Renganathan, K.; Davies, M. W.; Gu, X.; Crabb, J. S.; Kim, S. R.; Rozanowska, M. B.; Bonilha, V. L.; Rayborn, M. E.; Salomon, R. G.; Sparrow, J. R.; Boulton, M. E.; Hollyfield, J. G.; Crabb, J. W. *Mol. & Cell. Proteomics* **2008**, *7*.
- (84) Boulton, M.; Rozanowska, M.; Rozanowski, B.; T., W. *Photochem. Photobiol. Sci.* **2004**, *3*.

- (85) Cuervo, A. M.; Dice, J. R. *Exp. Gerontol.* **2000**, *35*, 119-131.
- (86) Yin, D. *Free Rad. Biol. Med.* **1996**, *21*, 871-888.
- (87) Asato, A. E.; Watanabe, C.; Li, X.-Y.; Liu, R. S. H. *Tetrahedron Lett.* **1992**, *33*, 3105-3108.
- (88) Peters, L.; Konig, G. M.; Wright, A. D.; Purkall, R.; Stackebrandt, E.; Eberl, L.; Riedel, K. *Appl. Environ. Microbiol.* **2003**, *69*, 3469-3475.
- (89) Peters, L.; Wright, A. D.; Krick, A.; Konig, G. M. *J. Chem. Ecol.* **2004**, *30*, 1165-1181.
- (90) Sparrow, J. R.; Boulton, M. *Exp. Eye Res.* **2005**, *80*, 595-606.
- (91) Fishkin, N. E.; Jang, Y.-P.; Itagak, Y.; Sparrow, J.; Nakanishi, K. *Org. Biomol. Chem.* **2003**, *1*, 1101-1105.
- (92) Sparrow, J. R.; Parish, C. A.; Hashimoto, M.; Nakanishi, K. *Invest. Ophthalmol. Vis. Sci.* **1999**, *40*, 2988-2995.
- (93) Das, A.; Mukhopadhyay, C. *J. Phys. Chem. B* **2008**, *112*, 7903-7908.
- (94) Sawyer, L.; Brownlow, S.; Polikarpov, I.; Wu, S.-Y. *International Dairy Journal* **1998**, *8*, 65-72.
- (95) Brinegar, A. C.; Kinsella, J. E. *Int. J. Pept. Protein Res.* **1981**, *18*, 18-25.
- (96) Brown, E. M.; Pfeffer, P. E.; Kumosinski, T. F.; Greenberg, R. *Biochemistry* **1988**, *27*, 5601-5610.
- (97) Mattarella, N. L.; Creamer, L. K.; Richardson, T. *J. Agric. Food Chem.* **1983**, *31*.
- (98) Rowley, B. O.; Lund, D. B.; Richardson, T. *J. Dairy Sci.* **1979**, *62*, 533-536.
- (99) Bairoch, A.; Apweiler, R. *Nucleic Acids Res.* **1999**, *27*, 49-54.
- (100) Tanumihardjo, S. A. *J. Labelled Cpd. Radiopharm.* **2001**, *44*, 365-372.
- (101) Creemers, A. F. L.; Lugtenburg, J. *J. Am. Chem. Soc.* **2002**, *124*, 6324-6334.
- (102) Uchikawa, O.; Fukatsu, K.; Tokunoh, R.; Kawada, M.; Matsumoto, K.; Imai, Y.; Hinuma, S.; Kato, K.; Nishikawa, H.; Hirai, K.; Miyamoto, M.; Ohkawa, S. *J. Med. Chem.* **2002**, *45*, 4222-4239.

- (103) Lugtenburg, J. *Pure Appl. Chem.* **1985**, *57*, 753-762.
- (104) Taber, D. F.; Raman, K.; Gaul, M. D. *The Journal of Organic Chemistry* **1987**, *52*, 28-34.
- (105) Valla, A.; Valla, B.; Le Guillou, R.; Cartier, D.; Dufosse, L.; Labia, R. *Helvetica Chimica. Acta.* **2007**, *90*, 512-520.
- (106) Caillard, I.; Tome, D. *Am. J. Physiol. Gastrointest. Liver Physiol.* **1994**, *266*, G1053-1059.
- (107) Marcon-Genty, D.; Tome, D.; Kheroua, O.; Dumontier, A. M.; Heyman, M.; Desjeux, J. F. *Am. J. Physiol. Gastrointest. Liver Physiol.* **1989**, *256*, G943-948.
- (108) Hu, H.; Harrison, T. J.; Wilson, P. D. *The Journal of Organic Chemistry* **2004**, *69*, 3782-3786.
- (109) Cogan, U.; Kopelman, M.; Mokady, S.; Shinitzky, M. *Eur. J. Biochem.* **1976**, *65*, 71-78.
- (110) Tucker, H.; Golding, G.; Purvis, S. R. *Tetrahedron Lett.* **1981**, *22*, 1373-1376.
- (111) Taneja, S. C.; Koul, S. K.; Dhar, K. L. *Indian J. Chem.* **1988**, *27B*, 769-770.
- (112) Verdegem, P. J. E.; Monnee, M. C. F.; Mulder, P. P. J.; Lugtenburg, J. *Tetrahedron Lett.* **1997**, *38*, 5355-5358.
- (113) Thomas, A. F.; Guntz-Dubini, R. *Helvetica Chimica Acta* **1976**, *59*, 2261-2267.
- (114) Valla, A.; Andriamialisoa, Z.; Labia, R. *Tetrahedron Lett.* **2000**, *41*, 3359-3362.
- (115) Duhamel, L.; Guillemont, J.; Poirier, J.-M.; Chabardes, P. *Tetrahedron Lett.* **1991**, *32*, 4495-4498.
- (116) Yamada, S.-i.; Shibasaki, M.; Terashima, S. *Tetrahedron Lett.* **1973**, *14*, 377-380.
- (117) Yamada, S.-i.; Shibasaki, M.; Terashima, S. *Tetrahedron Lett.* **1973**, *14*, 381-384.
- (118) Eder, U.; Sauer, G.; Wiechert, R. *Angew. Chem. Int. Ed. Engl.* **1971**, *10*, 496-497.
- (119) Hajos, Z. G.; Parrish, D. R., German Patent DE 2102623, 1971.

- (120) Dalko, P. I.; Moisan, L. *Angew. Chem., Int. Ed. Engl.* **2004**, *43*, 5138-5175.
- (121) Seayad, J.; List, B. *Org. Biomol. Chem.* **2005**, *3*, 719-724.
- (122) Alcaide, B.; Almendros, P. *Angew. Chem. Int.l Ed.* **2003**, *42*, 858-860.
- (123) Borgevig, A.; Kumaragurubaran, N.; Jorgensen, K. A. *Chem. Commun.* **2002**, 620-621.
- (124) Casas, J.; Engqvist, M.; Ibrahem, I.; Kaynak, B.; Armando Córdova *Angewandte Chemie International Edition* **2005**, *44*, 1343-1345.
- (125) Cordova, A.; Notz, W.; Barbas, C. F. *The Journal of Organic Chemistry* **2002**, *67*, 301-303.
- (126) List, B. *Tetrahedron* **2002**, *58*, 5573-5590.
- (127) List, B. *Acc. Chem. Res.* **2004**, *37*, 548-557.
- (128) List, B.; Hoang, L.; Martin, H. J. *Proc. Natl. Acad. Sci. U S A* **2004**, *101*, 5839-5842.
- (129) Northrup, A. B.; MacMillan, D. W. C. *J. Am. Chem. Soc.* **2002**, *124*, 6798-6799.
- (130) Northrup, A. B.; Mangion, I. K.; Hettche, F.; MacMillan, D. W. C. *Angewandte Chemie International Edition* **2004**, *43*, 2152-2154.
- (131) Notz, W.; Tanaka, F.; Barbas, C. F. *Acc. Chem. Res.* **2004**, *37*, 580-591.
- (132) Sakthivel, K.; Notz, W.; Bui, T.; Barbas, C. F. *J. Am. Chem. Soc.* **2001**, *123*, 5260-5267.
- (133) Ishihara, K.; Nakano, K. *J. Am. Chem. Soc.* **2005**, *127*, 10504-10505.
- (134) Lakner, F. J.; Negrete, G. R. *Synlett* **2002**, *4*, 2002.
- (135) Ramachary, D. B.; Chowdari, N. S.; Barbas III, C. F. *Tetrahedron Lett.* **2002**, *43*, 6743-6746.
- (136) Sabitha, G.; Fatima, N.; Reddy, E. V.; Yadav, J. S. *Advanced Synthesis & Catalysis* **2005**, *347*, 1353-1355.
- (137) Sundén, H.; Ibrahem, I.; Eriksson, L.; Córdova, A. *Angewandte Chemie International Edition* **2005**, *44*, 4877-4880.



- (138) Thayumanavan, R.; Dhevalapally, B.; Sakthivel, K.; Tanaka, F.; Barbas III, C. F. *Tetrahedron Lett.* **2002**, *43*, 3817-3820.
- (139) Betancort, J. M.; Sakthivel, K.; Thayumanavan, F. T.; Barbas III, C. F. *Synthesis* **2004**, *9*, 1509-1521.
- (140) Christoffers, J.; Baro, A. *Angewandte Chemie International Edition* **2003**, *42*, 1688-1690.
- (141) Halland, N.; Hansen, T.; Jørgensen, K. A. *Angewandte Chemie International Edition* **2003**, *42*, 4955-4957.
- (142) Halland, N.; Hazell, R. G.; Jorgensen, K. A. *J. Org. Chem.* **2002**, *67*, 8331-8338.
- (143) Horstmann, T. E.; Guerin, D. J.; Miller, S. J. *Angewandte Chemie* **2000**, *39*, 3635-3638.
- (144) Krause, N.; Hoffmann-Roder, A. *Synthesis* **2001**, *6*, 171-196.
- (145) Harada, N.; Nakanishi, K. *Acc. Chem. Res.* **1972**, *5*, 257-263.
- (146) Kyba, E. P.; Timko, J. M.; Kaplan, L. J.; De Jong, F.; Gokel, G. W.; Cram, D. J. *J. Am. Chem. Soc.* **1978**, *100*, 4555-4568.
- (147) Zhou, Z.; Tang, Y.; Wang, L.; Zhao, G.; Zhou, Q.; Tang, C. *Synthesis* **2004**, *2*.
- (148) Rabiller, C.; Danho, D. *Helvetica Chimica Acta* **1984**, *67*, 1254-1273.
- (149) Banker, G.; Goslin, K. *Culturing Nerve Cells*; 2nd ed.; MIT Press: Cambridge, MA, 2002.
- (150) Woodward, R. B.; Kohman, T. P.; Harris, G. C. *J. Am. Chem. Soc.* **1941**, *63*, 120-124.
- (151) Peters, L.; Konig, G. M.; Terlau, H.; Wright, A. D. *J. Nat. Prod.* **2002**, *65*, 1633-1637.
- (152) Peters, L.; Konig, G. M.; Wright, A. D.; Pukall, R.; Stackebrandt, E.; Eberl, L.; Reidel, K. *J. Cell Biol.* **2003**, *69*, 3369-3475.
- (153) Ramamurthy, V.; Tustin, G.; Yau, C. C.; Liu, R. S. H. *Tetrahedron* **1975**, *31*, 193-199.

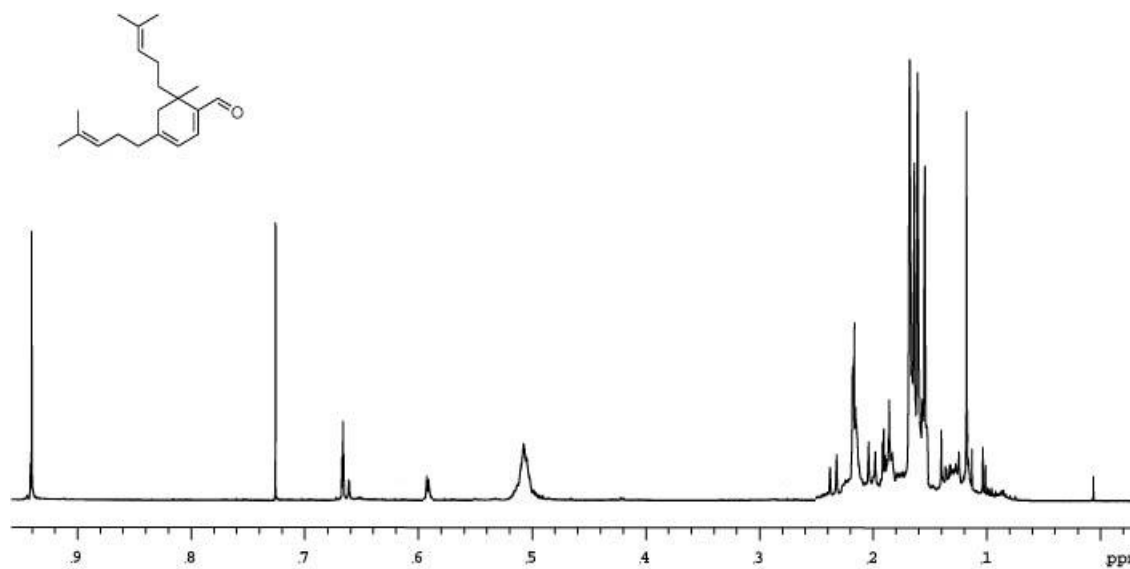
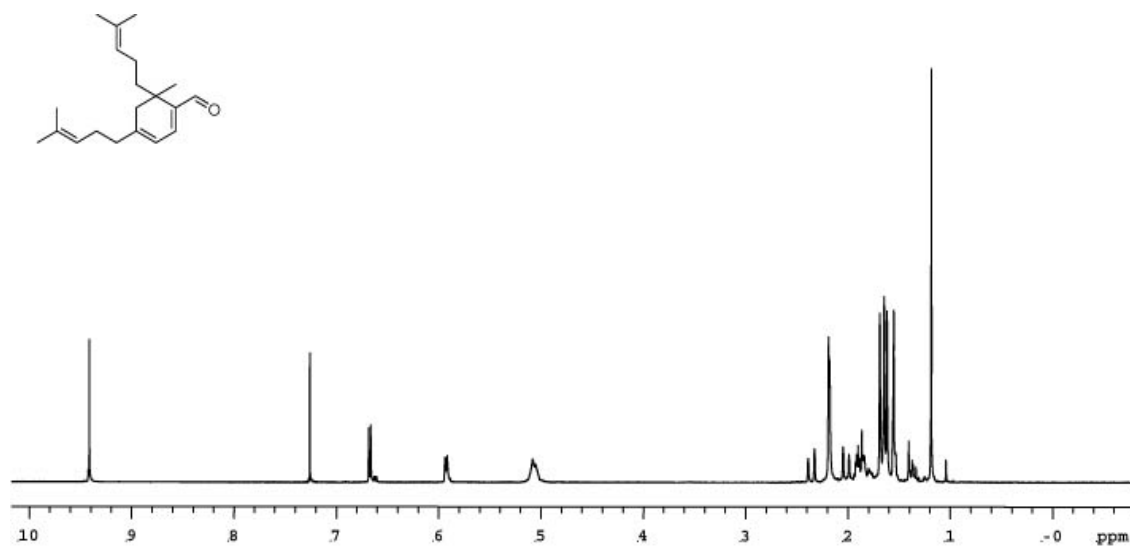
- (154) McFarland, J. W.; Conover, L. H.; Howes Jr., H. L.; Lynch, J. E.; Chisholm, D. R.; Austin, W. C.; Cornwell, R. L.; Danilewicz, J. C.; Courtney, W.; Morgan, D. H. *J. Med. Chem.* **1969**, *12*, 1066-1079.
- (155) Ouellet, S. G.; Tuttle, J. B.; MacMillan, D. W. C. *J. Am. Chem. Soc.* **2005**, *127*, 32.
- (156) Huang, Y.; Shi, L.; Li, B.; Ling, F. *Huaxue Xuebao* **1983**, *41*, 269-273.
- (157) Amann, A.; Vilhuber, H. G.; Kunze, J.; Giertz, H.; Frake, A. German Patent DE 2456958, 1975.
- (158) Lombardo, L. J.; Alessi, T. R. U.S. Patent 4895861, 1990.
- (159) Meyers, A. I.; Nabeya, A.; Adickes, H. W.; Politzer, I. R.; Malone, G. R.; Kovelesky, A. C.; Nolen, R. L.; Portnoy, R. C. *J. Org. Chem.* **1973**, *38*, 36-56.
- (160) Eberback, W.; Roser, J. *Tetrahedron Lett.* **1987**, *28*, 2685-2688.
- (161) Ramachandran, P. V.; Burghardt, T. E.; Reddy, M. V. R. *J. Org. Chem.* **2005**, *70*, 2329.
- (162) Ono, N.; Miyake, H.; Tanikaga, R.; Kaji, A. *J. Org. Chem.* **1982**, *47*, 5017-5019.
- (163) Syper, L. *J. Am. Chem. Soc.* **1987**, *43*, 2853-2871.
- (164) Anderson, P. L.; Brittain, D. A. German Patent 2439294, 1975.
- (165) Meyers, A. I.; Nabeya, A.; Adickes, H. W.; Fitzpatrick, J. M.; Malone, G. R.; Politzer, I. R. *J. Am. Chem. Soc.* **1969**, *91*, 764.
- (166) Asato, A. E.; Peng, A.; Hossain, M. Z.; Mirzadegan, T.; Bertram, J. S. *J. Med. Chem.* **1993**, *36*, 3137-3147.
- (167) Reddy, T. R. K.; Mutter, R.; Heal, W.; Guo, K.; Gillet, V. J.; Pratt, S.; Chen, B. *J. Med. Chem.* **2006**, *49*, 607-615.
- (168) Rhys Williams, A. T.; Winfield, S. A. *Analyst* **1983**, *108*, 1067-1071.
- (169) Okuyama, M.; Laman, H.; Kingsbury, S. R.; Visintin, C.; Leo, E.; Eward, K. L.; Stoeber, K.; Boshoff, C.; Williams, G. H.; Selwood, D. L. *Nat. Methods* **2007**, *4*, 153-159.
- (170) Gaussian 03, R. C.; Frisch, M. J.; Trucks, G. W.; Schlegel, H. B.; Scuseria, G. E.; Robb, M. A.; Cheeseman, J. R.; Montgomery, J., J. A.; Vreven, T.; Kudin, K. N.; Burant, J. C.; Millam, J. M.; Iyengar, S. S.; Tomasi, J.; Barone, V.; Mennucci,

- B.; Cossi, M.; Scalmani, G.; Rega, N.; Petersson, G. A.; Nakatsuji, H.; Hada, M.; Ehara, M.; Toyota, K.; Fukuda, R.; Hasegawa, J.; Ishida, M.; Nakajima, T.; Honda, Y.; Kitao, O.; Nakai, H.; Klene, M.; Li, X.; Knox, J. E.; Hratchian, H. P.; Cross, J. B.; Bakken, V.; Adamo, C.; Jaramillo, J.; Gomperts, R.; Stratmann, R. E.; Yazyev, O.; Austin, A. J.; Cammi, R.; Pomelli, C.; Ochterski, J. W.; Ayala, P. Y.; Morokuma, K.; Voth, G. A.; Salvador, P.; Dannenberg, J. J.; Zakrzewski, V. G.; Dapprich, S.; Daniels, A. D.; Strain, M. C.; Farkas, O.; Malick, D. K.; Rabuck, A. D.; Raghavachari, K.; Foresman, J. B.; Ortiz, J. V.; Cui, Q.; Baboul, A. G.; Clifford, S.; Cioslowski, J.; Stefanov, B. B.; Liu, G.; Liashenko, A.; Piskorz, P.; Komaromi, I.; Martin, R. L.; Fox, D. J.; Keith, T.; Al-Laham, M. A.; Peng, C. Y.; Nanayakkara, A.; Challacombe, M.; Gill, P. M. W.; Johnson, B.; Chen, W.; Wong, M. W.; Gonzalez, C.; and Pople, J. A.; Gaussian, Inc.: Wallingford, CT, 2004.
- (171) Parr, R. G.; Yang, W. *Density-Functional Theory of Atoms and Molecules*; Oxford University Press: Oxford, 1989.
- (172) Becke, A. J. *Chem. Phys.* **1993**, 98, 5648.
- (173) Lee, C.; Yang, W.; Parr, R. G. *Phys. Rev.* **1988**, 37, 785.
- (174) Foresman, J. B.; Frisch, A. E. *Exploring Chemistry with Electronic Structure Methods*; Gaussian Inc.: Pittsburgh, PA, 1996.
- (175) Hariharan, P. C.; Pople, J. A. *Theoret. Chimica Acta* **1973**, 28, 213.
- (176) Krishnan, R.; Binkley, J. S.; Seeger, R.; Pople, J. A. *J. Chem. Phys.* **1980**, 72, 650.
- (177) Spitznagel, G. W.; Clark, T.; Schleyer, P. V. R.; Hehre, W. J. *Comput. Chem.* **1987**, 8, 1109-1116.
- (178) Wolinski, K.; Hilton, J. F.; Pulay, P. *J. Am. Chem. Soc.* **1990**, 112, 8251.
- (179) Helgaker, T.; Watson, M.; Handy, N. C. *J. Chem. Phys.* **2000**, 113, 9402.
- (180) Albert, A.; Katritzky, A. R. In *Advances in Heterocyclic Chemistry*; Vol. 32, Academic Press: New York, NY, 1982, p 1-81.
- (181) Blaha, K.; Cervinka, O. *Adv. Org. Chem.* **1963**, 4, 1.
- (182) Erian, A. W. *Chem. Rev.* **1993**, 93, 1991-2005.
- (183) Hickmott, P. W. *Tetrahedron* **1982**, 38, 1975-2050.

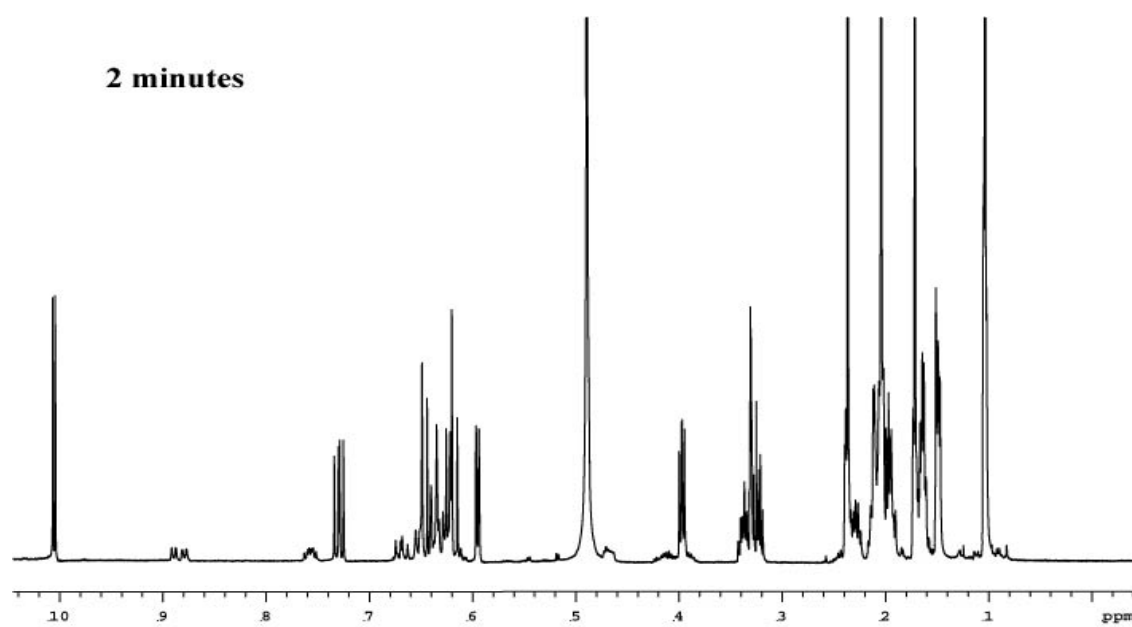
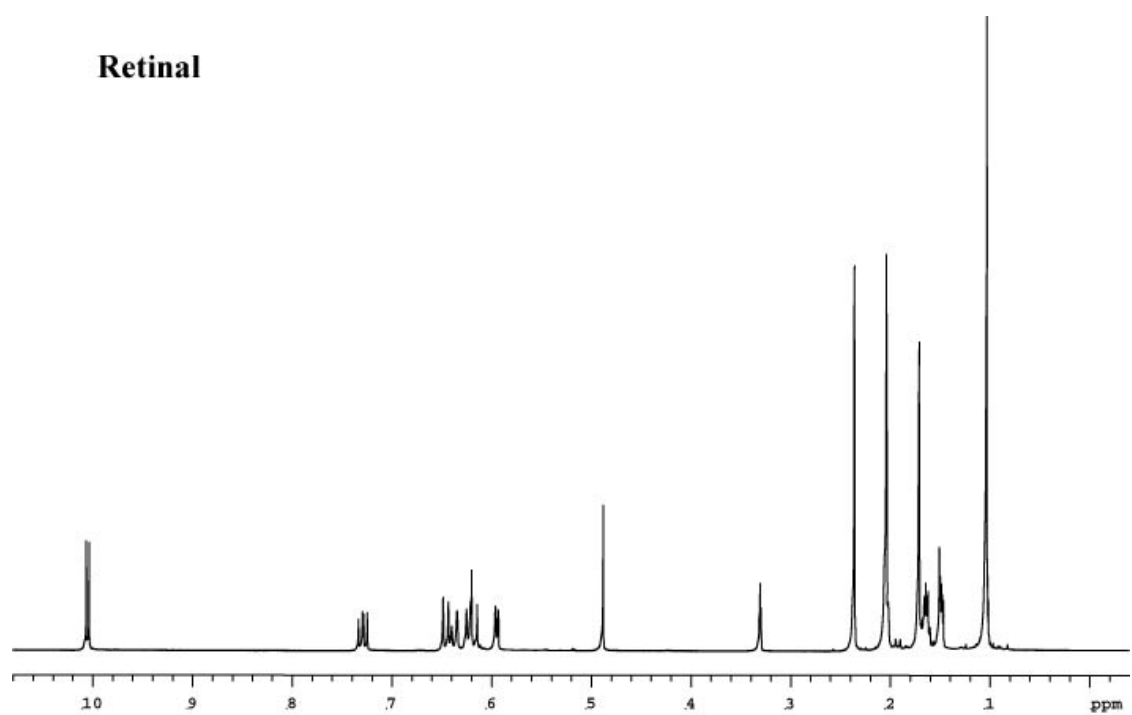
- (184) Wamhoff, H. *Adv. Heterocycl. Chem.* **1985**, 32, 1.
- (185) Prusiner, S. B. *Proc. Natl. Acad. Sci. U. S. A.* **1998**, 95, 13363.
- (186) Anderson, R. M.; Donnelly, C. A.; Ferguson, N. M.; Woolhouse, M. E. J.; Watt, C. J.; Udy, H. J.; MaWhinney, S.; Dunstan, S. P.; Southwood, T. R. E.; Wilesmith, J. W.; Ryan, J. B. M.; Hoinville, L. J.; Hillerton, J. E.; Austin, A. R.; Wells, G. A. H. *Nature* **1996**, 382, 779-788.
- (187) Collinge, J.; Sidle, K. C. L.; Meads, J.; Ironside, J.; Hill, A. F. *Nature* **1996**, 383, 685-690.
- (188) Will, R. G.; Ironside, J. W.; Zeidler, M.; Cousens, S. N.; Estibeiro, K.; Alperovitch, A.; Poser, S.; Pocchiari, M.; Hofman, A.; Smith, P. G. *Lancet* **1996**, 347, 921-925.
- (189) Weissmann, C.; Aguzzi, A. *Annu. Rev. Med.* **2005**, 56, 321-344.
- (190) Reddy, T. R. K.; Mutter, R.; Heal, W.; Guo, K.; Gillet, V. J.; Pratt, S.; Chen, B. *J. Med. Chem.* **2006**, 49, 607-615.
- (191) Tucker, H.; Golding, G.; Purvis, S. R. *Tetrahedron Lett.* **1981**, 22, 1373-1376.
- (192) Mlrek, J. A., M.; Mokrosz, M. *Synthesis* **1980**, 296.
- (193) Shabtai, J.; Ney-Igner, E.; Pines, H. *J. Chem. Soc., Perkin I* **1973**, 2230.
- (194) Asato, A. E.; Watanabe, C.; Li, X. Y.; Liu, R. S. H. *Tetrahedron Lett.* **1992**, 33, 3105-3108.
- (195) Ashton, W. T.; Walker, F. C.; Hynes, J. B. *J. Med. Chem.* **1973**, 16, 694-697.
- (196) Chern, J. W.; Tao, P. L.; Yen, M. H.; Lu, G. Y.; Shiau, C. Y.; Lai, Y. J.; Chien, S. L.; Chan, C. H. *J. Med. Chem.* **1993**, 36, 2196-2207.
- (197) Jen, T.; Dienel, B.; Bowman, H.; Petta, J.; Helt, A.; Loev, B. *J. Med. Chem.* **1972**, 15, 727-731.
- (198) Campbell, S. F.; Davey, M. J.; Hardstone, J. D.; Lewis, B. N.; Palmer, M. J. *J. Med. Chem.* **1987**, 30, 49-57.
- (199) Civantos Calzada, B.; Aleixandre de Artiñano, A. *Pharmacol. Res.* **2001**, 44, 195-208.
- (200) Docherty, J. R. *Pharmacol. Ther.* **1989**, 44, 241-284.

- (201) Katagiri, K.; Yoshida, T.; Sato, K. *Quinoxaline Antibiotics. Antibiotics: Mechanism of Action of Antimicrobial and Antitumor Agents*; Springer-Verlag: Heidelberg, 1975.
- (202) Waring, M. J.; Fox, K. R. *Molecular Aspects of Anti-cancer Drug Action*; Macmillan: New York, 1993.
- (203) Boger, D. L.; Ichikawa, S.; Tse, W. C.; Hedrick, M. P.; Jin, Q. J. *J. Am. Chem. Soc.* **2001**, *123*, 561-568.
- (204) Dell, A.; Williams, D. H.; Morris, H. R.; Smith, G. A.; Feeney, J.; Roberts, G. C. K. *J. Am. Chem. Soc.* **1975**, *97*, 2497-2502.
- (205) Phillips, D. R.; White, R. J.; Trist, H.; Cullinane, C.; Dean, D.; Crothers, D. M. *Anticancer Drug Res.* **1990**, *5*, 21-29.
- (206) May, L. G.; Madine, M. A.; Waring, M. J. *Nucleic Acids Res.* **2004**, *32*, 65-72.
- (207) Cuesta-Seijo, J. A.; Sheldrick, G. M. *Acta Crystallogr.* **2005**, *D61*, 442-448.
- (208) Ughetto, G.; Wang, A. H.; Quigley, G. J.; van der Marel, G. A.; van Boom, J. H.; Rich, A. *Nucleic Acids Res.* **1985**, *13*, 2305-2323.
- (209) Van Dyke, M. M.; B., D. P. *Science* **1984**, *225*, 653-657.
- (210) Waring, M. J.; Wakelin, L. P. G. *Nature* **1974**, *252*, 653-657.
- (211) Bench, B. J.; Liu, C. M.; Evett, C. R.; Watanabe, C. M. H. *Journal of Organic Chemistry* **2006**, *71*, 9458-9463.
- (212) Bench, B. J.; Tichy, S. E.; Perez, L. M.; Benson, J.; Watanabe, C. M. H. *Bioorg. Med. Chem.* **2008**.
- (213) Valla, A.; Andriamialisoa, Z.; Labia, R. *Tetrahedron Lett.* **2000**, *41*, 3359.

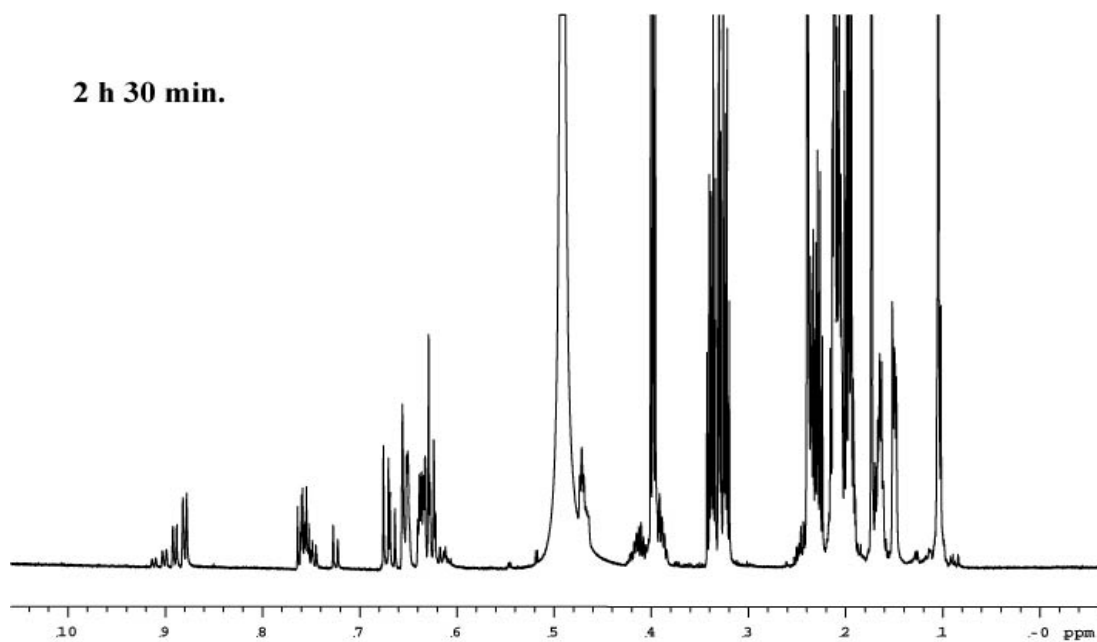
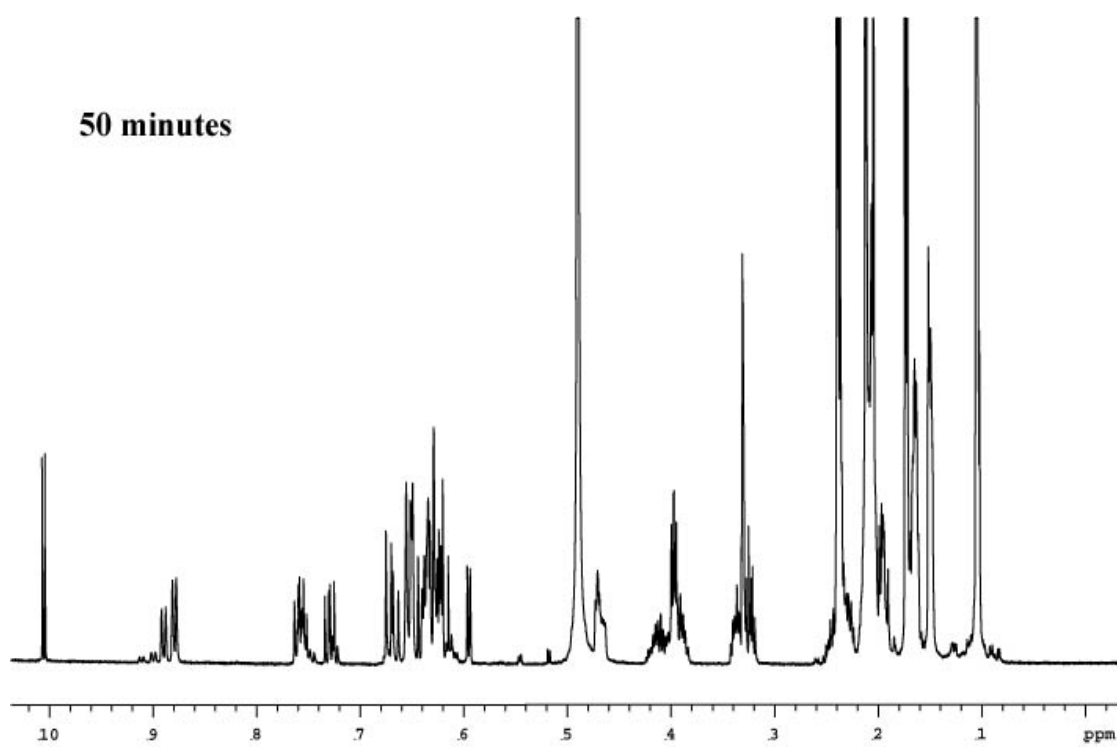
## APPENDIX A



**A-1.** <sup>1</sup>H-NMR spectra of natural cyclocitral (top) and deuterated cyclocitral.

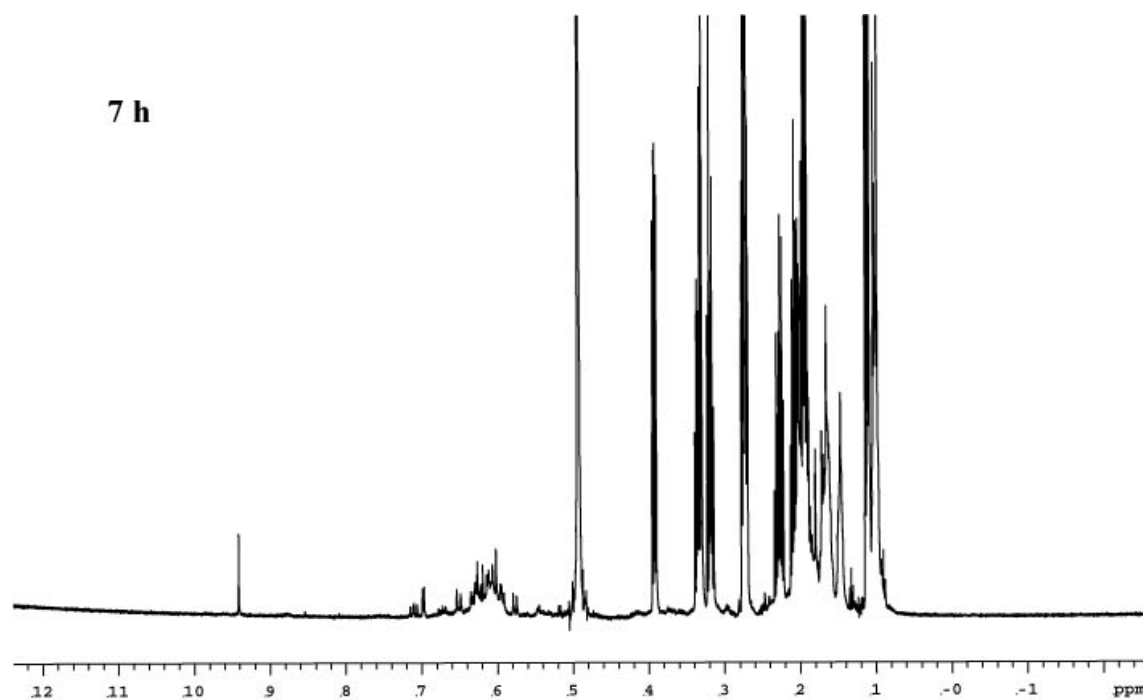
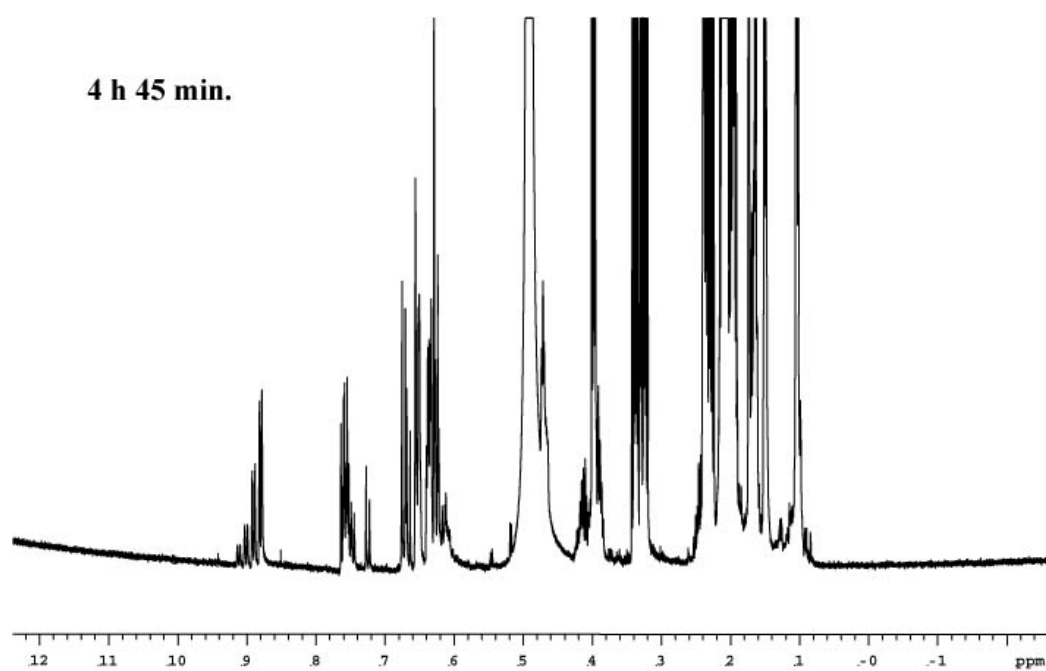


**A-2.** Full <sup>1</sup>H-NMR spectra at various time points for all-trans retinal self-condensation.

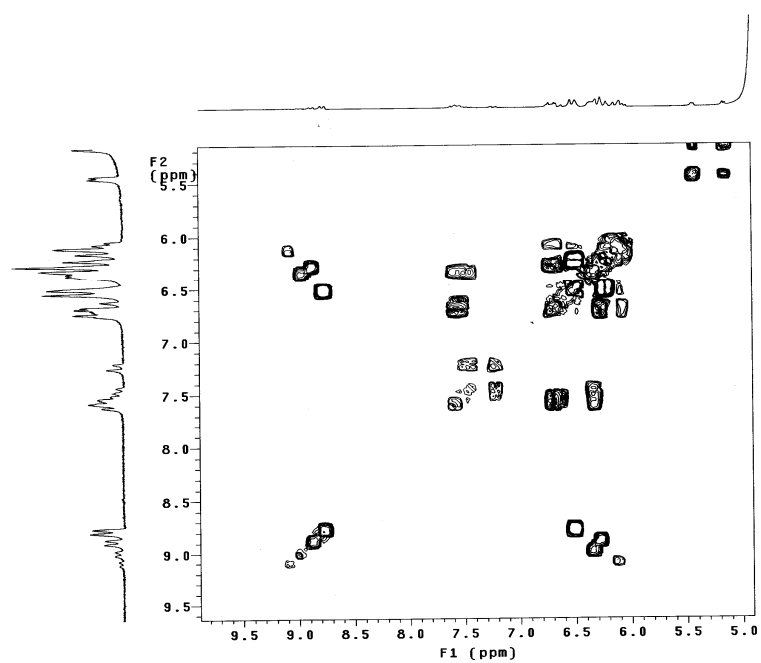
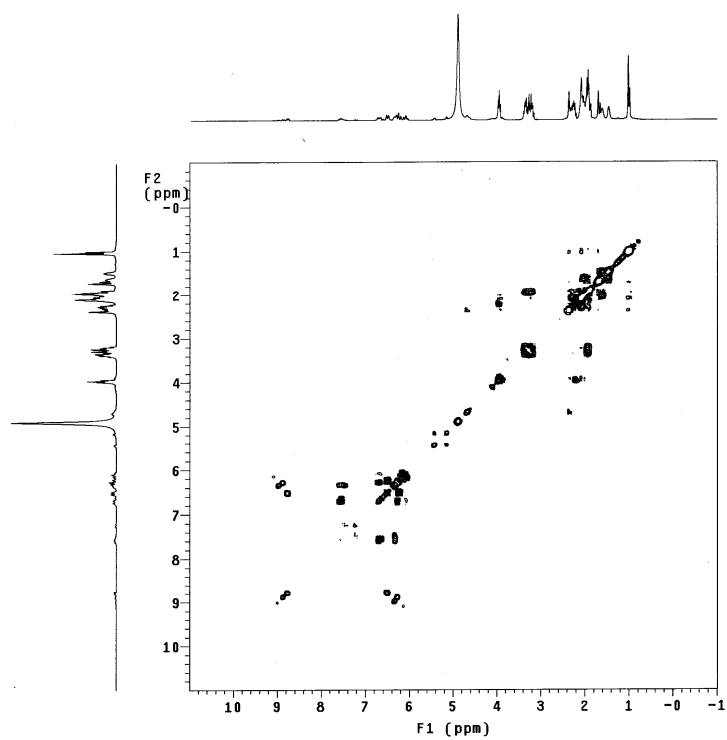


**A-2.** Continued.





A-2. Continued.



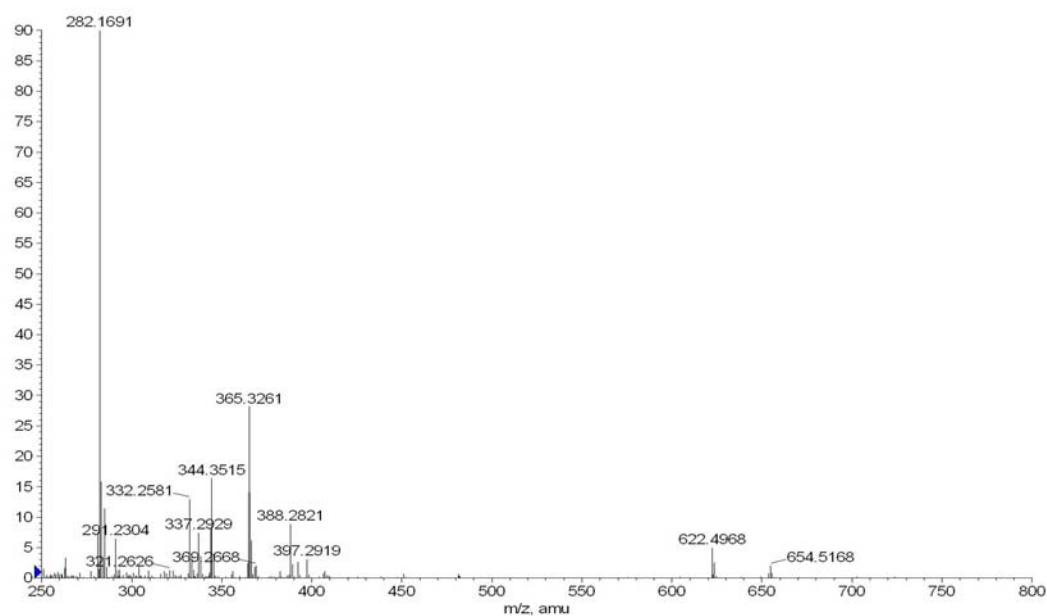
A-3.  $^1\text{H}$ ,  $^1\text{H}$ -COSY spectra of retinal reaction.

Full spectra on top with blow up of region of interest on bottom.

30 minutes

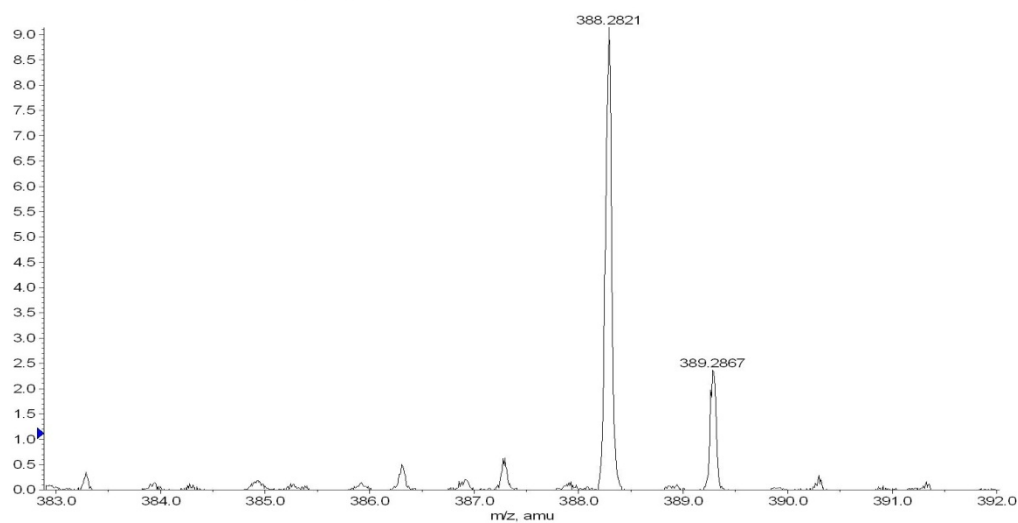
+TOF MS: 1.284 to 4.217 min from Sample 2 (30min 2) of 06230607.wiff  
a=3.55295067960074790e-004, t0=4.80865773630612240e+001

Max: 90.0 counts.



+TOF MS: 1.567 to 4.184 min from Sample 2 (30min 2) of 06230607.wiff  
a=3.55295067960074790e-004, t0=4.80865773630612240e+001

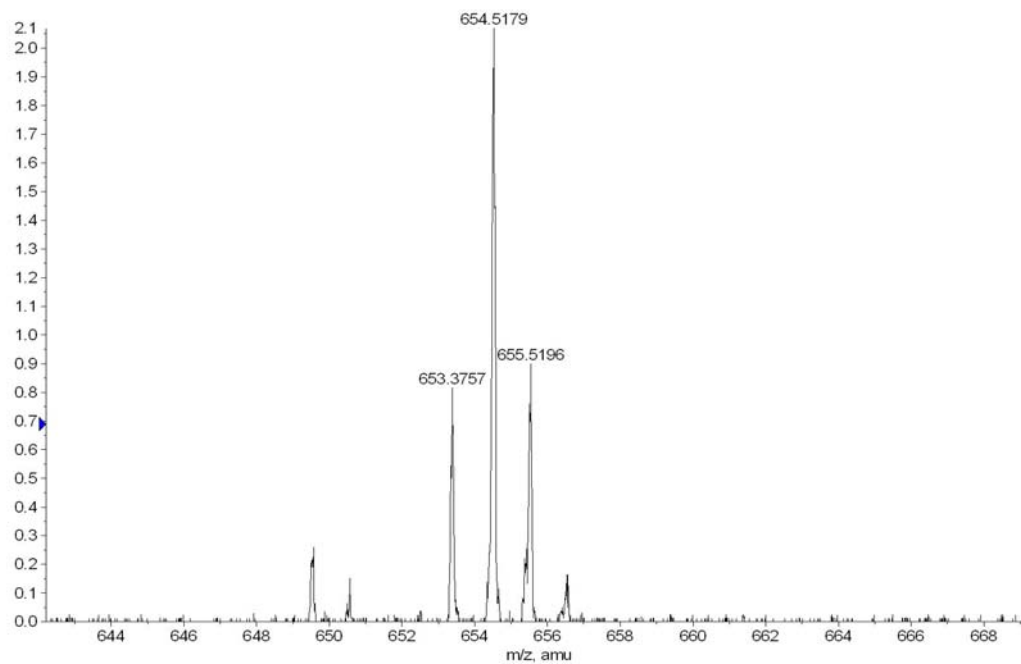
Max: 91.4 counts.



**A-4. Mass spectra correlating to NMR results for Schiff base formation and intermediate for *all-trans* retinal.**

+TOF MS: 1.567 to 4.184 min from Sample 2 (30min 2) of 06230607.wiff  
a=3.55295067960074790e-004, t0=4.80865773630612240e+001

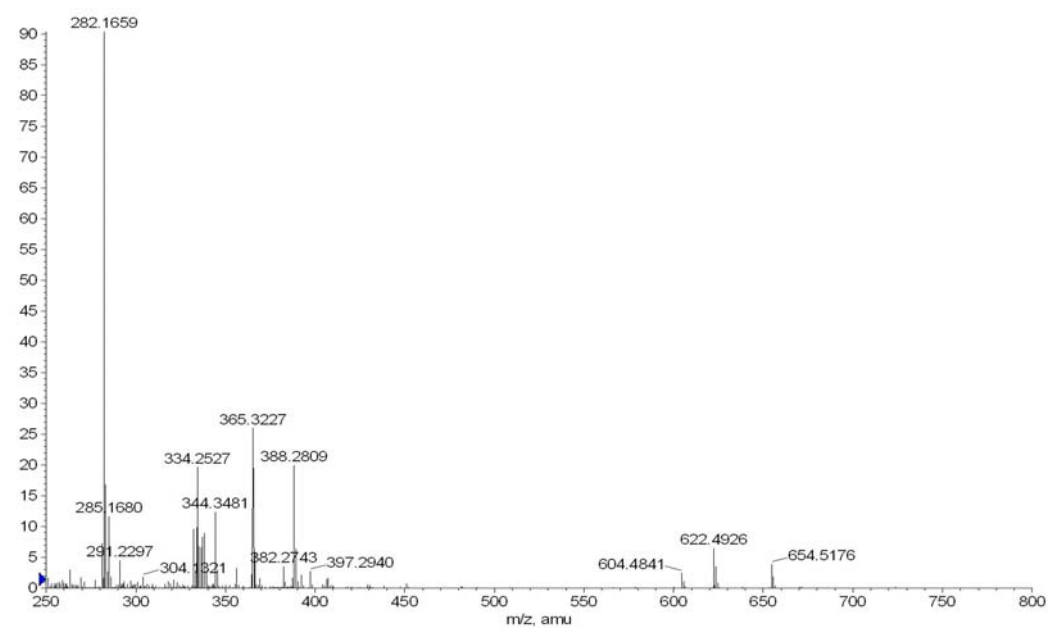
Max. 91.4 counts.



1 hour 30 minutes

+TOF MS: 1.450 to 3.200 min from 06230608.wiff  
a=3.55295067960074790e-004, t0=4.80865773630612240e+001

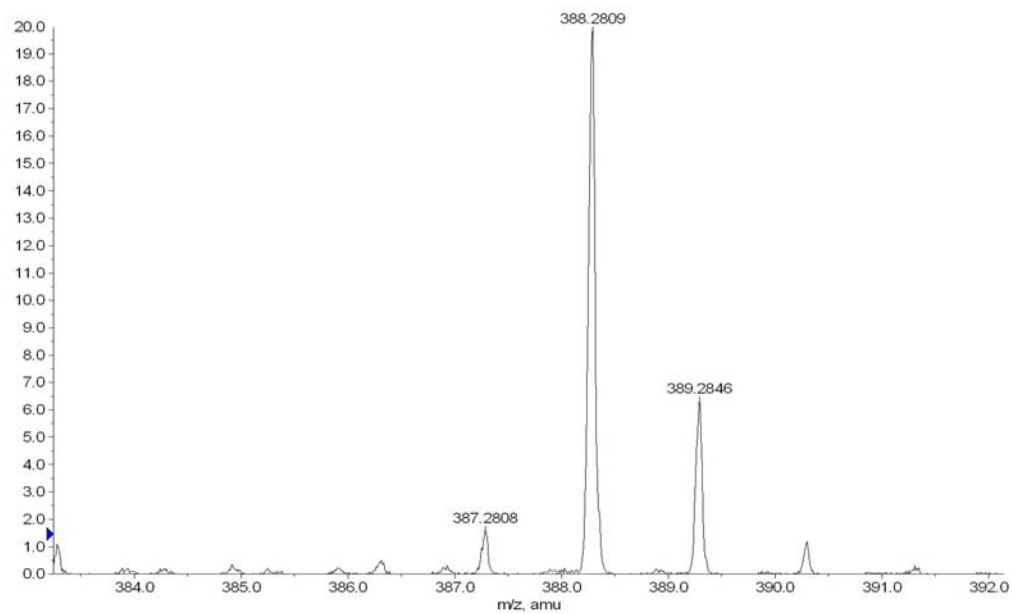
Max. 90.4 counts.



A-4. Continued.

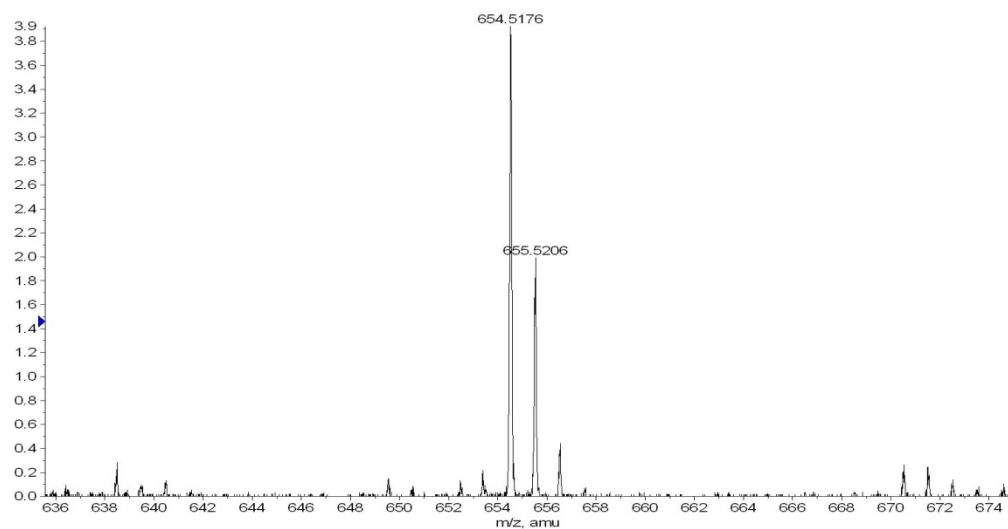
+TOF MS: 1.450 to 3.200 min from 06230608.wiff  
a=3.55295067960074790e-004, t0=4.80865773630612240e+001

Max. 90.4 counts.



+TOF MS: 1.450 to 3.200 min from 06230608.wiff  
a=3.55295067960074790e-004, t0=4.80865773630612240e+001

Max. 90.4 counts.

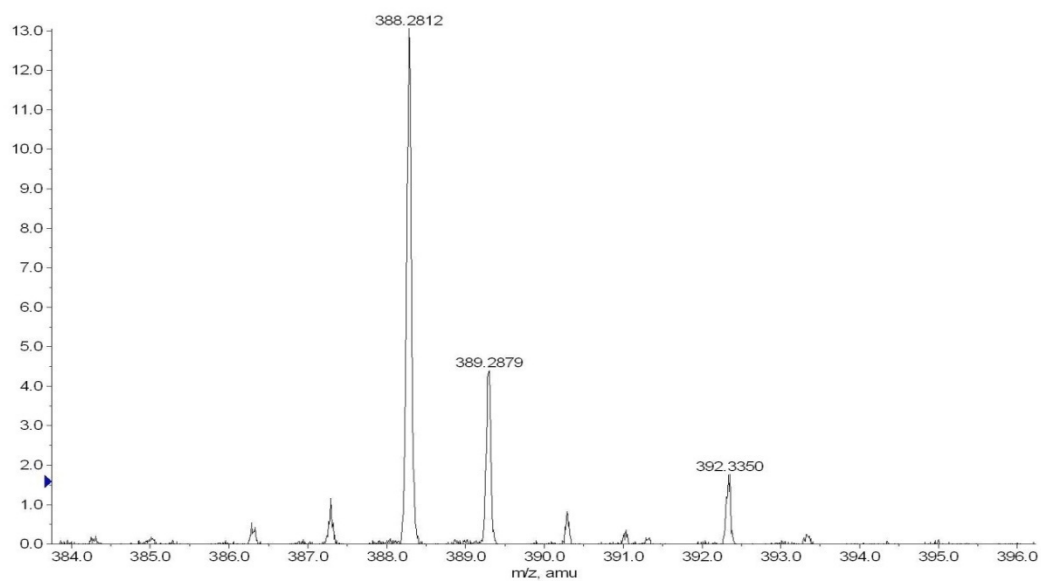
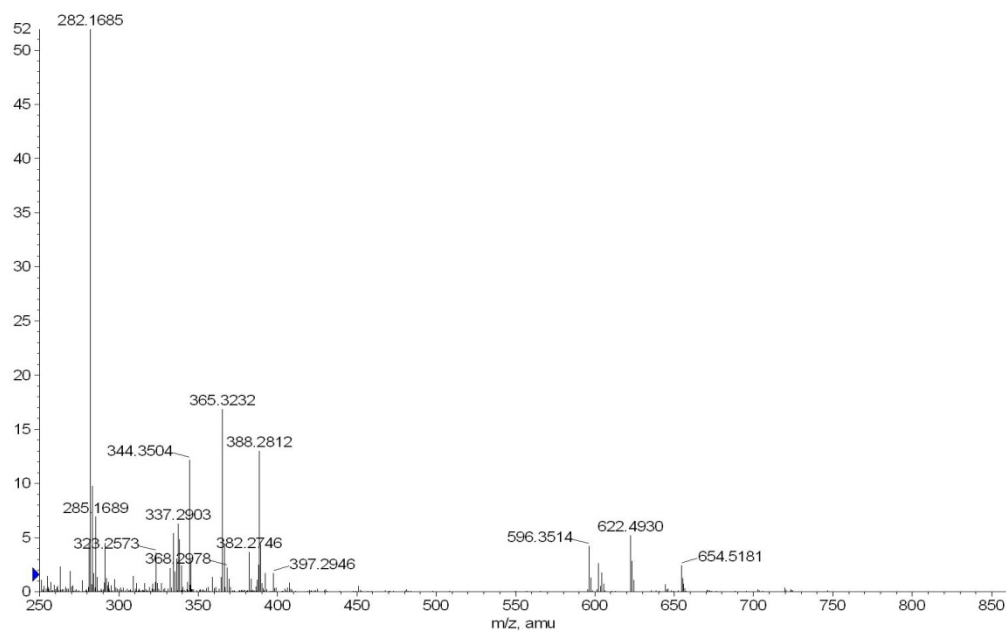


A-4. Continued.

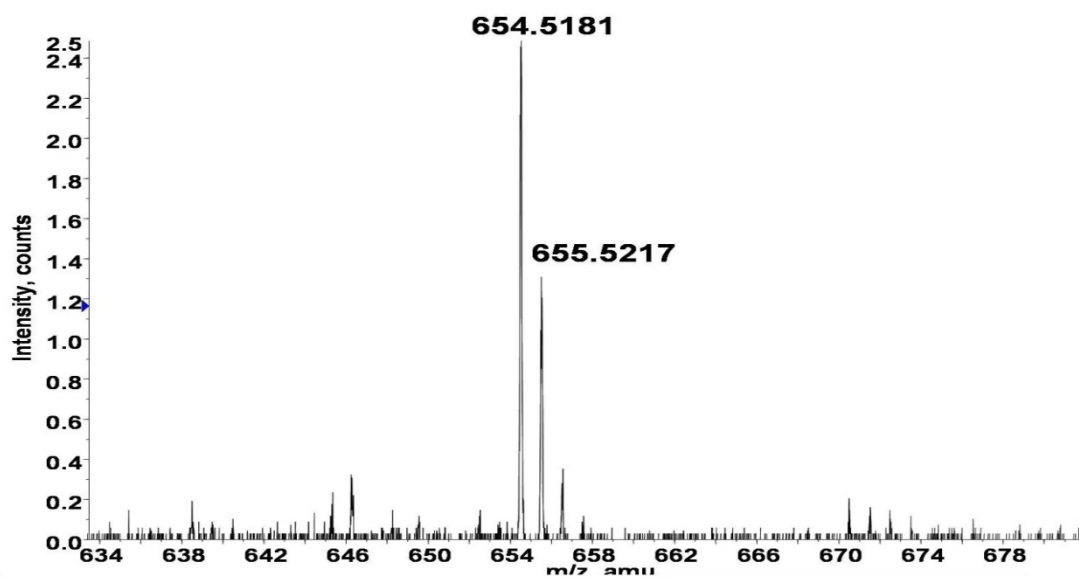
2 hours 30 minutes

+TOF MS: 0.233 to 1.350 min from 06230611.wiff  
a=3.55295067960074790e-004, t0=4.80865773630612240e+001

Max. 52.0 counts.



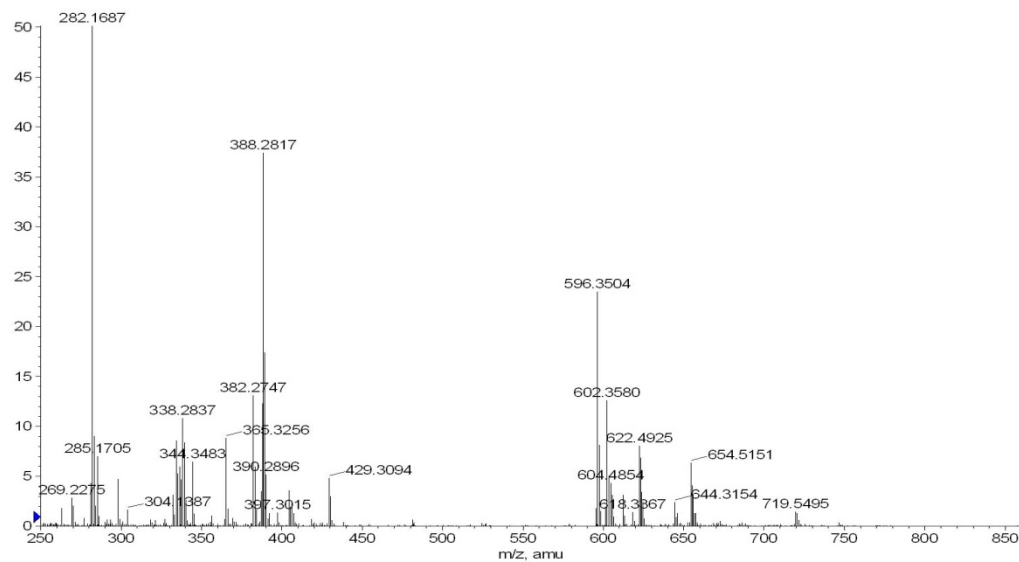
A-4. Continued.



4 hours 30 minutes

+TOF MS: 0.433 to 1.267 min from 06230610.wiff  
a=3.55295067960074790e-004, t0=4.80865773630612240e+001

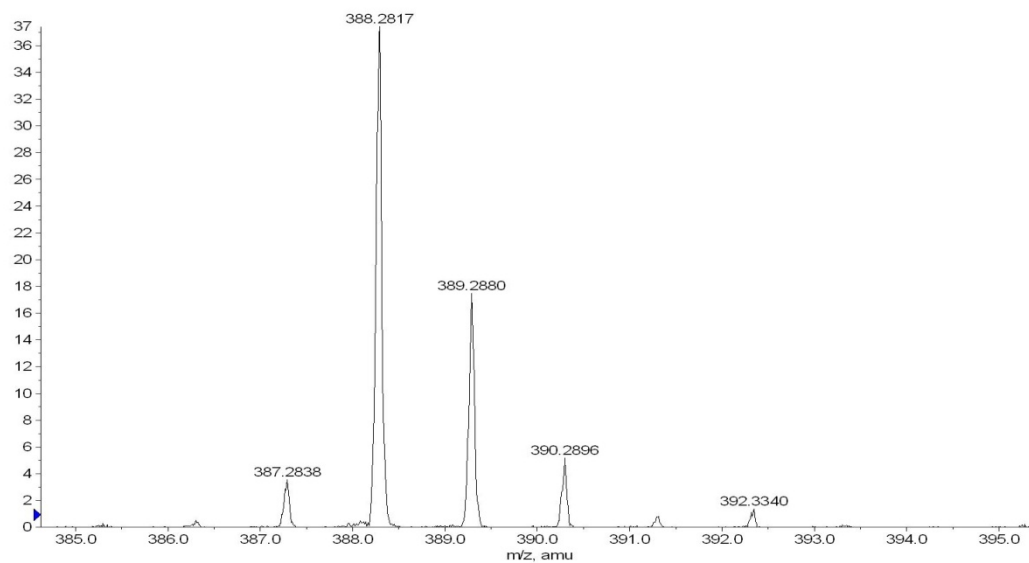
Max. 50.2 counts.



A-4. Continued.

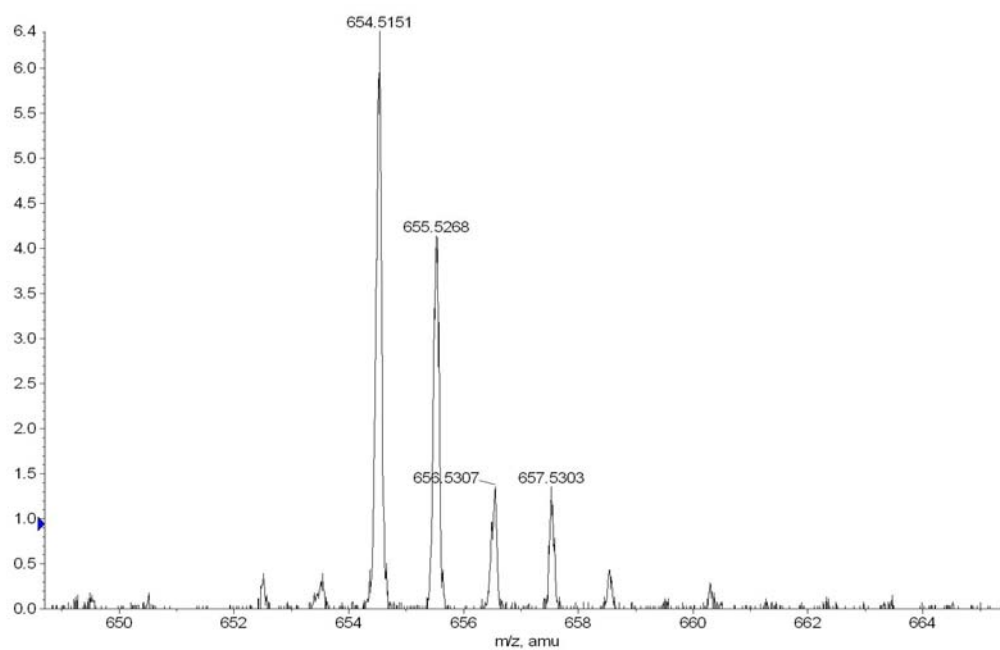
+TOF MS: 0.433 to 1.267 min from 06230610.wiff  
a=3.55295067960074790e-004, t0=4.80865773630612240e+001

Max. 50.2 counts.



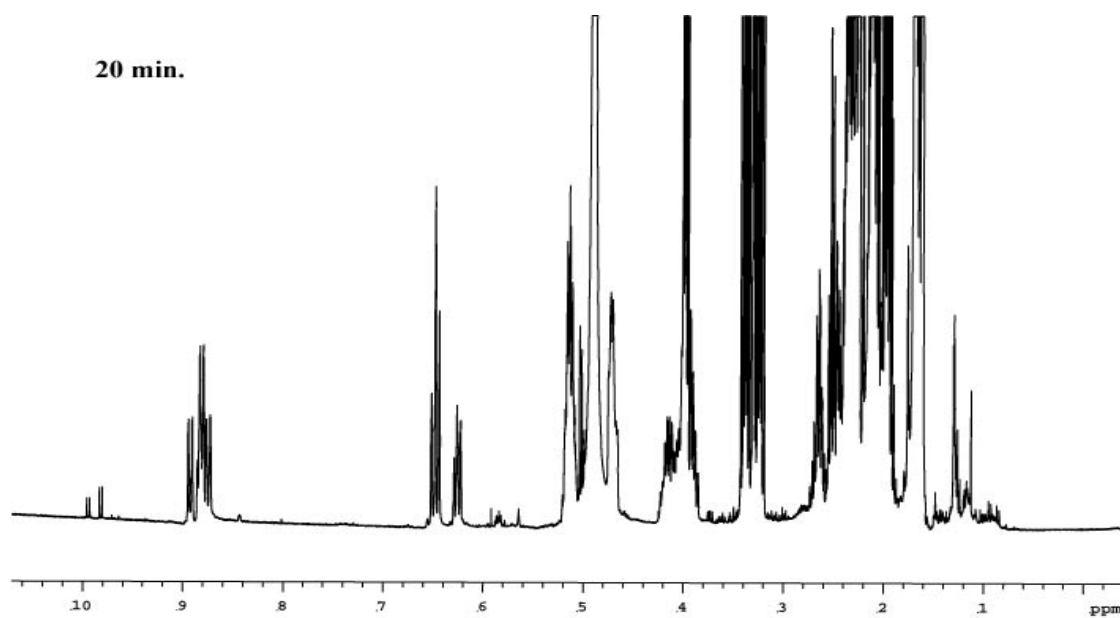
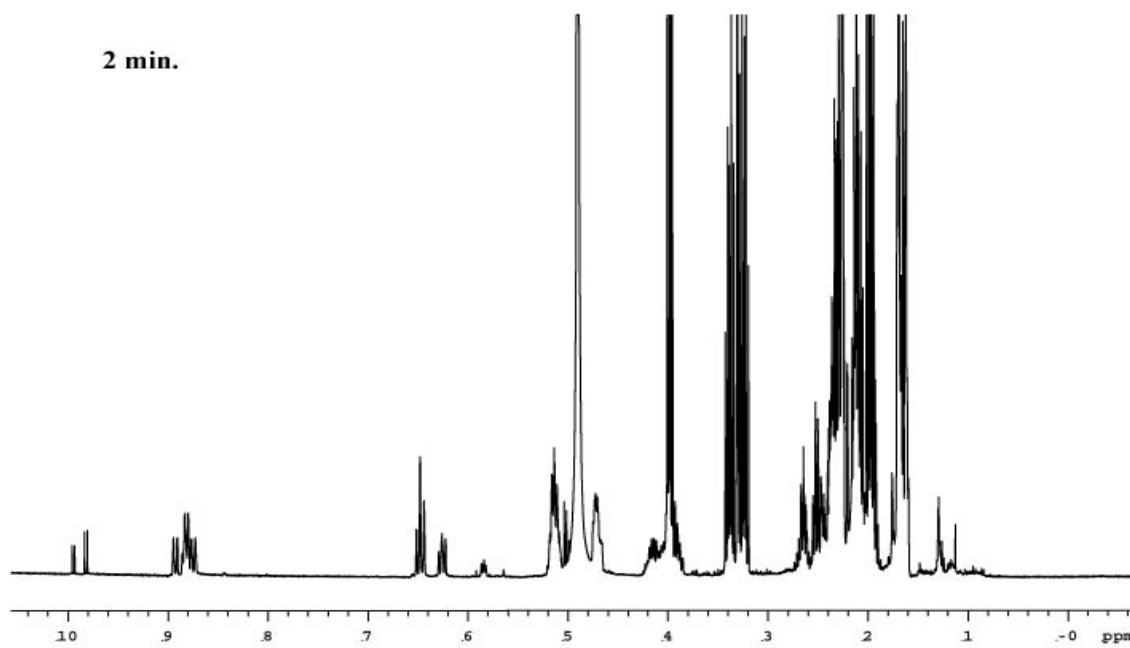
+TOF MS: 0.433 to 1.267 min from 06230610.wiff  
a=3.55295067960074790e-004, t0=4.80865773630612240e+001

Max. 50.2 counts.

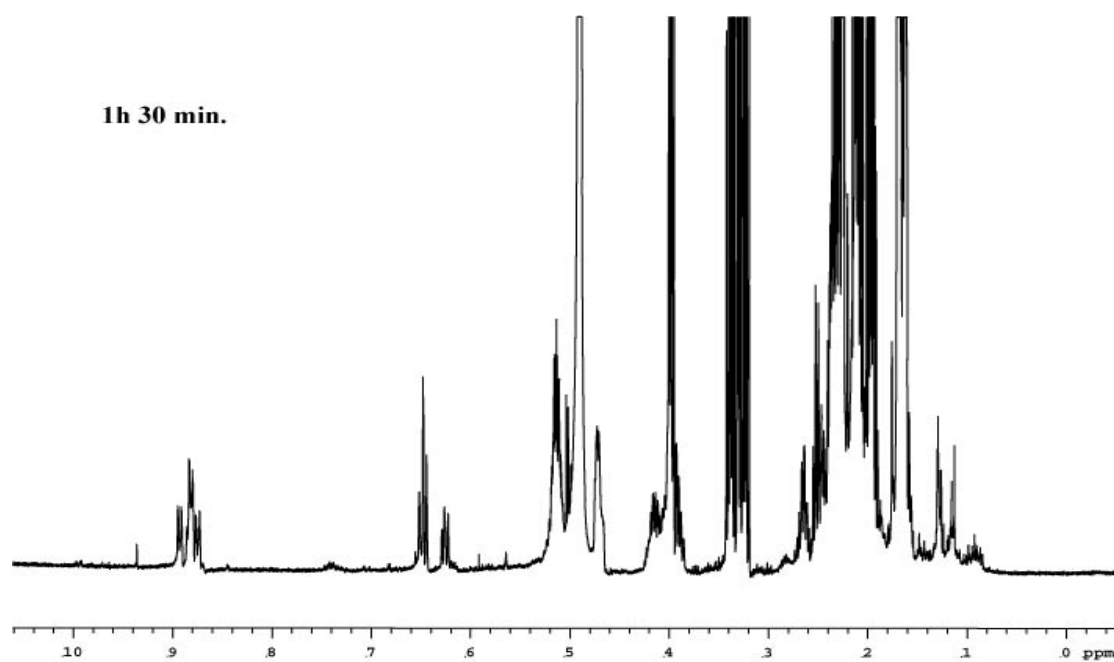
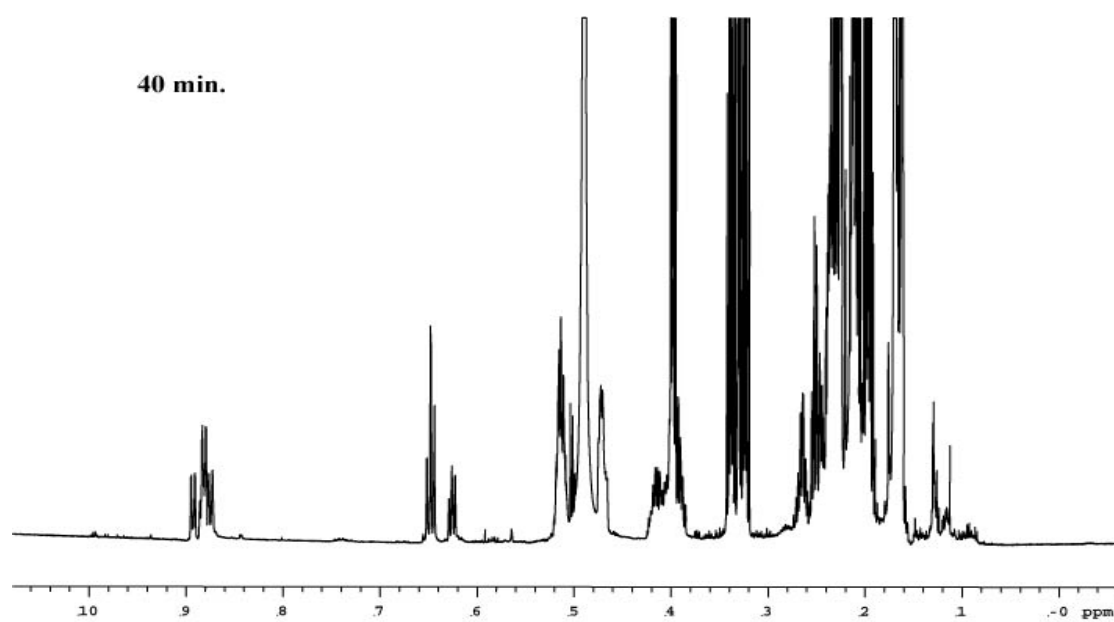


A-4. Continued.

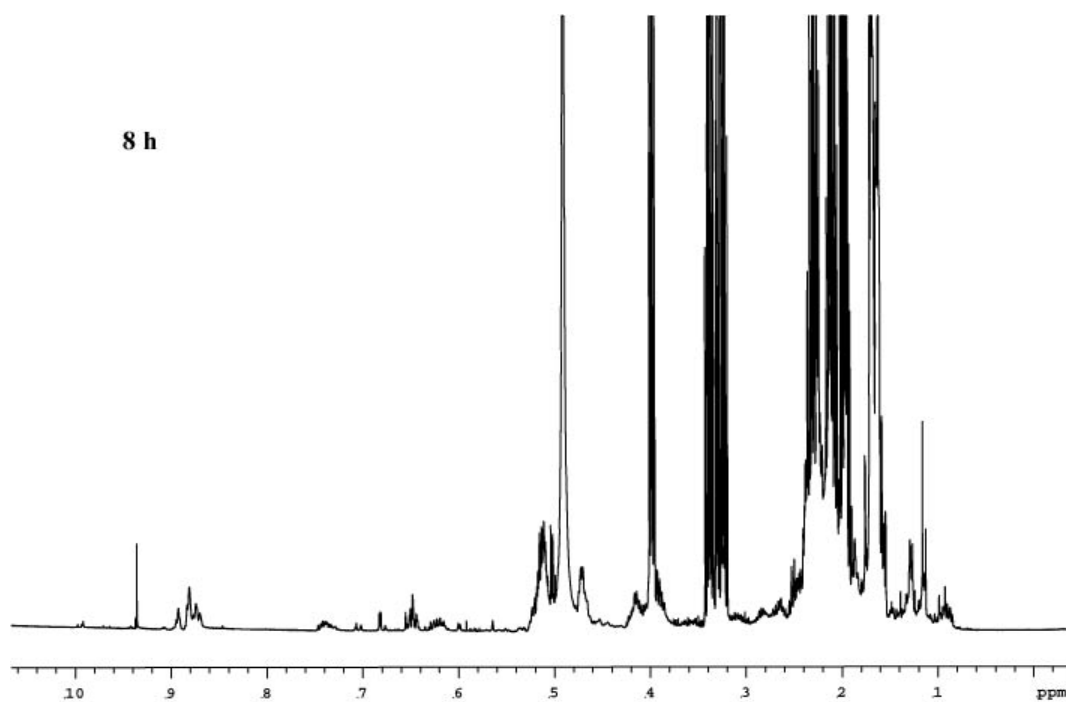
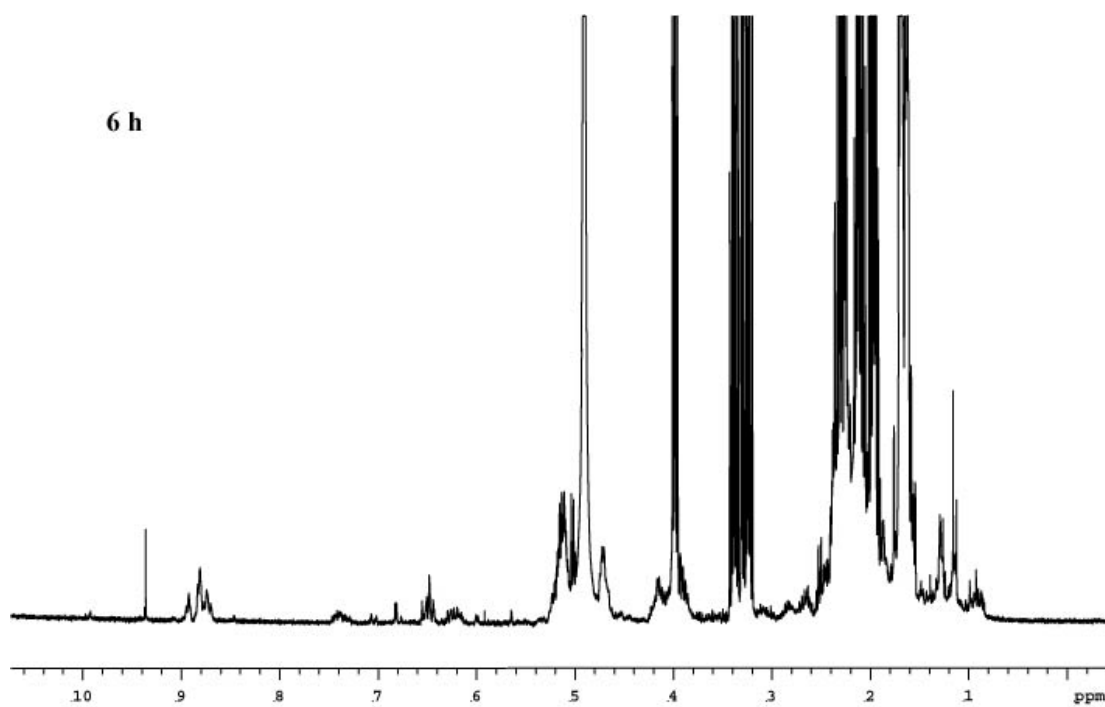




**A-5. Full <sup>1</sup>H-NMR spectra at various time points for citral self-condensation.**



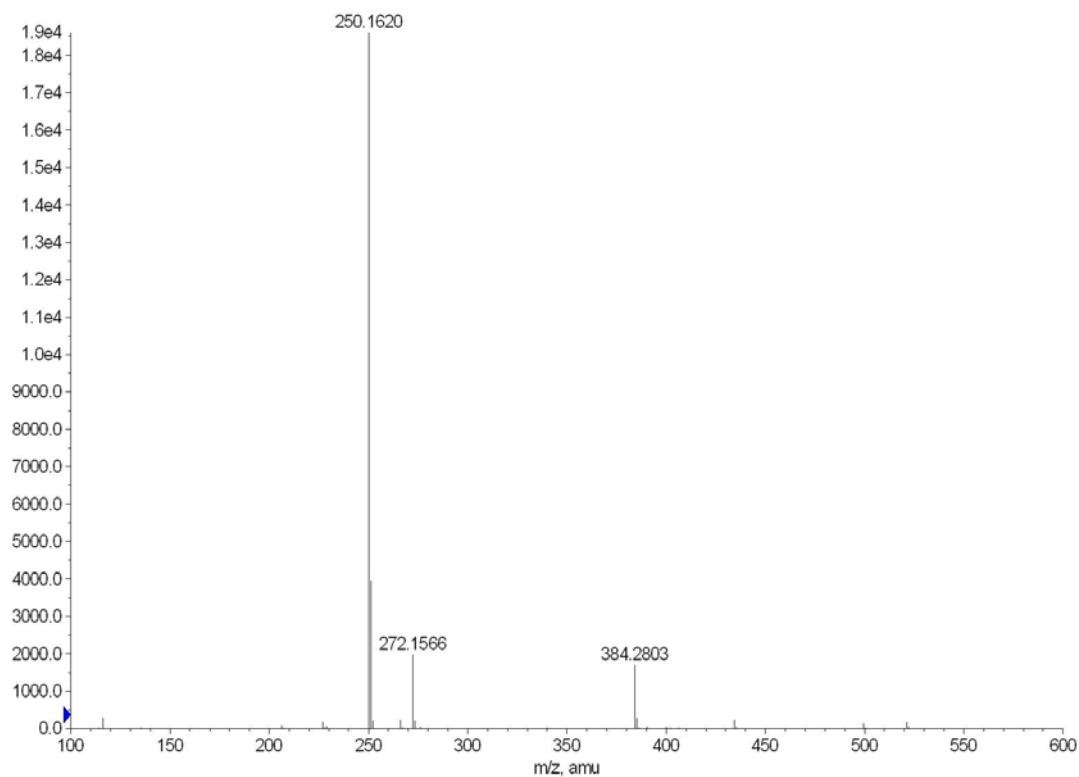
**A-5. Continued.**



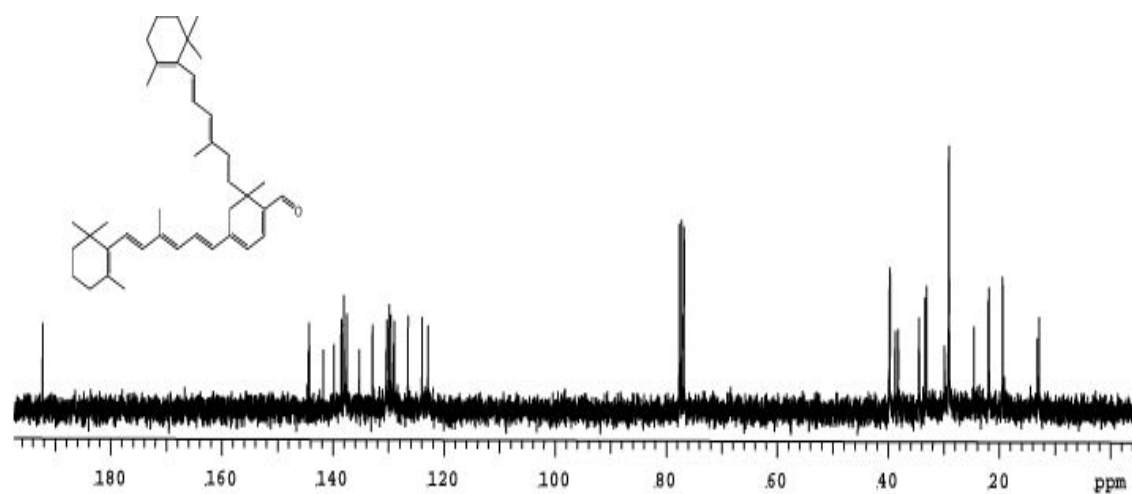
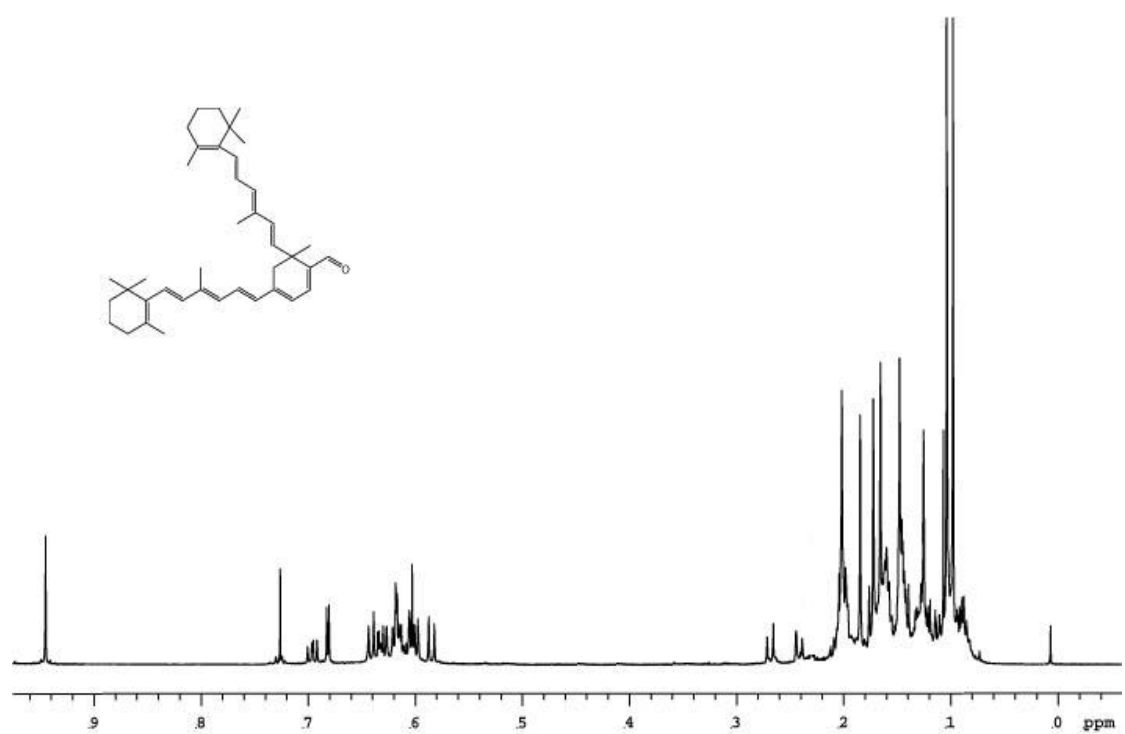
**A-5. Continued.**

+TOF MS: 4 MCA scans from 07180501.wiff  
a=3.55277723787620200e-004, t0=4.49306427987430650e+001

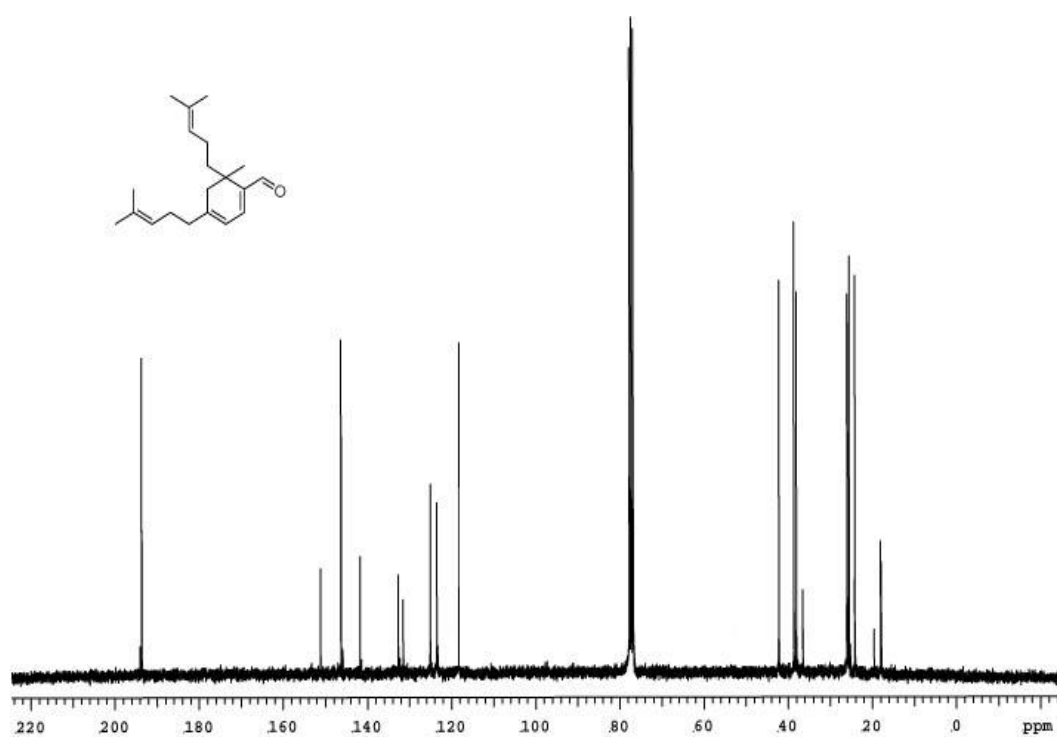
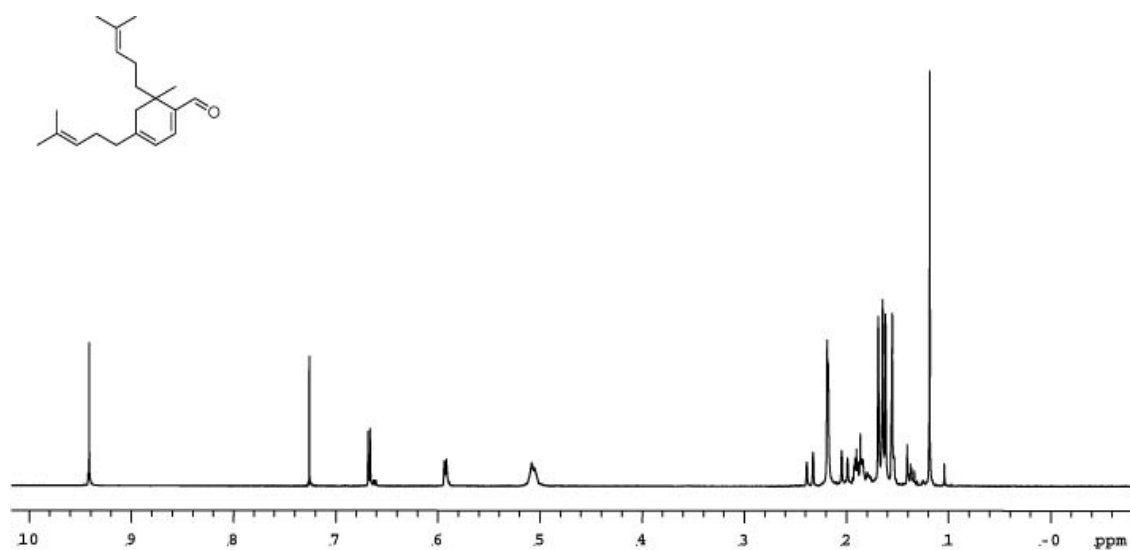
Max. 1.9e4 counts.



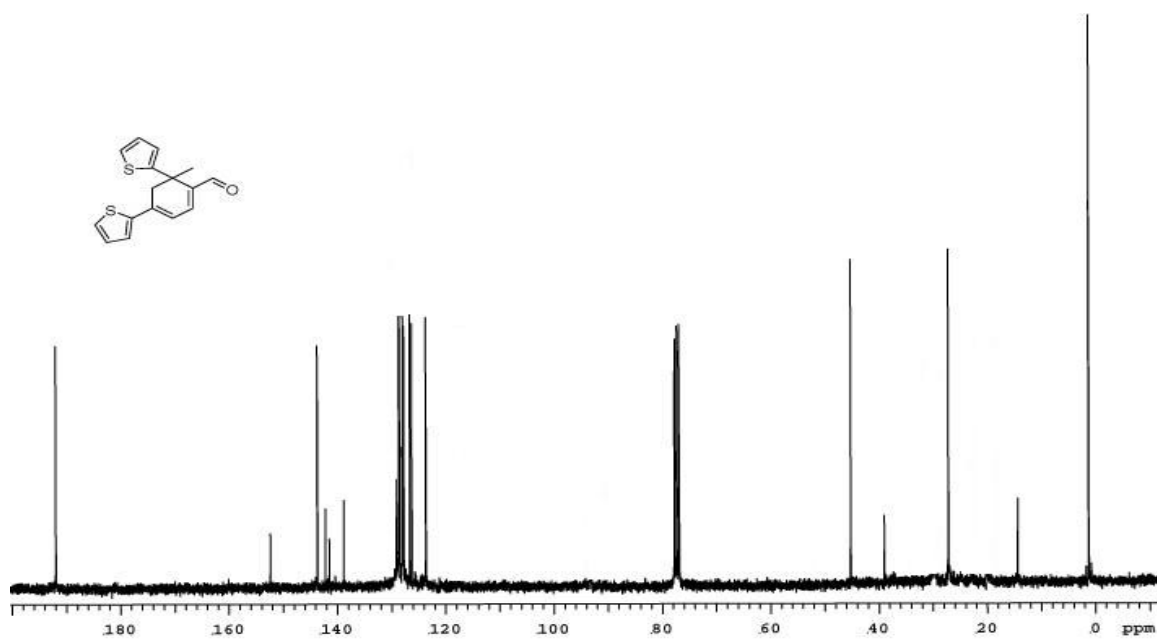
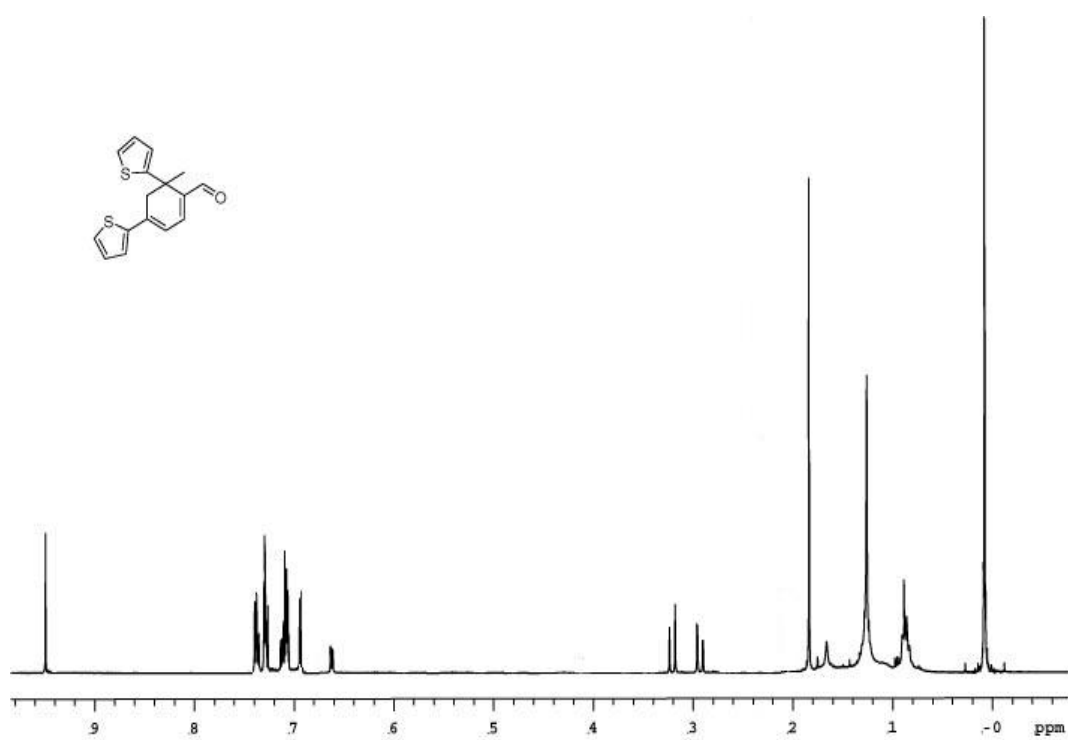
**A-6.** Mass spectra correlating to NMR results for Schiff base 57 and intermediate 59 for formation of cyclocitral from citral.



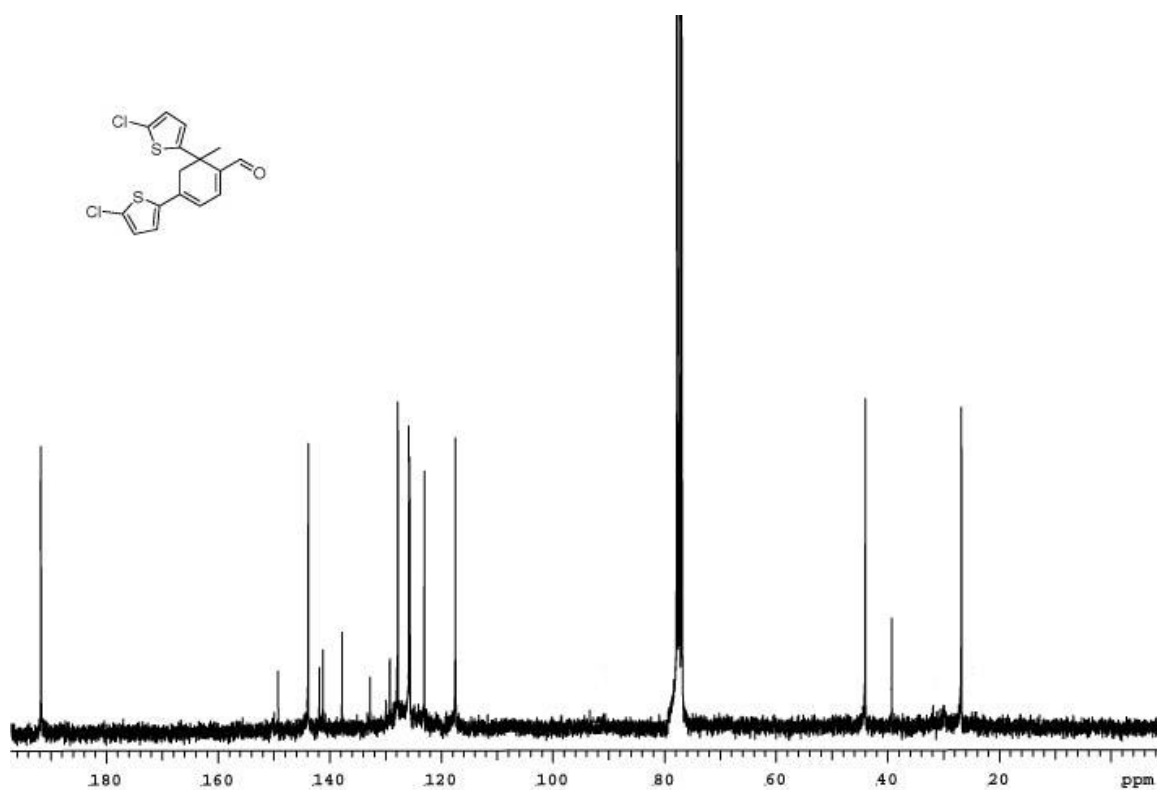
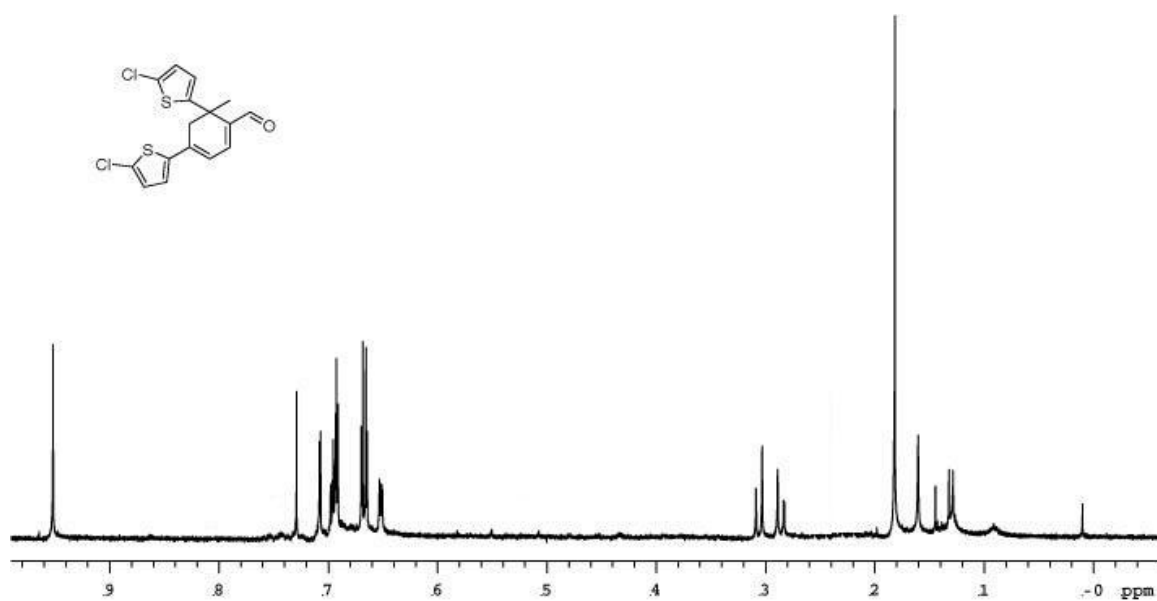
A-7. Spectra of 14.



A-8. Spectra of 15.

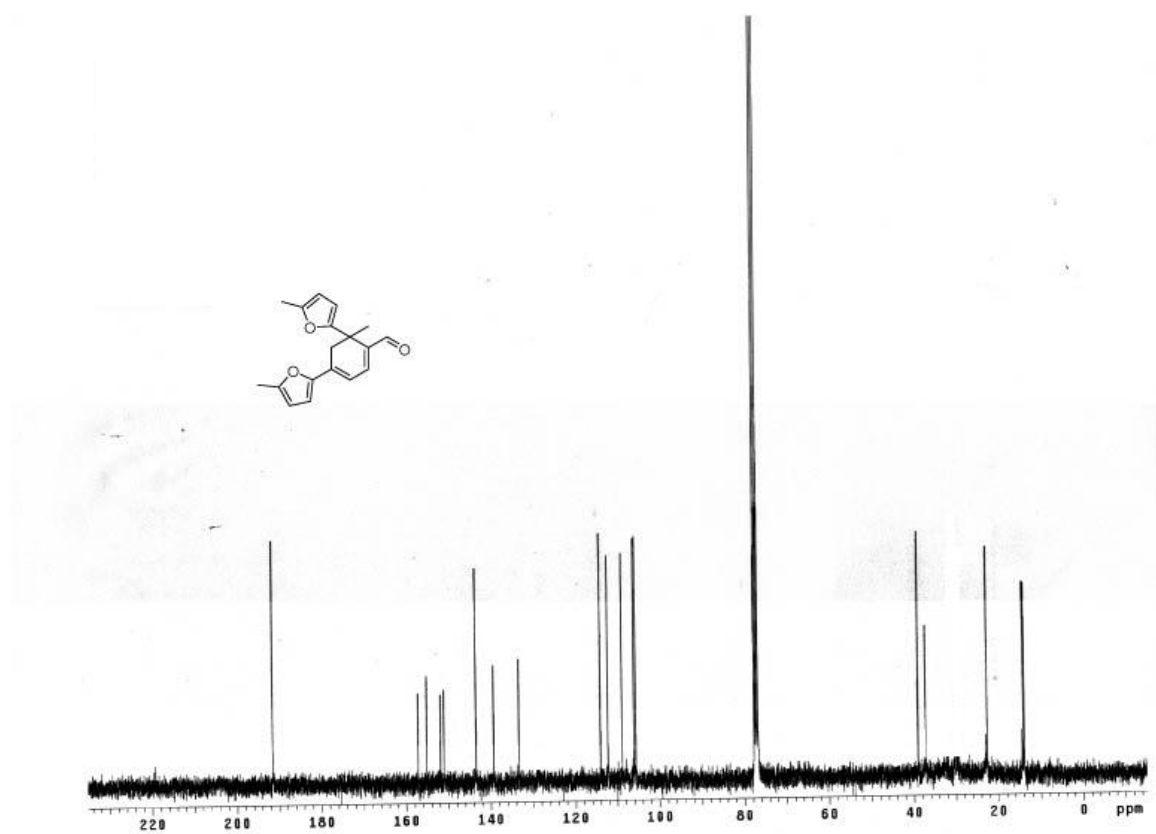
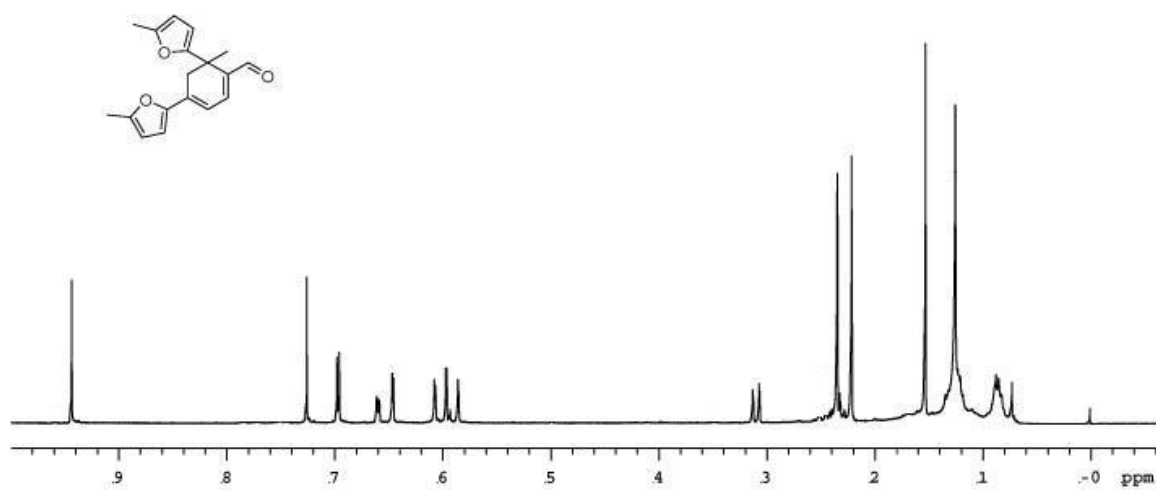


A-9. Spectra of 32.

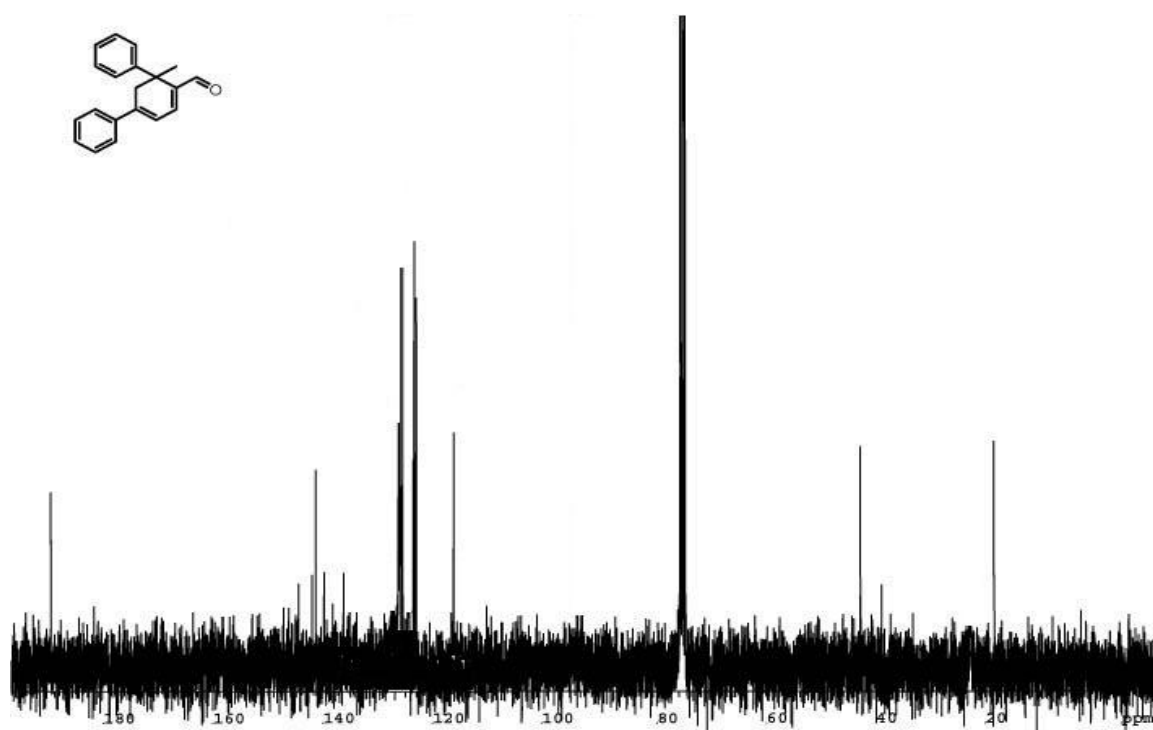
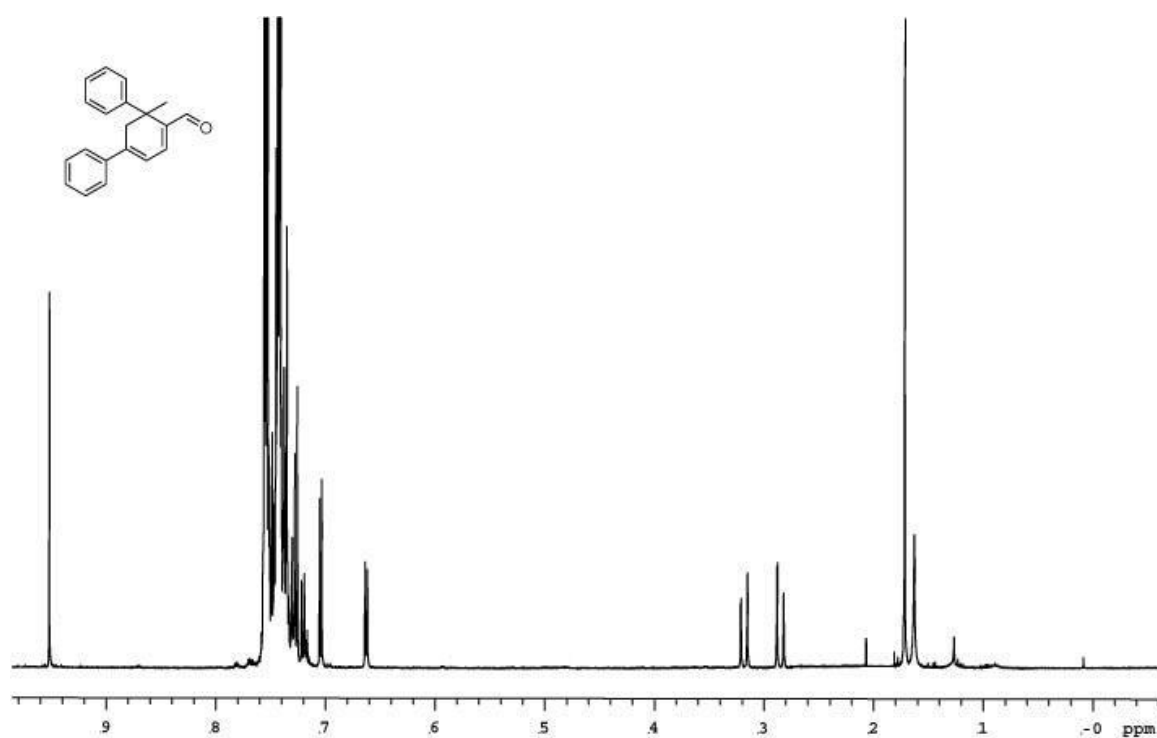


A-10. Spectra of 33.

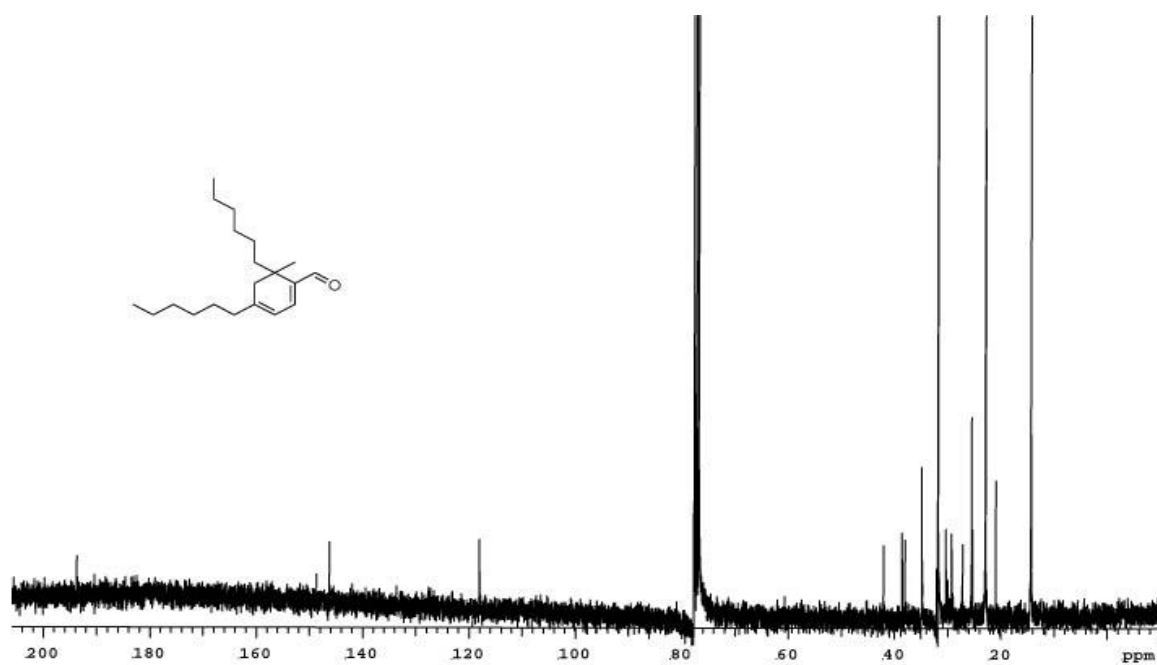
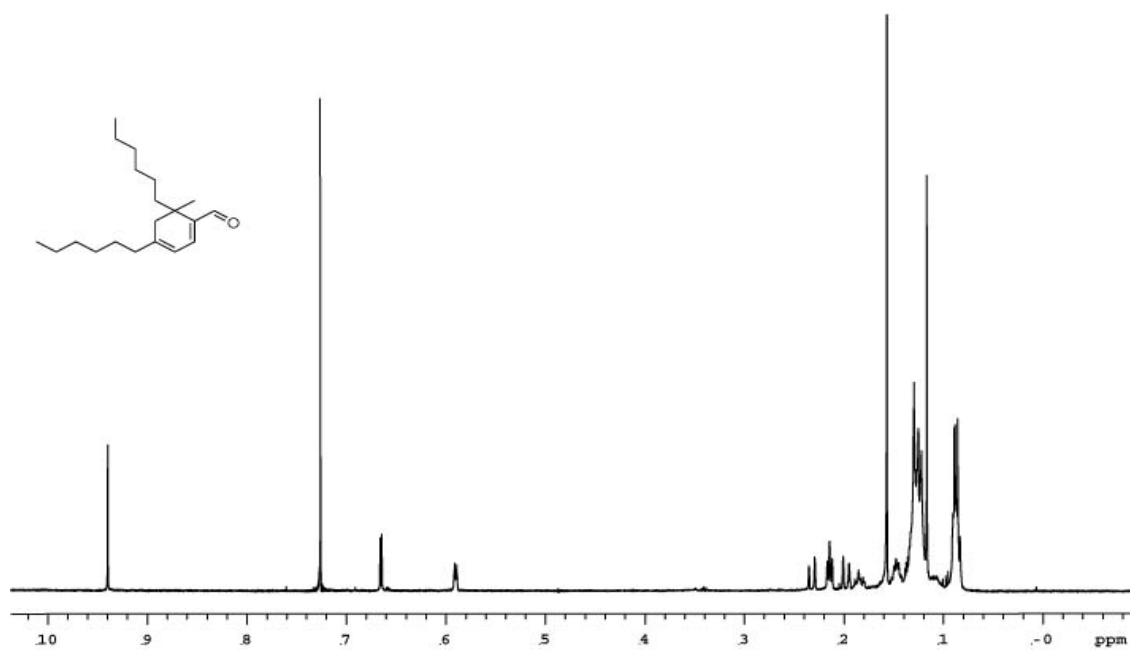




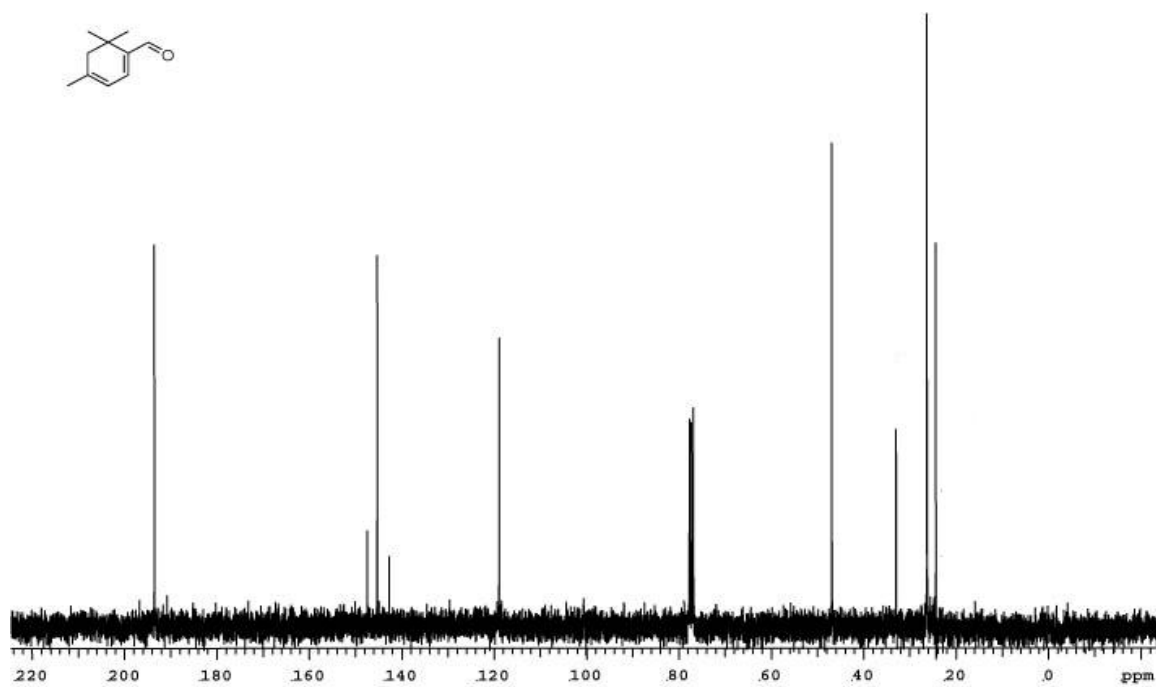
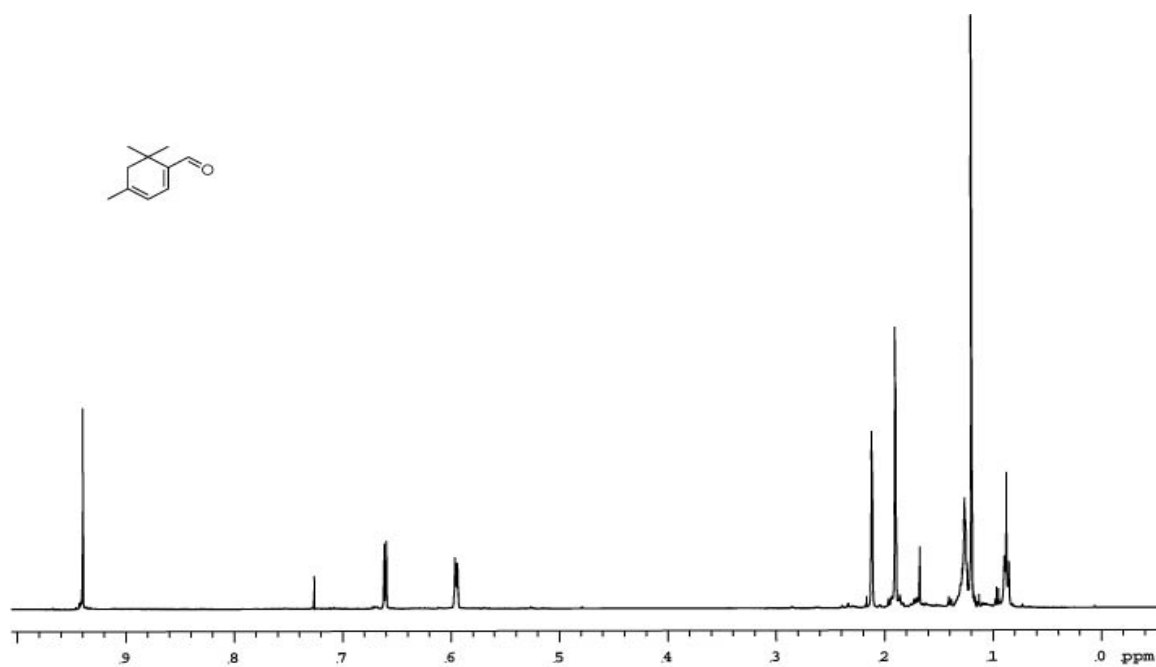
A-11. Spectra of 34.



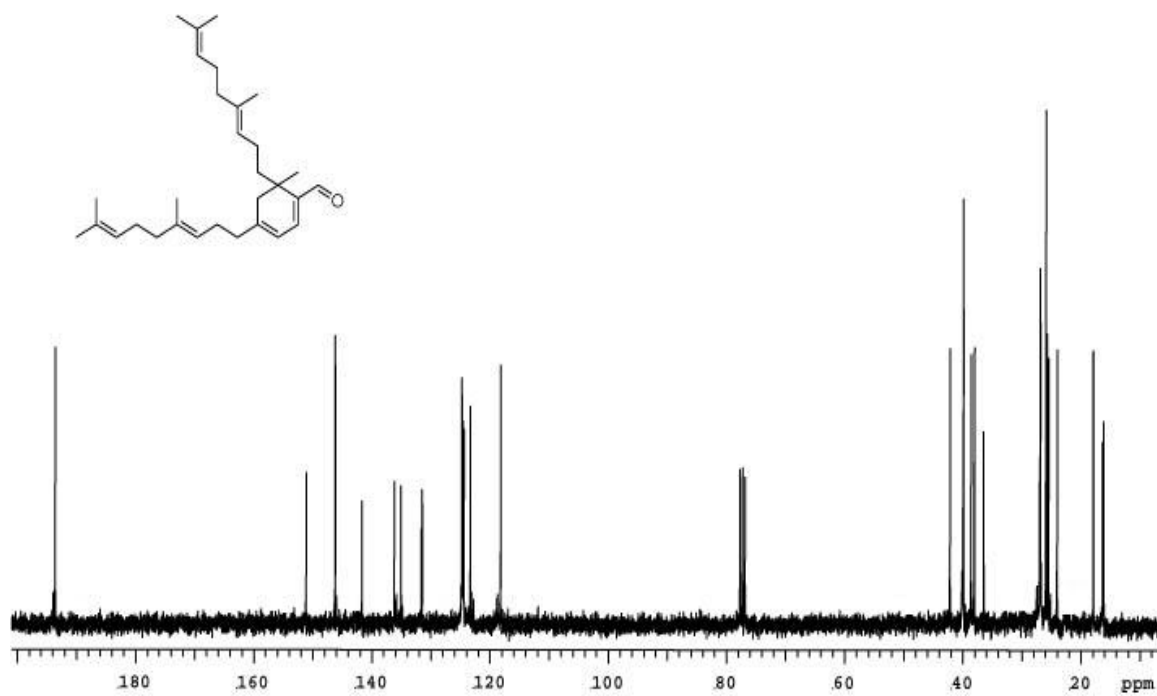
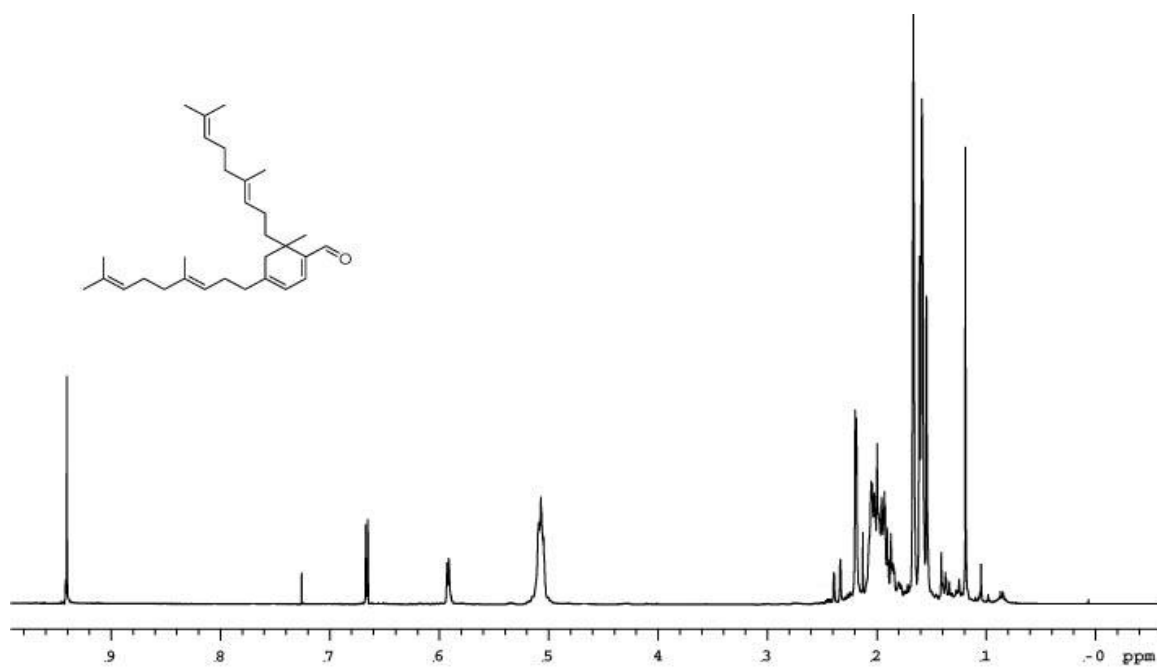
A-12. Spectra of 35.



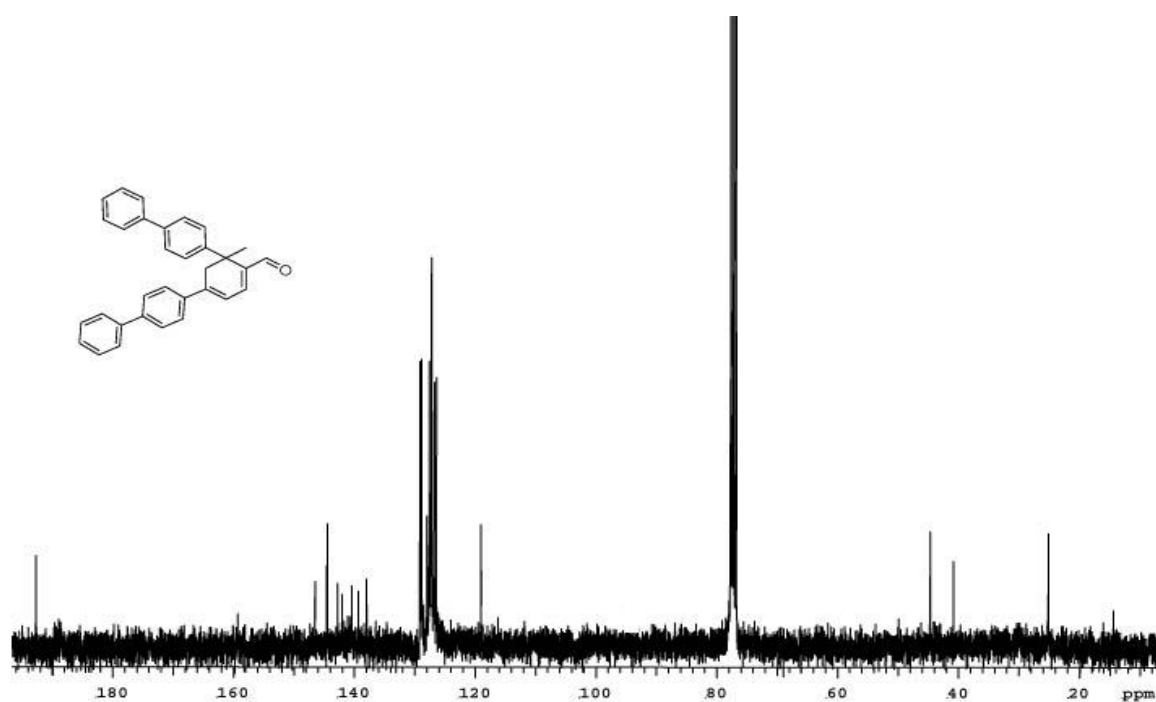
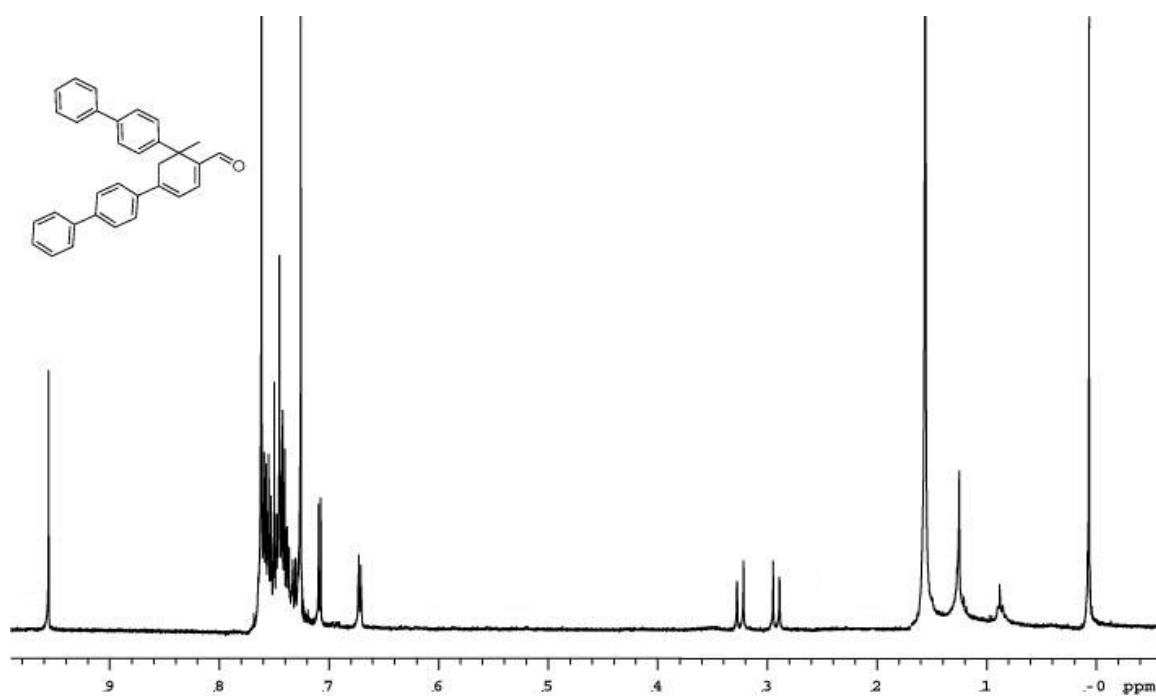
A-13. Spectra of 36.



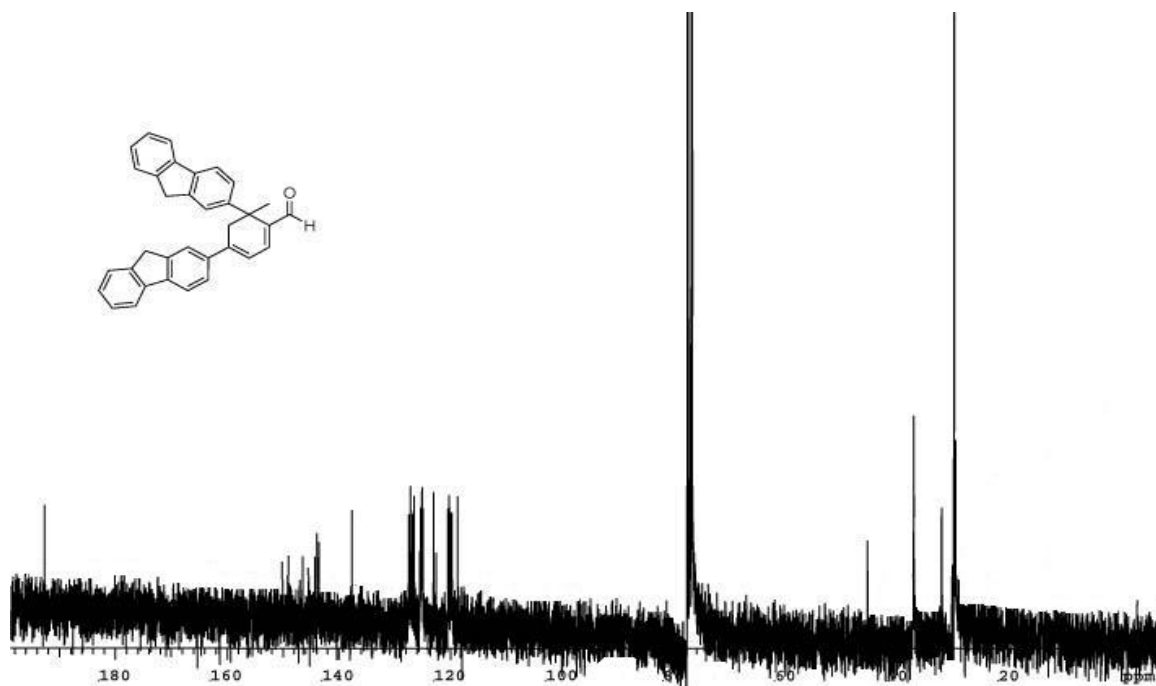
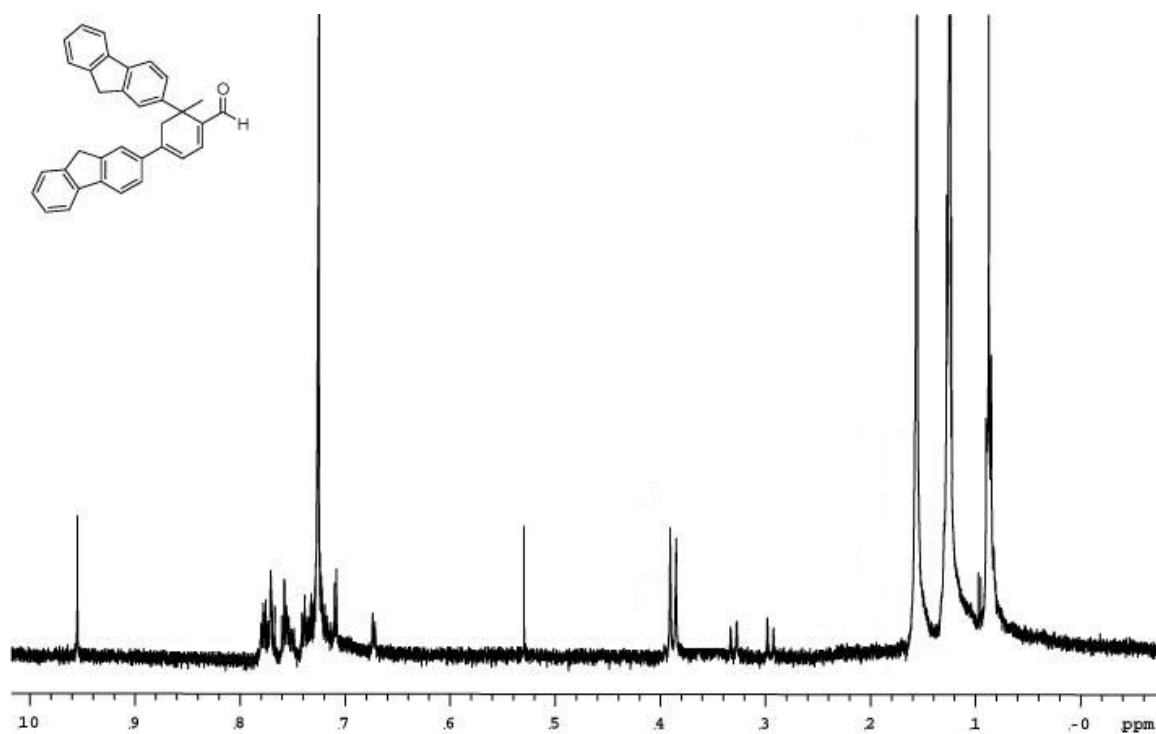
A-14. Spectra of 37.



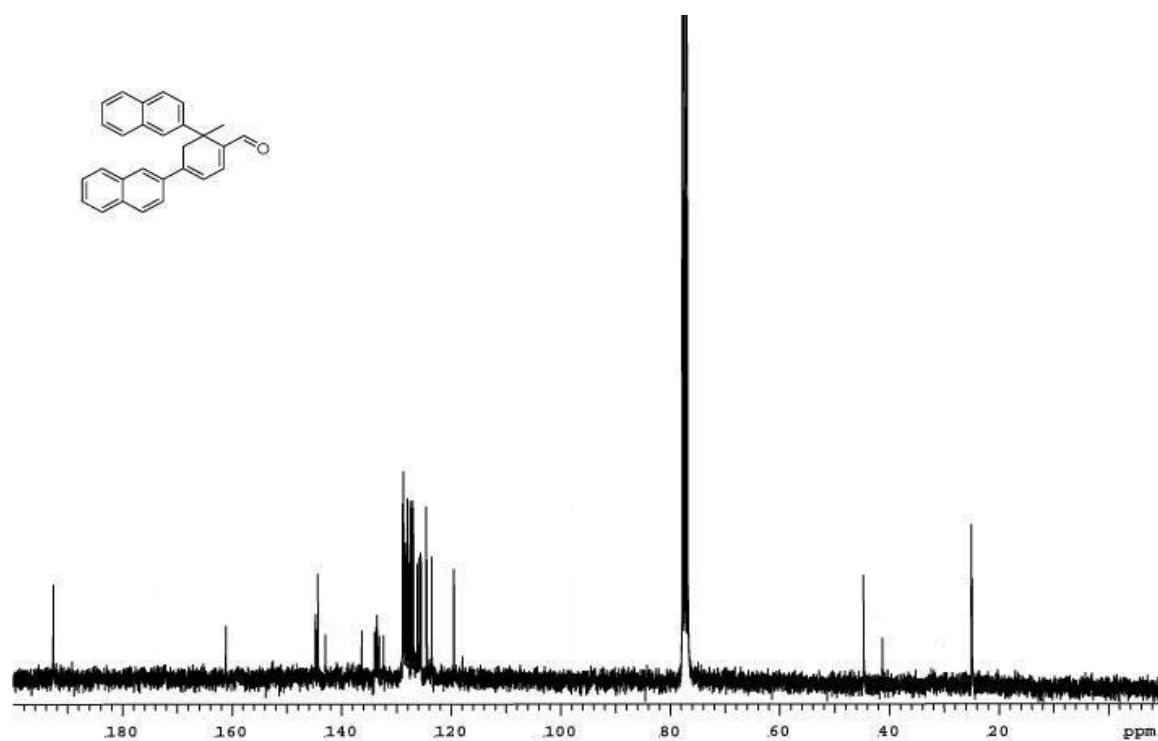
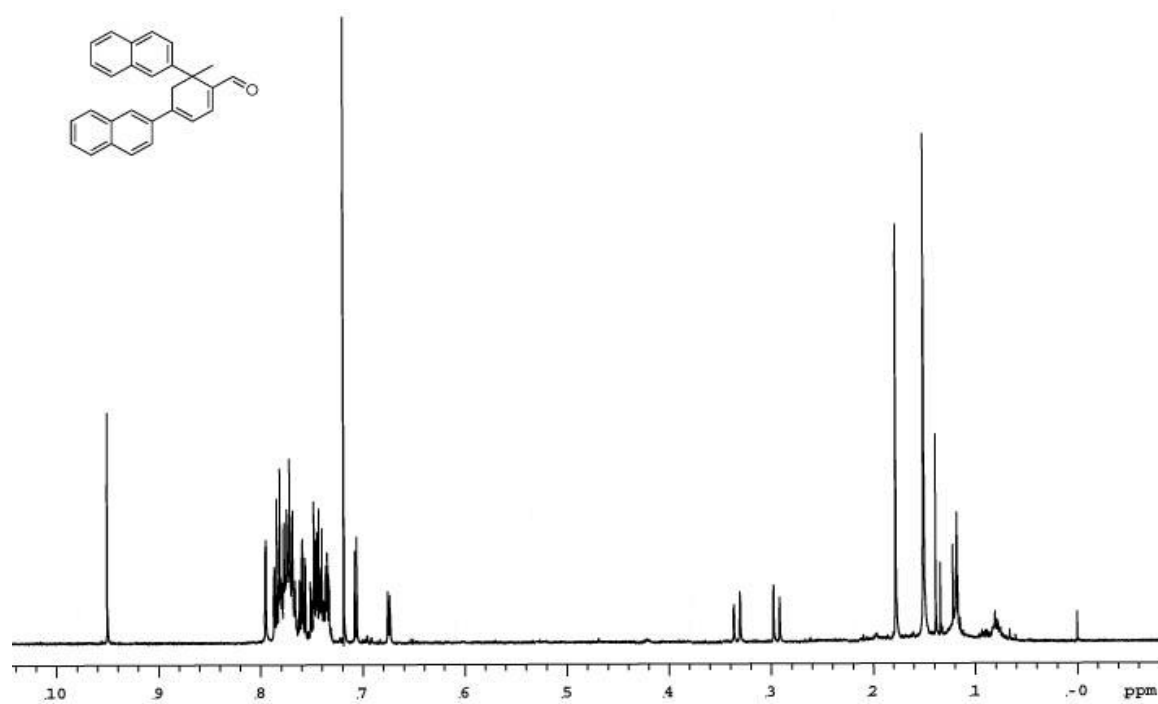
A-15. Spectra of 38.



A-16. Spectra of 39.

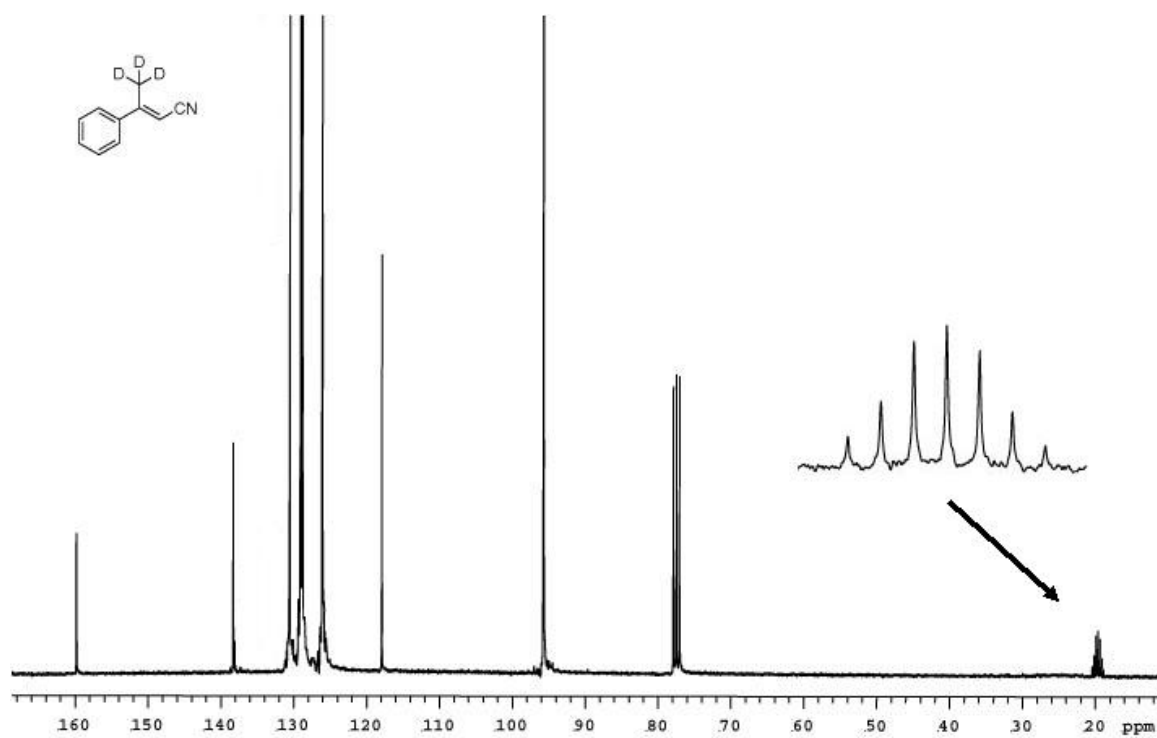
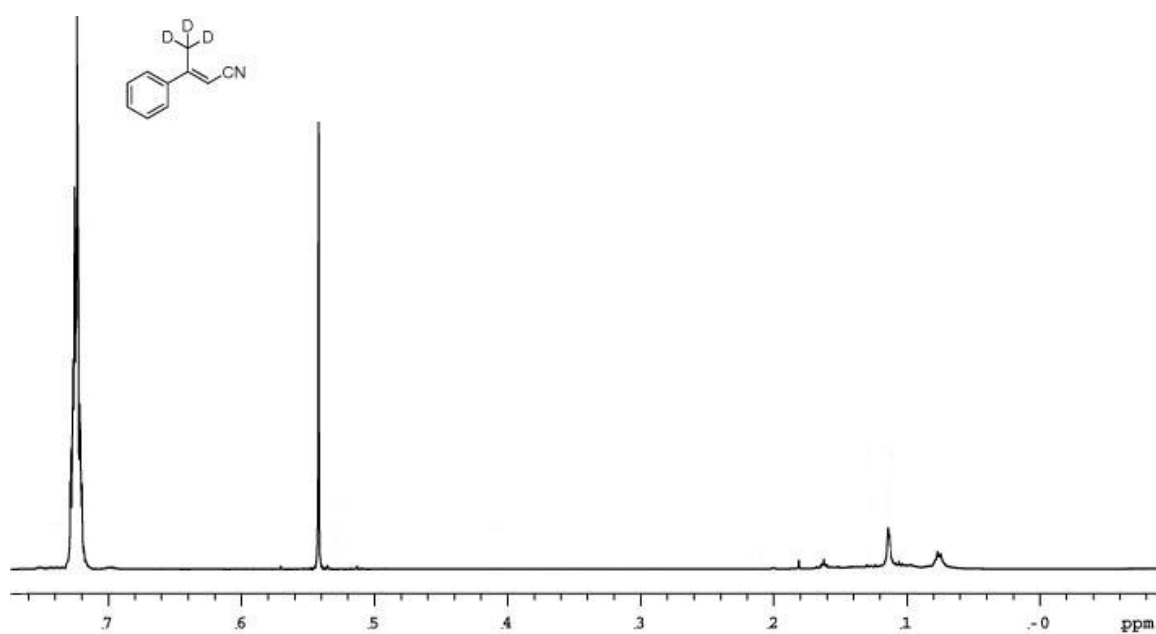


A-17. Spectra of 40.

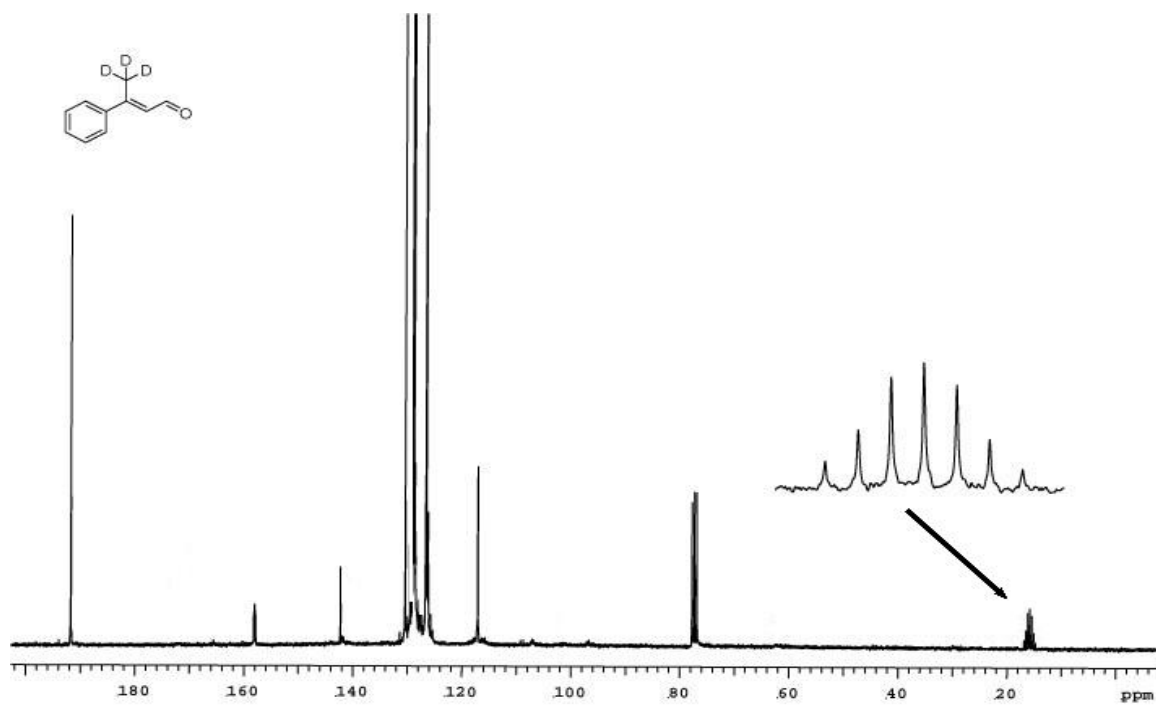
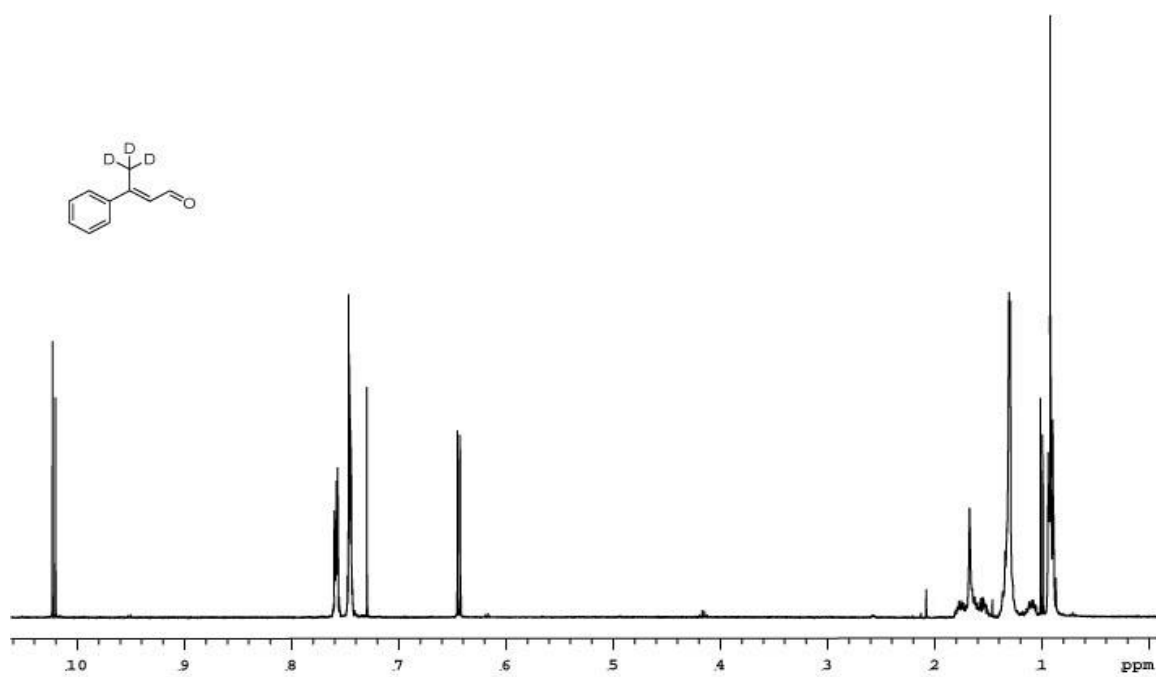


A-18. Spectra of 41.

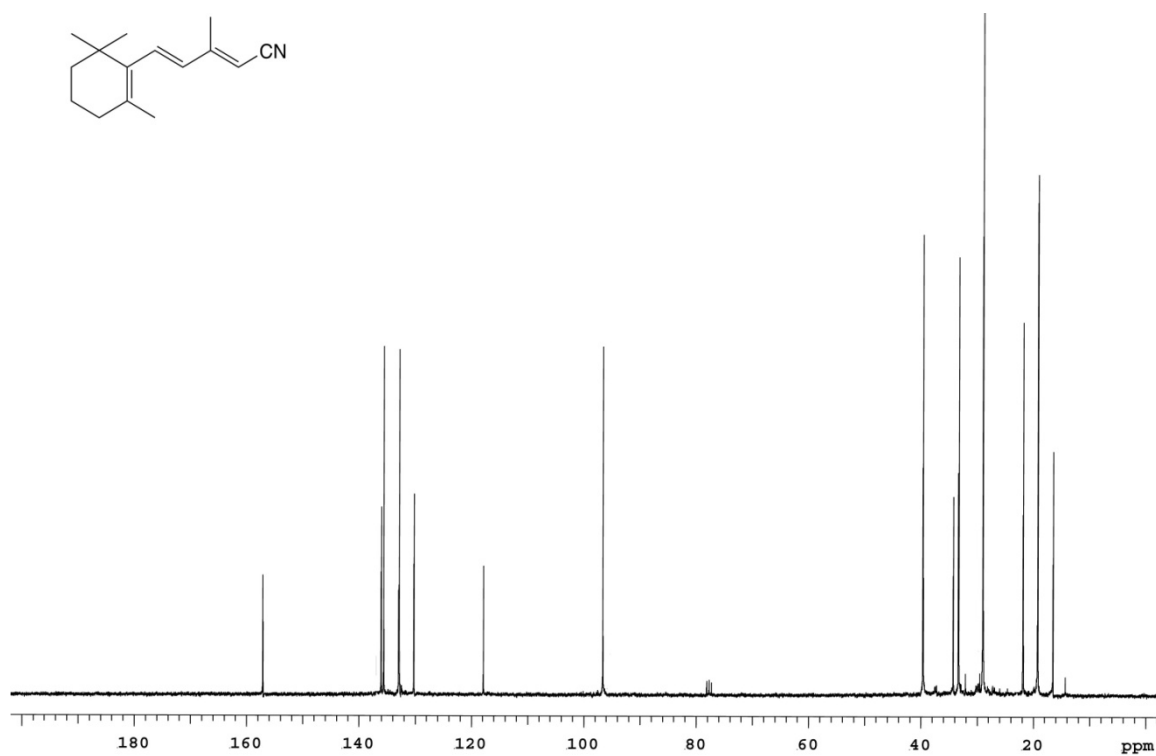
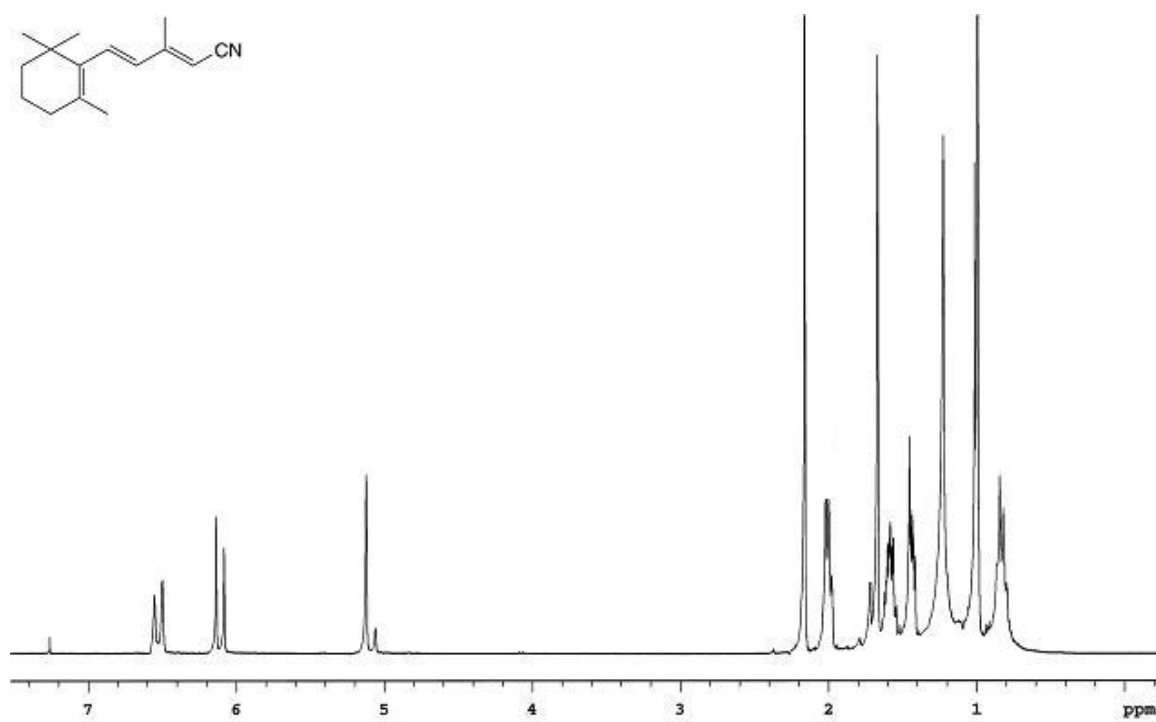




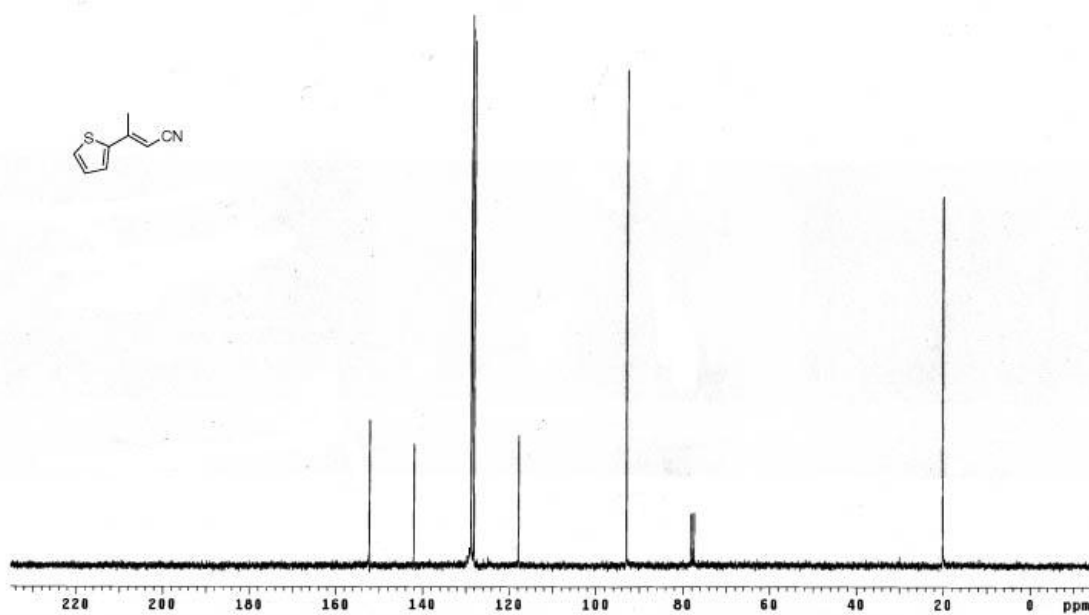
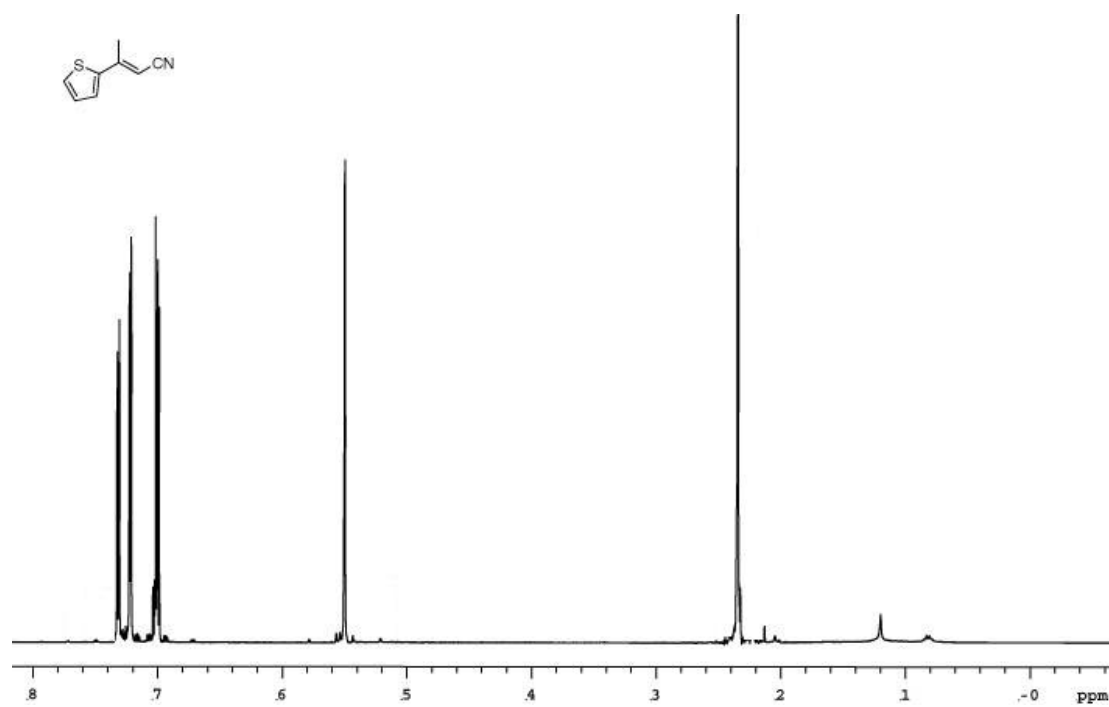
A-19. Spectra of 60.



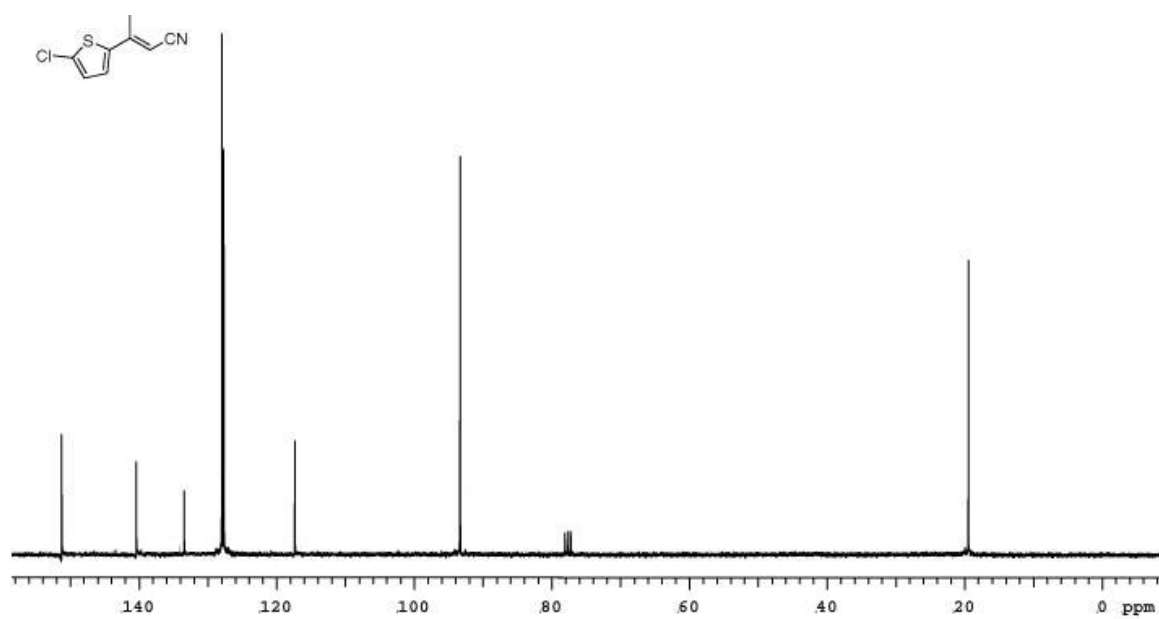
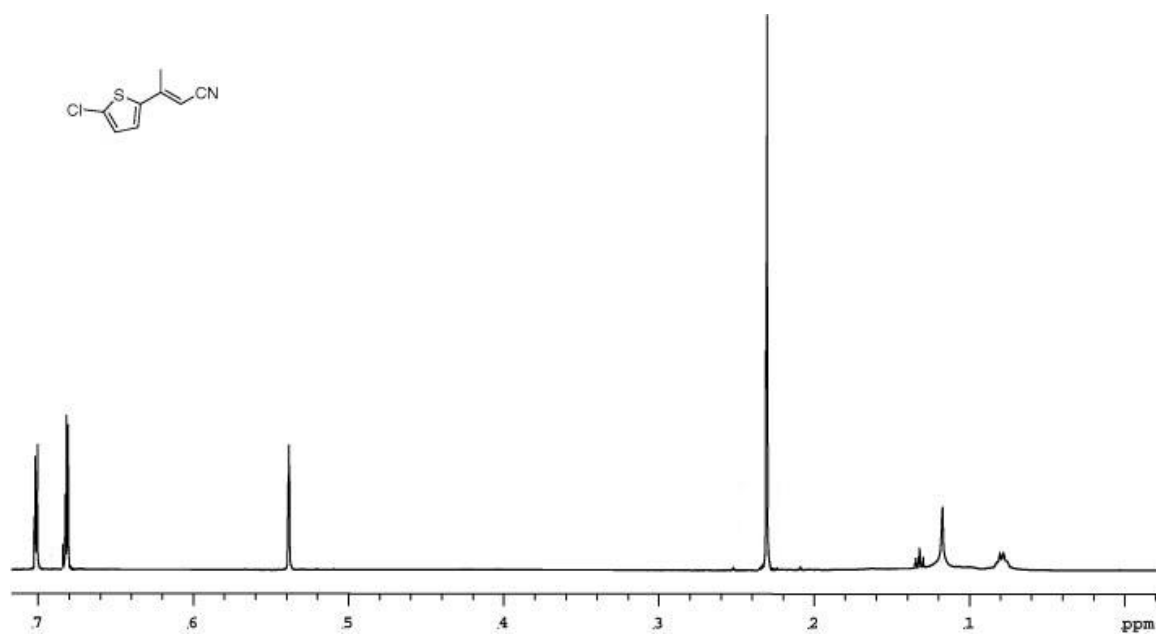
A-20. Spectra of 61.



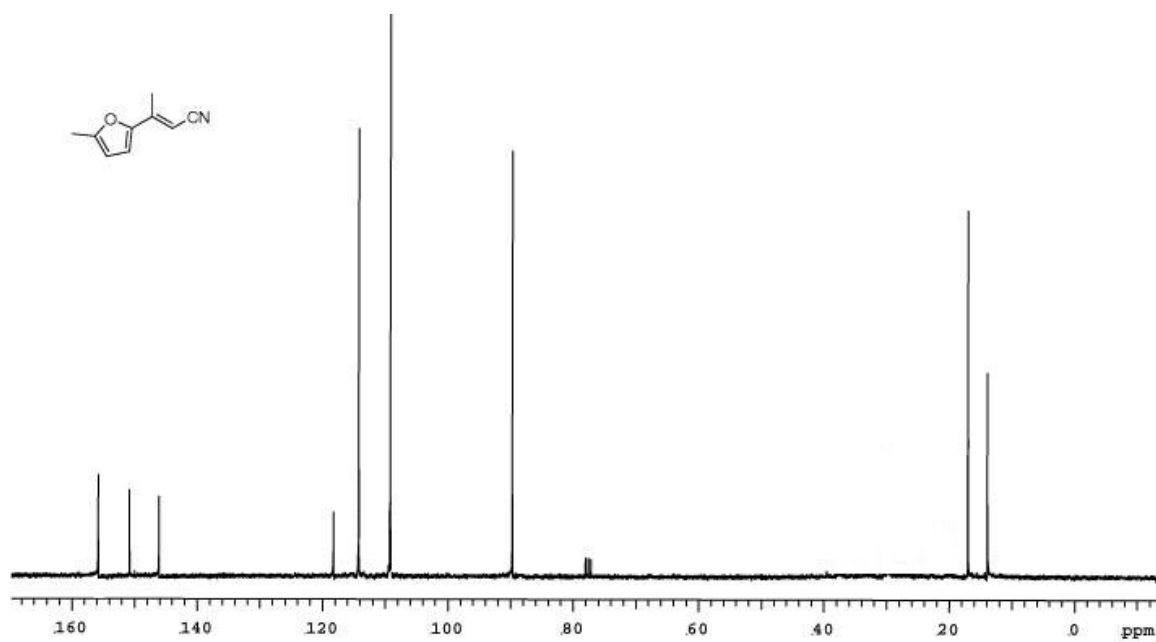
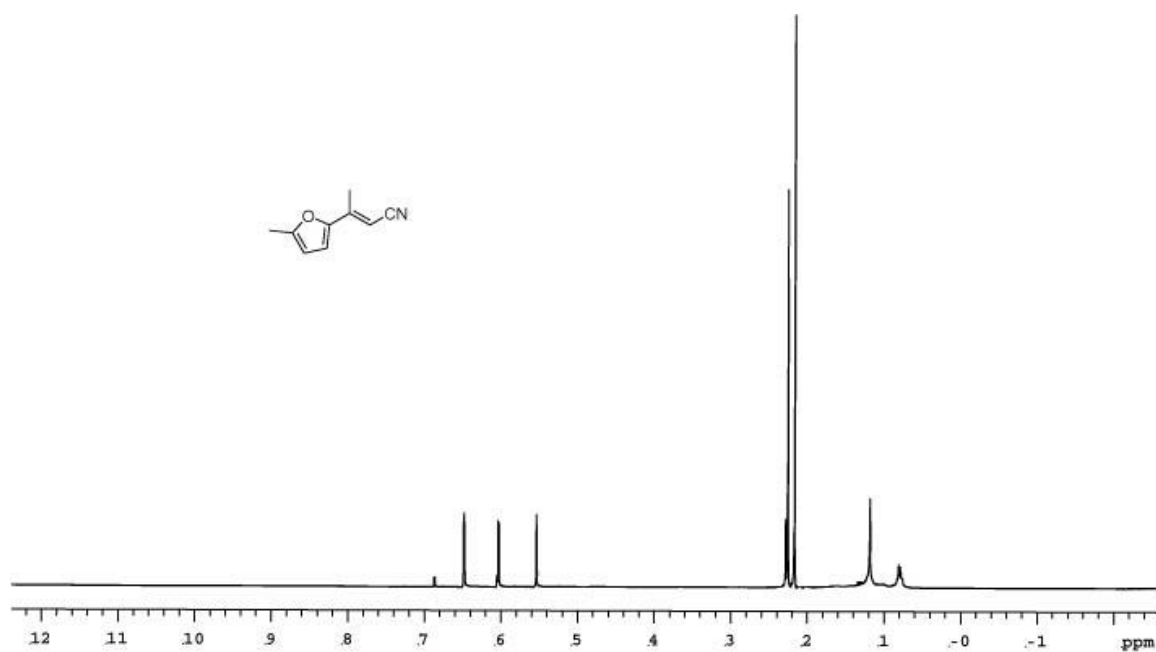
A-21. Spectra of 62.



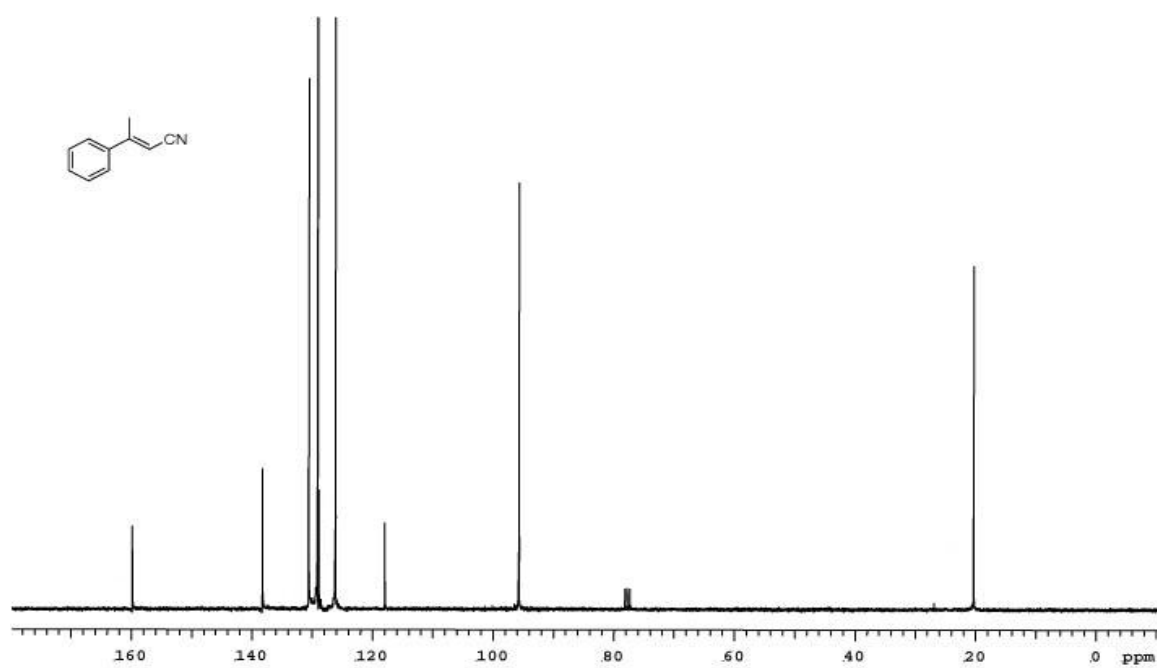
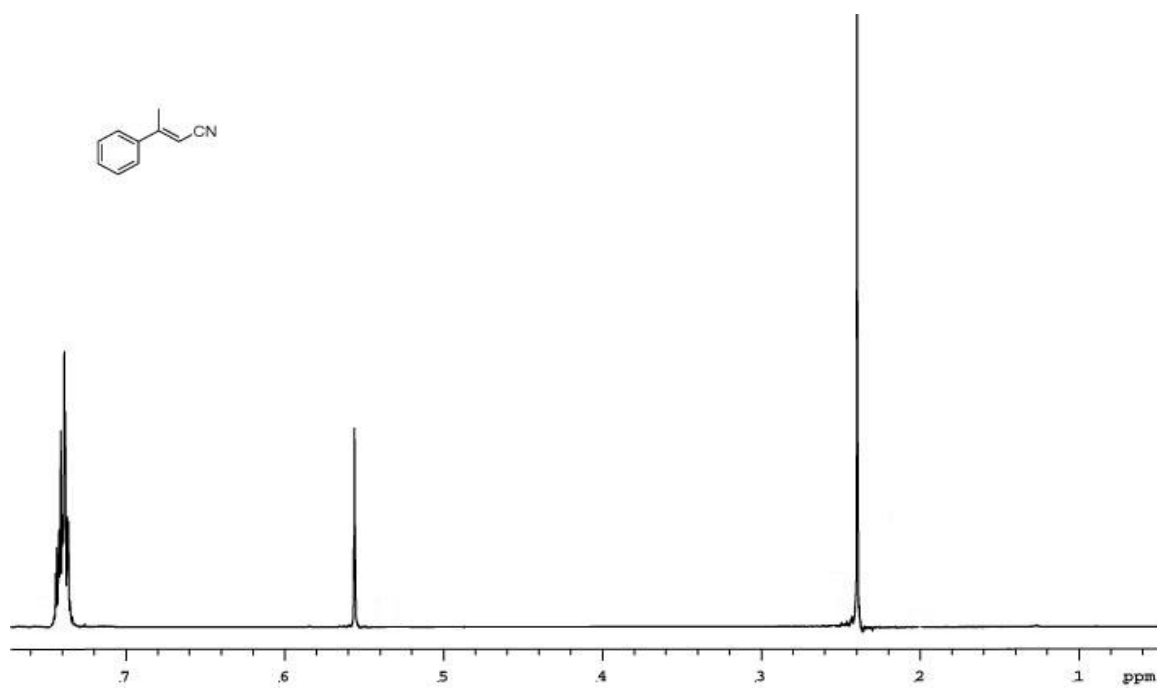
A-22. Spectra of 63.



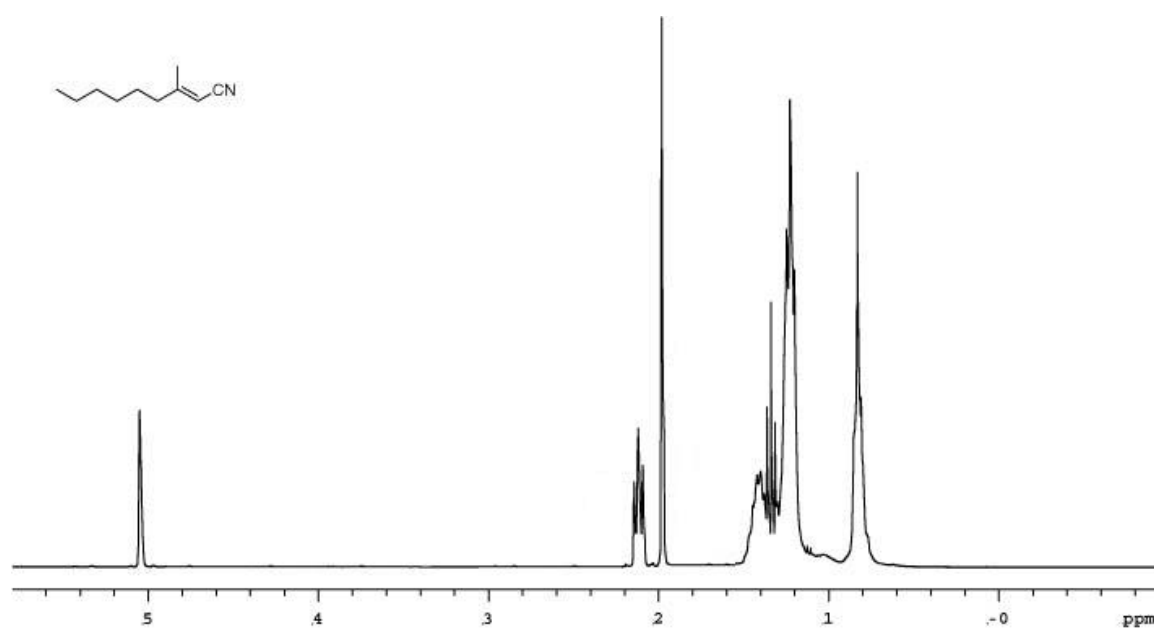
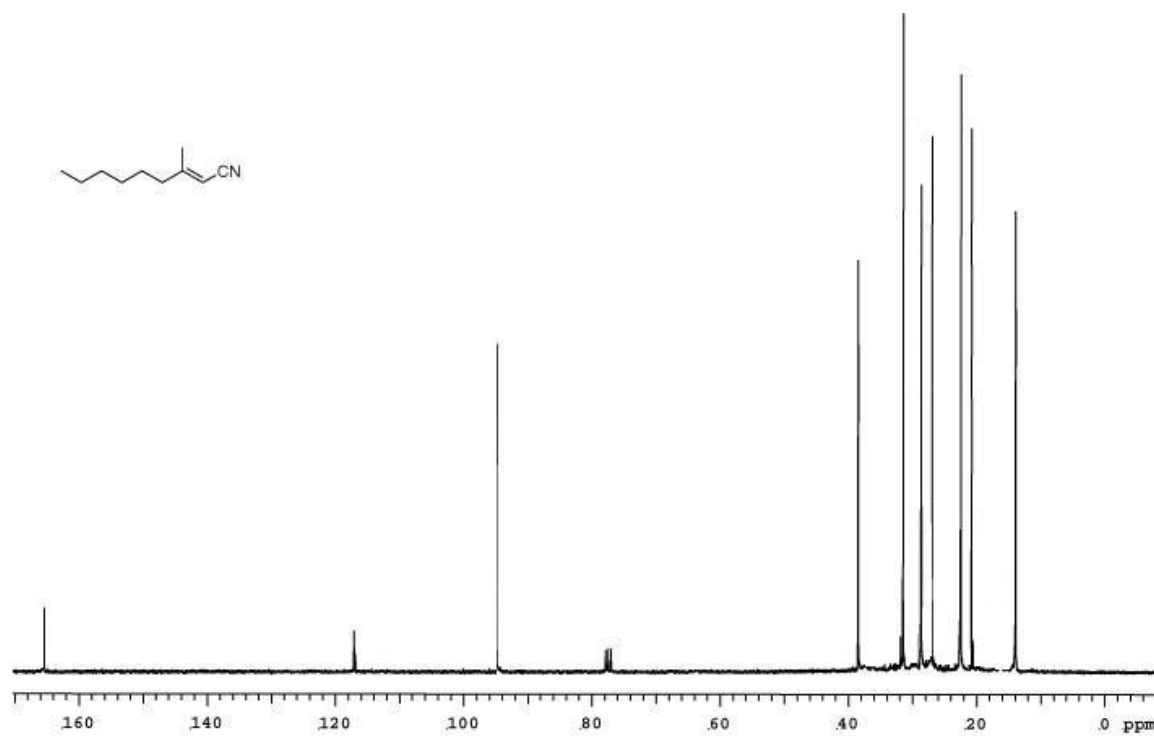
A-23. Spectra of 64.



A-24. Spectra of 65.

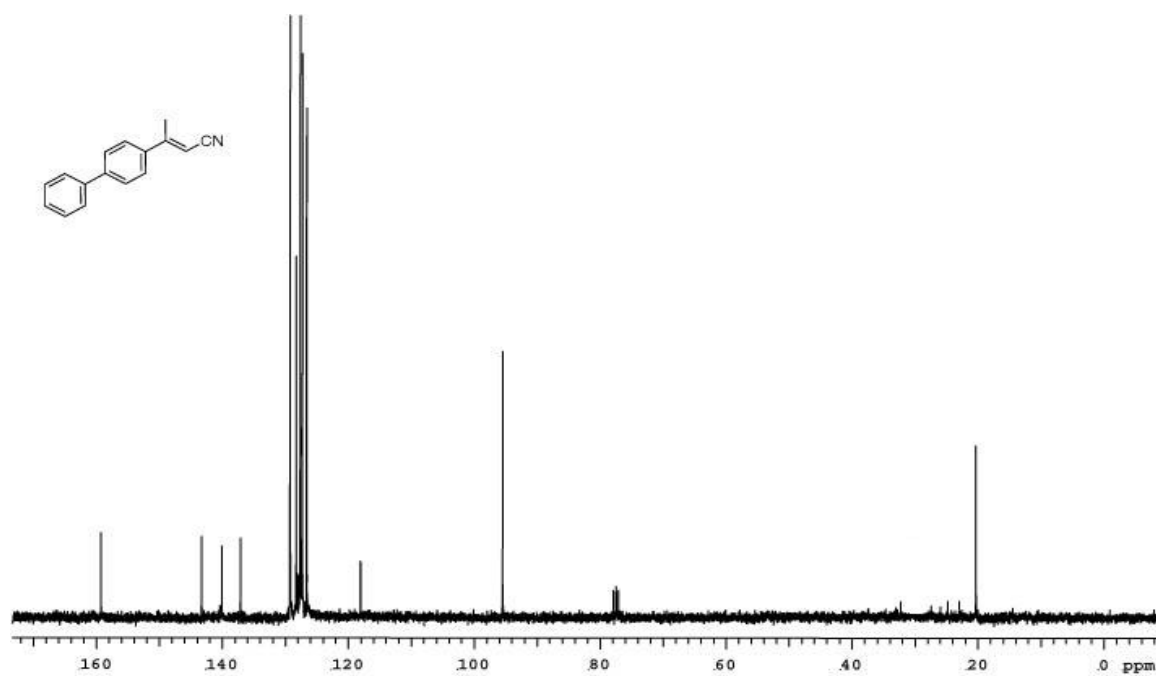
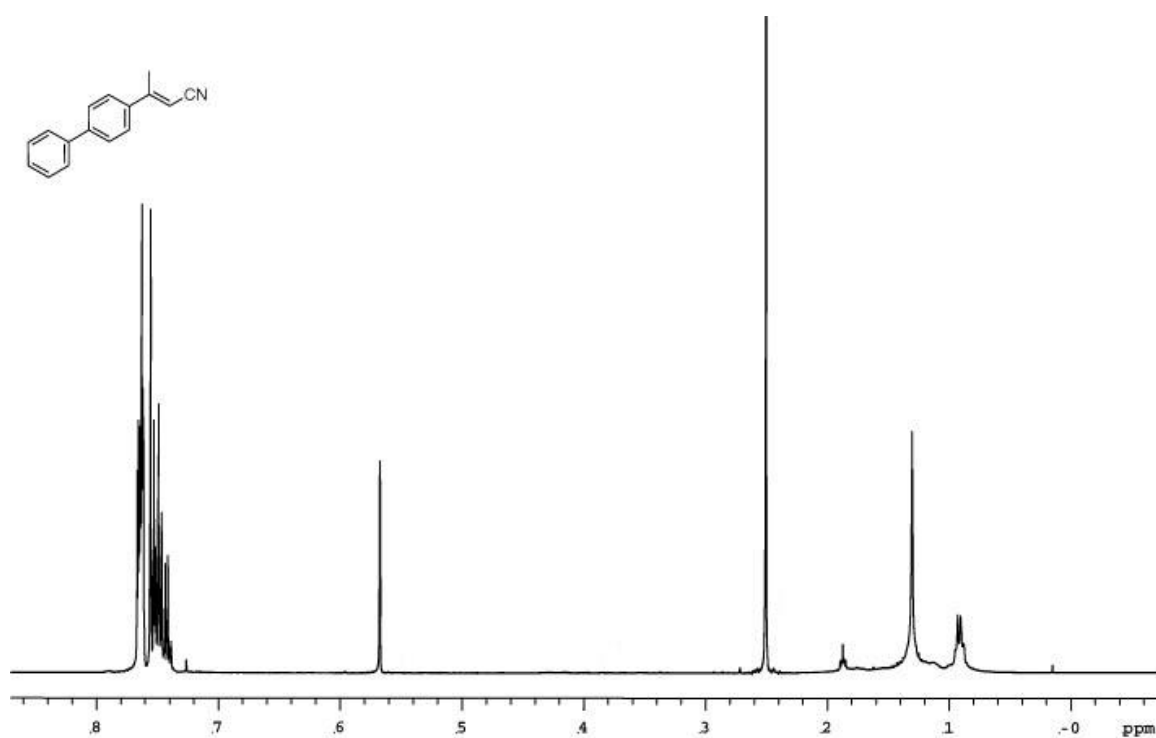


A-25. Spectra of 66.

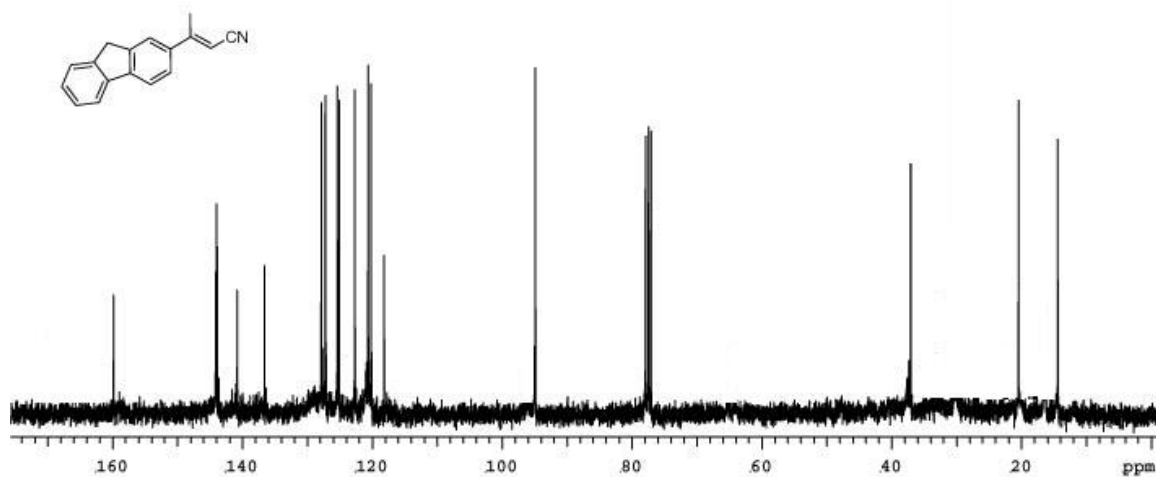
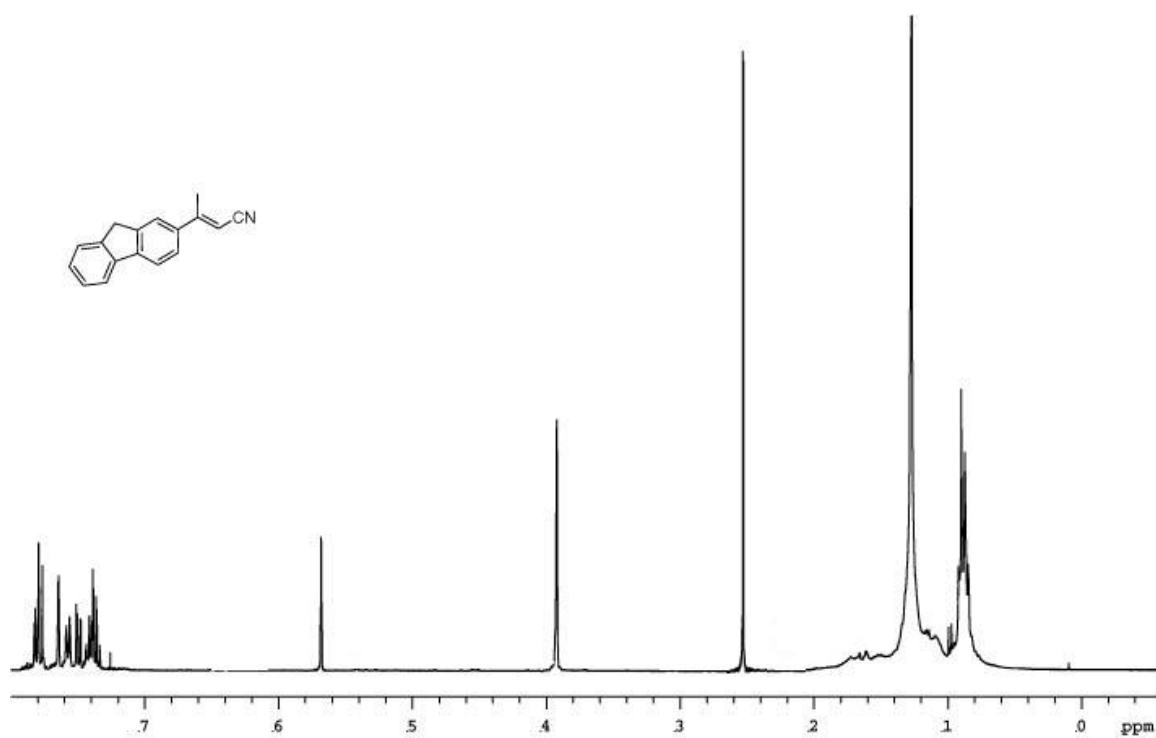


A-26. Spectra of 67.

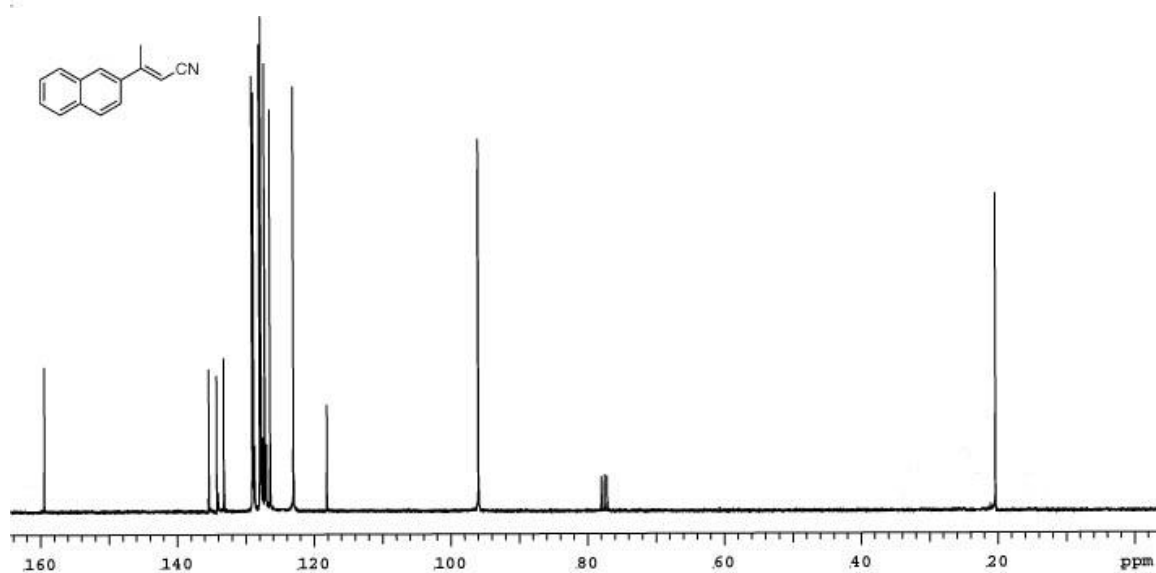
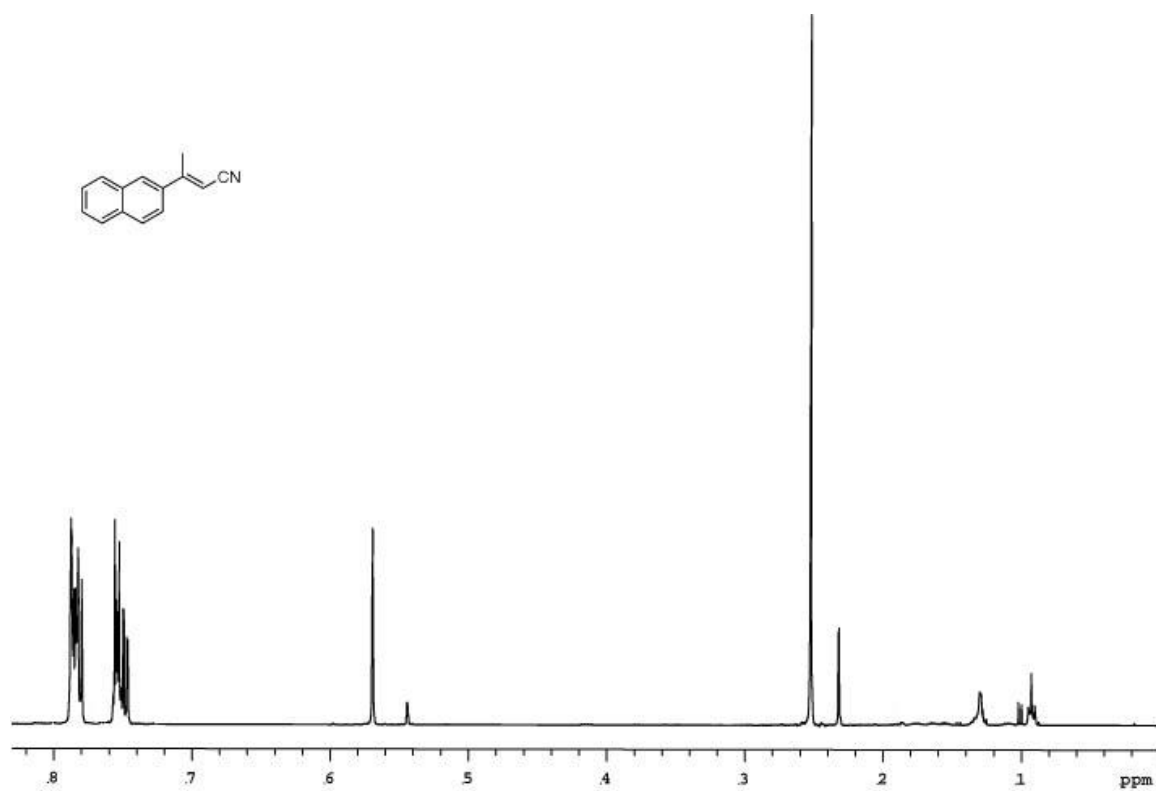




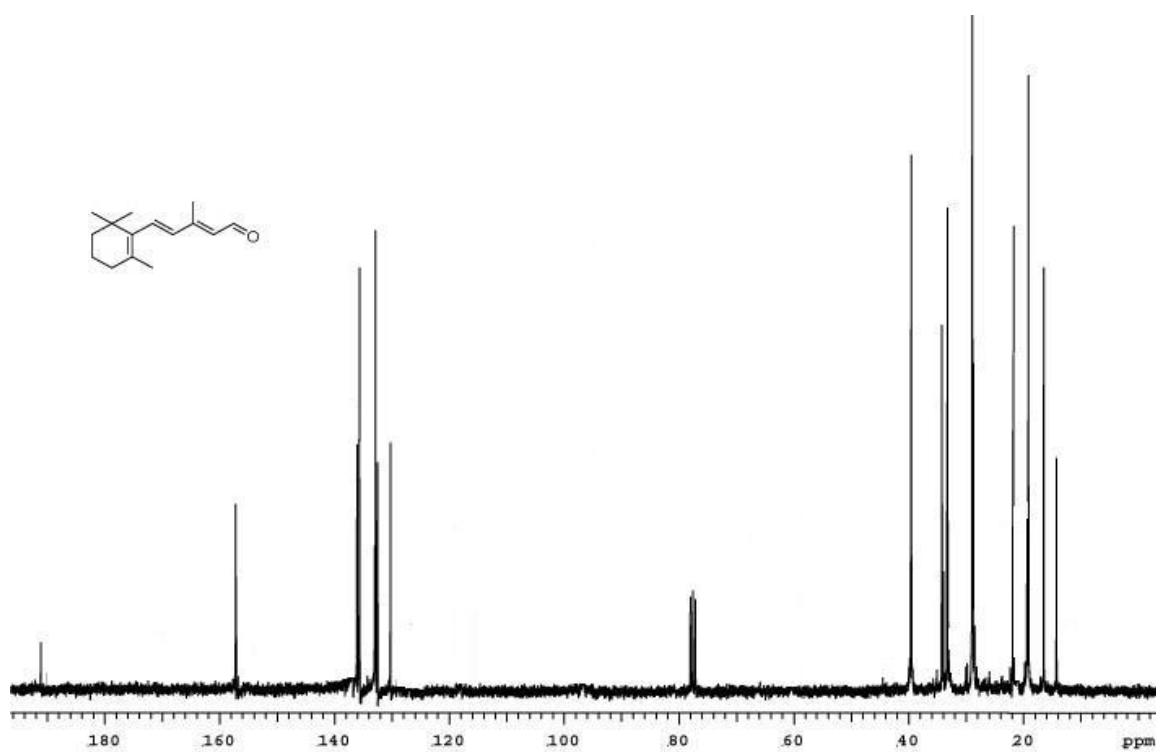
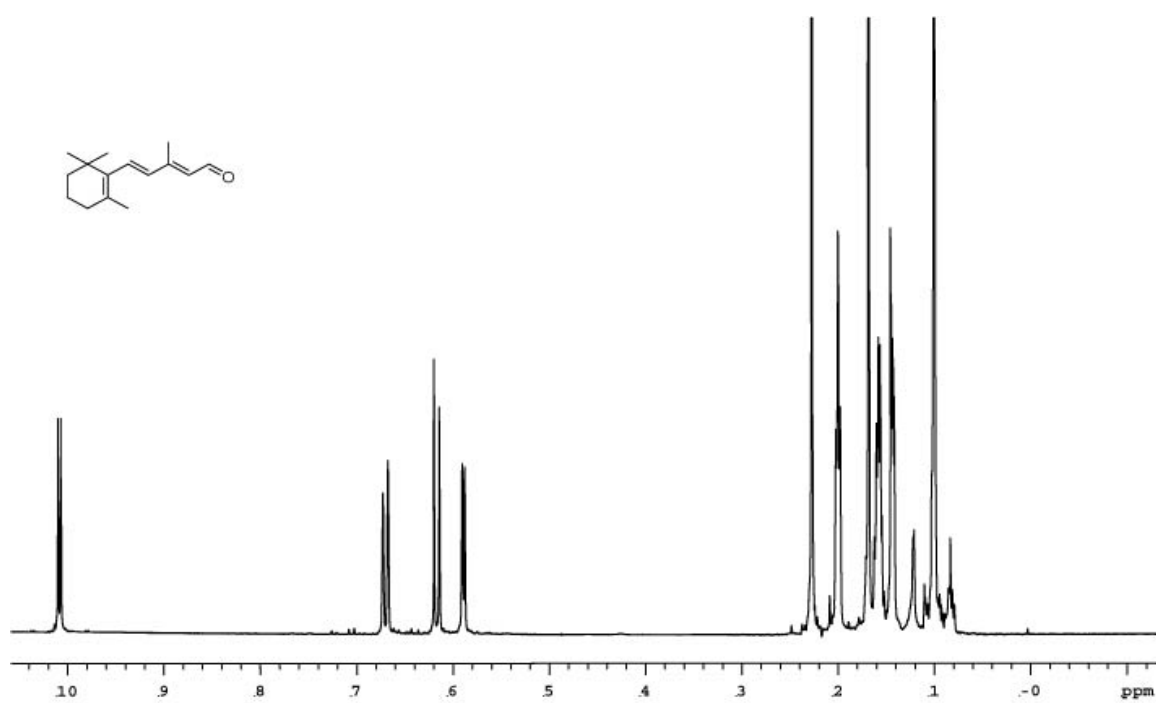
A-27. Spectra of 68.



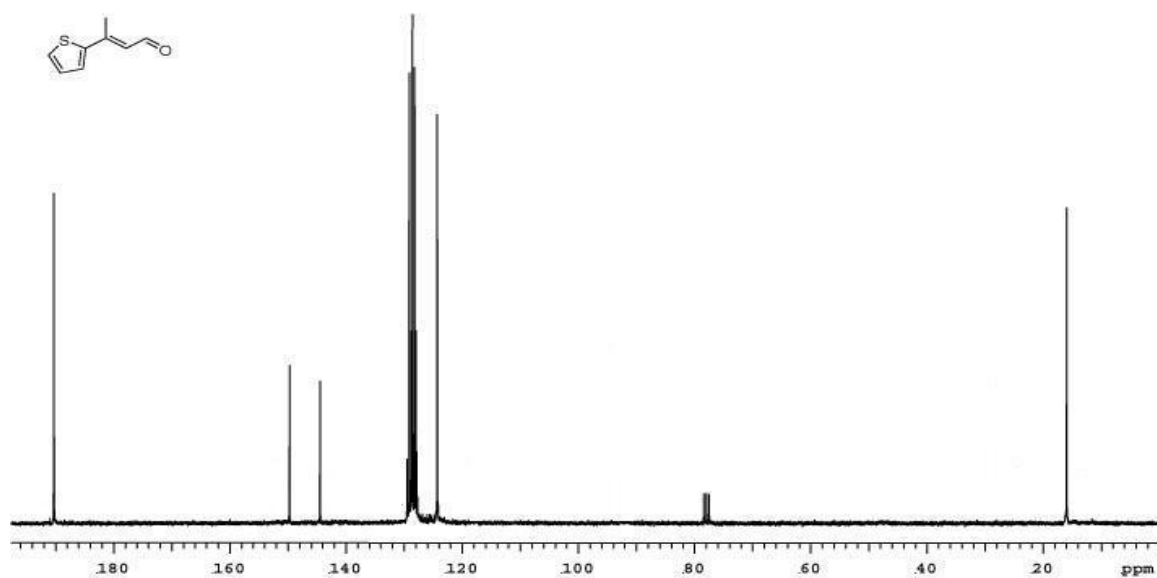
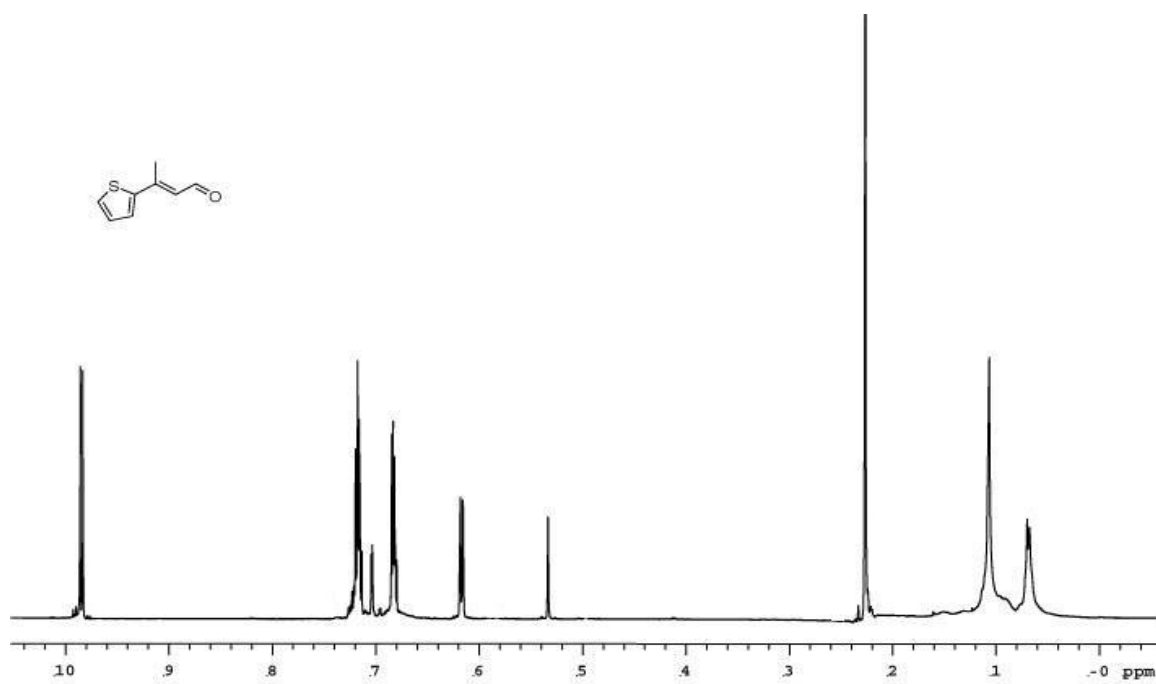
A-28. Spectra of 69.



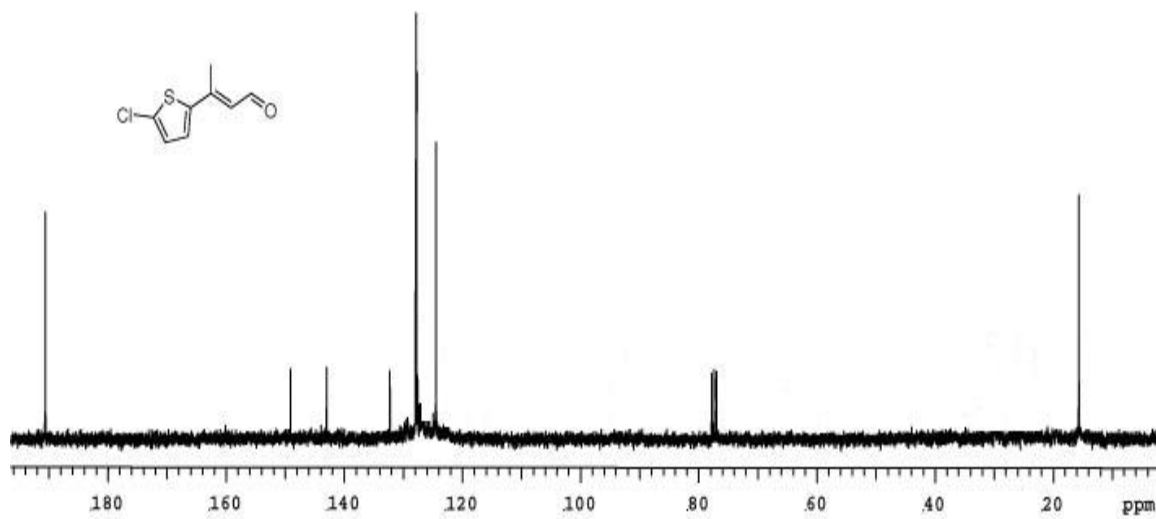
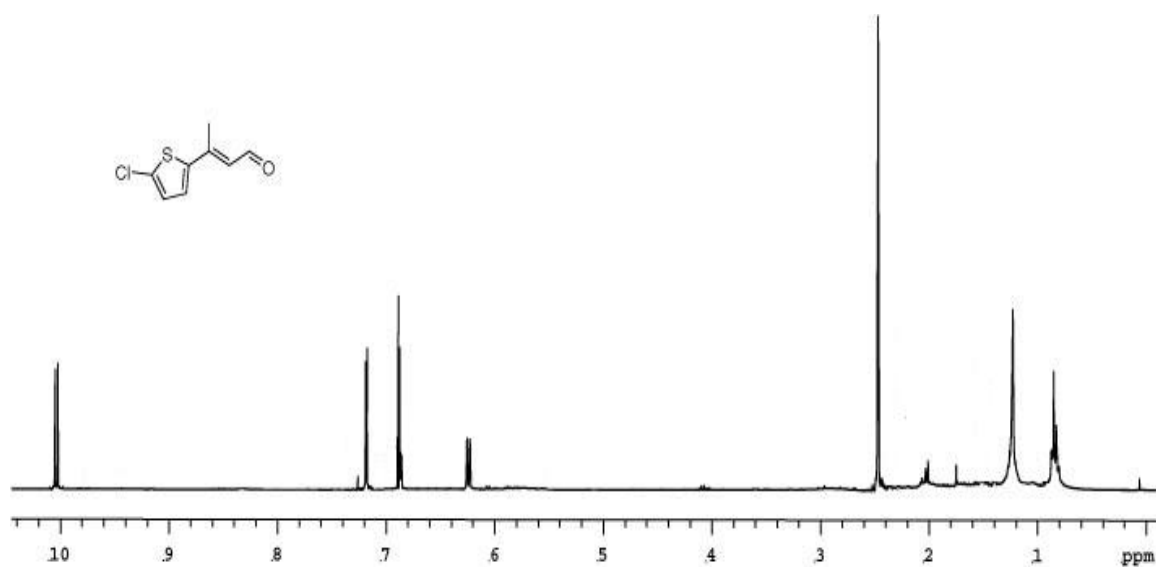
A-29. Spectra of 70.



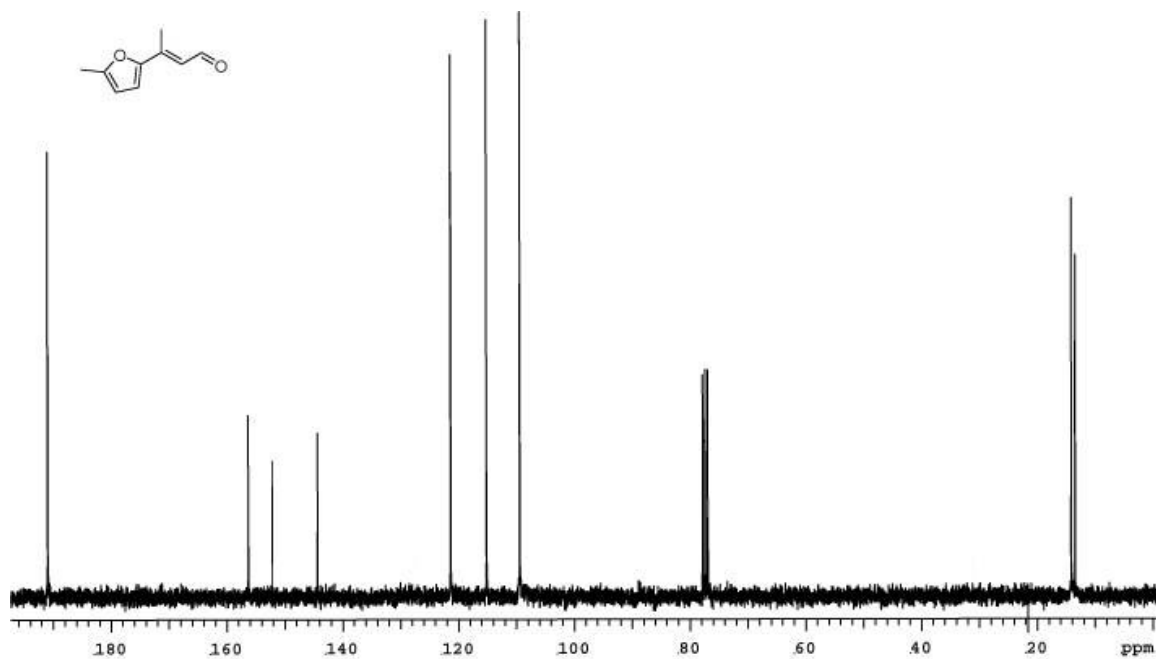
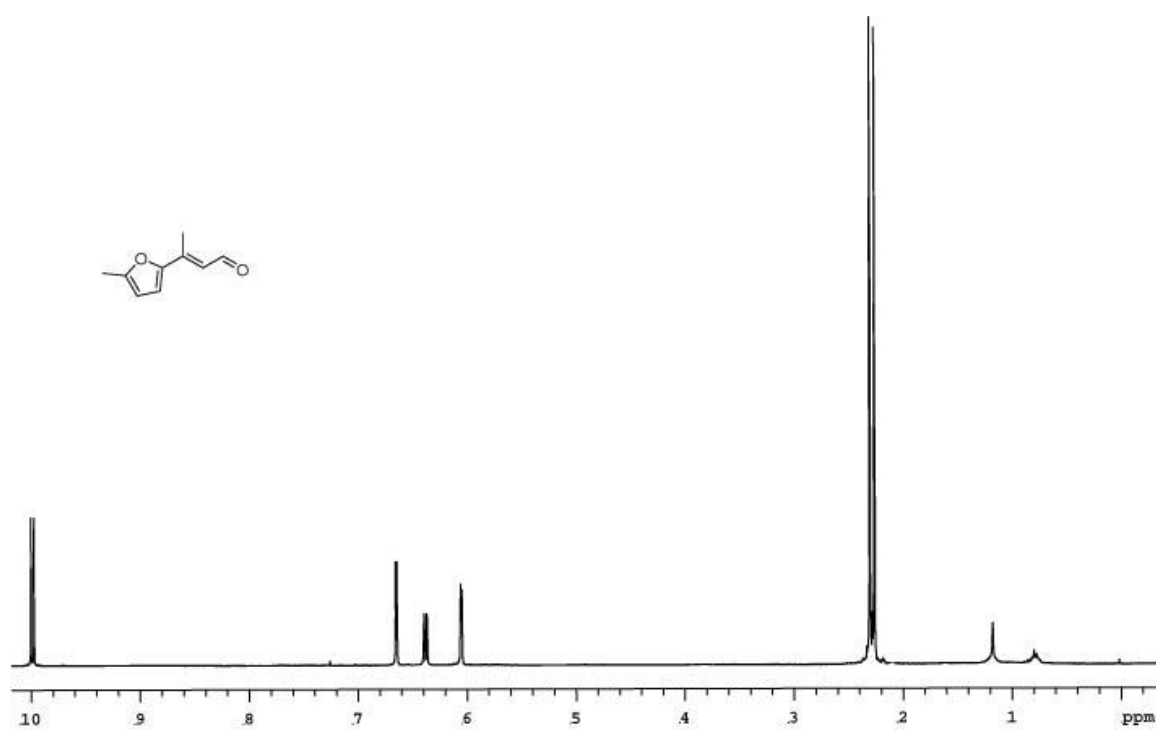
A-30. Spectra of 71.



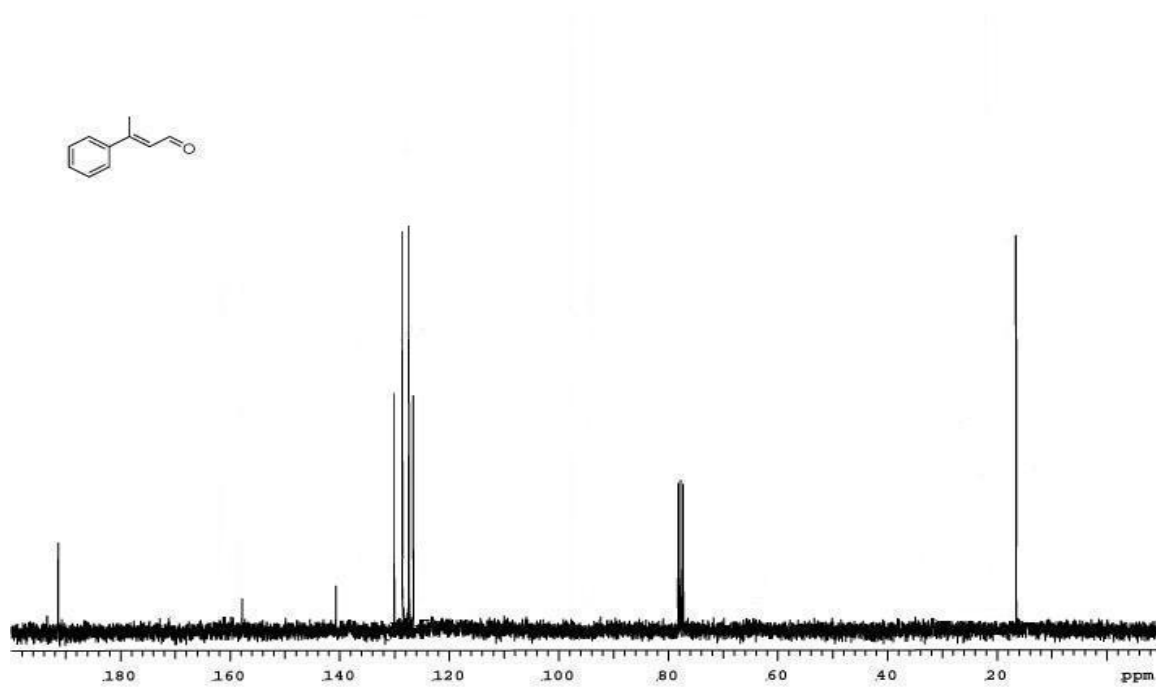
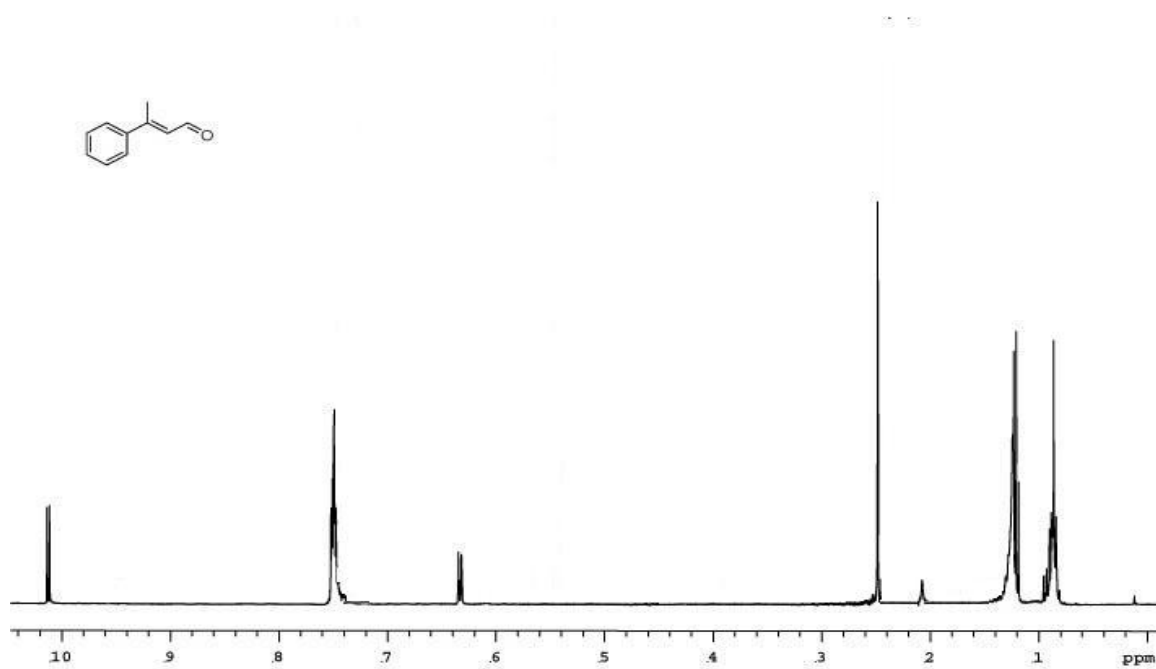
A-31. Spectra of 72.



A-32. Spectra of 73.

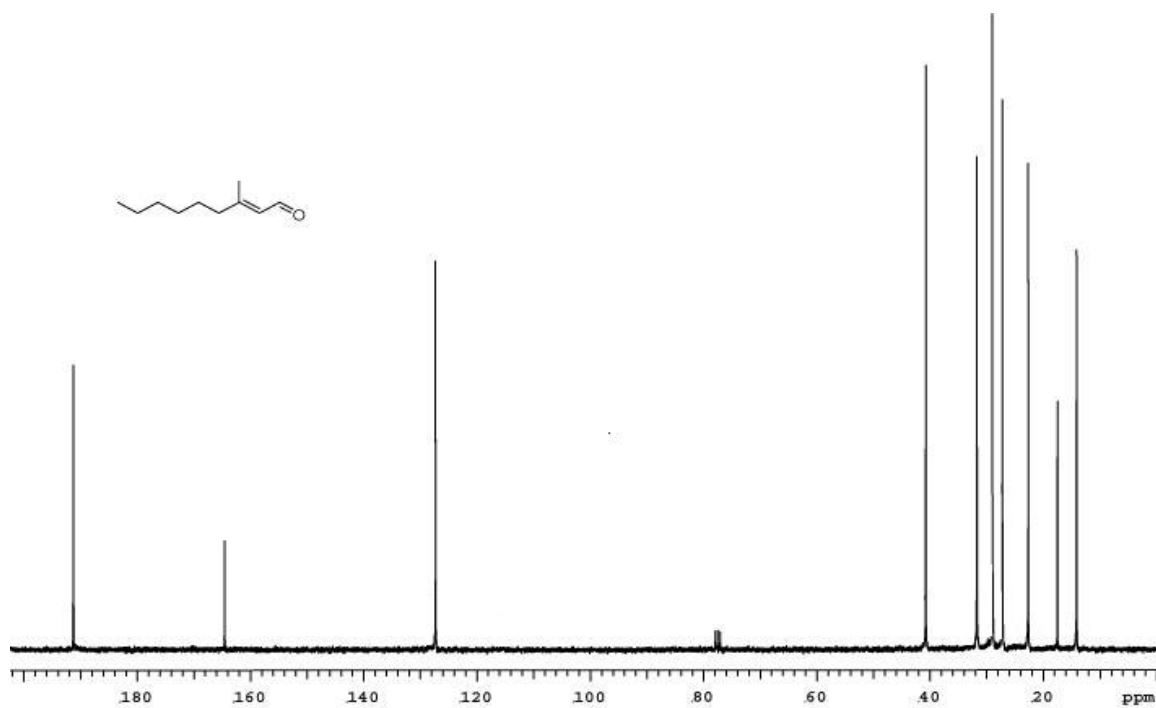
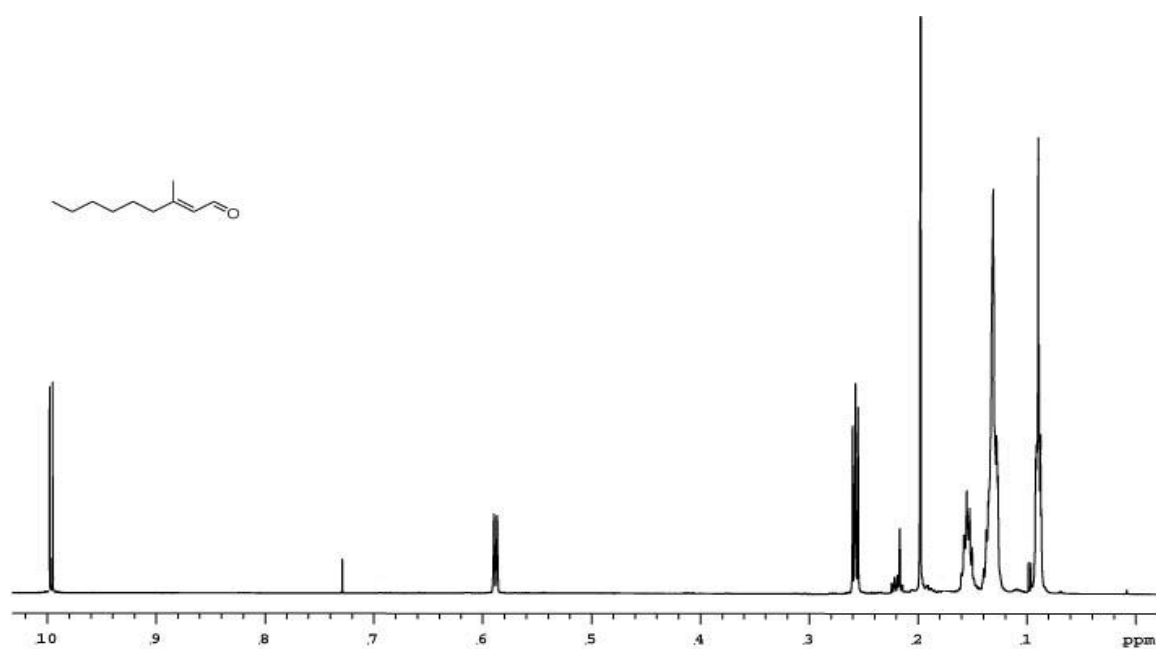


A-33. Spectra of 74.

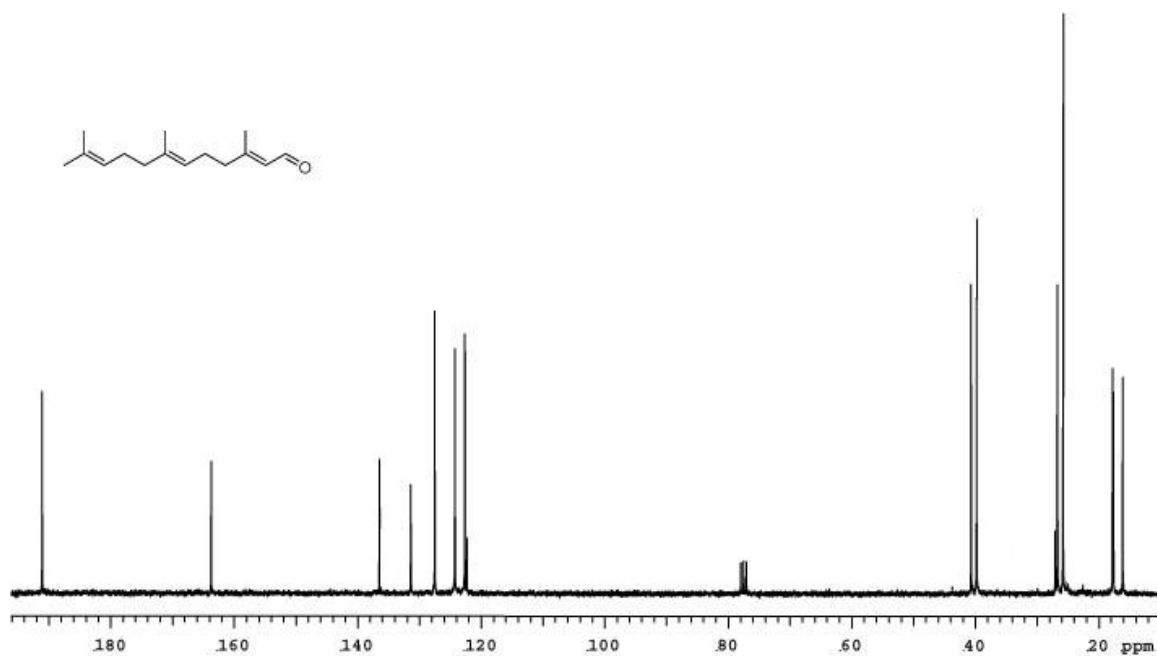
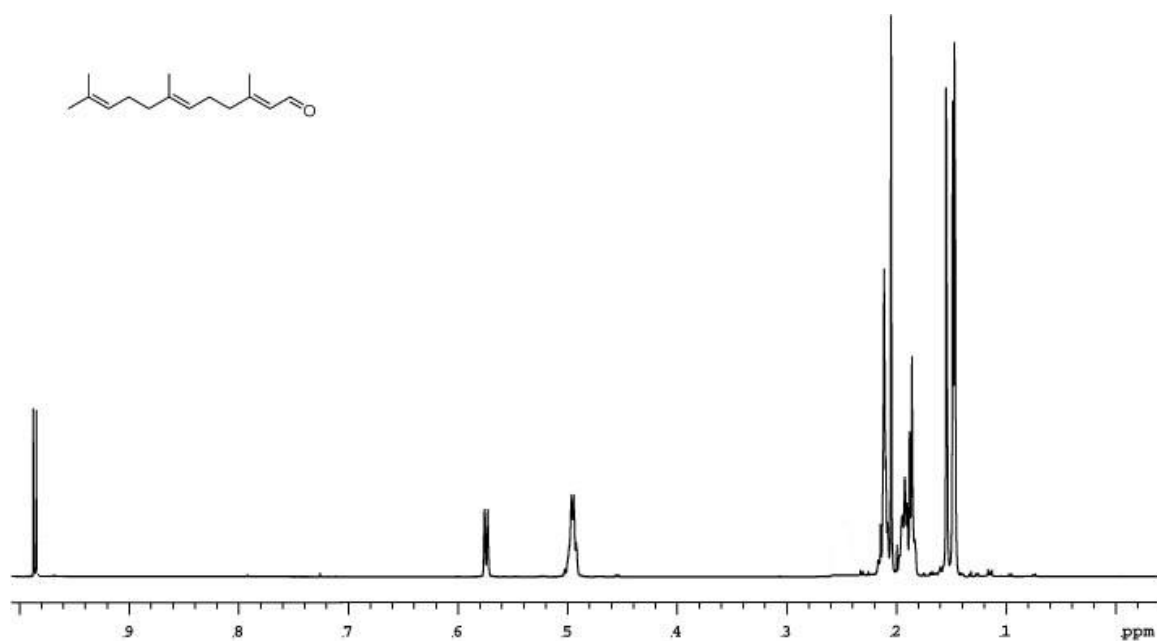


A-34. Spectra of 75.

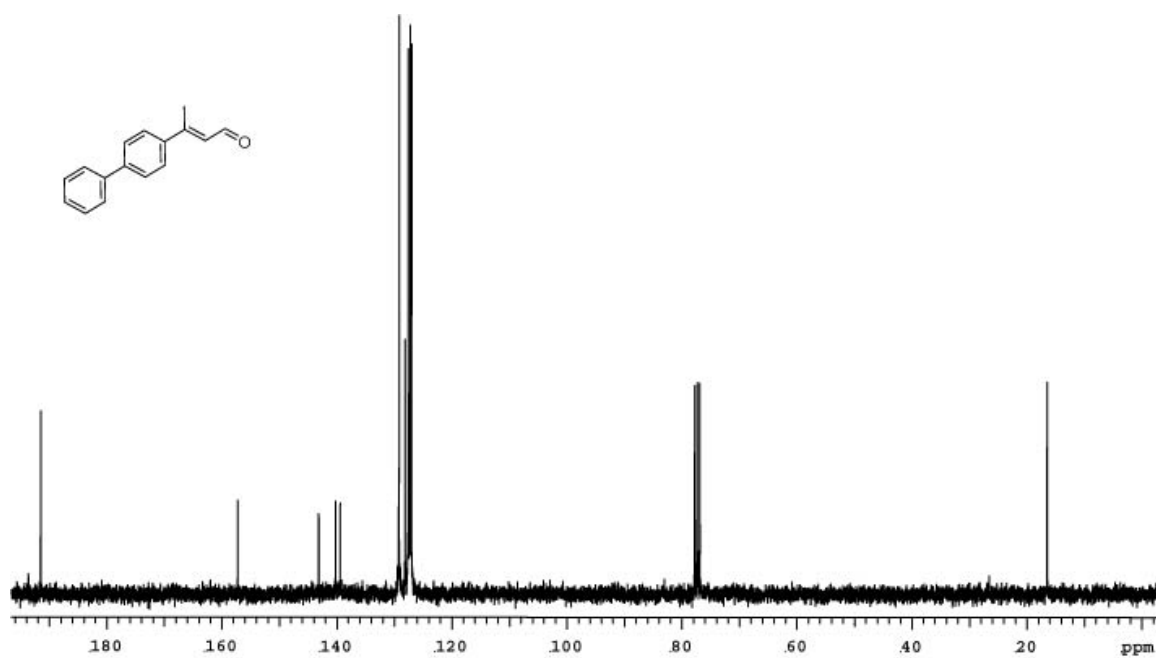
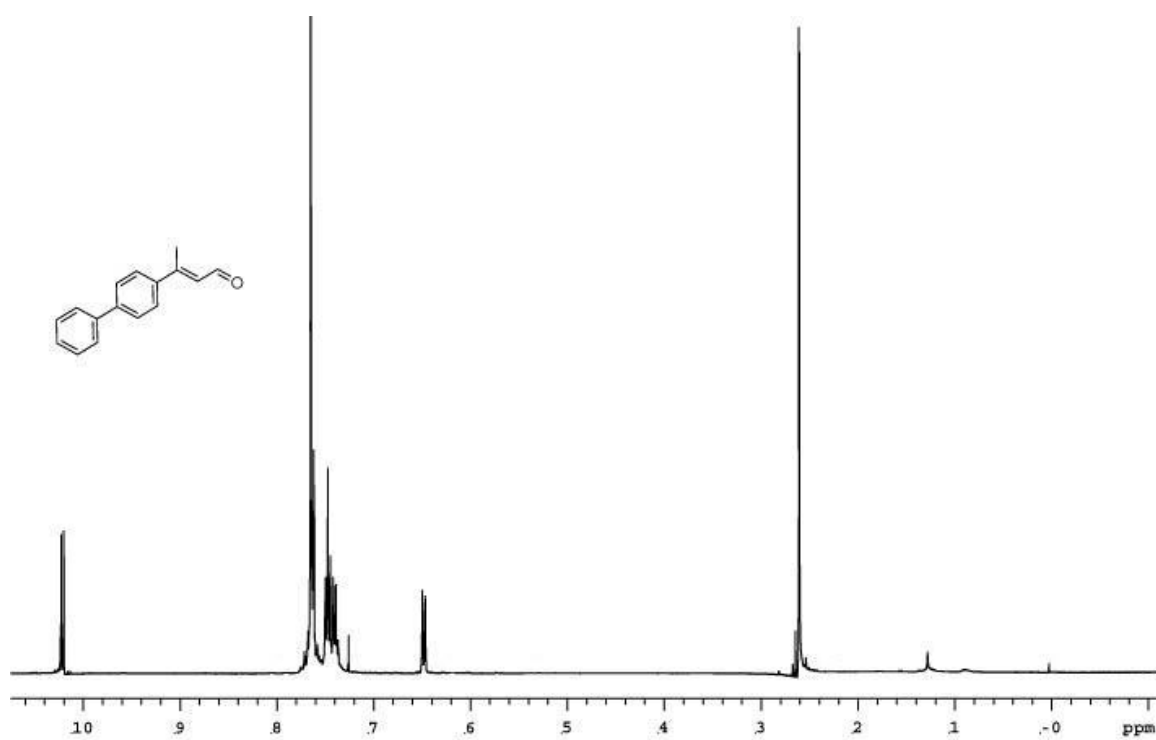




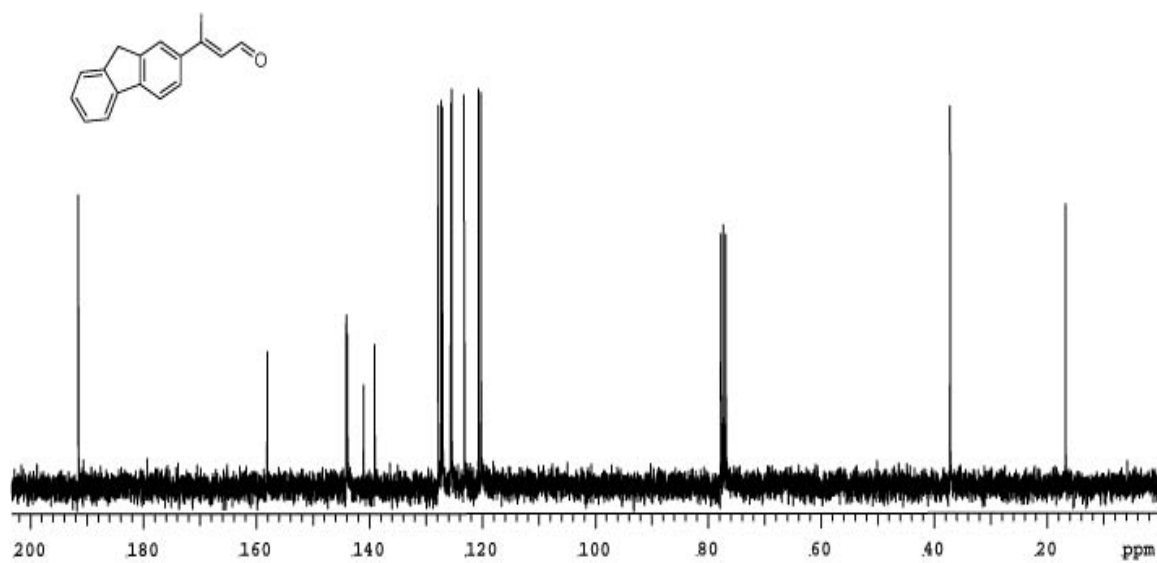
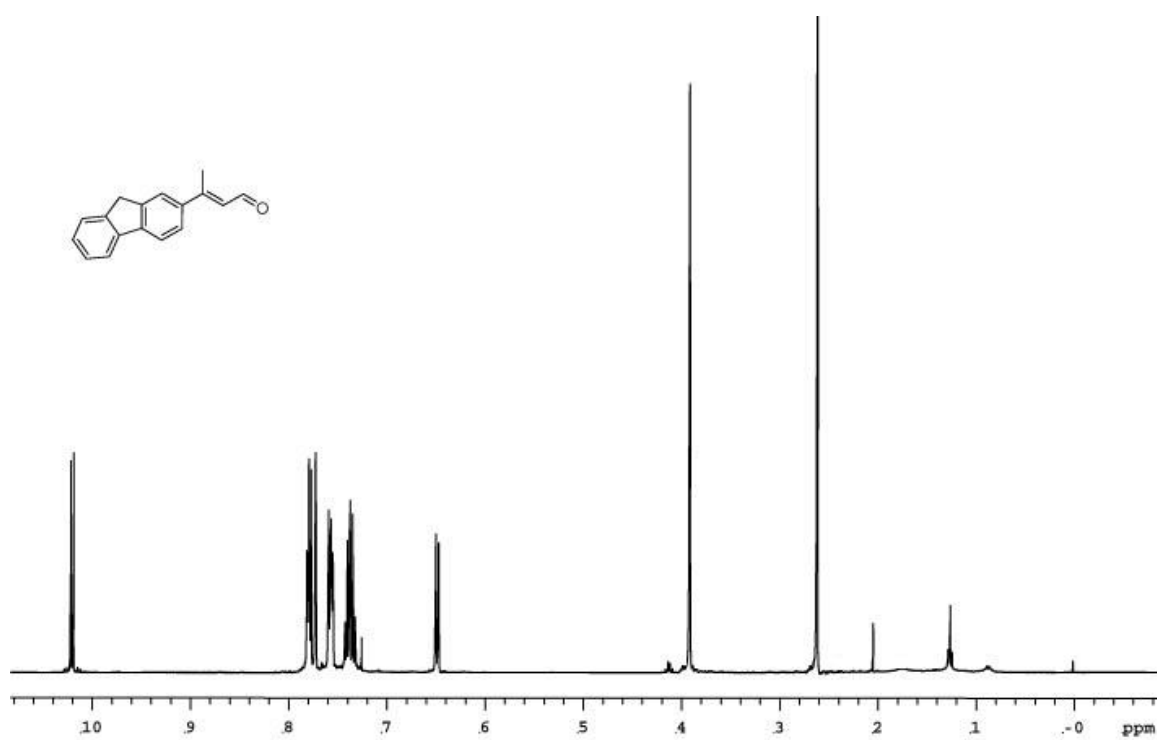
A-35. Spectra of 76.



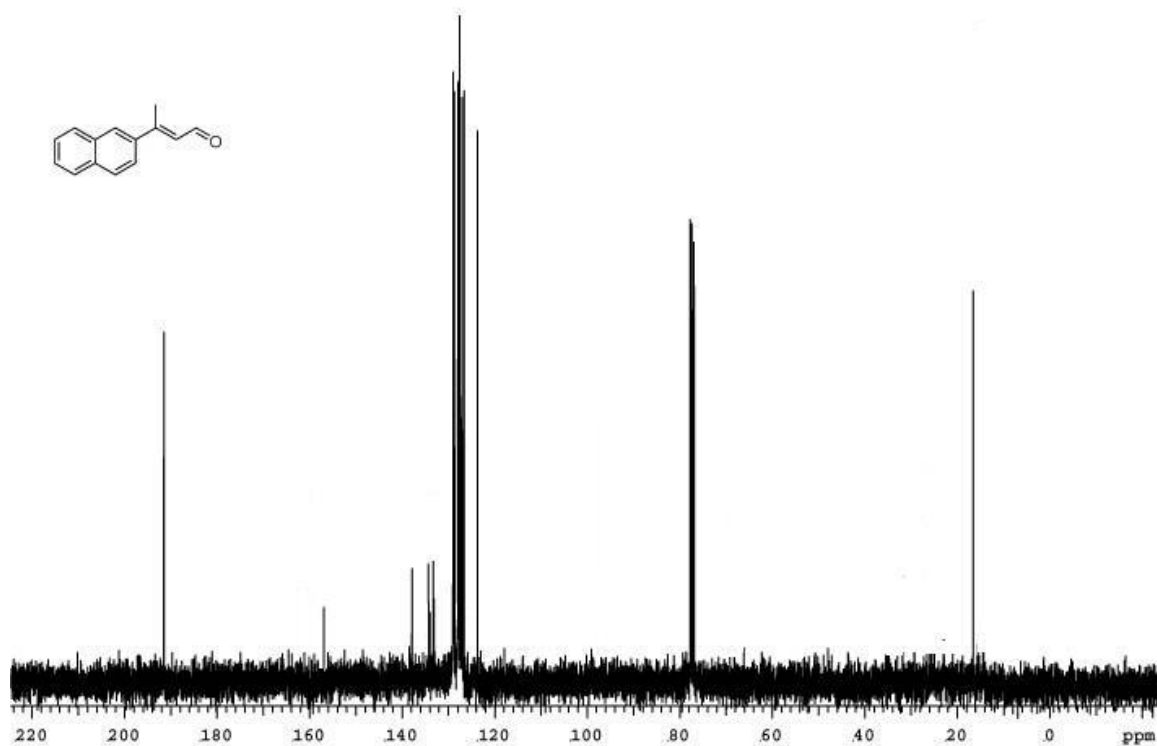
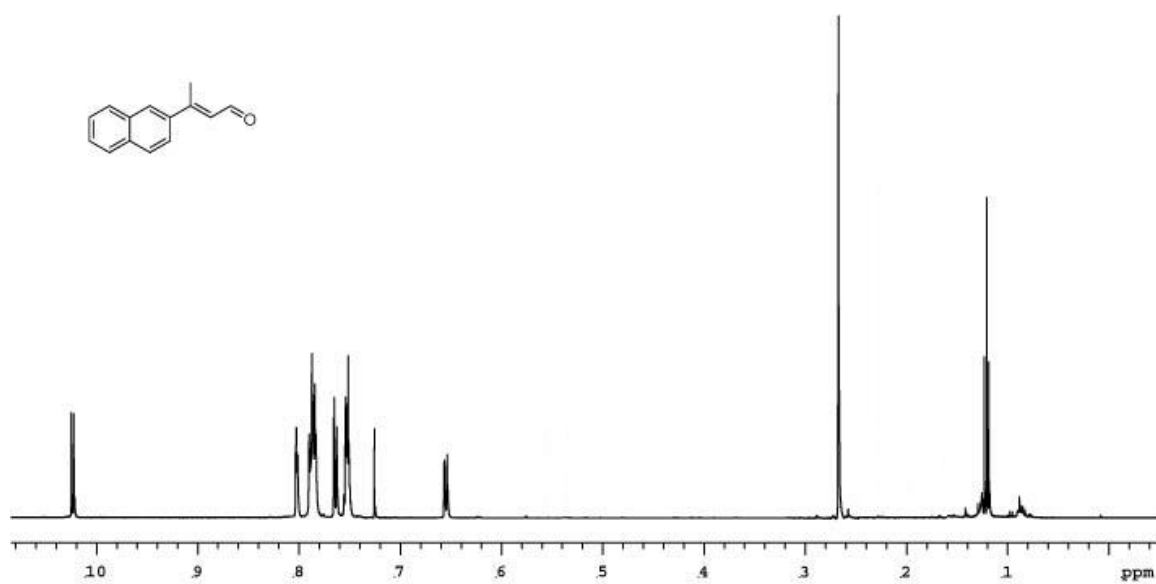
A-36. Spectra of 77.



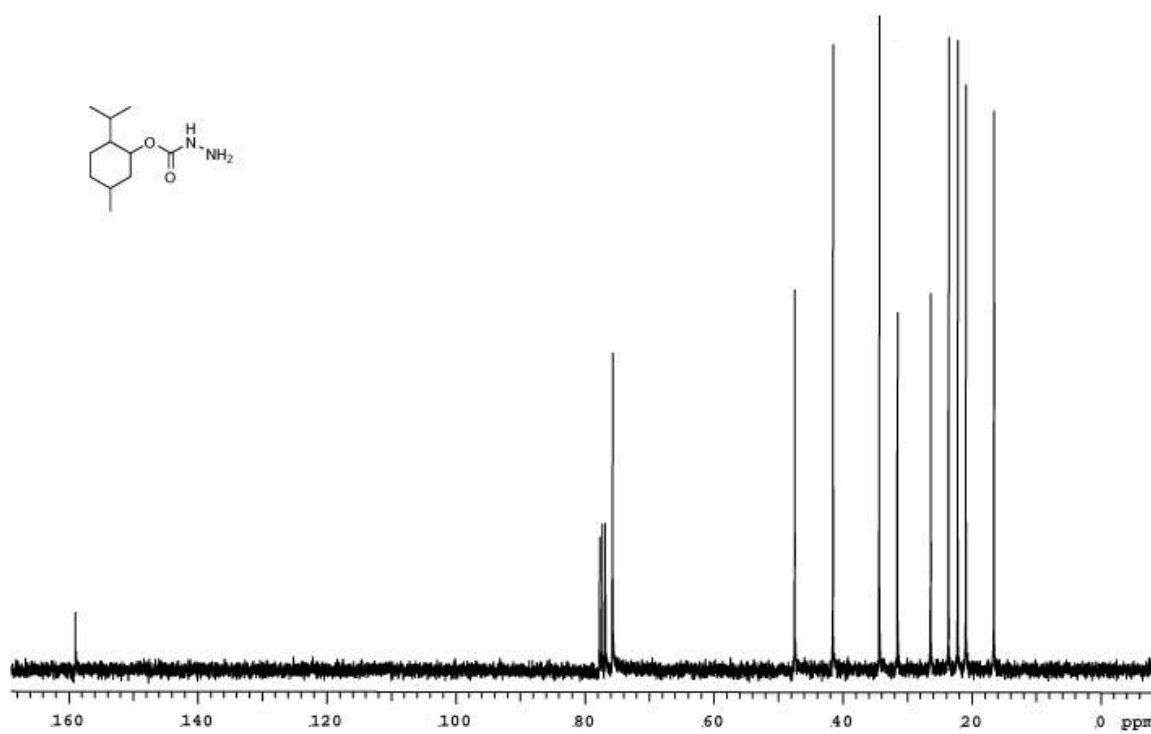
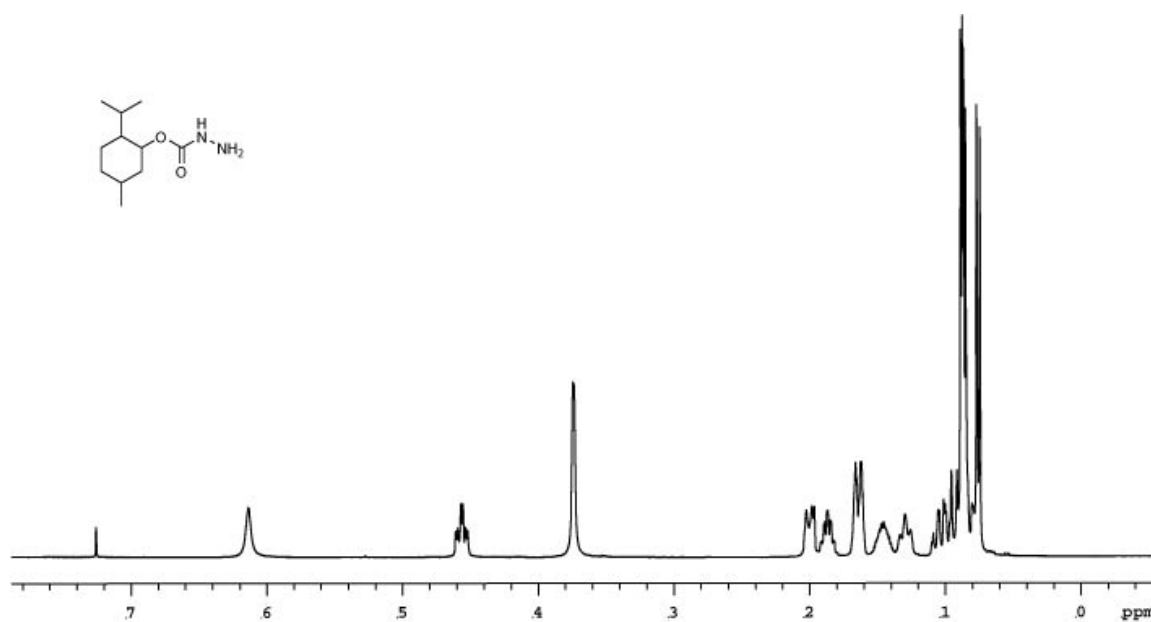
A-37. Spectra of 78.



A-38. Spectra of 79.

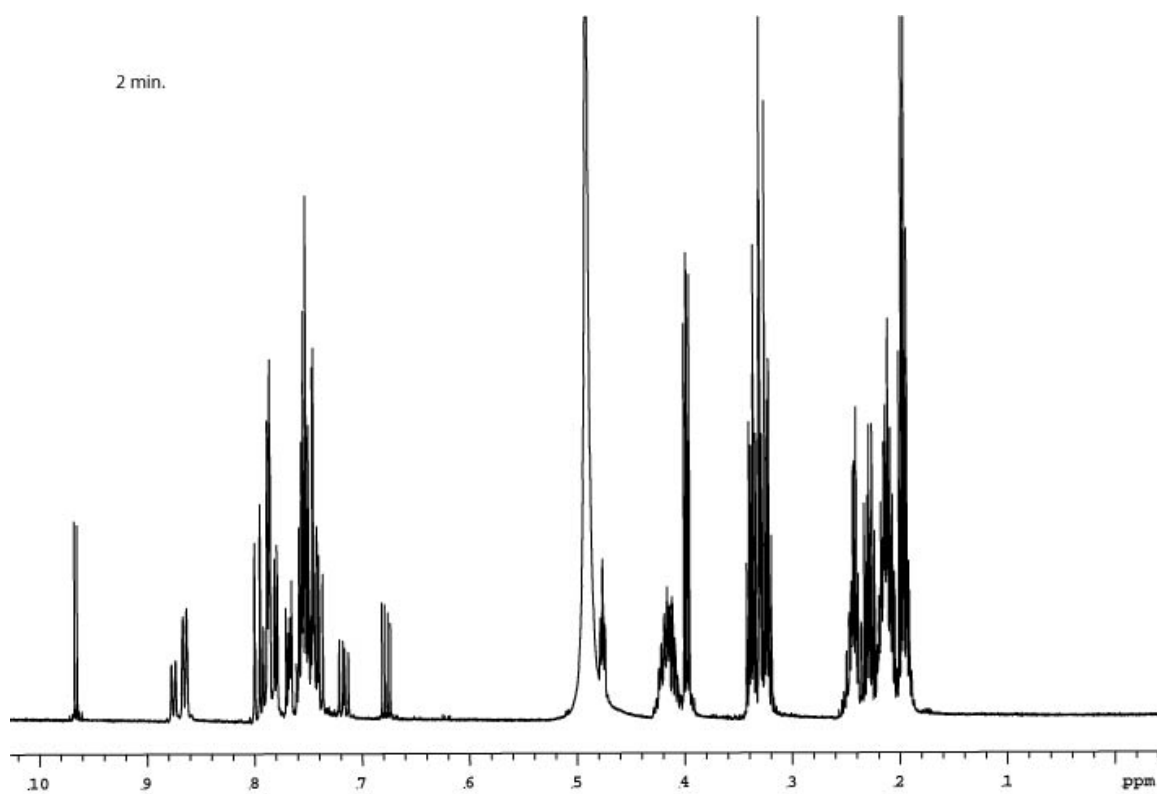
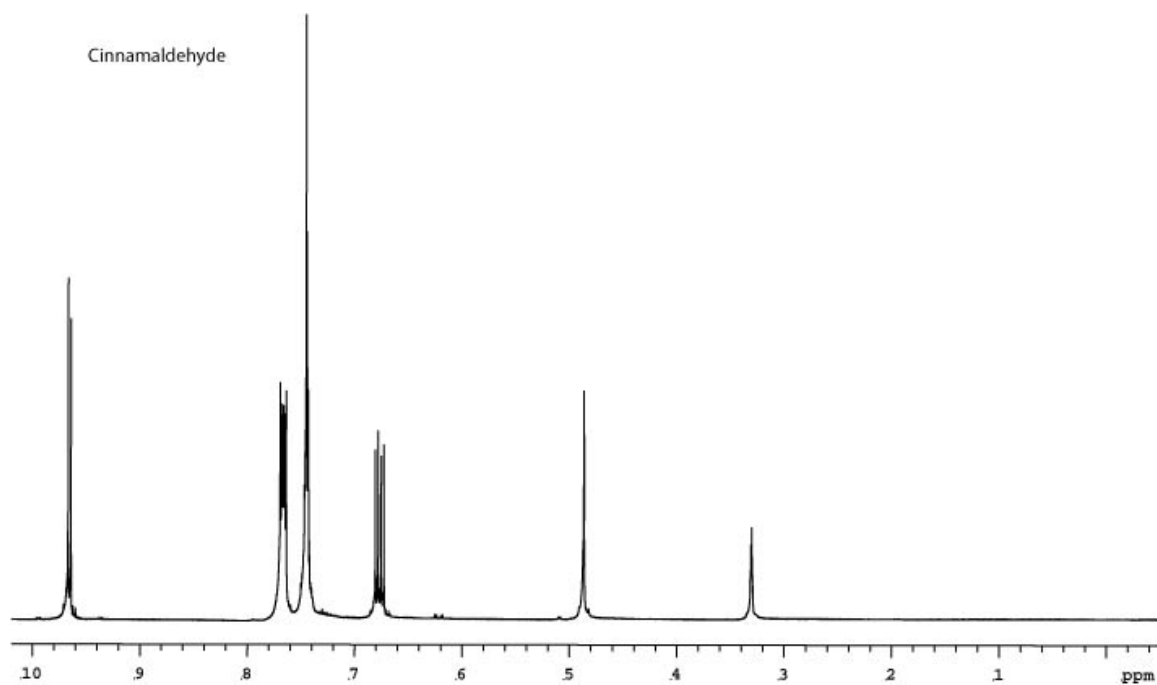


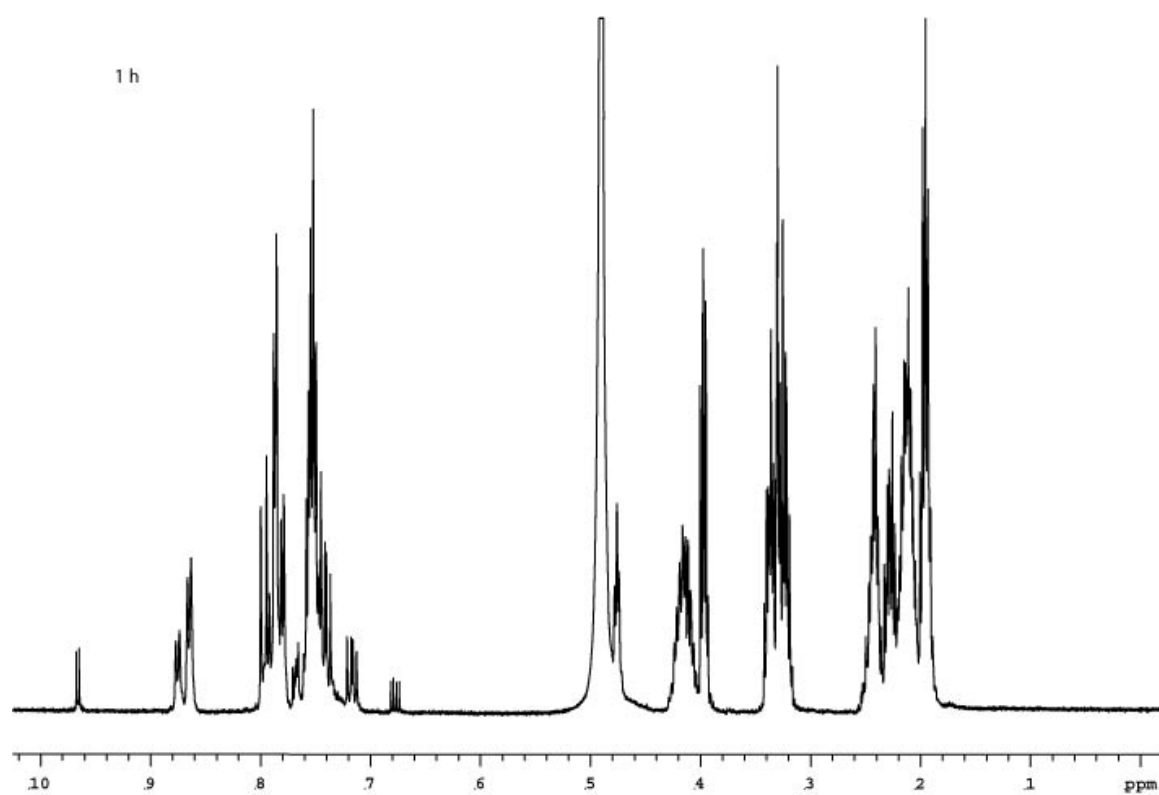
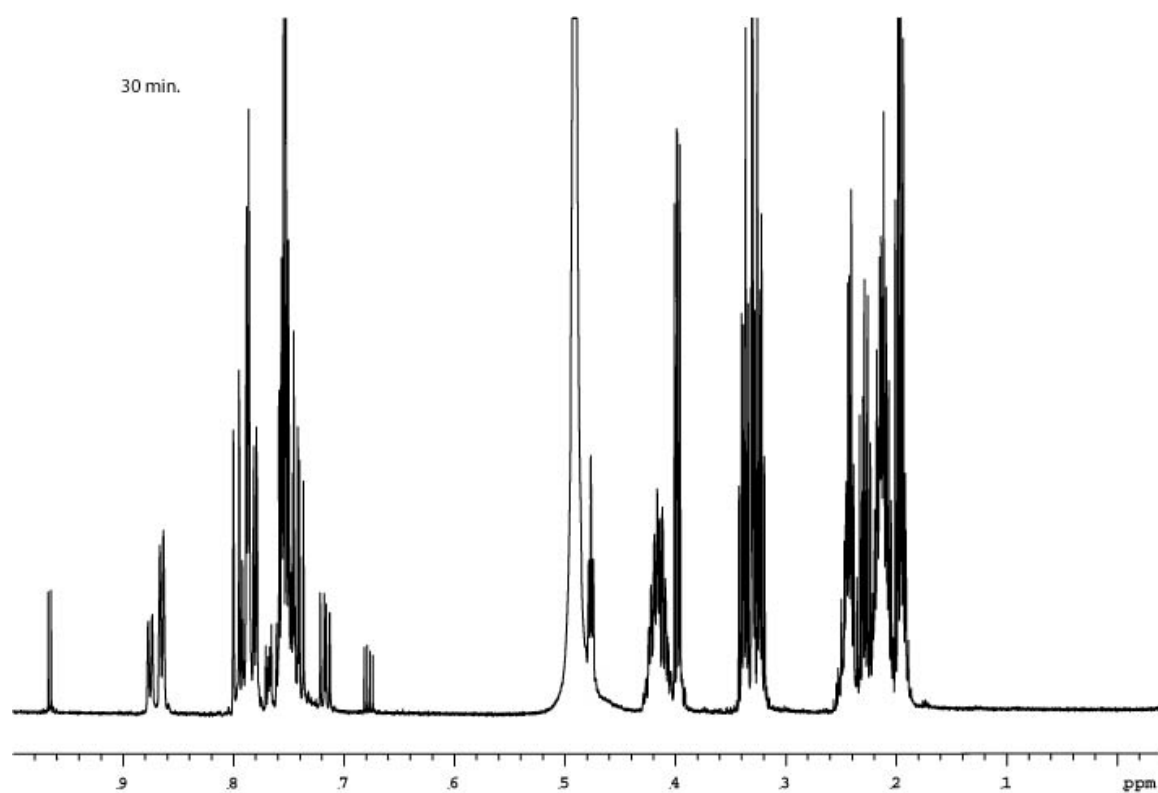
A-39. Spectra of 80.



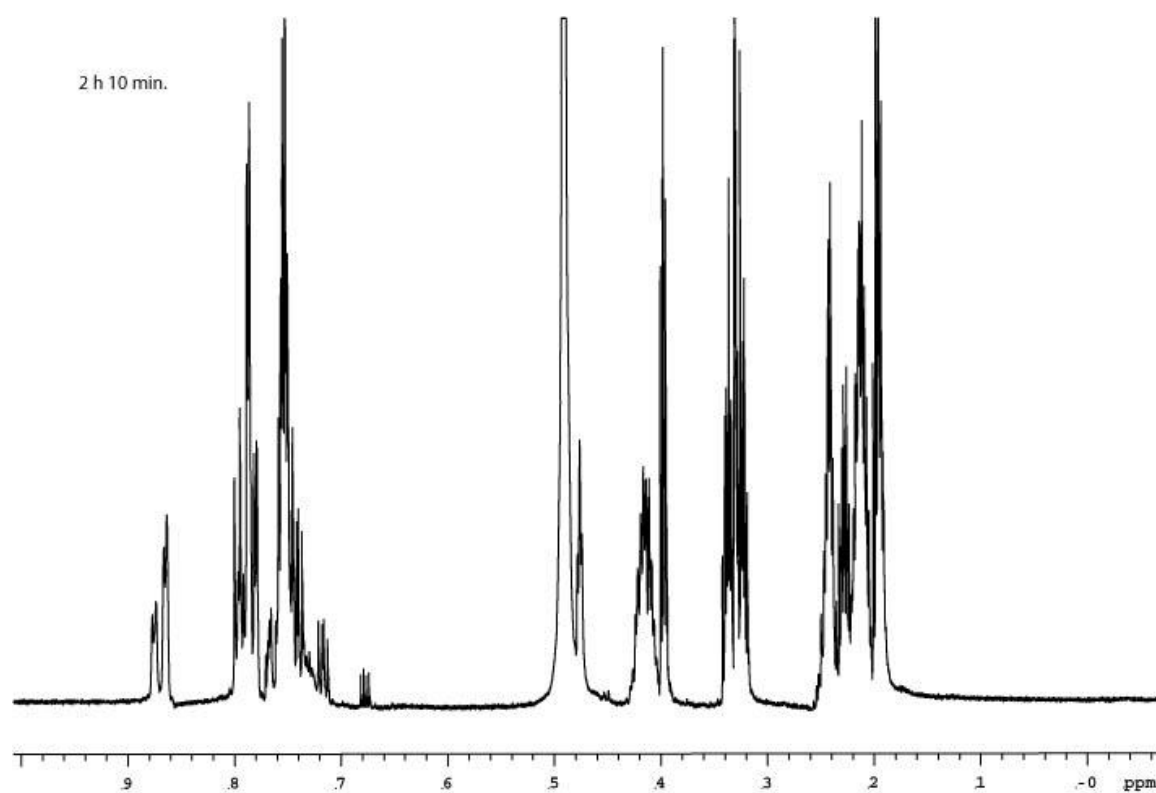
A-40. Spectra of 81.

## APPENDIX B

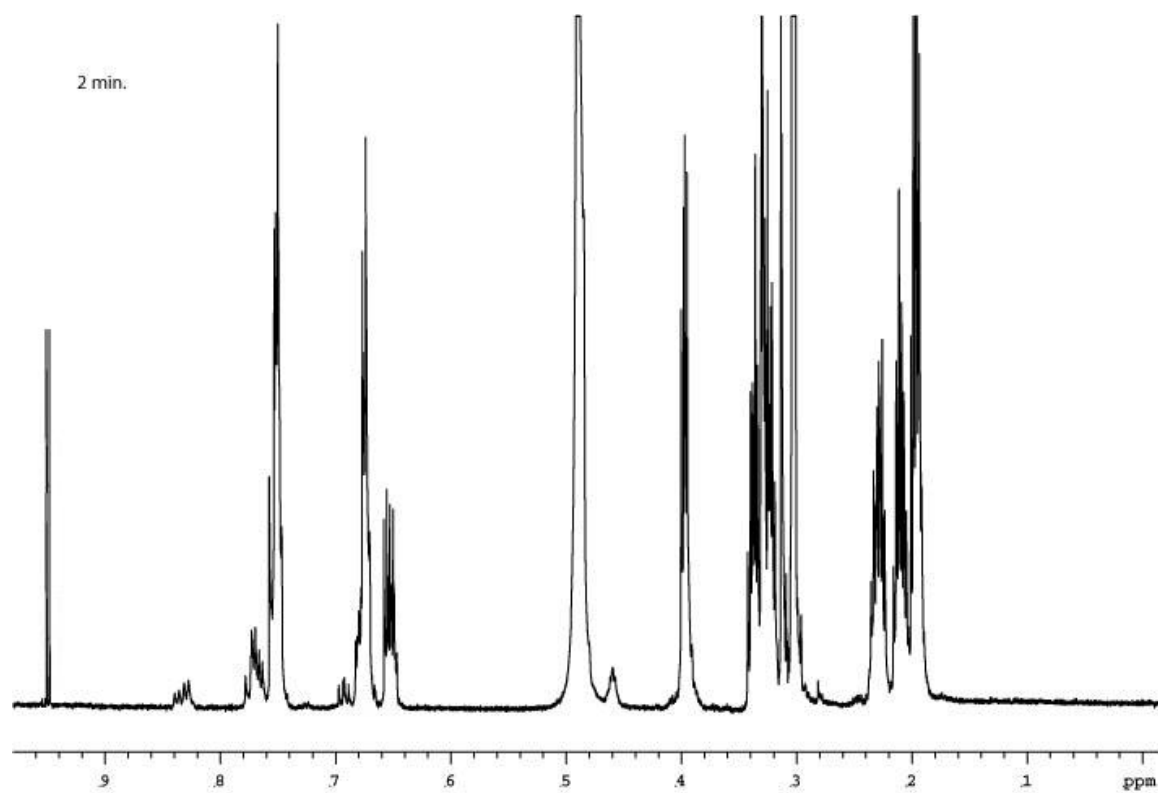
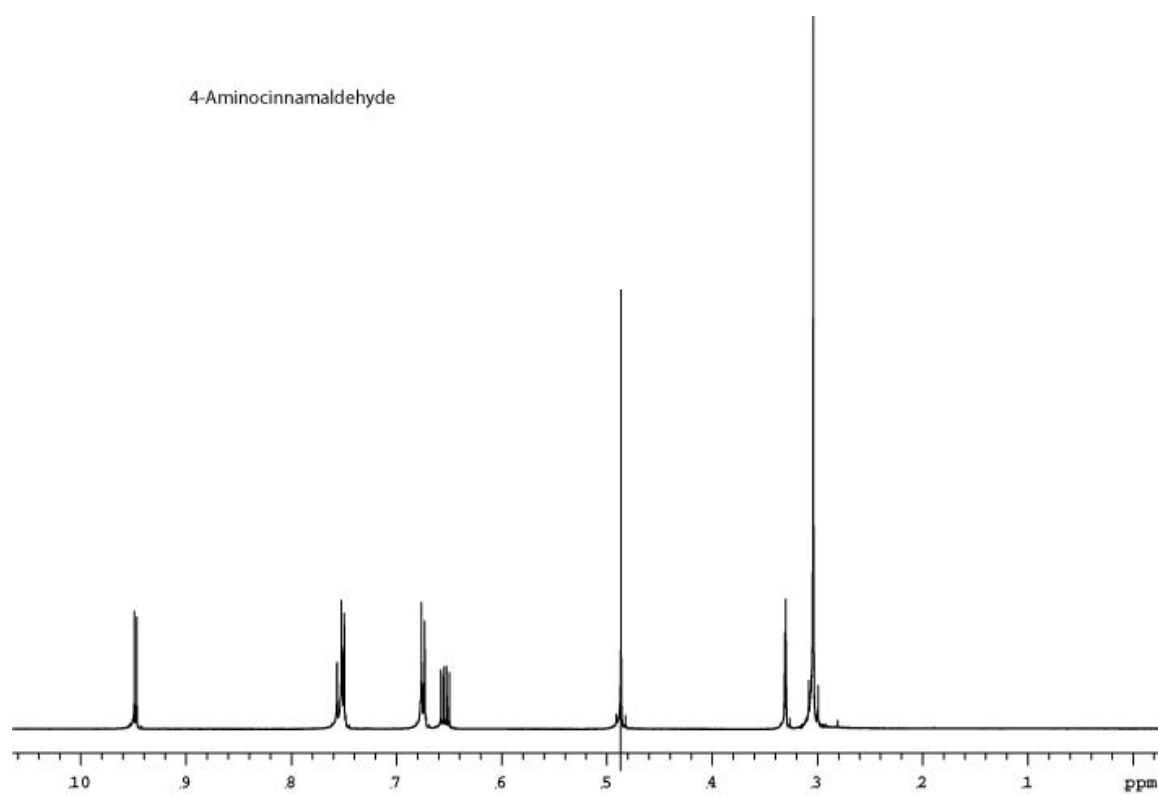


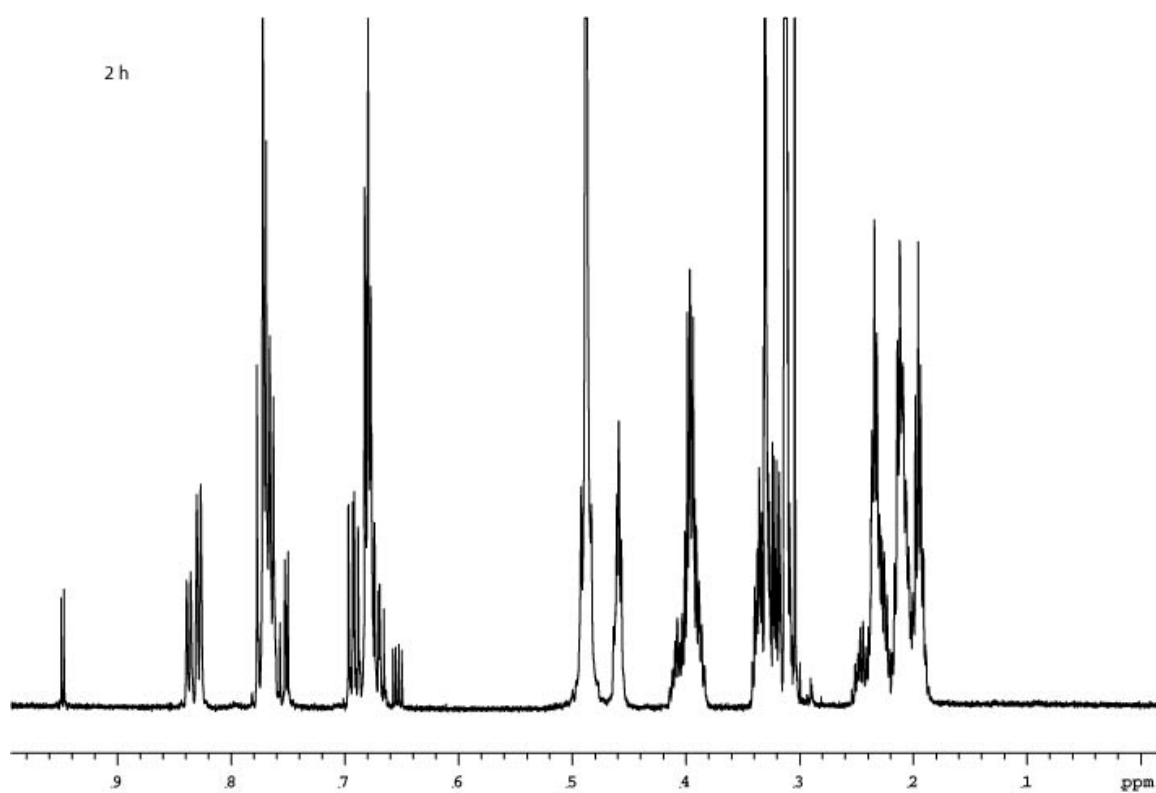
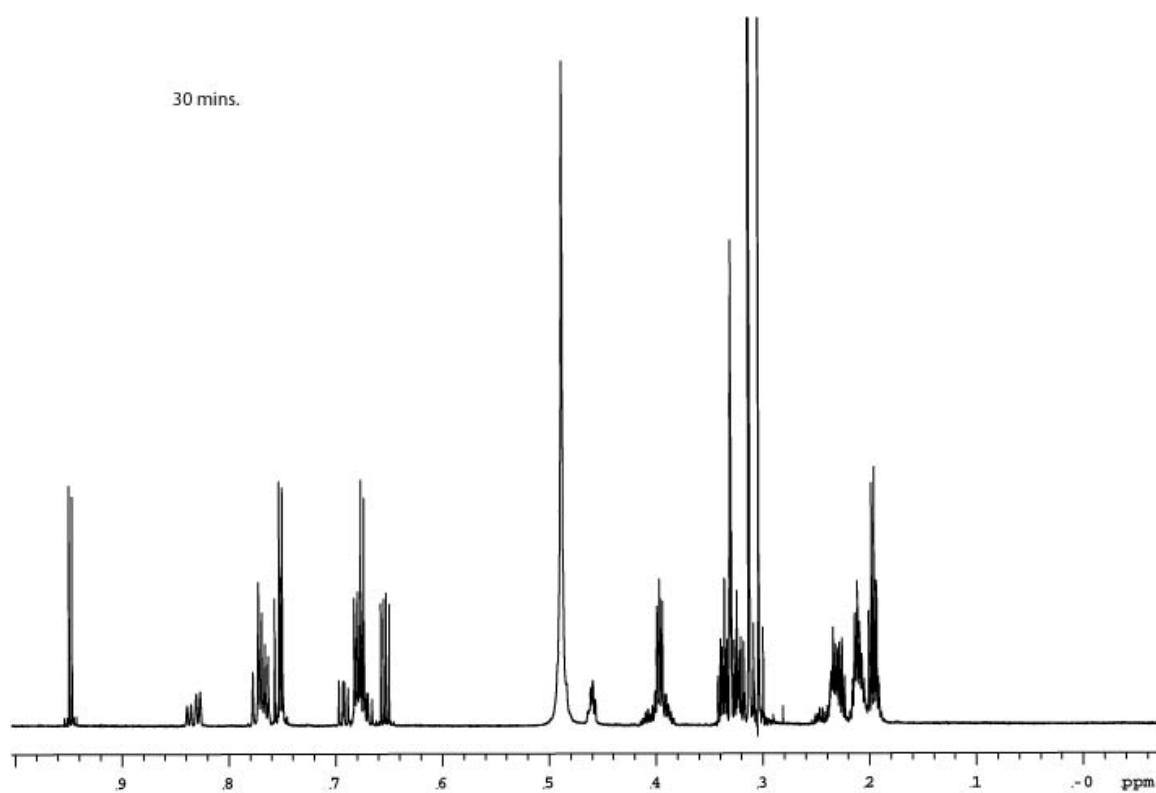


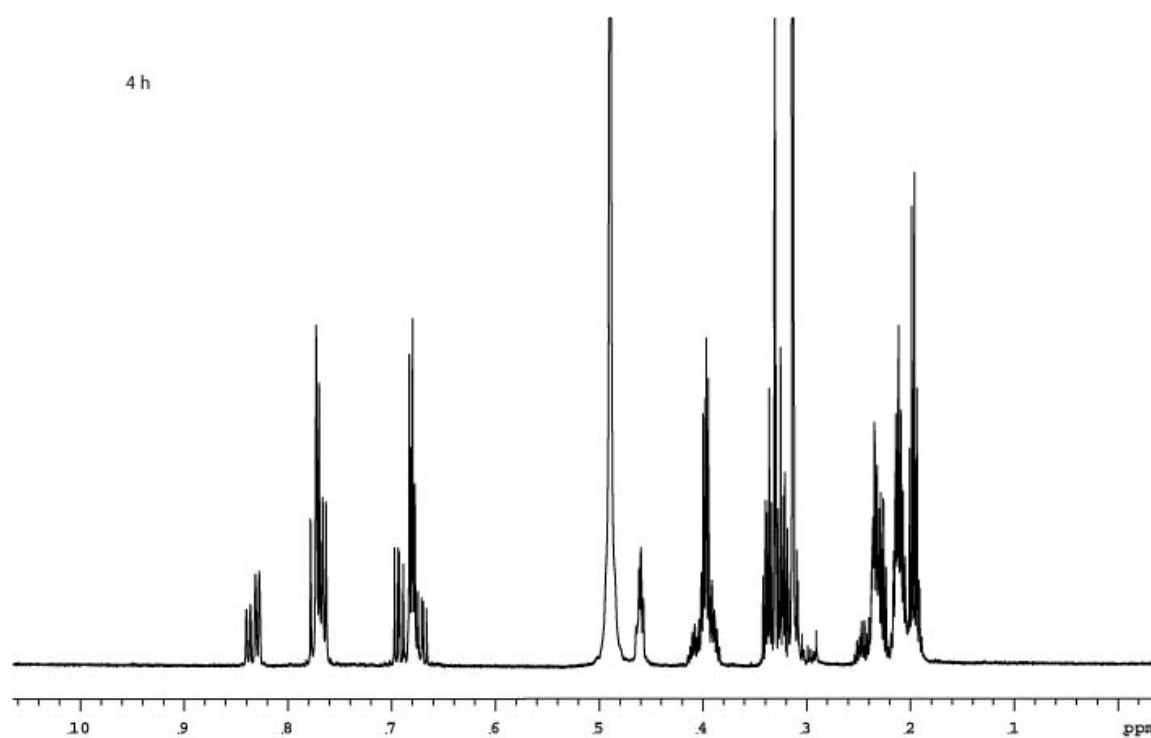




**B-1. Full <sup>1</sup>H spectra at various time points for cinnamaldehyde Schiff base.**

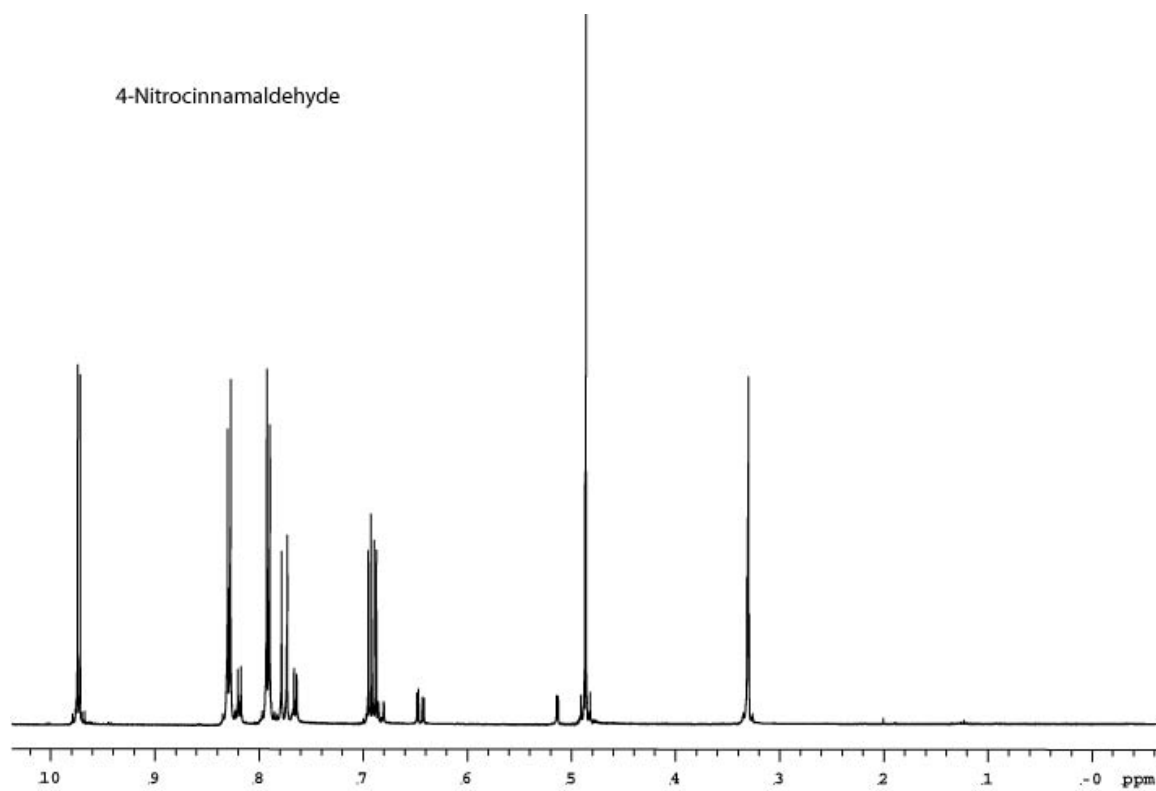
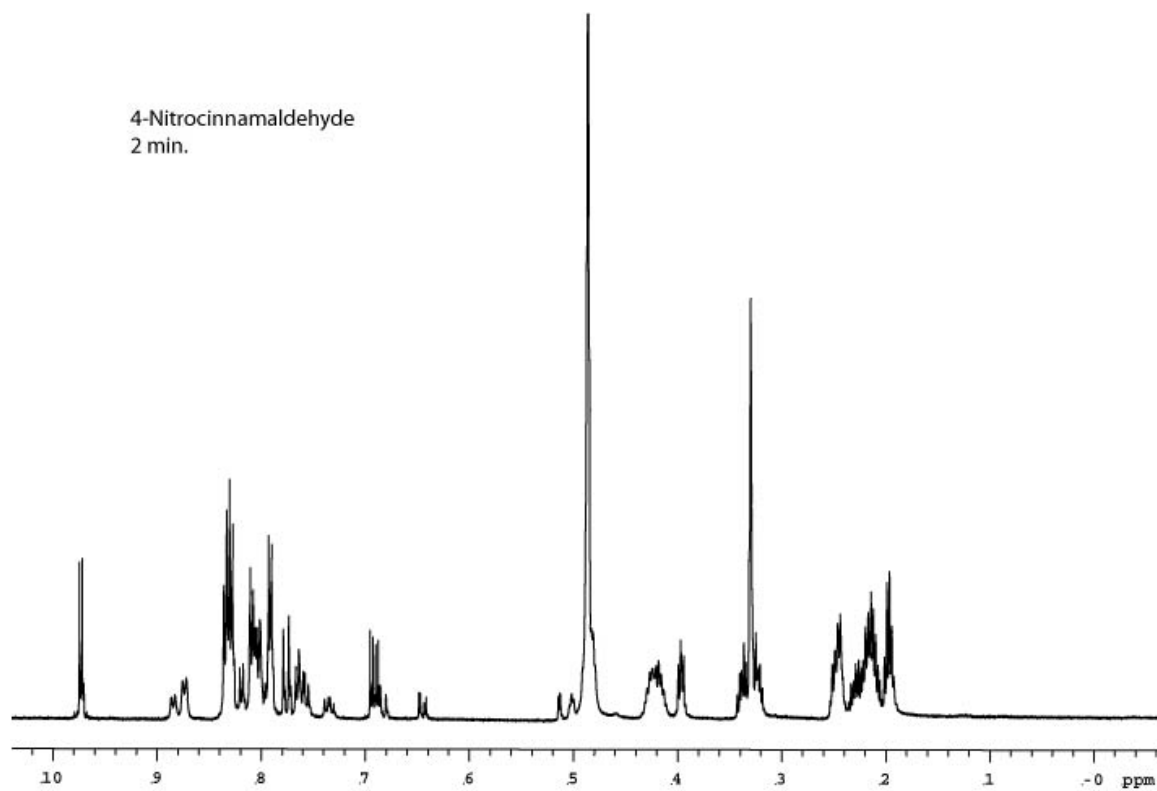


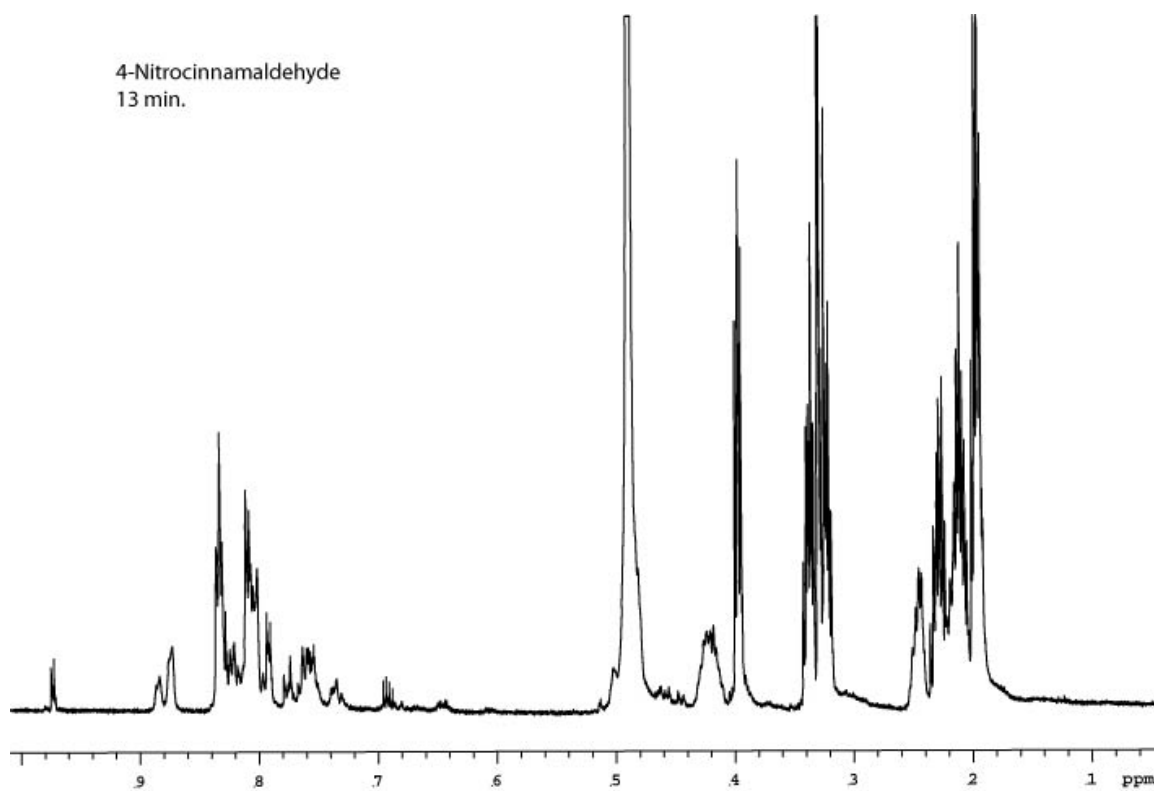
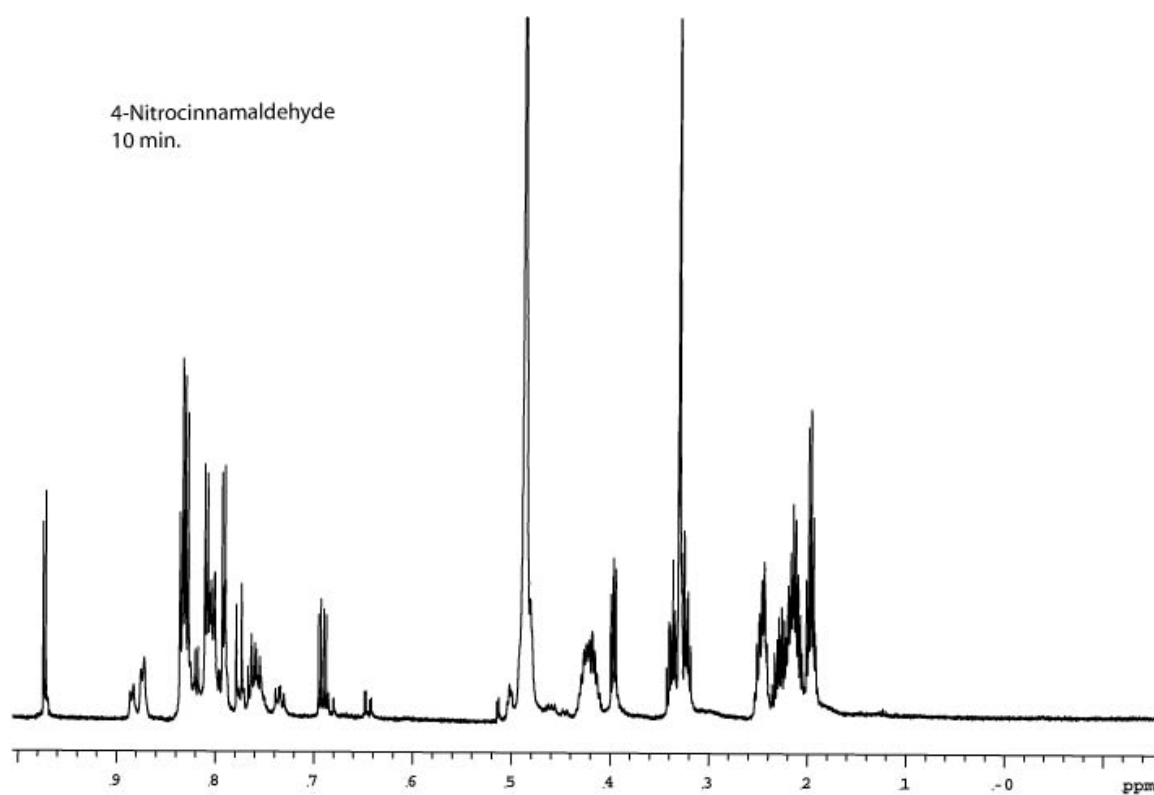


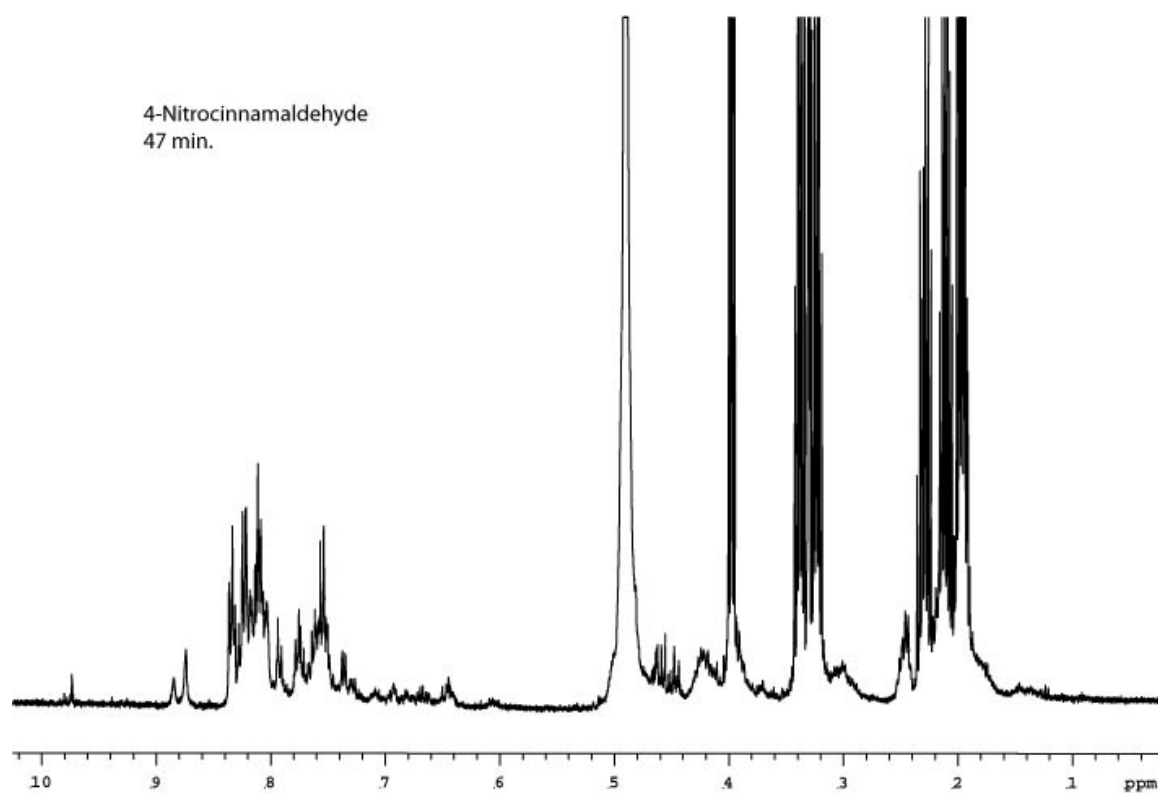
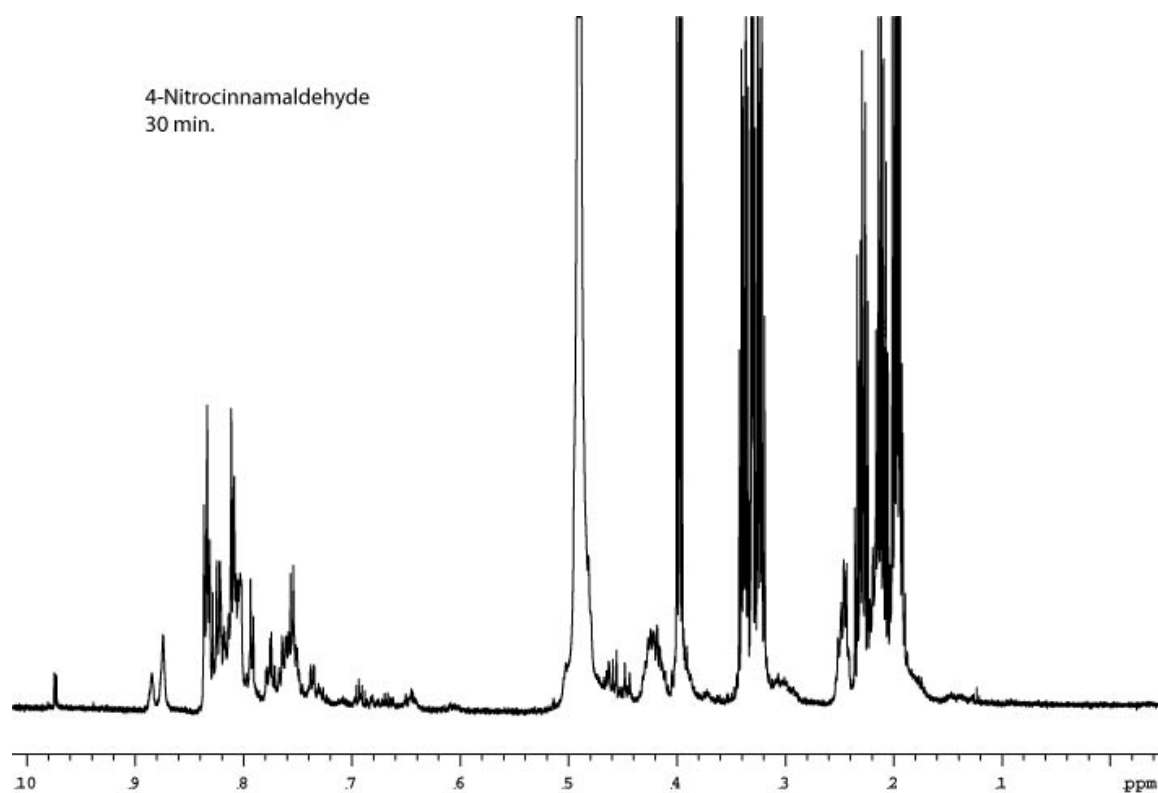


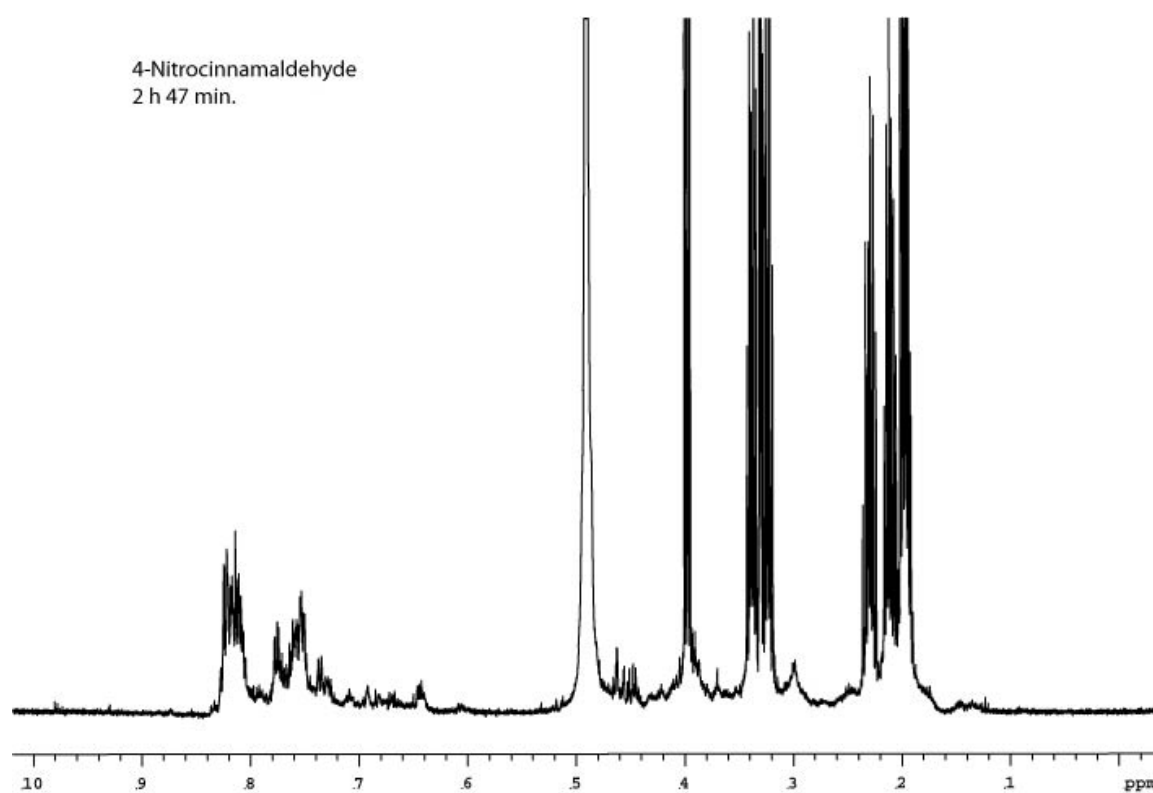
**B-2. Full <sup>1</sup>H Spectra at various time points for 4-dimethylamino-cinnamaldehyde Schiff base.**

4-Nitrocinnamaldehyde

4-Nitrocinnamaldehyde  
2 min.

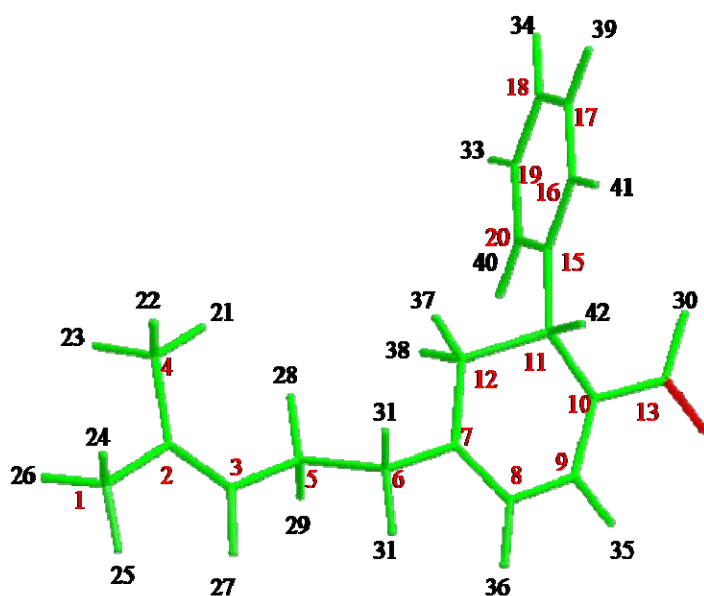




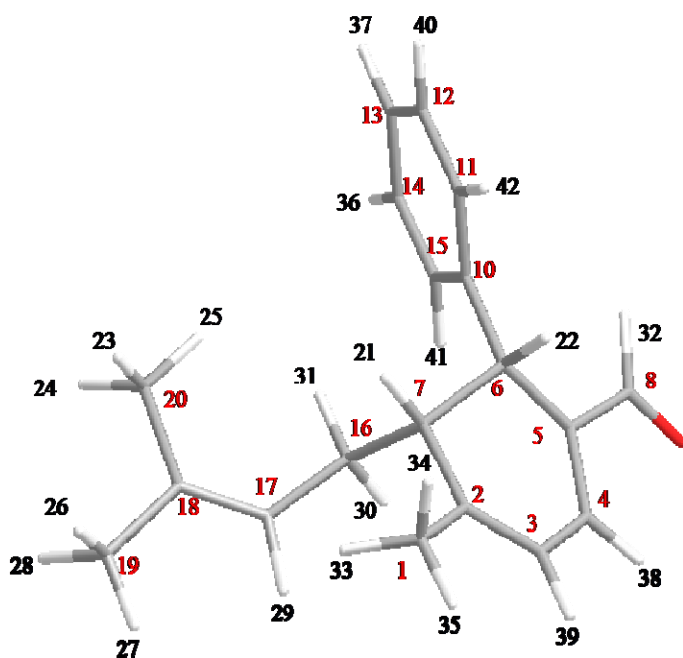


**B-3. Full <sup>1</sup>H Spectra at Various Time Points for 4-Nitro-Cinnamaldehyde Schiff Base.**





B-4. Numbering scheme for  $\beta$ -methyl product.



B-5. Numbering scheme for  $\gamma$ -methylene cis and trans products.

**B-6.** Table of bond distance between desired atoms thru space.

Distances between atoms		
	Atoms	Distance
cis	H(21)-H(22)	3.0424
	H(22)-H(31)	3.0474
	H(22)-H(30)	2.5894
	H(39)-H(38)	2.5022
trans	H(22)-H(21)	2.3793
	H(31)-H(21)	2.4651
	H(30)-H(21)	3.0566
	H(39)-H(38)	2.5199
Desired	H(42)-H(37)	2.4055
	H(42)-H(38)	3.0544
	H(38)-H(32)	3.4743
	H(38)-H(31)	3.9748
	H(37)-H(32)	2.5532
	H(37)-H(31)	3.7381
	H(36)-H(35)	2.5131

**B-7.** Table of NMR predictions of citral plus cinnamaldehyde products.

NMR predictions					
cis-isomer_cit+		desired_cit+cin		trans-isomer_ci	
C 1	0.00	C 1	0.00	C 1	0.00
C 2	0.00	C 2	0.00	C 2	0.00
C 3	0.00	C 3	0.00	C 3	0.00
C 4	0.00	C 4	0.00	C 4	0.00
C 5	0.00	C 5	0.00	C 5	0.00
C 6	0.00	C 6	0.00	C 6	0.00
C 7	0.00	C 7	0.00	C 7	0.00
C 8	0.00	C 8	0.00	C 8	0.00
O 9	0.00	C 9	0.00	O 9	0.00
C 10	0.00	C 10	0.00	C 10	0.00
C 11	0.00	C 11	0.00	C 11	0.00
C 12	0.00	C 12	0.00	C 12	0.00
C 13	0.00	C 13	0.00	C 13	0.00
C 14	0.00	O 14	0.00	C 14	0.00
C 15	0.00	C 15	0.00	C 15	0.00
C 16	0.00	C 16	0.00	C 16	0.00
C 17	0.00	C 17	0.00	C 17	0.00

C 18	0.00	C 18	0.00	C 18	0.00
C 19	0.00	C 19	0.00	C 19	0.00
C 20	0.00	C 20	0.00	C 20	0.00
H 21	1.78	H 21	2.08	H 21	3.63
H 22	4.40	H 22	1.32	H 22	2.71
H 23	1.07	H 23	1.33	H 23	0.76
H 24	1.12	H 24	1.67	H 24	0.59
H 25	1.44	H 25	1.57	H 25	0.81
H 26	1.68	H 26	1.81	H 26	1.62
H 27	1.66	H 27	5.48	H 27	1.64
H 28	1.61	H 28	2.62	H 28	1.53
H 29	5.34	H 29	1.59	H 29	5.74
H 30	2.15	H 30	9.56	H 30	2.45
H 31	2.12	H 31	2.28	H 31	1.83
H 32	9.83	H 32	2.15	H 32	9.23
H 33	2.17	H 33	7.59	H 33	2.06
H 34	2.04	H 34	7.49	H 34	2.19
H 35	1.89	H 35	7.52	H 35	1.90
H 36	7.63	H 36	6.25	H 36	7.65
H 37	7.50	H 37	2.25	H 37	7.52
H 38	7.53	H 38	2.77	H 38	7.36
H 39	6.39	H 39	7.58	H 39	6.01

H 40	7.58	H 40	7.70	H 40	7.58
H 41	7.68	H 41	7.40	H 41	7.61
H 42	7.54	H 42	4.06	H 42	7.53

**B-8.** Table of dihedral Angles and J-values of Selected Bonds.

## Dihedral Angles

	Bonds	Dihedrals	J-value
	H(29)-C(17)-C(16)-H(30)	-147.65	9.98
	H(29)-C(17)-C(16)-H(31)	-32.446	8.28
	H(30)-C(16)-C(7)-H(22)	-81.237	2.08
	H(31)-C(16)-C(7)-H(22)	165.21	12.31
Trans			
product	H(41)-C(15)-C(14)-H(36)	0.3983	11
	H(36)-C(14)-C(13)-H(37)	0.2499	11
	H(37)-C(13)-C(12)-H(40)	0.0839	11
	H(40)-C(12)-C(11)-H(42)	-0.2413	11
	H(22)-C(7)-C(6)-H(21)	160.2	11.79
	H(38)-C(4)-C(3)-H(39)	6.3471	10.88

	H(29)-C(17)-C(16)-H(31)	157.1	11.41
	H(29)-C(17)-C(16)-H(30)	40.64	7
	H(31)-C(16)-C(7)-H(21)	61.883	3.75
	H(30)-C(16)-C(7)-H(21)	176.59	12.96
Cis			
product	H(41)-C(15)-C(14)-H(36)	0.11	11
	H(37)-C(13)-C(12)-H(40)	-0.1052	11
	H(40)-C(12)-C(11)-H(42)	0.0087	11
	H(21)-C(7)-C(6)-H(22)	55.602	4.63
	H(38)-C(4)-C(3)-H(39)	11.676	10.61
	H(35)-C(9)-C(8)-H(36)	9.3054	10.75
	H(32)-C(6)-C(5)-H(29)	178.09	12.99
	H(32)-C(6)-C(5)-H(28)	62.709	3.64
Desired	H(31)-C(6)-C(5)-H(29)	-66.222	3.22
	H(31)-C(6)-C(5)-H(28)	178.4	12.99
	H(29)-C(5)-C(3)-H(27)	56.755	4.48
	H(28)-C(5)-C(3)-H(27)	174.02	12.89

**B-9.** Table of total Nuclear Spin-Spin Couplings for Cis Product.

Cis Product

Total nuclear spin-spin coupling J(Hz)

	1	2	3	4	5
1	0.000000				
2	41.862800	0.000000			
3	2.612210	71.893900	0.000000		
4	5.136900	-2.937690	53.219600	0.000000	
5	-1.208270	7.516430	-2.825330	70.385500	0.000000
6	2.183560	-2.246380	5.249840	0.129298	41.589400
7	1.676650	38.531300	0.040648	4.804590	-2.557860
8	0.693838	-1.858610	4.903180	0.658931	54.475000
9	0.166942	-2.068580	1.160440	-6.593110	1.688840
10	0.106285	3.633080	-0.451467	2.556150	-1.203260
11	0.054285	-0.095191	0.102004	0.345540	2.790520
12	-0.025429	-0.014007	0.004850	0.117538	0.271804
13	0.021175	0.041142	-0.038651	0.031568	0.167495
14	-0.036791	0.067195	-0.004024	-0.032640	-0.158761
15	-0.006239	0.170241	-0.022400	-0.100456	1.221040
16	0.636831	-2.435420	2.140770	-1.407760	2.490880

17	0.142680	0.896143	-0.069963	0.015173	-0.148480
18	0.385495	-0.146360	0.058912	-0.036266	0.091555
19	-0.153877	0.033133	-0.009640	-0.000947	-0.010167
20	-0.129436	0.039566	0.009145	-0.015354	0.010791
21	3.770460	-5.034930	4.295770	-0.793500	6.779000
22	-1.189920	4.765760	-3.479080	5.035080	-8.022380
23	0.405810	-0.016263	-0.010704	-0.023084	-0.018845
24	0.343816	-0.124683	0.019370	-0.050681	0.014804
25	-0.002197	0.001021	-0.014732	-0.018641	0.000963
26	0.261355	-0.107005	0.019666	-0.034553	-0.007111
27	0.044085	-0.008361	0.025626	-0.017544	0.002785
28	0.217588	-0.093787	0.012423	-0.019760	0.008306
29	1.344940	-0.114493	0.223788	-0.068768	0.095023
30	-0.208177	1.972950	-0.196544	0.272156	-0.047372
31	0.016065	7.040730	0.242549	-0.242776	0.031247
32	-0.009953	0.006962	1.257720	2.760480	22.268600
33	120.956000	-8.009170	7.137510	-2.354040	2.255700
34	119.509000	-8.294150	6.099510	-3.244080	2.783100
35	120.464000	-3.600730	5.771890	0.138248	-0.025408
36	-0.004624	0.022976	-0.038940	0.013119	0.024014
37	-0.048813	-0.041598	-0.044680	-0.020489	-0.192522
38	0.156911	7.386420	2.309190	154.020000	-1.991150



39	5.983860	-0.645620	150.797000	2.626490	5.812110
40	0.006893	0.014816	-0.017420	0.026241	0.173843
41	-0.056723	0.073608	-0.107725	0.180322	-0.204997
42	-0.019076	-0.038329	-0.000619	-0.002593	-0.129723
	6.00	7.00	8.00	9.00	10.00
6	0.000000				
7	32.283100	0.000000			
8	4.244610	1.987000	0.000000		
9	-0.210710	0.307581	34.989500	0.000000	
10	43.919500	-1.798860	2.102250	0.127505	0.000000
11	3.703460	1.186870	-0.222416	0.051622	59.983900
12	3.723640	-0.937777	0.037020	0.009595	-1.693050
13	-0.758126	0.907480	-0.012039	0.027450	9.154140
14	2.974890	-0.906011	0.037888	0.000332	-1.744370
15	1.669250	0.878206	0.507589	-0.000481	58.130300
16	-0.951551	31.709000	-0.551637	-0.325896	1.426180
17	3.783570	-2.083750	0.112478	0.001097	-0.084204
18	0.003548	2.607100	-0.020573	-0.034197	-0.010468
19	0.195802	-0.889258	0.006247	0.001931	-0.003675
20	-0.023357	-0.814940	-0.001580	0.000932	0.015821
21	-2.453040	128.223000	0.909011	-0.143036	1.002520
22	118.336000	-6.794620	1.832650	1.071560	-6.480860

23	0.026554	1.607630	-0.013356	0.014654	0.018892
24	-0.013213	1.496120	-0.023304	-0.001986	0.025246
25	0.028397	0.095135	-0.000026	0.015586	0.090962
26	0.132689	2.645490	-0.016492	0.003477	0.001556
27	0.000089	0.062361	-0.007423	-0.002501	-0.003767
28	-0.040197	2.059730	-0.016611	-0.003233	-0.002362
29	-0.092959	0.807794	-0.014090	-0.057526	0.099028
30	2.181890	-5.148880	0.159571	-0.054320	-0.250075
31	1.435820	-3.931040	-0.043387	-0.004310	0.140554
32	-0.077705	-0.157623	162.583000	-4.176310	0.138306
33	-1.576620	3.144520	-1.271590	-0.496692	0.295734
34	-1.791010	2.250810	-1.574620	-0.606709	0.216340
35	0.697796	7.157510	-0.077945	0.023629	0.187045
36	0.594056	0.243879	-0.028885	0.011271	6.767750
37	0.530886	-0.694656	0.006607	0.036197	-1.356680
38	6.466750	-1.265690	5.325740	-0.104002	0.137673
39	-1.152300	5.828710	-0.027341	-0.071419	-0.033038
40	0.379792	0.322239	-0.082333	0.050663	6.706050
41	2.709250	-0.737425	0.532786	-0.119920	0.330187
42	4.574030	-0.765870	-0.018125	0.113844	0.197976
11		12	13	14	15
11	0.000000				

12	59.304600	0.000000			
13	-2.163410	58.898800	0.000000		
14	9.065780	-1.672300	58.987500	0.000000	
15	-0.412134	8.932370	-2.185450	59.340300	0.000000
16	-0.161650	0.098384	-0.046934	0.080722	0.510308
17	-0.004732	0.009109	-0.012176	0.022971	0.103076
18	0.000400	-0.007858	-0.001467	-0.006346	0.012322
19	-0.001451	0.001283	-0.001745	0.002111	0.000411
20	0.012083	0.007072	0.007155	0.009846	0.000157
21	-0.115367	0.075995	-0.069526	0.040837	-0.064903
22	5.805440	0.095648	0.168905	0.421870	5.587560
23	0.022447	0.018809	0.012870	0.009066	0.036199
24	0.012252	0.008932	0.015016	0.024111	0.032733
25	0.073225	0.055784	0.052716	0.073087	0.082378
26	0.004940	-0.004477	-0.000604	-0.005065	0.009550
27	-0.005589	-0.009523	-0.009760	-0.005257	-0.001178
28	-0.003192	-0.006323	-0.001418	0.002773	0.032441
29	-0.024343	-0.010344	-0.031015	0.001028	0.118706
30	0.043672	-0.062940	-0.008284	0.034715	0.112228
31	0.069209	0.033807	-0.026137	0.208630	0.511960
32	0.165363	0.009719	-0.005209	0.159548	0.621782
33	-0.039049	0.000346	0.001647	-0.006325	0.021080

34	-0.038578	0.006056	-0.000789	-0.006622	0.056732
35	-0.003456	-0.024675	-0.006630	-0.033159	-0.011548
36	-1.252050	7.204800	1.237250	148.899000	1.426680
37	6.981790	1.329230	149.626000	1.472750	7.027740
38	0.368389	0.054860	-0.035127	-0.050114	0.027899
39	-0.053179	-0.024561	-0.031081	-0.029335	-0.022027
40	1.359680	148.262000	1.082440	7.075810	-1.252210
41	6.270240	-1.055180	6.797330	0.830806	148.241000
42	146.614000	1.007490	6.803660	-0.920210	5.704800
16		17	18	19	20
16	0.000000				
17	44.397200	0.000000			
18	0.765667	79.710900	0.000000		
19	4.430460	3.730160	42.255100	0.000000	
20	3.489760	2.397180	41.726600	4.554290	0.000000
21	-4.237940	1.734450	-0.166763	0.112481	0.056737
22	9.920080	0.116135	0.274737	-0.042638	-0.064738
23	-1.006370	5.233390	-6.157350	2.255100	117.764000
24	-1.066240	4.968870	-6.379290	2.114260	117.842000
25	0.369370	3.456150	-3.194530	8.639030	120.053000
26	-0.667640	5.607770	-6.118790	117.287000	1.986670
27	0.165368	5.780000	-3.481970	120.050000	7.934250

28	-1.025940	5.354670	-6.235540	117.886000	2.202750
29	3.860720	143.412000	-0.584974	7.525340	7.385940
30	122.046000	-5.754340	6.433780	-0.853525	-0.525116
31	120.951000	-5.037460	4.605070	-0.617888	0.117319
32	-0.051504	-0.008396	-0.023907	-0.009802	-0.005413
33	-1.667670	0.241448	0.354217	-0.001505	0.000177
34	-1.871750	0.254673	0.066289	-0.007003	-0.013540
35	-0.205017	-0.108688	0.074955	-0.036673	-0.041350
36	-0.051439	-0.030552	-0.017271	-0.007375	0.003533
37	0.040201	-0.014838	-0.024778	-0.008304	0.001235
38	0.450852	-0.037273	-0.012234	-0.017773	-0.020048
39	-1.533930	0.076593	-0.039798	-0.004340	-0.030120
40	-0.112828	-0.036732	-0.018592	-0.010506	0.000546
41	0.757721	0.125701	-0.027842	-0.000655	0.003341
42	0.042567	0.000211	-0.022985	-0.006771	0.003625
21		22	23	24	25
21	0.000000				
22	6.934080	0.000000			
23	0.018433	0.131631	0.000000		
24	-0.184064	0.158631	-17.432800	0.000000	
25	0.226299	-0.004193	-12.502100	-12.474200	0.000000
26	-0.152877	0.232675	-1.507150	-1.737080	-0.318410

27	-0.035506	-0.043638	-0.278958	-0.314821	2.725150
28	-0.214825	0.066208	-1.694110	-1.601630	-0.375354
29	-0.316401	-0.013797	-2.582500	-2.342780	-0.636441
30	10.511400	-1.070440	1.779910	1.309130	-0.062297
31	4.211070	-0.521701	0.288089	0.599402	-0.082441
32	-0.174358	0.029779	-0.043800	-0.040453	0.004064
33	-0.560510	2.881380	0.070208	-0.094316	0.010163
34	-0.667508	3.355130	0.030907	-0.115990	-0.008331
35	0.197758	0.047876	-0.039227	-0.052572	-0.079336
36	-0.131977	0.115770	-0.045468	0.008399	0.046820
37	-0.031841	-0.382851	-0.030433	-0.016621	0.016515
38	-0.087213	-4.168710	-0.083026	-0.059057	-0.061486
39	-0.168470	1.141450	-0.077963	-0.113196	-0.078998
40	-0.042111	0.121063	-0.004740	-0.039621	0.018352
41	0.033345	-0.577010	-0.043232	0.006179	0.087714
42	0.265718	-0.135026	0.011653	-0.052712	0.049678
26		27	28	29	30
26	0.000000				
27	-12.004200	0.000000			
28	-16.803300	-12.488700	0.000000		
29	-2.309130	-0.018469	-2.426640	0.000000	
30	1.300030	0.024880	2.301770	6.328950	0.000000

31	0.593404	-0.113051	0.525603	9.495170	-12.377900
32	-0.049743	-0.046056	-0.046822	-0.072539	-0.022796
33	0.120913	0.174192	-0.041082	0.374684	0.190997
34	-0.012828	-0.020382	-0.096062	0.016970	0.121169
35	0.015055	0.026754	-0.022146	0.053542	-0.108337
36	-0.042572	-0.041641	-0.019363	-0.075951	0.014527
37	-0.041518	-0.053574	-0.034626	-0.082333	-0.085911
38	-0.060348	-0.033953	-0.056579	-0.032181	-0.062214
39	-0.073870	-0.003065	-0.078704	0.015092	0.092166
40	-0.027266	-0.052231	-0.042066	-0.096057	-0.097528
41	-0.039815	-0.016490	-0.006628	0.055803	0.280346
42	-0.019059	-0.040065	-0.049117	-0.069406	-0.094614
31	32	33	34	35	
31	0.000000				
32	-0.003985	0.000000			
33	-0.609595	-0.139333	0.000000		
34	-0.481941	-0.139538	-20.643200	0.000000	
35	-0.037365	-0.082964	-11.748800	-12.739900	0.000000
36	0.029556	-0.006436	-0.049673	-0.060974	-0.065816
37	-0.031751	-0.050241	-0.037789	-0.031831	-0.084936
38	-0.046955	-0.259110	1.496610	1.272460	-0.010976
39	-0.045924	0.697035	-2.803240	-3.022560	-0.089471

40	-0.091664	-0.064831	-0.045110	-0.018212	-0.052821
41	0.467426	0.650222	0.018187	0.025113	-0.068174
42	-0.012896	0.012836	-0.001279	0.092147	-0.051668
	36	37	38	39	40
36	0.000000				
37	6.509510	0.000000			
38	-0.072232	-0.121959	0.000000		
39	-0.088267	-0.078440	5.418680	0.000000	
40	0.993945	6.593980	-0.051401	-0.086072	0.000000
41	6.984630	0.778221	-0.079963	-0.054194	0.513859
42	0.451278	0.806012	-0.080215	-0.063650	6.808880
	41	42			
41	0.000000				
42	1.482740	0.000000			

**B-10.** Table of total Nuclear Spin-Spin Couplings for Desired Product.  
Desired product

Total nuclear spin-spin coupling J(Hz)

	1	2	3	4	5
1	0.000000				
2	42.304200	0.000000			
3	3.715680	81.086700	0.000000		



4	4.614660	42.156700	2.460630	0.000000	
5	4.430720	0.353378	43.987300	3.606950	0.000000
6	-1.033460	3.496870	-1.629490	-0.906829	31.562200
7	0.122472	0.317023	5.081840	-0.086201	-3.001990
8	-0.008534	0.115621	-0.001583	-0.016499	3.234180
9	-0.008226	-0.047432	0.099212	-0.013737	-1.755950
10	0.001844	0.046288	0.009776	0.000679	1.571570
11	-0.006499	-0.009238	-0.066466	-0.003355	-0.910864
12	0.009009	0.008362	-0.101604	0.022858	1.997660
13	-0.005069	-0.029299	-0.019110	-0.003154	-0.804358
14	0.002409	-0.010580	0.010473	0.002625	-0.420337
15	0.000312	0.002969	0.005035	0.004133	0.266075
16	-0.000746	-0.001155	-0.001446	0.002034	-0.015178
17	-0.000964	-0.002267	-0.002078	0.001289	0.001702
18	-0.001314	-0.001375	-0.002362	0.000919	0.006975
19	-0.000715	-0.002539	-0.001167	0.001908	-0.001909
20	-0.000411	-0.001092	-0.000749	0.002993	0.009540
21	8.572300	-3.225190	3.385510	119.315000	0.442919
22	2.260340	-6.158250	5.200250	118.053000	-0.992646
23	2.089010	-6.335050	4.917760	118.352000	-0.956512
24	117.578000	-6.104250	5.554010	2.076020	-0.642503
25	120.509000	-3.468370	5.881390	8.034230	0.189339

26	117.710000	-6.206270	5.323140	2.119690	-0.946514
27	7.605580	-0.714848	142.698000	7.166930	4.038160
28	-0.426348	4.147260	-4.105040	0.278144	119.556000
29	-1.290720	5.827430	-6.053910	-0.972711	122.286000
30	-0.007979	-0.013826	-0.008950	-0.005777	-0.052955
31	0.050592	-0.200547	2.773100	0.153128	-3.678220
32	0.102881	-0.127601	1.724610	0.068203	-6.124090
33	-0.005492	-0.009798	-0.008235	-0.000110	0.001016
34	-0.006775	-0.011047	-0.011863	-0.002586	-0.004630
35	-0.004145	0.029853	0.088156	-0.016488	0.932272
36	-0.017930	-0.060266	-0.011181	-0.021715	-1.679960
37	-0.002514	-0.012617	0.012944	0.024681	-0.543074
38	-0.004875	-0.123377	0.102277	0.007024	-2.291790
39	-0.006133	-0.009144	-0.010999	-0.001741	-0.009441
40	-0.002653	-0.010471	0.001076	0.004936	0.027584
41	-0.003858	-0.006574	-0.006073	0.001905	-0.006358
42	-0.003344	0.049686	0.000872	0.001898	1.467130
	6.00	7.00	8.00	9.00	10.00
6	0.000000				
7	41.618200	0.000000			
8	2.433200	72.891400	0.000000		
9	4.761060	-3.244530	54.239600	0.000000	

10	-1.180950	8.093060	-2.979760	71.979100	0.000000
11	2.275470	-2.379450	5.180780	0.146365	41.223600
12	2.490510	38.133000	0.211353	5.570800	-2.364220
13	0.686604	-1.848980	4.841930	0.899026	55.277800
14	0.161376	-2.472700	1.307690	-6.755820	1.607260
15	0.003194	4.159400	-0.764201	2.473880	-2.085070
16	0.094301	0.013459	0.084306	0.303319	2.317380
17	-0.018405	-0.024733	0.000549	0.082094	-0.029305
18	0.022440	0.106111	-0.036240	0.039945	0.327216
19	-0.031922	-0.082003	0.006764	-0.036108	-0.338523
20	0.020729	-0.031104	0.011619	-0.078319	1.175440
21	0.040398	0.029002	-0.002514	-0.011111	-0.009287
22	1.880140	0.182900	0.024195	-0.008032	-0.011927
23	1.927140	0.096198	0.044760	-0.013736	-0.000201
24	2.800200	0.272788	0.087760	-0.004291	0.004457
25	0.074643	0.010401	-0.011123	-0.004257	-0.013995
26	2.236590	0.047311	0.033241	-0.000263	-0.012991
27	2.446980	-0.174430	-0.019224	0.006403	-0.038758
28	-3.242210	1.661340	-0.308310	0.072902	-0.098027
29	-5.170160	1.949920	-0.161458	0.100695	-0.058156
30	-0.000363	-0.057617	1.318890	2.773290	22.229600
31	122.653000	-3.787800	5.835510	0.115889	0.002560

32	123.062000	-6.793020	5.928820	-1.902490	1.884540
33	-0.004245	0.047949	-0.039241	0.026884	0.072856
34	-0.040162	-0.098567	-0.030953	-0.038880	-0.288138
35	0.142773	7.182940	2.229620	153.065000	-2.092200
36	5.590100	-0.232925	150.484000	2.915650	5.585970
37	3.387120	-5.062410	4.768580	-0.831964	7.743320
38	1.433070	-7.673080	5.005450	-3.735360	3.976230
39	0.006664	0.044540	-0.023028	0.021507	0.175362
40	-0.027708	-0.064431	-0.049346	0.233226	-0.277147
41	-0.019070	-0.085867	-0.017905	0.002138	-0.239264
42	-1.163860	3.587920	-3.404630	4.704850	-7.309180
	11	12	13	14	15
11	0.000000				
12	33.618300	0.000000			
13	4.957670	2.323940	0.000000		
14	-0.225818	0.300335	35.014600	0.000000	
15	43.494900	-1.934610	2.306040	0.176736	0.000000
16	3.767620	1.554590	-0.110758	0.038928	60.500000
17	3.696750	-0.764550	-0.030924	0.024566	-1.726970
18	-0.731976	0.880305	0.030786	0.009838	9.059440
19	3.197050	-0.920799	-0.025008	0.004549	-1.693750
20	2.091750	1.683470	0.144967	0.019255	59.151300

21	0.013534	0.022611	0.001748	0.013927	0.023820
22	-0.003373	-0.000297	-0.008258	0.014521	0.005583
23	-0.013072	-0.006514	-0.013202	0.007199	0.003705
24	-0.016897	-0.009372	-0.017190	0.006814	-0.000682
25	-0.006599	-0.007048	-0.006534	0.011457	-0.004836
26	-0.006987	-0.010484	-0.007554	0.009282	-0.004459
27	0.075918	0.247144	-0.002762	0.026361	-0.013600
28	0.143595	0.156787	0.064529	0.031079	0.007815
29	0.084925	-0.161795	0.050544	-0.003510	-0.023611
30	0.124880	-0.170397	161.850000	-4.093030	0.080995
31	0.560711	6.745880	-0.093848	0.030831	0.339833
32	-1.086440	2.528620	-1.102640	-0.383575	0.301062
33	0.544672	0.271506	0.008389	0.002658	6.674400
34	0.539031	-0.671552	-0.027475	0.033690	-1.347330
35	6.486560	-1.231550	5.323280	-0.119023	-0.188218
36	-0.911063	6.117330	-0.022026	-0.050691	0.143559
37	-2.701830	125.428000	0.761937	-0.152377	0.735672
38	-6.027710	119.762000	-1.546730	-0.511089	5.039670
39	0.411277	0.301445	-0.022559	0.057001	6.775330
40	3.174100	-0.515649	0.134391	-0.028431	-0.195236
41	4.559260	-0.745660	-0.060904	0.124910	0.281710
42	119.675000	-6.059240	1.549850	1.019420	-5.790570

	16	17	18	19	20
16	0.000000				
17	59.179400	0.000000			
18	-2.163890	59.335900	0.000000		
19	8.921580	-1.669420	59.065300	0.000000	
20	-0.239325	8.909600	-2.155740	60.028600	0.000000
21	0.018780	0.011915	0.010270	0.016515	0.022857
22	0.006198	0.003567	0.000582	0.000921	0.003778
23	0.000484	-0.000813	0.000019	0.002995	0.004042
24	-0.001203	-0.002655	-0.004376	-0.004069	-0.002711
25	-0.004526	-0.006280	-0.007402	-0.005264	-0.004125
26	-0.003834	-0.004819	-0.004687	-0.002907	-0.002387
27	-0.006565	-0.011407	-0.011715	-0.009040	-0.007323
28	0.018070	0.002344	0.002013	0.017049	0.023740
29	-0.003790	-0.013353	-0.012379	0.002420	0.003093
30	0.319026	0.011096	0.042283	0.056775	0.382317
31	0.017384	-0.019073	-0.003732	-0.032568	-0.004515
32	-0.022626	-0.003145	0.000485	-0.019575	-0.003436
33	-1.253730	7.159920	1.292450	148.511000	1.428330
34	7.008630	1.350480	149.419000	1.462090	7.066110
35	0.307735	0.016727	-0.017858	-0.054904	0.036527
36	-0.052249	-0.034445	-0.023866	-0.035792	-0.074247

37	-0.105293	0.028456	-0.020169	0.023534	-0.020896
38	-0.169583	-0.004321	0.016501	0.047135	0.092983
39	1.354100	148.266000	1.089390	7.104160	-1.256080
40	6.148050	-1.035230	6.873540	0.755469	147.210000
41	147.089000	1.127520	6.727920	-0.941009	5.717100
42	5.870820	0.269376	-0.030482	0.680796	4.808790
21	22	23	24	25	
21	0.000000				
22	-12.346000	0.000000			
23	-12.594000	-17.296100	0.000000		
24	-0.360513	-1.479910	-1.726630	0.000000	
25	2.714330	-0.265094	-0.324623	-12.255400	0.000000
26	-0.357888	-1.656540	-1.567780	-16.652100	-12.345400
27	-0.702640	-2.469670	-2.526720	-2.313910	-0.035365
28	-0.179822	-0.019375	0.045284	0.030266	-0.152754
29	-0.040923	2.422890	2.073590	2.272940	0.043487
30	-0.007224	-0.027654	-0.033419	-0.031165	-0.031623
31	-0.089620	0.015211	-0.229137	-0.140458	0.028094
32	0.096547	-0.060236	-0.216541	-0.141083	-0.023555
33	0.018146	-0.021900	-0.008954	-0.025679	-0.027203
34	0.000722	-0.019990	-0.019996	-0.025279	-0.032945
35	-0.043353	-0.045154	-0.038286	-0.014013	-0.025010

36	-0.035412	-0.053979	-0.064243	-0.043786	0.005629
37	0.197922	0.064726	-0.003842	0.004952	-0.025204
38	0.146951	-0.010960	-0.012345	-0.055286	-0.029049
39	0.005383	-0.007886	-0.024096	-0.017612	-0.030021
40	0.053793	-0.014627	-0.000449	-0.020861	-0.015895
41	0.030750	0.008339	-0.022635	-0.006672	-0.019972
42	0.021672	0.002574	-0.021005	0.007285	-0.025026
26	27	28	29	30	
26	0.000000				
27	-2.374010	0.000000			
28	0.014363	9.899620	0.000000		
29	3.401610	4.443640	-12.722600	0.000000	
30	-0.034172	-0.046210	-0.028763	-0.046422	0.000000
31	-0.169503	0.033504	11.759200	3.585760	-0.074537
32	-0.213763	-0.291109	4.342220	11.407200	-0.123625
33	-0.018812	-0.038731	0.015746	-0.005568	-0.019129
34	-0.025427	-0.048451	-0.016057	-0.042350	-0.055998
35	-0.035226	-0.027894	-0.166405	-0.091074	-0.199647
36	-0.033110	0.068594	-0.014818	0.208257	0.607447
37	-0.024188	-0.037418	0.272900	-0.011919	-0.178378
38	-0.027374	0.003325	0.725867	0.336848	-0.151487
39	-0.026594	-0.045408	-0.016827	-0.051473	-0.027598



40	-0.013365	-0.021013	0.095321	0.068546	0.271530
41	-0.024509	-0.033852	0.015109	-0.043126	0.100755
42	-0.033860	-0.049818	-0.114120	-0.179200	0.054390
	31	32	33	34	35
31	0.000000				
32	-12.058900	0.000000			
33	-0.058155	-0.047456	0.000000		
34	-0.081671	-0.046955	6.463250	0.000000	
35	0.059301	0.792271	-0.061999	-0.124383	0.000000
36	-0.098532	-2.016030	-0.075008	-0.087150	5.509320
37	-0.232211	-0.670265	-0.096903	-0.034420	-0.066961
38	-0.987392	-2.764380	0.041329	-0.043688	1.316630
39	-0.050927	-0.026144	0.960827	6.593690	-0.054990
40	-0.065796	-0.024387	7.013800	0.786700	-0.047034
41	-0.054897	0.039486	0.456780	0.797750	-0.091155
42	0.111416	2.164090	0.109868	-0.200427	-3.835470
	36	37	38	39	40
36	0.000000				
37	-0.520195	0.000000			
38	-3.690340	-17.341700	0.000000		
39	-0.086301	-0.058219	-0.109903	0.000000	
40	-0.091721	0.005198	0.246469	0.505476	0.000000

41	-0.084545	0.164314	-0.085279	6.706110	1.482990
42	0.962861	8.535670	19.353300	0.032708	-0.484783
	41	42			
41	0.000000				
42	0.005386	0.000000			

**B-11.** Table of total Nuclear Spin-Spin Couplings for Trans Product.  
trans product

Total nuclear spin-spin coupling J(Hz)

	1	2	3	4	5
1	0.000000				
2	41.768200	0.000000			
3	2.775880	72.878600	0.000000		
4	5.170370	-3.236780	54.438400	0.000000	
5	-1.285520	8.507780	-2.847080	71.415000	0.000000
6	2.423270	-1.774130	4.898170	0.095340	40.901900
7	1.976600	39.315300	0.201101	4.727510	-1.854660
8	0.698849	-1.904320	5.008490	0.928840	55.832800
9	0.170761	-2.687270	1.370900	-6.690110	1.616710
10	0.001183	3.634260	-0.845491	2.545350	-2.390090
11	0.120866	0.197256	0.035867	0.264950	2.056160
12	-0.016792	0.086878	0.001175	0.053823	-0.157006

13	0.025284	0.030020	-0.033559	0.042099	0.384814
14	-0.034434	-0.041094	0.009963	-0.037188	-0.398900
15	0.024002	-0.076874	0.007267	-0.057736	1.279610
16	1.330800	-1.268680	2.313800	-0.847086	3.498690
17	0.847858	0.066596	-0.090079	-0.024487	0.516678
18	0.161019	-0.136483	0.071534	-0.020222	0.054741
19	-0.019220	0.029726	-0.029586	-0.008828	0.024970
20	0.060687	0.021878	-0.012472	-0.011076	-0.011018
21	-1.237930	3.242110	-3.414080	4.761650	-7.591970
22	1.530700	-7.759510	4.827690	-3.577740	3.032640
23	0.217499	-0.079126	0.022733	-0.011253	0.042134
24	-0.011200	0.002076	-0.021343	-0.020177	0.004505
25	0.035829	-0.114792	0.008219	-0.020516	0.016465
26	0.061097	-0.104462	0.041731	-0.003467	0.063782
27	0.072283	-0.092073	0.029138	-0.009290	-0.000121
28	0.012155	-0.004791	-0.007039	-0.016939	-0.018397
29	1.550470	-0.171942	-0.011471	-0.026500	0.049167
30	-0.207178	8.178730	0.785014	-0.014088	0.275489
31	0.051146	4.220690	-0.192034	0.037047	-0.300281
32	0.005694	-0.064387	1.294350	2.641880	21.888900
33	120.737000	-7.770750	7.146620	-2.484370	2.395280
34	119.919000	-8.085420	6.227100	-2.962720	2.606770

35	120.673000	-3.646460	6.539460	0.352552	-0.008983
36	-0.003257	0.018217	-0.036477	0.033025	0.091337
37	-0.044007	-0.063664	-0.021936	-0.053948	-0.317360
38	-0.022145	7.166890	2.323290	153.197000	-2.021730
39	6.646370	-0.534765	149.831000	2.561470	5.870030
40	0.005816	0.018133	-0.026055	0.016437	0.162886
41	-0.024421	0.000776	-0.027828	0.250087	-0.284932
42	-0.030308	0.037416	-0.031429	-0.005589	-0.282977
	6.00	7.00	8.00	9.00	10.00
6	0.000000				
7	33.349200	0.000000			
8	4.842260	2.287080	0.000000		
9	-0.171599	0.301307	34.997900	0.000000	
10	43.271600	-1.693100	2.396520	0.212437	0.000000
11	3.017220	1.860390	-0.021600	0.027642	59.614200
12	3.426530	-0.418831	-0.063129	0.025244	-1.711700
13	-0.715101	0.653020	0.049099	0.004517	8.989790
14	3.209210	-0.690943	-0.040982	0.002124	-1.634010
15	2.166520	1.610080	0.101070	0.011988	59.095200
16	0.716011	34.969700	0.323964	-0.093314	0.397766
17	4.300470	-2.588900	0.333216	-0.007498	-0.106795
18	-0.085680	2.555850	0.000347	0.003463	0.040015

19	0.201778	-0.997391	-0.001670	0.004014	0.005191
20	-0.032507	-0.907325	-0.001174	0.006336	0.102786
21	119.792000	-6.108140	1.623920	1.030690	-6.043650
22	-5.736800	122.799000	-1.509950	-0.488637	5.807680
23	0.020244	1.855020	0.015460	0.016412	0.044708
24	0.023270	0.133058	-0.003506	0.042230	0.215173
25	-0.009209	1.640150	0.019886	0.024453	0.039948
26	0.110465	2.861670	0.032134	0.010151	-0.004491
27	-0.051846	2.308800	0.002247	0.018355	-0.001518
28	0.005376	0.080534	-0.004257	0.018755	0.003868
29	0.021360	1.041770	0.013510	0.039180	0.082472
30	4.464170	-4.434450	0.168048	0.091135	-0.022267
31	0.634979	-4.462260	-0.007661	0.084000	-0.109722
32	0.097193	-0.173166	161.381000	-4.099390	0.069243
33	-1.384000	2.804570	-1.388180	-0.521365	0.686514
34	-1.414280	1.751550	-1.493260	-0.555883	0.576304
35	0.736873	6.316630	-0.079365	0.039300	0.254464
36	0.524185	0.195830	0.017259	-0.003749	6.621440
37	0.517233	-0.506522	-0.044509	0.032068	-1.344040
38	6.505830	-1.037770	5.293870	-0.145208	-0.443818
39	-0.830194	6.211990	0.093638	-0.034595	0.165527
40	0.413945	0.212347	-0.000605	0.058428	6.731780

41	3.121420	-0.273272	0.063058	-0.016737	-0.363718
42	4.023980	-0.466123	-0.087401	0.129680	0.236871
	11	12	13	14	15
11	0.000000				
12	58.084200	0.000000			
13	-2.099500	58.609400	0.000000		
14	8.924510	-1.569280	58.417300	0.000000	
15	-0.143063	8.861700	-2.122760	59.330900	0.000000
16	0.015206	-0.006633	-0.021690	0.025669	-0.081488
17	0.038287	-0.001398	-0.008372	-0.007563	0.004532
18	0.013432	-0.004197	0.003011	0.007873	0.000194
19	0.000658	0.004182	0.001008	0.007862	0.008893
20	0.027517	0.016853	0.003191	0.040532	0.127131
21	5.984300	0.272376	-0.045503	0.754042	4.795810
22	-0.191497	-0.003022	0.032403	0.040320	0.159307
23	0.037899	0.019842	0.036407	0.072078	0.043959
24	0.172957	0.116257	0.103232	0.170014	0.239289
25	0.018419	0.045322	0.026465	0.041151	0.039539
26	0.001055	-0.004970	0.005211	0.007715	0.012585
27	0.011959	0.001853	0.005533	0.000909	0.011557
28	0.000772	-0.006120	-0.006638	-0.002328	0.004294
29	0.078315	-0.013603	-0.022477	-0.010295	-0.013298

30	0.432589	0.108631	-0.000900	-0.010294	0.126472
31	-0.011283	-0.017263	-0.013927	-0.016795	0.167888
32	0.451238	0.032391	0.063657	0.018387	0.354067
33	-0.032942	-0.008873	0.001296	-0.013100	0.010907
34	-0.041536	-0.014559	0.000468	-0.030688	-0.003547
35	0.025562	-0.022700	-0.006197	-0.032410	-0.009151
36	-1.252840	7.153100	1.275500	148.730000	1.452480
37	6.996100	1.331080	149.881000	1.436940	7.036950
38	0.263829	-0.001048	-0.007805	-0.054920	0.044015
39	-0.048423	-0.032319	-0.029117	-0.027991	-0.076000
40	1.385150	148.545000	1.094750	7.102380	-1.253510
41	6.167580	-1.008530	6.909690	0.714482	148.144000
42	148.337000	1.168380	6.736530	-0.934315	5.759350
16		17	18	19	20
16	0.000000				
17	43.858100	0.000000			
18	0.558311	79.673300	0.000000		
19	4.604260	3.877170	42.202700	0.000000	
20	3.273270	2.271350	41.213900	4.386240	0.000000
21	7.190170	0.050788	0.026621	0.015533	0.055596
22	-5.363020	3.508450	-0.080402	0.159398	0.054637
23	-1.114570	5.152000	-6.289390	2.087570	117.449000

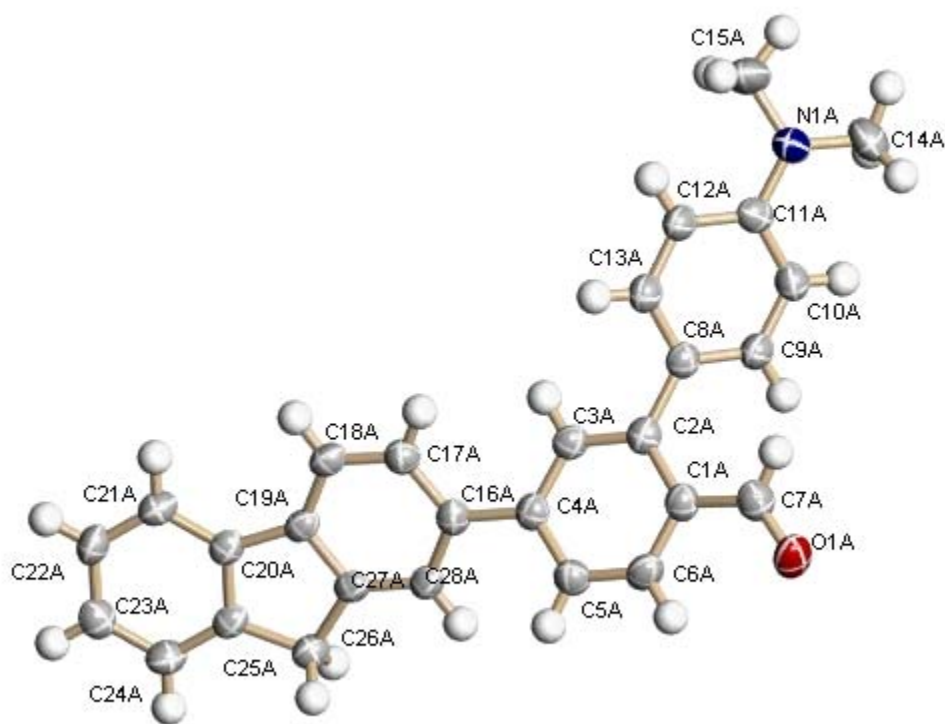
24	0.275073	3.413130	-3.017740	8.821260	120.580000
25	-1.057800	5.126450	-6.431630	2.372950	117.642000
26	-0.682840	5.580890	-6.208760	117.507000	2.006800
27	-1.027510	5.487900	-6.140800	117.732000	2.183040
28	0.152843	5.866730	-3.458870	119.957000	7.778330
29	4.393490	144.152000	-0.798962	7.554250	7.540500
30	120.470000	-5.829770	4.787290	-0.830116	-0.075488
31	119.743000	-4.701120	6.587830	-0.503543	-0.235248
32	-0.060049	-0.026615	-0.024584	-0.009178	0.008543
33	-0.679011	0.628915	0.286697	-0.057185	-0.037842
34	-0.746009	1.097750	0.098563	-0.000805	0.010392
35	0.168831	0.907359	0.202639	-0.060493	-0.025112
36	-0.047662	-0.028610	-0.011843	-0.008100	-0.007472
37	-0.016101	-0.027772	-0.019384	-0.008643	0.003681
38	0.277842	-0.024562	-0.018691	-0.012663	-0.010082
39	-0.324281	-0.008632	-0.033101	-0.014962	-0.025951
40	-0.020702	-0.029168	-0.023620	-0.009130	0.003047
41	0.015858	-0.005809	-0.012572	-0.006000	-0.014654
42	0.132201	0.008698	-0.034208	-0.011228	-0.003391
21		22	23	24	25
21	0.000000				
22	17.063000	0.000000			



23	-0.091223	0.046233	0.000000		
24	0.035862	0.262579	-12.844600	0.000000	
25	-0.047791	-0.184746	-17.725100	-12.349300	0.000000
26	-0.079130	-0.030311	-1.598040	-0.298760	-1.703010
27	-0.080556	-0.183655	-1.763890	-0.362974	-1.511910
28	-0.043690	-0.010769	-0.334831	2.805030	-0.246580
29	-0.006645	-0.306005	-2.692830	-0.591918	-2.278680
30	0.051884	1.791810	0.763146	0.048944	1.115180
31	-0.142070	8.865430	1.123830	-0.063332	0.664207
32	0.090941	-0.135447	-0.026396	0.021700	-0.036618
33	2.632370	-3.945910	0.169702	-0.002578	0.035894
34	2.917730	-4.048230	-0.038552	-0.032075	-0.085915
35	-0.064101	-0.745506	0.093499	-0.072025	-0.034893
36	0.113851	0.061077	0.071154	0.020618	-0.042360
37	-0.167779	-0.044196	-0.015370	0.001508	-0.001717
38	-3.732060	1.264180	-0.067434	-0.060205	-0.086672
39	0.923129	-3.417940	-0.067143	-0.068760	-0.098829
40	0.030500	-0.088510	-0.068659	0.019092	-0.005148
41	-0.427517	0.199838	0.090554	0.102002	-0.051291
42	0.052246	-0.092888	-0.072408	0.069880	-0.015044
26		27	28	29	30
26	0.000000				

27	-16.794100	0.000000			
28	-12.177800	-12.310900	0.000000		
29	-2.406360	-2.409260	-0.016319	0.000000	
30	1.146040	1.054000	-0.085115	8.510900	0.000000
31	0.611513	1.376680	-0.025441	6.889320	-13.464800
32	-0.039454	-0.040844	-0.044575	-0.068339	0.001052
33	0.179361	0.057936	0.140635	0.658931	-0.045617
34	-0.037714	-0.043438	0.079072	0.241827	0.106700
35	0.048196	0.021746	-0.011749	0.454742	-0.302843
36	-0.001700	-0.034154	-0.053224	-0.092574	-0.081749
37	-0.033622	-0.030112	-0.061051	-0.092833	-0.042475
38	-0.063888	-0.080151	-0.058842	-0.098619	-0.127393
39	-0.045048	-0.068977	-0.034662	-0.062927	0.393990
40	-0.048849	-0.026090	-0.056586	-0.088333	0.024903
41	0.011171	-0.045194	-0.033555	-0.065827	-0.009964
42	-0.054037	-0.027223	-0.042878	-0.027295	0.314124
31		32	33	34	35
31	0.000000				
32	-0.031617	0.000000			
33	0.053767	-0.138541	0.000000		
34	0.297255	-0.158959	-19.820200	0.000000	
35	-0.099789	-0.083717	-12.260600	-12.492900	0.000000

36	-0.107761	-0.027147	-0.020655	-0.060722	-0.054234
37	-0.098347	-0.055090	-0.056633	-0.072128	-0.086267
38	-0.198282	-0.167117	1.471640	1.169160	0.041181
39	0.188045	0.590085	-2.862350	-2.660220	-0.047118
40	-0.035408	0.001452	-0.060596	-0.052081	-0.061578
41	-0.078342	0.129804	0.045485	-0.048620	-0.051027
42	0.087468	0.187156	-0.059607	-0.015660	-0.075022
36		37	38	39	40
36	0.000000				
37	6.483990	0.000000			
38	-0.053049	-0.122318	0.000000		
39	-0.074686	-0.088898	5.706080	0.000000	
40	0.999817	6.608710	-0.059562	-0.094000	0.000000
41	7.072020	0.810039	-0.030935	-0.078705	0.491120
42	0.458035	0.824012	-0.096538	-0.087256	6.715570
41		42			
41	0.000000				
42	1.494660	0.000000			




---

**B-12. X-ray crystal determination of 146.**
**Table 21. Crystal data and structure refinement for cw02a.**

Identification code	cw02a	
Empirical formula	C <sub>28</sub> H <sub>23</sub> N O	
Formula weight	389.47	
Temperature	90(2) K	
Wavelength	0.71073 Å	
Crystal system	Triclinic	
Space group	P-1	
Unit cell dimensions	a = 10.116(5) Å	∠ = 90.844(6)°.
	b = 10.160(5) Å	∠ = 97.738(6)°.
	c = 21.595(10) Å	∠ = 110.128(6)°.
Volume	2060.5(17) Å <sup>3</sup>	
Z	4	

Density (calculated)	1.256 Mg/m <sup>3</sup>
Absorption coefficient	0.075 mm <sup>-1</sup>
F(000)	824
Crystal size	0.50 x 0.04 x 0.04 mm <sup>3</sup>
Theta range for data collection	1.91 to 25.00°.
Index ranges	-11 ≤ h ≤ 12, -12 ≤ k ≤ 12, -25 ≤ l ≤ 25
Reflections collected	16109
Independent reflections	7096 [R(int) = 0.0533]
Completeness to theta = 25.00°	98.0 %
Absorption correction	Semi-empirical from equivalents
Max. and min. transmission	0.9970 and 0.9633
Refinement method	Full-matrix least-squares on F <sup>2</sup>
Data / restraints / parameters	7096 / 0 / 545
Goodness-of-fit on F <sup>2</sup>	1.003
Final R indices [I > 2σ(I)]	R1 = 0.0530, wR2 = 0.1048
R indices (all data)	R1 = 0.1127, wR2 = 0.1295
Largest diff. peak and hole	0.368 and -0.199 e.Å <sup>-3</sup>

Atomic coordinates ( × 10<sup>4</sup>) and equivalent isotropic displacement parameters (Å<sup>2</sup> × 10<sup>3</sup>) for cw02a. U(eq) is defined as one third of the trace of the orthogonalized U<sup>ij</sup> tensor.

	x	y	z	U(eq)
O(1A)	2551(2)	1103(2)	1336(1)	45(1)
N(1A)	8261(2)	7471(2)	592(1)	41(1)
C(1A)	4513(3)	2256(3)	2127(1)	32(1)
C(2A)	5868(3)	3330(2)	2285(1)	29(1)
C(3A)	6584(3)	3418(2)	2886(1)	29(1)
C(4A)	6027(3)	2528(2)	3345(1)	28(1)
C(5A)	4662(3)	1518(3)	3186(1)	33(1)
C(6A)	3937(3)	1386(3)	2586(1)	35(1)
C(7A)	3751(3)	1929(3)	1481(1)	39(1)
C(8A)	6478(3)	4399(2)	1841(1)	29(1)

C(9A)	5678(3)	5070(3)	1482(1)	32(1)
C(10A)	6247(3)	6084(3)	1083(1)	34(1)
C(11A)	7692(3)	6510(3)	1017(1)	33(1)
C(12A)	8529(3)	5880(3)	1394(1)	33(1)
C(13A)	7930(3)	4863(3)	1792(1)	34(1)
C(14A)	7373(3)	8114(3)	224(1)	50(1)
C(15A)	9786(3)	8134(3)	638(2)	67(1)
C(16A)	6824(3)	2649(2)	3984(1)	28(1)
C(17A)	8317(3)	3147(2)	4086(1)	32(1)
C(18A)	9097(3)	3257(2)	4670(1)	31(1)
C(19A)	8387(3)	2862(2)	5183(1)	27(1)
C(20A)	8901(3)	2773(2)	5841(1)	27(1)
C(21A)	10280(3)	3095(2)	6164(1)	33(1)
C(22A)	10462(3)	2833(3)	6789(1)	36(1)
C(23A)	9296(3)	2293(3)	7099(1)	37(1)
C(24A)	7926(3)	2000(3)	6786(1)	34(1)
C(25A)	7736(3)	2235(2)	6158(1)	27(1)
C(26A)	6372(3)	1973(3)	5712(1)	31(1)
C(27A)	6893(3)	2372(2)	5096(1)	25(1)
N(1B)	3251(3)	7268(2)	522(1)	44(1)
O(1B)	-2442(2)	785(2)	1233(1)	75(1)
C(1B)	-418(3)	1885(3)	2005(1)	40(1)
C(2B)	856(3)	3047(3)	2177(1)	33(1)
C(3B)	1556(3)	3159(3)	2792(1)	33(1)
C(4B)	1078(3)	2185(3)	3233(1)	35(1)
C(5B)	-135(3)	1008(3)	3031(1)	43(1)
C(6B)	-859(3)	861(3)	2435(1)	45(1)
C(7B)	-1386(3)	1794(3)	1418(1)	50(1)
C(8B)	1456(3)	4128(3)	1740(1)	32(1)
C(9B)	2059(3)	5551(3)	1942(1)	33(1)
C(10B)	2640(3)	6587(3)	1550(1)	34(1)
C(11B)	2658(3)	6253(3)	919(1)	33(1)
C(12B)	2065(3)	4815(3)	708(1)	36(1)
C(13B)	1496(3)	3808(3)	1110(1)	35(1)

C(14B)	3118(3)	6902(3)	-140(1)	55(1)
C(15B)	3855(3)	8740(3)	739(1)	55(1)
C(16B)	1791(3)	2436(3)	3899(1)	33(1)
C(17B)	2493(3)	3804(3)	4167(1)	37(1)
C(18B)	3097(3)	4089(3)	4800(1)	39(1)
C(19B)	2970(3)	2970(3)	5165(1)	35(1)
C(20B)	3456(3)	2929(3)	5839(1)	33(1)
C(21B)	4218(3)	3999(3)	6305(1)	34(1)
C(22B)	4553(3)	3609(3)	6900(1)	38(1)
C(23B)	4174(3)	2231(3)	7042(1)	43(1)
C(24B)	3422(3)	1178(3)	6590(1)	41(1)
C(25B)	3050(3)	1500(3)	5997(1)	33(1)
C(26B)	2263(3)	561(3)	5411(1)	41(1)
C(27B)	2286(3)	1591(3)	4920(1)	30(1)
C(28B)	1693(3)	1309(3)	4282(1)	40(1)
C(28A)	6122(3)	2281(2)	4504(1)	28(1)

Bond lengths [Å] and angles [°] for cw02a.

O(1A)-C(7A)	1.210(3)
N(1A)-C(11A)	1.381(3)
N(1A)-C(14A)	1.446(3)
N(1A)-C(15A)	1.445(4)
C(1A)-C(6A)	1.389(3)
C(1A)-C(2A)	1.421(3)
C(1A)-C(7A)	1.472(3)
C(2A)-C(3A)	1.383(3)
C(2A)-C(8A)	1.486(3)
C(3A)-C(4A)	1.395(3)
C(4A)-C(5A)	1.402(3)
C(4A)-C(16A)	1.482(3)
C(5A)-C(6A)	1.382(3)
C(8A)-C(9A)	1.396(3)

C(8A)-C(13A)	1.399(4)
C(9A)-C(10A)	1.374(3)
C(10A)-C(11A)	1.402(4)
C(11A)-C(12A)	1.411(4)
C(12A)-C(13A)	1.382(3)
C(16A)-C(28A)	1.397(3)
C(16A)-C(17A)	1.402(4)
C(17A)-C(18A)	1.377(3)
C(18A)-C(19A)	1.391(3)
C(19A)-C(27A)	1.404(3)
C(19A)-C(20A)	1.462(3)
C(20A)-C(25A)	1.393(3)
C(20A)-C(21A)	1.399(3)
C(21A)-C(22A)	1.378(3)
C(22A)-C(23A)	1.385(4)
C(23A)-C(24A)	1.387(4)
C(24A)-C(25A)	1.380(3)
C(25A)-C(26A)	1.511(3)
C(26A)-C(27A)	1.506(3)
C(27A)-C(28A)	1.389(3)
N(1B)-C(11B)	1.378(3)
N(1B)-C(14B)	1.447(3)
N(1B)-C(15B)	1.450(3)
O(1B)-C(7B)	1.212(3)
C(1B)-C(6B)	1.402(4)
C(1B)-C(2B)	1.416(3)
C(1B)-C(7B)	1.475(4)
C(2B)-C(3B)	1.402(3)
C(2B)-C(8B)	1.480(4)
C(3B)-C(4B)	1.394(3)
C(4B)-C(5B)	1.399(4)
C(4B)-C(16B)	1.496(4)
C(5B)-C(6B)	1.370(4)
C(8B)-C(9B)	1.399(3)



C(8B)-C(13B)	1.403(3)
C(9B)-C(10B)	1.379(3)
C(10B)-C(11B)	1.404(3)
C(11B)-C(12B)	1.416(3)
C(12B)-C(13B)	1.373(3)
C(16B)-C(17B)	1.400(3)
C(16B)-C(28B)	1.406(4)
C(17B)-C(18B)	1.402(4)
C(18B)-C(19B)	1.373(4)
C(19B)-C(27B)	1.391(3)
C(19B)-C(20B)	1.478(4)
C(20B)-C(21B)	1.404(3)
C(20B)-C(25B)	1.427(4)
C(21B)-C(22B)	1.381(4)
C(22B)-C(23B)	1.370(4)
C(23B)-C(24B)	1.373(4)
C(24B)-C(25B)	1.363(4)
C(25B)-C(26B)	1.522(3)
C(26B)-C(27B)	1.498(3)
C(27B)-C(28B)	1.409(4)

C(11A)-N(1A)-C(14A)	119.8(2)
C(11A)-N(1A)-C(15A)	119.9(2)
C(14A)-N(1A)-C(15A)	117.9(2)
C(6A)-C(1A)-C(2A)	118.9(2)
C(6A)-C(1A)-C(7A)	118.0(2)
C(2A)-C(1A)-C(7A)	122.8(2)
C(3A)-C(2A)-C(1A)	118.1(2)
C(3A)-C(2A)-C(8A)	119.8(2)
C(1A)-C(2A)-C(8A)	121.9(2)
C(2A)-C(3A)-C(4A)	123.3(2)
C(3A)-C(4A)-C(5A)	117.6(2)
C(3A)-C(4A)-C(16A)	121.9(2)
C(5A)-C(4A)-C(16A)	120.5(2)

C(6A)-C(5A)-C(4A)	120.3(2)
C(5A)-C(6A)-C(1A)	121.7(2)
O(1A)-C(7A)-C(1A)	124.5(3)
C(9A)-C(8A)-C(13A)	115.7(2)
C(9A)-C(8A)-C(2A)	122.9(2)
C(13A)-C(8A)-C(2A)	121.3(2)
C(10A)-C(9A)-C(8A)	123.0(3)
C(9A)-C(10A)-C(11A)	121.1(3)
N(1A)-C(11A)-C(10A)	121.7(3)
N(1A)-C(11A)-C(12A)	121.6(3)
C(10A)-C(11A)-C(12A)	116.8(2)
C(13A)-C(12A)-C(11A)	121.0(3)
C(12A)-C(13A)-C(8A)	122.4(3)
C(28A)-C(16A)-C(17A)	117.8(2)
C(28A)-C(16A)-C(4A)	121.5(2)
C(17A)-C(16A)-C(4A)	120.8(2)
C(18A)-C(17A)-C(16A)	122.6(2)
C(17A)-C(18A)-C(19A)	119.1(2)
C(18A)-C(19A)-C(27A)	119.5(2)
C(18A)-C(19A)-C(20A)	131.8(2)
C(27A)-C(19A)-C(20A)	108.6(2)
C(25A)-C(20A)-C(21A)	119.8(2)
C(25A)-C(20A)-C(19A)	108.9(2)
C(21A)-C(20A)-C(19A)	131.4(2)
C(22A)-C(21A)-C(20A)	119.3(2)
C(21A)-C(22A)-C(23A)	120.5(3)
C(22A)-C(23A)-C(24A)	120.6(3)
C(25A)-C(24A)-C(23A)	119.1(3)
C(24A)-C(25A)-C(20A)	120.7(2)
C(24A)-C(25A)-C(26A)	129.5(2)
C(20A)-C(25A)-C(26A)	109.8(2)
C(27A)-C(26A)-C(25A)	102.9(2)
C(28A)-C(27A)-C(19A)	120.6(2)
C(28A)-C(27A)-C(26A)	129.6(2)

C(19A)-C(27A)-C(26A)	109.7(2)
C(11B)-N(1B)-C(14B)	120.2(2)
C(11B)-N(1B)-C(15B)	120.8(2)
C(14B)-N(1B)-C(15B)	118.5(2)
C(6B)-C(1B)-C(2B)	119.1(3)
C(6B)-C(1B)-C(7B)	118.4(3)
C(2B)-C(1B)-C(7B)	122.1(3)
C(3B)-C(2B)-C(1B)	117.3(2)
C(3B)-C(2B)-C(8B)	119.7(2)
C(1B)-C(2B)-C(8B)	123.0(2)
C(4B)-C(3B)-C(2B)	123.7(2)
C(3B)-C(4B)-C(5B)	116.9(3)
C(3B)-C(4B)-C(16B)	121.1(2)
C(5B)-C(4B)-C(16B)	121.9(2)
C(6B)-C(5B)-C(4B)	121.3(3)
C(5B)-C(6B)-C(1B)	121.4(3)
O(1B)-C(7B)-C(1B)	124.5(3)
C(9B)-C(8B)-C(13B)	115.7(2)
C(9B)-C(8B)-C(2B)	121.0(2)
C(13B)-C(8B)-C(2B)	123.3(2)
C(10B)-C(9B)-C(8B)	122.7(2)
C(9B)-C(10B)-C(11B)	121.0(2)
N(1B)-C(11B)-C(10B)	121.9(2)
N(1B)-C(11B)-C(12B)	120.9(2)
C(10B)-C(11B)-C(12B)	117.1(2)
C(13B)-C(12B)-C(11B)	120.6(2)
C(12B)-C(13B)-C(8B)	123.0(2)
C(17B)-C(16B)-C(28B)	118.3(3)
C(17B)-C(16B)-C(4B)	120.7(2)
C(28B)-C(16B)-C(4B)	120.9(2)
C(18B)-C(17B)-C(16B)	122.6(3)
C(19B)-C(18B)-C(17B)	117.9(3)
C(18B)-C(19B)-C(27B)	121.7(3)
C(18B)-C(19B)-C(20B)	130.6(2)

C(27B)-C(19B)-C(20B)	107.7(2)
C(21B)-C(20B)-C(25B)	119.2(2)
C(21B)-C(20B)-C(19B)	131.9(2)
C(25B)-C(20B)-C(19B)	108.9(2)
C(22B)-C(21B)-C(20B)	117.9(2)
C(23B)-C(22B)-C(21B)	122.3(3)
C(24B)-C(23B)-C(22B)	120.2(3)
C(25B)-C(24B)-C(23B)	120.1(3)
C(24B)-C(25B)-C(20B)	120.3(2)
C(24B)-C(25B)-C(26B)	131.0(2)
C(20B)-C(25B)-C(26B)	108.6(2)
C(27B)-C(26B)-C(25B)	103.0(2)
C(19B)-C(27B)-C(28B)	120.2(2)
C(19B)-C(27B)-C(26B)	111.7(2)
C(28B)-C(27B)-C(26B)	128.0(2)
C(16B)-C(28B)-C(27B)	119.3(2)
C(27A)-C(28A)-C(16A)	120.3(2)

---

Symmetry transformations used to generate equivalent atoms:

Anisotropic displacement parameters ( $\text{\AA}^2 \times 10^3$ ) for cw02a. The anisotropic displacement factor exponent takes the form:  $-2\pi^2 [h^2 a^{*2} U^{11} + \dots + 2 h k a^* b^* U^{12}]$

	U <sup>11</sup>	U <sup>22</sup>	U <sup>33</sup>	U <sup>23</sup>	U <sup>13</sup>	U <sup>12</sup>
O(1A)	43(1)	37(1)	44(1)	-4(1)	-10(1)	6(1)
N(1A)	38(2)	40(1)	39(1)	11(1)	4(1)	5(1)
C(1A)	33(2)	29(1)	32(2)	0(1)	-1(1)	11(1)
C(2A)	31(2)	26(1)	32(2)	-3(1)	2(1)	13(1)
C(3A)	29(2)	23(1)	33(2)	-3(1)	1(1)	5(1)
C(4A)	29(2)	25(1)	32(2)	0(1)	1(1)	12(1)
C(5A)	35(2)	28(1)	34(2)	4(1)	3(1)	8(1)
C(6A)	29(2)	26(1)	44(2)	0(1)	-2(1)	4(1)

C(7A)	43(2)	32(2)	36(2)	0(1)	-1(1)	10(2)
C(8A)	29(2)	27(1)	29(2)	-2(1)	-1(1)	7(1)
C(9A)	27(2)	36(2)	30(2)	1(1)	0(1)	8(1)
C(10A)	36(2)	35(2)	32(2)	4(1)	1(1)	13(1)
C(11A)	35(2)	30(1)	25(2)	-2(1)	1(1)	3(1)
C(12A)	28(2)	39(2)	28(2)	2(1)	-1(1)	7(1)
C(13A)	33(2)	36(2)	31(2)	0(1)	-1(1)	12(1)
C(14A)	60(2)	54(2)	39(2)	16(2)	9(2)	21(2)
C(15A)	46(2)	67(2)	65(2)	25(2)	2(2)	-9(2)
C(16A)	32(2)	18(1)	31(2)	-2(1)	-1(1)	7(1)
C(17A)	32(2)	28(1)	33(2)	2(1)	4(1)	9(1)
C(18A)	24(2)	27(1)	40(2)	-1(1)	4(1)	6(1)
C(19A)	21(2)	21(1)	37(2)	-1(1)	3(1)	7(1)
C(20A)	27(2)	19(1)	33(2)	-5(1)	0(1)	6(1)
C(21A)	26(2)	30(1)	40(2)	-3(1)	6(1)	8(1)
C(22A)	28(2)	38(2)	38(2)	-1(1)	-5(1)	12(1)
C(23A)	44(2)	33(2)	31(2)	-2(1)	0(1)	11(1)
C(24A)	31(2)	34(2)	36(2)	-2(1)	9(1)	7(1)
C(25A)	24(2)	19(1)	36(2)	-3(1)	2(1)	6(1)
C(26A)	26(2)	30(1)	34(2)	-3(1)	5(1)	7(1)
C(27A)	25(2)	15(1)	35(2)	0(1)	6(1)	6(1)
N(1B)	56(2)	33(1)	38(2)	3(1)	5(1)	12(1)
O(1B)	59(2)	57(1)	73(2)	-6(1)	-19(1)	-14(1)
C(1B)	37(2)	33(2)	44(2)	-3(1)	1(2)	7(1)
C(2B)	31(2)	32(1)	36(2)	-2(1)	1(1)	12(1)
C(3B)	27(2)	31(1)	38(2)	0(1)	5(1)	9(1)
C(4B)	28(2)	32(2)	46(2)	5(1)	11(1)	11(1)
C(5B)	40(2)	38(2)	51(2)	5(1)	8(2)	11(2)
C(6B)	37(2)	34(2)	54(2)	-3(2)	1(2)	0(1)
C(7B)	41(2)	45(2)	51(2)	-8(2)	-3(2)	3(2)
C(8B)	30(2)	32(1)	32(2)	-3(1)	-4(1)	11(1)
C(9B)	30(2)	34(2)	34(2)	-3(1)	1(1)	11(1)
C(10B)	31(2)	30(1)	38(2)	-5(1)	0(1)	8(1)
C(11B)	33(2)	33(2)	32(2)	1(1)	-1(1)	12(1)

C(12B)	39(2)	41(2)	29(2)	-4(1)	-3(1)	16(1)
C(13B)	36(2)	27(1)	38(2)	-2(1)	-3(1)	9(1)
C(14B)	62(2)	61(2)	33(2)	9(2)	6(2)	11(2)
C(15B)	61(2)	37(2)	61(2)	2(2)	17(2)	8(2)
C(16B)	25(2)	40(2)	40(2)	13(1)	12(1)	14(1)
C(17B)	33(2)	40(2)	39(2)	5(1)	9(1)	13(1)
C(18B)	31(2)	32(2)	55(2)	7(1)	13(2)	10(1)
C(19B)	21(2)	28(1)	55(2)	-5(1)	12(1)	7(1)
C(20B)	19(2)	52(2)	33(2)	2(1)	6(1)	18(1)
C(21B)	27(2)	30(1)	48(2)	0(1)	8(1)	12(1)
C(22B)	28(2)	47(2)	35(2)	-6(1)	3(1)	9(1)
C(23B)	30(2)	53(2)	47(2)	8(2)	6(1)	15(2)
C(24B)	33(2)	40(2)	54(2)	11(2)	11(2)	13(1)
C(25B)	19(2)	31(1)	45(2)	-10(1)	5(1)	4(1)
C(26B)	37(2)	31(2)	53(2)	0(1)	5(2)	10(1)
C(27B)	26(2)	32(1)	37(2)	9(1)	10(1)	12(1)
C(28B)	27(2)	39(2)	53(2)	-1(1)	11(1)	7(1)
C(28A)	25(2)	22(1)	35(2)	1(1)	2(1)	8(1)

Hydrogen coordinates (  $\times 10^4$ ) and isotropic displacement parameters ( $\text{\AA}^2 \times 10^3$ ) for cw02a.

	x	y	z	U(eq)
H(3A)	7500	4119	2990	35
H(5A)	4232	923	3493	40
H(6A)	3022	681	2484	42
H(7A)	4235	2400	1156	46
H(9A)	4695	4814	1514	39
H(10A)	5653	6504	847	41
H(12A)	9519	6159	1373	40
H(13A)	8525	4464	2041	40
H(14A)	6525	7380	2	76

H(14B)	7909	8694	-80	76
H(14C)	7083	8703	502	76
H(15A)	10171	8639	1049	101
H(15B)	10009	8797	309	101
H(15C)	10214	7415	586	101
H(17A)	8809	3419	3737	38
H(18A)	10108	3599	4722	37
H(21A)	11082	3489	5956	39
H(22A)	11394	3024	7008	43
H(23A)	9437	2123	7530	45
H(24A)	7129	1641	7001	41
H(26A)	5749	973	5690	37
H(26B)	5845	2567	5838	37
H(3B)	2404	3942	2915	39
H(5B)	-462	296	3312	52
H(6B)	-1676	47	2311	55
H(7B)	-1167	2579	1167	60
H(9B)	2068	5816	2367	40
H(10B)	3033	7540	1710	41
H(12B)	2060	4545	284	44
H(13B)	1113	2852	954	42
H(14D)	3655	6282	-199	82
H(14E)	3496	7758	-360	82
H(14F)	2112	6418	-309	82
H(15D)	3124	9029	895	82
H(15E)	4201	9307	392	82
H(15F)	4649	8878	1078	82
H(17B)	2564	4570	3911	44
H(18B)	3579	5027	4970	47
H(21B)	4495	4961	6215	41
H(22B)	5064	4321	7220	46
H(23B)	4433	2003	7455	52
H(24B)	3160	224	6691	50
H(26C)	2759	-79	5304	49

H(26D)	1274	-3	5465	49
H(28B)	1232	368	4113	48
H(28A)	5112	1967	4453	34

---

**B-13.** Cytotoxicity data for microbes.

<b>Compound</b>	<b>B. subtilis 6633</b>	<b>E. coli</b>	<b>Yeast</b>	<b>Jurkats</b>
<b>Control</b>	0.382	1.067	1.34	1352.5
<b>86A</b>	0.0945	1.2715	1.0585	1142.8
<b>86B</b>	0.242	1.2805	1.0815	1219.8
<b>86C</b>	0.289	1.3255	1.1465	1416.6
<b>87A</b>	0.2105	1.0755	1.07	661.84
<b>87B</b>	0.2225	1.268	1.19	1197.7
<b>87C</b>	0.265	1.335	1.2185	1408.7
<b>88A</b>	0.0905	1.145	1.043	459.03
<b>88B</b>	0.248	1.3505	1.1815	796.19
<b>88C</b>	0.28	1.3805	1.85	1099.9
<b>89A</b>	0.156	0.7	1.607	180.61
<b>89B</b>	0.1875	0.7455	1.746	544.36
<b>89C</b>	0.5535	0.89	1.764	935.13
<b>90A</b>	0.126	0.7925	1.536	199.45
<b>90B</b>	0.5315	0.811	1.715	248.05
<b>90C</b>	0.5415	0.8185	1.771	1181



<b>91A</b>	0.047	1.1945	1.1075	926.01
<b>91B</b>	0.297	1.2075	1.166	1360.1
<b>91C</b>	0.3455	1.3035	1.1705	1413.4
<b>92A</b>	0.1795	0.889	1.238	228.05
<b>92B</b>	0.27	1.013	1.29	324.4
<b>92C</b>	0.32	1.155	1.4155	410.67
<b>93A</b>	0.4765	0.7715	1.828	574.25
<b>93B</b>	0.523	0.8365	1.872	1211.5
<b>93C</b>	0.537	0.849	1.902	1391.4
<b>94A</b>	0.1805	0.959	1.276	109.025
<b>94B</b>	0.2495	0.971	1.264	275.045
<b>94C</b>	0.346	1.061	1.3755	312.05
<b>95A</b>	0.335	0.876	1.2825	668.885
<b>95B</b>	0.4375	0.9385	1.3285	712.825
<b>95C</b>	0.6705	1.0575	1.4785	867.21
<b>96A</b>	0.1535	1.295	1.1	971.36
<b>96B</b>	0.268	1.0385	1.162	1201.7
<b>96C</b>	0.3325	1.341	1.1795	1523.1
<b>97A</b>	0.3505	0.9865	1.3165	151.93
<b>97B</b>	0.3545	1.049	1.3435	2615.85
<b>97C</b>	0.4375	1.0815	1.369	2799.1
<b>98A</b>	0.216	1.013	1.271	55.5

<b>98B</b>	0.2205	1.072	1.319	126.722
<b>98C</b>	0.251	1.083	1.357	213.175
<b>99A</b>	0.1145	0.5805	1.478	119.79
<b>99B</b>	0.183	0.941	1.833	375.32
<b>99C</b>	0.704	0.947	1.862	1577
<b>100A</b>	0.6095	0.707	1.759	787.17
<b>100B</b>	0.6435	0.7495	1.796	1543.3
<b>100C</b>	0.689	0.783	1.844	1660.1
<b>101A</b>	0.017	1.0905	1.0645	1063
<b>101B</b>	0.197	1.293	1.2045	1330.3
<b>101C</b>	0.224	1.3375	1.259	1351.8
<b>102A</b>	0.2015	1.2545	0.6295	775.14
<b>102B</b>	0.2705	1.3425	1.031	808.445
<b>102C</b>	0.2895	1.413	1.035	1077.62
<b>103A</b>	0.1675	1.176	0.808	927.85
<b>103B</b>	0.246	1.3115	1.016	1295.05
<b>103C</b>	0.3375	1.38	1.0245	1824.1
<b>104A</b>	0.3485	0.935	1.337	476.675
<b>104B</b>	0.363	0.9345	1.349	925.455
<b>104C</b>	0.385	1.0245	1.389	793.995
<b>105A</b>	0.141	1.245	0.7245	526.79
<b>105B</b>	0.1755	1.134	1.128	702.42

<b>105C</b>	0.303	1.355	1.13	1319.6
<b>106A</b>	0.18	1.019	1.2415	63.7075
<b>106B</b>	0.2945	1.038	1.334	166.115
<b>106C</b>	0.3205	1.251	1.484	315.35
<b>107A</b>	0.3385	0.9345	1.3265	624.28
<b>107B</b>	0.351	0.9765	1.3715	1153
<b>107C</b>	0.5745	1.194	1.4075	1184.9
<b>108A</b>	0.104	1.027	1.388	995.515
<b>108B</b>	0.2385	1.0465	1.392	1182.1
<b>108C</b>	0.2915	1.157	1.524	1300.7
<b>109A</b>	0.205	1.0065	1.346	262.315
<b>109B</b>	0.2505	1.0215	1.352	318.73
<b>109C</b>	0.375	1.141	1.479	856.985
<b>110A</b>	0.27	1.023	1.335	291.72
<b>110B</b>	0.2905	1.0285	1.354	1131.5
<b>110C</b>	0.345	1.211	1.508	1523.3
<b>111A</b>	0.1045	0.73	1.709	348.72
<b>111B</b>	0.506	0.754	1.808	1065.9
<b>111C</b>	0.554	0.864	1.845	1454.2
<b>112A</b>	0.302	0.9595	1.343	29.9465
<b>112B</b>	0.3385	1.03	1.3665	729.675
<b>112C</b>	0.386	1.2255	1.6095	898.63

<b>113A</b>	0.1285	1.347	1.066	693.29
<b>113B</b>	0.1755	1.407	1.133	735.37
<b>113C</b>	0.1885	1.486	1.1815	956.85
<b>26A</b>	0.1325	0.995	1.344	47.7535
<b>26B</b>	0.45	1.037	1.045	446.6
<b>26C</b>	0.5145	1.139	1.438	516.2
<b>114A</b>	0.1055	0.7925	1.536	199.45
<b>114B</b>	0.5425	0.811	1.715	248.05
<b>114C</b>	0.5875	0.8185	1.771	1181
<b>115A</b>	0.096	1.1845	1	655.13
<b>115B</b>	0.2735	1.3445	1.1105	885.45
<b>115C</b>	0.2925	1.387	1.1835	1107.4
<b>116A</b>	0.0356	1.2515	0.9995	1318.2
<b>116B</b>	0.0985	1.355	1.028	1459.6
<b>116C</b>	0.1775	1.376	1.0325	1478
<b>117A</b>	0.2645	0.939	1.2405	99.0895
<b>117B</b>	0.272	1.002	1.2855	232.865
<b>117C</b>	0.2915	1.146	1.3775	715.45
<b>118A</b>	0.087	1.151	1.019	734.525
<b>118B</b>	0.1825	1.2765	1.025	1680.2
<b>118C</b>	0.2205	1.504	1.063	1715.45
<b>119A</b>	0.3745	0.9745	1.3445	603.33

<b>119B</b>	0.3835	1.021	1.447	605.64
<b>119C</b>	0.5085	1.0465	1.4675	638.36
<b>120A</b>	0.021	0.9205	1.324	499.145
<b>120B</b>	0.069	1.0615	1.3245	756.75
<b>120C</b>	0.378	1.106	1.4375	958.04
<b>121A</b>	0.1385	1.039	1.301	558.81
<b>121B</b>	0.1815	1.054	1.311	1051.4
<b>121C</b>	0.3185	1.066	1.427	1188.73
<b>122A</b>	0.0565	1.029	1.2475	59.7755
<b>122B</b>	0.249	1.052	1.403	244.86
<b>122C</b>	0.344	1.058	1.4325	257.55
<b>123A</b>	0.435	0.5575	1.459	938.53
<b>123B</b>	0.5855	0.824	1.691	1305.6
<b>123C</b>	0.5915	0.9025	1.812	1566.2
<b>124A</b>	0.1665	1.374	0.9595	718.03
<b>124B</b>	0.247	1.384	1.0995	1245.7
<b>124C</b>	0.3465	1.369	1.1715	1296.7
<b>125A</b>	0.3715	0.961	1.275	872.96
<b>125B</b>	0.402	1.1165	1.286	880.355
<b>125C</b>	0.4125	1.1525	1.313	1076.85
<b>126A</b>	0.1815	1.4615	0.7915	359.593
<b>126B</b>	0.197	1.4635	1.016	470.015

<b>126C</b>	0.2295	1.474	1.0285	1443.05
<b>127A</b>	0.3265	0.991	1.3465	691.315
<b>127B</b>	0.356	0.9915	1.391	761.965
<b>127C</b>	0.372	1.0185	1.438	1007.865
<b>128A</b>	0.104	1.027	1.388	558.81
<b>128B</b>	0.2385	1.0465	1.92	1015.4
<b>128C</b>	0.2915	1.157	1.524	1188.73
<b>129A</b>	0.2005	0.9995	1.298	420.065
<b>129B</b>	0.273	0.977	1.326	668.42
<b>129C</b>	0.2725	1.03	1.35	752.02
<b>130A</b>	0.1615	1.0585	0.5925	285.24
<b>130B</b>	0.235	1.07	0.977	312.065
<b>130C</b>	0.2825	1.148	1.0495	808.91
<b>131A</b>	0.168	0.968	1.185	60.125
<b>131B</b>	0.178	0.991	1.2825	125.915
<b>131C</b>	0.182	1.026	1.369	719.6
<b>132A</b>	0.3335	1.003	1.2555	653.74
<b>132B</b>	0.3455	1.0945	1.3245	789.945
<b>132C</b>	0.368	1.2395	1.33	854.43
<b>27A</b>	0.223	1.191	0.6805	501.92
<b>27B</b>	0.3135	1.466	1.068	623.935
<b>27C</b>	0.3465	1.5585	1.0715	1379.85

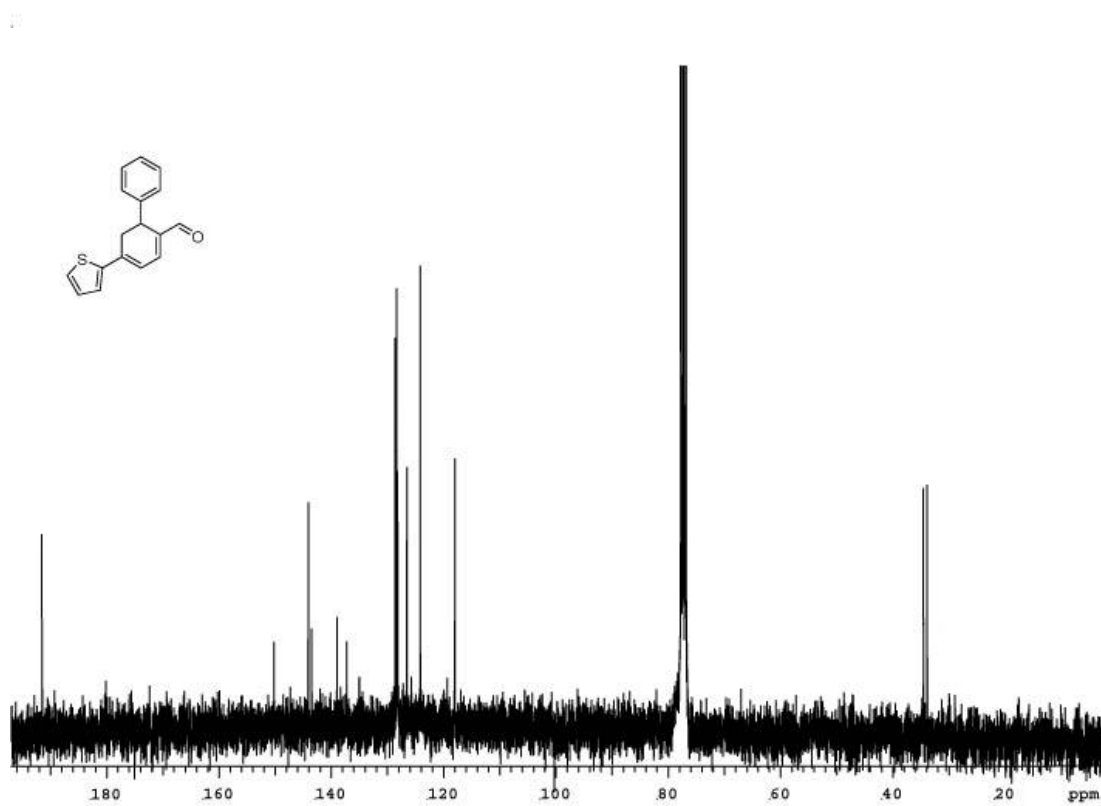
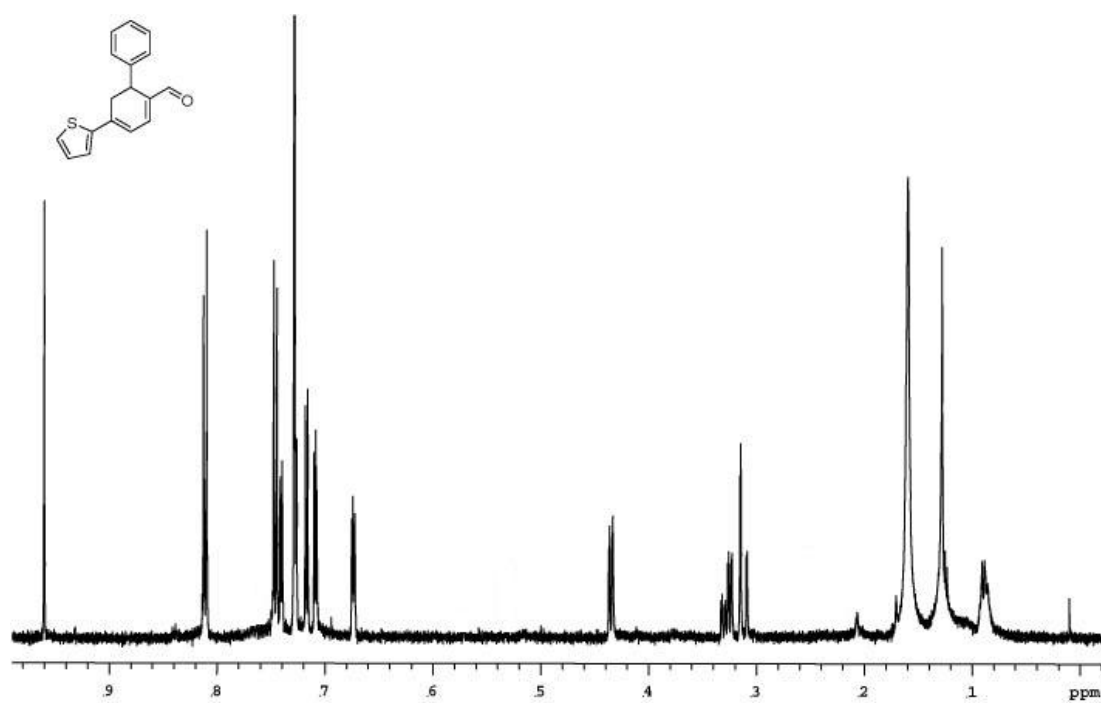
<b>28A</b>	0.1955	1.034	1.095	131.772
<b>28B</b>	0.2655	1.049	1.286	321.3
<b>28C</b>	0.281	1.19	1.3535	489.9
<b>133A</b>	0.1685	0.7905	1.522	525.05
<b>133B</b>	0.3605	0.876	1.694	814.23
<b>133C</b>	0.3825	0.928	1.74	1741.3
<b>134A</b>	0.1685	0.7905	1.522	525.05
<b>134B</b>	0.3605	0.876	1.694	814.23
<b>134C</b>	0.3825	0.928	1.74	1741.3
<b>135A</b>	0.038	1.067	0.783	610.73
<b>135B</b>	0.1035	1.396	1.174	673.98
<b>135C</b>	0.213	1.373	1.2	1081.4
<b>136A</b>	0.1105	1.019	1.3465	450.585
<b>136B</b>	0.347	1.029	1.373	830.41
<b>136C</b>	0.3565	1.084	1.5285	1251.45
<b>137A</b>	0.2585	1.301	0.998	656.75
<b>137B</b>	0.2896	1.333	1.0435	1079.7
<b>137C</b>	0.347	1.342	1.1625	1568.4
<b>138A</b>	0.332	0.9955	1.321	110.65
<b>138B</b>	0.3375	1.038	1.351	370.58
<b>138C</b>	0.459	1.0695	1.353	483.41
<b>139A</b>	0.364	0.996	1.213	1968

<b>139B</b>	0.3745	0.9955	1.3205	2311.5
<b>139C</b>	0.5055	1.0435	1.353	2650.2
<b>140A</b>	0.312	0.9625	1.3	553.955
<b>140B</b>	0.321	0.951	1.35	673.625
<b>140C</b>	0.3355	0.991	1.361	675.48
<b>141A</b>	0.325	0.929	1.323	241.88
<b>141B</b>	0.365	0.978	1.375	420.755
<b>141C</b>	0.3705	0.9335	1.377	663.42
<b>142A</b>	0.2185	1.403	0.4755	670.39
<b>142B</b>	0.248	1.6365	1.05	817.695
<b>142C</b>	0.3645	1.595	1.109	966.04
<b>143A</b>	0.182	0.992	1.231	345.45
<b>143B</b>	0.247	1.04	1.299	375.4
<b>143C</b>	0.4335	1.149	1.3185	417.035
<b>144A</b>	0.2545	1.056	1.299	494.525
<b>144B</b>	0.281	1.127	1.339	1053.91
<b>144C</b>	0.33	1.2715	1.446	1789.6
<b>145A</b>	0.2605	1.066	1.27	802.78
<b>145B</b>	0.307	1.075	1.305	831.34
<b>145C</b>	0.506	1.133	1.444	1013.03
<b>146A</b>	0.2555	1.026	0.467	370.46
<b>146B</b>	0.269	1.054	1.324	631.655

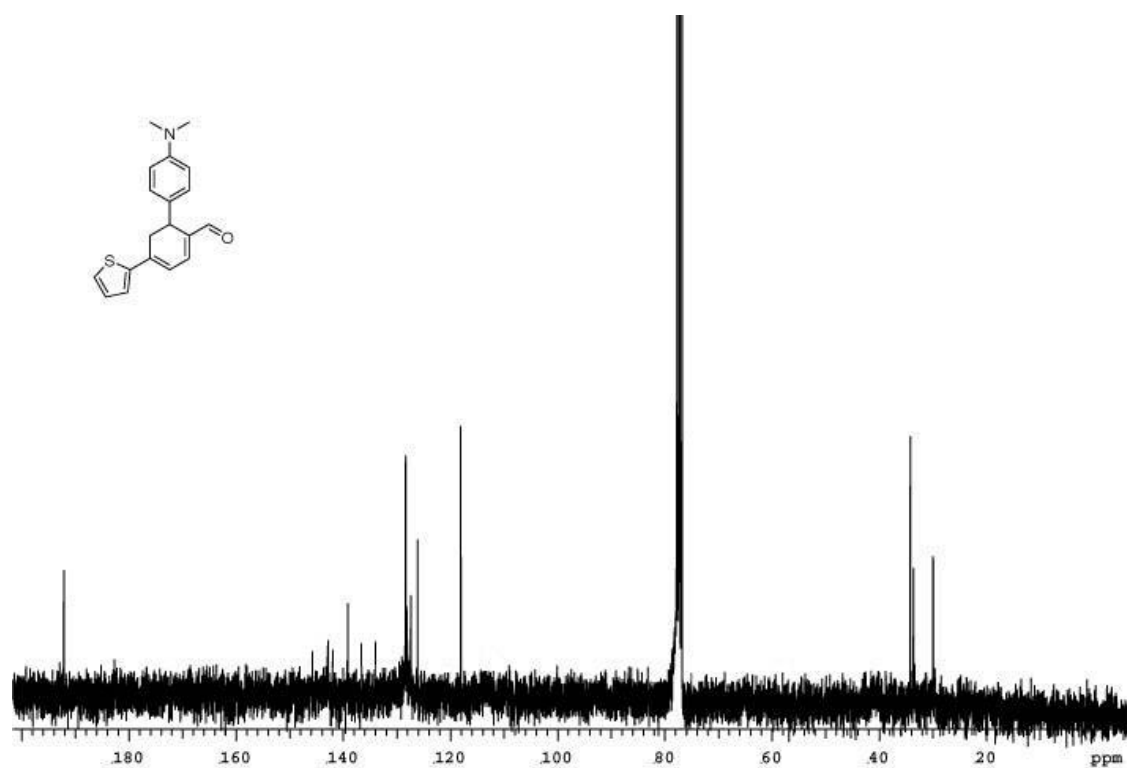
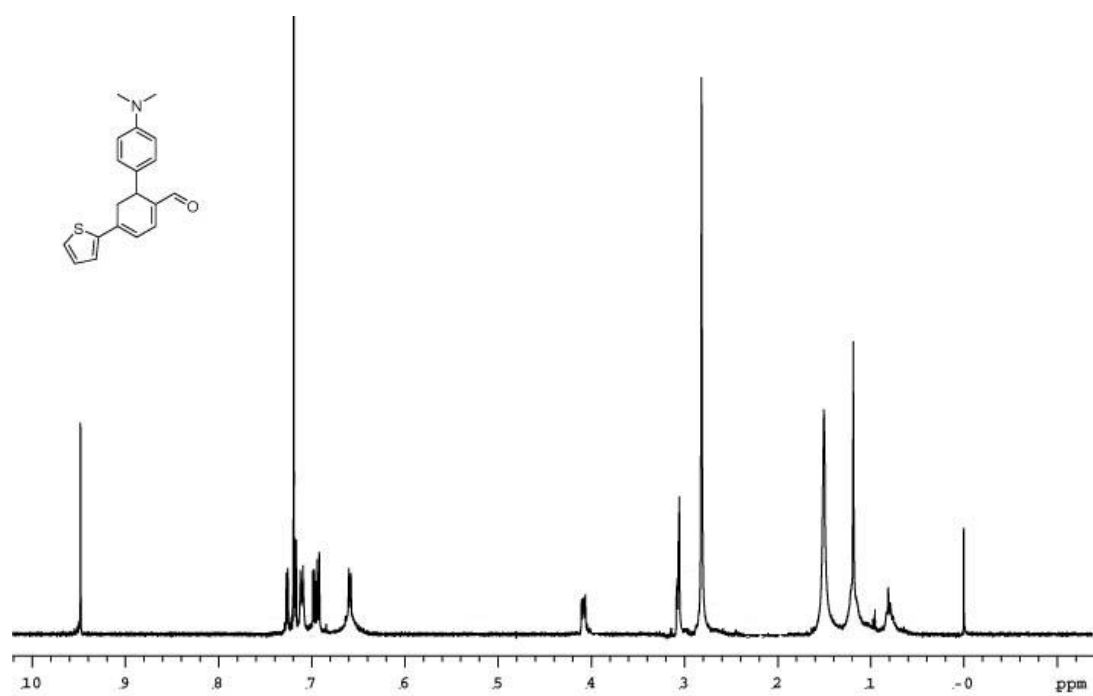


<b>146C</b>	0.409	1.0605	1.398	939.52
<b>147A</b>	0.0535	1.2355	0.606	1433
<b>147B</b>	0.115	1.43	1.01	1563.9
<b>147C</b>	0.2535	1.568	1.03	1541.5
<b>148A</b>	0.1385	1.038	0.8515	624.485
<b>148B</b>	0.152	1.438	1.0305	1044.89
<b>148C</b>	0.316	1.542	1.046	1209.85
<b>149A</b>	0.3235	1.066	1.282	669.1
<b>149B</b>	0.3535	1.0775	1.337	869.12
<b>149C</b>	0.6065	1.2095	1.348	992.495
<b>150A</b>	0.1145	1.1675	0.981	348.49
<b>150B</b>	0.207	1.385	1.197	673.74
<b>150C</b>	0.352	1.379	1.2145	846.95
<b>151A</b>	0.0495	1.215	0.9935	391.965
<b>151B</b>	0.2315	1.3715	1.0335	901.74
<b>151C</b>	0.237	1.64	1.074	1225.93
<b>152A</b>	0.2885	1.014	1.361	638.705
<b>152B</b>	0.294	1.056	1.368	684.64
<b>152C</b>	0.416	1.074	1.48	1015.3
<b>153A</b>	0.2575	1.036	1.32	314.845
<b>153B</b>	0.2865	1.076	1.335	399.595
<b>153C</b>	0.378	1.08	1.341	414.5

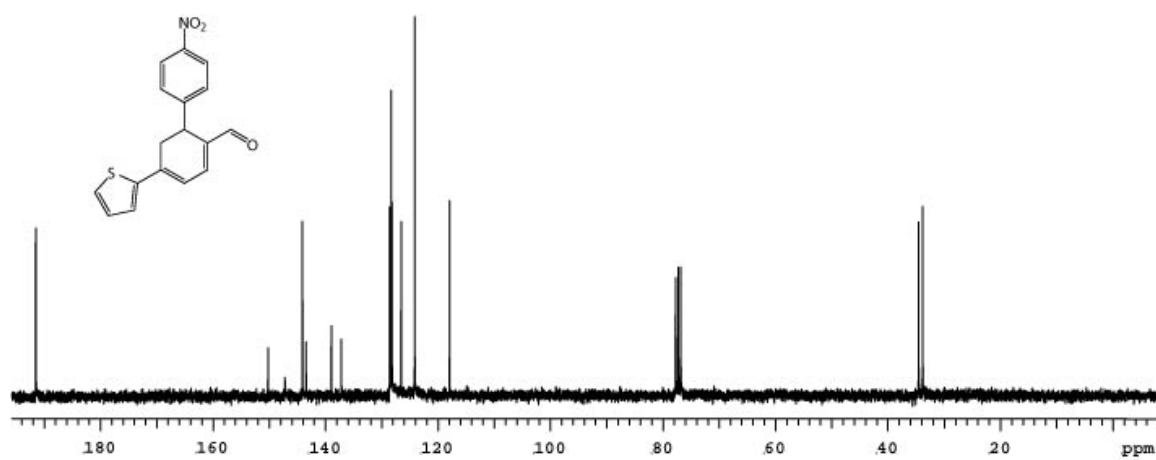
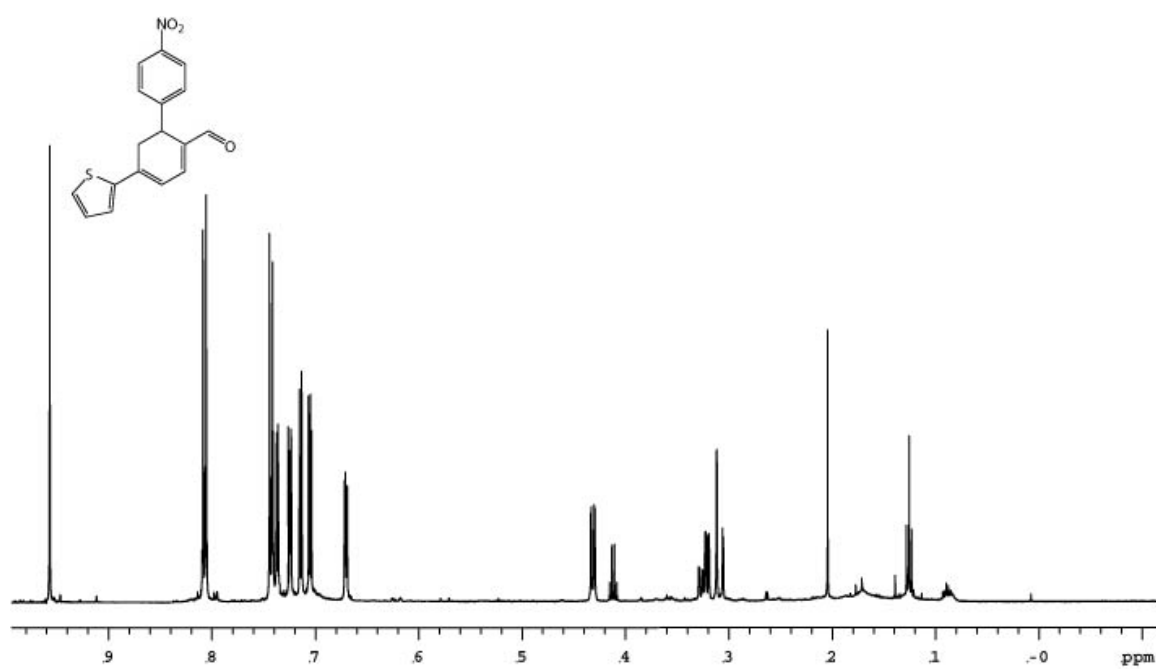
<b>154A</b>	0.0195	1.2265	1	890.5
<b>154B</b>	0.2105	1.573	1.0345	1350.65
<b>154C</b>	0.3655	1.5475	1.0495	1827.5



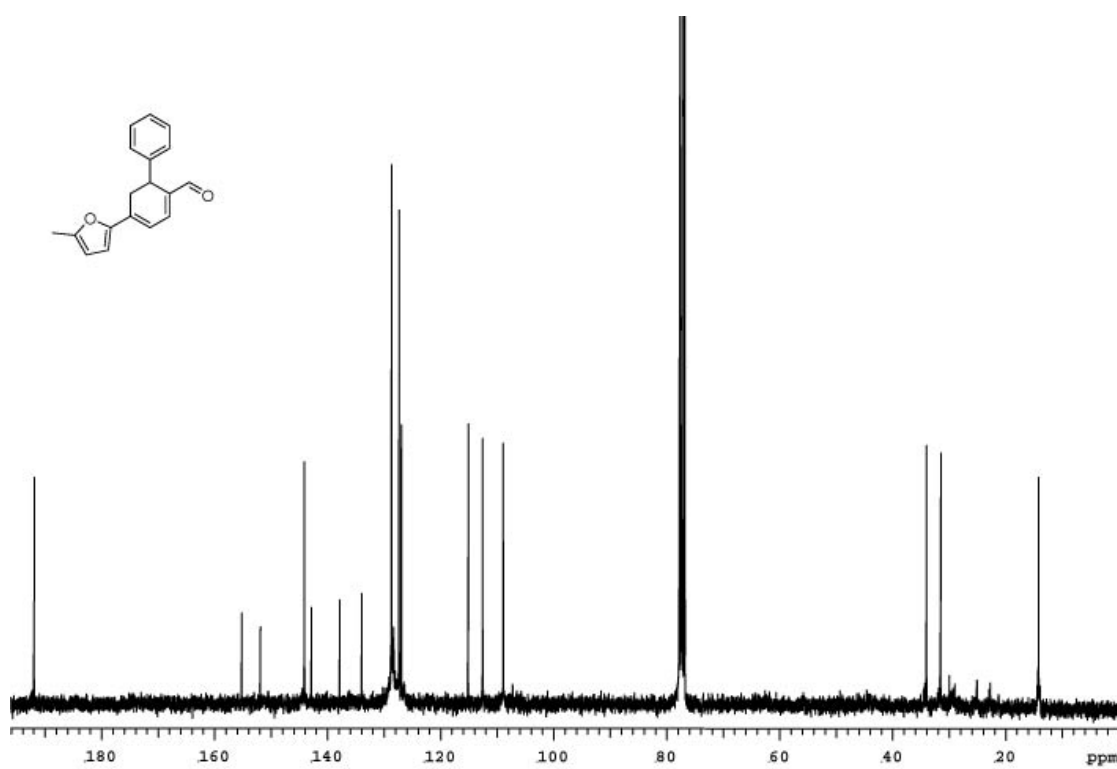
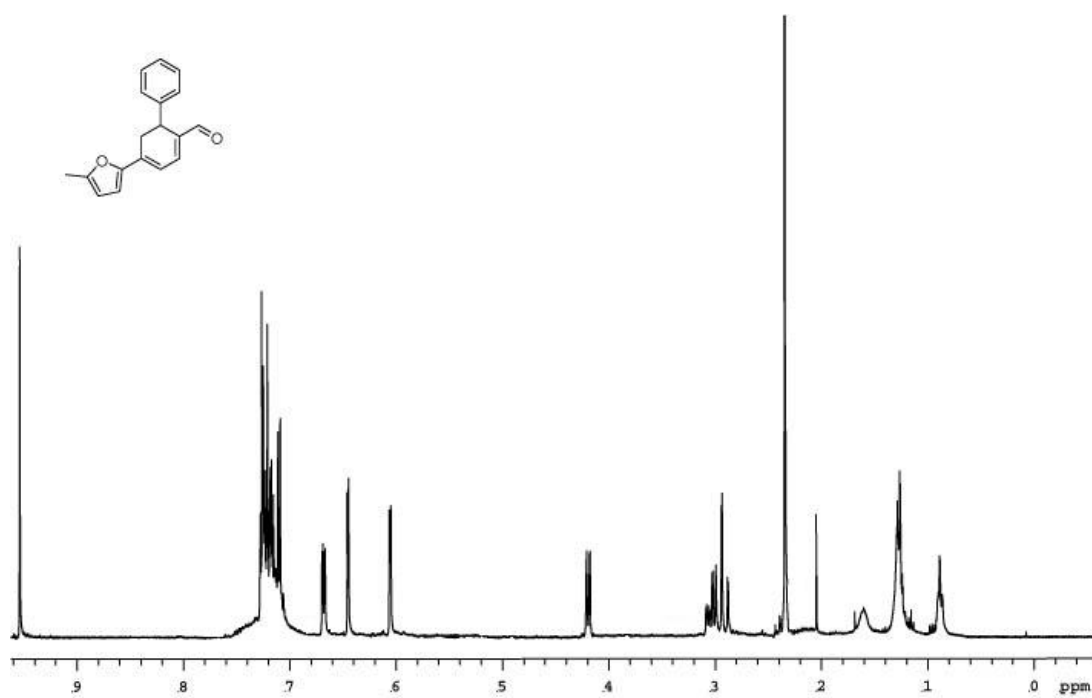
B-14. Spectra of 86.



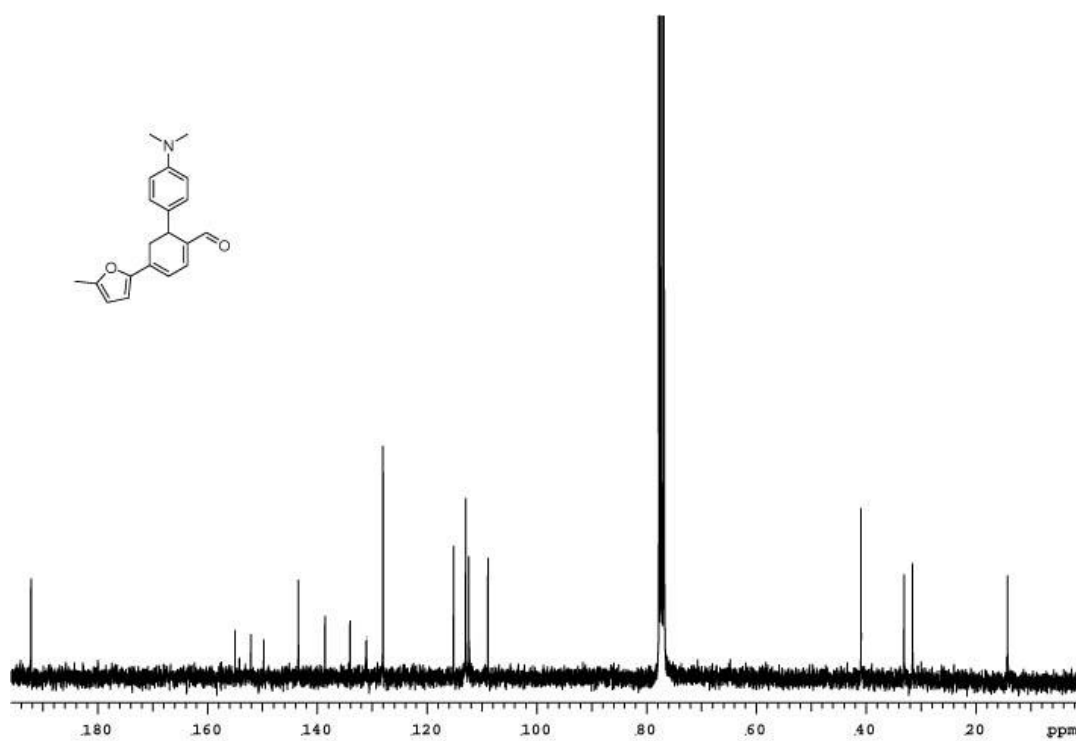
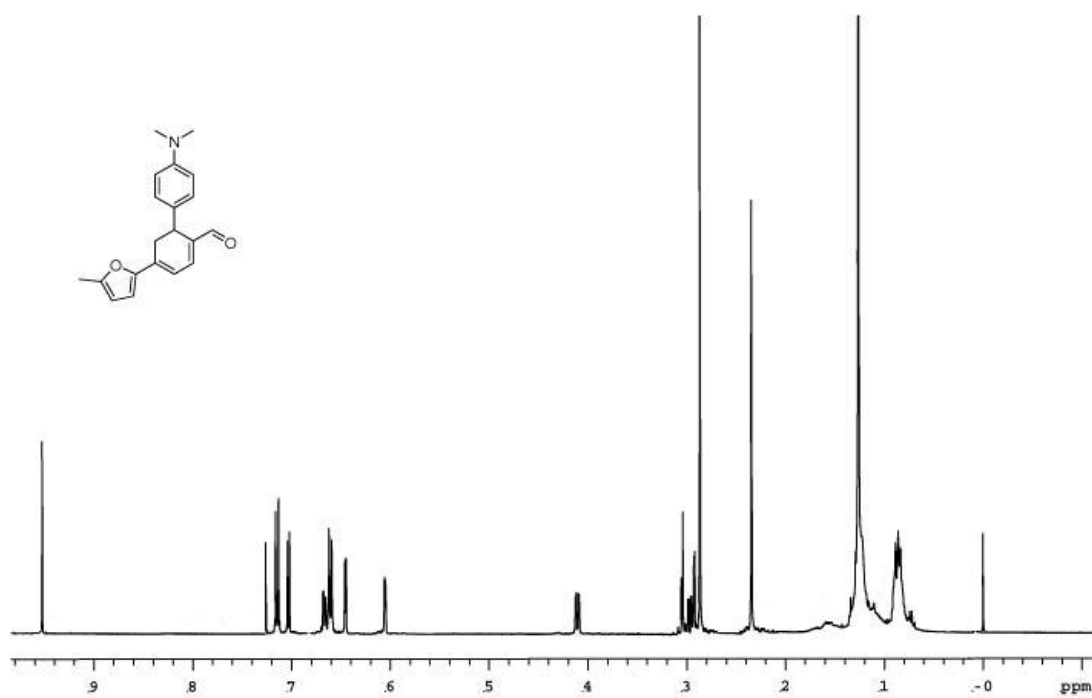
B-15. Spectra of 87.



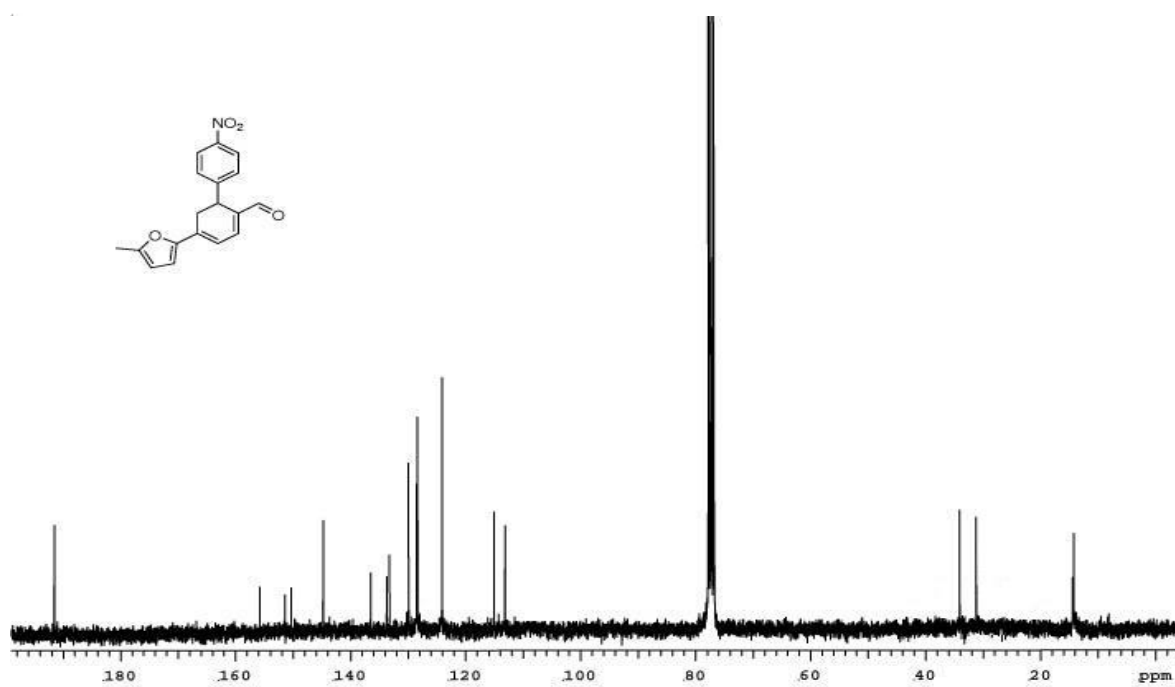
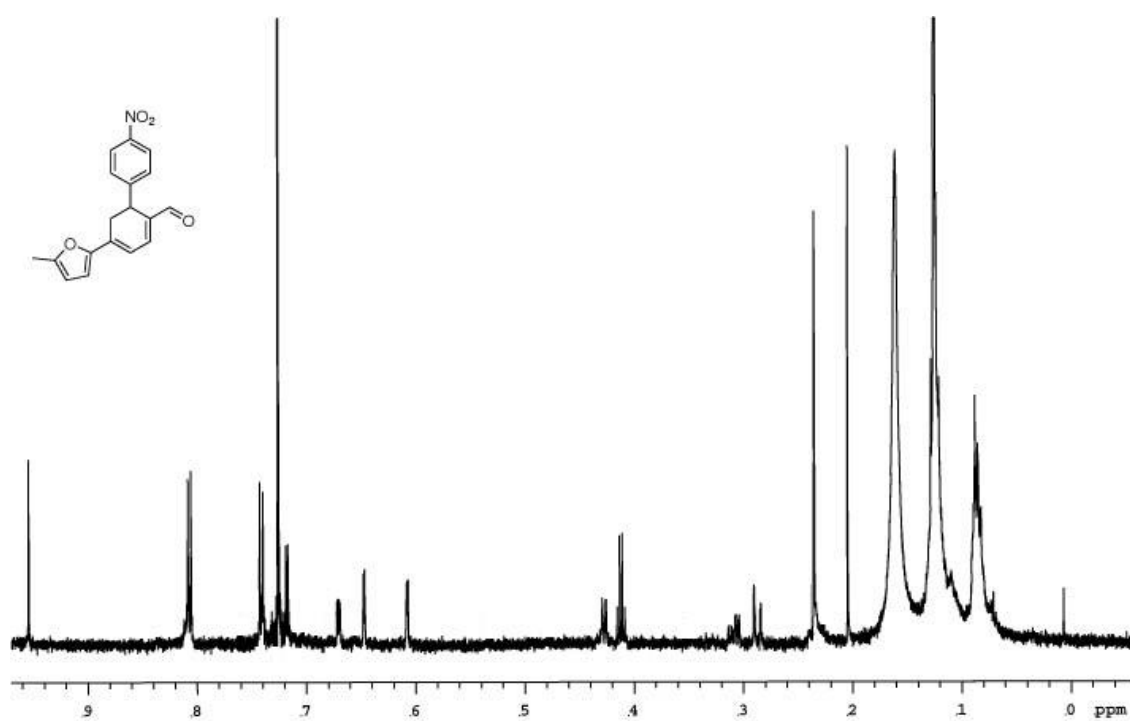
B-16. Spectra of 88.



B-17. Spectra of 89.

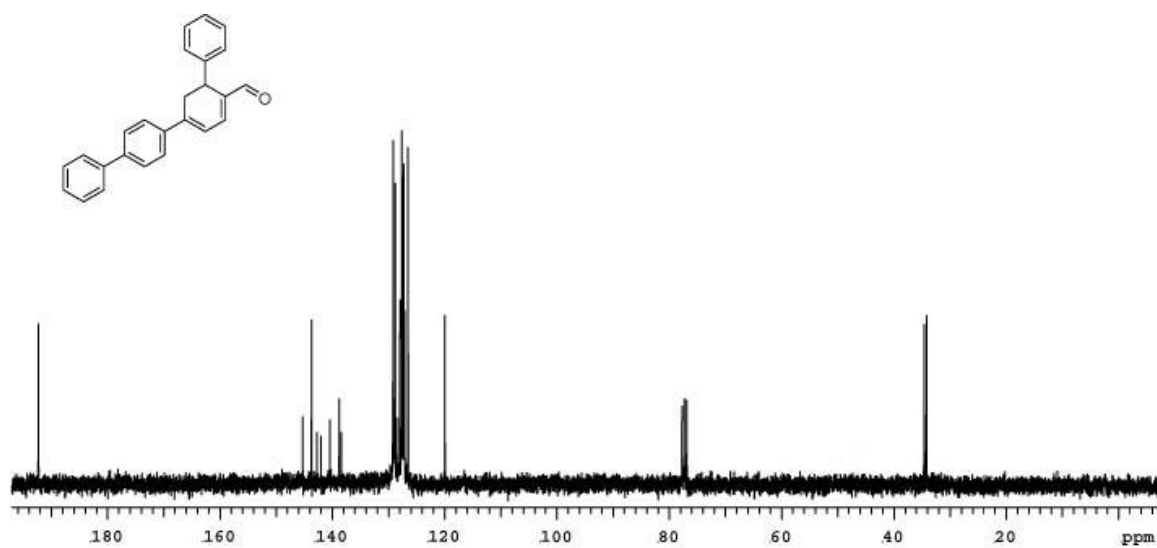
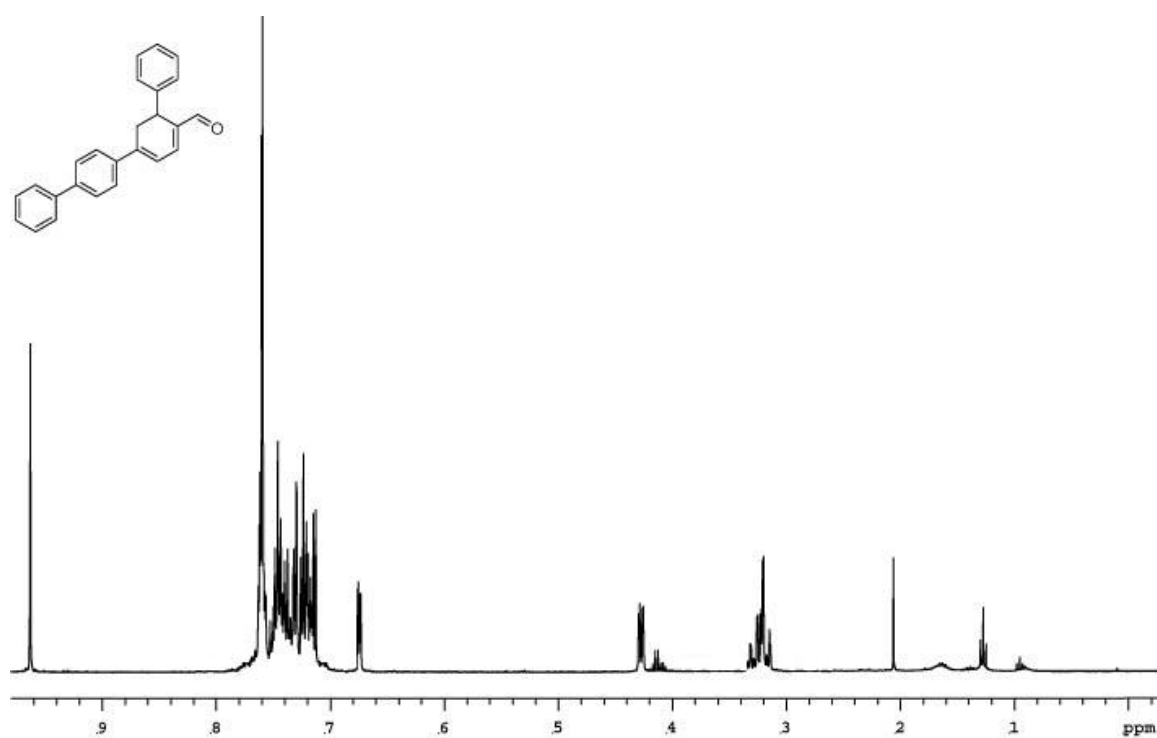


B-18. Spectra of 90.

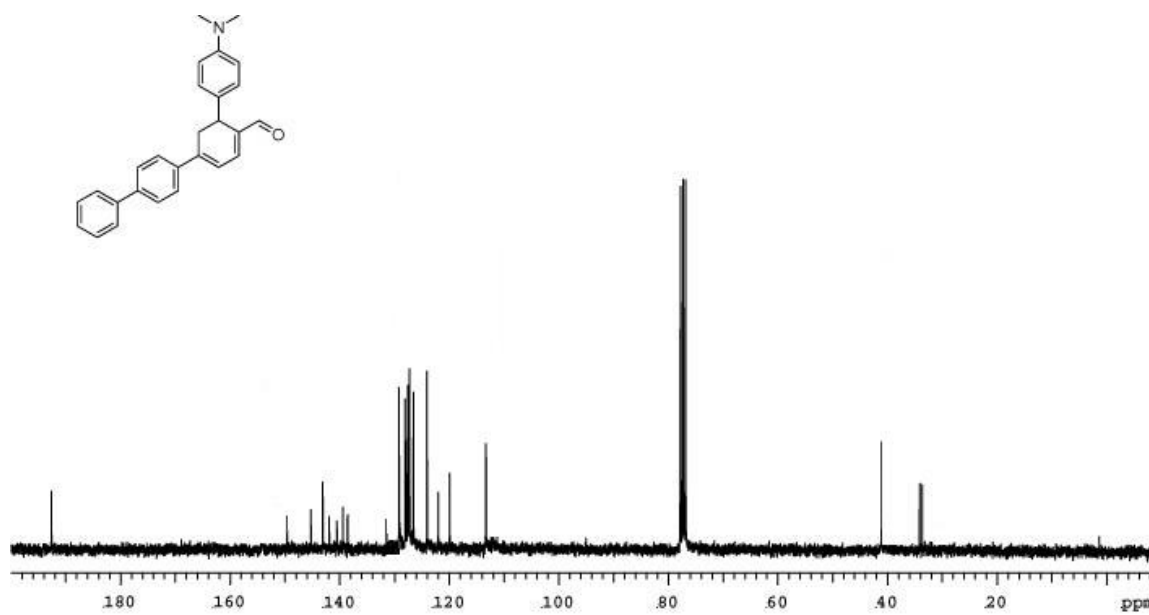
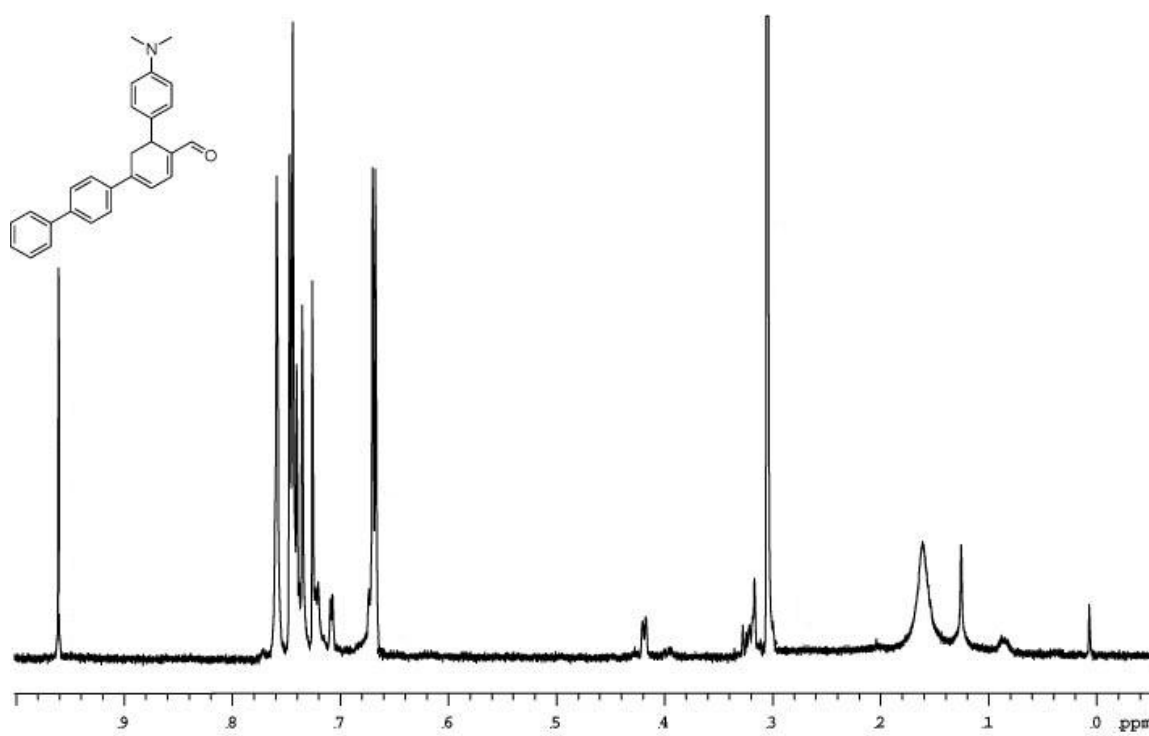


B-19. Spectra of 91.

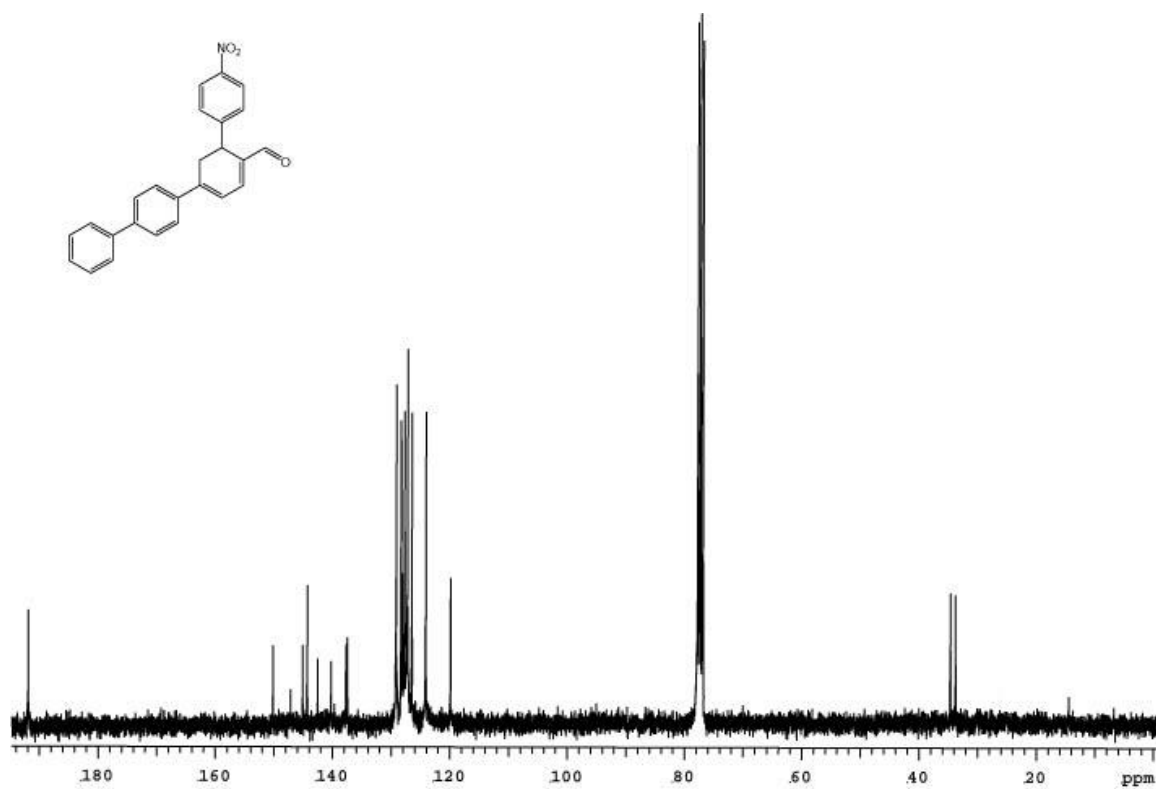
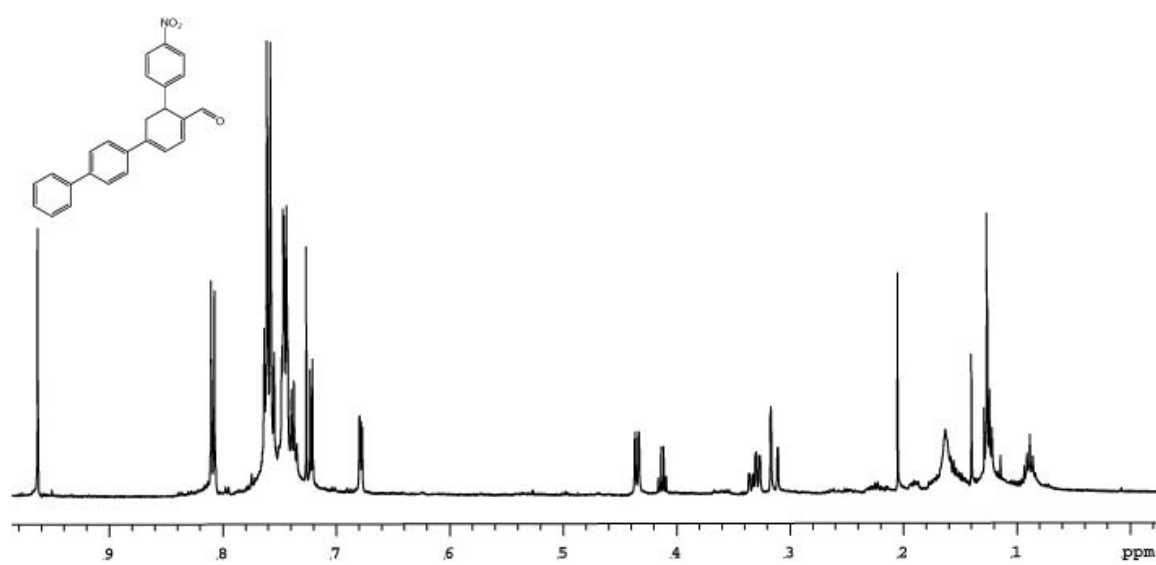




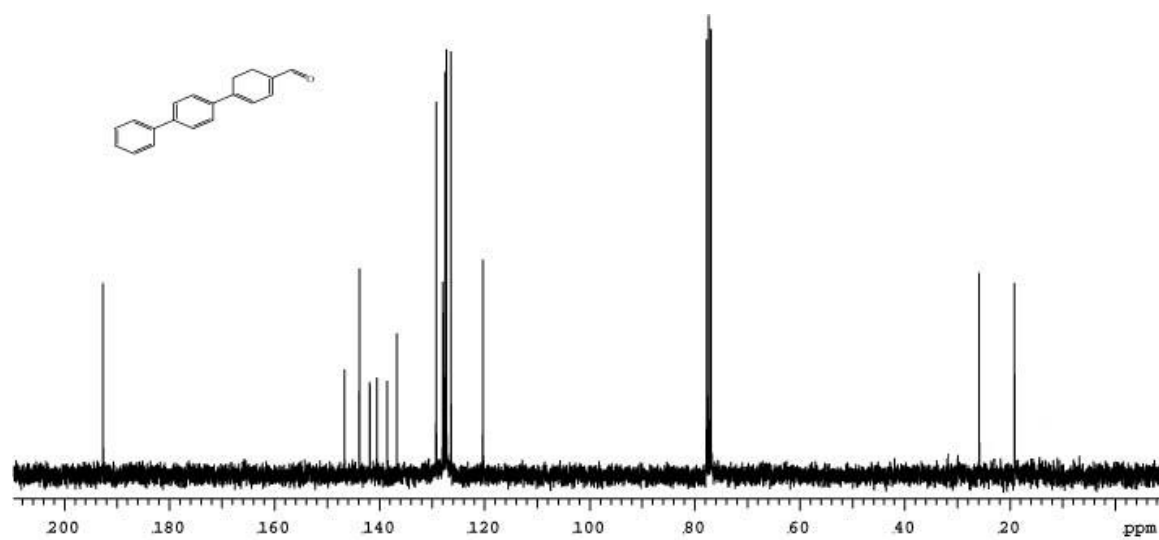
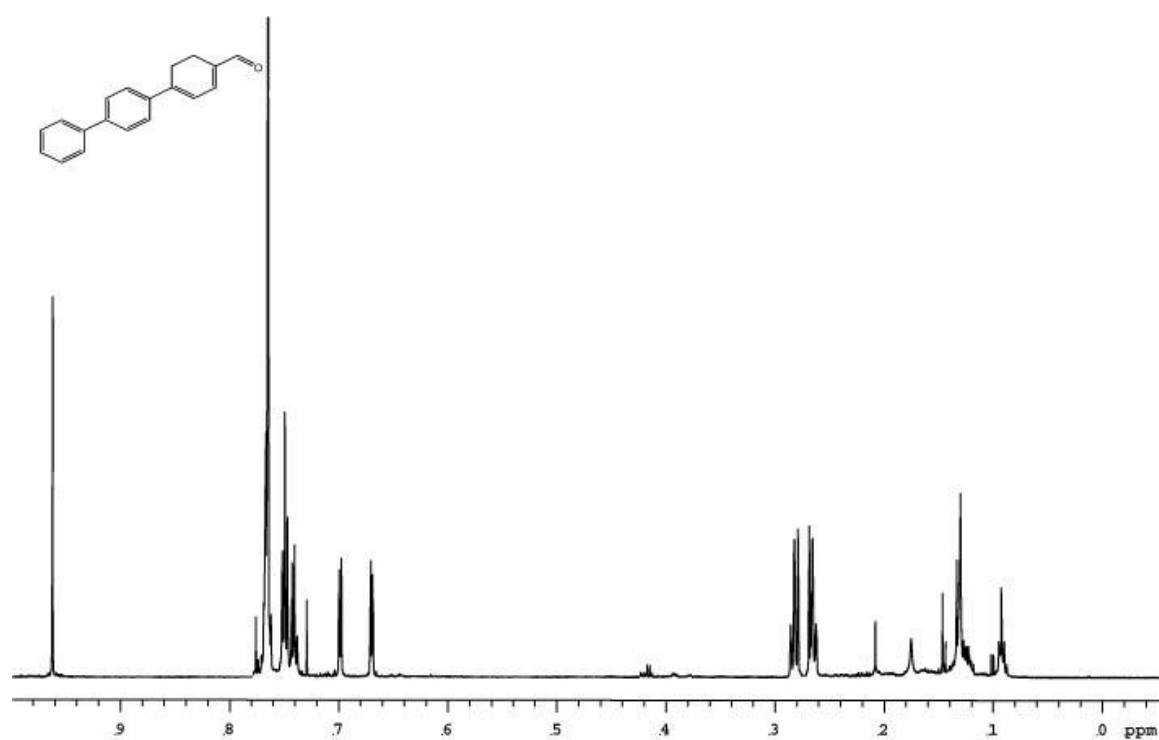
B-20. Spectra of 92.



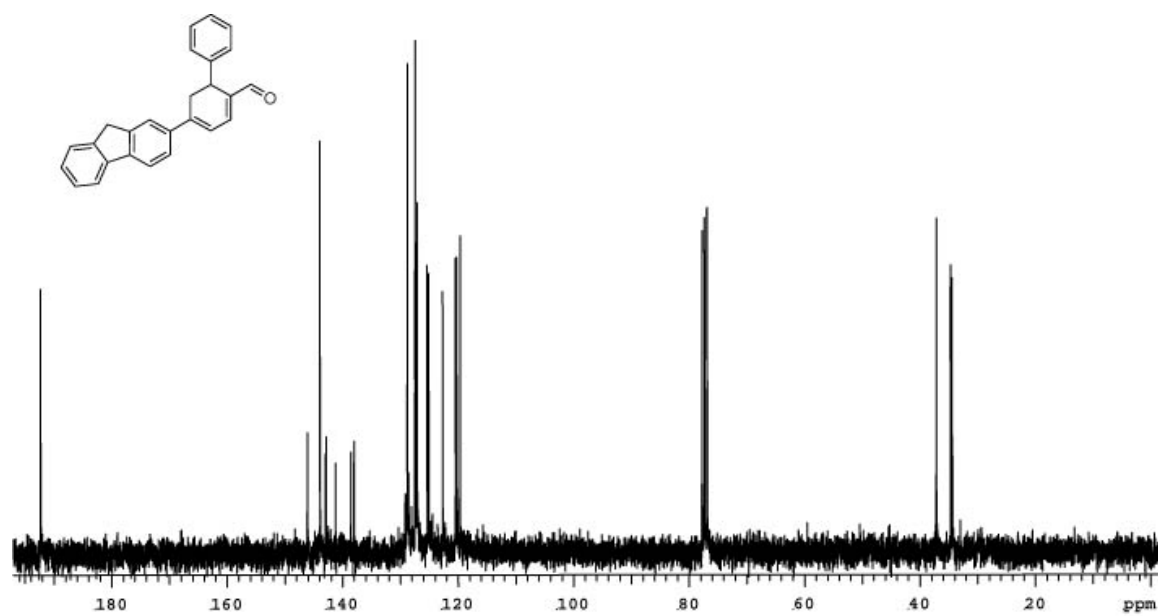
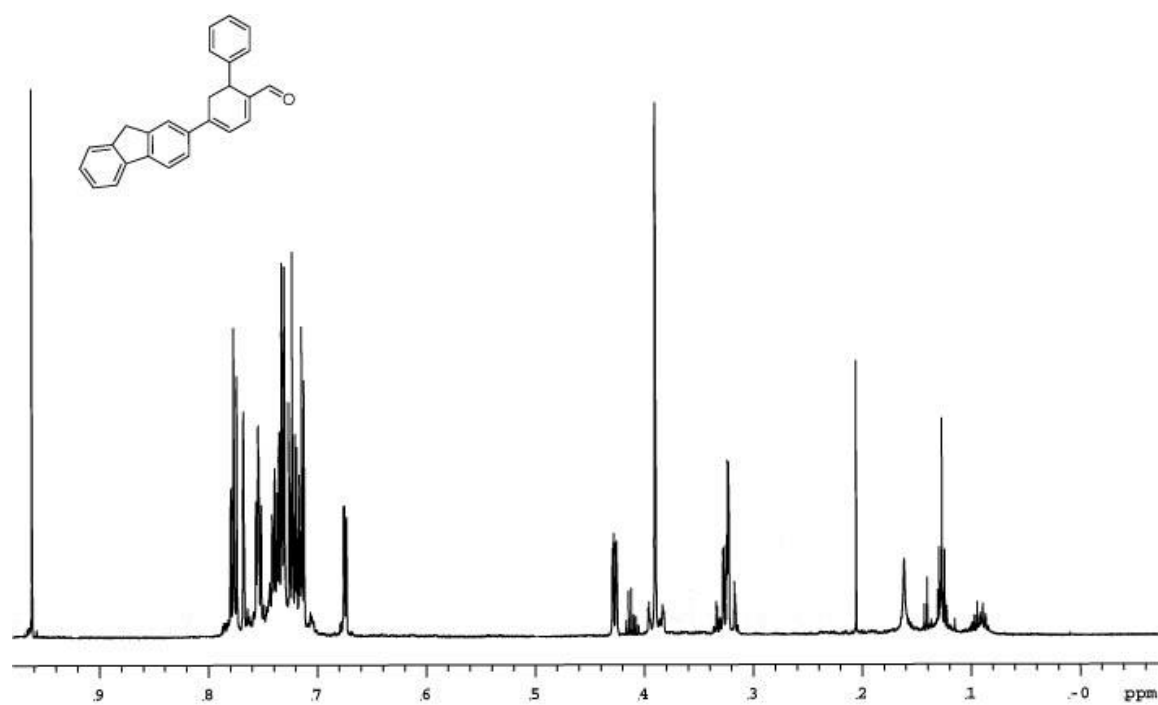
B-21. Spectra of 93.



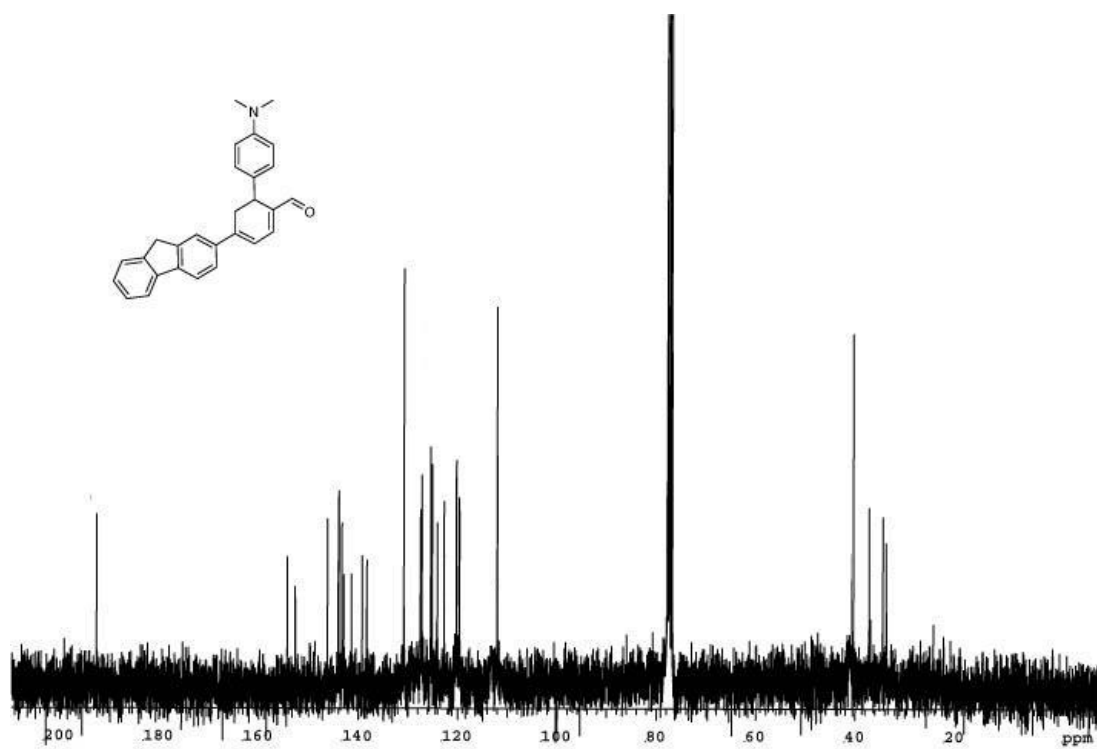
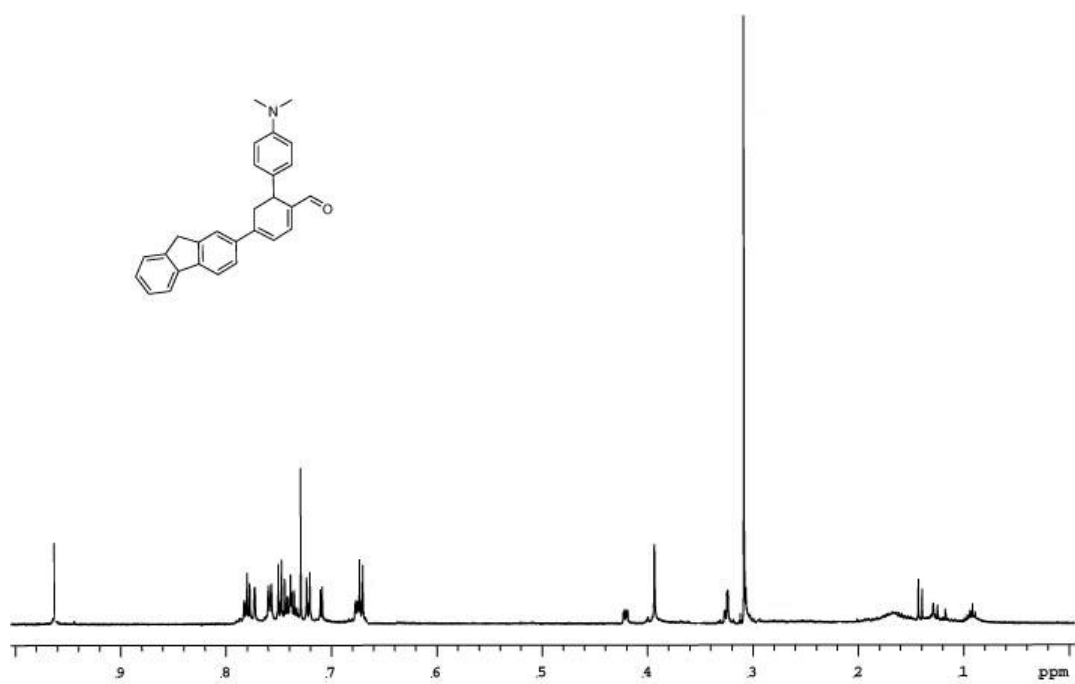
B-22. Spectra of 94.



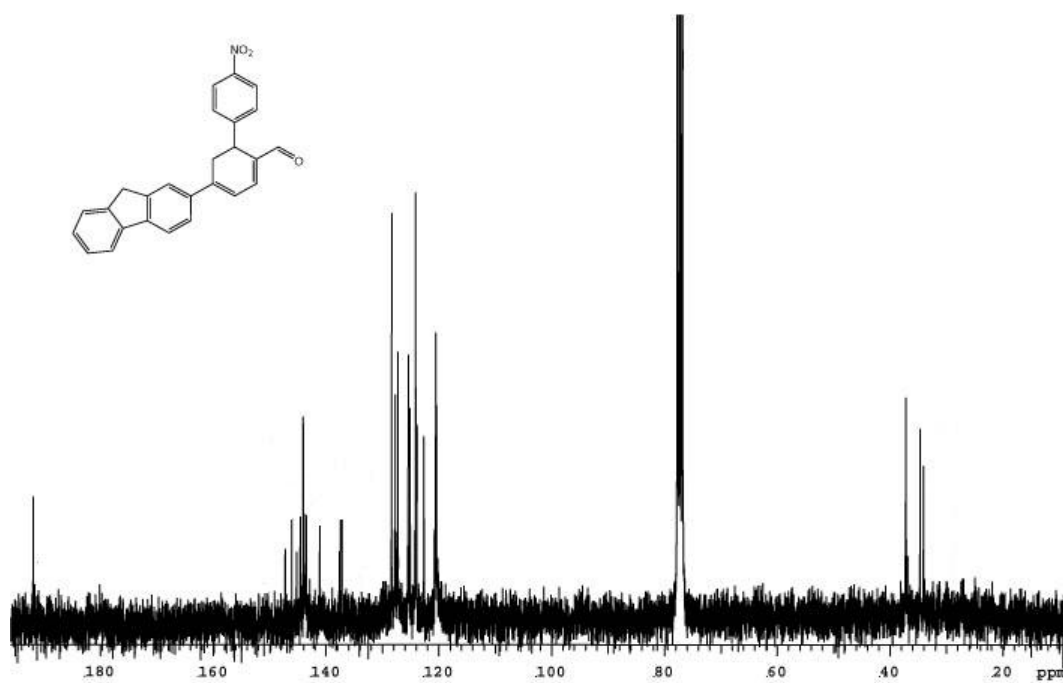
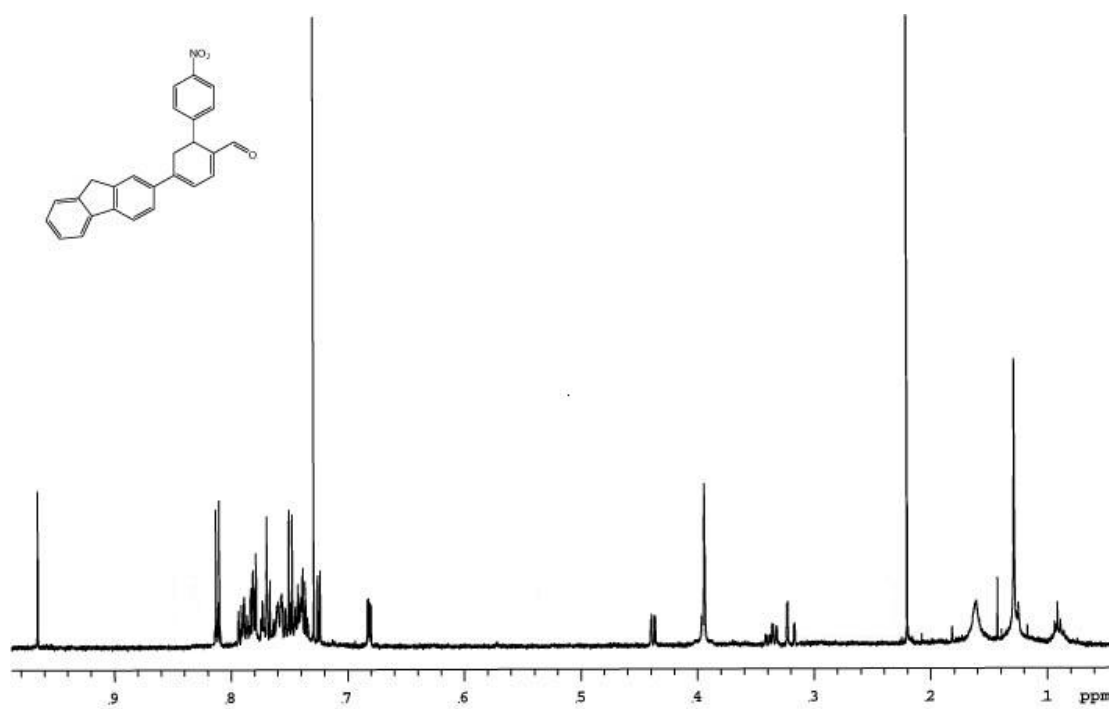
B-23. Spectra of 95.



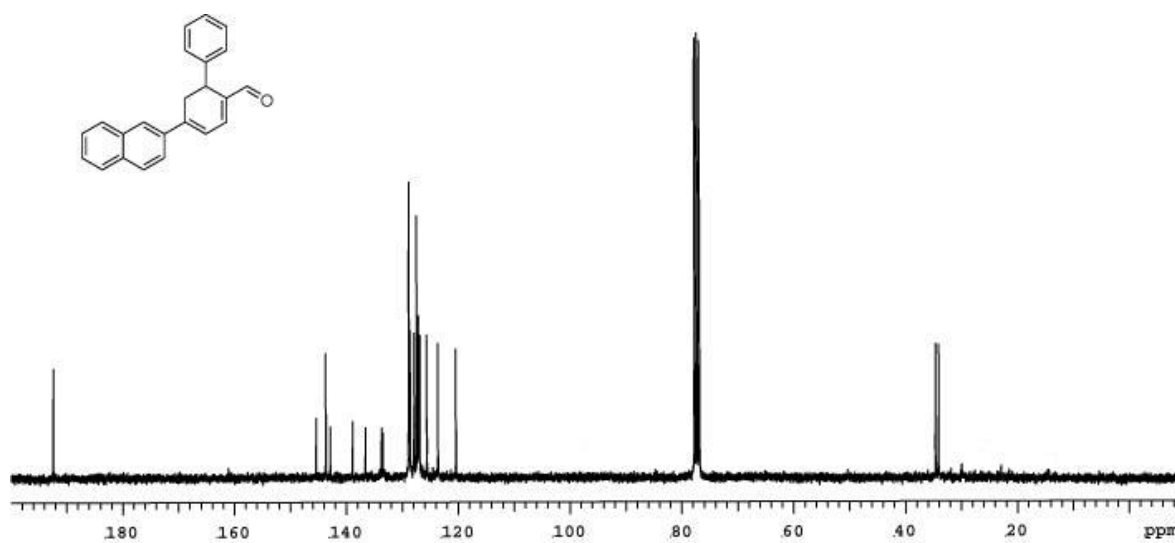
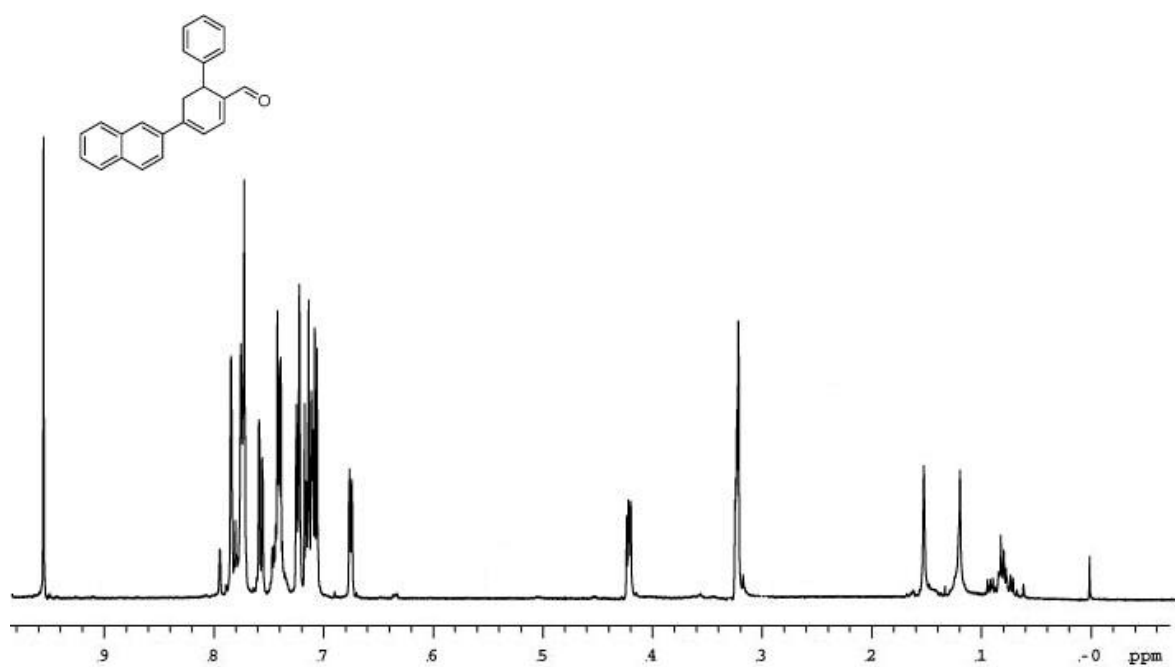
B-24. Spectra of 96.



B-25. Spectra of 97.

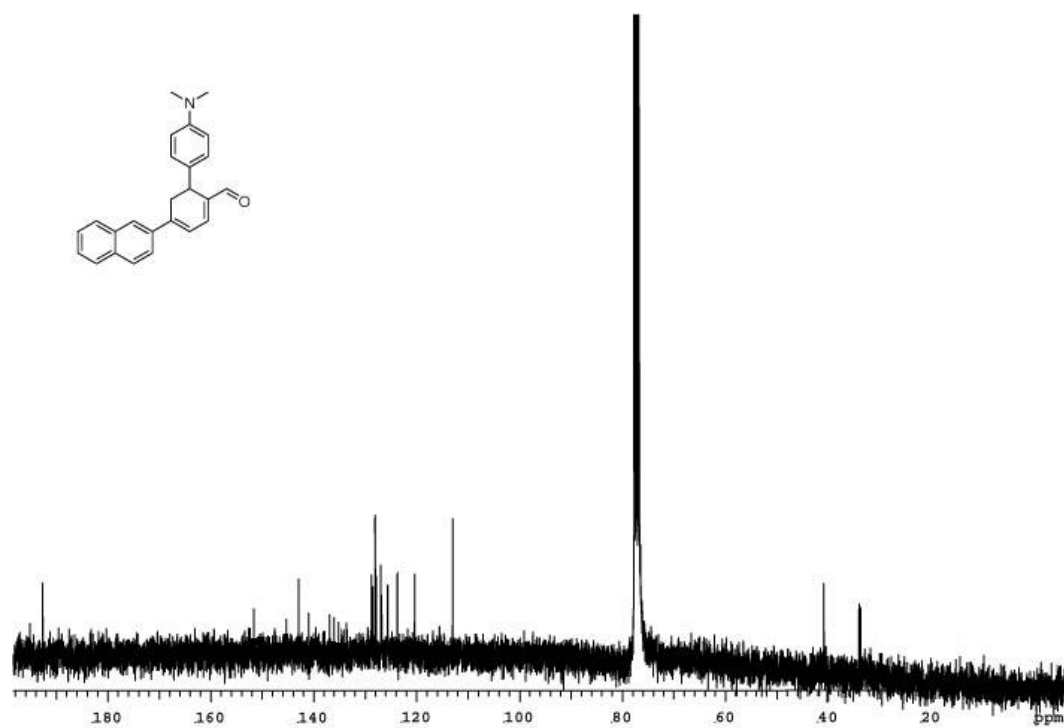
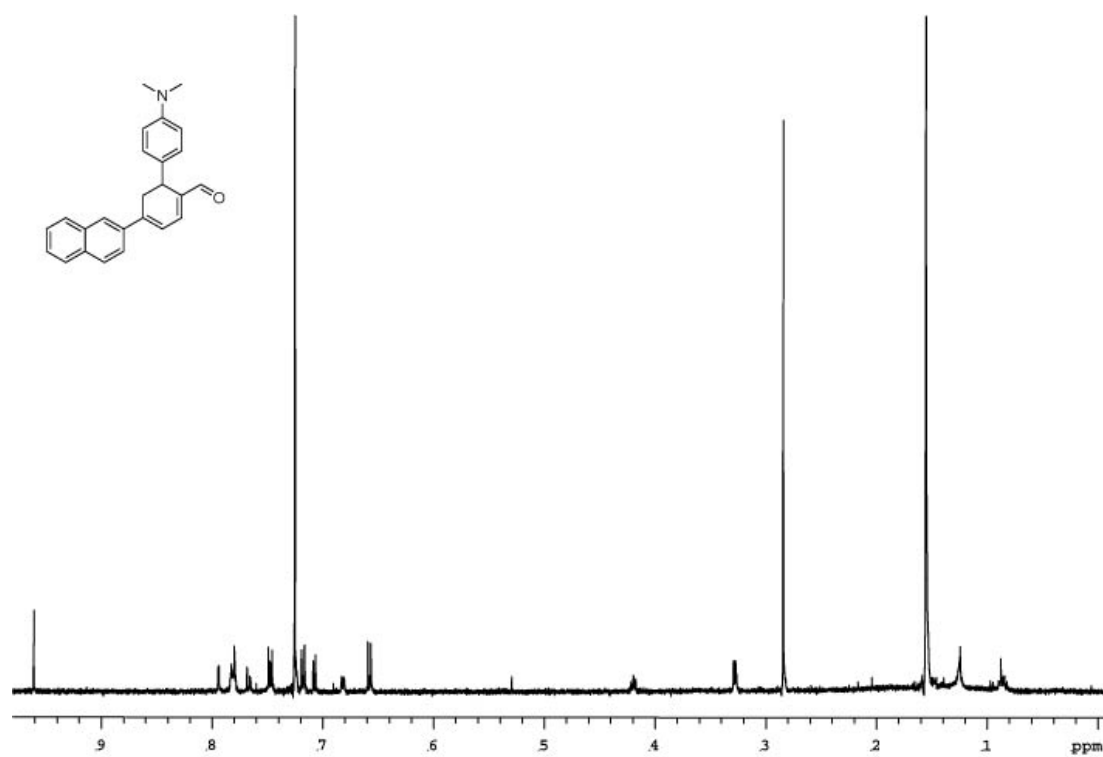


B-26. Spectra of 98.

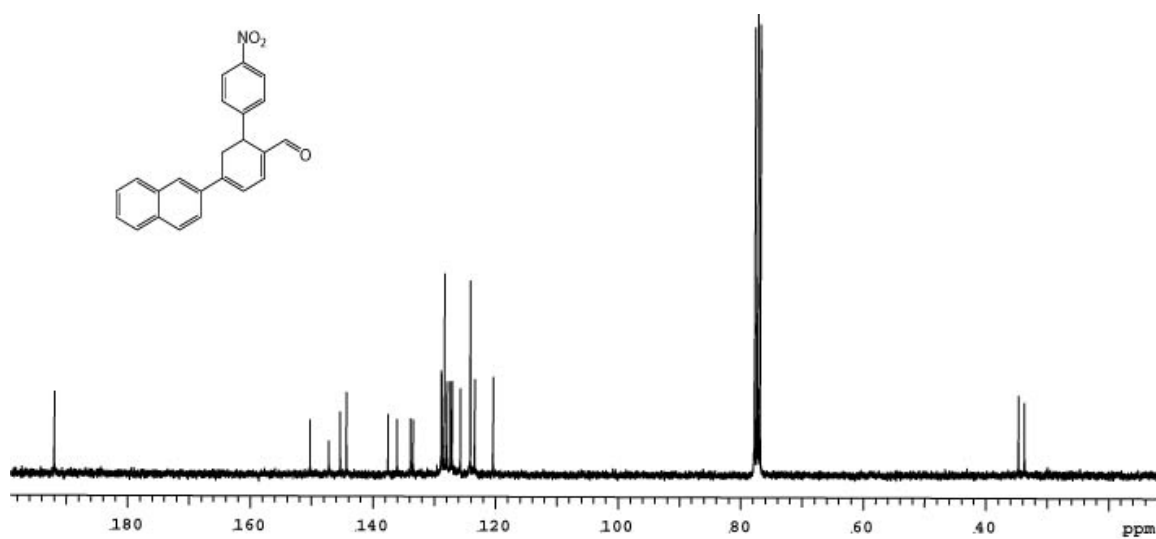
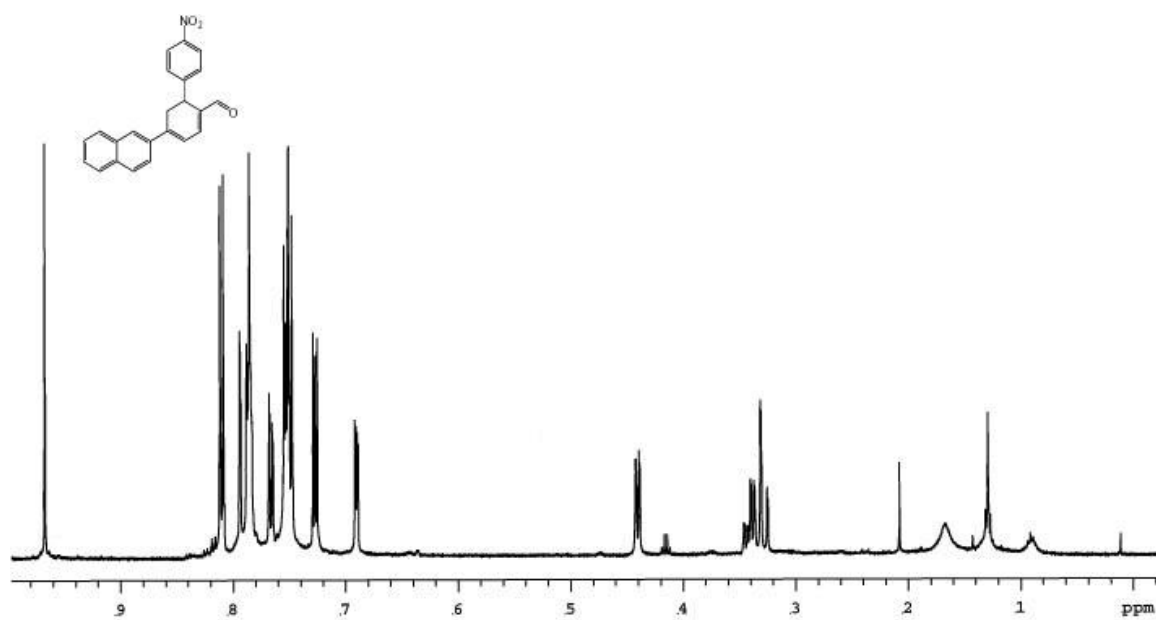


**B-27. Spectra of 99.**

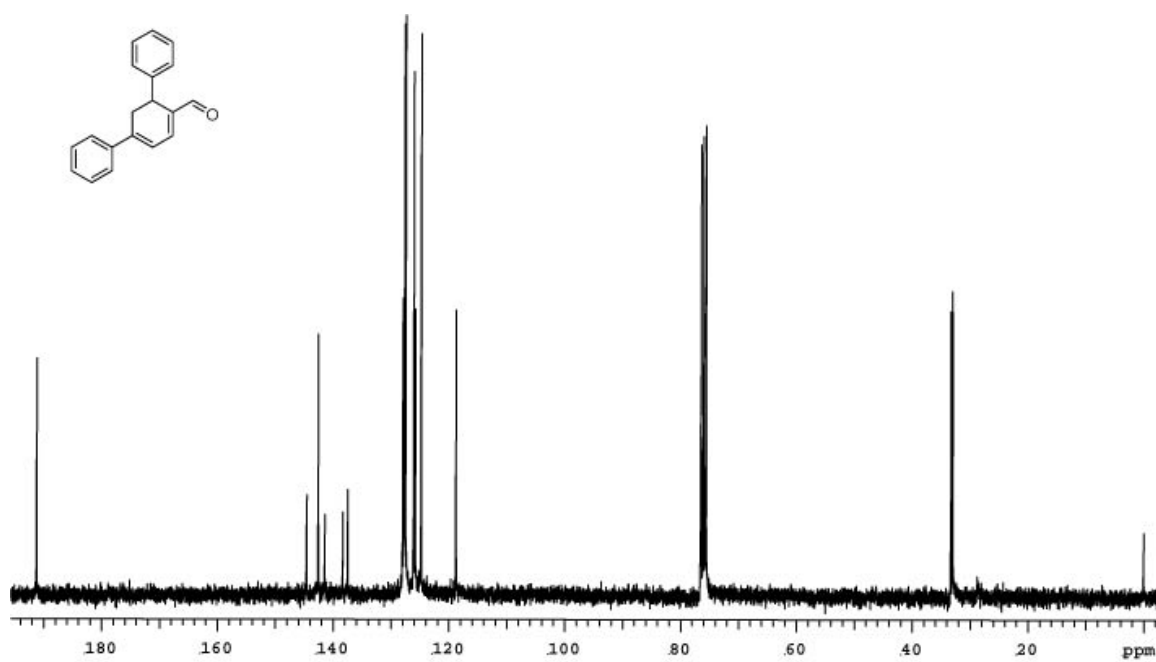
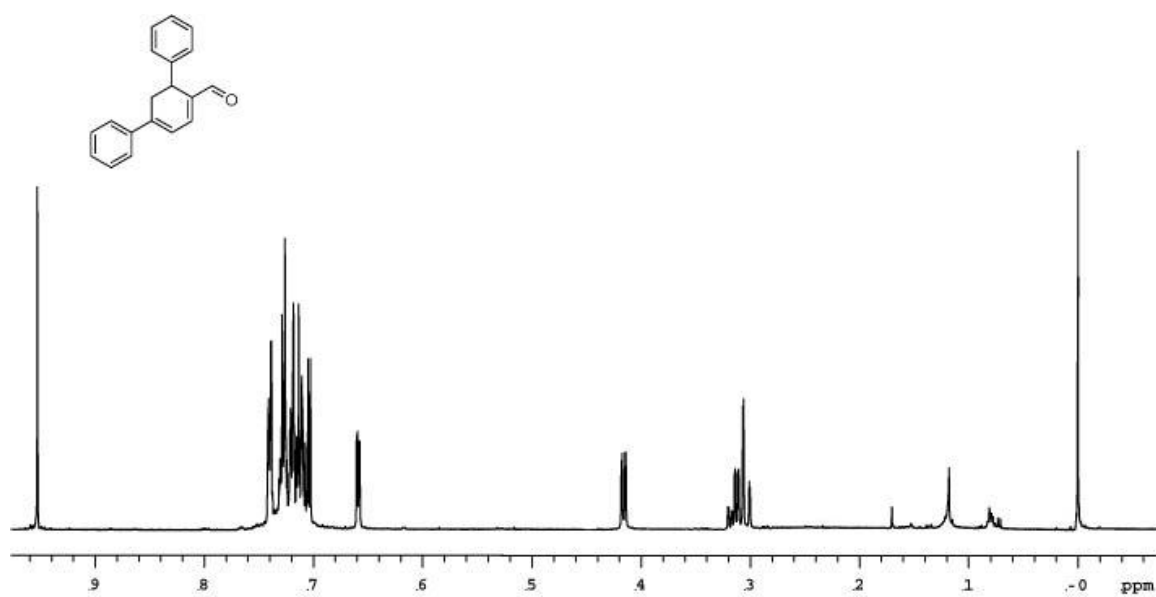




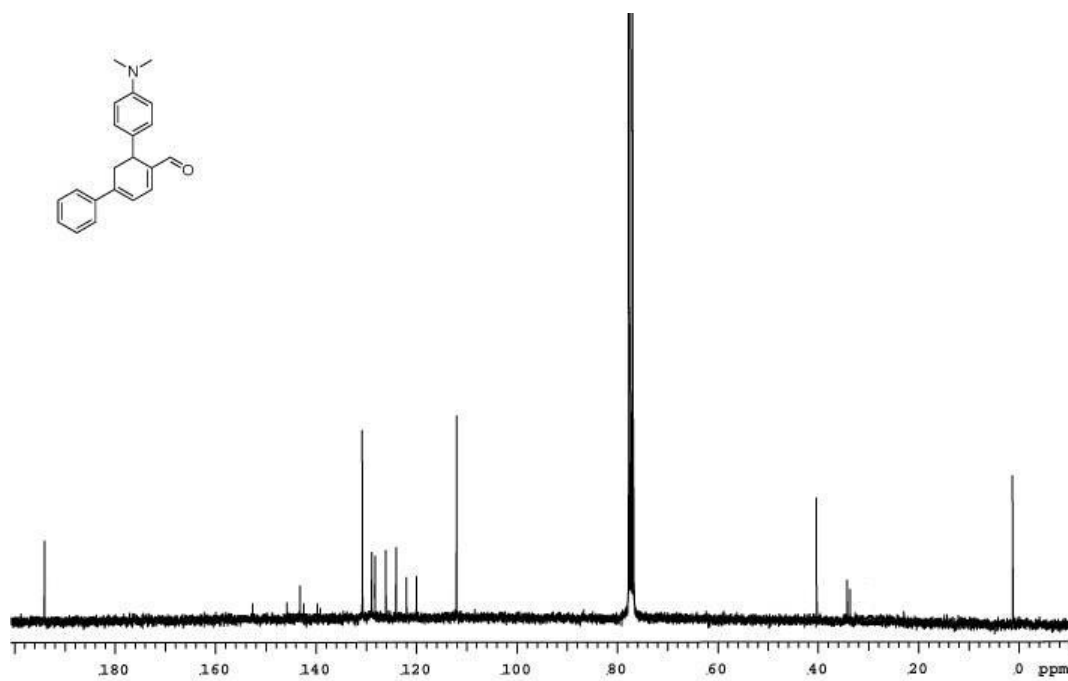
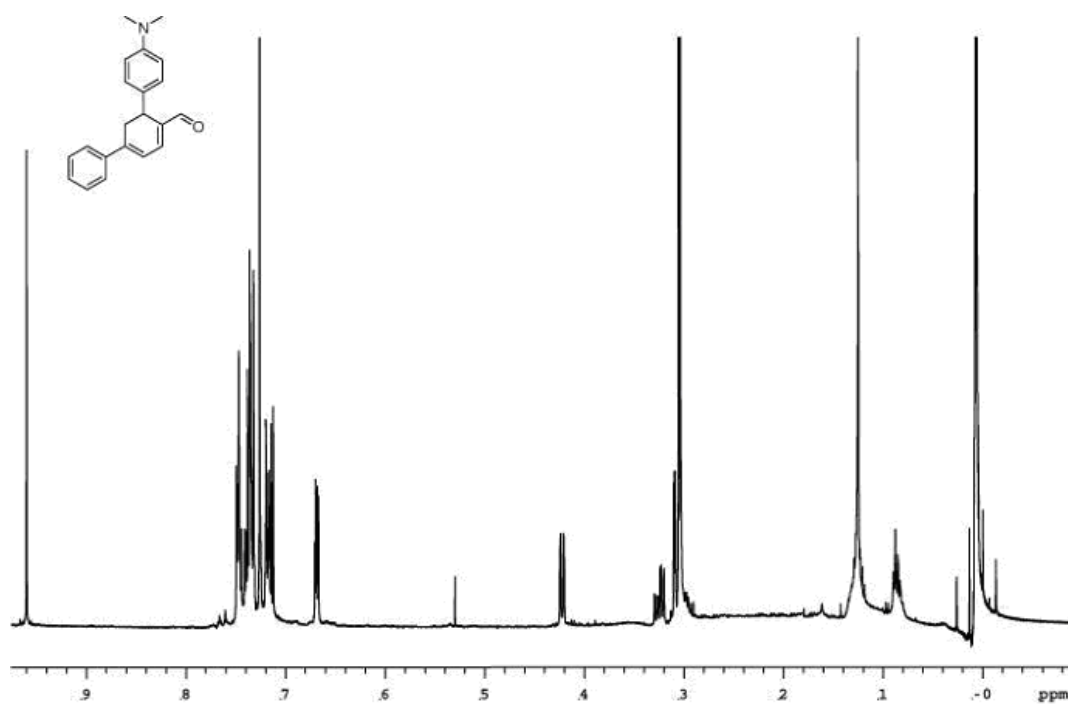
B-28. Spectra of 100.



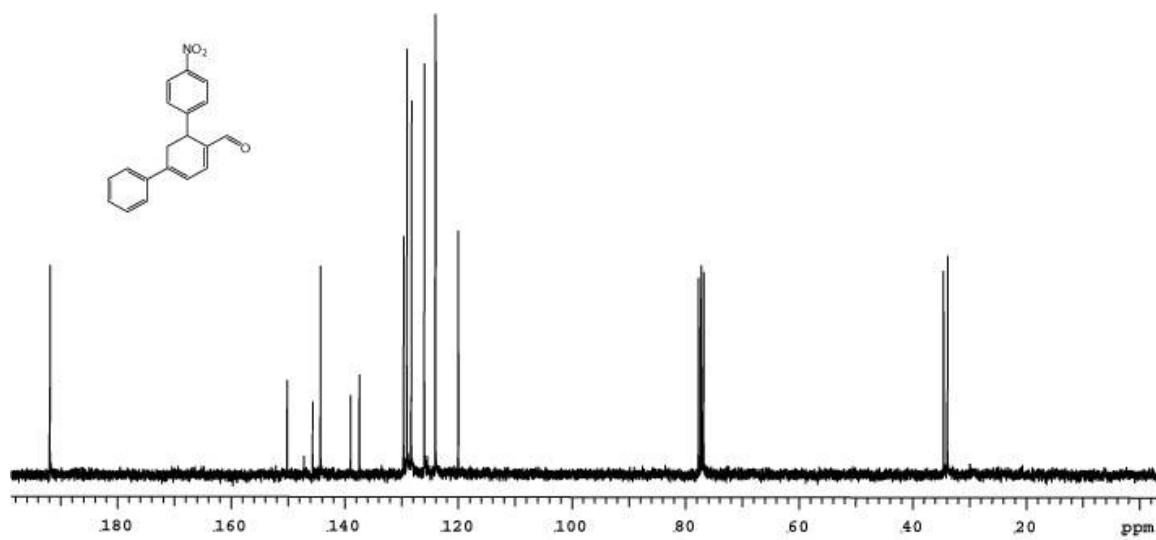
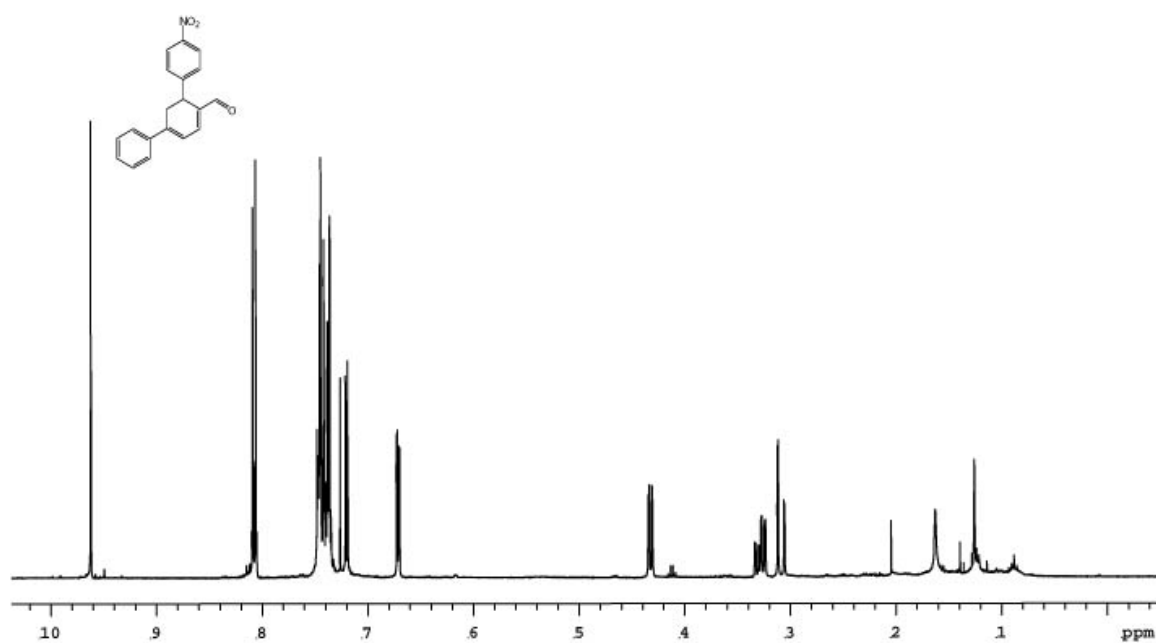
B-29. Spectra of 101.



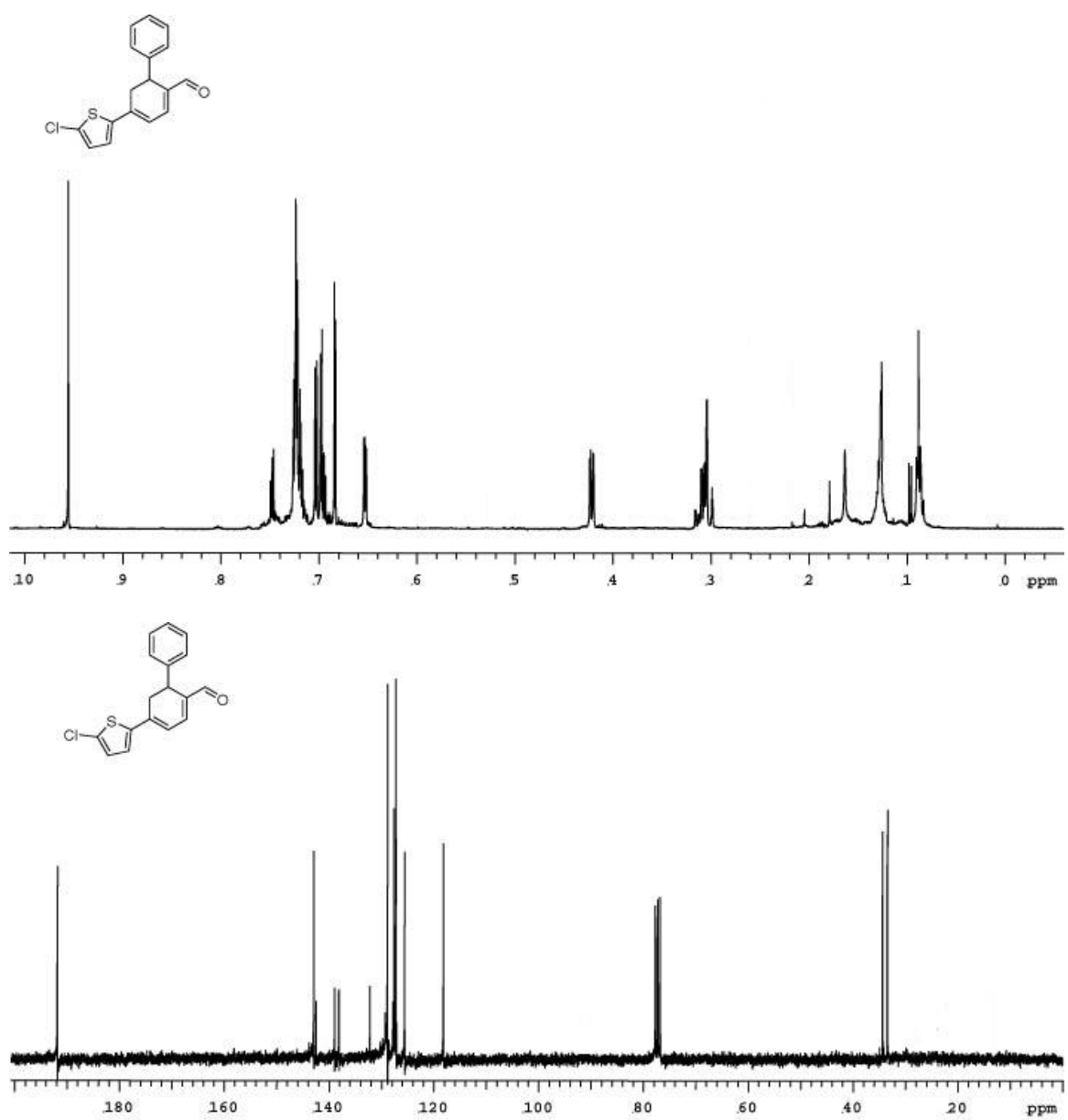
**B-30. Spectra of 102.**



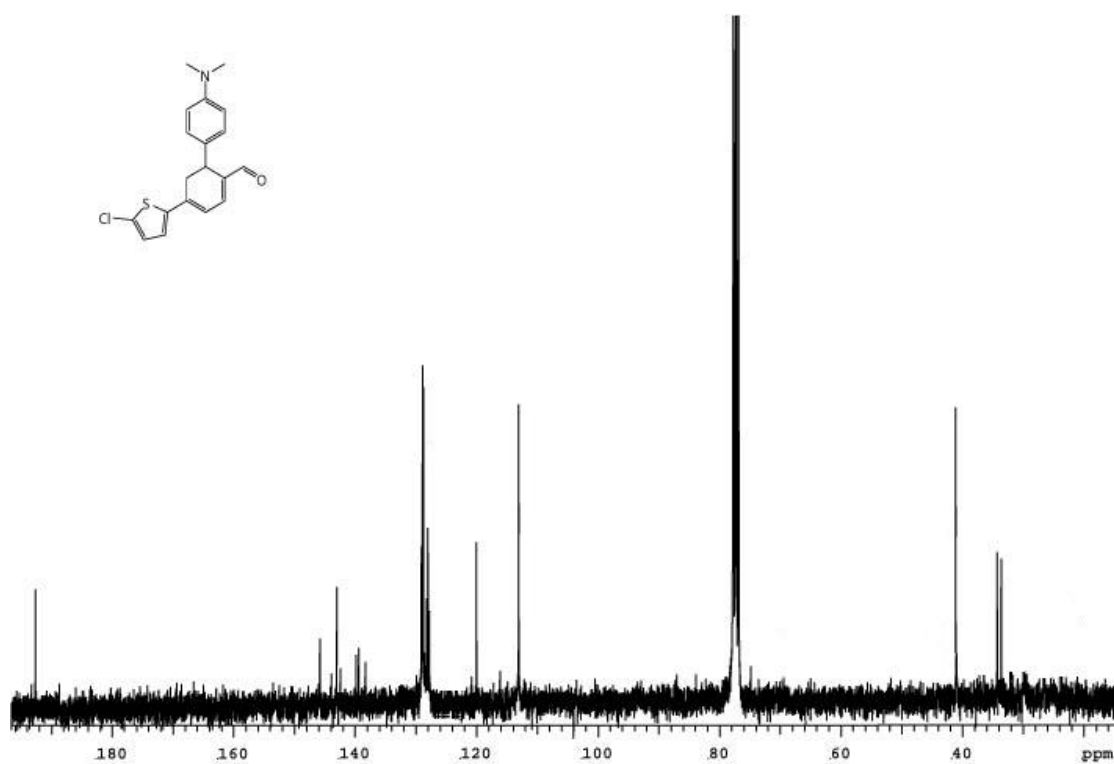
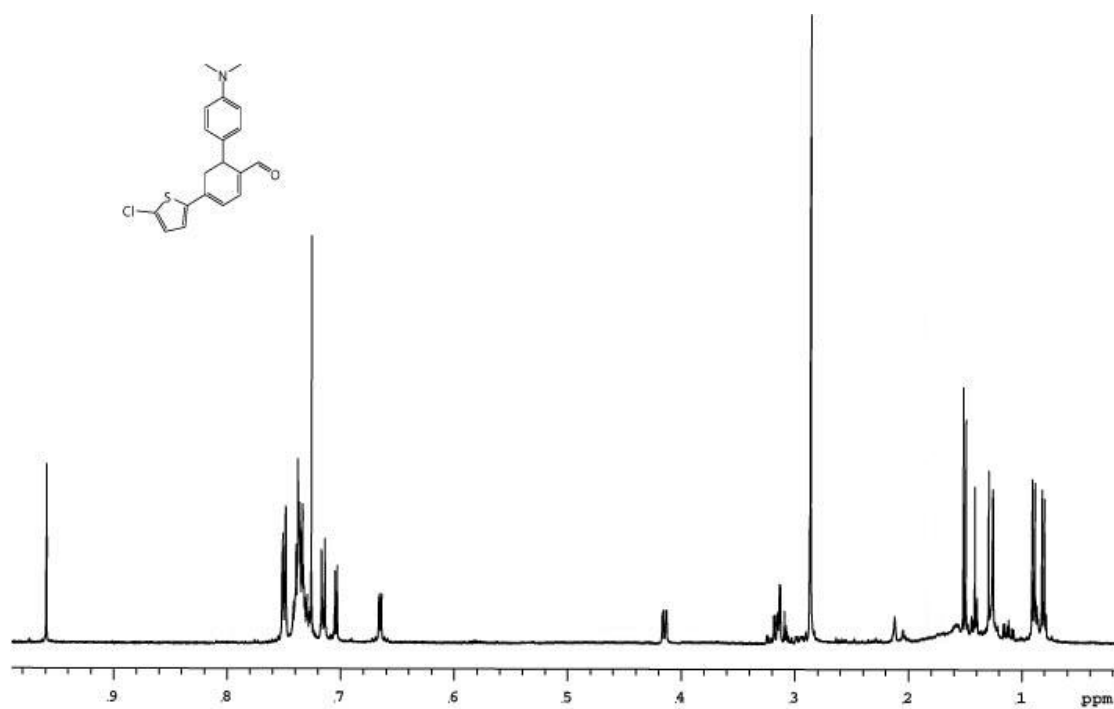
**B-31. Spectra of 103.**



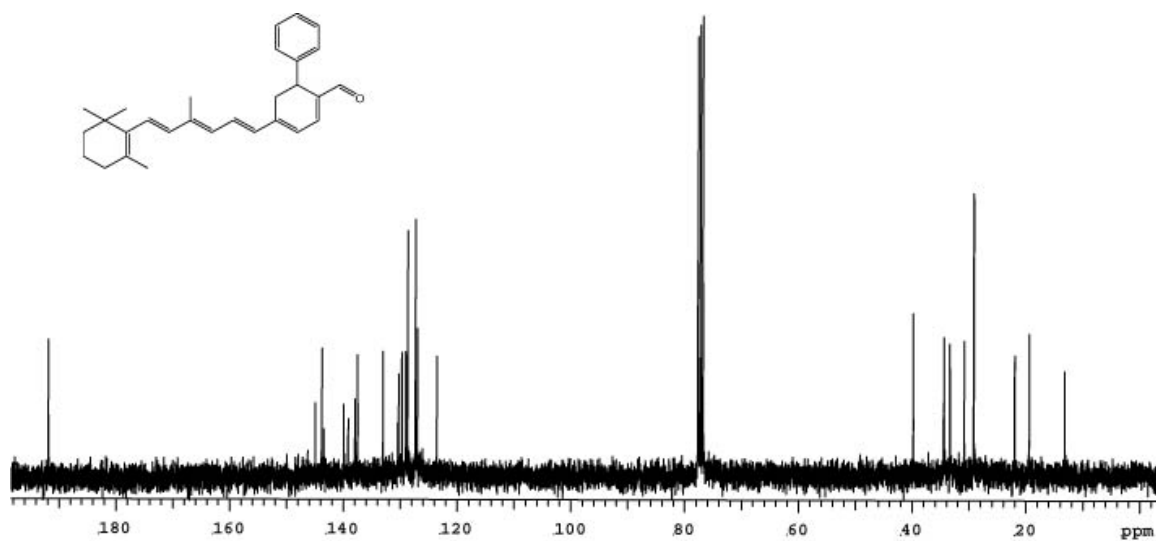
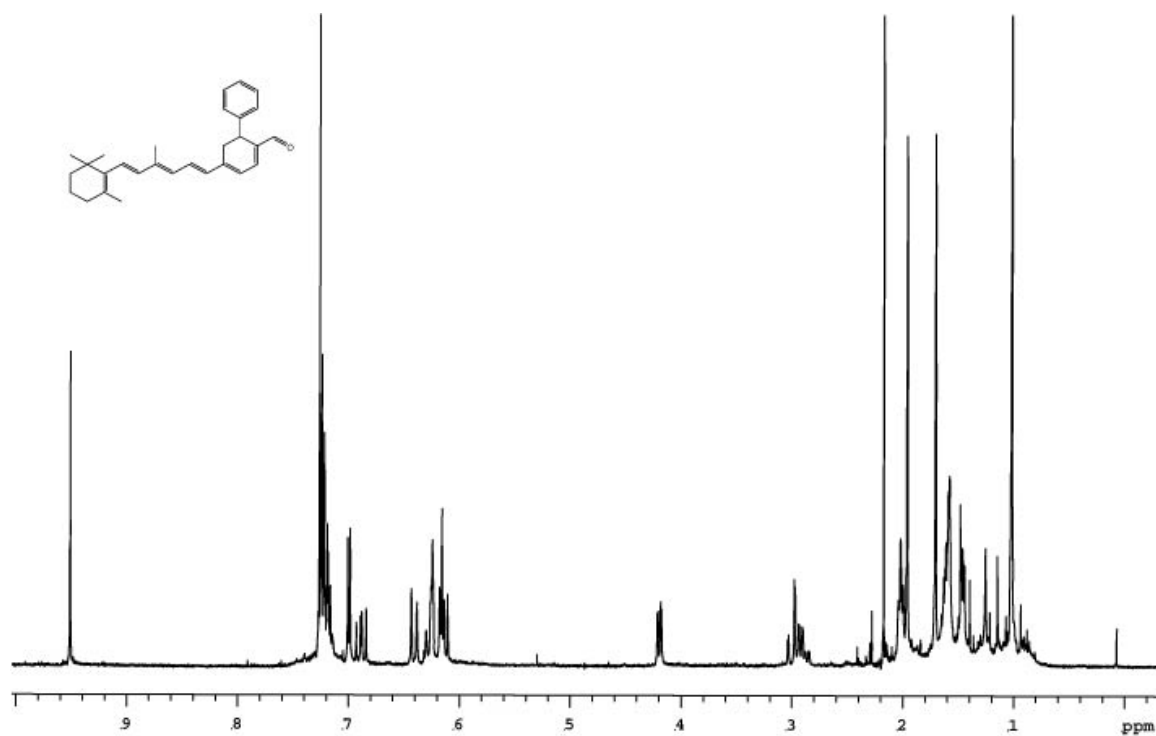
B-32. Spectra of 104.



B-33. Spectra of 105.

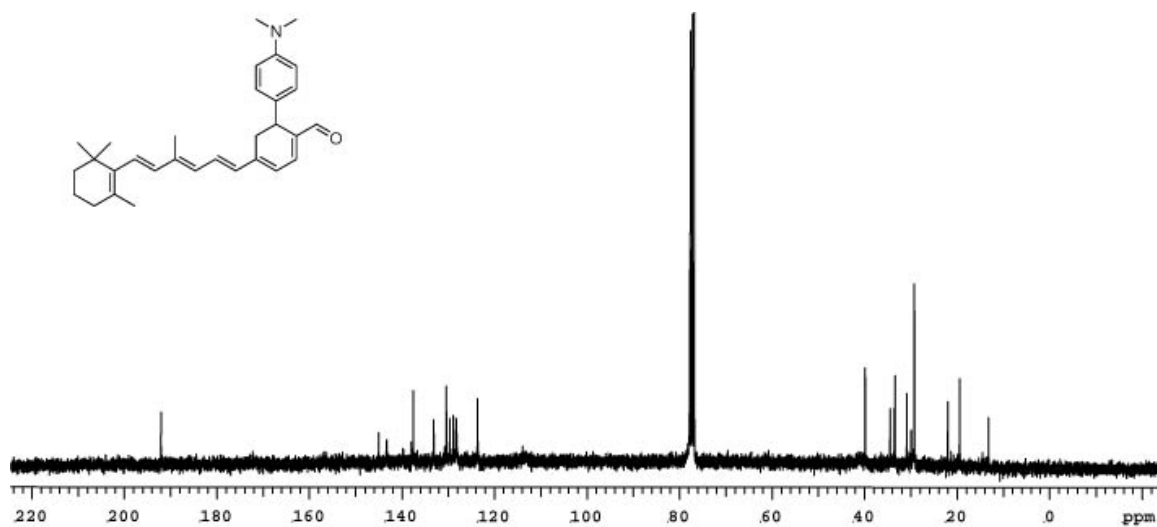
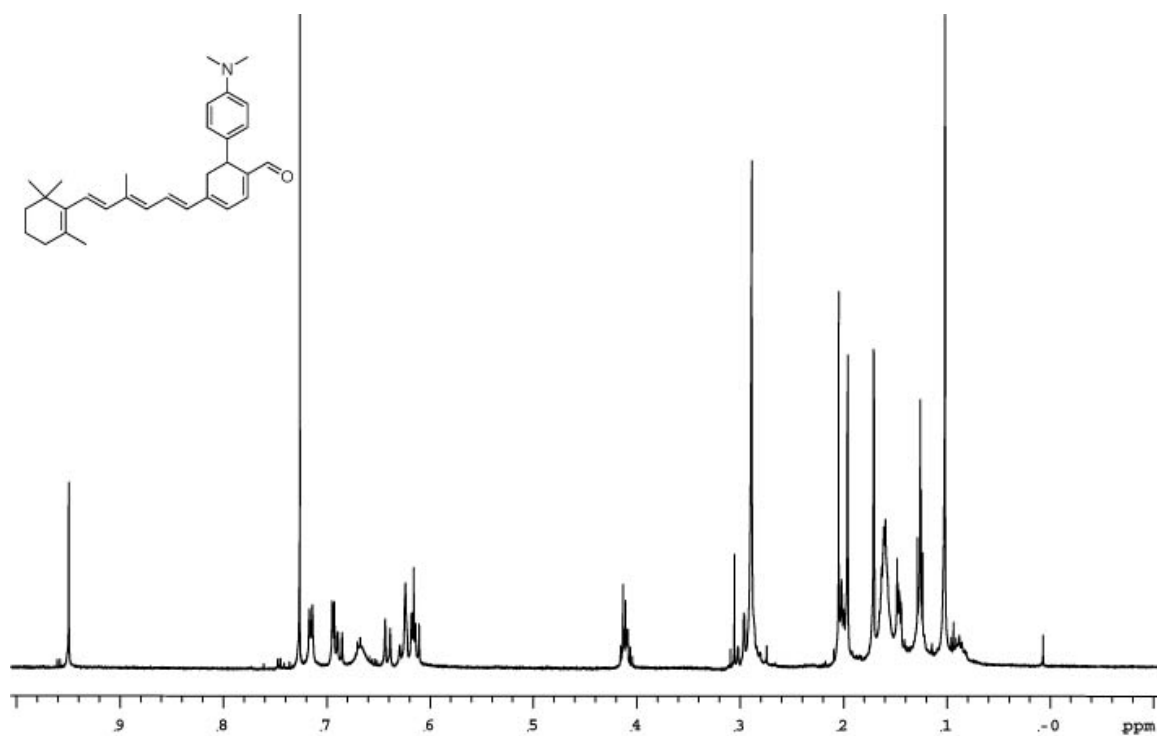


B-34. Spectra of 106.

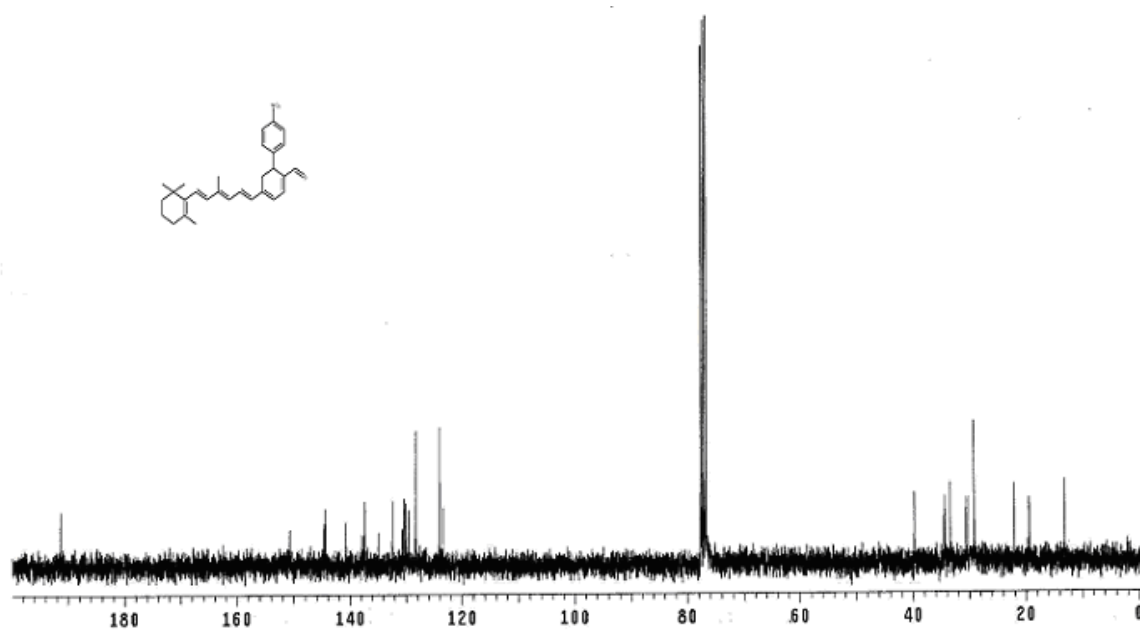
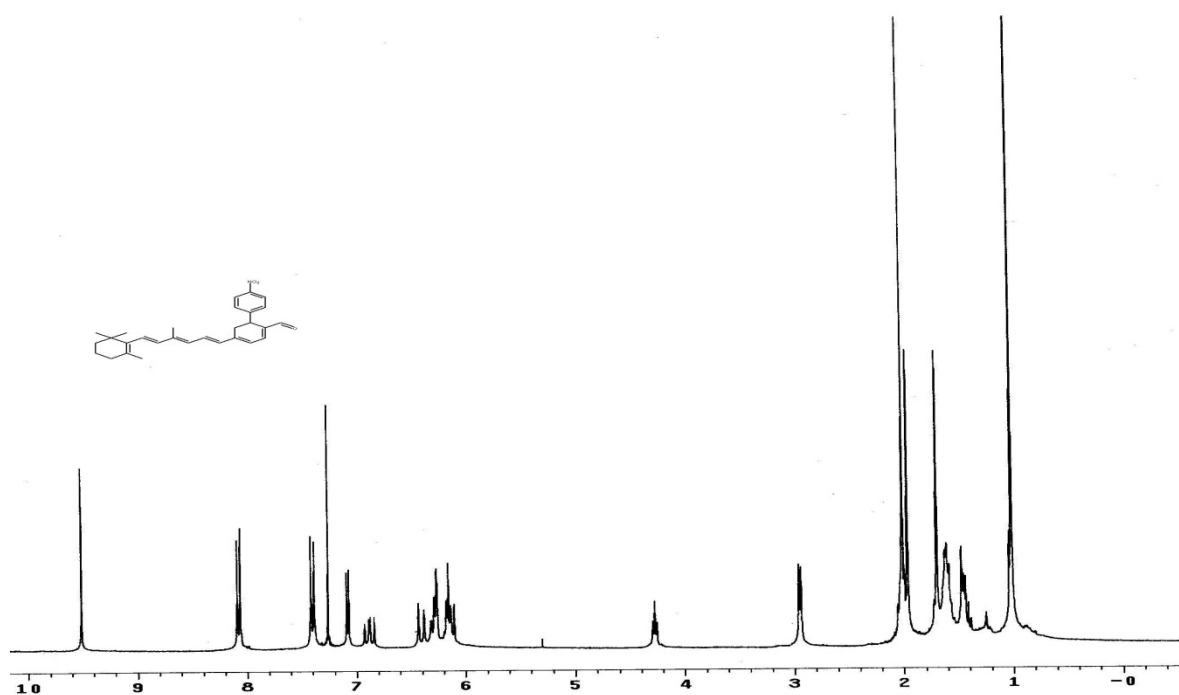


B-35. Spectra of 107.

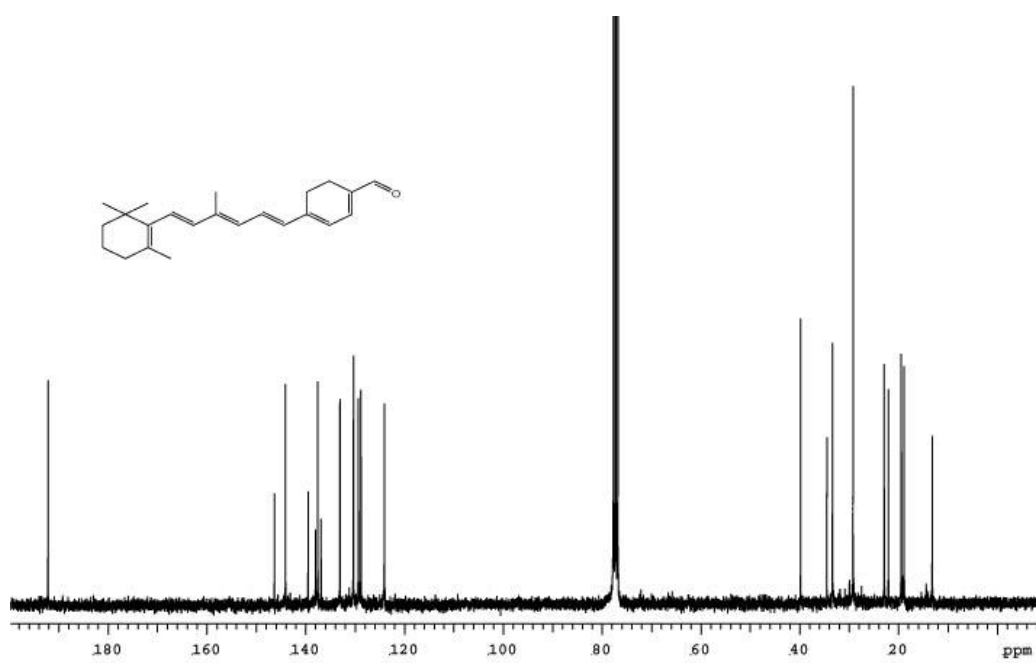
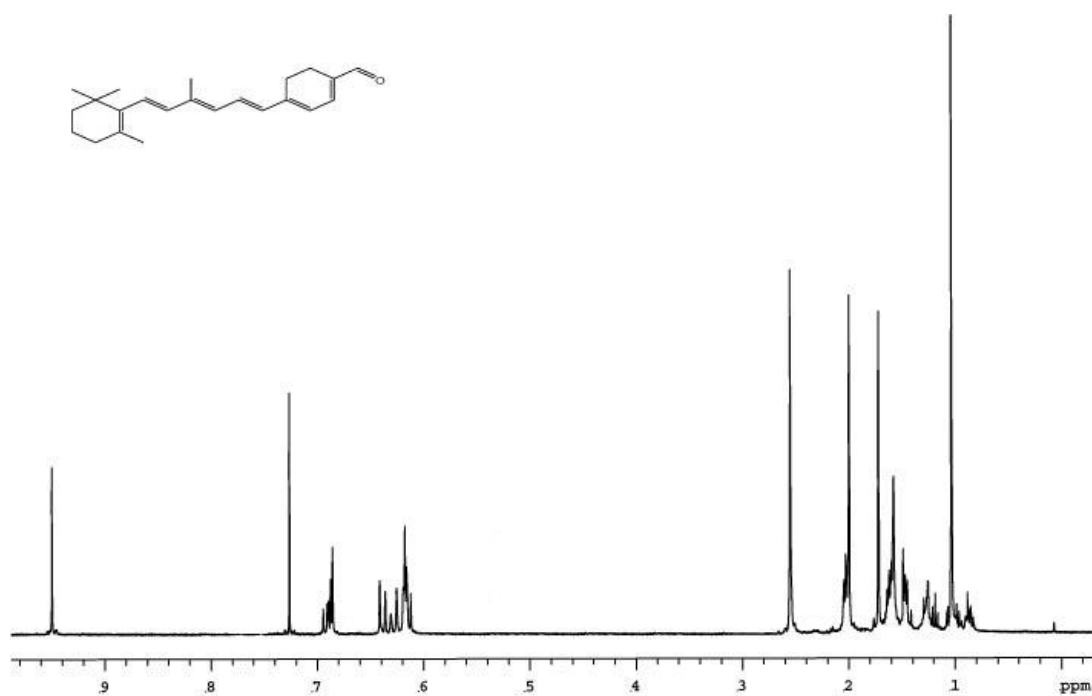




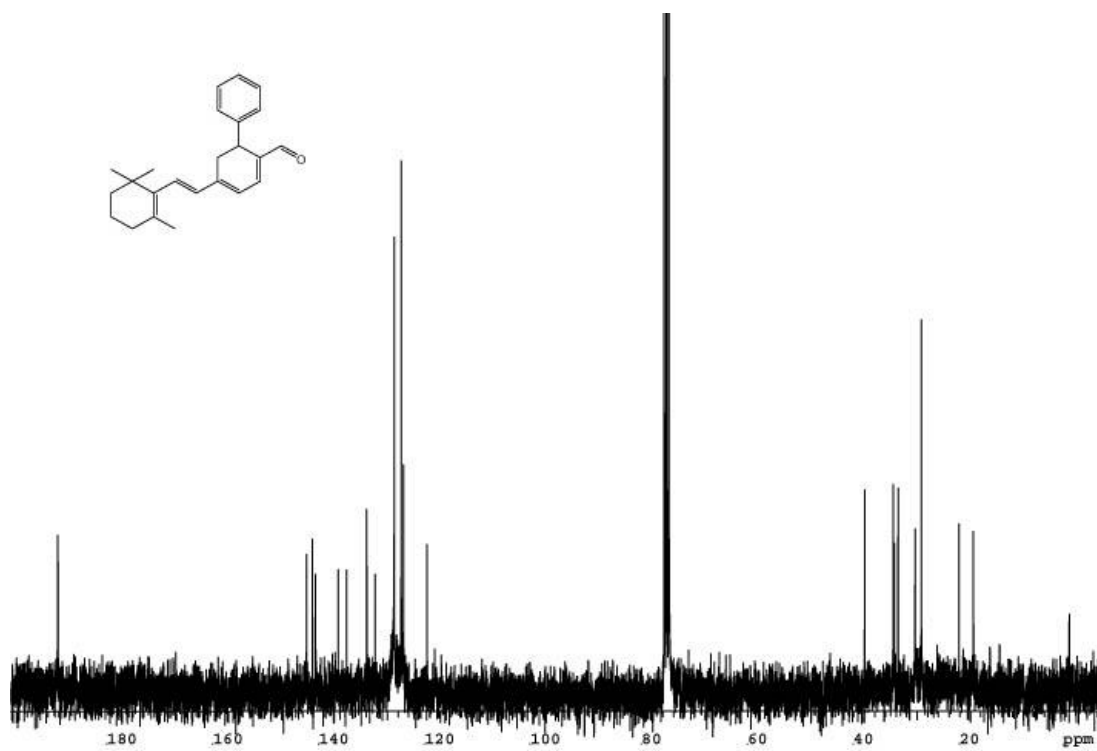
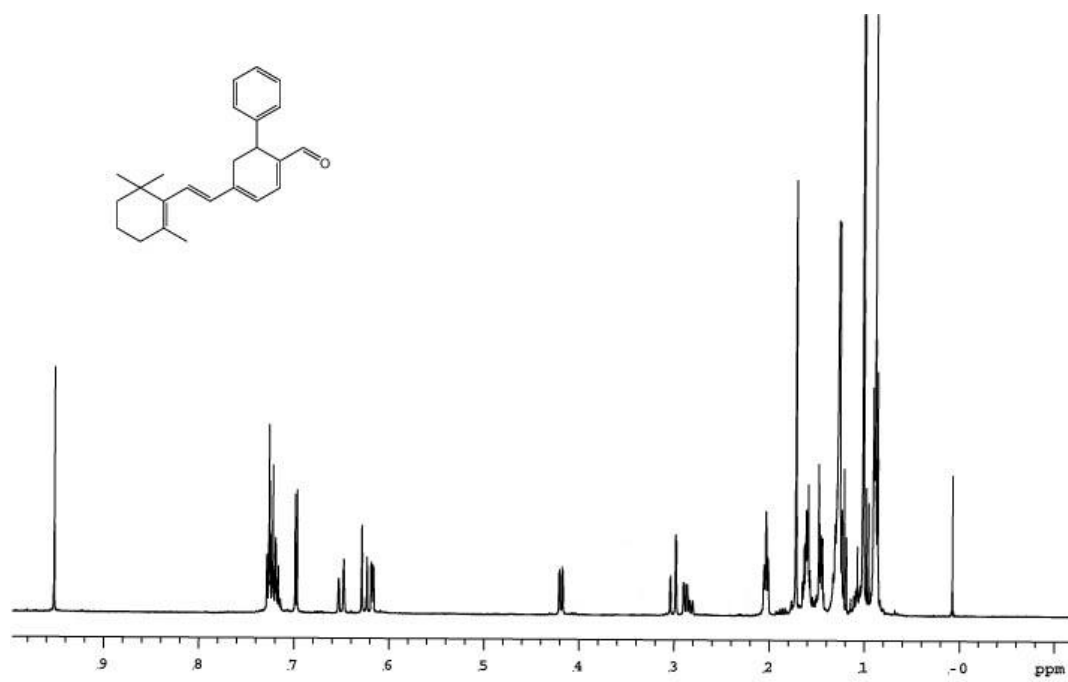
B-36. Spectra of 108.



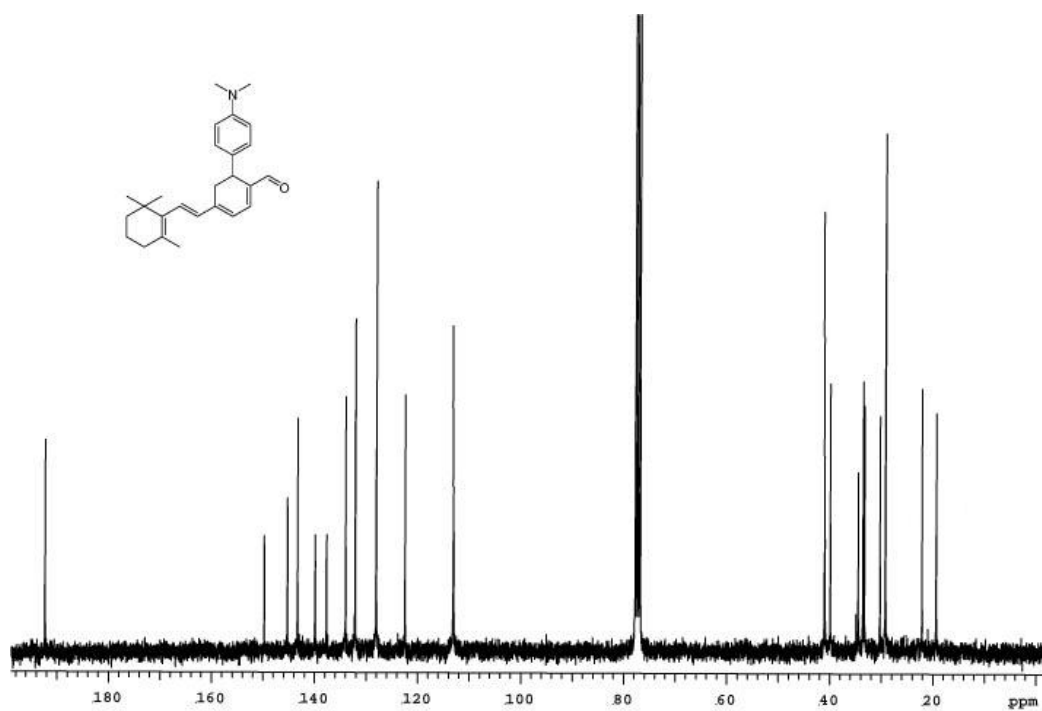
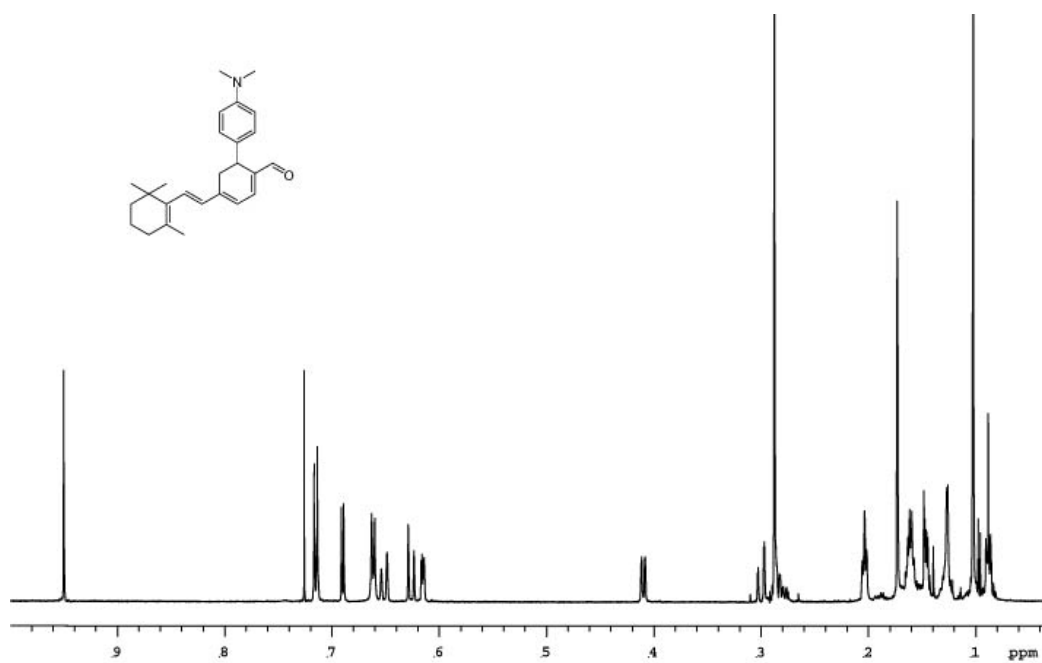
B-37. Spectra of 109.



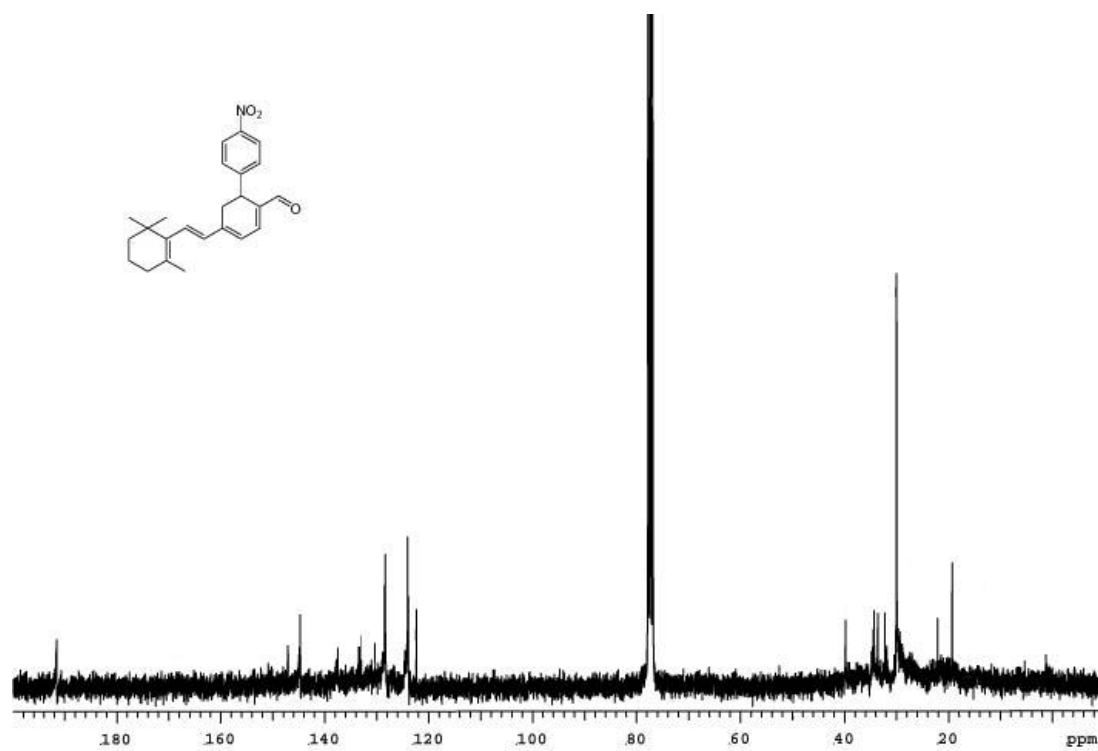
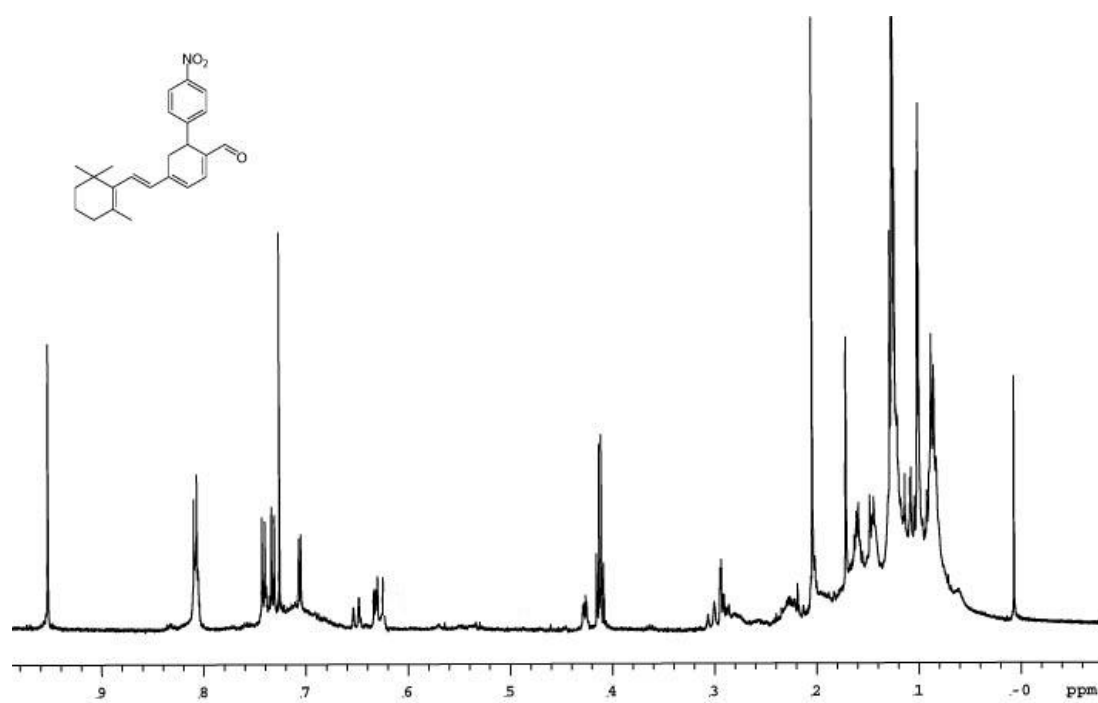
B-38. Spectra of 110.



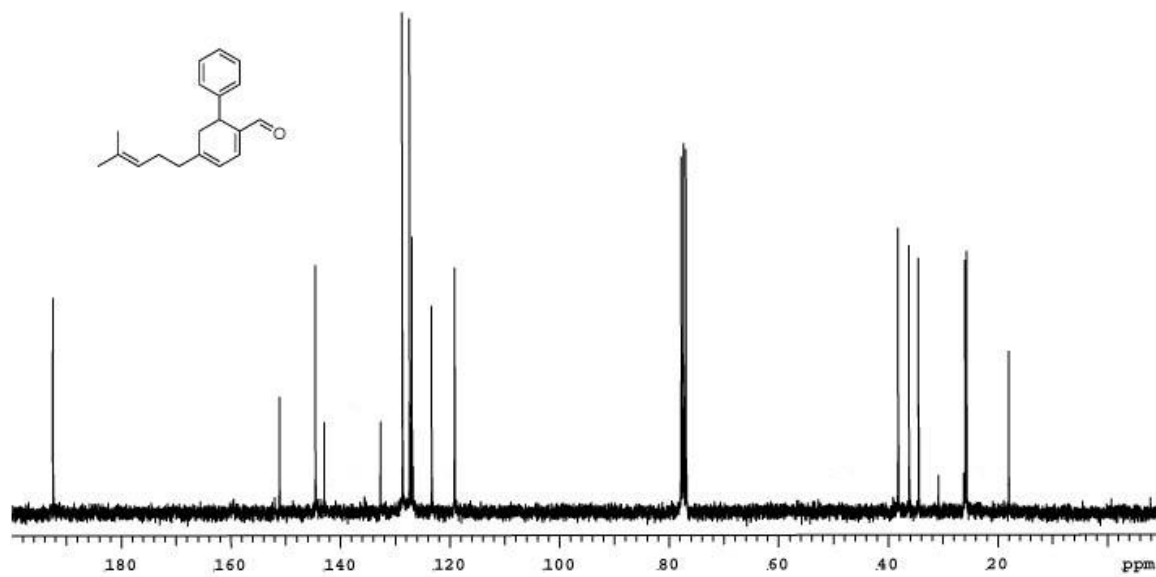
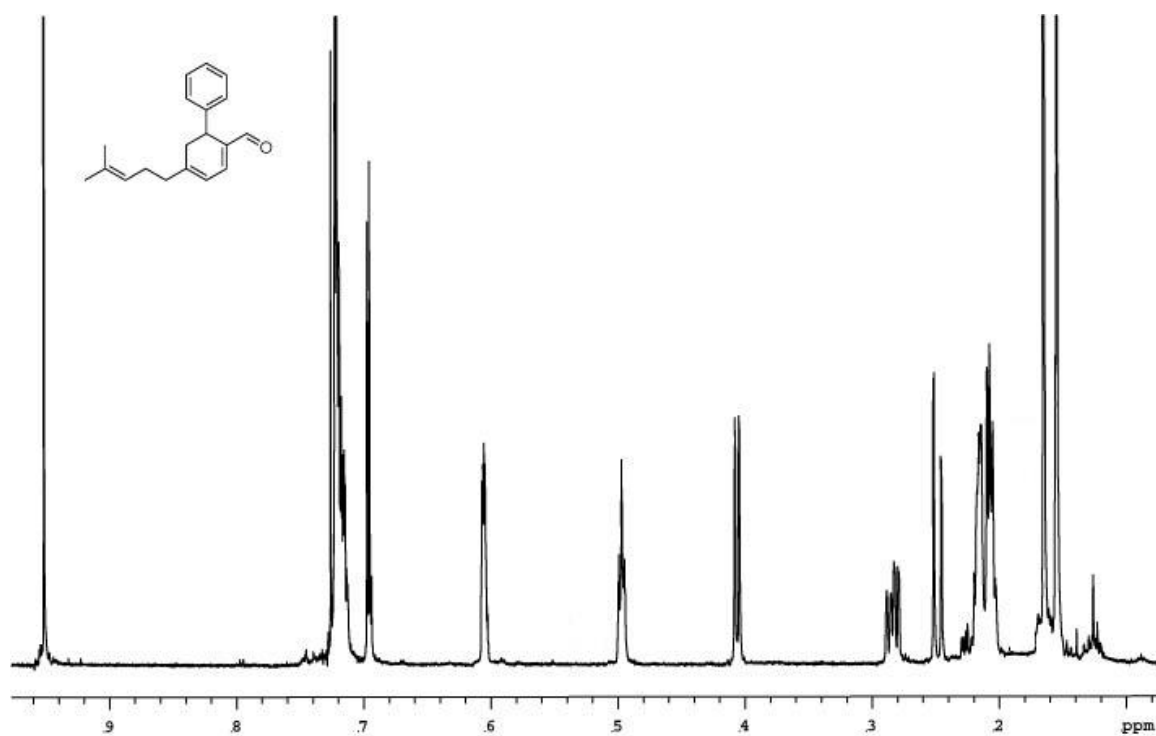
**B-39. Spectra of 111.**



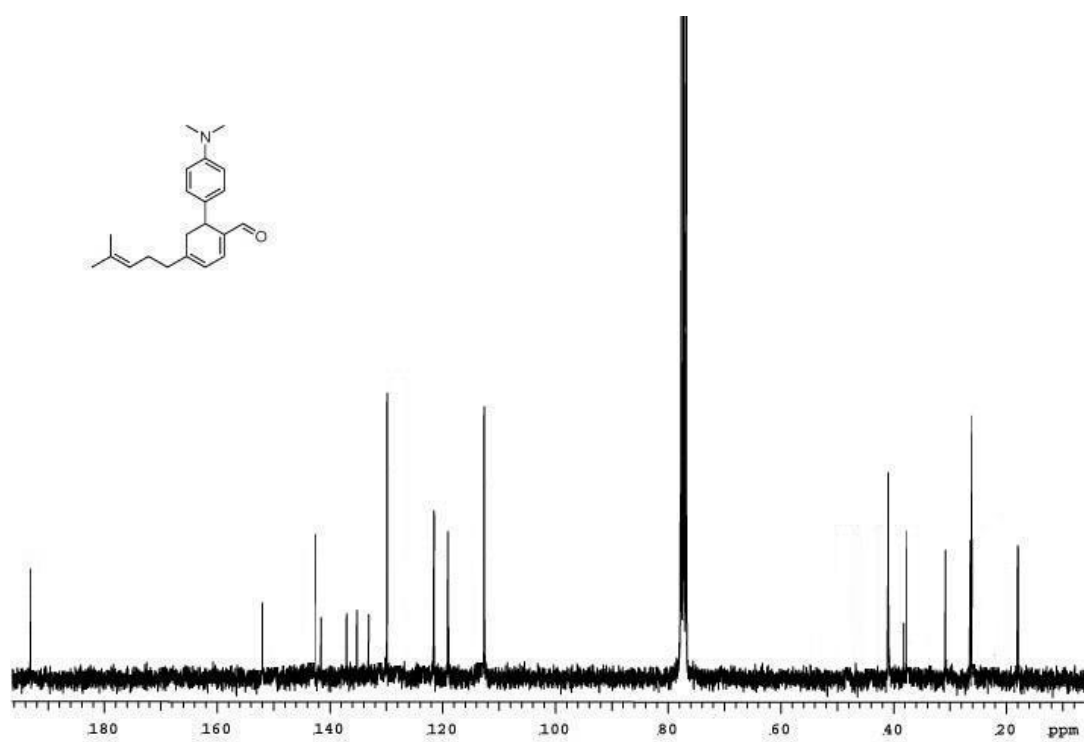
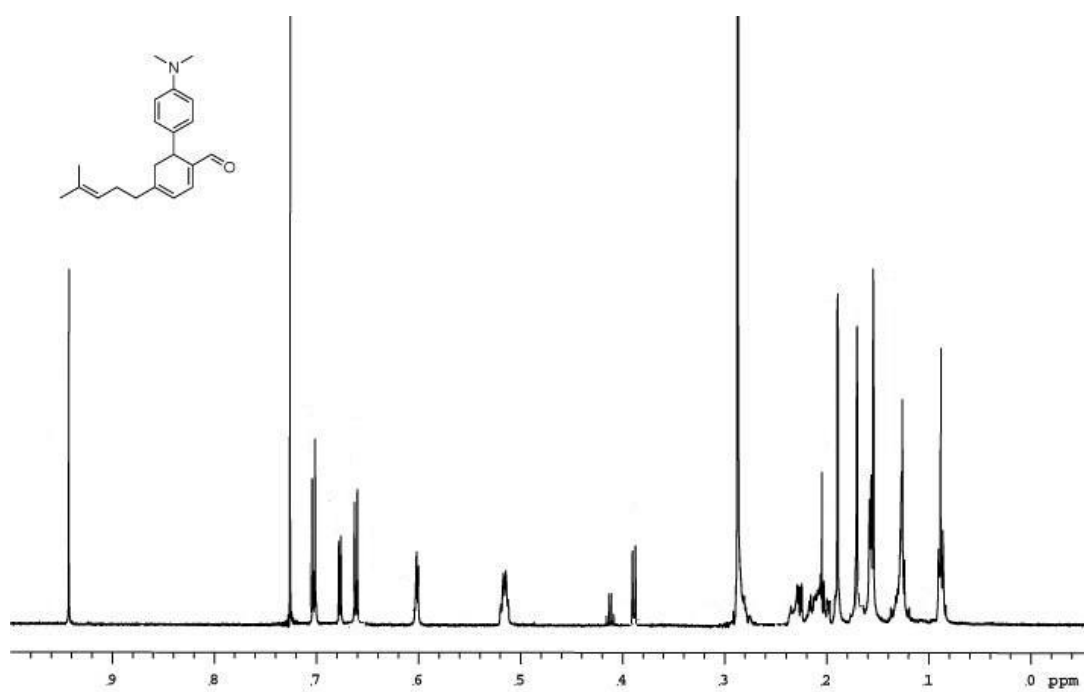
B-40. Spectra of 112.



**B-41. Spectra of 113.**

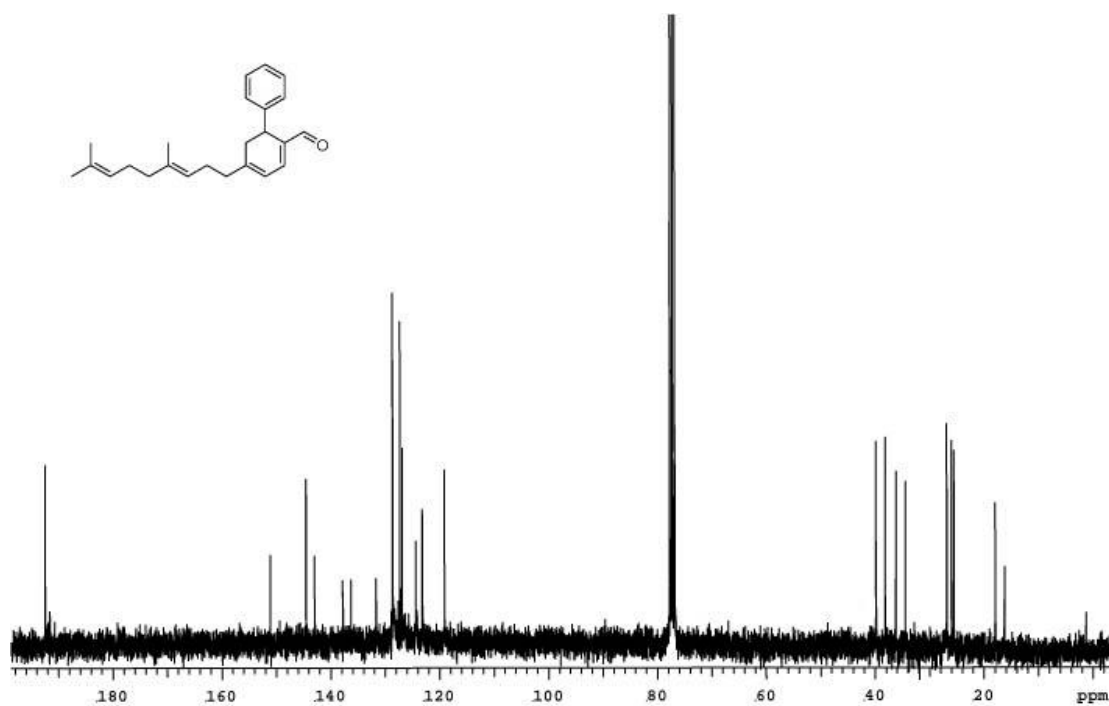
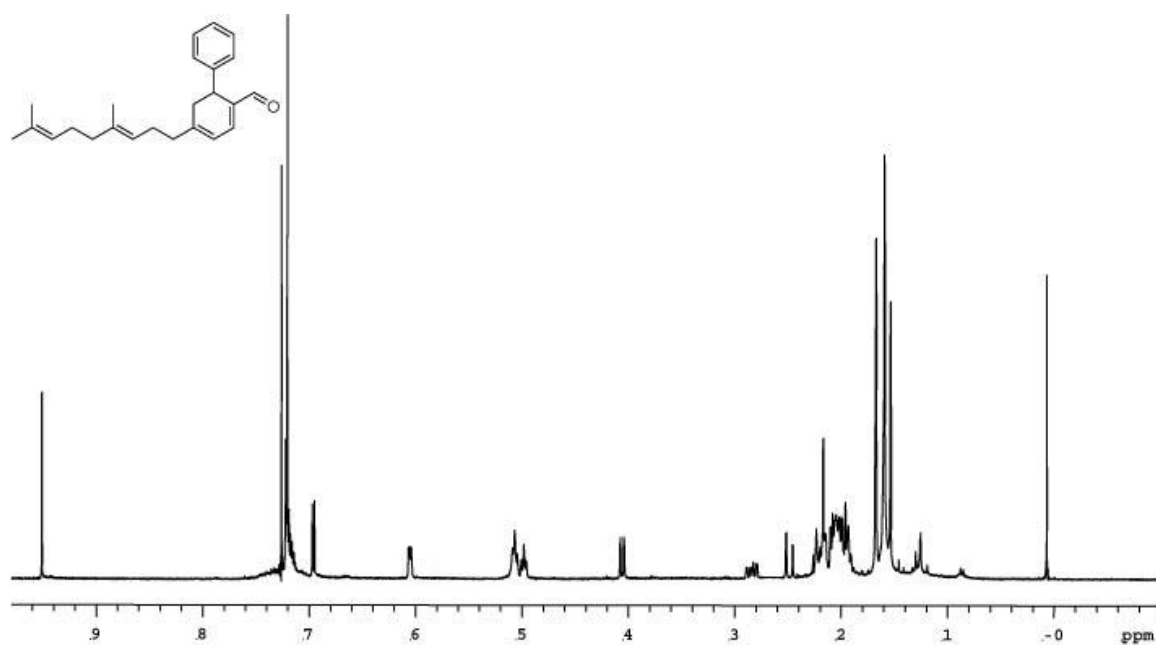


**B-42. Spectra of Error! Bookmark not defined.**

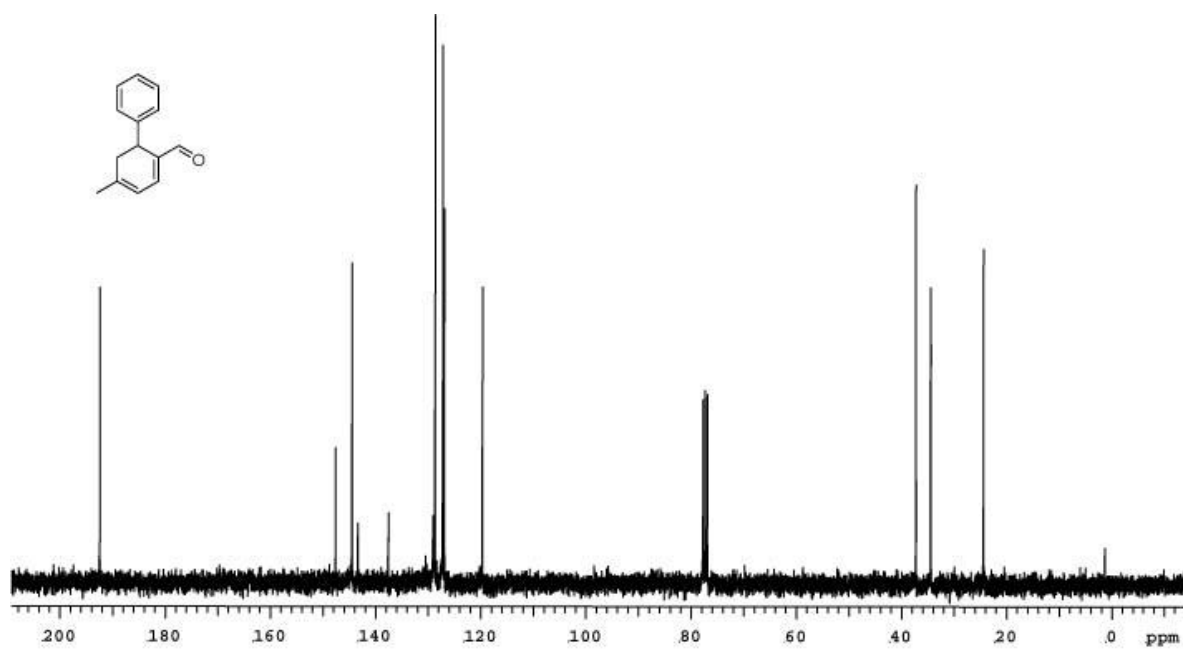
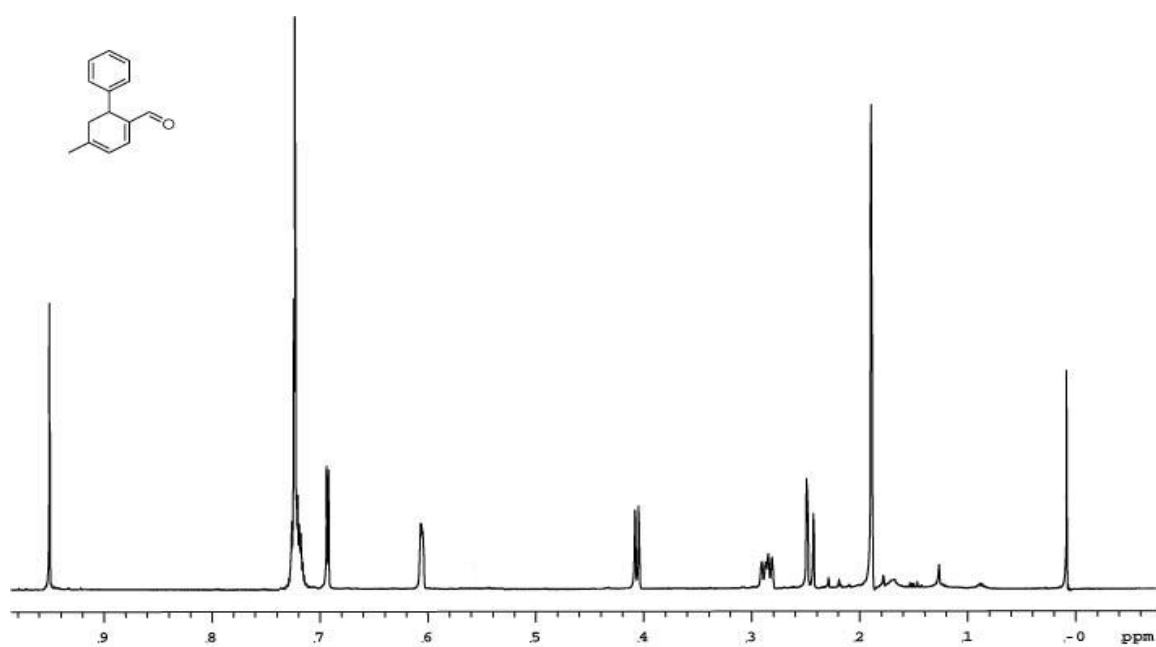


**B-43. Spectra of 114.**

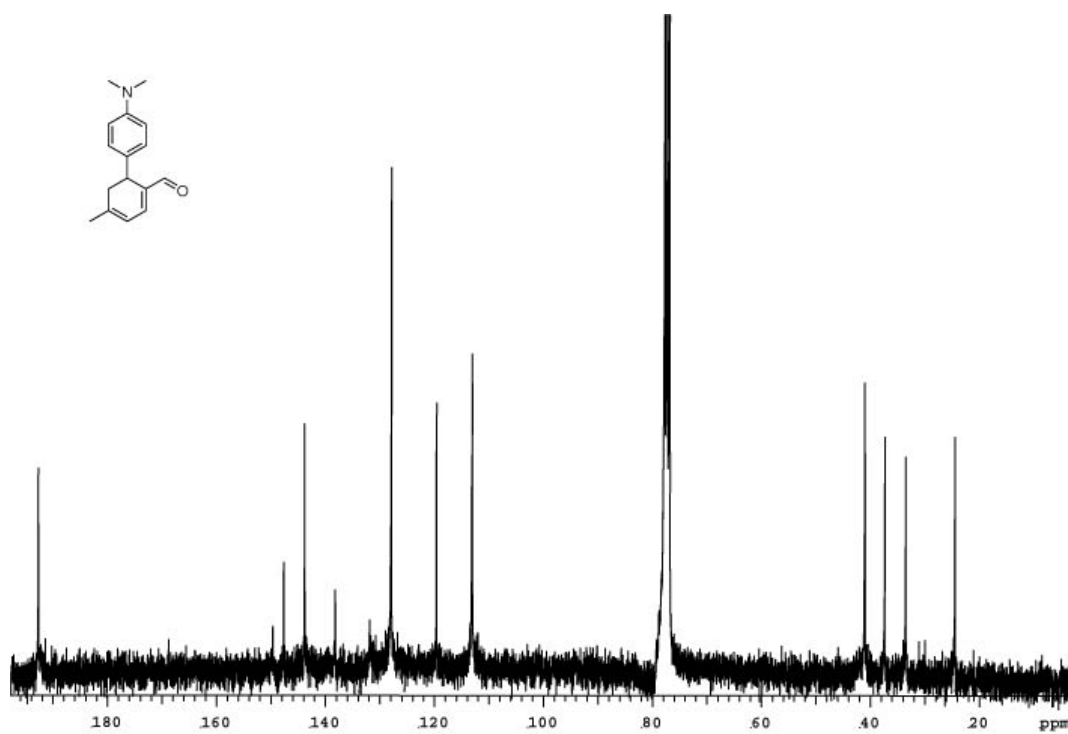
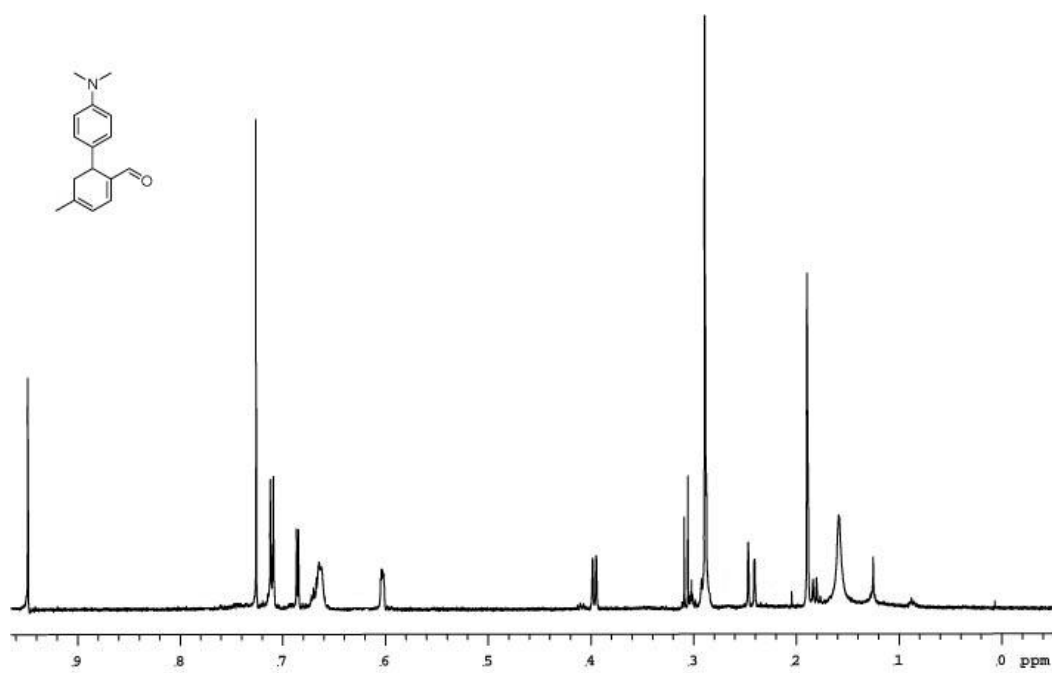




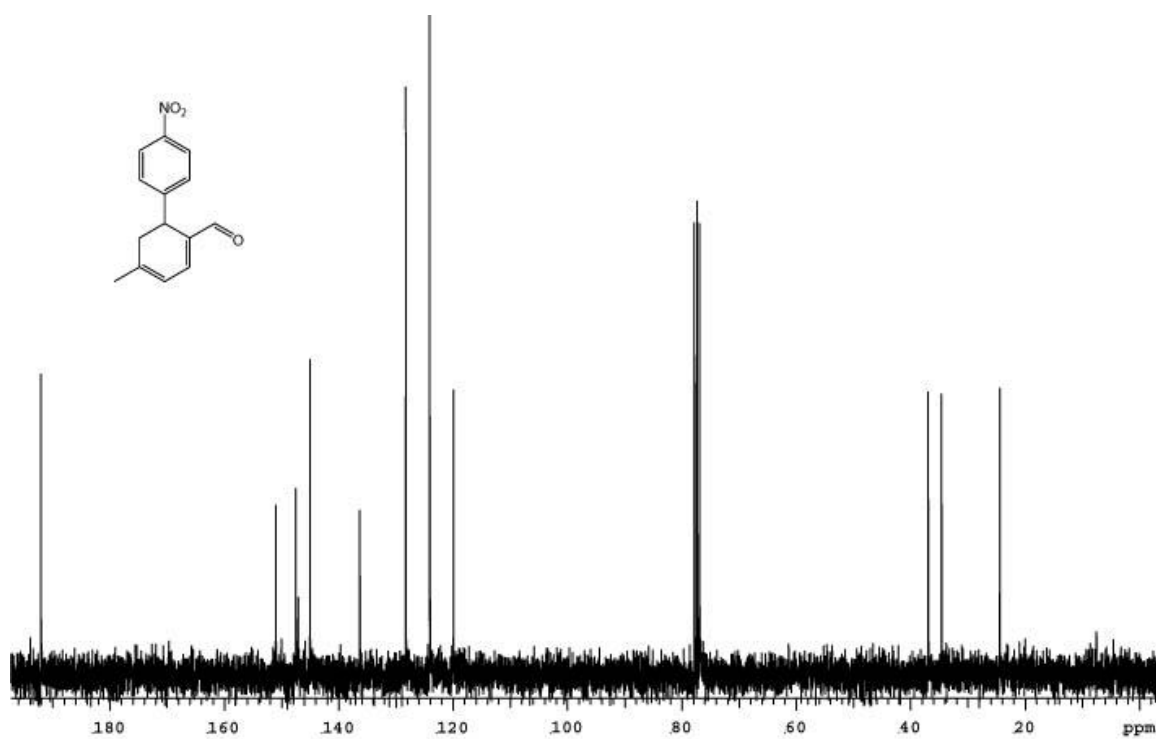
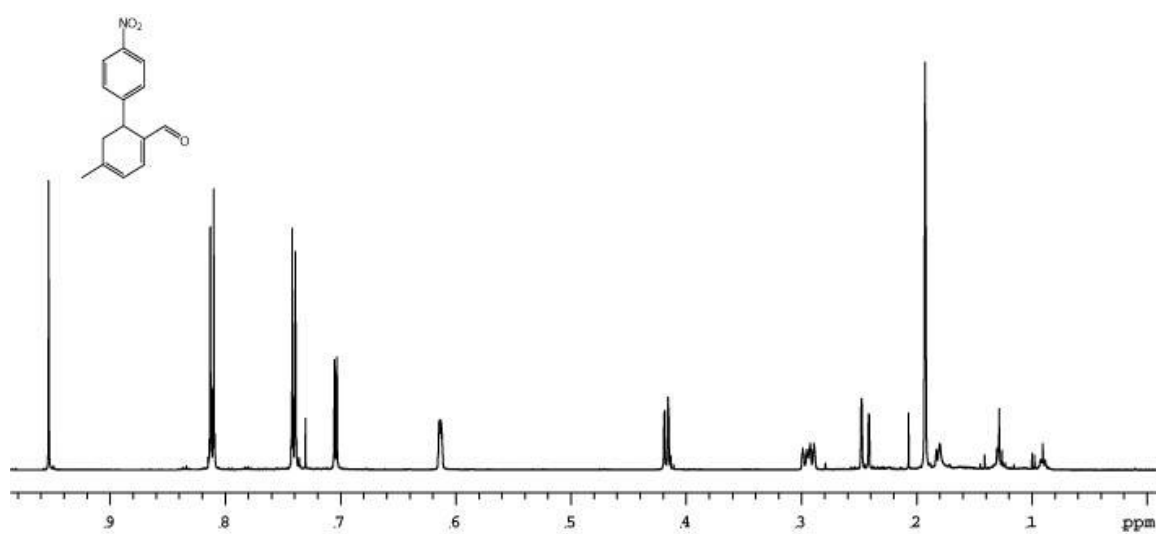
B-44. Spectra of 115.



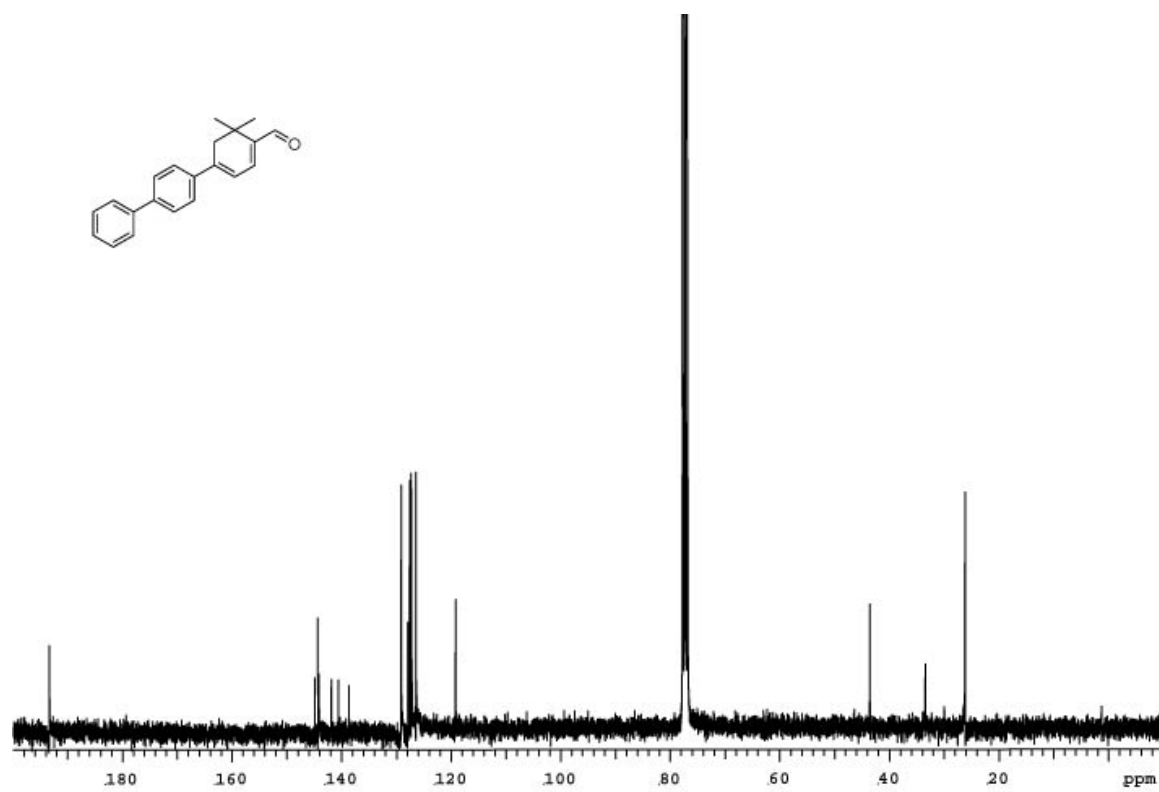
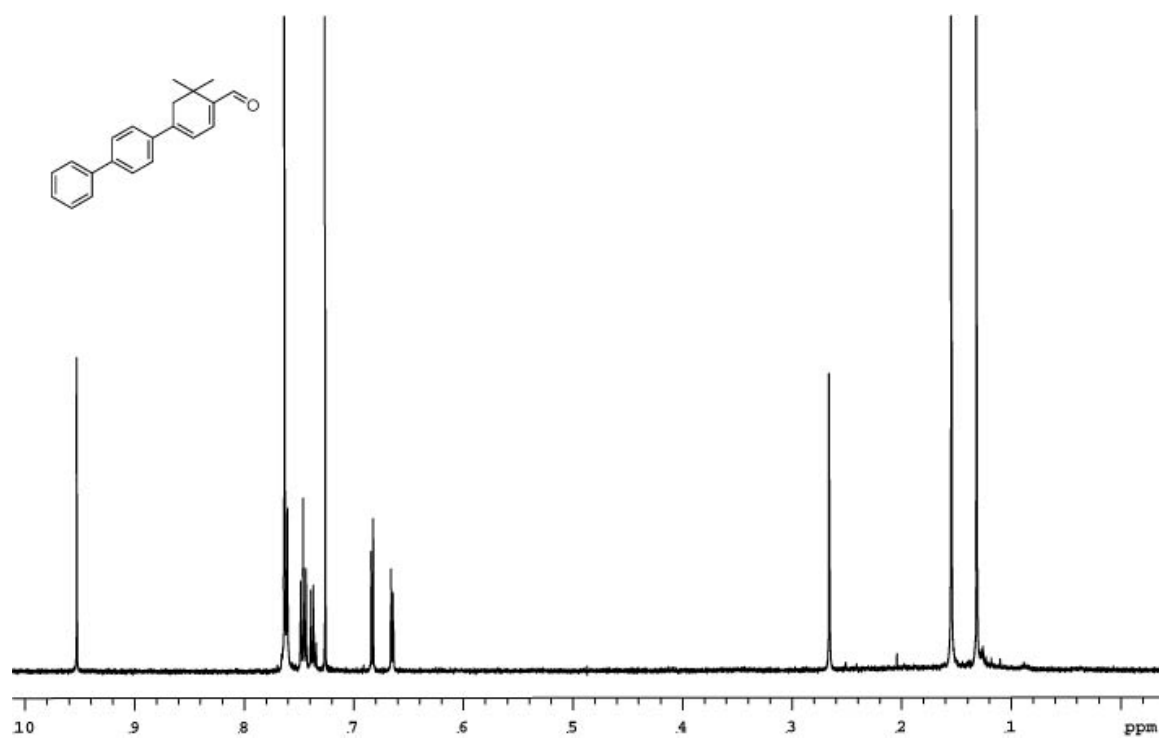
B-45. Spectra of 116.



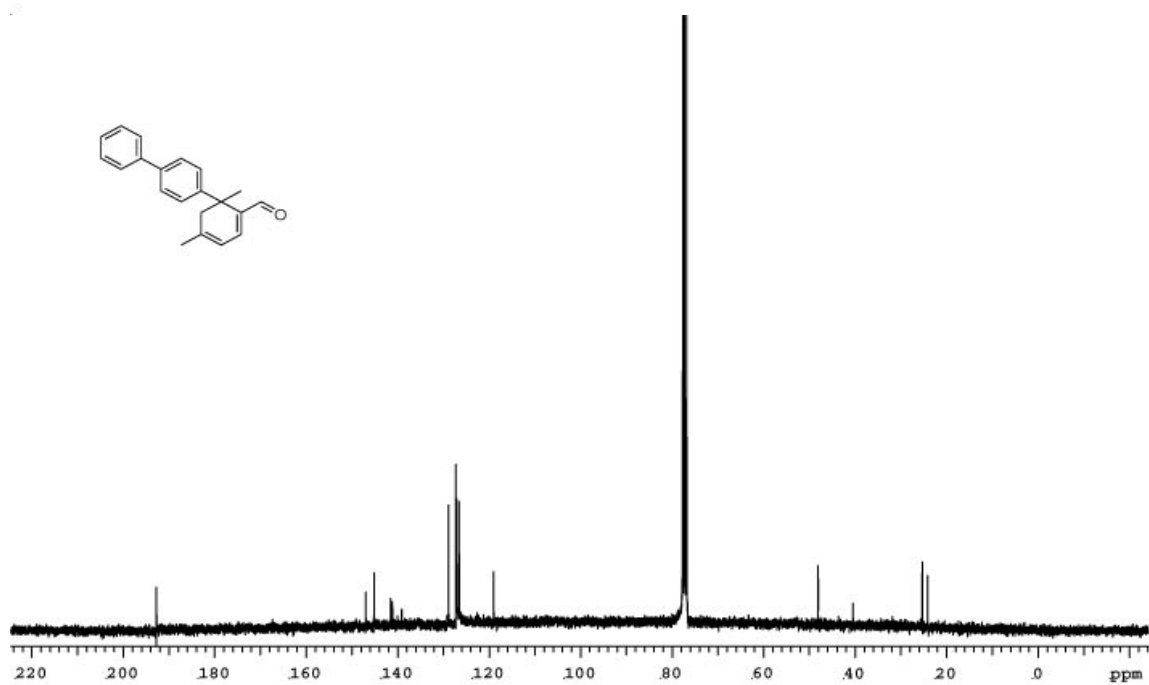
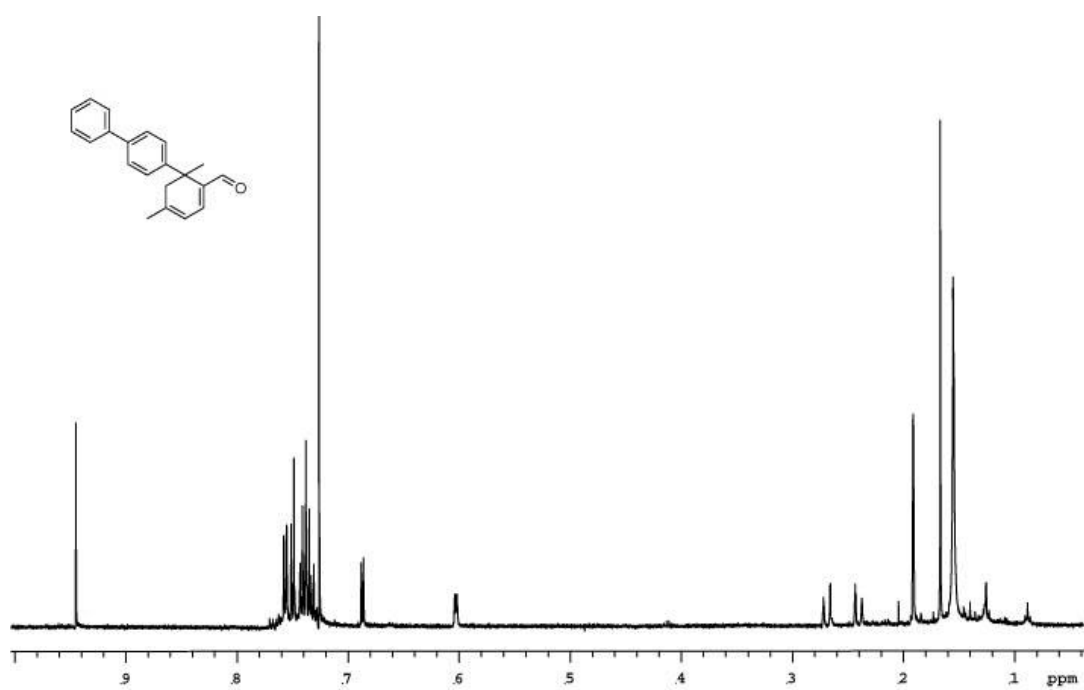
B-46. Spectra of 117.



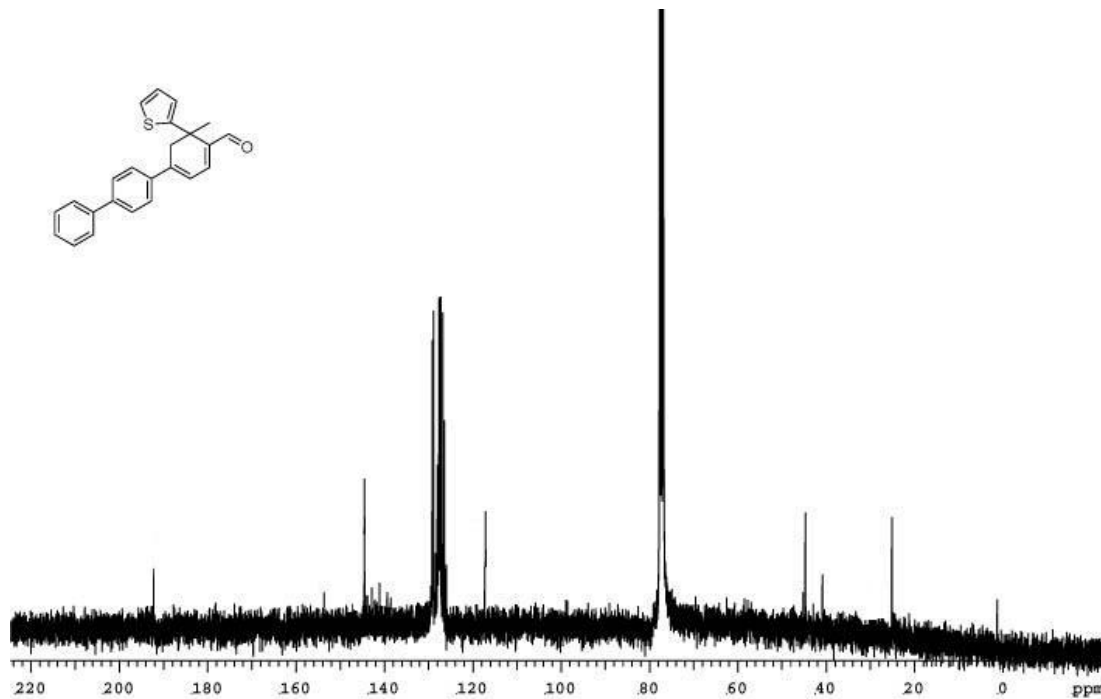
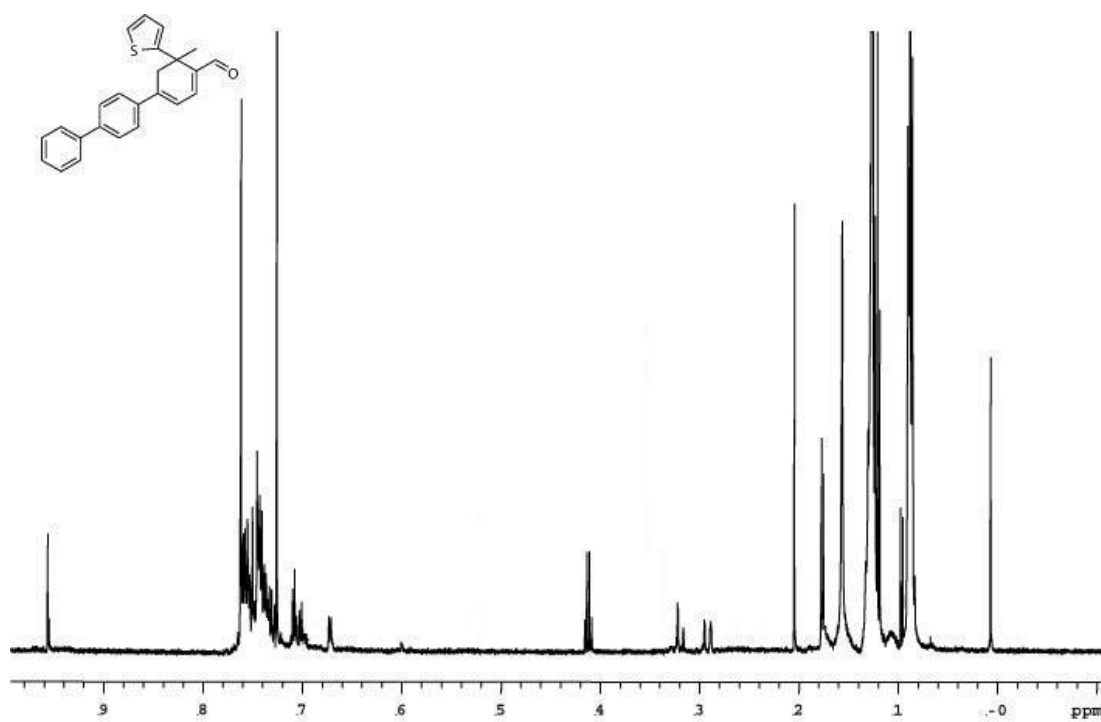
B-47. Spectra of 118.



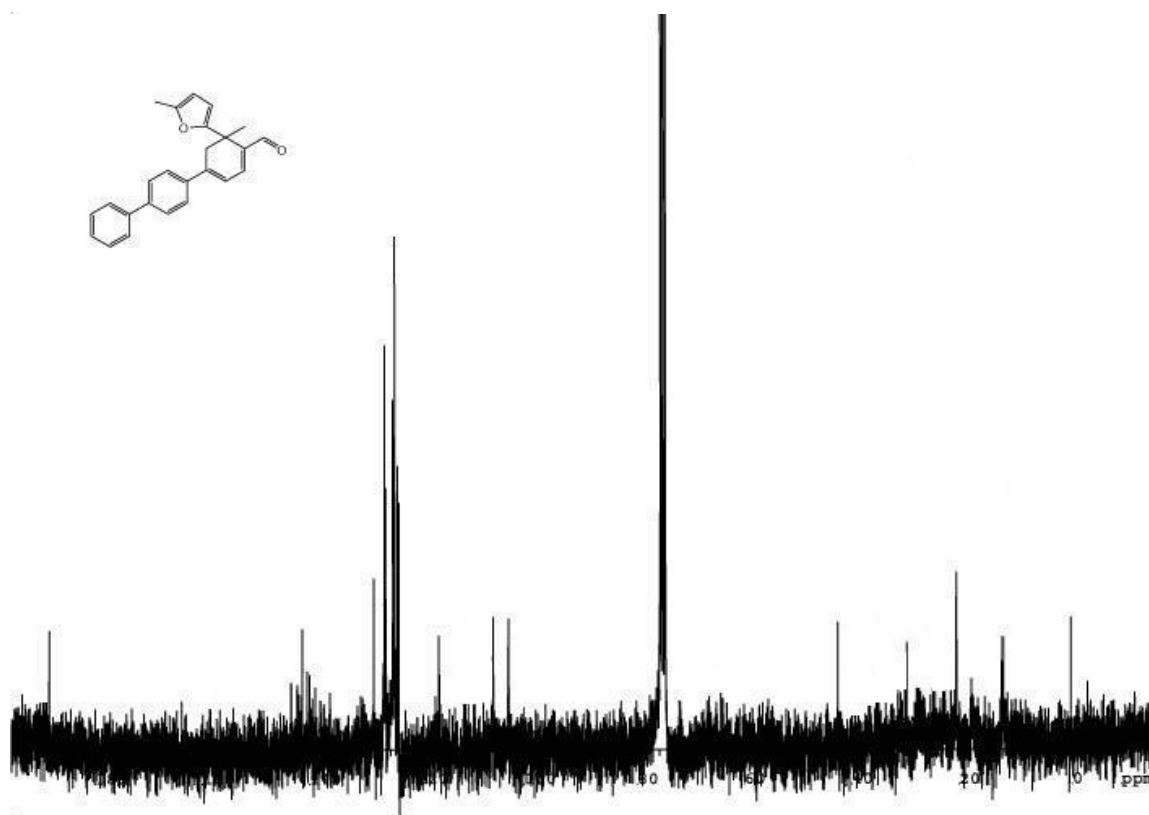
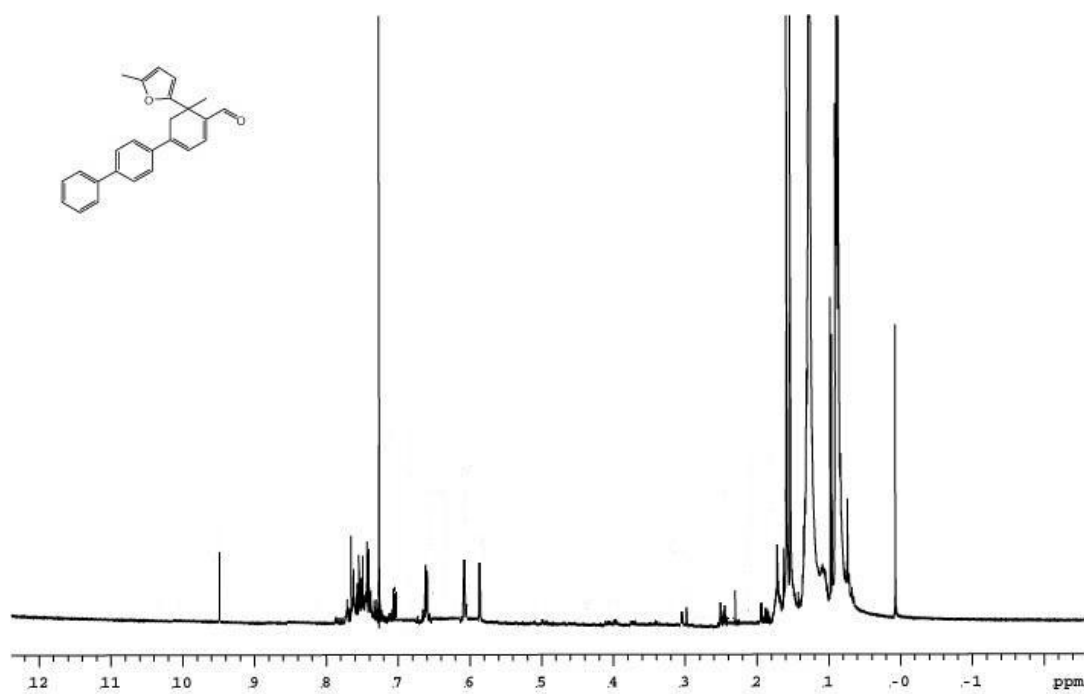
**B-48. Spectra of 119.**



B-49. Spectra of 120.

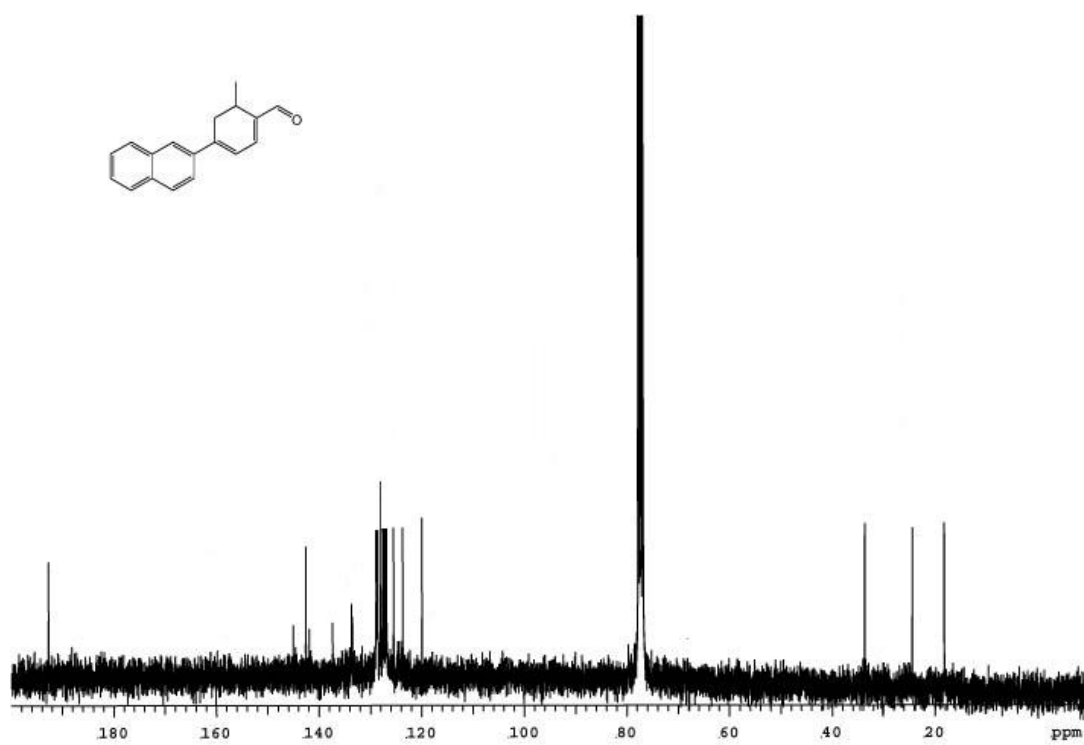
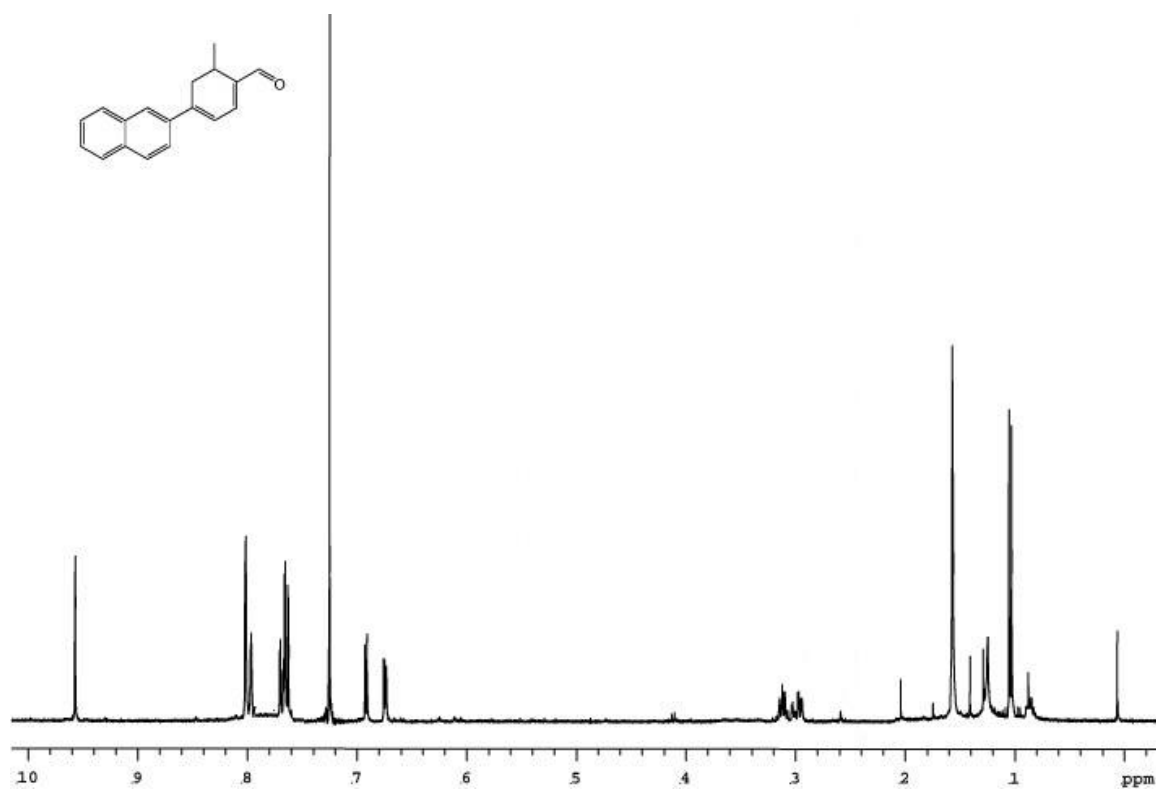


B-50. Spectra of 121.

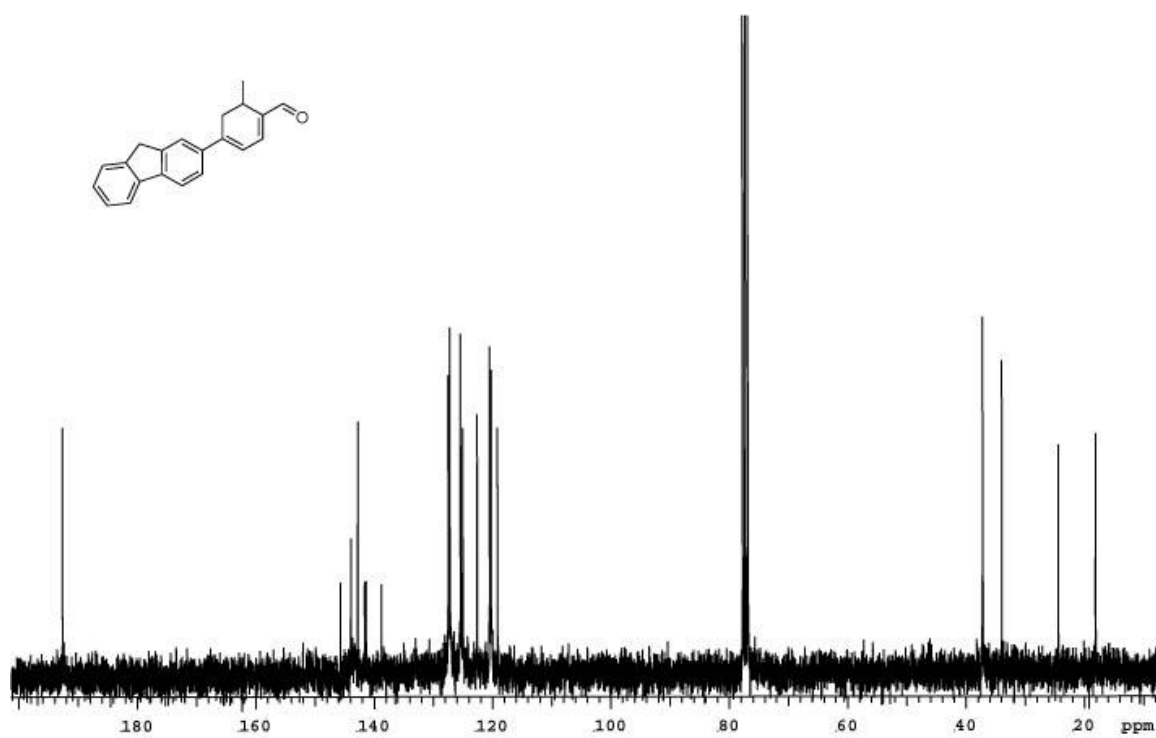
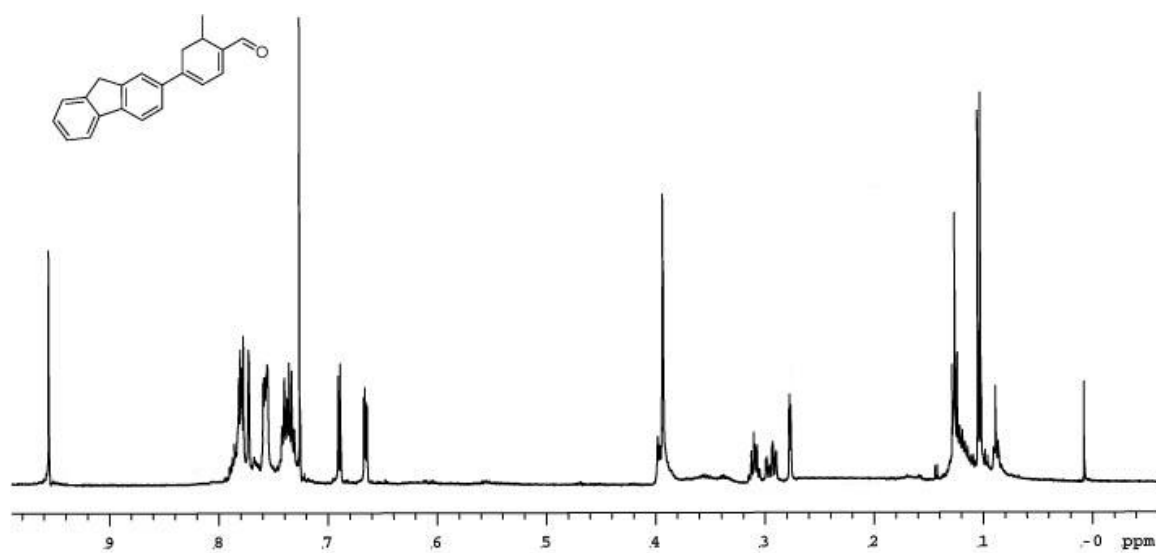


B-51. Spectra of 122.

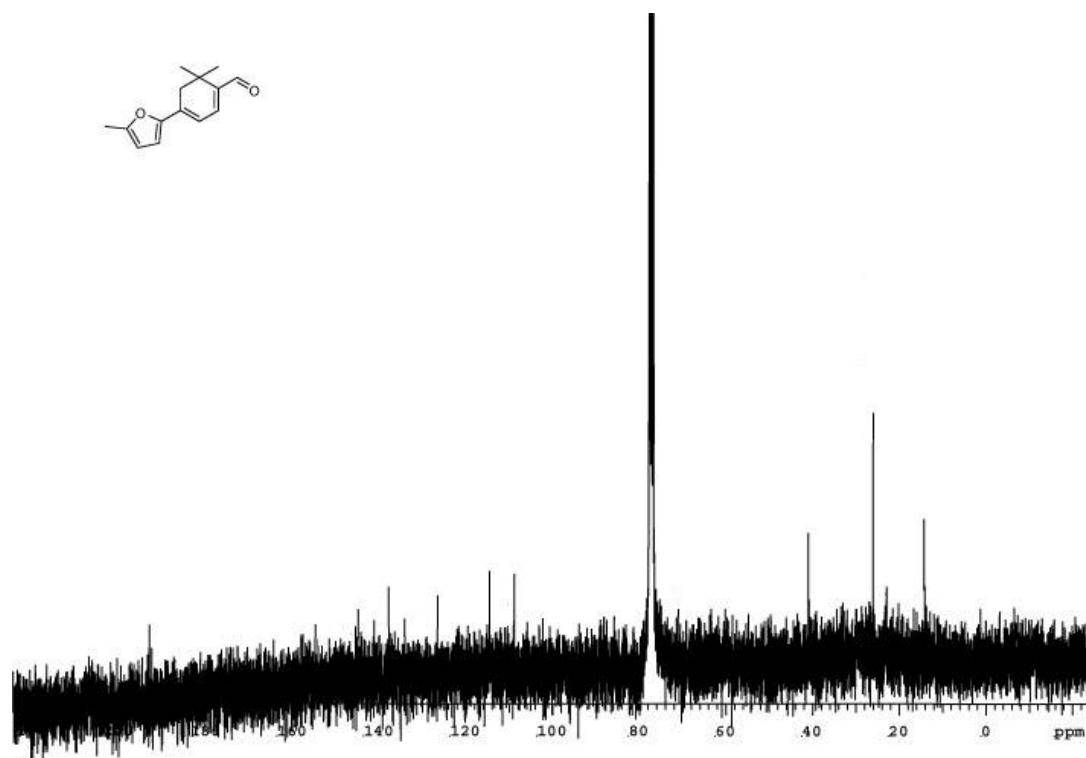
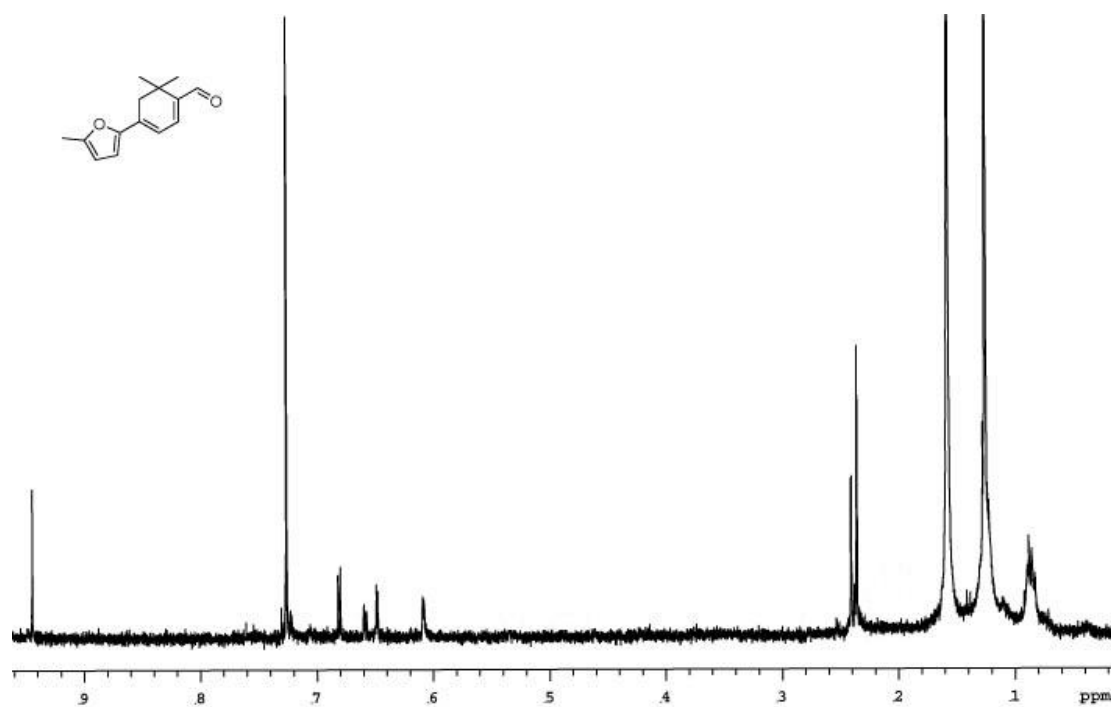




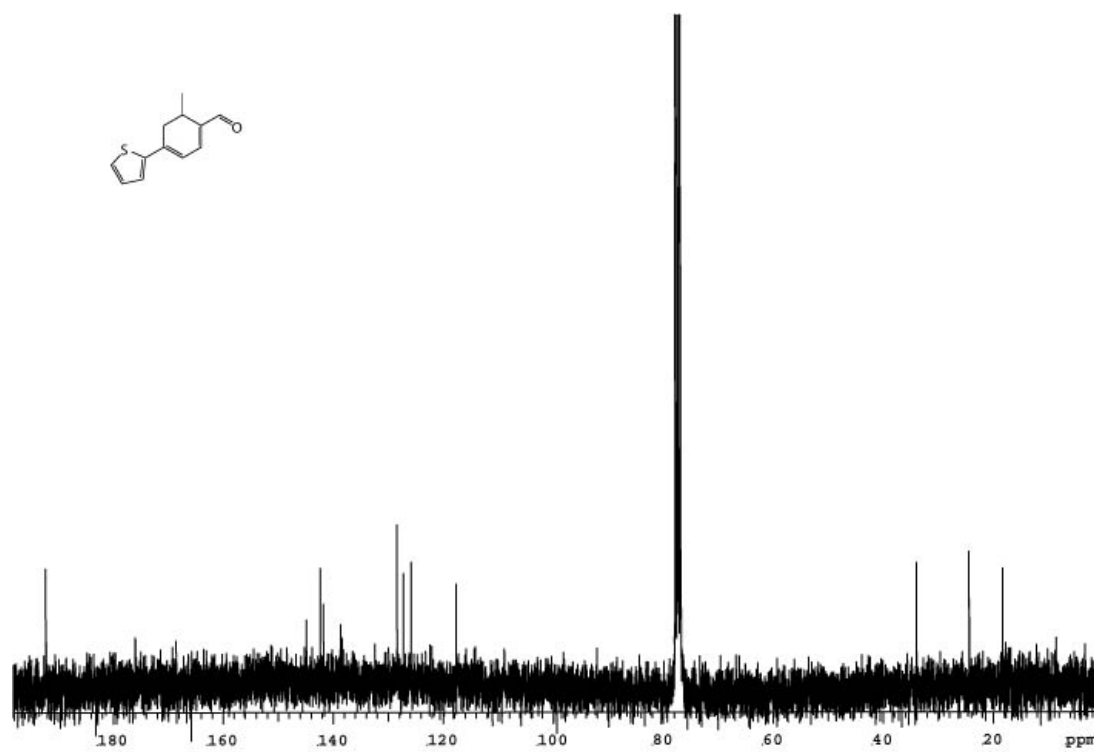
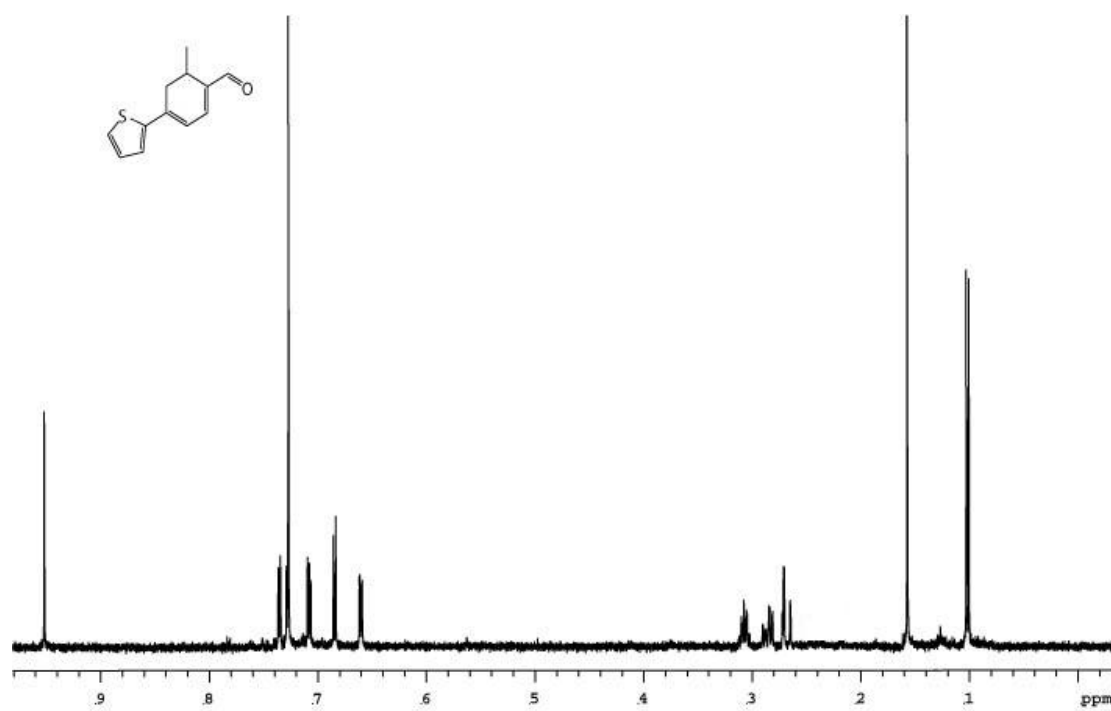
**B-52. Spectra of 123.**



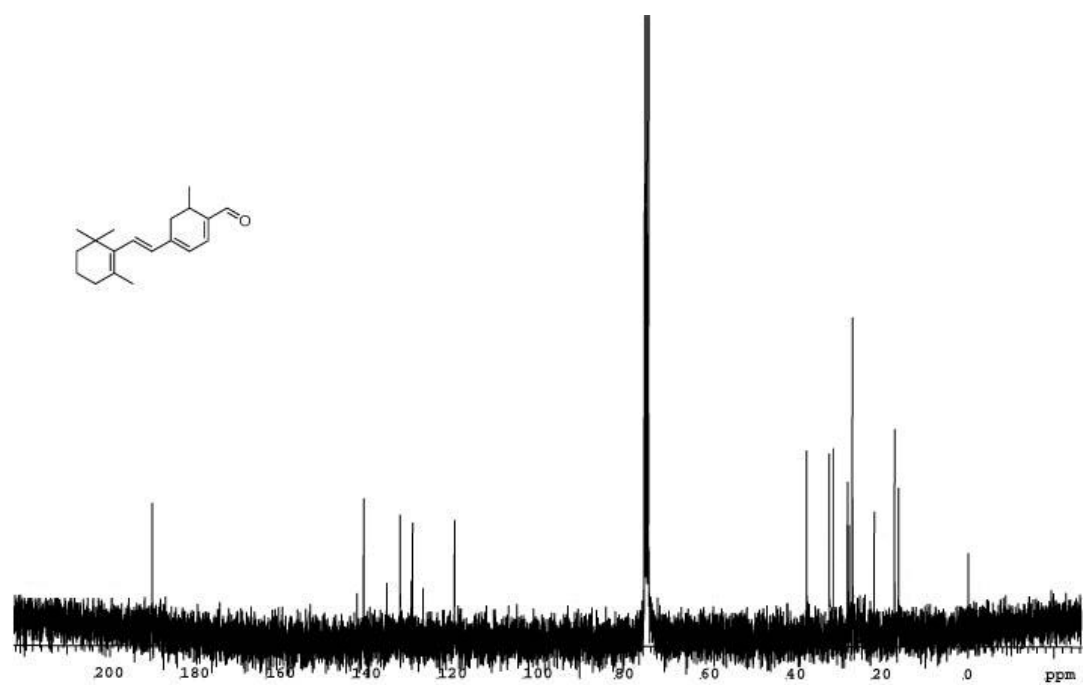
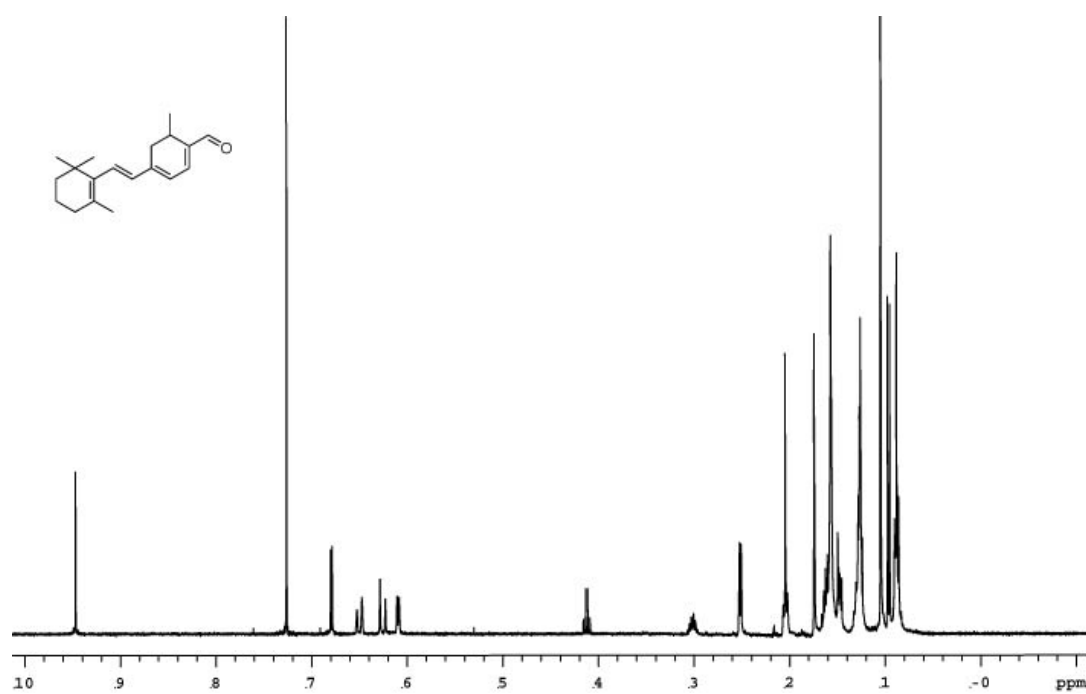
**B-53. Spectra of 124.**



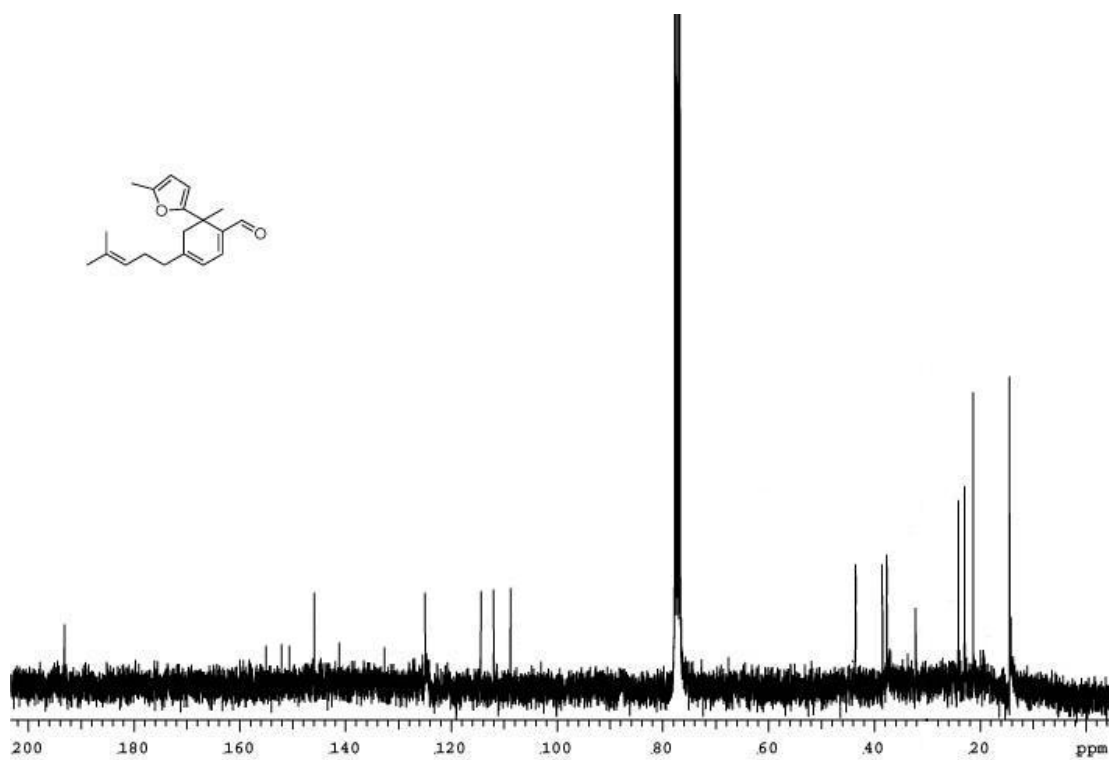
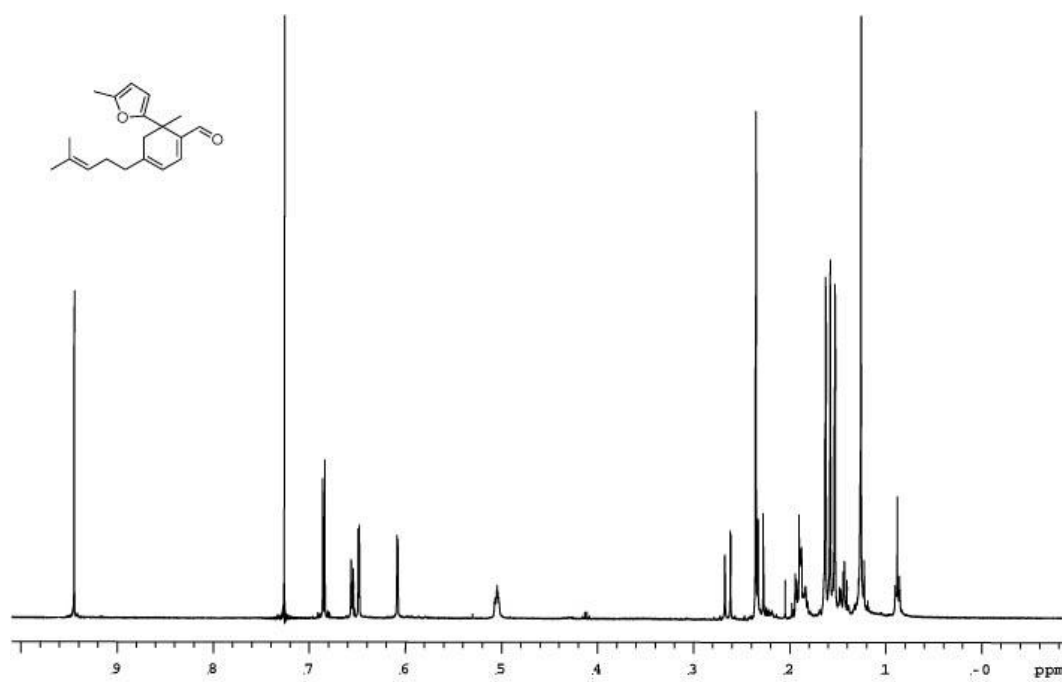
B-54. Spectra of 125.



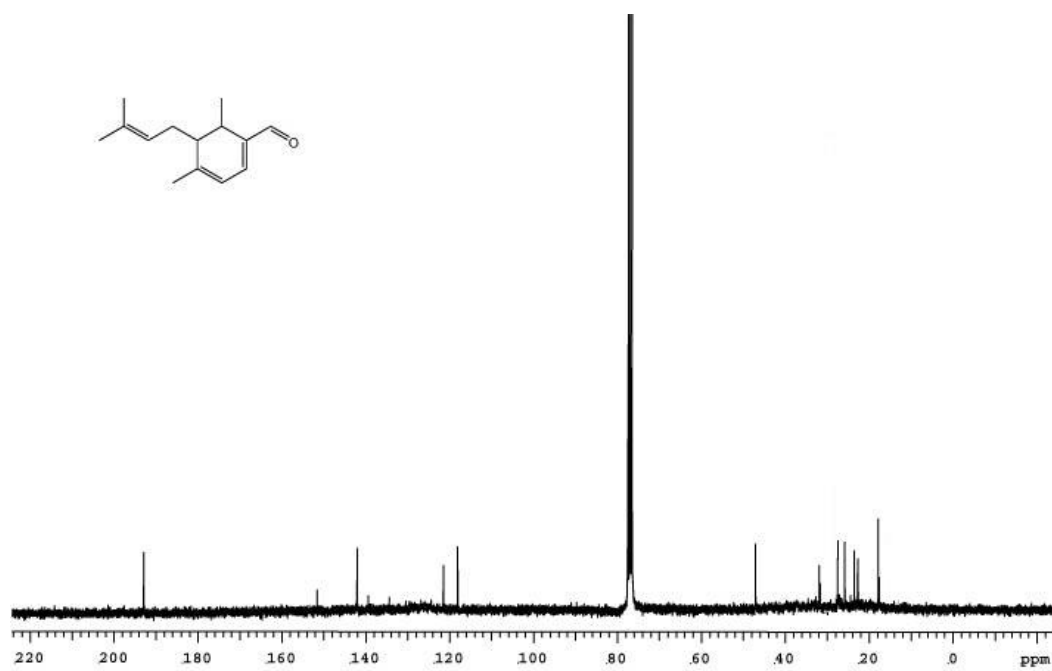
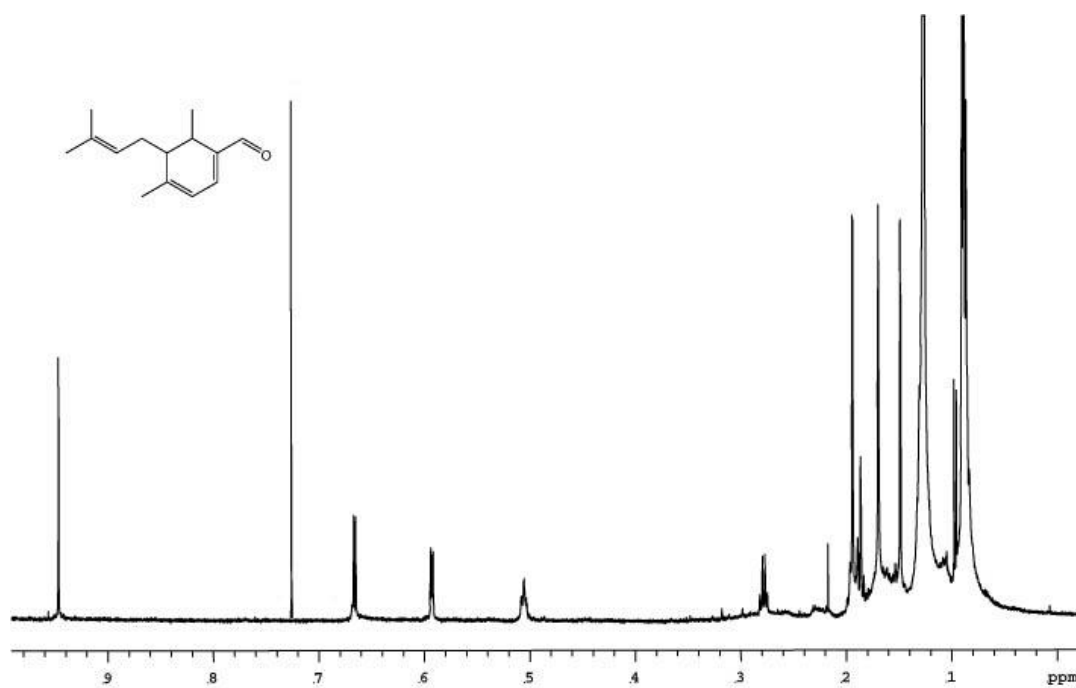
B-55. Spectra of 126.



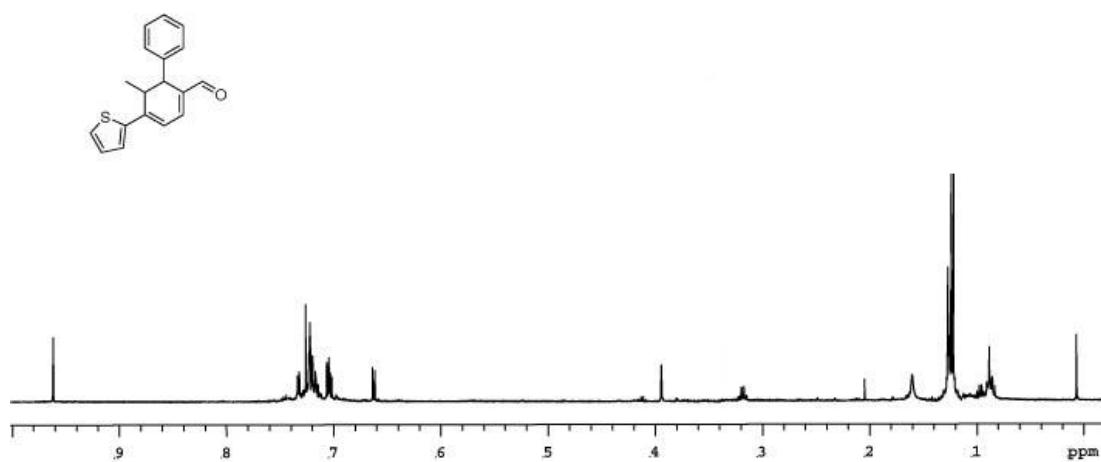
**B-56. Spectra of 127.**



**B-57. Spectra of 128.**

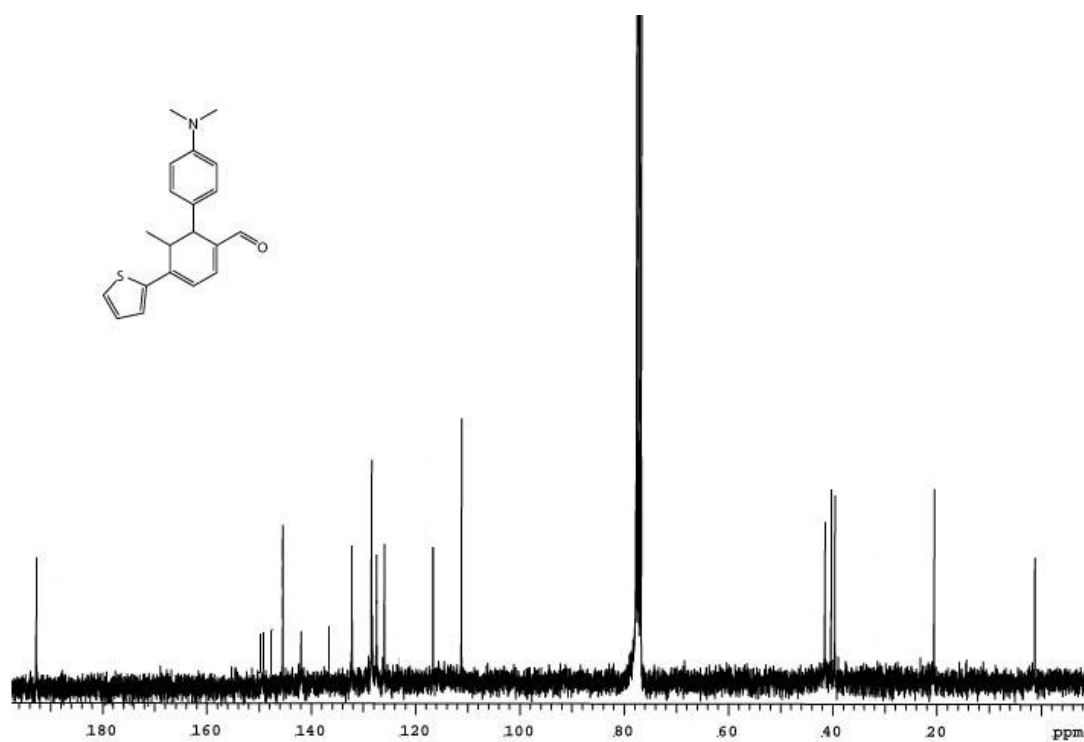
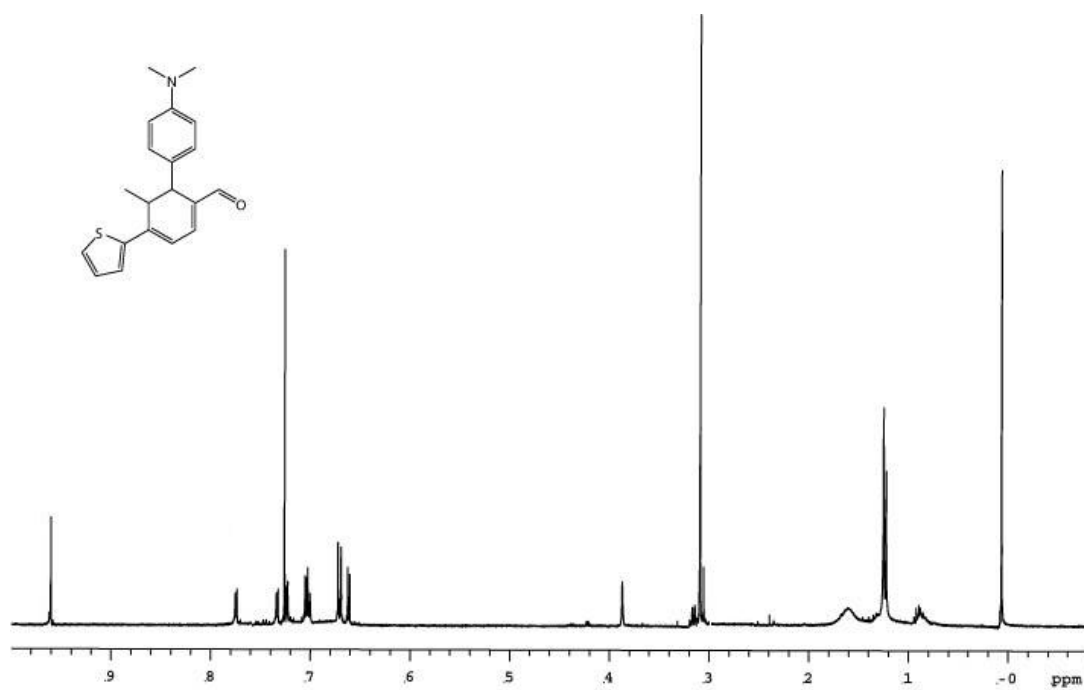


B-58. Spectra of 129.

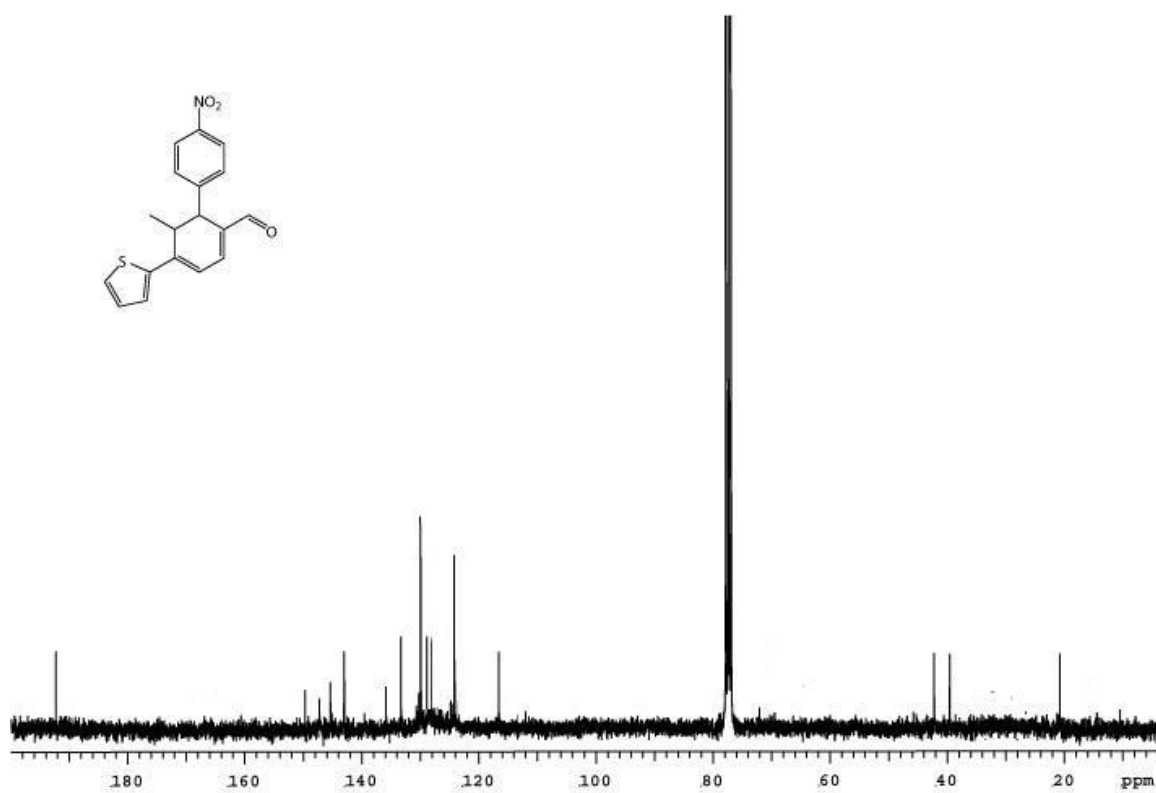
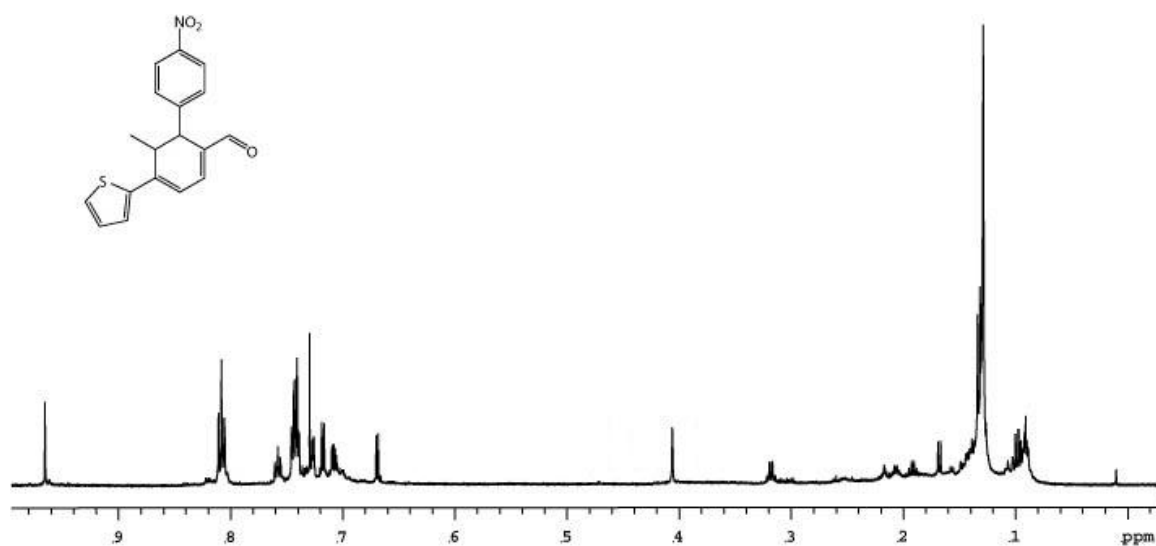


**B-59. Spectra of 130.**

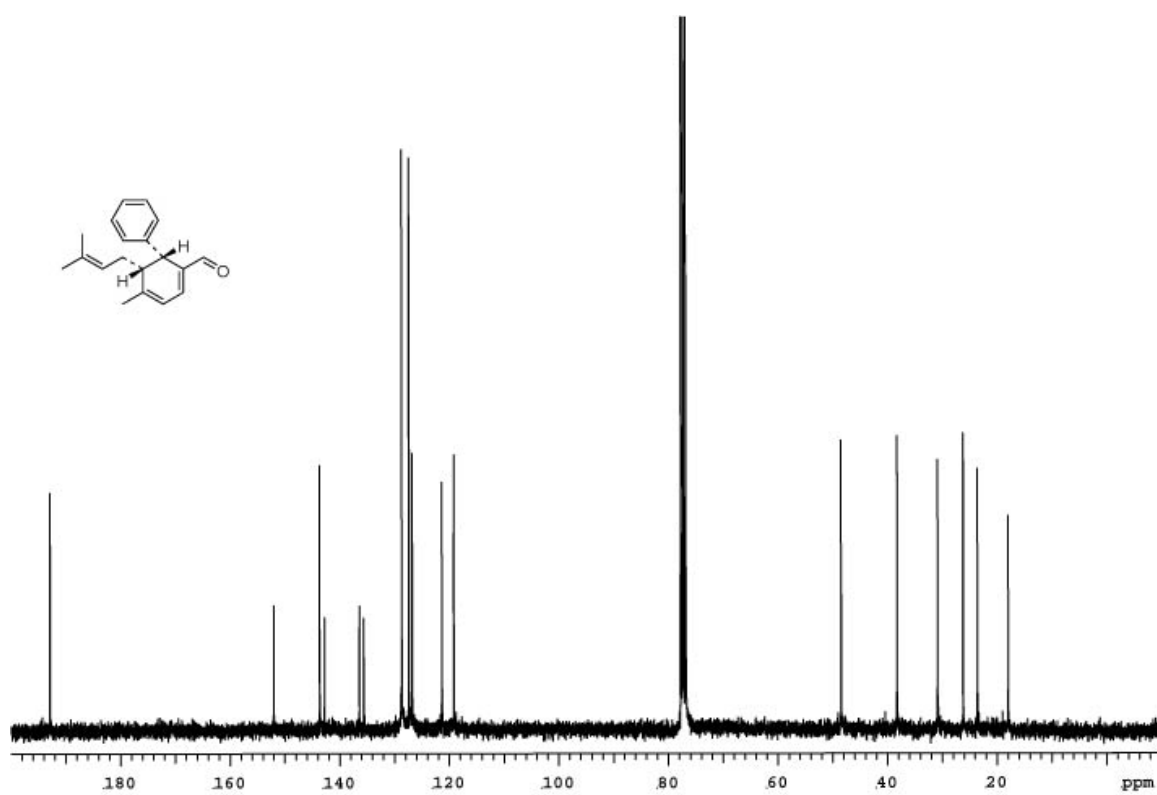
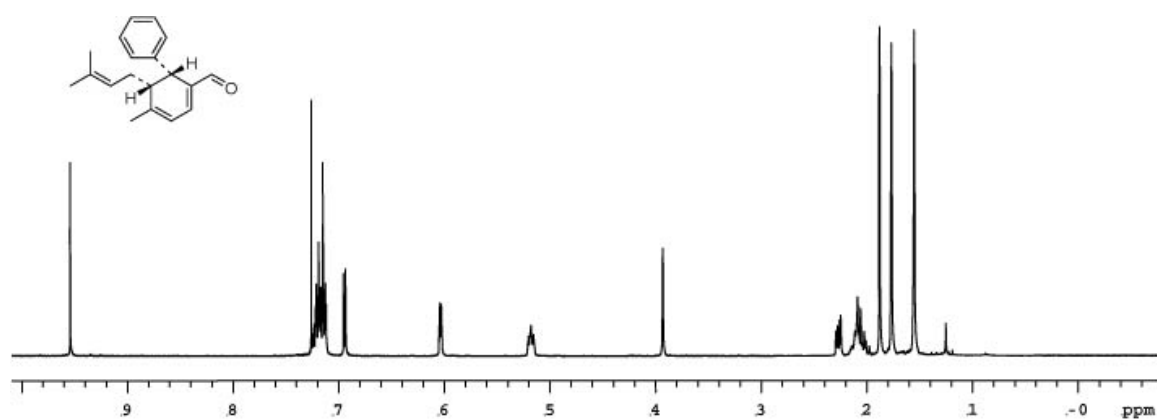




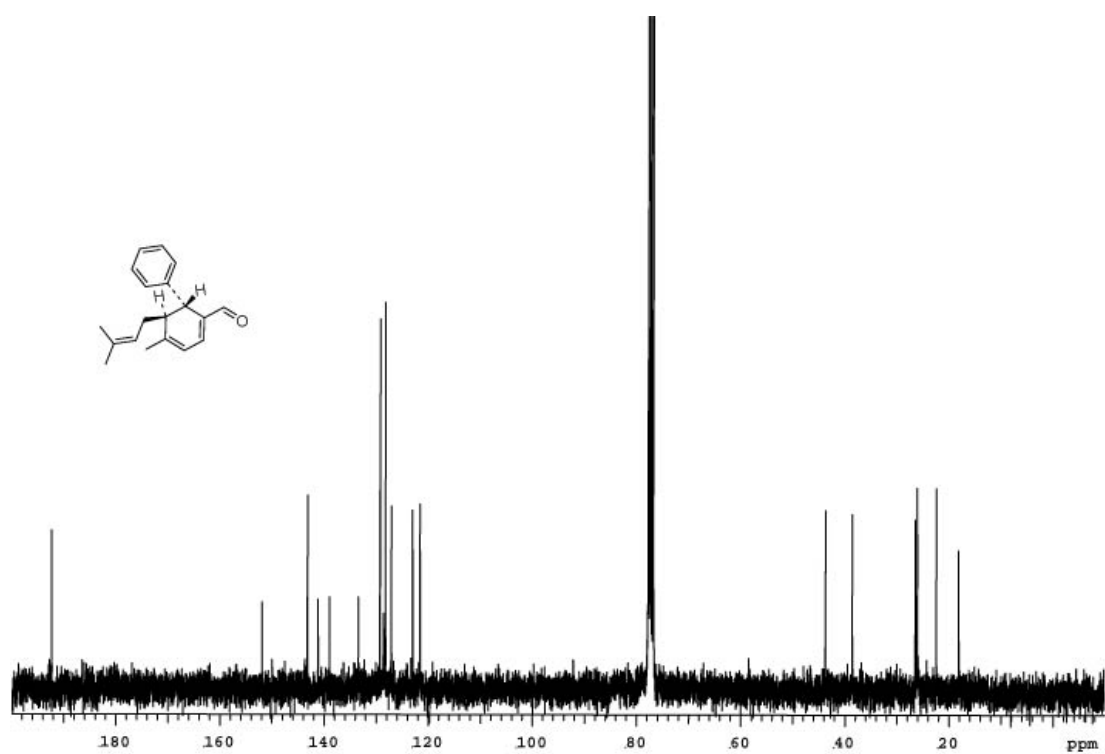
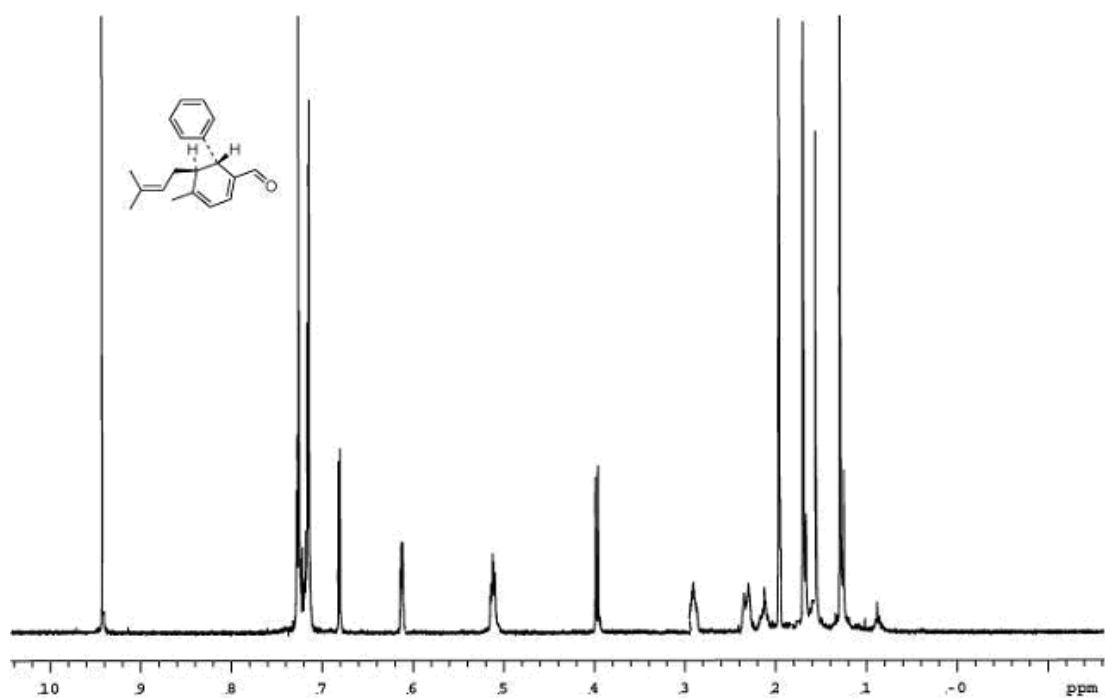
**B-60. Spectra of 131.**



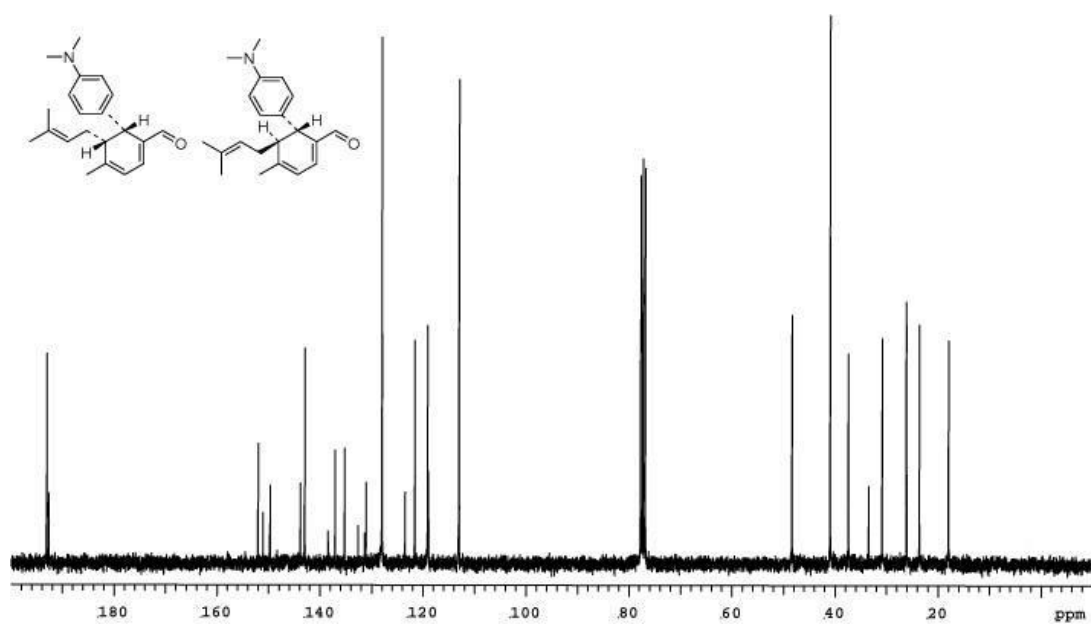
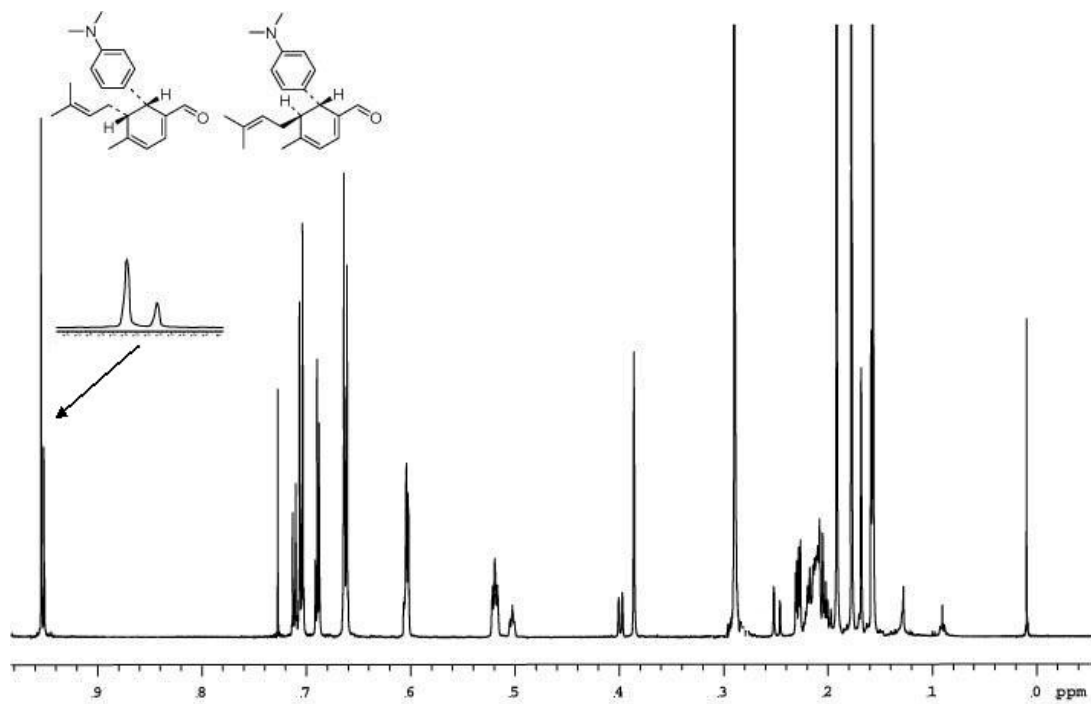
B-61. Spectra of 132.



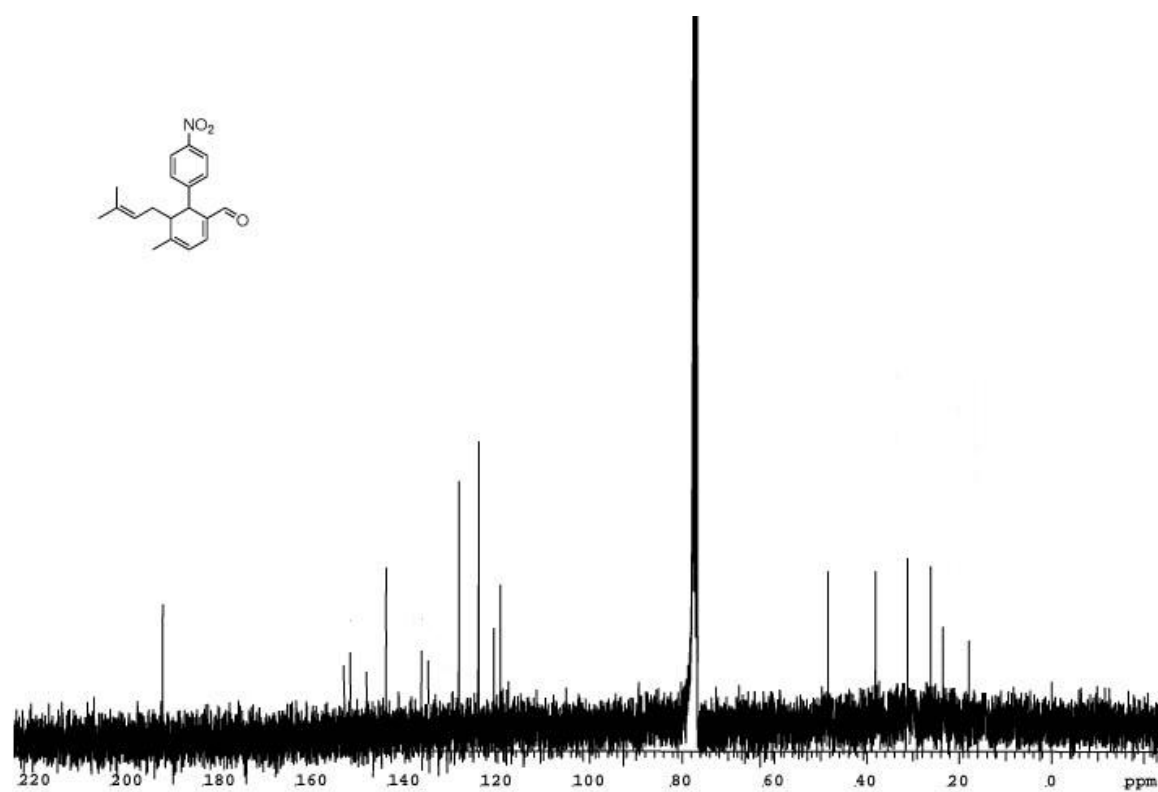
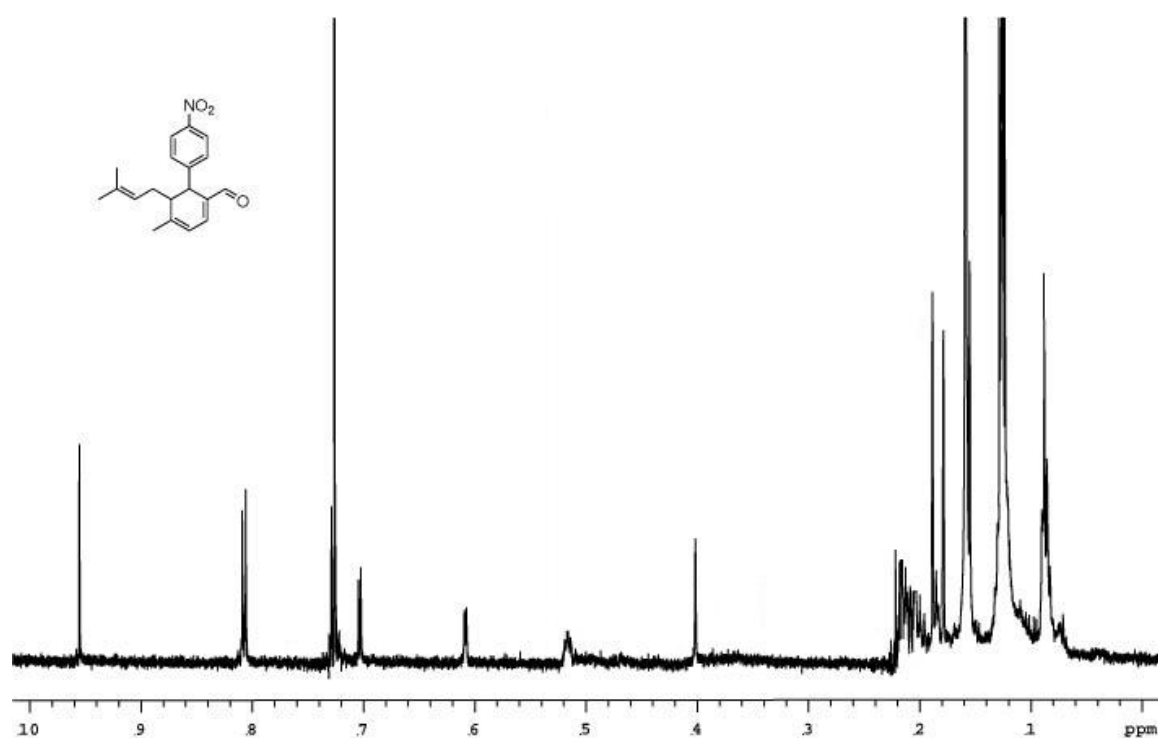
B-62. Spectra of 27.



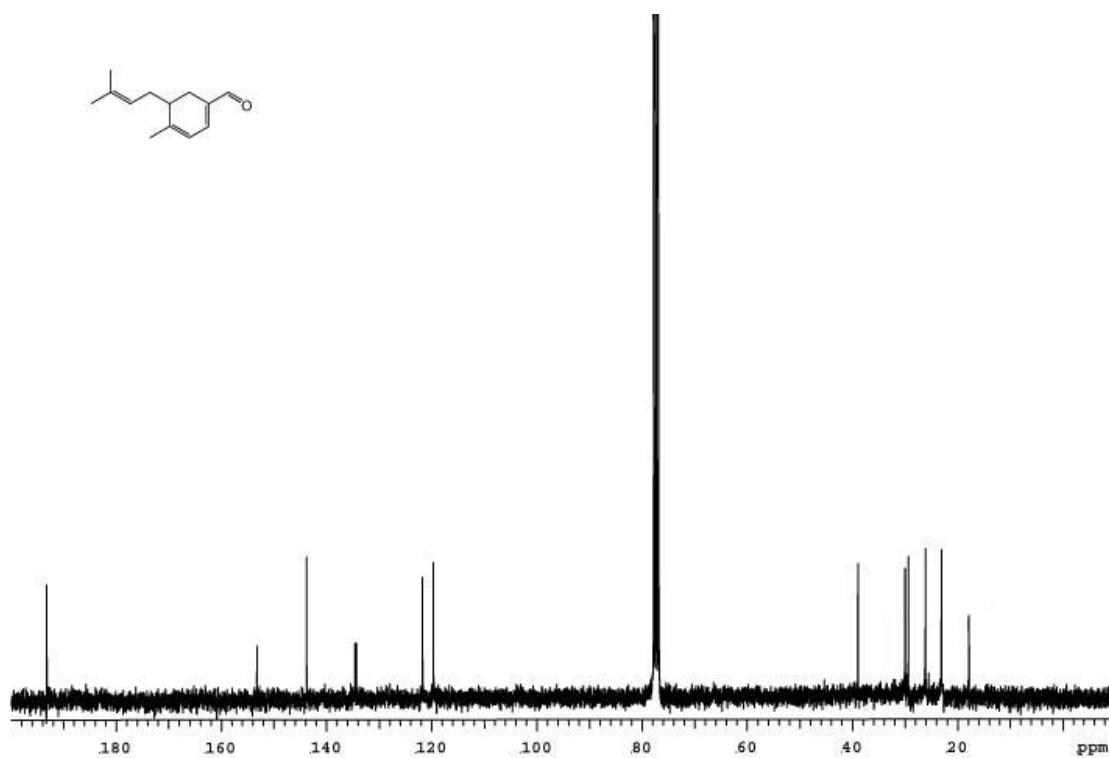
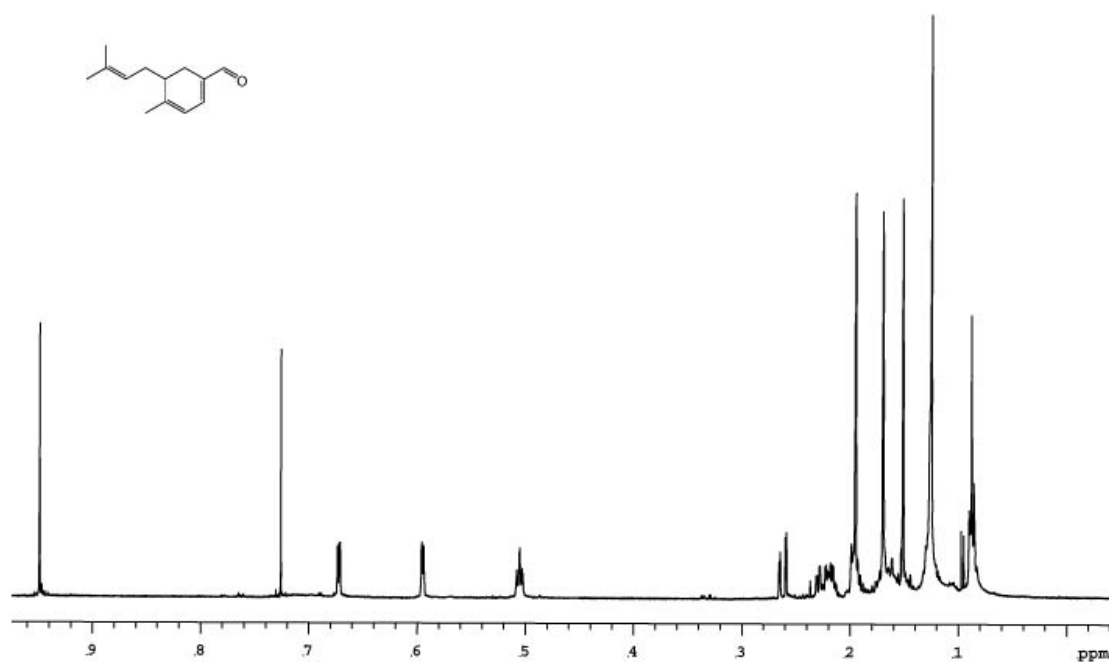
B-63. Spectra of 28.



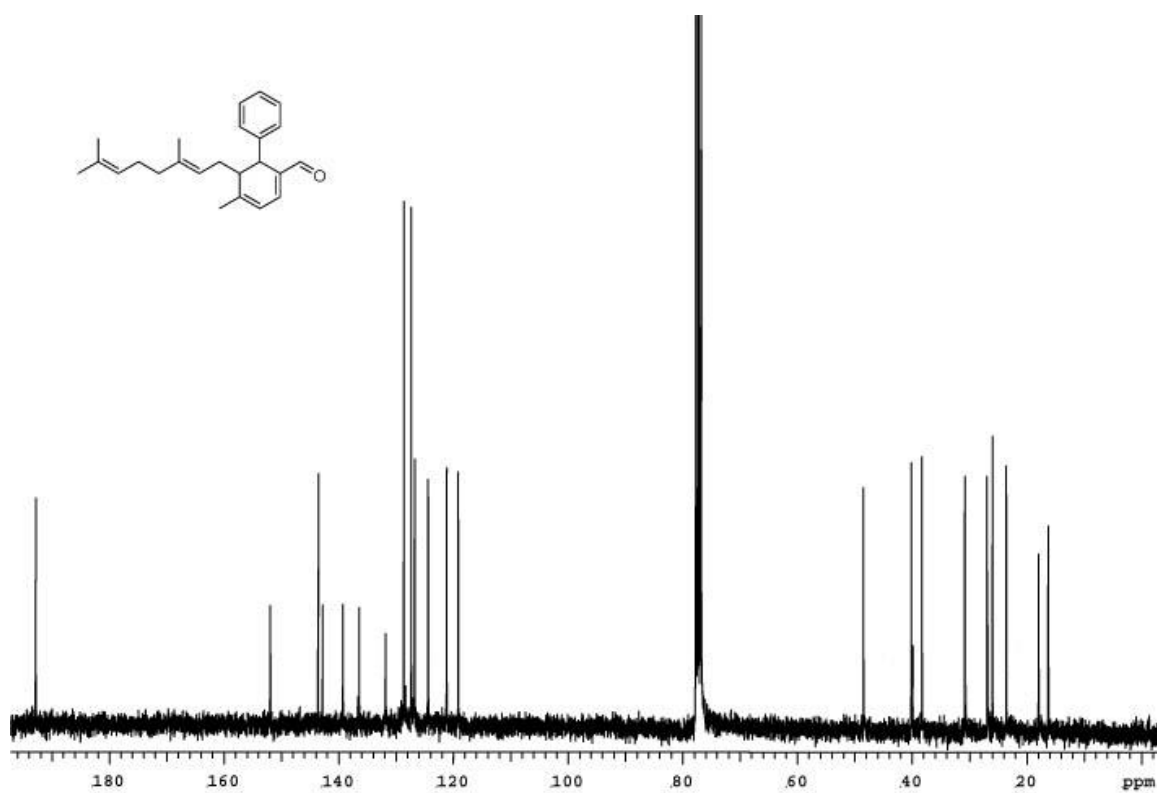
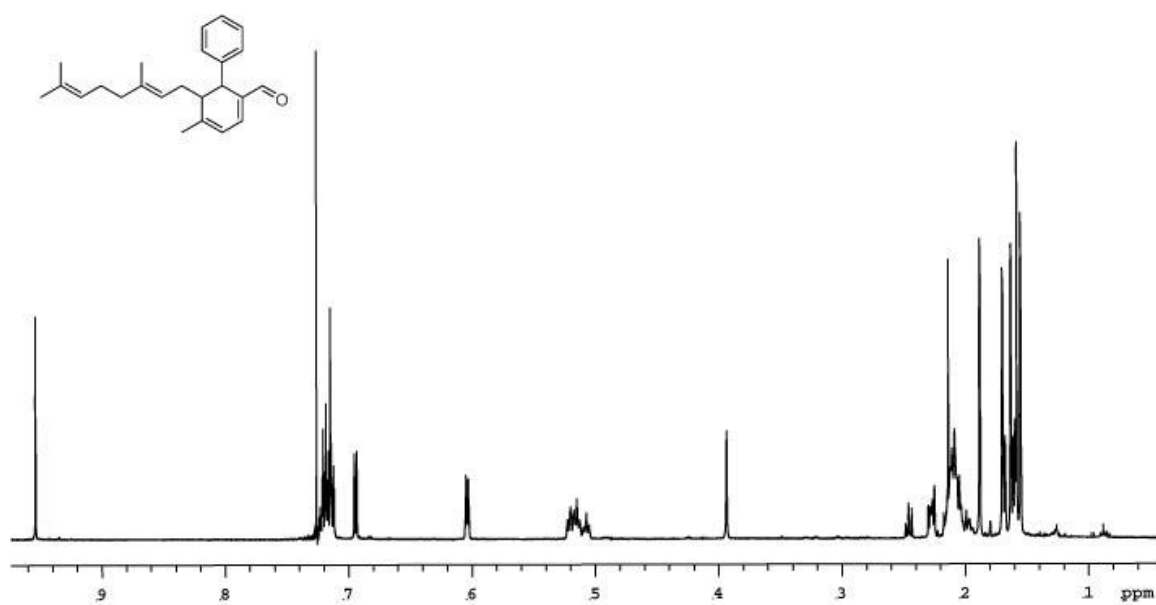
B-64. Spectra of 133 and 134.



**B-65. Spectra of 135.**

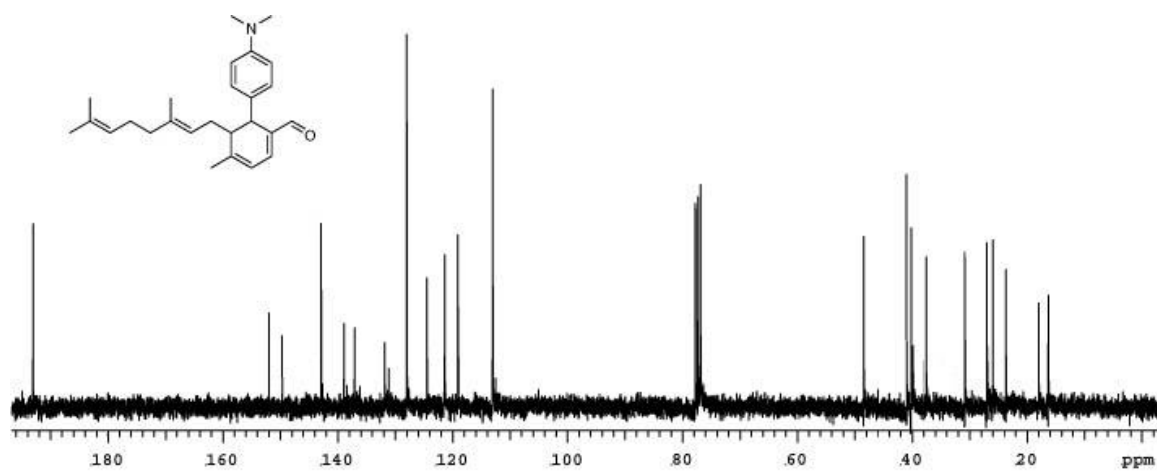
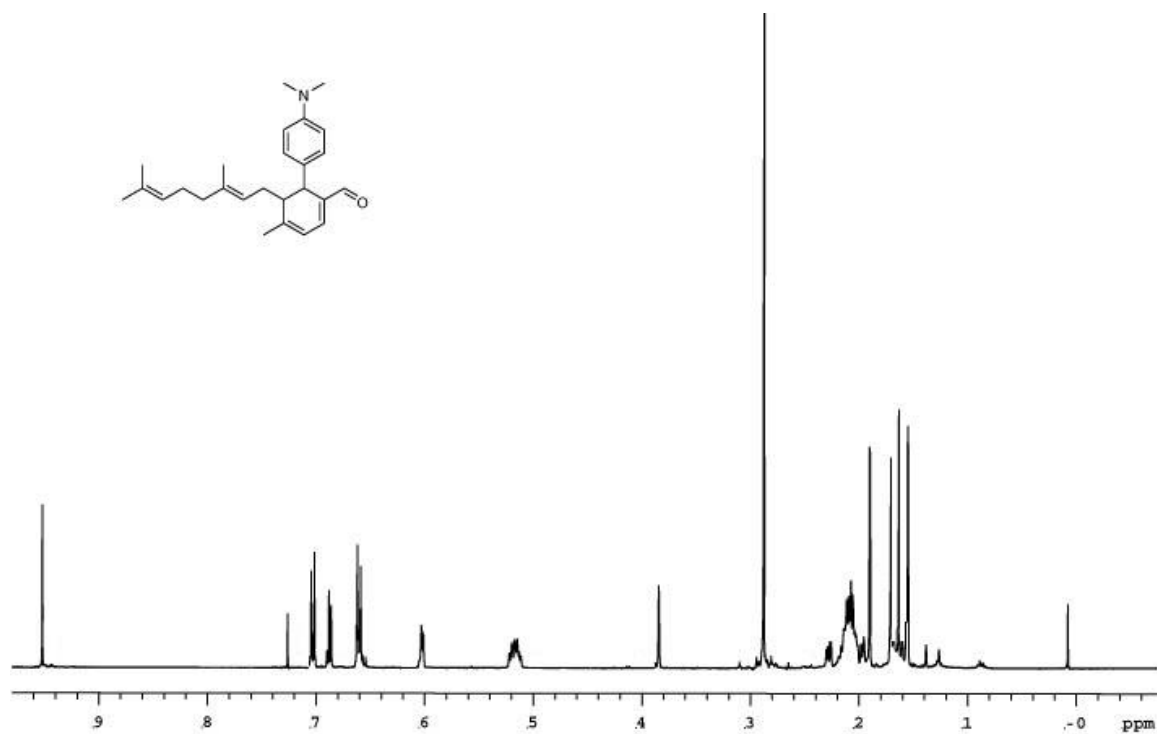


**B-66. Spectra of 136.**

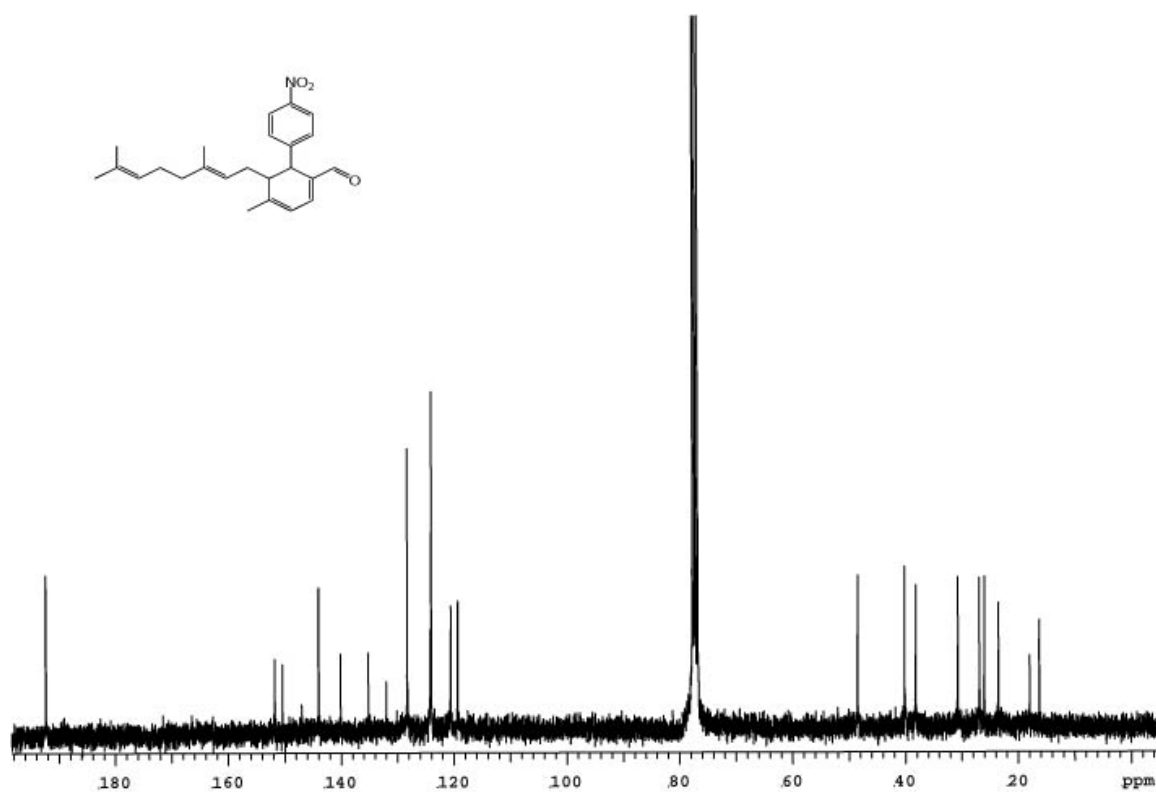
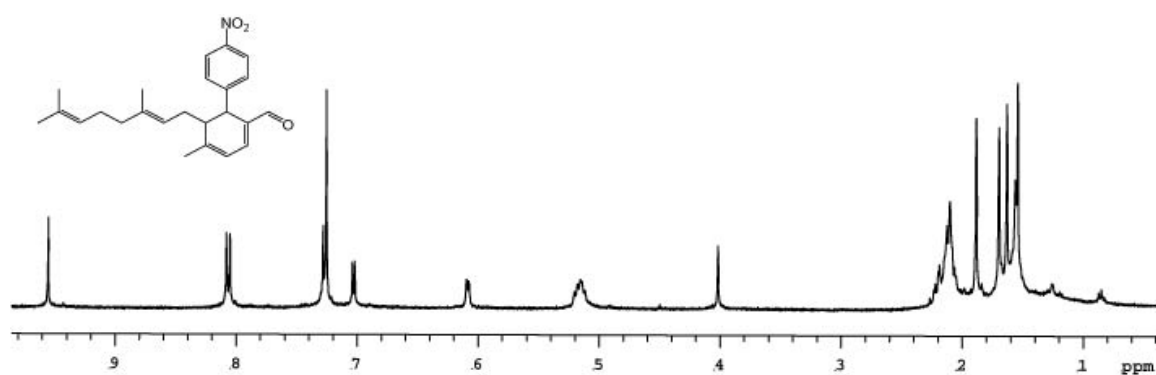


B-67. Spectra of 137.

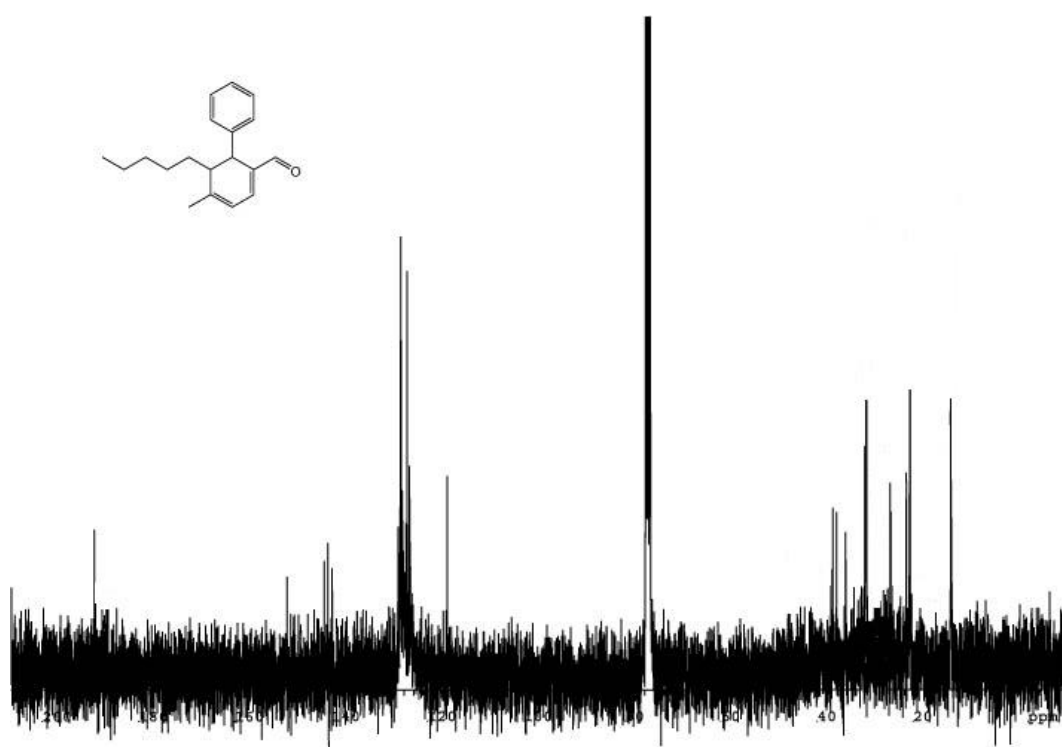
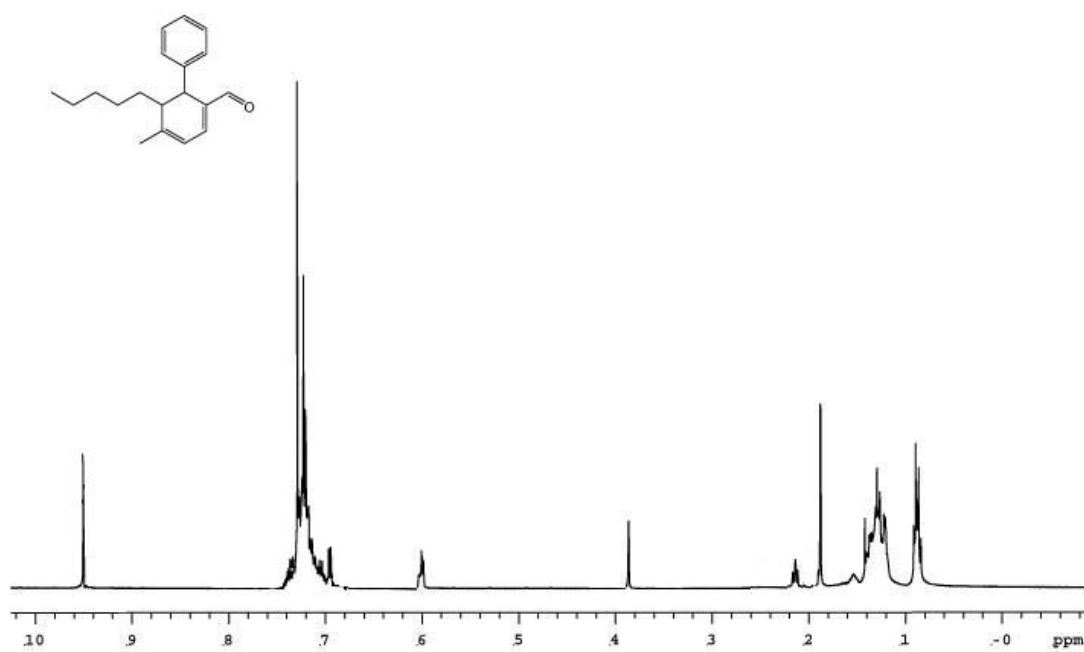




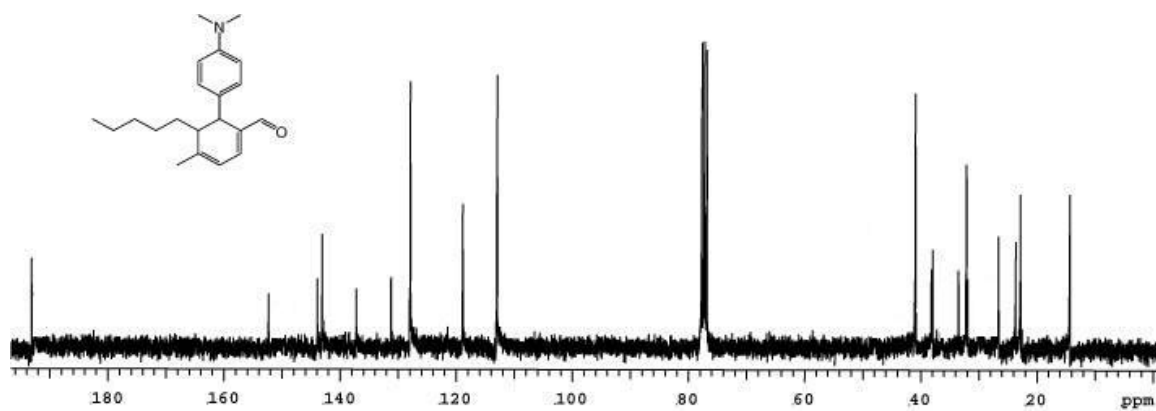
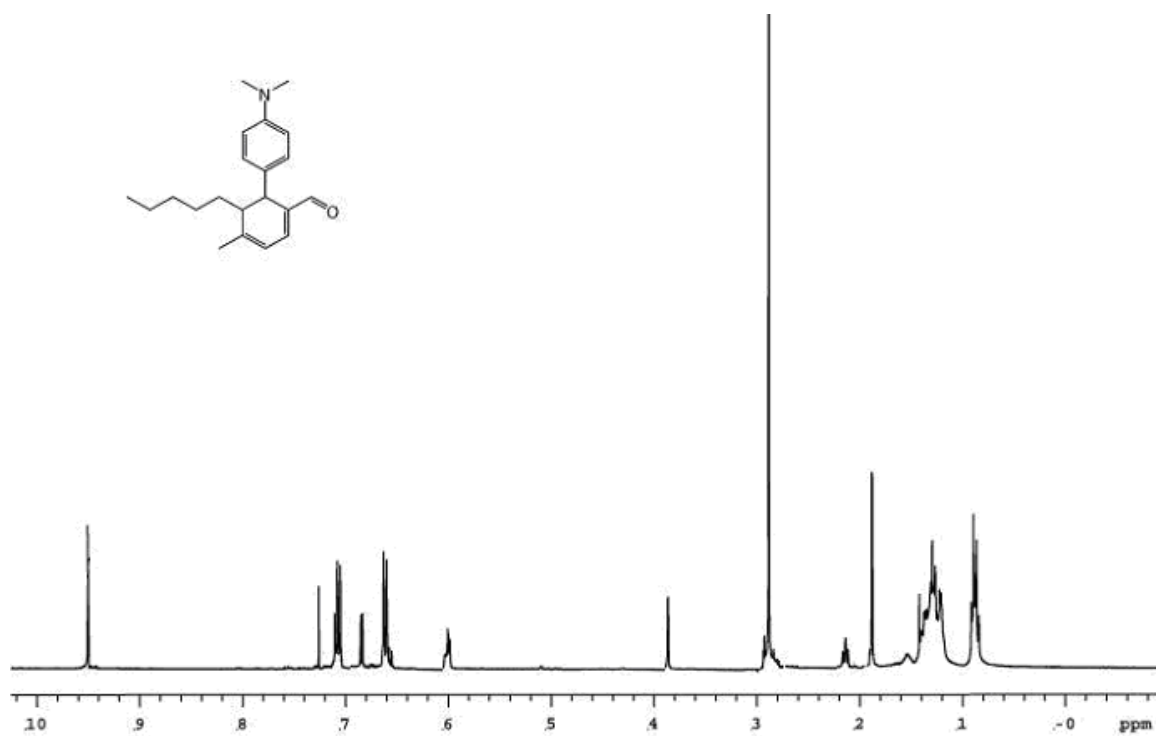
B-68. Spectra of 138.



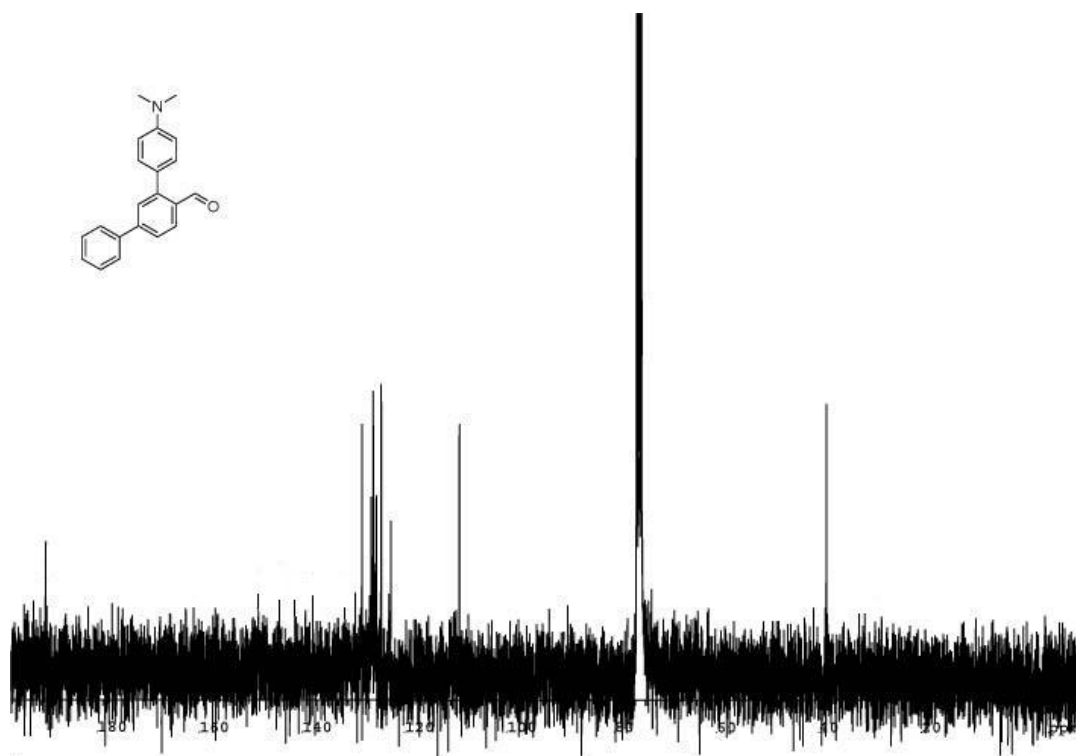
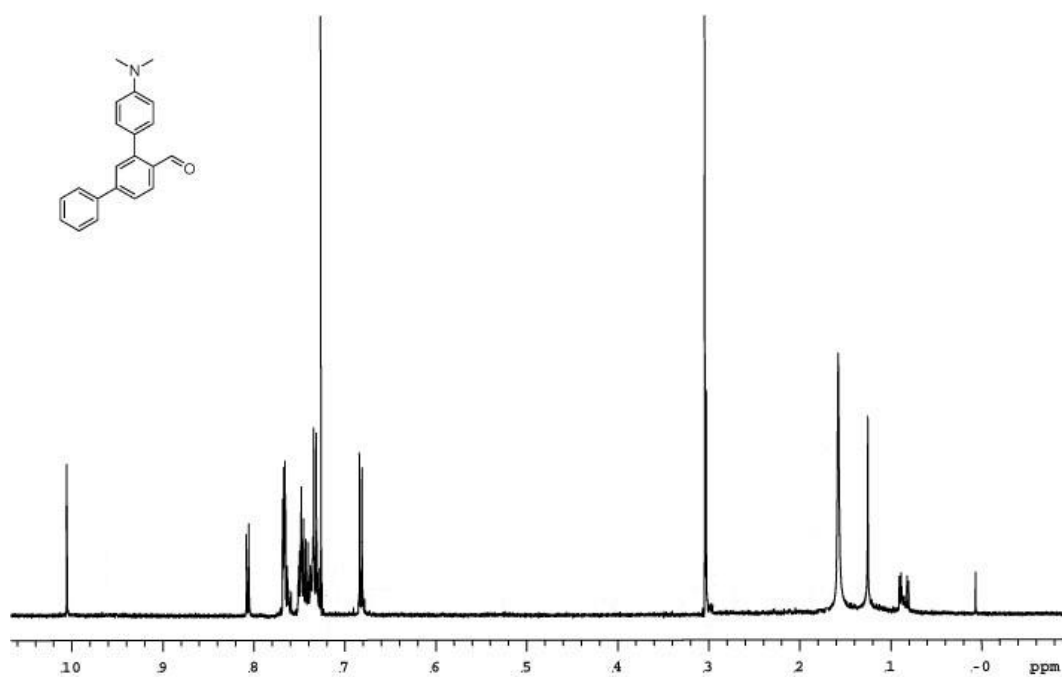
**B-69. Spectra of 139.**



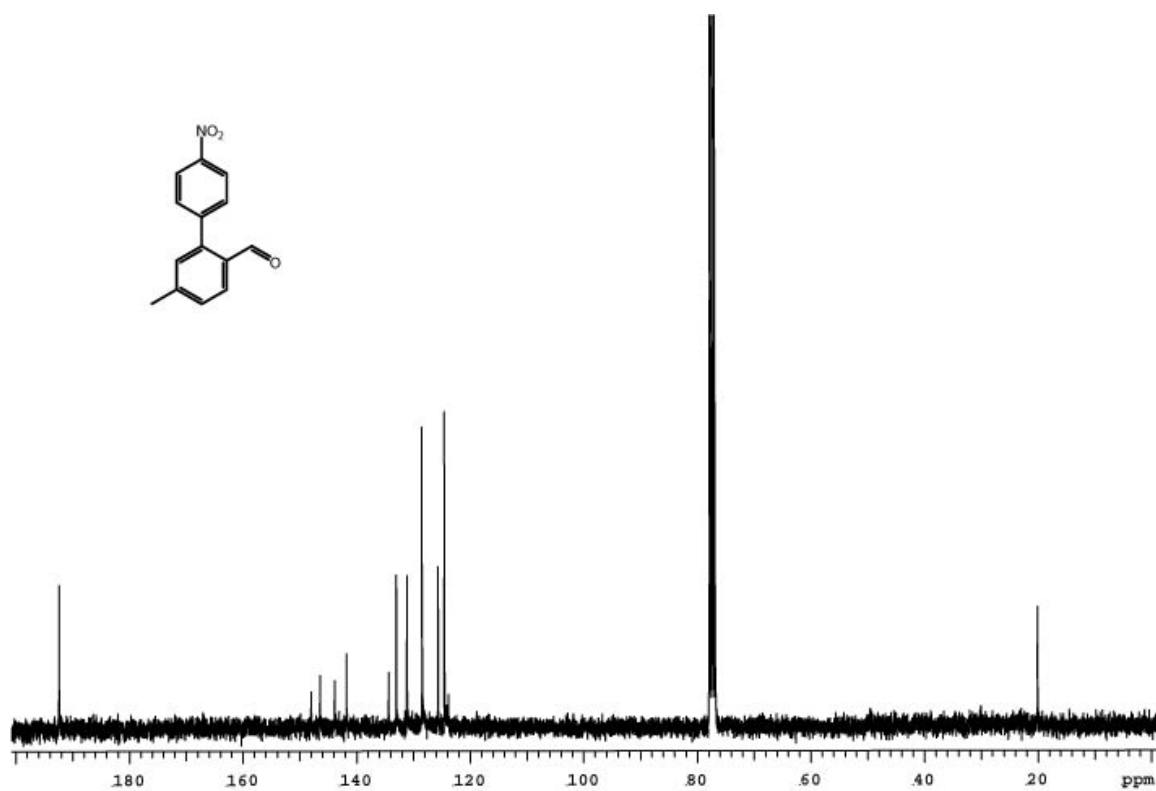
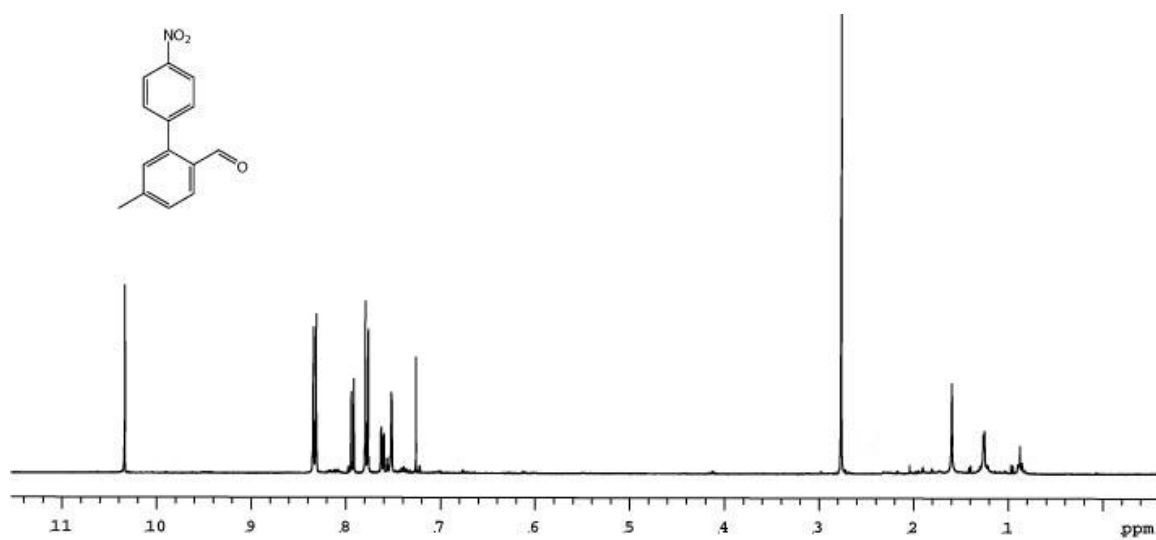
**B-70. Spectra of 140.**



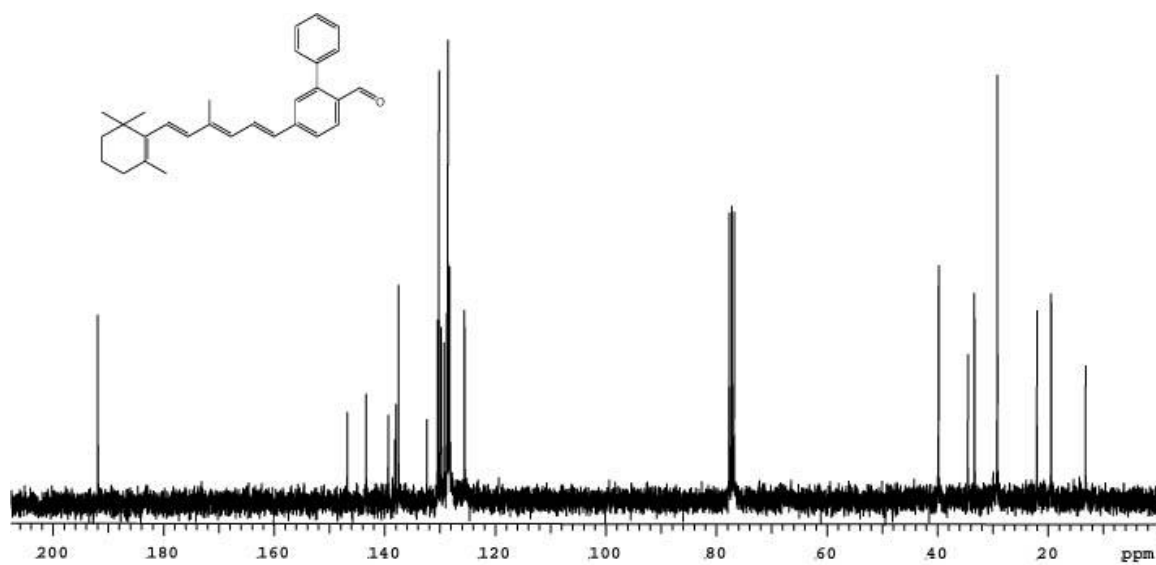
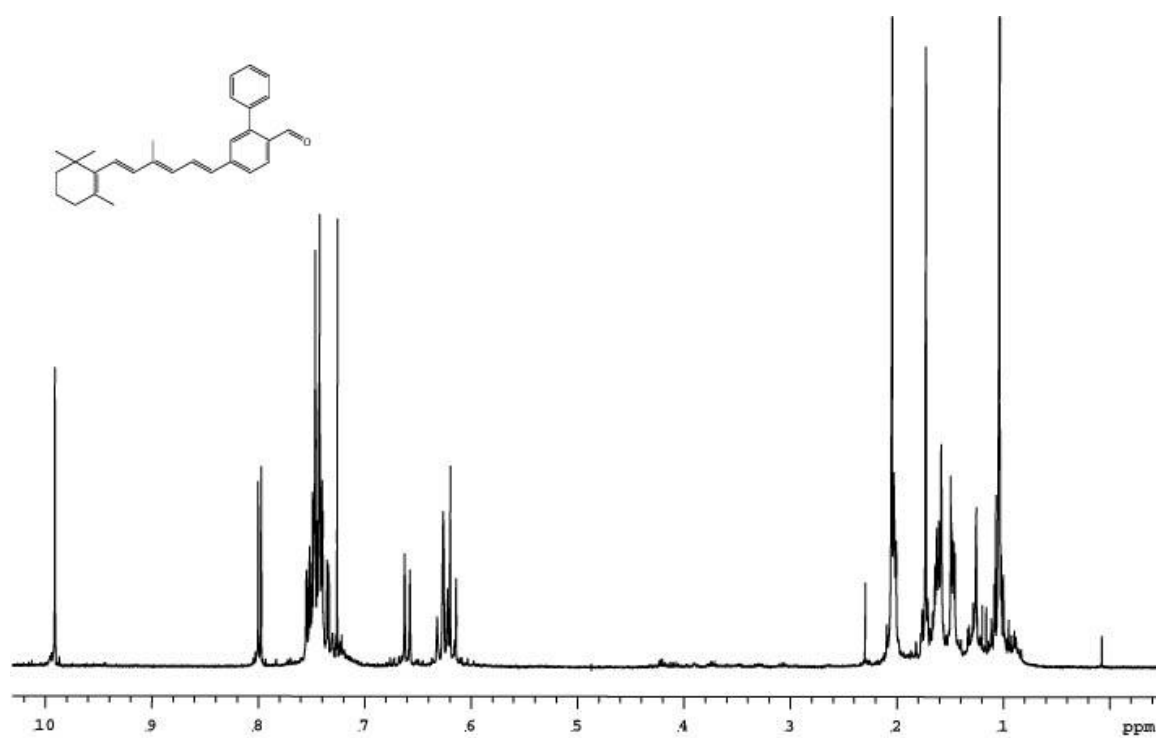
**B-71. Spectra of 141.**



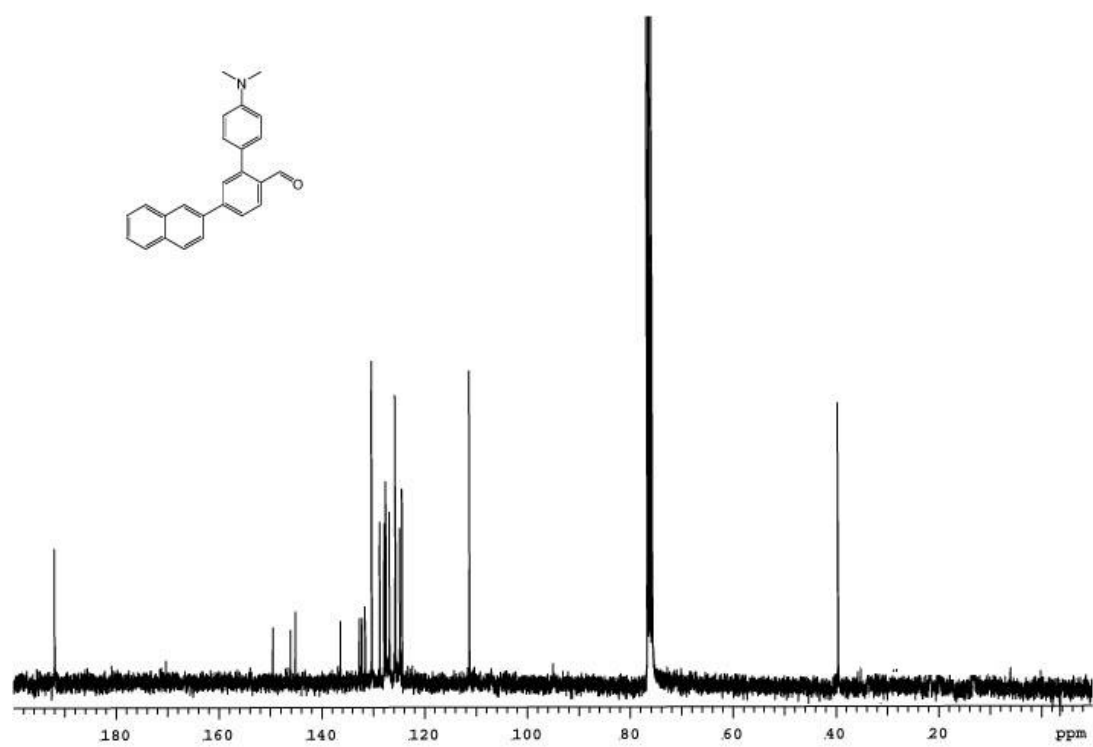
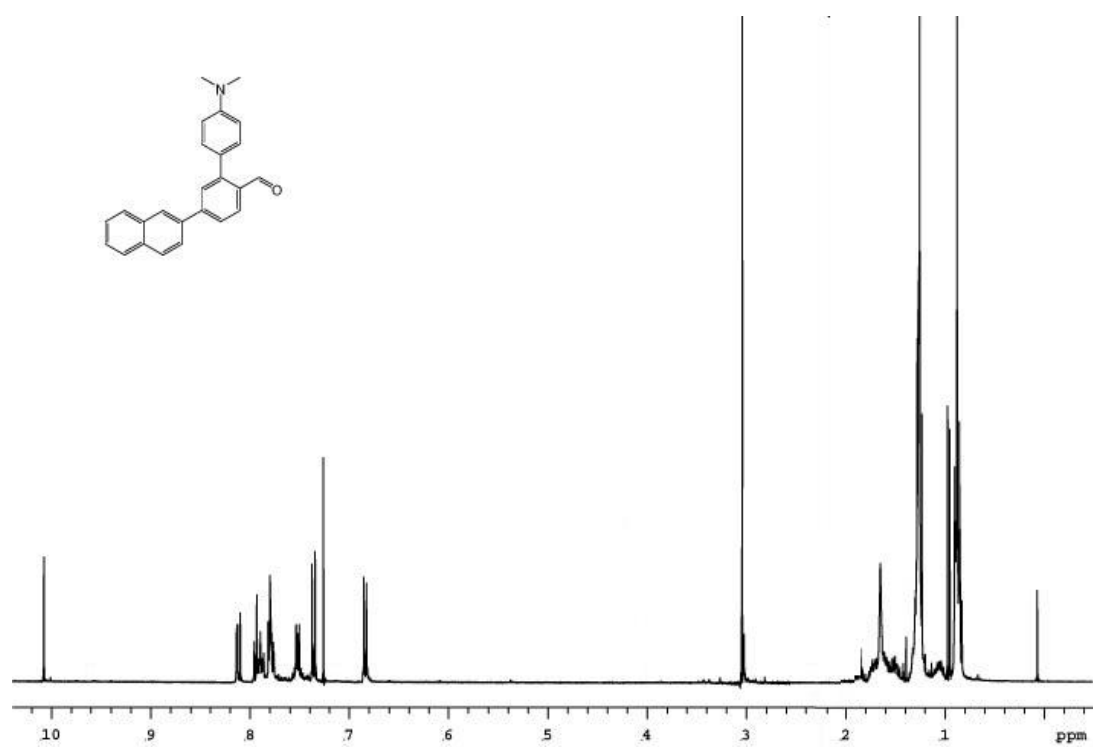
B-72. Spectra of 142.



B-73. Spectra of 143.

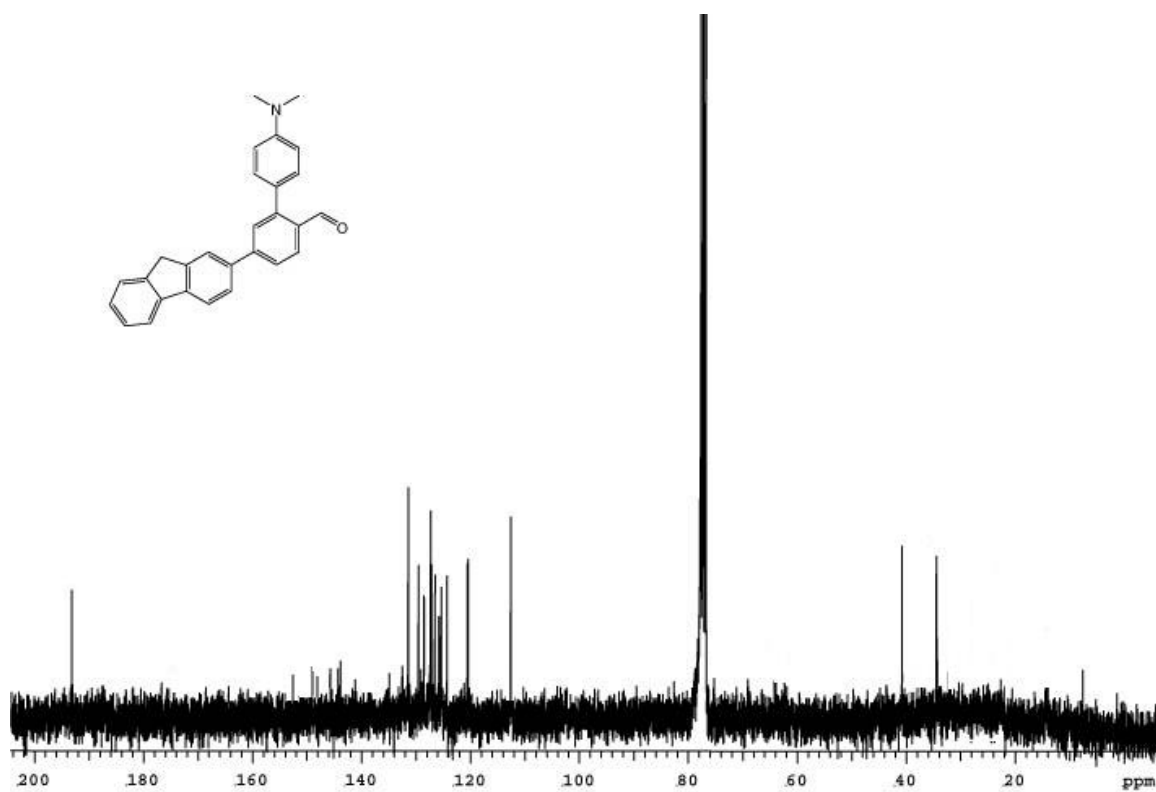
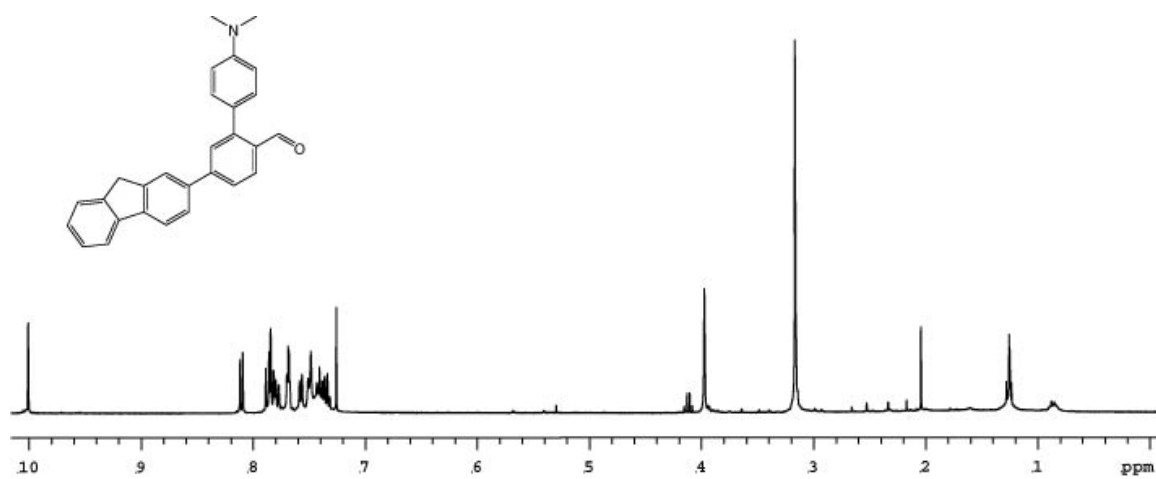


**B-74. Spectra of 144.**

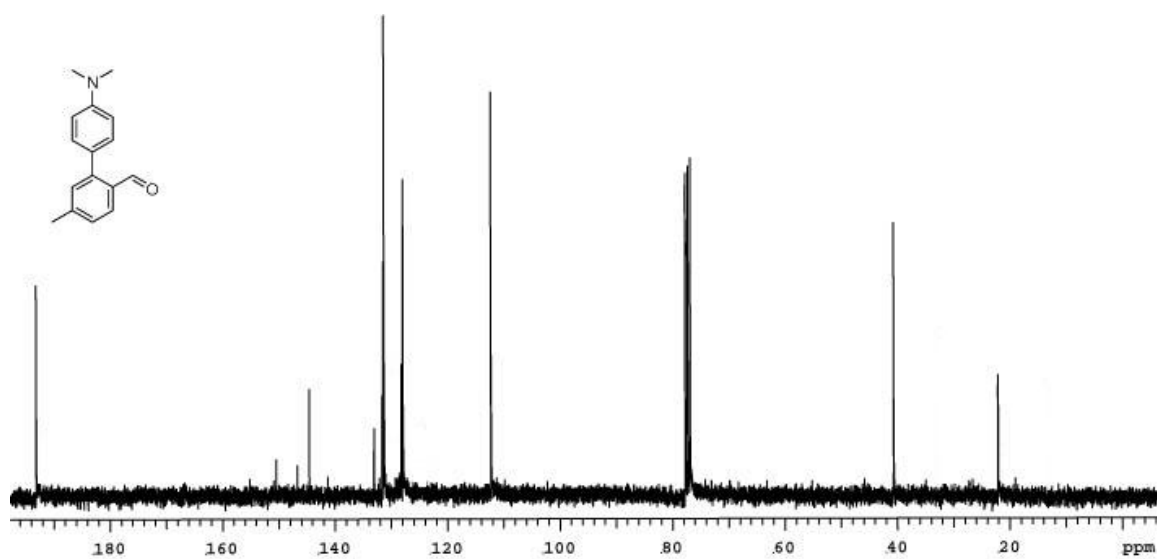
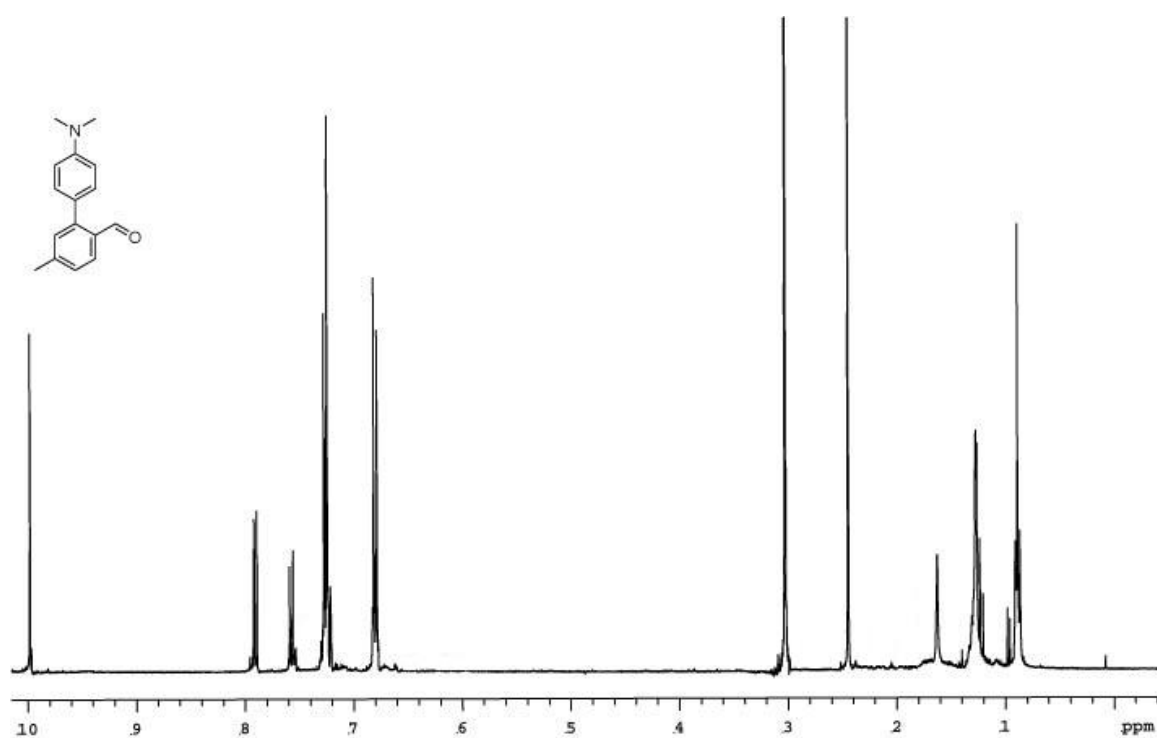


B-75. Spectra of 145.

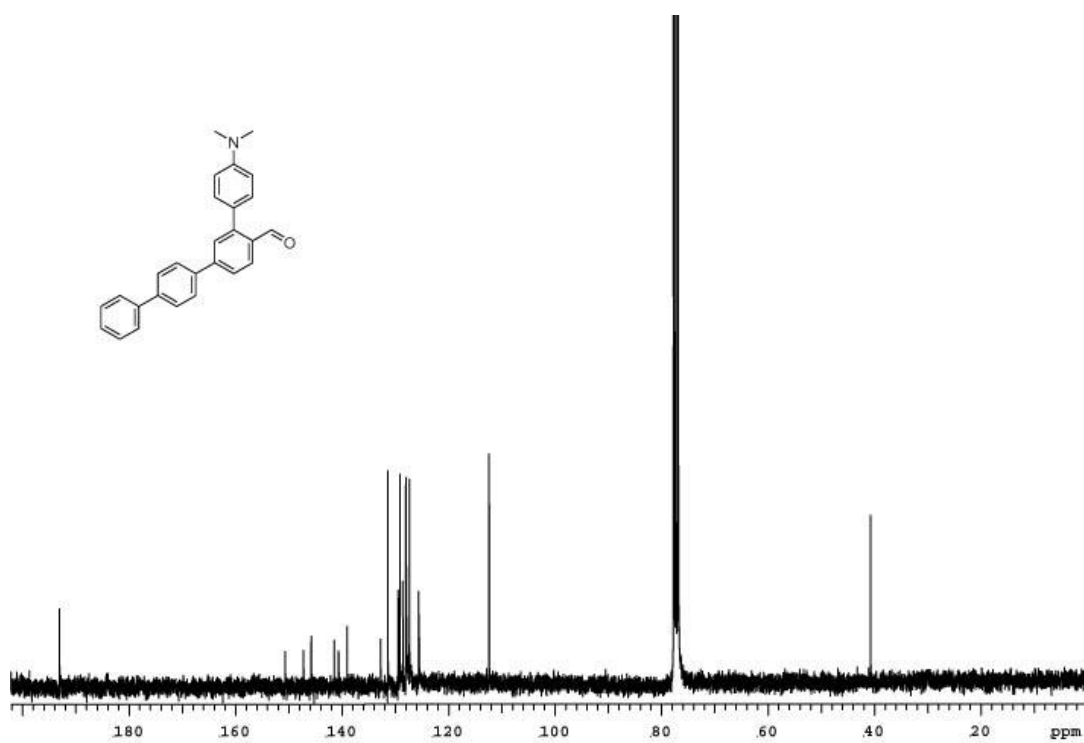
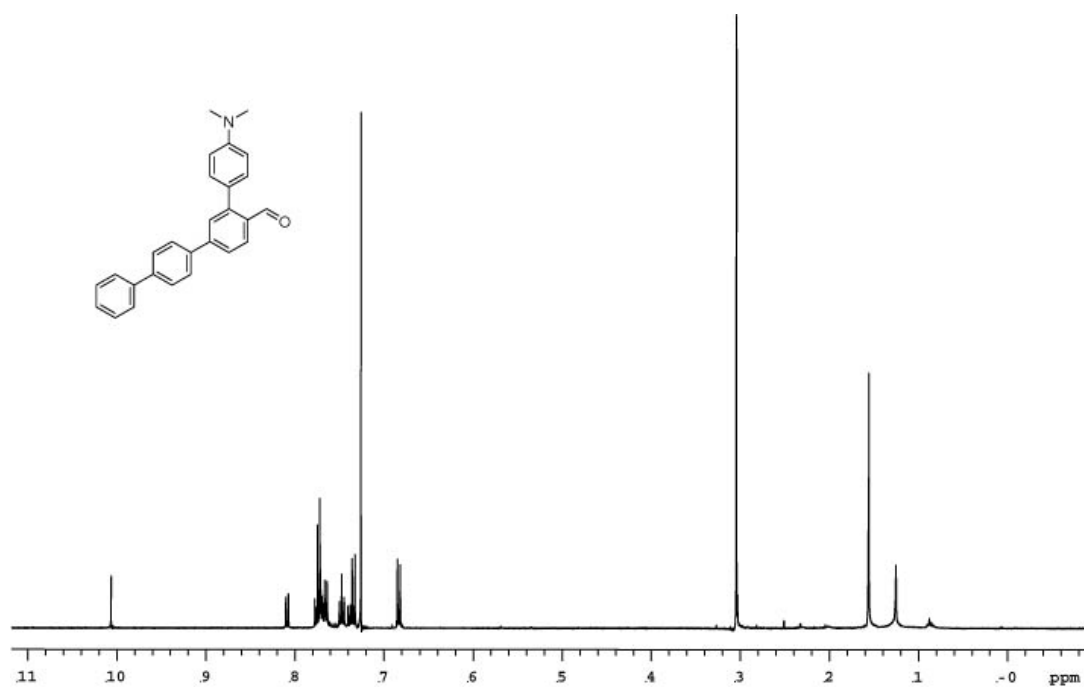




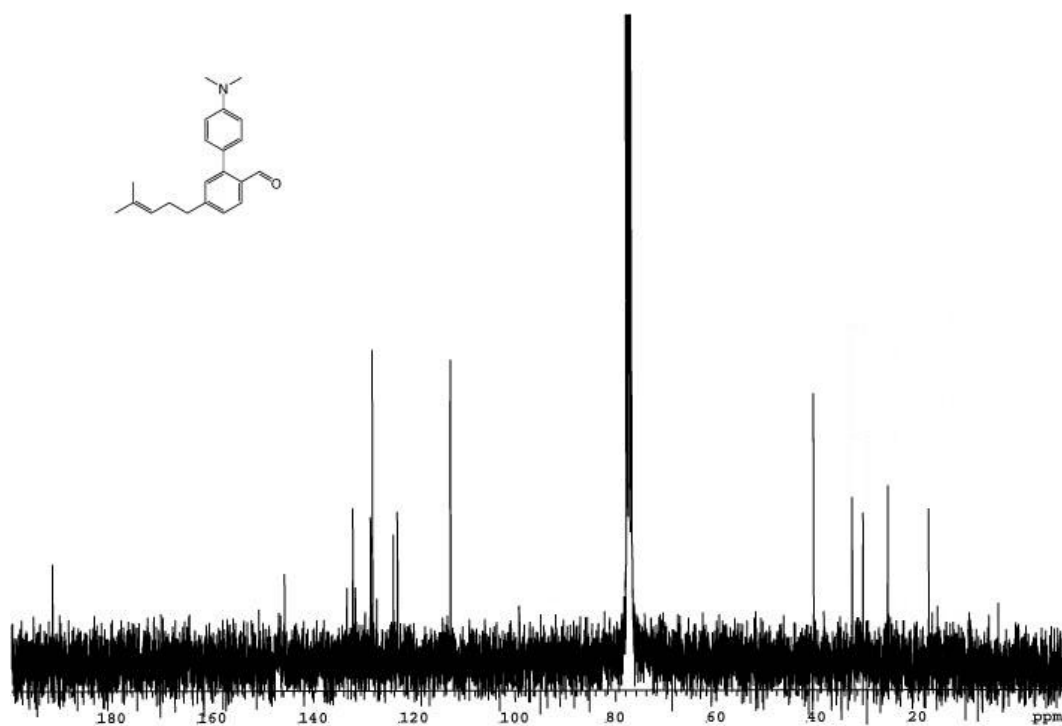
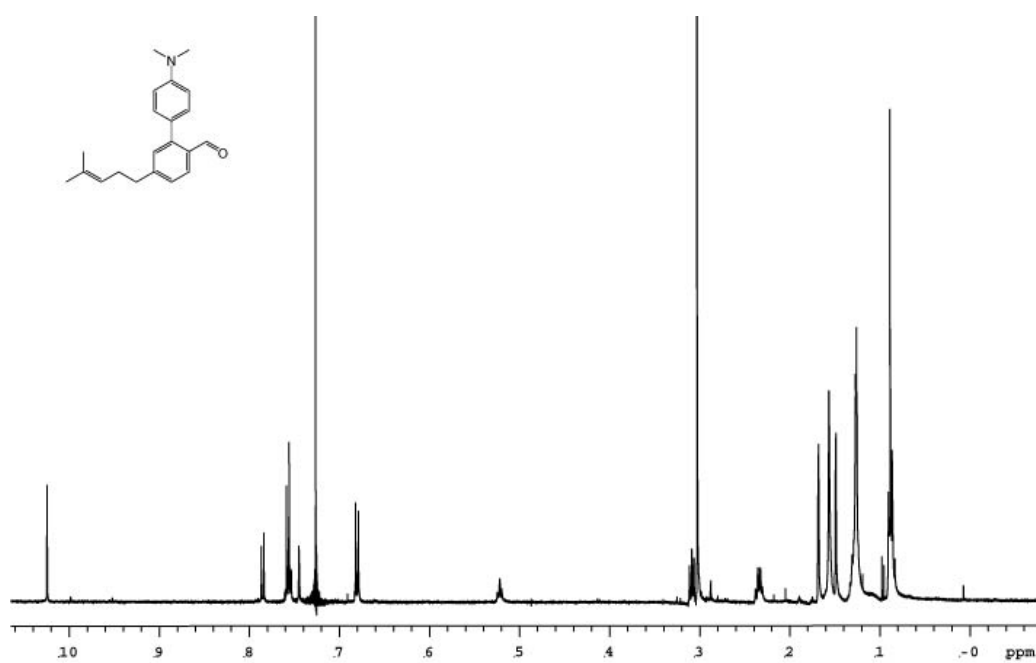
**B-76. Spectra of 146.**



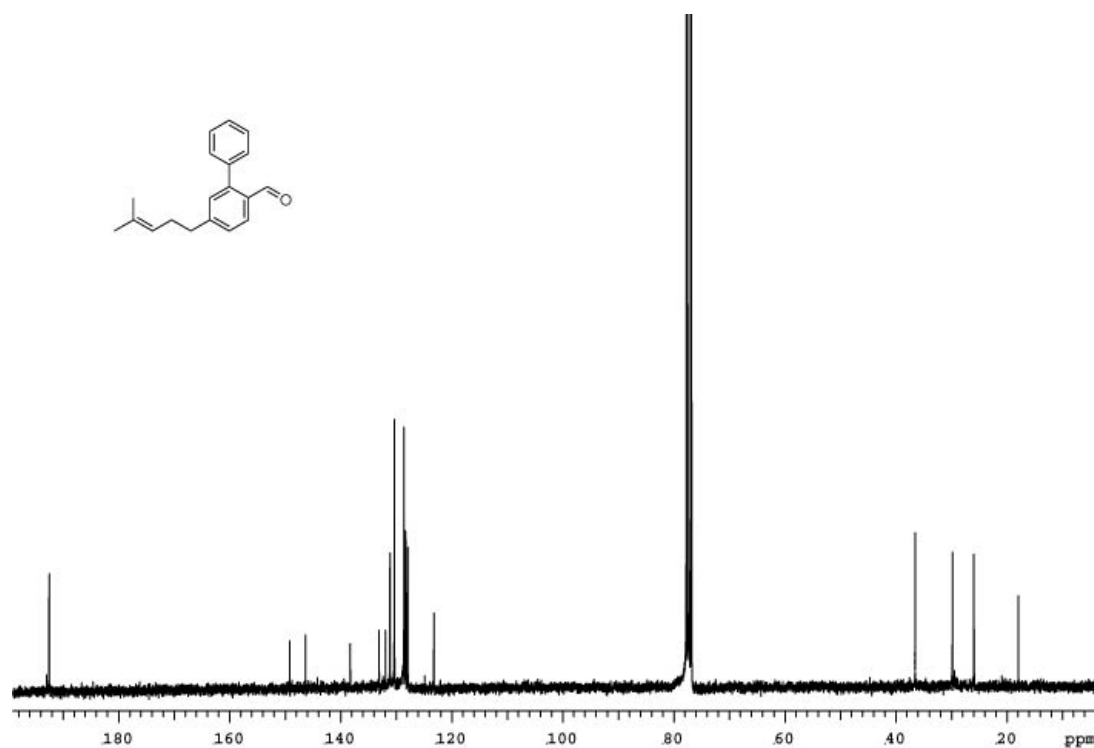
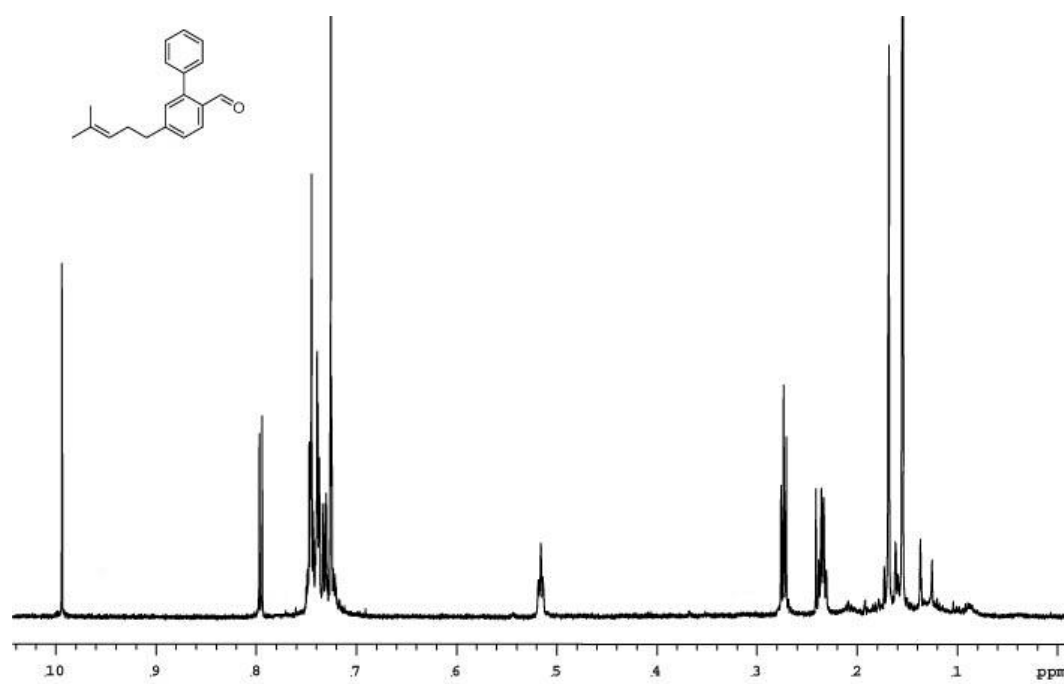
B-77. Spectra of 147.



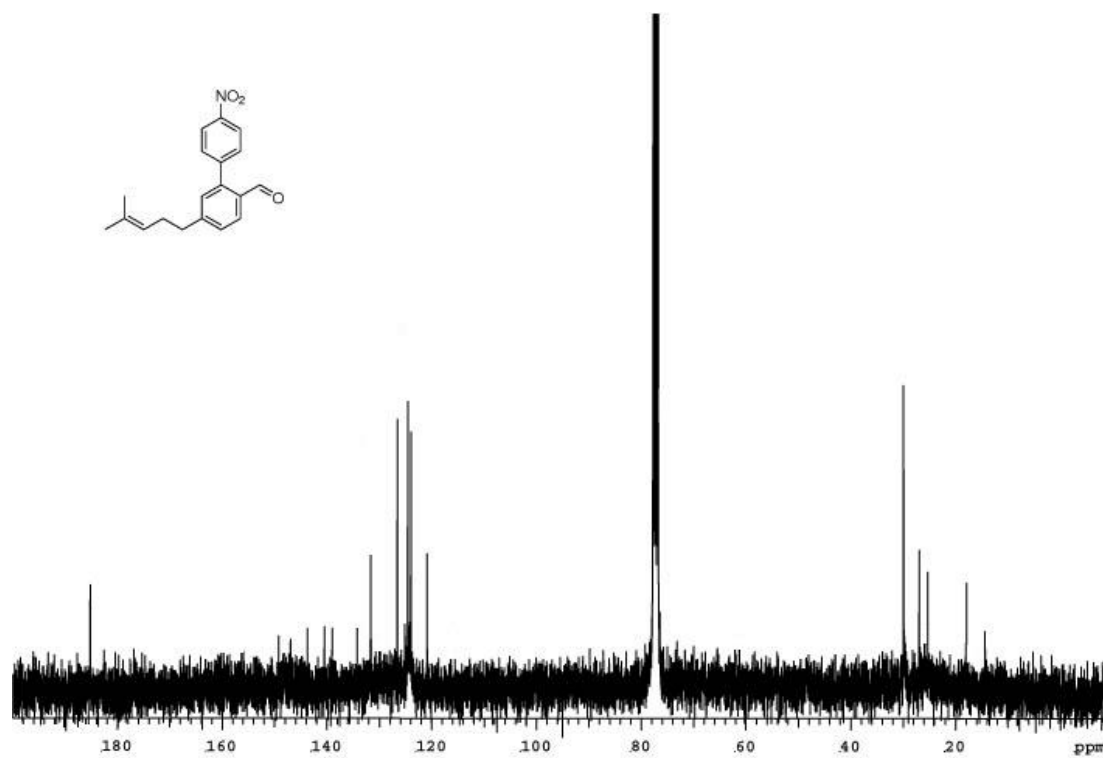
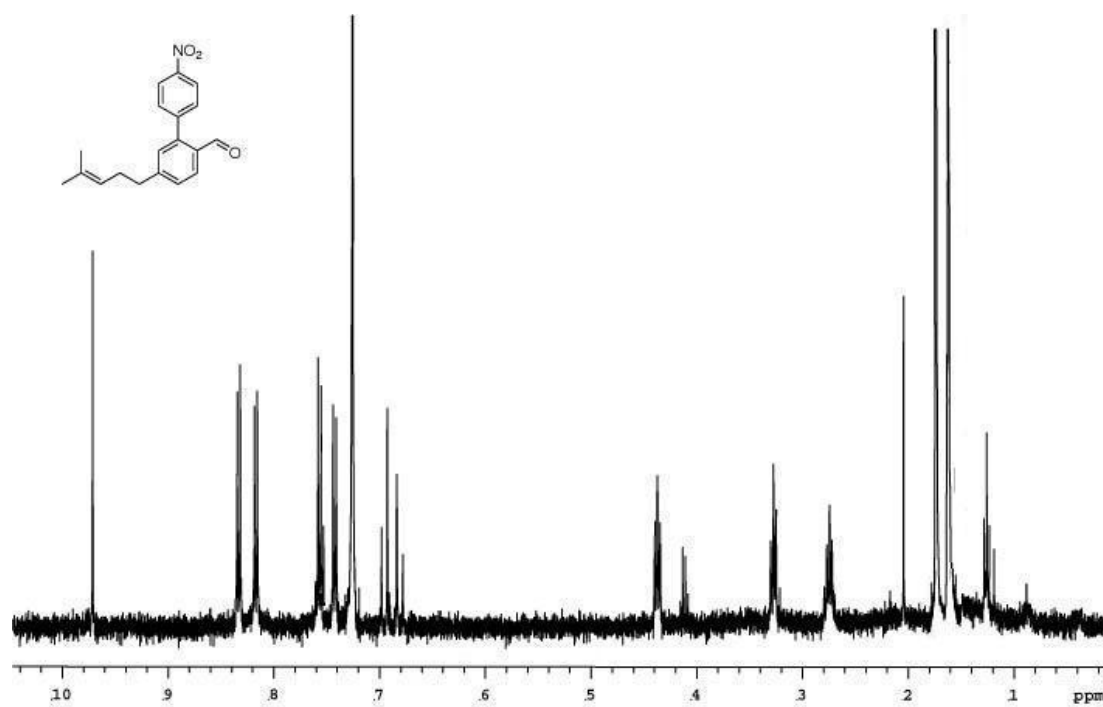
**B-78. Spectra of 148.**



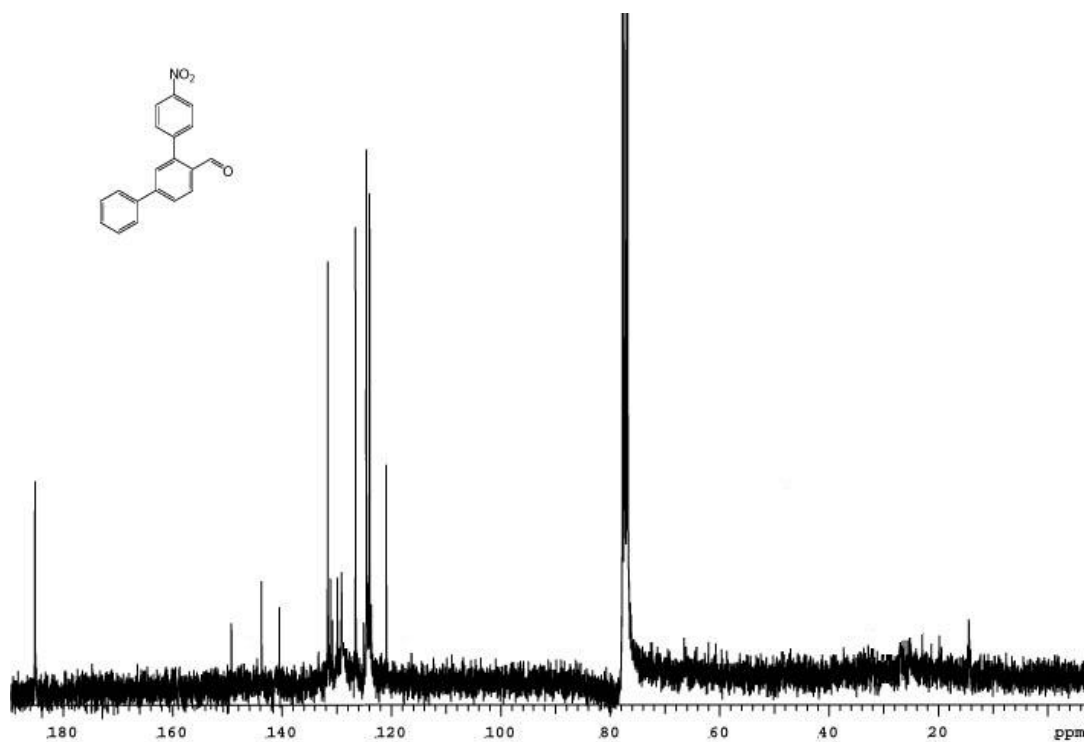
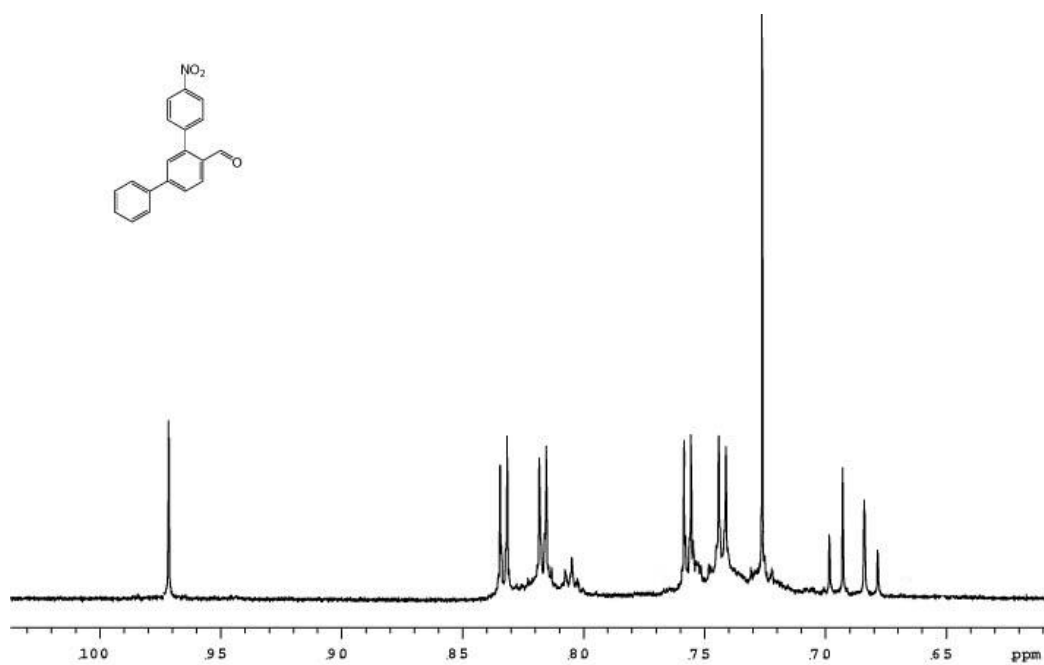
**B-79. Spectra of 149.**



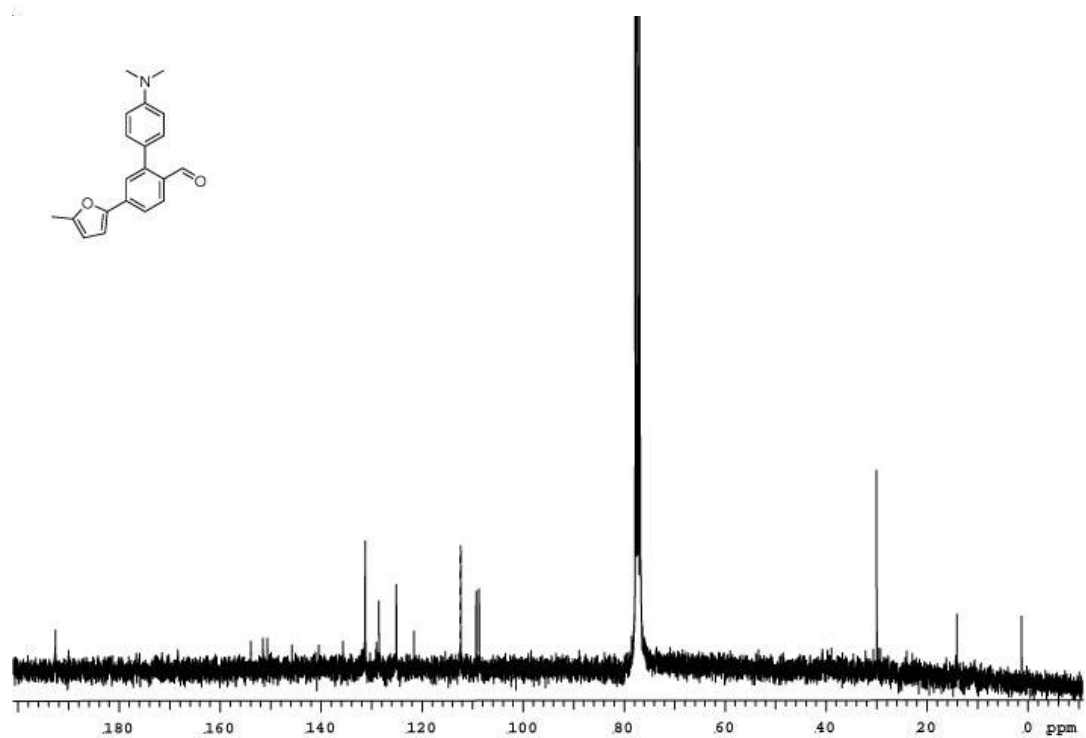
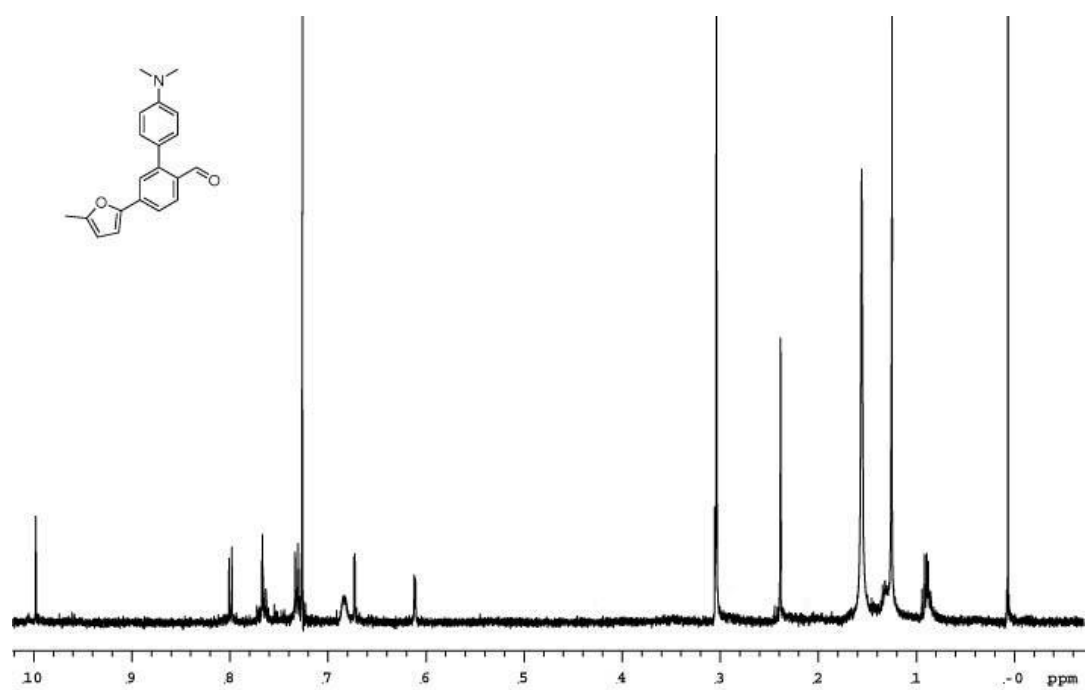
**B-80. Spectra of 150.**



B-81. Spectra of 151.

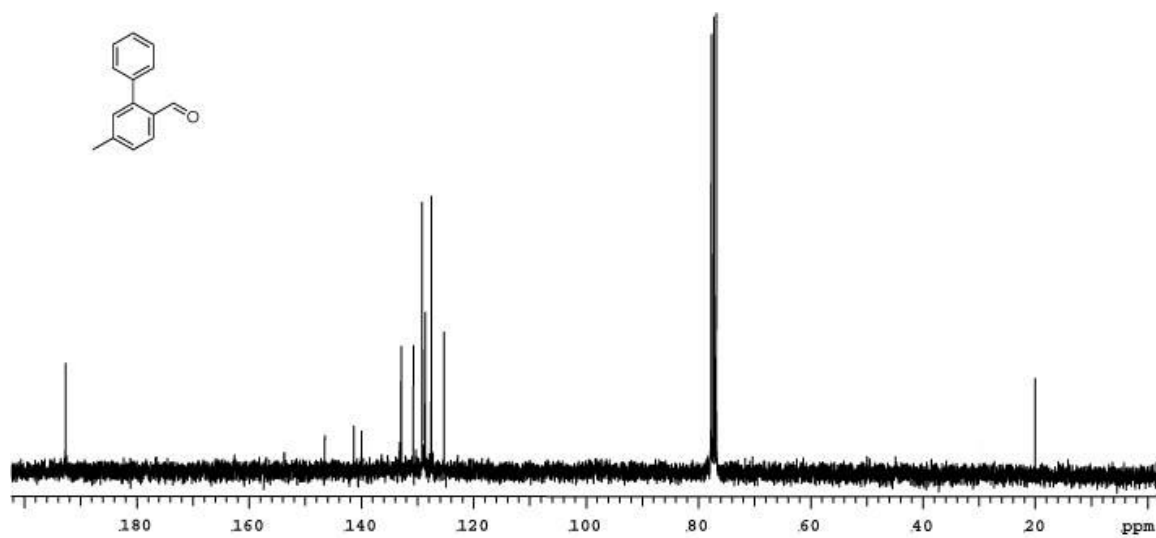
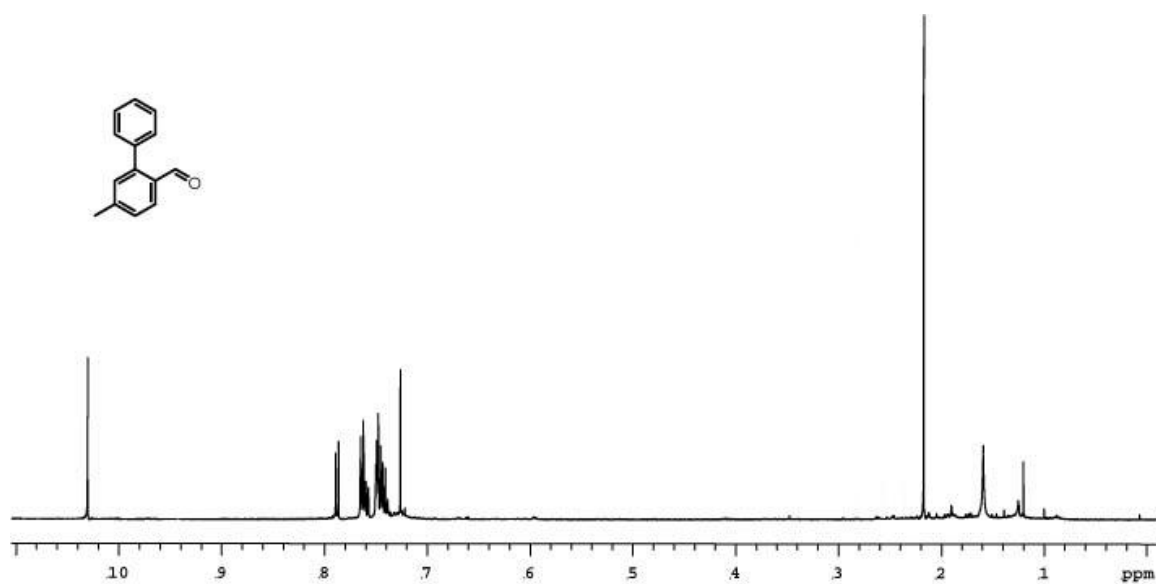


B-82. Spectra of 152.

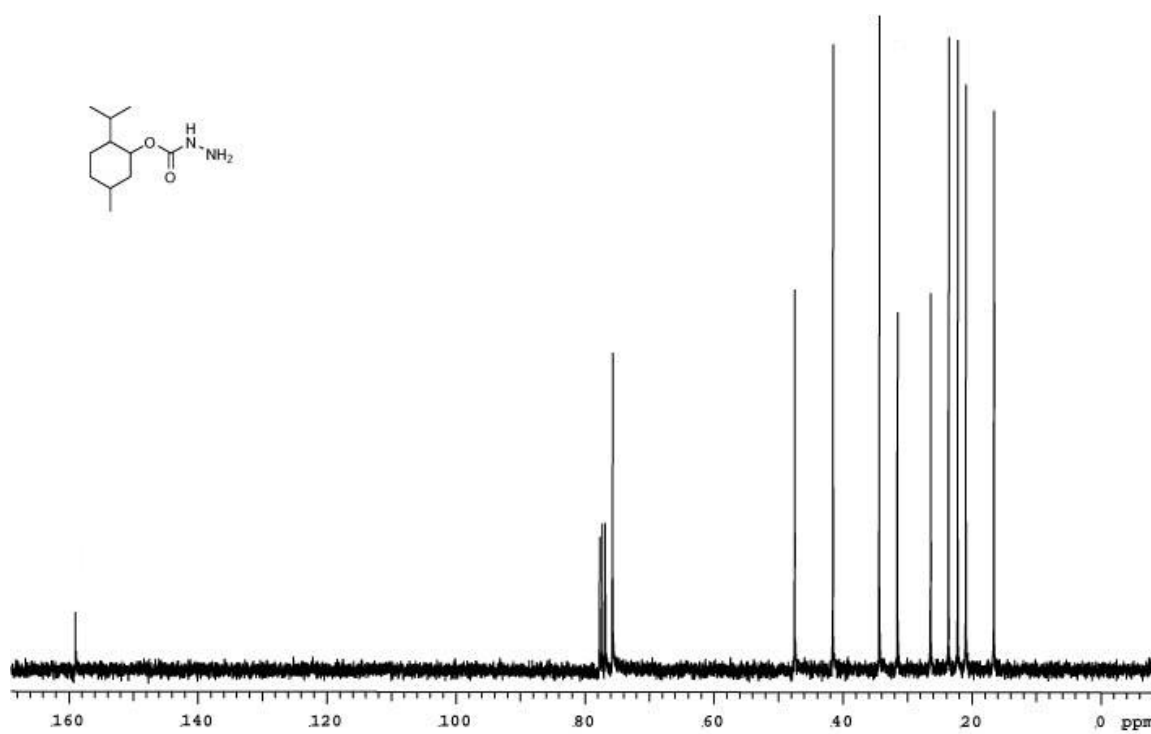
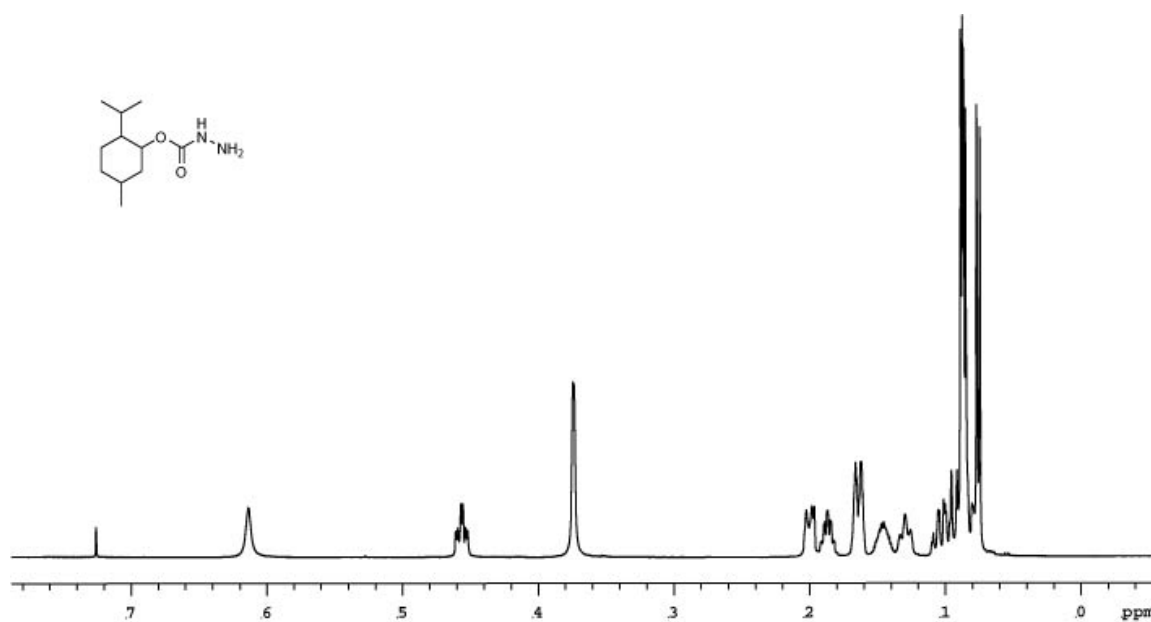


**B-83. Spectra of 153.**



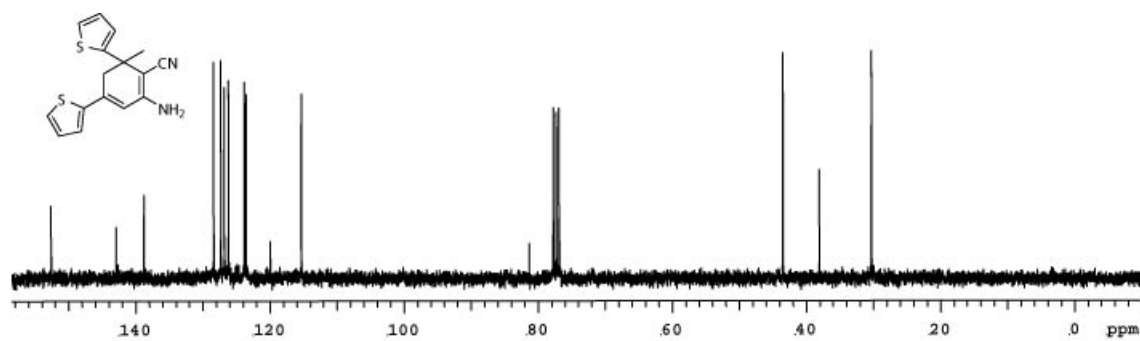
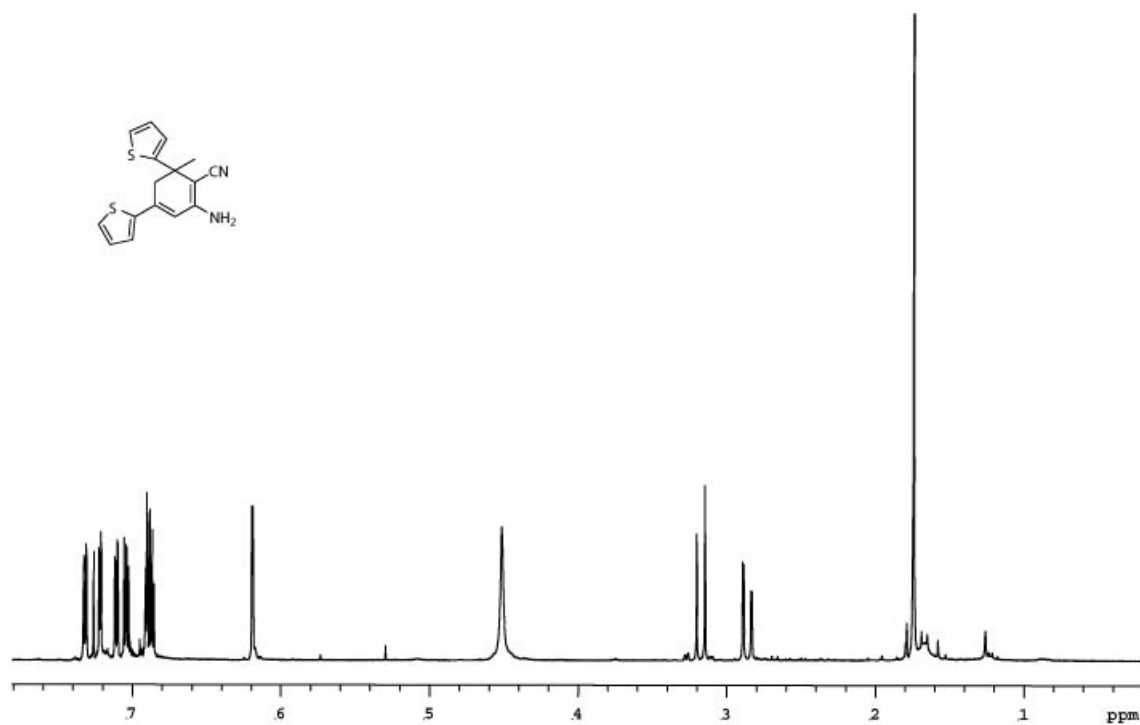


**B-84. Spectra of 154.**

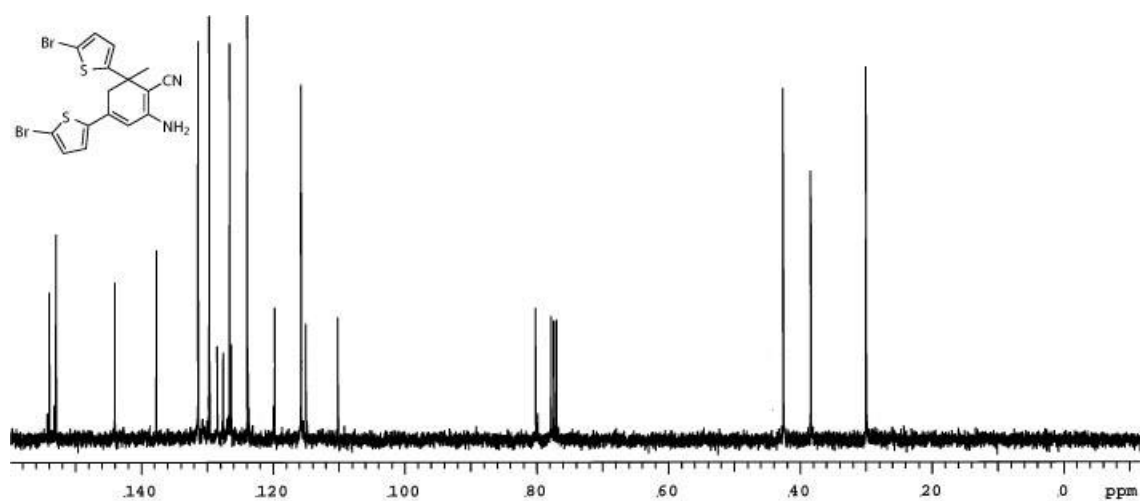
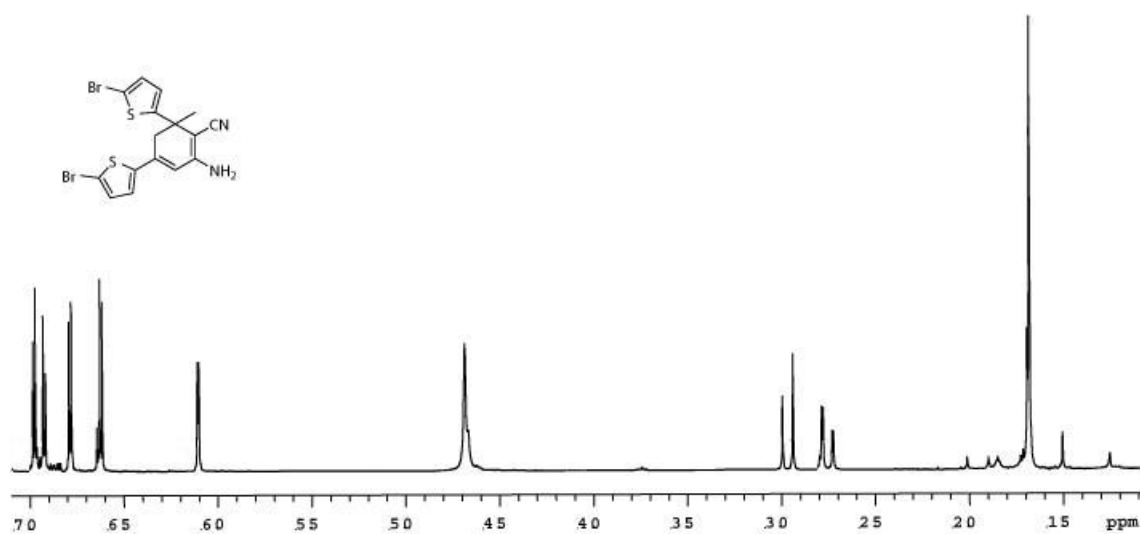


**B-85. Spectra of 81.**

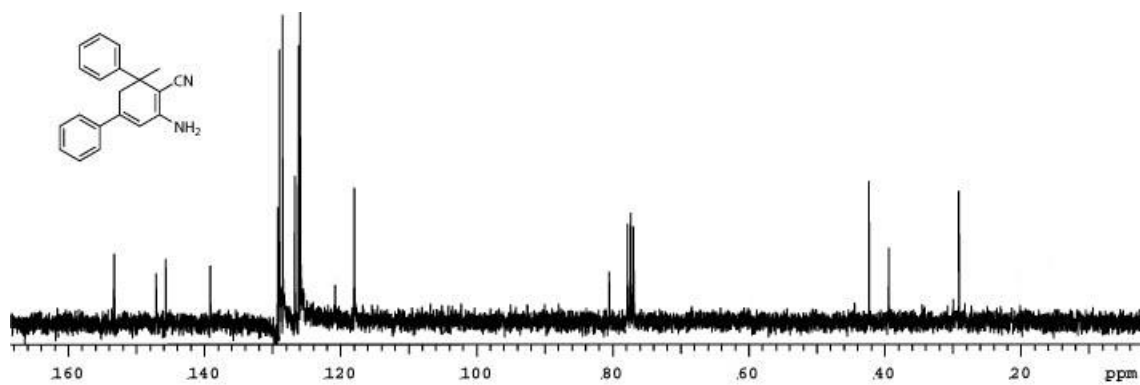
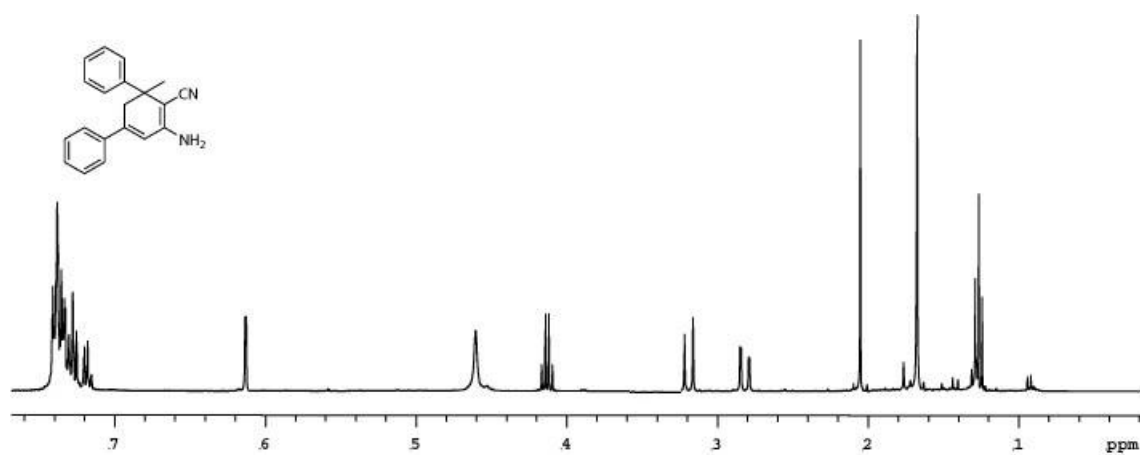
## APPENDIX C



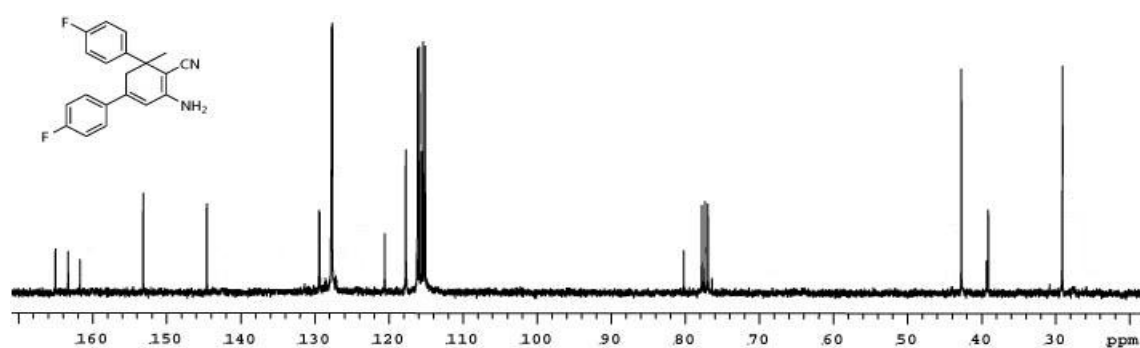
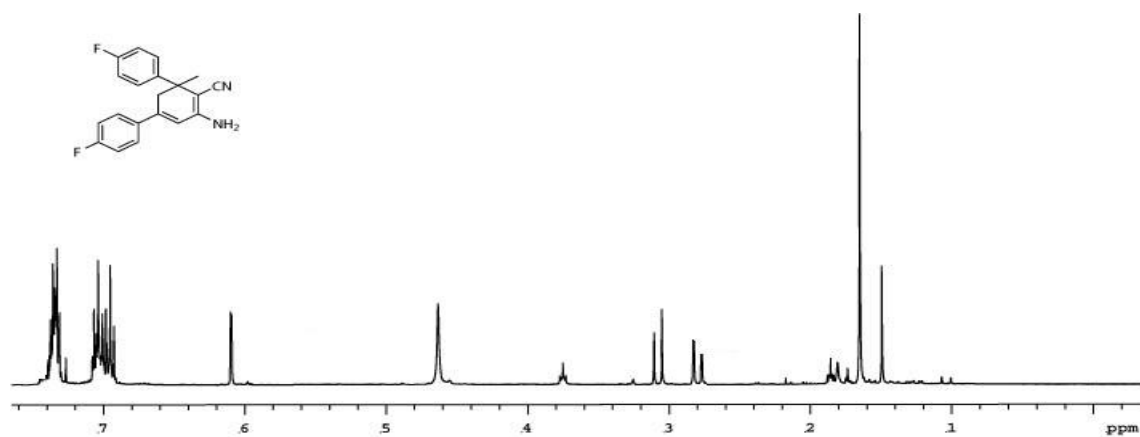
C-1. Spectra of 166.



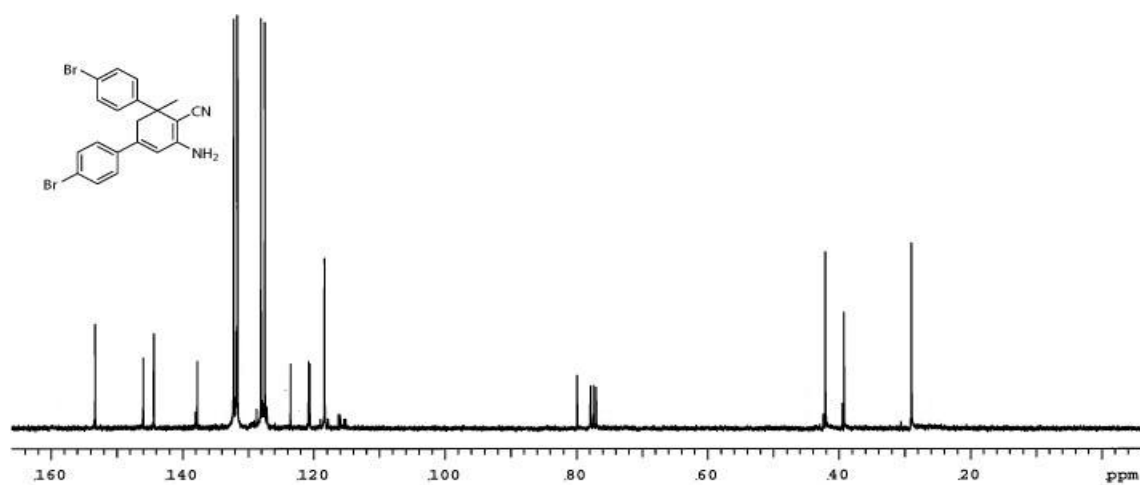
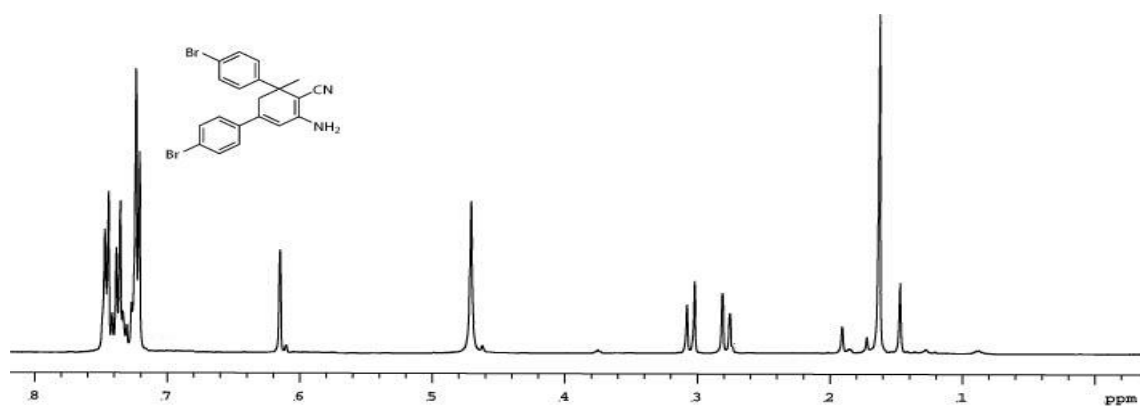
C-2. Spectra of 167.



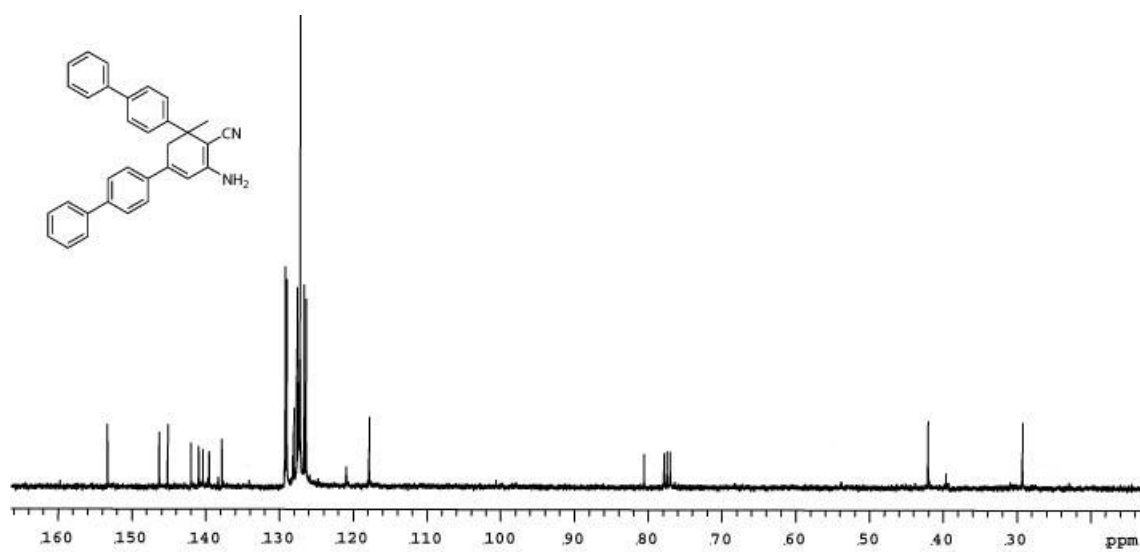
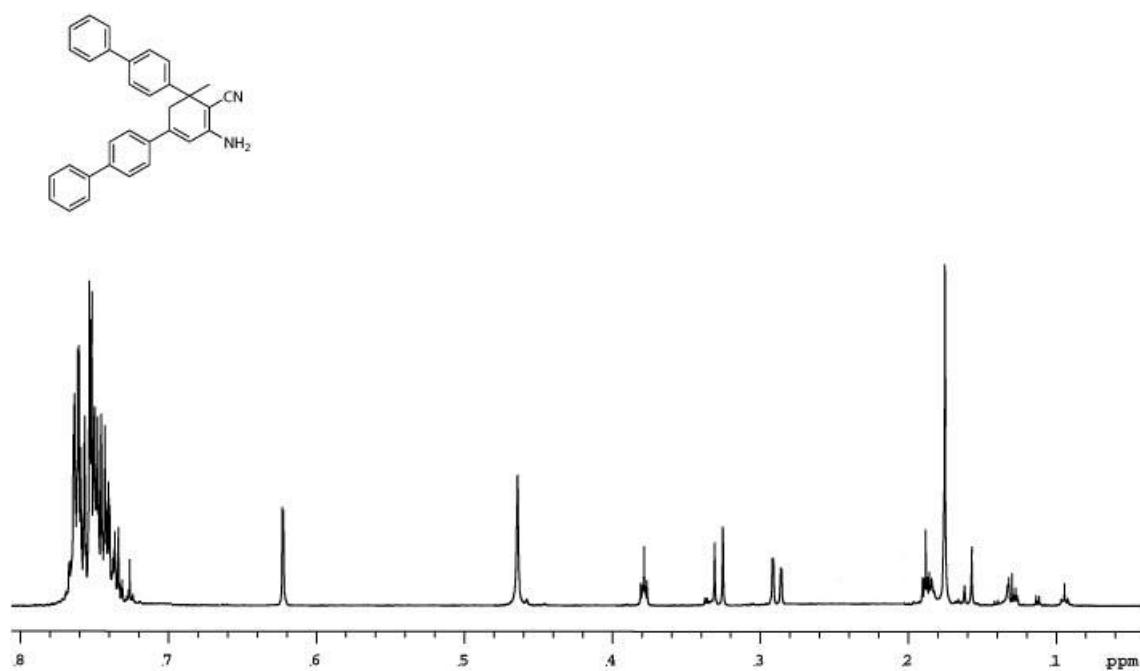
### C-3. Spectra of 168.



C-4. Spectra of 169.

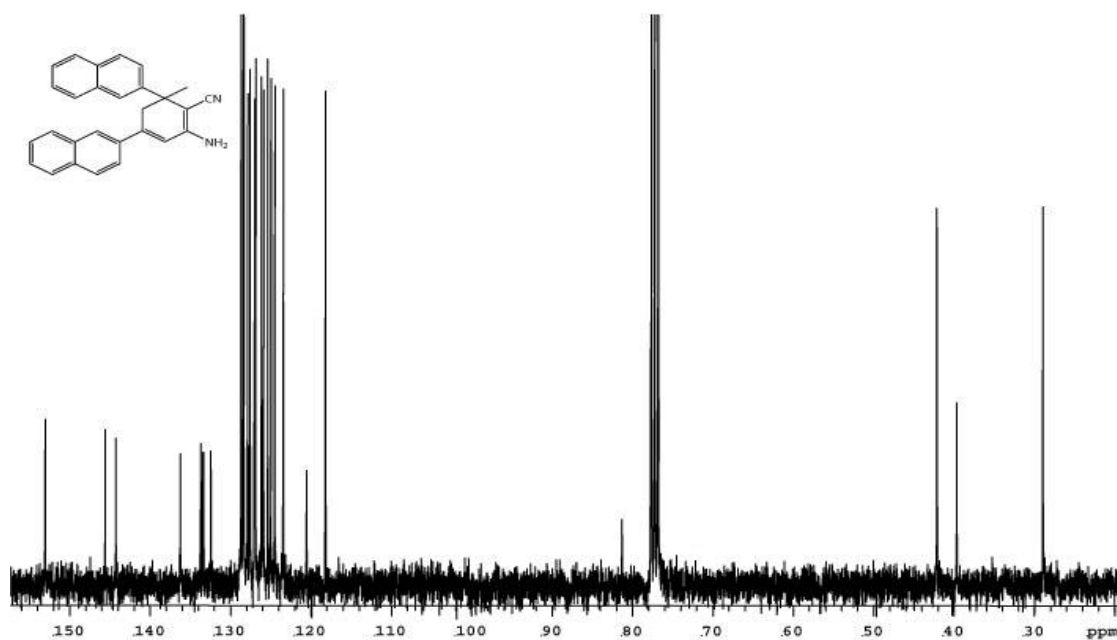
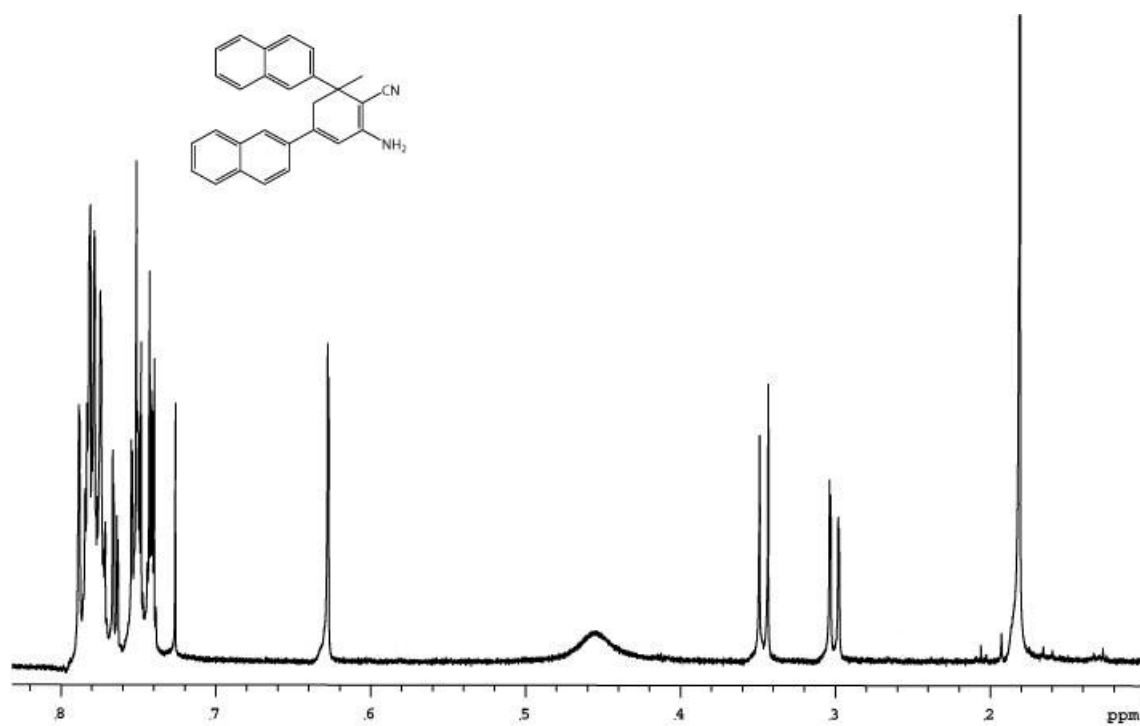


C-5. Spectra of 170.

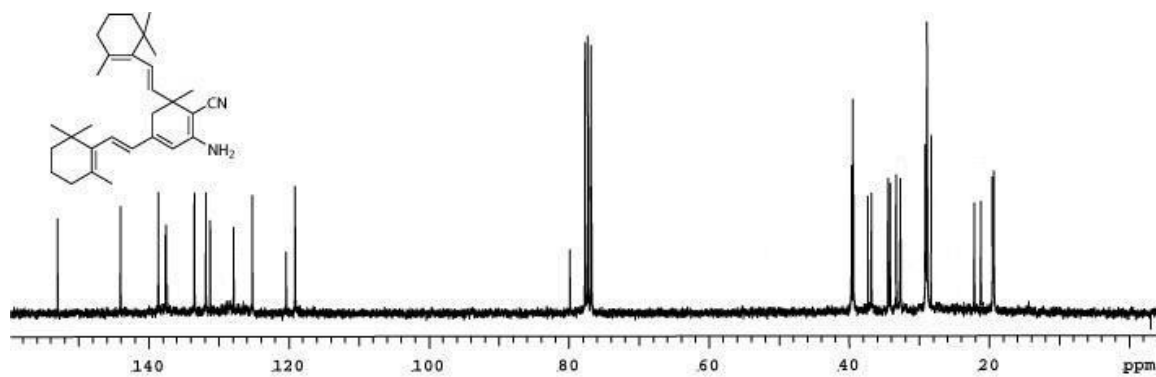
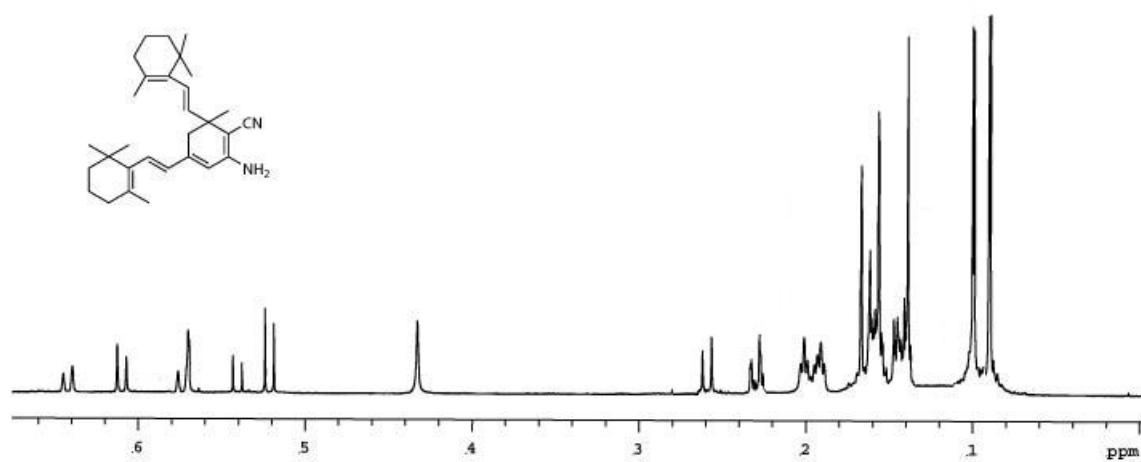


C-6. Spectra of 171.

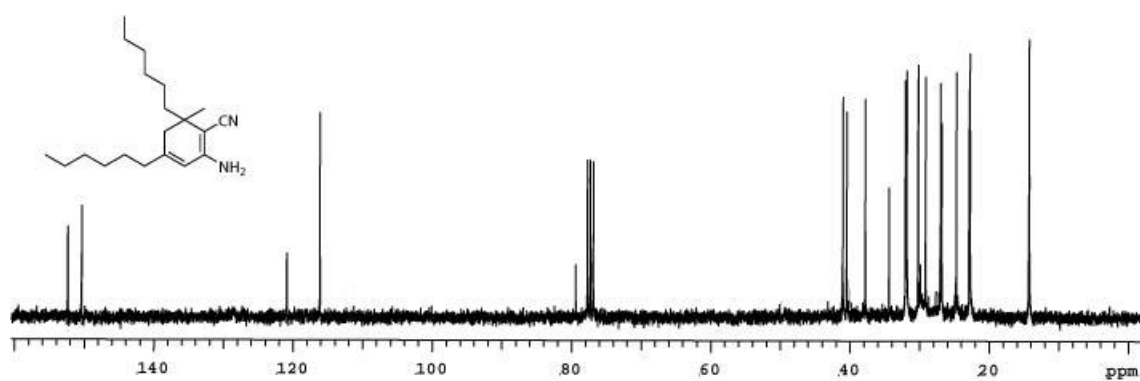
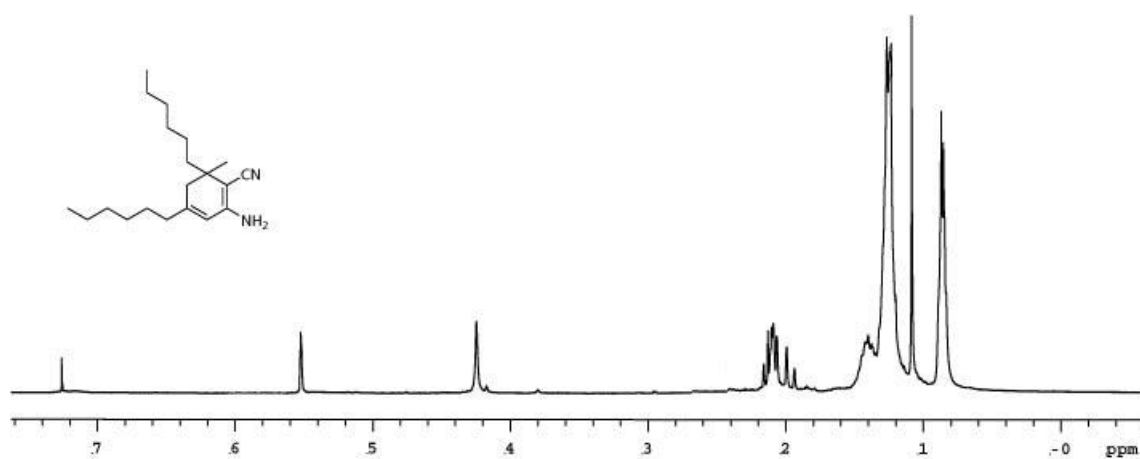




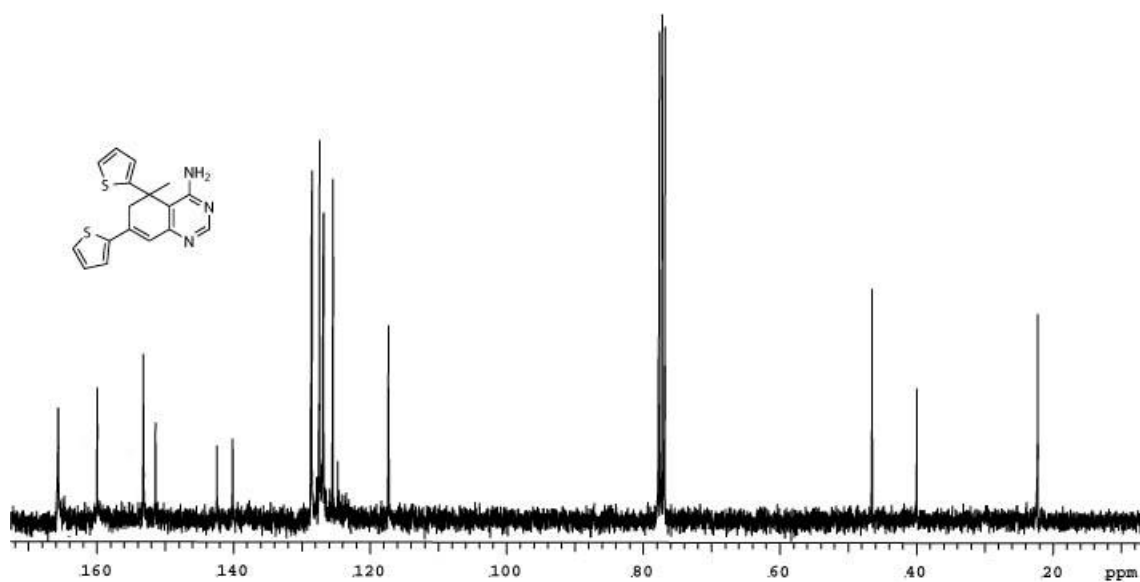
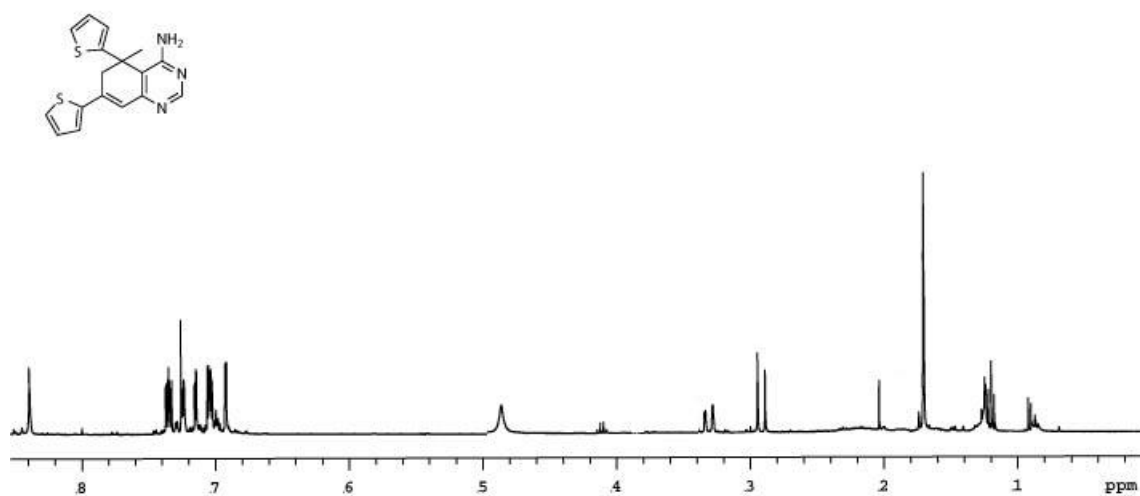
C-7. Spectra of 172.



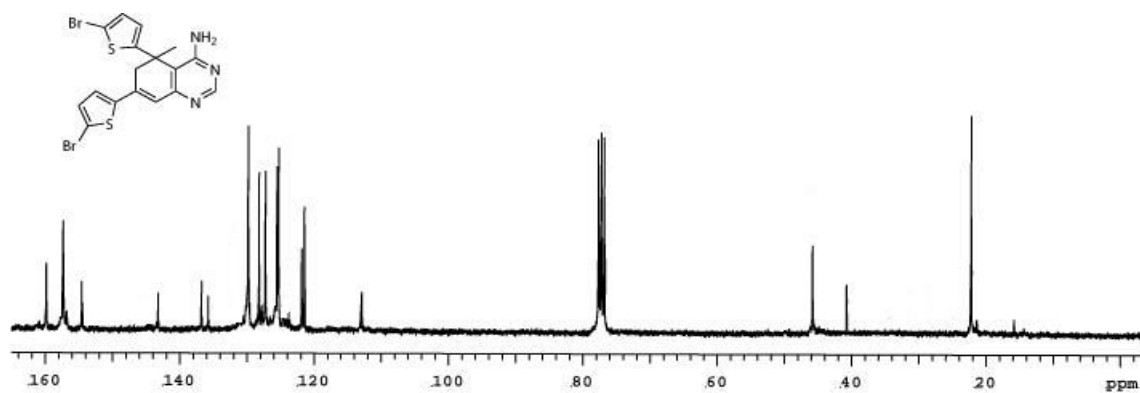
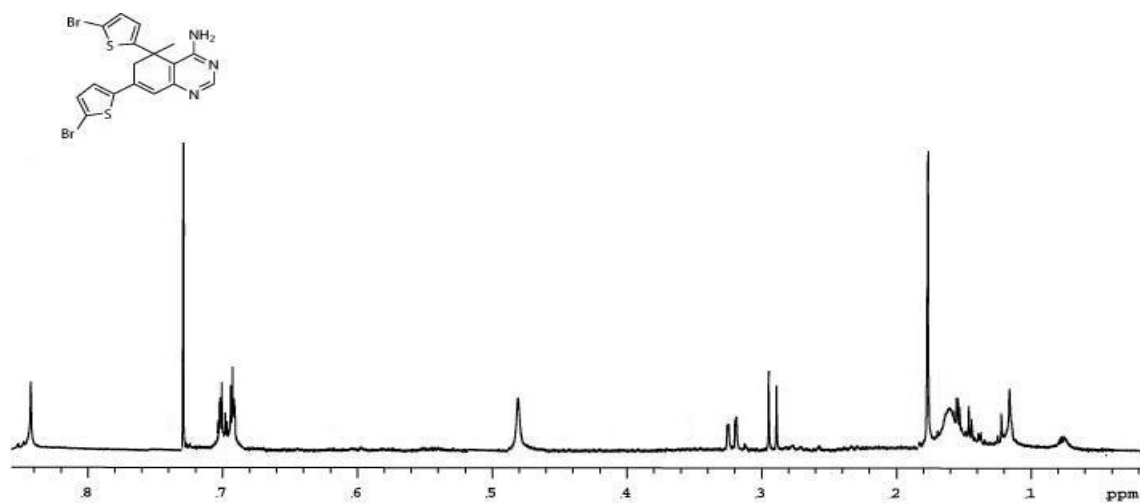
**C-8. Spectra of 173.**



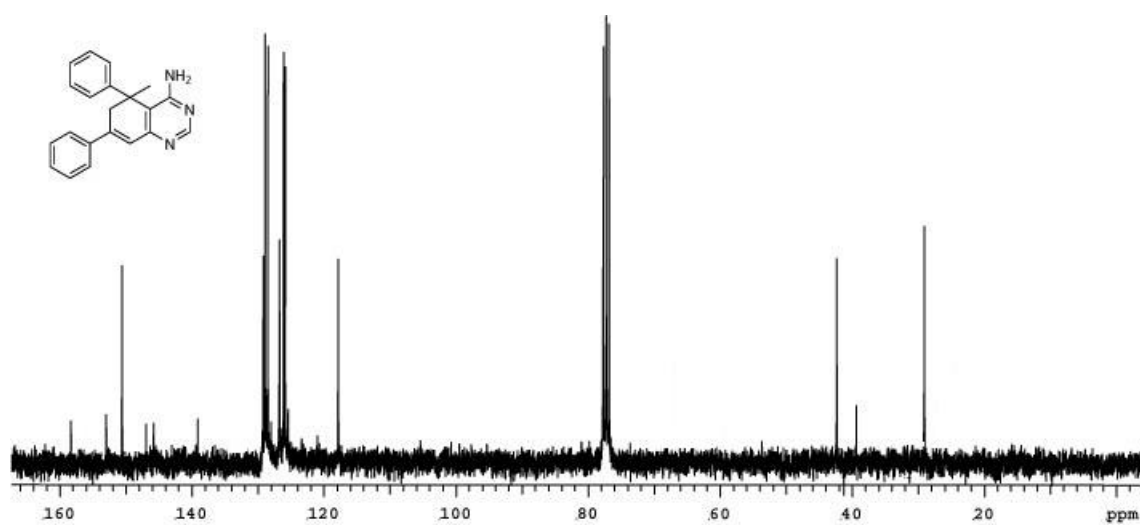
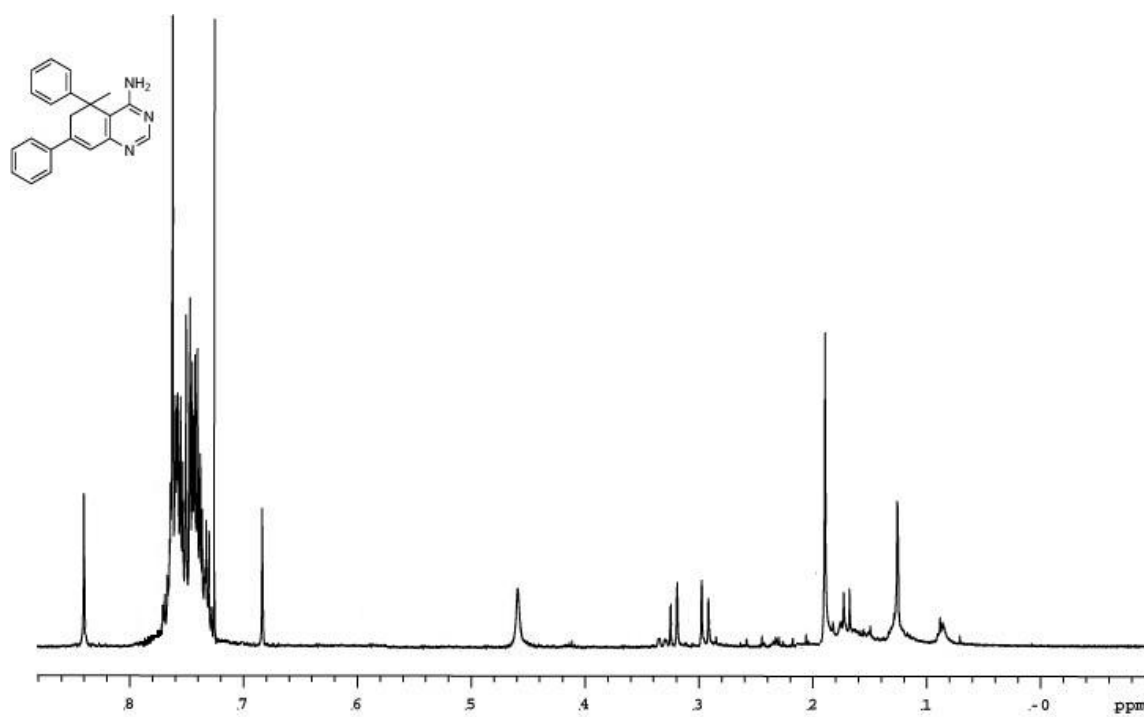
C-9. Spectra of 174.



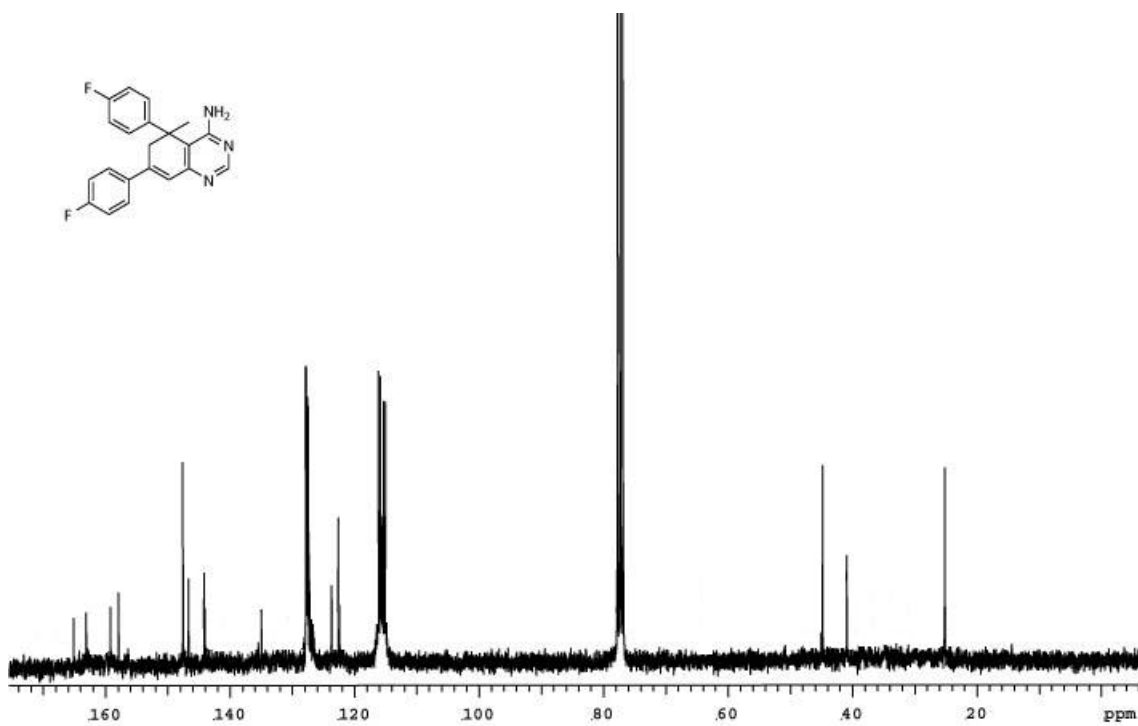
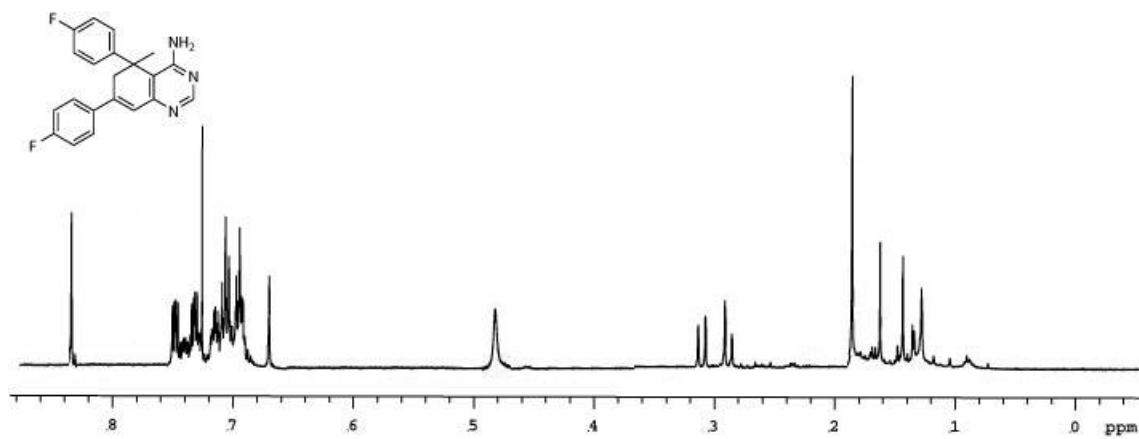
**C-10. Spectra of 175.**



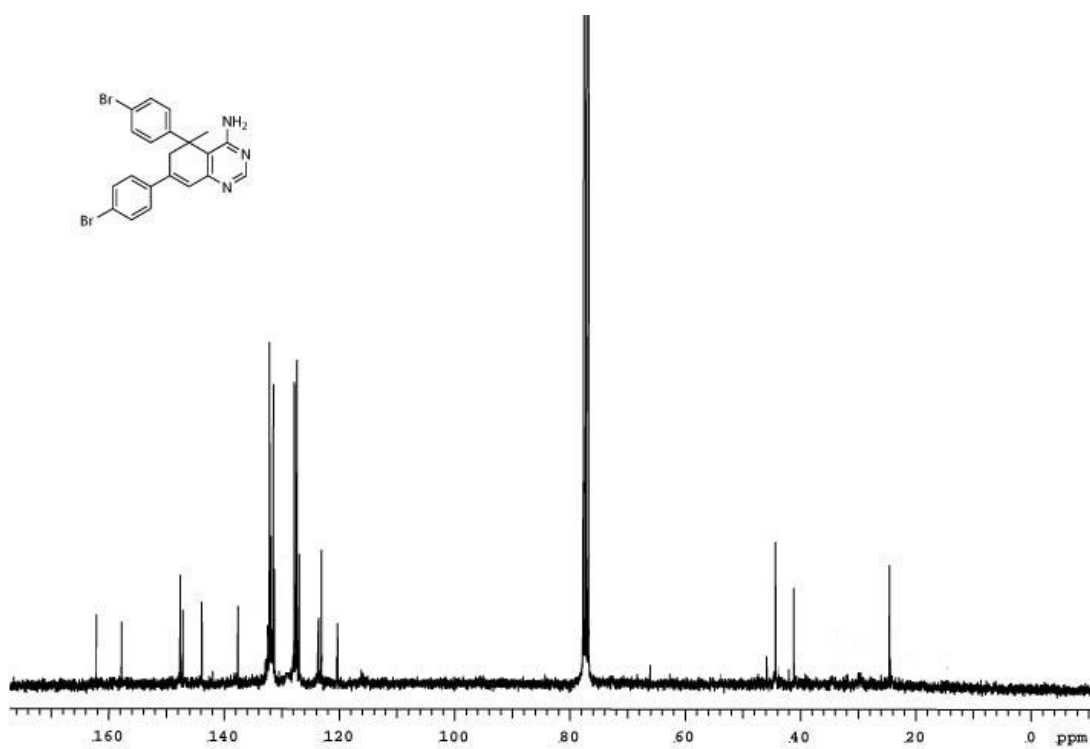
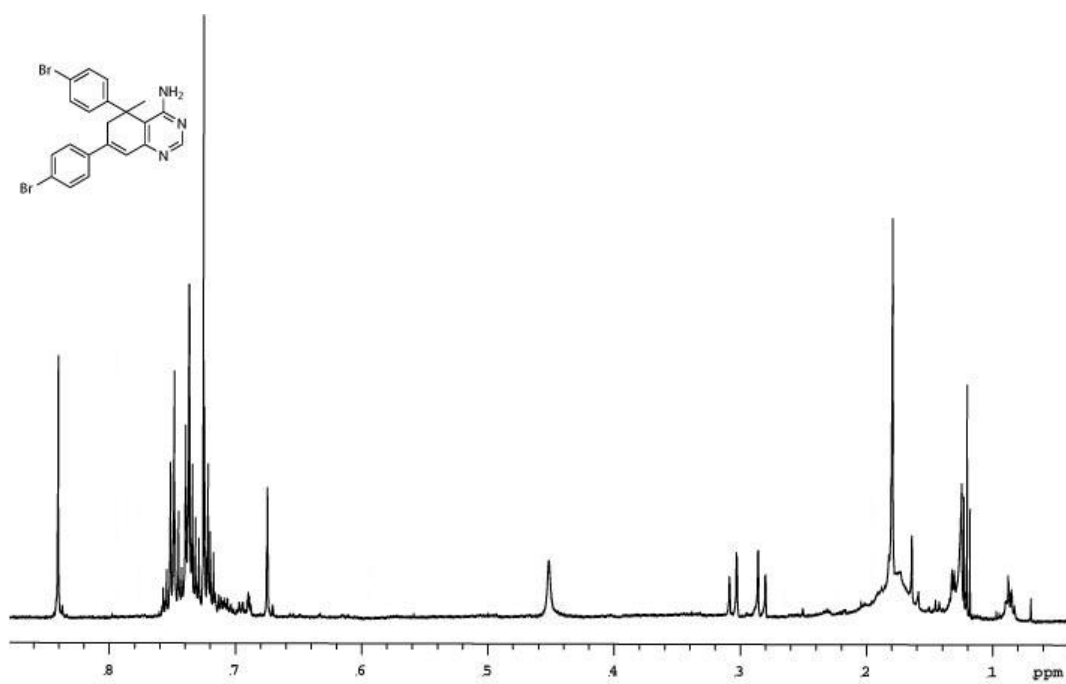
C-11. Spectra of 176.



C-12. Spectra of 177.

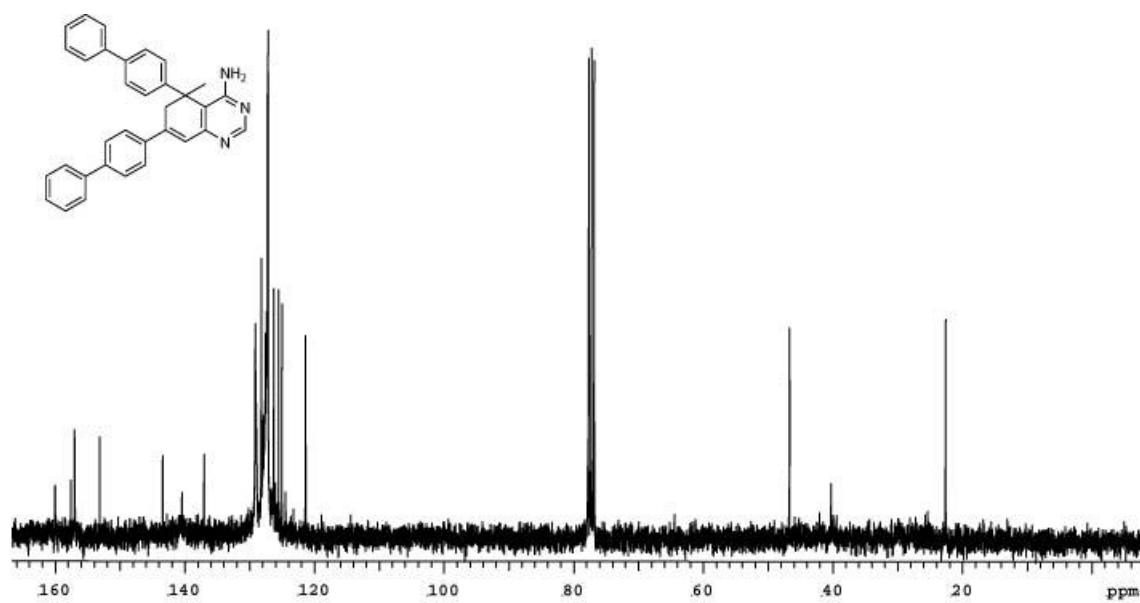
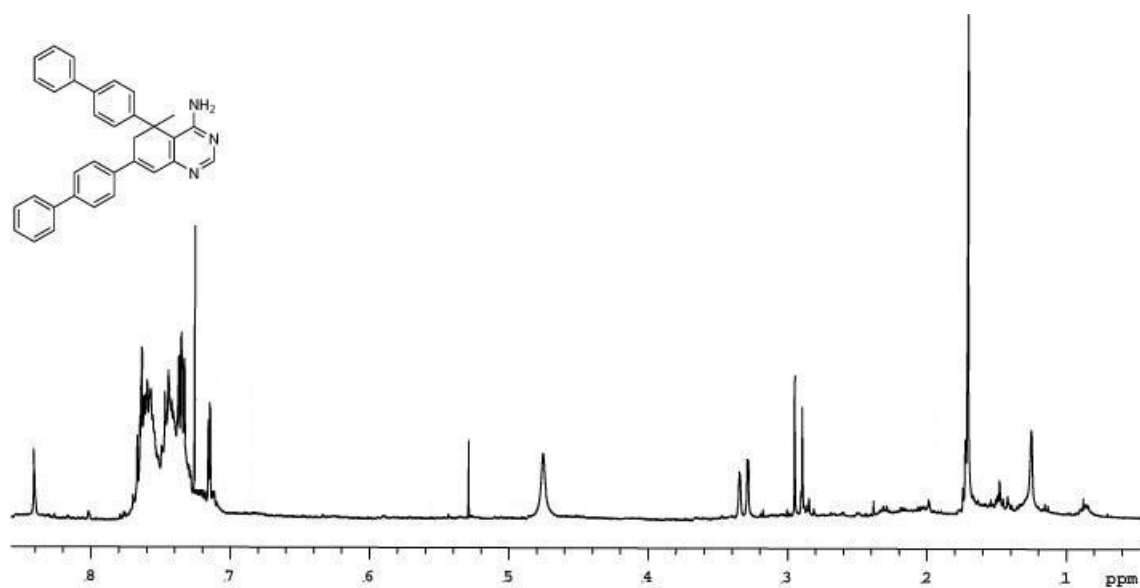


C-13. Spectra of 178.

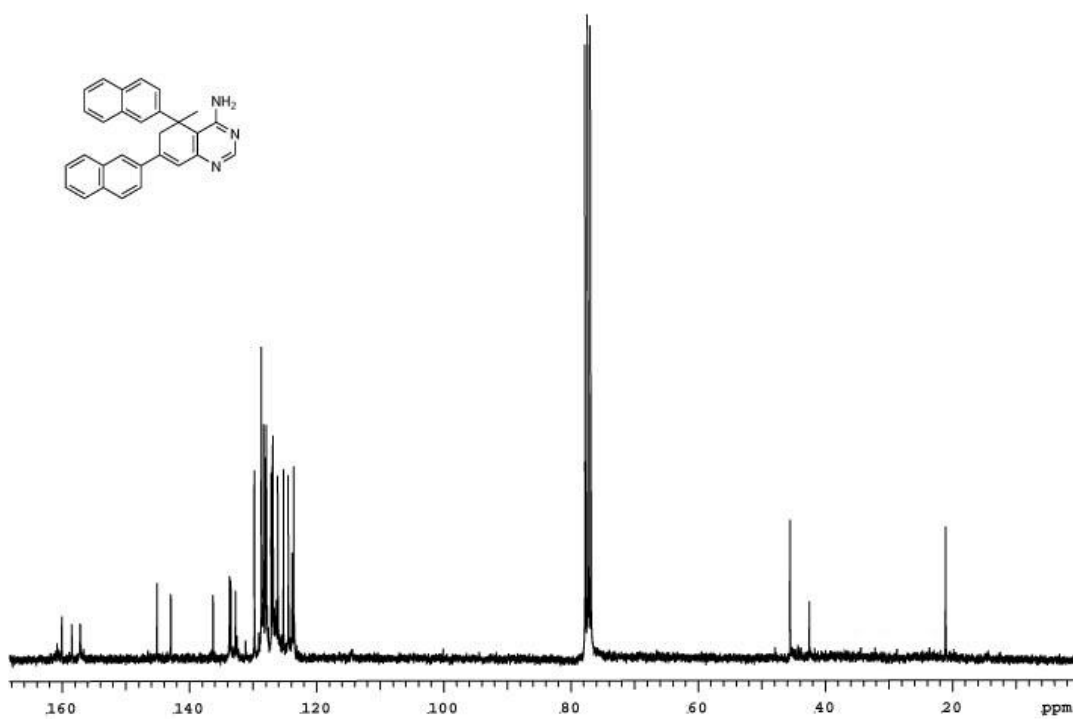
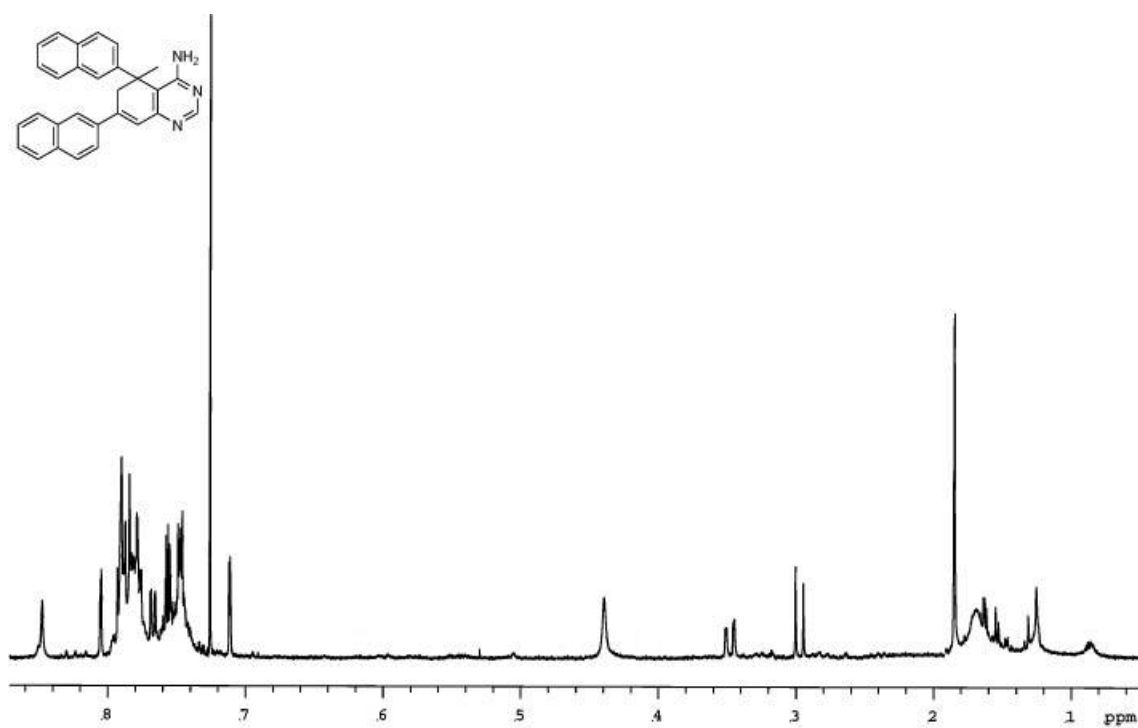


C-14. Spectra of 179.

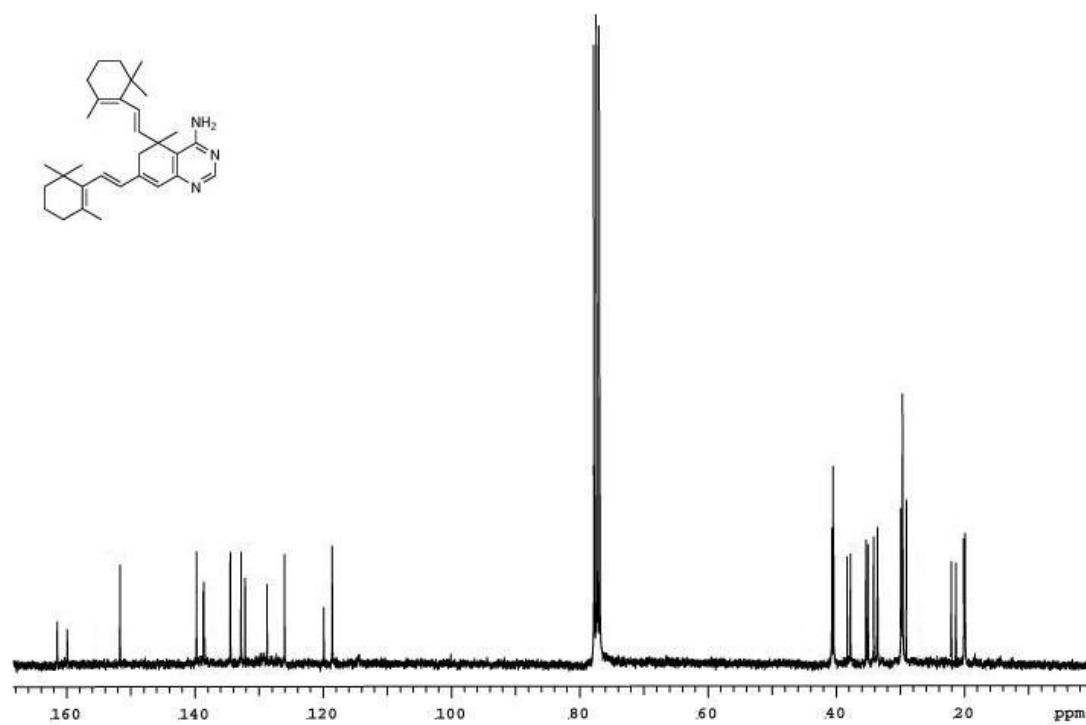
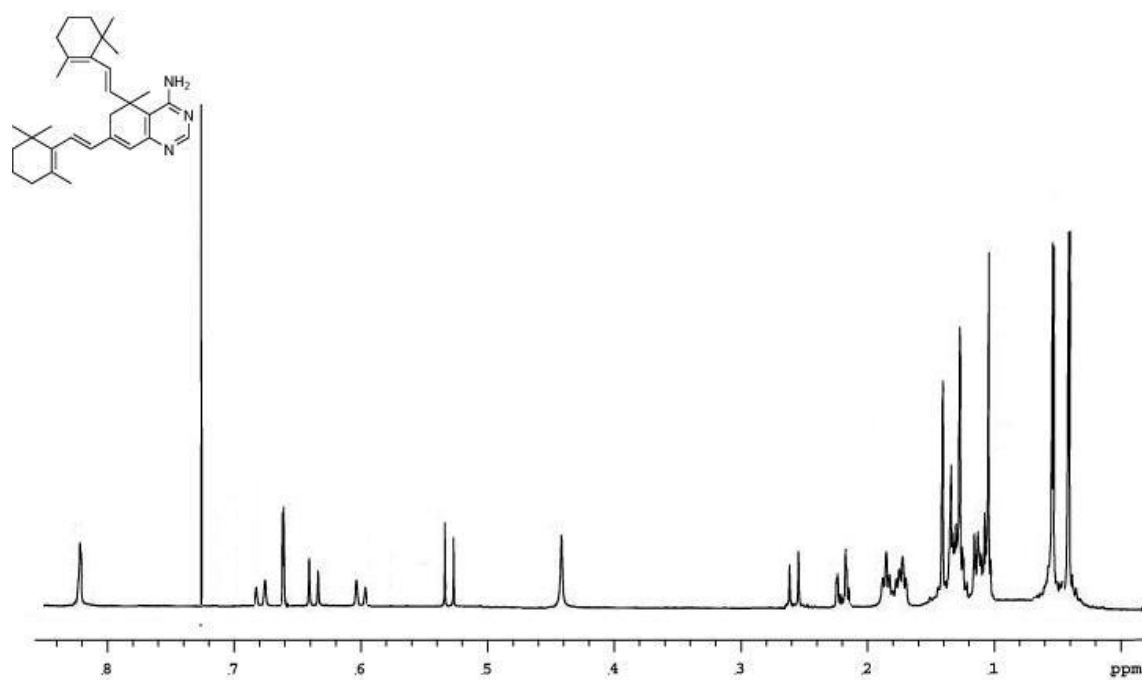




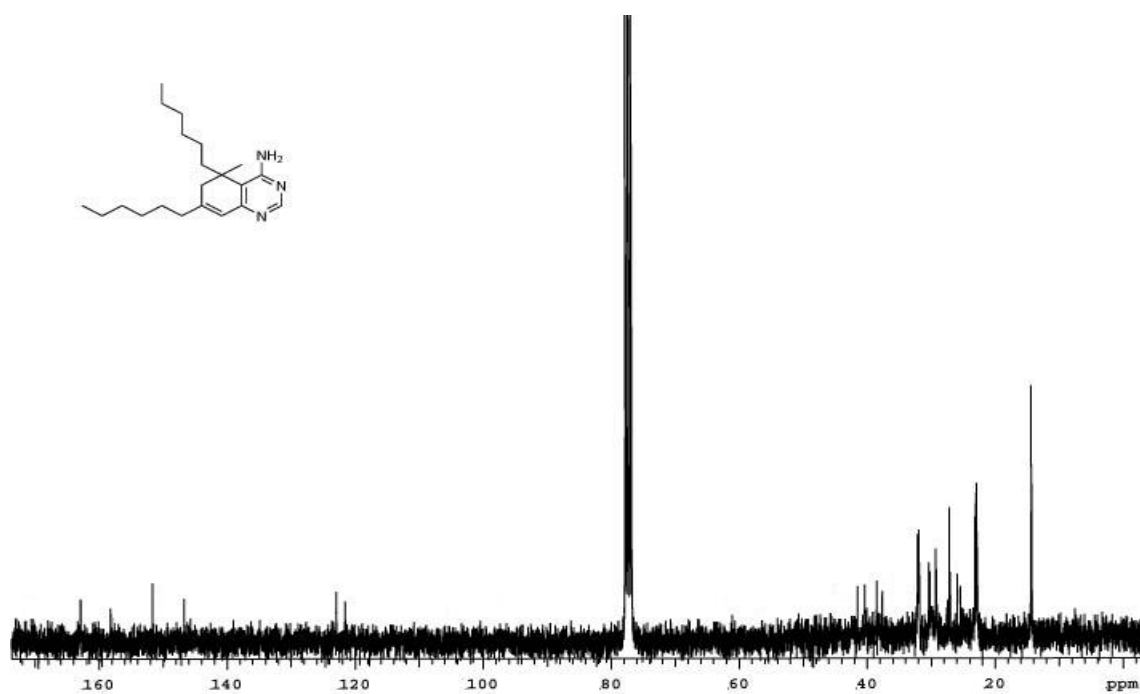
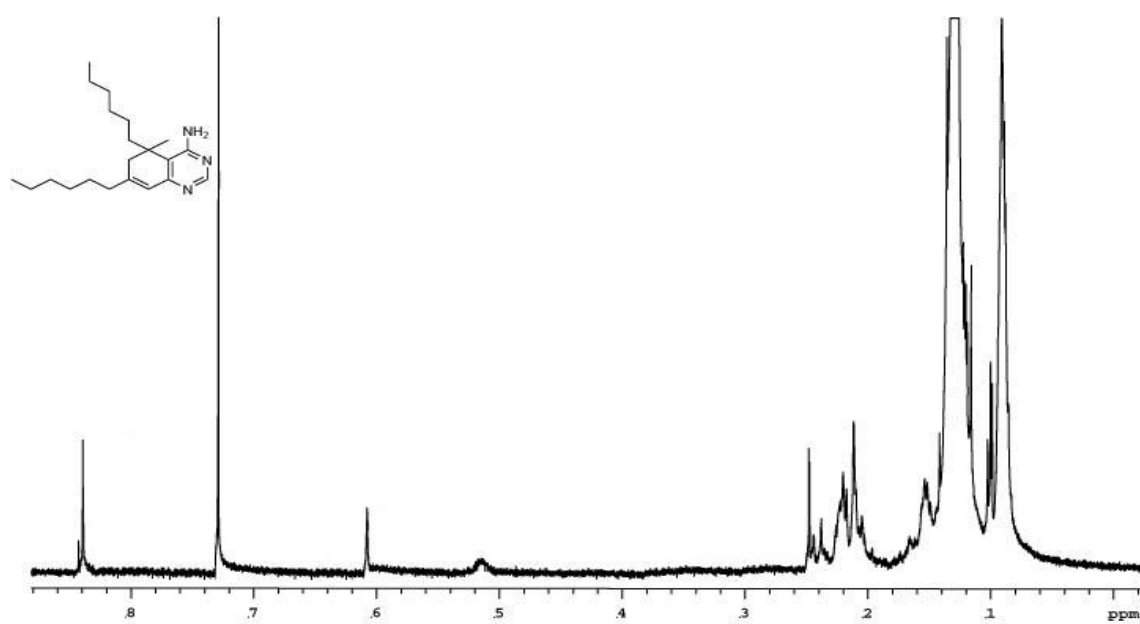
C-15. Spectra of 180.



C-16. Spectra of 181.



C-17. Spectra of 182.



C-18. Spectra of 183.

## VITA

Name: Bennie John Bench

Education: B.S. Chemistry

Southeastern Oklahoma State University, 2003

Ph.D. Chemistry, Texas A&M University, 2009

Permanent Address: Department of Chemistry

M.S. 3255

Texas A&M University

College Station, TX 77843

### Publications:

Angell, S.; Bench, B. J.; Watanabe, C. M. H. *Chem. Biol.*, **2006**, *13*, 1349-1359.

Bench, B. J.; Liu, C.; Evett, C. R.; Watanabe, C. M. H. *J. Org. Chem.*, **2006**, *71*, 9458-9463.

Daniel, S.; Diaz, A. J.; Martinez, K. M.; Bench, B. J.; Albertorio, F.; Cremer, P. S. *J. Am. Chem. Soc.*, **2007**, *129*, 8072-8073.

Bench, B. J.; Suarez, V. H.; Watanabe, C. M. H. *Bioorg. Med. Chem. Lett.*, **2008**, *18*, 3126-3130.

Bench, B. J.; Tichy, S. E.; Perez, L. M.; Benson, J.; Watanabe, C. M. H. *Bioorg. Med. Chem.*, **2008**, *16*, 7573-7581.